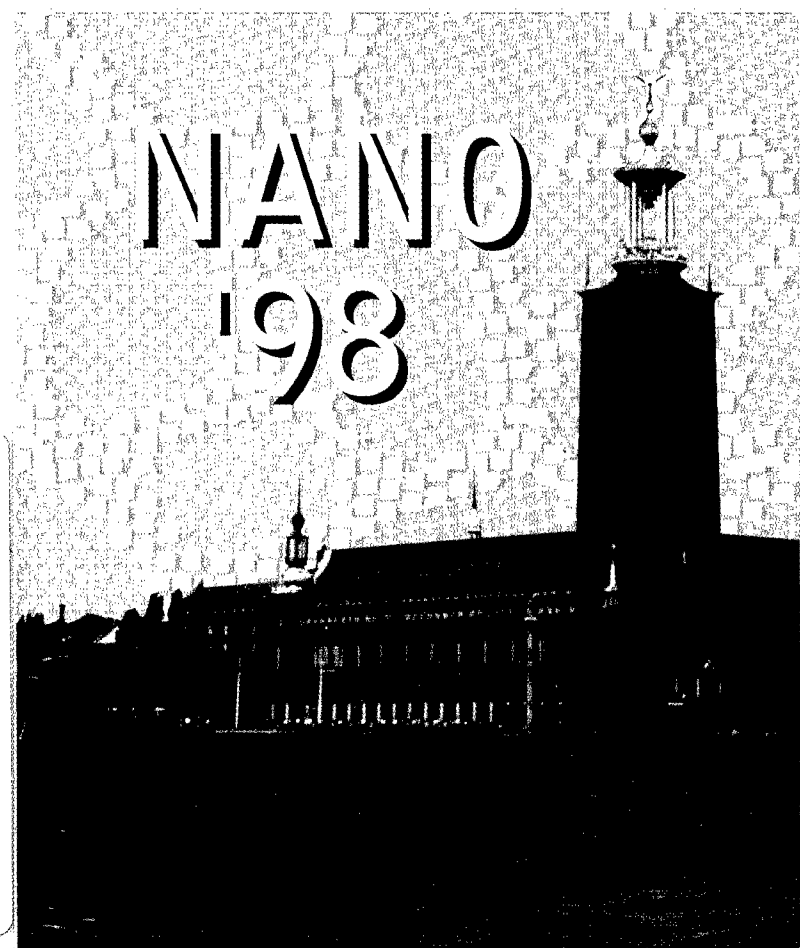


DISTRIBUTION STATEMENT A:  
Approved for Public Release -  
Distribution Unlimited



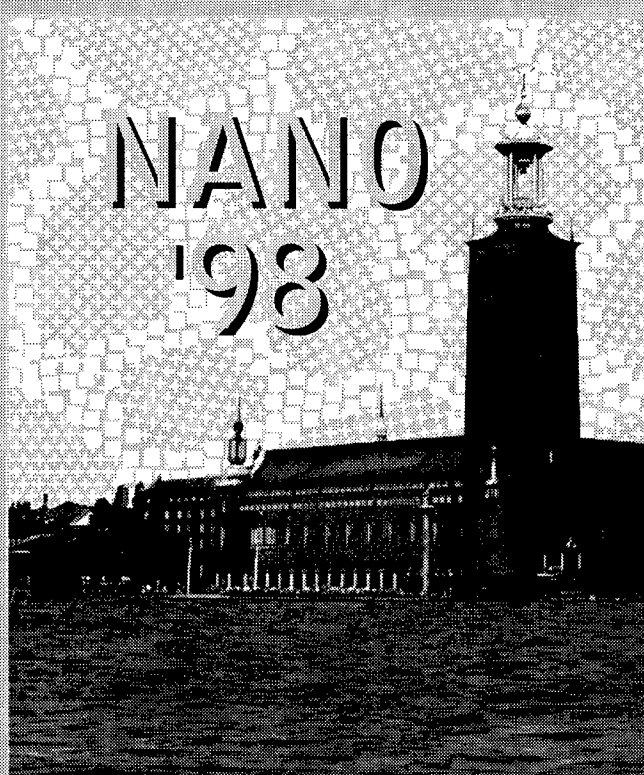
# Book of Abstracts

June 14-19, 1998  
Stockholm, Sweden

20000118102

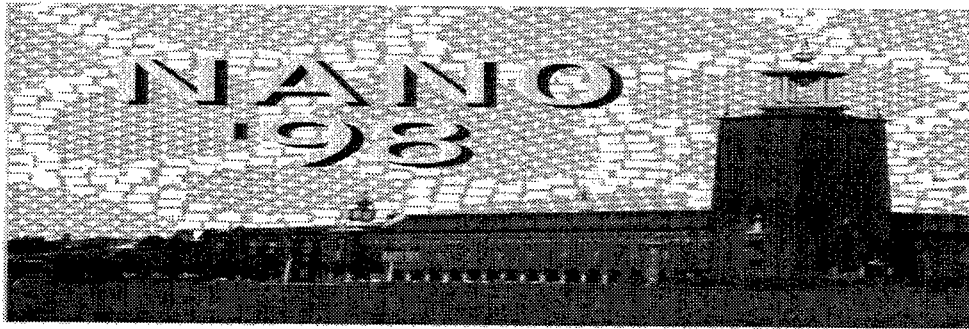
---

Fourth International Conference  
on Nanostructured Materials



Book of Abstracts

June 14-19, 1998  
Stockholm, Sweden



*Welcome to Stockholm and NANO'98,  
.... on the eve of Swedish Midsummer!*

*A remarkable group of interdisciplinary scientists from 40 countries have "self-assembled" here at Stockholm on the eve of the fascinating Scandinavian midsummer. The over 600 abstracts being presented in this conference indeed signal the emergence of new challenges as well as opportunities in materials science. We see clear trends as a result of the coming together of chemists, physicists, materials scientists, engineers, and architects of 'life-science' exploiting the driving force of nanotechnology into the limits of imagination. Chemistry is getting closer to post modern alchemy wherein dream materials are being modelled and synthesized almost at a molecule by molecule level, while the physicists have engineered atom by atom features.*

*The art of developing functionalized nanostructured materials exploiting unusual interfacial properties has not only produced new hitherto unknown man-made materials but almost seem to lead to the world of 'self-assembled systems' - a step closer to mimicking nature! Exploitation of the size-related properties of nanostructured materials, like transparency of opaque ceramics, superplasticity, enhanced mechanical properties, and complex tailored multilayer systems have produced value added components of promise like the GMR heads, unusual soft and hard magnetics, quantum dots, catalysts, and unusually hard material tools etc to name a few.*

*In addition to the invited and oral presentations, we hope the added feature of 'invited posters' and extensive poster sessions will provide many an opportunity to meet and discuss with your colleagues, to gain insight into new vistas of health, wealth, and benefits of mankind.*

*We certainly want you to enjoy the innumerable cultural activities being organized all over Stockholm, the 1998-culture capital of Europe. We sincerely hope that you will richly benefit from the sessions, and the cultural environment will remain a memorable experience.*



Mamoun Muhammed

Conference Co-Chairs



K. V. Rao

---

## **CONFERENCE CHAIRS**

**Mamoun Muhammed**

**K.V. Rao**

## **LOCAL ORGANIZING COMMITTEE,**

*Royal Institute of Technology*

Gonzalez, Maria José  
Hjelm, Sara  
Koo, Sang Mo  
Kim, Hyon-ju  
Northon, Anita  
Palmqvist, Anders

Shourie, Sheveta  
Turkki, Tarja  
Wahlberg, Sverker  
Wang, Mingshing  
Zhang, Yu  
Zagorodni, Andrei

## **SCIENTIFIC PROGRAMME COMMITTEE**

Dahlberg, Dan,  
Gleiter, Herbert,  
Grishin, Alexander,  
Hofmann, Heinrich,  
Muhammed, M.,  
Rao, K.V. ,  
Shull, Robert D.,  
Siegel, Richard W.,  
Thölén, Anders,  
Tsakalakos, Thomas,

*University of Minnesota, MN, USA*  
*Forschungszentrum Karlsruhe, Germany*  
*Royal Institute of Technology; Sweden*  
*EPFL, Switzerland*  
*Royal Institute of Technology,Sweden*  
*Royal Institute of Technology, Sweden*  
*NIST, MD , USA*  
*Rensselaer Polytechnic Institute, NY, USA*  
*Chalmers Institute of Technology, Sweden*  
*Rutgers University, NJ, USA*

## **PUBLICATION COMMITTEE**

M. Muhammed  
K.V. Rao

B. Kear  
T. Tsakalakos

## **NATIONAL ADVISORY COMMITTEE**

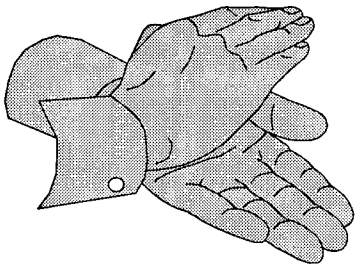
Brandt, Gunnar,  
Claeson, Tord,  
Eriksson, Torsten,  
Granqvist, Claes-Göran,  
Grinder, Olle,  
Grishin, Alexander,  
Haviland, David,  
Holmberg, Krister,  
Karlsson, Ulf  
Mårtensson, Nils,  
Nygren, Mats,  
Petersson, Sture,

*Sandvik AB*  
*Chalmers Institute of Technology*  
*Linköping Technical University*  
*Uppsala University*  
*Powder Metallurgy AB*  
*Royal Institute of Technology*  
*Royal Institute of Technology*  
*Institute of Surface Chemistry*  
*Royal Institute of Technology*  
*Uppsala University*  
*Stockholm University*  
*Royal Institute of Technology*

Roeraade, Johan,	<i>Royal Institute of Technology</i>
Rosén, Arne,	<i>Chalmers Institute of Technology</i>
Rowcliffe, David,	<i>Royal Institute of Technology</i>
Salwén, Anders,	<i>Institute of Metals Research (IM)</i>
Samuelsson, Lars,	<i>Lund Technical University</i>
Sandström, Rolf,	<i>Royal Institute of Technology</i>
Savage, Steven,	<i>Swedish National Defense Laboratories (FOA)</i>
Sterte, Johan,	<i>Luleå Technical University</i>
Sundgren, Jan-Erik,	<i>Linköping Technical University</i>
Sundqvist, Bertil,	<i>Umeå University</i>
Thölén, Anders,	<i>Chalmers Institute of Technology</i>
Warren, Richard,	<i>Luleå Technical University</i>
Wendin, Göran,	<i>Chalmers Institute of Technology</i>
Wilander, Magnus,	<i>Chalmers Institute of Technology</i>

## INTERNATIONAL ADVISORY COMMITTEE

Awschalom, David D.,	<i>Univ. of California, USA</i>
Bennemann, K.H.,	<i>Freie Universität Berlin, Germany</i>
Chantrell, R.W.,	<i>University of Keele, U.K.</i>
Chien, C.L.,	<i>Johns Hopkins University, USA</i>
Fiorani, Dino,	<i>ITSE, CNR, Italy</i>
Garcia, Nicolas,	<i>Lab de Fisica de Sistemas, Spain</i>
Gleiter, Herbert,	<i>Forschungszentrum Karlsruhe, Germany</i>
Hadjipanayis, G.C.,	<i>Univ. of Delaware, USA</i>
Hofmann, Heinrich,	<i>EPFL, Switzerland</i>
Inoue, Akihisa,	<i>Tohoku University, Japan</i>
Jena, Purushottam,	<i>Virginia Commonwealth Univ., USA</i>
Kear, Bernard H.,	<i>Rutgers University, USA</i>
Kozec, Marija,	<i>Jozef Stefan Institute, Slovenia</i>
Leppävuori, Seppo,	<i>Univ. of Oulu, Finland</i>
Makino, A.	<i>Alps Electric Company, Japan.</i>
Magini, M.,	<i>ENEA, Italy</i>
Multani, Manu,	<i>T.I.F.R Mumbai, India</i>
Muñoz, Juan S.,	<i>Univ. Autònoma de Barcelona, Spain</i>
Mörup, Steen,	<i>Techincal University of Denmark, Denmark</i>
Niarchos, Dimitri,	<i>DEMOKRITOS, Greece</i>
O'Grady, K.,	<i>University of Wales, U.K.</i>
Schmidt, G.,	<i>Univ. Essen, Germany</i>
Schultz, L.,	<i>IFW, Germany</i>
Scott, J.F.,	<i>Univ. of New South Wales, Australia</i>
Shull, Robert D.,	<i>NIST, MD, USA</i>
Siegel, Richard W.,	<i>Rensselaer Polytechnic Institute, USA</i>
St. Pierre,Timothy,	<i>Univ. of Western Australia, Australia</i>
Thomas, Gareth,	<i>University of California, USA</i>
Weller, Dieter	<i>IBM, San Jose, USA</i>
Wolf, Stuart A.,	<i>DARPA, USA</i>
Yavari, A.R.,	<i>LTPCM-CNRS, France</i>
Yu, Seong-Cho,	<i>Chungbuk Nat'l. Univ., Cheong-Ju, Korea</i>



## **SPONSORS**

Royal Institute of Technology, Sweden

Swedish Consortium on Clusters and Ultrafine Particles, Sweden

Brinell Center, Royal Institute of Technology, Sweden

European Consortium for Nanophase Materials, Switzerland

Acta Metallurgica Inc., USA

Alps Electric Company, Japan

Canon Centre City, Sweden

Carl Tryggers Stiftelse, Sweden

European Research Office of the US Army, USARDSD-UK

Elsevier Science Inc., Switzerland

Finnair, Finland

The Office of Naval Research ONR, USA

Swedish Natural Science Research Council, NFR, Sweden

Swedish Research Council for Engineering Sciences, (TFR), Sweden

Swedish Royal Academy of Science, Nobel Committee for Chemistry, Sweden

Swedish Royal Academy of Science, Nobel Committee for Physics, Sweden

Swedish National Board for Industrial and Technical Development (NUTEK)



## NANO 98 Program Overview

Time (approx.)	Monday	Tuesday	Wednesday	Thursday	Friday
0830-0915	<b>Plenary I</b> Giaver	<b>Plenary II</b> Esaki	<b>Plenary III</b> Sonojai	<b>Session 20</b> Theory II	<b>Session 24</b> Applications III
0915-1000	<b>Session 1</b> Novelties	<b>Session 5</b> Nanostructure, Multilayers & Thin Films I	<b>Session 8</b> Theory I	<b>Session 11</b> Optical Properties	<b>Session 16</b> Nanotechnology
1030-1230	<b>Session 2</b> Synthesis I	<b>Session 6</b> Nanostructure, Multilayers & Thin Films II	<b>Session 9</b> Fullerenes	<b>Session 12</b> Nanopowders	<b>Session 17</b> Magnetic Prop. I
1400-1530	<b>Session 3</b> Synthesis II	<b>Session 7</b> Nanoparticles	<b>Session 10</b> Size Effects	<b>Session 13</b> Mechanical prop.	<b>Session 18</b> Magnetic Prop. II
1600-1730	<b>Session 4</b> Synthesis III		<b>Invited Poster Session</b>	<b>Session 15</b> Struct. & Prop. I	<b>Session 19</b> Struct. & Prop. II
1900-2130	<b>Poster Session I</b>		<b>City Hall Reception</b>	<b>Poster Session II</b>	<b>Poster Session III</b>

# NANO 98

## Scientific Program

Monday 1998-06-15

08:15 OPENING SESSION

PL 1 **PLENARY LECTURE I:** Giaever, I., USA

08:30 *Nanostructures: Immunology, Tissue Culture and Biosensors*

### Session 1: Novelties in Nano Materials

1-1 (I) Fendler, J.H. USA

09:15 *High Energy Density Rechargeable Lithium- Ion Battery Prepared by the Self-Assembly of Graphite Oxide Nanoplatelets and Polyelectrolytes Nanolayers.*

1-2 (I) Krill,C.E., Michels,A., Helfen,L., Birninger,R., Germany

09:40 *Measuring and Modelling the Kinetics of Grain Growth in Nanocrystalline Materials*

1-3 (I) Wakayama, Y., Tanaka, S., Japan

10:05 *Fabrication of Nanoscale Heterojunction of Si/Au and Si/Ag by Surface Droplet Epitaxy*

10:30 to 10:50 Coffee Break

### Session 2: Synthesis I: General

2-1 (I) Magini, M., Iasonna, A., Padella, F., Italy

10:50 *Panel on Mechanical Alloying Process. Theoretical Framework and Experimental Supports*

2-2 (I) Shafi, Kurikka.V.P.M., Gedanken, A., Israel

11:10 *Sonochemical Approach for the Preparation of Nanostructured Ferrite Particles*

2-3 (I) Valiev, R.Z., Russia

11:30 *Nanostructured Materials Processed by Severe Plastic Deformation*

2-4 Kitamoto,Y., ABE Masanori, Japan

11:50 *Nanostructured Oxide Films by Ferrite Plating with Sonochemistry*

2-5 Deppert, K., Magnusson, M.H., Malm, J.-O., Bovin, J.-O., and Samuelson, L. Sweden

12:05 *Size-Selected Gold Nanoparticles by Aerosol Technology*

2-6 Fissan, H., Kruis, F.E., Rellinghaus, B., Otten, F., Wassermann, E.F., Germany

12:20 *Gas Phase Synthesis and Characterization of Equal-Sized Nanoscale Semiconductor Particles*

12:35 to 14:00 Lunch Break

### Session 3: Synthesis II: Self-assembly

3-1 (I) Schoeman, B.J., Higberg, K., Sterte, J., Sweden

14:00 *Nanoparticles of Microporous Materials*

3-2 (I) Anuradha, T.V. and Ranganathan, S., India

14:20 *Synthesis of Mesoporous TiO<sub>2</sub> and Tin*

3-3 (I) Kotov, N.A., Magonov, S., Tropsha, Y., USA

14:40 *Control Over the Film Structure in Layer-By-Layer Self-Assembled Films*

3-4 Smirnov, V. M., RUSSIA

15:00 *The Modern Synthetic Possibilities for Topological Organization of Oxide Nanostructures and Nanostructured Materials*

**15:15 to 15:40 Coffee Break**

**Session 4: Synthesis III: Chemical Methods**

- 4-1 (I) Trudeau, M. L., Canada  
15:40 *Nanocrystalline Fe and Fe-Riched Fe-Ni Through Electrodeposition*
- 4-2 Fernandez, A., Reddy, E.P., Rojas, T.C., Sanchez Lopez, J.C., Dominguez, M., Roldan, E., Campora, J., Palma, P., Spain  
16:00 *Preparation and Characterisation of Cobalt Oxide Nanosized Particles Obtained by An Electrochemical Method*
- 4-3 (I) O'Connor, C. J., Seip, Candace, T., Carpenter, E.E., Li,S., John,V.T., USA  
16:15 *Synthesis and Reactivity of Nanophase Ferrites in Reverse Micellar Solutions*
- 4-4 Hempelmann, R., Meyer, F., Dierstein, A., Beck, Ch., Wagner, J., Härti, W., Mathur,S., Veith, M., Germany  
16:35 *Size-Controlled Synthesis of Nanoscale Aluminate Spinels Via W/O Microemulsions Using Heterobimetallic Alkoxide Precursors*
- 4-5 Tsuzuki, T., McCormic, P.G., Australia  
16:50 *Mechanochemical Synthesis of Metal Sulphides Nanoparticles*
- 4-6 Bartz, K., Veith, M., Altherr, A., Blin, J., Heintz, M., Pillong, F., Germany  
17:05 *Glow Discharge Mass Spectrometry (GDMS) - A Powerful Tool in the Analysis of Nano-Scaled Materials*
- 4-7 Elihn, K., Boman, M., Kruis, E., Fissan, H., Carlsson, J-O, Sweden  
17:20 *Formation of Iron-Containing Nanoparticles By Laser-Assisted Photocatalytical Dissociation of Ferrocene*

**17:35 to 19:00 Dinner Break**

**POSTER SESSION I**

**Tuesday 1998-06-16**

- PL 2** PLENARY LECTURE II: Esaki, L., Japan  
08:30 *The Evolution of Nanoscale in Semiconductor Physics*

**Parallel section A**

**Session 5: Nanostructure, Multilayers &Thin Films I**

- 5-1 (I) Falco, C.M., Murayama, A., Hyomi, K., Eickman, J., USA  
09:15 *Magnetic Anisotropy of Ultrathin Co Films and Co-Based Sandwich Structures*
- 5-2 (I) Tsakalacos, T., Simopoulos, A., Jankowski, A., Kioussis, N., USA  
09:35 *Structure and Properties of Nanoscale Multilayers*
- 9:55 **Discussions**

**10:00 to 10:30 Coffee Break**

**Session 6: Nanostructure, Multilayers &Thin Films II**

- 6-1 (I) Schuller, I., USA  
10:30 *Arrays of Submicron Magnetic Dots: Hysteresis and Flux Pinning*
- 6-2 Brinznak, R., Jensen, P.J., Bennemann, K.H., Germany  
10:50 *Simulation of the Magnetic Properties During the Nanostructural Growth of Ultrathin Films*

<b>6-3</b>	<u>Melinon, P., Keghelian, P., Perez, A., France</u>
<b>11:05</b>	<i>Properties of Silicon and Silicon-Carbon Cluster Assembled Films</i>
<b>6-4</b>	<u>Eibeck, P., Spatz, J.P., Möller, M., Germany</u>
<b>11:20</b>	<i>Ultrathin Diblock Copolymer Films. A Tool for Nanolithography</i>
<b>6-5</b>	<u>Josell, D., Carter, W.C., USA</u>
<b>11:35</b>	<i>Stability of Multilayer Structures: Capillary Effects</i>
<b>6-6</b>	<u>Suda, Y., Ebihara, K., Baba, K., Abe, H., Grishin, A.M., Japan</u>
<b>11:50</b>	<i>Epitaxial Silicon Nitride Thin Films Grown by Pulsed YAG Laser Deposition</i>
<b>6-7</b>	<u>Cottam, M.G., Costa Filho, R.N., Russia</u>
<b>12:05</b>	<i>Energy Shift and Damping of Dipole-Exchange Spin Waves in Ultrathin Ferromagnetic Films</i>
<b>12:20</b>	<b>Discussions</b>

**12:30 to 14:00 Lunch Break**

### **Session 7: Nanoparticles**

<b>7-1 (I)</b>	<u>Hofmann, H., Houriet, R., Hofmeister, H., Dutta, J., Switzerland</u>
<b>14:00</b>	<i>Crystallization and Reaction Behavior of Nano-Sized Amorphous Silicon Powders</i>
<b>7-2 (I)</b>	<u>Baughman, R.H., Zakhidov, A.A., Cui, C., Khairullin, I., Liu, L.M., Iqbal, Z., Dantas, S.O., Ralchenko, V.G., USA</u>
<b>14:20</b>	<i>Three-Dimensionally Periodic Nanostructured Foams and Hybrid Materials From Opals</i>
<b>7-3 (I)</b>	<u>Vollath, D., Szabo, D. V., Fuchs, J., Germany</u>
<b>14:40</b>	<i>Synthesis and Properties of Ceramic – Polymer Composites</i>
<b>7-4 (I)</b>	<u>Klabunde, K. J., Zhang, D., Sorenson, C., USA</u>
<b>15:00</b>	<i>Encapsulated Iron, Cobalt, and Nickel Nanocrystals; Effect of Coating Material (<math>Mg</math>, <math>MgF_2</math>) on Magnetic Properties</i>
<b>7-5</b>	<u>Erb, U., Robertson, A., Palumbo, G., Canada</u>
<b>15:20</b>	<i>Practical applications for electrodeposited nanocrystalline materials</i>
<b>15:35</b>	<b>Discussions</b>

### **Parallel section B**

### **Session 8: Theory I**

<b>8-1 (I)</b>	<u>Doyama, M., Nozaki, T., Kogure, Y., Yokotsuka, T., Japan</u>
<b>09:15</b>	<i>Plastic Deformation of Pure Silicon Nanocrystals by Molecular Dynamics</i>
<b>8-2 (I)</b>	<u>Jena, P., Nayak, S.K., Reddy, B.V., Khanna, S.N., Rao, B.K., USA</u>
<b>09:40</b>	<i>Magnetism at the Nanoscale</i>

**10:00 Discussions**

**10:10 to 10:30 Coffee Break**

### **Session 9: Fullerenes**

<b>9-1 (I)</b>	<u>Eklund, P.C., USA</u>
<b>10:30</b>	<i>Carbon Nanotubes-Science and Applications</i>
<b>9-2 (I)</b>	<u>Hornyak, G.L., Schneider, J.J., Czap, N., Jones, K.M., Hasoon, F.S., Heben, M.J., USA</u>
<b>10:55</b>	<i>Template Synthesis of Carbon Nanotubes</i>

<b>9-3 (I)</b>	<u>Billas, I.M.L.</u> , Branz, W., Malinowski, N., Tast, F., Heinebrodt, M., Martin, T.P., Massobrio, C., Boero, M., Parrinello, M., <i>Germany</i>
<b>11:15</b>	<i>Experimental and Computational Studies of Heterofullerenes</i>
<b>9-4</b> <u>Oku, T.</u> , Schmid, G., Niihara, K., Suganuma, K., <i>Japan</i>	
<b>11:35</b>	<i>Formation of Carbon Nanocapsules with Clusters</i>
<b>9-5</b>	<u>Keblinski, P.</u> , Wolf, D., Phillpot, S.R., Gleiter, H., <i>USA</i>
<b>11:55</b>	<i>Nature of Grain Boundaries in Nanocrystalline Diamond by Atomistic Simulations</i>
<b>9-6</b>	<u>Meng, G.W.</u> , Zhang, L.D., <i>China</i>
<b>12:10</b>	<i>Synthesis of Beta-SiC Nanowires with SiO<sub>2</sub> Wrappers</i>
<b>12:25</b>	<b>Discussions</b>

**12:30 to 14:00   Lunch Break**

### **Session 10: Size Effects**

<b>10-1 (I)</b>	<u>Yacaman, M.J.</u> , Ascencio, J.A., Alvarez, M.P., <i>Mexico</i>
<b>14:00</b>	<i>A Novel Structure Observed in Nanoparticles of Gold</i>
<b>10-2 (I)</b>	<u>Iqbal, Z.</u> , Vijayalakshmi, S., White, C.W., Federeci, J.C., Grebel, H., <i>USA</i>
<b>14:20</b>	<i>Nanoclustered Silicon-Based Artificial Dielectrics and Superlattices: Fabrication, Characterization and Photophysics</i>
<b>10-3 (I)</b>	<u>Ayyub, P.</u> , Chattopadhyay, S., Sheshadri, K., Lahiri, R., <i>India</i>
<b>14:40</b>	<i>The Nature of Ferroelectric Order in Finite Systems</i>
<b>10-4</b>	<u>Chen, Y.Y.</u> , Yao, Y.D., Lee, T.K., Liu, W.C., Chang, H.C., Lin, K.Y., Lin, Y.S., Wang, Z.C., Li, W.H., <i>Taiwan</i>
<b>15:00</b>	<i>Heavy-Fermion Behaviour in CeAl<sub>2</sub> Nanoparticles</i>
<b>10-5 (I)</b>	<u>Niklasson, G.A.</u> , Bobbert, P.A., Craighead, H.G., <i>Sweden</i>
<b>15:15</b>	<i>Optical Properties of Square Lattices of Gold Nanoparticles</i>
<b>15:35</b>	<b>Discussions</b>
<b>15:45 to 16:00</b>	<b>Coffee Break</b>
<b>16:00</b>	
<b>to</b>	<b>INVITED POSTERS' SESSION</b>
<b>17:30</b>	

**17:30-19:00   Dinner Break**

<b>19:00</b>	
<b>to</b>	
<b>21:30</b>	<b>CITY HALL RECEPTION</b>

**Wednesday 1998-06-17**

- PL 3 PLENARY LECTURE III:** Somorjai, G. USA  
**08:30** *Transition Metal (Pt, Ag) Nano-Cluster Arrays Fabricated by Electron Beam Lithography (2-5-50 nm range): Structure, Stability, and Catalytic Reaction Studies*

**Parallel section C**

**Session 11: Optical Properties**

- 11-1 (I)** El-Shall, M.S., Li, S., Germanenko, I., USA  
**09:15** *Synthesis and Charactrization of Silicon Nanocrystals and Incorporation in Polymer Films*
- 11-2** Stietz, F., Germany  
**9:35** *Optical Properties of Metal Nanoparticles: Adsorbate Induced Modifications*
- 11-3** Milovzorov, D., Inokuma, T., Kurata, Y., Hasegawa, S. Japan  
**9:50** *Correlation Between Structural and Optical Properties of Nanocrystal Particles Prepared at Low Temperature by Plasma-Enhanced Chemical Vapor Deposition*

**10:05 to 10:30 Coffee Break**

**Session 12: Mechanical Alloying**

- 12-1 (I)** Arrot, A. S., USA  
**10:30** *Can Ball-Milling Yield Superior Soft Magnetic Materials?*
- 12-2** Ma, E., He, L., Allard, Jr, USA  
**10:50** *Full-Density (I)Situ Cu-Fe Nanocomposites Consolidated From Mechanically Alloyed Solid Solution Precursors*
- 12-3** Enzo, S., Frattini, R., Canton, P., Mulas, G., Radaelli, P., Italy  
**11:05** *A Study of Al-Mo Alloys Synthesized by Mechanical Treatment and Annealed In-Situ*
- 12-4** Glezer A.M., Russia  
**11:20** *Structure and Plastic Flow Mechanisms of Melt-Quenched Nanocrystals*
- 12-5** Jiang, J.Z., Wynn, P., Morup, S., Okada, T., Berry, F.J., Denmark  
**11:35** *Magnetic Structure Evolution in Mechanically Milled Nanostructured ZnFe<sub>2</sub>O<sub>4</sub> Particles*

**Session 13: Nano Powders**

- 13-1** Sergeev, G.B., Nemukhin, A.V., Sergeev, B.M., Shabatina, T.I., Zagorskii, V.V., Russia  
**11:55** *Cryosynthesis and Properties of Metal-Organic Nanomaterials*
- 13-2** Schwitzgebel, G., Heim, U., Germany  
**12:10** *Electrochemistry of Nanocrystalline Copper*
- 12:25** **D i s c u s s i o n s**

**12:30 to 14:00 Lunch Break**

**Session 14: Mechanical Properties**

- 14-1 (I)** Fitz-Gerald, J. and Singh, R.K., USA  
**14:00** *Synthesis and Properties of Nano-functionalized Particulate Materials.*

<b>14-2 (I)</b>	Inoue, A., Fan, C., Takeuchi, A., <i>Japan</i>
<b>14:25</b>	<i>High-Mechanical Strength of Bulk Nanostructure Alloys Consisting of Compound and Amorphous Phases</i>
<b>14-3 (I)</b>	Sastry, S. M. L., <i>USA</i>
<b>14:45</b>	<i>Microstructural Refinement and Mechanical Property Improvement of Copper and Copper-Al<sub>2</sub>O<sub>3</sub> Specimens Processed by Equal Channel Angular Extrusion (ECAE)</i>
<b>14-4 (I)</b>	Tanimoto Hisanori, Sakai,S., Mizubayashi,H., <i>Japan</i>
<b>15:05</b>	<i>Mechanical Properties of High Density Nanocrystalline Gold Prepared by Gas Deposition Method</i>
<b>15:25</b>	<b>Discussions</b>

**15:30 to 16:00 Coffee Break**

### **Session 15: Structures & Properties I**

<b>15-1 (I)</b>	Andrievski, R.A., <i>Russia</i>
<b>16:00</b>	<i>Physical Properties of Nanostructured High Melting Point Compounds</i>
<b>15-2 (I)</b>	Merzbacher, C.I., Barker, J.G., Anderson, M. L., Long, J.W., Rolison, D.R., <i>USA</i>
<b>16:20</b>	<i>Characterization of Composite Aerogels by Contrast-Matched Small-Angle Neutron Scattering</i>
<b>15-3</b>	Würschum,R., Michel,T., Scharwaechter,P., Frank,W., Schaefer,H.E., <i>Germany</i>
<b>16:40</b>	<i>Fe Diffusion in Nanocrystalline Alloys and the Influence of Amorphous Intercrystalline Layers</i>
<b>15-4</b>	Lu, K., <i>China</i>
<b>16:55</b>	<i>Experimental Evidences of Lattice Distortion in Nanocrystalline Materials</i>
<b>15-5</b>	Segers,D., Petteghem,S.V., Löffler,J.F., Swygenhoven,H.V., Wagner,W., Dauwe,C., <i>Belgium</i>
<b>17:10</b>	<i>Positron Annihilation Study of Nanocrystalline Iron</i>
<b>17:25</b>	<b>Discussions</b>

### **Parallel Section D**

#### **Session 16: Nanotechnology**

<b>16-1 (I)</b>	Garcia, N., <i>Spain</i>
<b>09:15</b>	<i>Nanowires; Theory and Experiments.</i>
<b>16-2 (I)</b>	Chou, S.Y., Zhang, W., Zhuang, L., Guo, L., <i>USA</i>
<b>09:40</b>	<i>Nanoimprint Lithography -- A New Low-cost High-Throughput Sub-10-nm Lithography</i>
<b>10:00</b>	<b>Discussions</b>

**10:05 to 10:30 Coffee Break**

#### **Session 17: Magnetic Properties I**

<b>17-1 (I)</b>	Roshko, R.M., Mitchler, P. D., Wesseling, E., Dahlberg, Dan E., <i>USA</i>
<b>10:30</b>	<i>Magnetic Nanoparticles, Henkel Plots, and Preisach Models; Interactions and Dynamics</i>

<b>17-2 (I)</b>	<u>Fiorani, D.</u> , Dormann, J.L., Cherkaoui, R., Spinu, L., Lucari, F., D'Orazio, F., Nogues, M.,
<b>10:50</b>	Tronc, E., Jolivet, J.P., Garcia, A., <i>Italy/France</i>
<i>Collective Glass State in Magnetic Nanoparticles Systems</i>	
<b>17-3 (I)</b>	<u>Majetich, S.</u> , <i>USA</i>
<b>11:10</b>	<i>Nanoscale Magnetic Characterization of Nanoparticles</i>
<b>17-4 (I)</b>	<u>Berkowitz, A.E.</u> , Kodama, R.H., Takano, K., Foner, S., McNiff, E.J., Makhlouf, S.H., Parker, F.T., <i>USA</i>
<b>11:30</b>	<i>Anomalous Properties of Magnetic Nanoparticles</i>
<b>17-5</b>	<u>Edelstein, A.S.</u> , Kodama, R.H., Miller, M.M., Browning, V., Lubitz, P., Sieber, H., <i>USA</i>
<b>11:45</b>	<i>Ferromagnetic/Antiferromagnetic Structures with Ferromagnetic Interlayer Coupling</i>
<b>17-6 (I)</b>	<u>Schultz, L.</u> , Neu, V., Bauer, H.-D., <i>Germany</i>
<b>12:00</b>	<i>Grain Size Dependence of Remanence Enhancement of Nano-Crystalline Nd-Fe-B Powders</i>
<b>17-7</b>	<u>Varga, L.K.</u> , Rao, K.V., <i>Hungary</i>
<b>12:20</b>	<i>Thermomagnetic Study of Metastable Nanograins in Soft Magnetic Nanocrystalline Alloys</i>
<b>12:35</b>	<b>D i s c u s s i o n s</b>
<b>12:40 to 14:00      Lunch Break</b>	
<b>Session 18: Magnetic Properties II</b>	
<b>18-1 (I)</b>	<u>Aliev, F.G.</u> , Moshchalkov, V.V., Bruynseraede, Y., <i>Belgium</i>
<b>14:00</b>	<i>Anomalous Electron Transport in Magnetic Multilayers Tuned by Electric and Magnetic Fields</i>
<b>18-2 (I)</b>	<u>Madurga, V.</u> , Vergara, J., Perez de Landazabal, I., Ortega, R.J., <i>Spain</i>
<b>14:20</b>	<i>Nanostructured Laser Ablated CuCo Thin Films: Magnetic and Magneto resistive Properties.</i>
<b>18-3</b>	<u>Ivchenko, V.A.</u> , Uimin, M.A., Yermakov, A. Ye, Korobeinikov, A.Yu, <i>Russia</i>
<b>14:40</b>	<i>Field Ion Microscopy and Magnetic Properties of the Cu<sub>80</sub>Co<sub>20</sub> Nanophase Compounds by Mechanical Milling</i>
<b>18-4</b>	<u>Chiriac, H.</u> , Ovari, T. A., Marinescu, C.S., <i>Romania</i>
<b>14:55</b>	<i>Giant Magneto-Impedance Effect in Nanocrystalline Ribbons</i>
<b>18-5</b>	<u>Swagten, H.J.M.</u> , Van de Veerdonk, R.J.M., Kuijpers, N.C.W., Moodera, J.S., de Jonge, W.J.M., <i>Netherlands</i>
<b>15:10</b>	<i>Influence of Oxidation Time on the Magneto-transport Properties of Magnetic Tunnel Junctions</i>
<b>15:25</b>	<b>D i s c u s s i o n s</b>
<b>15:30-16:00    Coffee Break</b>	
<b>Session 19: Structures &amp; Properties II</b>	
<b>19-1 (I)</b>	<u>Shull, R.D.</u> , Shapiro, A.J., Chopra, H.D., Nikitenko, V., Gornakov, V., Khapikov, A., Dedukh, L.M., Kabanov, Y.P., Chaiken, A., Michel, R.P., <i>USA</i>
<b>16:00</b>	<i>Magnetic Domains in Nanocrystalline and Nanocomposite Materials?</i>
<b>19-2 (I)</b>	<u>Hadjipanayis, G.C.</u> , Prados, C., <i>USA</i>
<b>16:20</b>	<i>Nanocrystalline Sm-(Co, Cu, Ni) Thin Films with Giant Coercivity</i>
<b>19-3 (I)</b>	<u>Salmeron, Miquel.</u> , <i>USA</i>
<b>16:40</b>	<i>Studies of Tribology and Liquid Structures Using Scanning Probe Microscopy</i>
<b>19-4</b>	<u>Kester, E.</u> , Rabe, U., Arnold, W., <i>Germany</i>
<b>17:00</b>	<i>Measurement of Mechanical Properties of Nanoscaled Ferrites Using Atomic Force Microscopy at Ultrasonic Frequencies</i>

19-5	<u>Löffler, J.F.</u> , Wagner, W., Braun, H-B., Kostorz, G., Wiedenmann, A., Switzerland
17:15	<i>Grain Size Dependence of Intergranular Magnetic Correlations in Nanostructured Metals</i>
<b>17:30 Discussions</b>	
17:35 to 19:00 Dinner Break	
19:00 to 21:30 <b>POSTER SESSION II</b>	

## Thursday 1998-06-18

### Session 20: Theory II

20-1 (I)	<u>Kresin, V.Z.</u> , Kresin, V.V., USA <i>Unusual Low-Energy Collective Excitations (I) Nanoclusters and Nanocluster Compounds</i>
08:30	
20-2	<u>Herr, U.</u> , Germany <i>Molecular Dynamics Simulations of Nanocrystalline Glass Forming Alloys</i>
08:55	
20-3	<u>Saenger, D.U.</u> , Germany <i>Optical Absorption by An Ensemble of Semiconducting Nanoparticles</i>
09:10	
20-5	<u>Gupta, V.V.</u> , Lau, M.L., Lavernia, E.J., USA <i>A Mathematical Model to Trace the Genesis of Nanocrystallinity in Coatings Obtained Via High Velocity Oxygen Fuel Thermal Spray</i>
09:25	
20-6	<u>Swygenhoven, H. Van</u> , Spaczer, M., El Azzaoui, M., Hou, M., Caro, A., Switzerland <i>The Influence of Grain Boundary Structure on the Density of Nanophase Ni: a Molecular Dynamics Computer Simulation.</i>
09:40	
09:55	<b>Discussions</b>
10:00 to 10:30 Coffee Break	

### Session 21: Processing

21-1 (I)	<u>Groza, J.R.</u> , USA <i>Nanosintering</i>
10:30	
21-2	<u>Kopylov, V.I.</u> , Belorussia <i>Producing Nano- and Microcrystalline Materials by ECAP-Process</i>
10:50	
21-3 (I)	<u>Yoo, S.H.</u> , Sudarshan, T.S., Sethuram, K., Kalyanaraman, R., Subbash, G., Dowding, R.J., USA <i>Consolidation and High Rate Mechanical Behavior of Nanocrystalline Tantalum Powders</i>
11:05	
21-4 (I)	<u>Kiss, L.B.</u> , Söderlund, J., Niklasson, G.A., Granqvist, C.G., Sweden <i>The Real Origin of Log-normal Size Distribution of Nanoparticles Ar Vapour Growth Processes</i>
11:25	

## **Session 22: Applications I**

- 22-1 (I) Ying, J. Y., USA  
11:45 *Nanostructure Processing of Advanced Catalytic Materials*
- 22-2 Wilcoxon, J.P., Thurston, T.R., Martin, J.E., USA  
12:05 *Applications of Metal and Semiconductor Nanoclusters as Thermal and Photo-Catalysts*
- 22-3 Hernando A., Del Bianco L., Rojo J.M., Ballesteros C., Spain  
12:20 *An Overview on Nanophase Materials and Magnetic Applications*

**12:35 to 14:00 Lunch Break**

- 22-4 Gleeson, D., Burch,R., Tsang,S.C.E., UK  
14:00 *Thin FilmDeposition in Mesoporous Channels as Novel Sensor and Catalyst Methods*
- 22-5 Voronov, O.A., Sandagi, R.K., Kear, B.H., USA  
14:15 *WC/Co/Diamond Nanocomposites*

**14:30 Discussions**

## **Session 23: Applications II**

- 23-1 (I) Zakhidov, A.A., Baughman, R.H., Cui, C., Khairullin, I., Shkunov, M., Vardeny, V.Z., USA  
14:40 *Periodic Nanocomposites and Nanoporous Structures for Photonic Crystals and Advanced Thermoelectrics.*
- 23-2 (I) Provenzano,V., Valiev,R.Z., Rickerby,D.G., Valdre,G., Italy  
15:00 *Mechanical Properties of Nanostructured Chromium-Based Alloys*
- 23-3 Venkatasubramanian, R., Siivola, E., USA  
15:20 *Factorial Enhancement in Thermoelectric Figure of Merit with Si/Ge Superlattice Structures*

**15:35-16:00 Coffee Break**

- 23-4 (I) Vogel, V., Dennis, J.R., Howard, J., USA  
16:00 *Molecular Shuttles and Nanotracks*
- 23-5 Ginley,D.S., Schulz,D.L., Curtis,C.J., USA  
16:20 *Nano-Cu-In-Se as a Precursor to CIS Solar Cells*
- 23-6 Hedberg, L., Petronis, S., Kasemo, B., Sweden  
16:35 *Nanofabricated substrates for probing single biomolecules by surface enhanced raman scattering*
- 23-7 Webster, T.J., Siegel, R.W., Bizios, R., USA  
16:50 *Osteoblast Function on Nanophase Alumina*
- 23-8 Yavari, A.R., Tousimi, K., France  
17:05 *Ceramic-Copper Metal-Matrix Nanocomposites Prepared by Reactive Milling*
- 23-9 Kislov, V.V., Kolesov, V.V., Gubin, S.P., Soldatov, E.S., Trifonov, A.S., Russia  
17:20 *The Molecular Cluster-Materials for Nanoelectronics*
- 17:35 **Discussions**

**17:40-19:00 Dinner Break**

- 19:00  
to  
21:30
- POSTER SESSION III**

**Friday 1998-06-19**

**Session 24: Applications III**

- 24-1 (I) Menon, A., USA  
09:00 *Nanotechnology: A Data Storage Perspective*
- 24-2 (I) Sellmyer, D.J., Yu, M., Luo, C.P., Thomas, R., Liu, Y., USA  
09:30 *Nano Structured Films for Extremely High Density Magnetic Recording*
- 24-3 (I) Weller, D., Moser, A., Beat, M., Doerner, M., Folks, L., Jones, B., Kaufman, J., USA  
09:55 *Superparamagnetism and Dynamic Coercivity in Magnetic Recording Media*
- 24-4 Scott, J.F., Alexe, M., Curran, C., Pignolet, A., Hesse, D., Zakharov, N.D., Germany  
10:15 *1 Gigabit Nanoscale Bismuth Oxide Electrode Self-Patterning Ferroelectric Thin Films for Memory Application*
- 11:00 to 12:30 **10:30 to 11:00 Coffee Break**  
**PANEL SESSION ON FUTURE TRENDS IN NANOS**  
Siegel, D., Glieter H., Kear, B., ...
- 12:30 **CLOSING SESSION - Glieter, H. - Inoue A.**
- 12:45 **Conference ends**
- 12:45 Onwards **Conference picnic**  
**Swedish Mid-Summer Festivities...**

**Invited Poster Session**

- IP-1 Sivamohan, R.; Takahashi, H.; Kasuya, A.; Tsunekawa, S.; Ito, S.; Tohji, K.; Jeyadevan, B.; Japan  
*Liquid Chromatography Used to Size-Separate the Amphiphilic-Molecules Stabilised Nano-Particles of CdS in the 1-10 nm Range*
- IP-2 Josell, D.; Van Heerden, D.; Scechtman, D.; Read, D.; USA  
*Mechanical Properties of Multilayer Materials*
- IP-3 Petrov, Y.I.; Russia  
*Preparation, Some Properties and Applications of Ultrafine Aerosol Particles of Metals, Their Alloys and Compounds*
- IP-4 Ohnuma, M.; Hono, K.; Onodera, H.; Japan  
*Microstructure of Sputter-Deposited Co-Al-O Granular Thin Films*
- IP-5 Lau, M.L.; Huang, B.; Lavernia, E.J.; USA  
*Synthesis and Characterization of Nanocrystalline WC-Co Coatings*
- IP-6 Olde Riekerink, M.B.; Terlingen, J.G.A.; Engbers, G.H.M.; Feijen, J.; Netherlands  
*Nanostructuring of Polymer Surfaces by Gas Plasma Treatment*
- IP-7 Sorokin, L.M.; Hutchison, J.L.; Bogomolov, V.N.; Zaslavskaya, T.N.; Russia  
*TEM and HREM Study of the 3D Superlattices Consisting of Nanoclusters in Synthetic Opal Matrix*
- IP-8 Osmolovski, M.G.; Ivanova, L.Y.; Russia  
*Ultrafine Chromium Dioxide Powders*
- IP-9 Schurack, F.; Eckert, J.; Schultz, L.; Germany  
*High Strength Al-Alloys with Nano-Quasicrystalline Phase as Main Component*
- IP-10 Yermakov, A.Y.; Zajkov, N.K.; Mushnikov, N.V.; Gasivo, V.S.; Serikov, V.V.; Russia  
*Nanostructural State and Magnetism of RFe<sub>2</sub>H<sub>x</sub> Hydrides Obtained by Hydrogen-Induced Amorphization*
- IP-11 Sweeney, S.M.; Mayo, M.J.; USA  
*Green Density Effects in the Sintering of Nanocrystalline and Near-Nanocrystalline Ceramics*
- IP-12 Chen, Y.; Australia  
*Investigation of Nanosized Ceramic Powders Produced by Mechanochemistry*
- IP-13 Rao, B.K.; Khanna, S.N.; Jena, P.; USA  
*Designing Atomic Clusters as Super Atoms*
- IP-14 Baró, M.D.; Amils, X.; Nogués, J.; Suriñach, S.; Muñoz, J.S.; Galianella, S.; Spain  
*Order-Disorder Transitions in Nanocrystalline Ball Milled Fe-40Al At.% Alloy*
- IP-15 Kusano, E.; Kitagawa, M.; Satoh, A.; Kobayashi, T.; Nanto, H.; Kinbara, A.; Japan  
*Hardness of Compositionally Nano-Modulated TiN Films*
- IP-16 Beck, Ch.; Hempelmann, R.; Burch, Ch.; Unruh, H.G.; Germany  
*Phonon Confinement in Nanocrystalline Y<sub>2</sub>O<sub>3</sub> Studied by Raman Light Scattering*
- IP-17 Crnjak-Orel, Z.; Muevi, I.; Slovenia  
*Characterization of Vanadium Oxide and New V/Ce Oxide Films Prepared by Sol Gel Process*
- IP-18 Lang, M.; Arnold, W.; Germany  
*Measurement of Elastic and Anelastic Properties of Nanocrystalline Metals*

- IP-19 Kolobkova, E.V.; Lipovskii, A.A.; Petrikov, V.D.; Russia  
*PbSe, PbS Quantum Dots: Synthesis and Physical Properties*
- IP-20 Wu, X.; Tan, G.; Wang, Y.; Li, Z.; China  
*Mechanical Explosion Synthesis of Nanocrystalline Tungsten Carbides Powders*
- IP-21 Yu, S.C.; Kim, K.S.; Song, I.Y.; Kim, H.J.; Korea  
*The Low Temperature Dependence of Magnetization of As-Deposited Fe-Hf-N Nanocrystalline Thin Films.*
- IP-22 Oku, T.; Bovin, J-O; Nakajima, S.; Kubota, H.; Ohgami, T.; Suganuma, K.; Japan  
*Nanostructural Characterization of Solid Clusters and Oxide by HREM with Residual Indices*
- IP-23 Toppari, J.J.; Kauppinen, J.P.; Hirvi, K.P.; Kinnunen, K.M.; Pekola, J.P.; Finland  
*Coulomb Blockade Nanothermometer*
- IP-24 Pasquini, L.; Bonetti, E.; Campari, E.G.; Sampaolesi, E.; Scipione, G.; Italy  
*Magnetoelasticity and Internal Strains in Nanocrystalline Nickel*
- IP-25 Mishra, P.; Jain, K.P.; India  
*Raman and Photoluminescence Studies of Nanocrystalline Silicon Processed by CW-Laser Annealing*
- IP-26 Göthelid, M.; Haglund, S.; Ågren, J.; Sweden  
*WC(0001)-Co and WC(0001)-CoOx Studied by STM and AES*
- IP-27 Youngdahl, C.J.; Agnew, S.R.; Elliott, B.R.; Sanders, P.G.; Weertman, J.R.; Eastman, J.A.; USA  
*Mechanical Properties of Nanocrystalline Metals in Compression*
- IP-28 Westergren, J.; Grönbeck, H.; Rosén, A.; Nordholm, S.; Sweden  
*Metal Cluster Cooling and Heating in Noble Gas Atmosphere*
- IP-29 Weissmuller, J.; Michels, A.; Barker, J.; Shull, R.D.; McMichael, R.D.; Erb, U.; Germany  
*Measuring Magnetic Microstructure by Spin -Polarized Small -Angle Neutron Scattering*
- IP-30 Ramasamy, S.; Viswanath, R.N.; India  
*Sol-Gel Derived YSTZ-Al<sub>2</sub>O<sub>3</sub> and YSTZ-Al<sub>2</sub>O<sub>3</sub>-SiO<sub>2</sub> Nanocomposites*
- IP-31 Persson, S. H.M.; Olofsson, L.; Hedberg, L.; Sweden  
*Self-Assembled Single Electron Tunnelling Devices*
- IP-32 Boikov, Y.A.; Danilov, V.A.; Claeson, T.; Erts, D.; Sweden  
*Ultrathin A<sub>2</sub>(V)B<sub>3</sub>(VI) Thermoelectric Films Confine Charge Carriers to Move in Two Dimensions*
- IP-33 Vijayalakshmi, R.; Kapoor, S.; Kulshreshtha.S.K.; Mittal, J.P.; India  
*Nanophase Platinum Particles on Na Zeolite a Surface by Gamma Radiolysis*
- IP-34 Noskova, N.I.; Volkova, E.G.; Russia  
*The Deformation and Peculiarities of the Destruction of Nanophase Materials*
- IP-35 Shih, H.C.; Tsai, S.H.; Tsai, T.G.; Taiwan  
*Synthesis of Carbon Nanotubes on Porous Anodic Alumina by ECR/CVD*
- IP-36 Srdic, V.V.; Winterer, M.; Hahn, H.; Germany  
*Modification of Chemical Vapor Synthesis Process for Different Zirconia-Alumina Nanoparticles*
- IP-37 Obraztsova, E.D.; Bonard, J.-M.; Kuznetsov, V.L.; Zaikovskii, V.I.; Pimenov, S.M.; Pozarov, A.S.; Karabutov, A.V.; Frolov, V.D.; Konov, V.I.; Russia  
*Structural Measurements for Single-Wall Carbon Nanotubes by Raman Scattering Technique*

- IP-38 Levoska, J.; Tyunina, M.; Leppävuori, S.; Finland  
*Laser Ablation Deposition of Silicon Nanostructures*
- IP-39 Kreibig, U.; Gartz, M.; Hilger, A.; Neuendorf, R.; Germany  
*Interfaces in Nanostructures: Optical Investigations on Cluster-Matter*
- IP-40 Makino, A.; Inoue, A.; Masumoto, T.; Japan  
*Nanocrystalline Soft Magnetic Fe-M-B(M=Zr, Hf, Nb),  
Fe-M-O(M=Zr, Hf, Rare Earth) Alloys and Their Applications*
- IP-41 Stavroyiannis, S.; Panagiotopoulos, I.; Niarchos, D.; Christodoulides, J.; Hadjipanayis,  
G.C.; Greece  
*New CoPt/Ag Granular Films for High Density Recording Media*

**Poster Session I**

- P1-1 Curcic, R.; Zivanovic, P.; Djurkovic, G.; Jokanovic, V.; Yugoslavia  
*Application of Specific Metallothermic Method in Wolfram Powder Obtaining from Scheelite*
- P1-2 Sun, X.; Bi, H.; Sun, X.; Wei, W.; José-Yacamán, M.; China  
*Preliminary Studies on Wear Resistance of Bulk AlN<sub>p</sub>/Al Nanocomposite Materials*
- P1-3 Sun, X.; Sun, X.; Wei, W.; José-Yacamán, M.; China  
*Study on Thermal Oxidation Behavior and Products of Bulk AlN<sub>p</sub>/Al Nanocomposite Materials*
- P1-4 Mordkovich, V.Z.; Japan  
*Synthesis of Carbon/Oxide Nanocomposites by Intercalation /Deintercalation of Nanostructured Carbons*
- P1-5 Zeng, W.; Gui, L.; Wang, J.; Guo, J.; China  
*Synthesis of Al<sub>2</sub>O<sub>3</sub> Nanopowders Using Inorganic Salt and Its Thermodynamics*
- P1-6 Kear, B.H.; Xiao, T.D.; Strutt, P.R.; USA  
*Synthesis of High Active-Site Density Nanofibrous MnO<sub>2</sub>-Based Materials with Enhanced Permeabilities*
- P1-7 Liao, S.-C.; Chen, Y.-J.; Kear, B.H.; Mayo, W.E.; USA  
*High Pressure/Low Temperature Sintering of Bulk Nanocrystalline Alumina*
- P1-8 Kear, B.H.; Chen, Y.-J.; Glumac, N.; Skandan, G.; USA  
*Particle Size Control During Flat-Flame Synthesis of Nanophase Oxide Powders*
- P1-9 Moskovits, M.; Ravi, B.G.; Chaim, R.; Israel  
*Sintering of Bimodal ZrO<sub>2</sub> - 4 wt% Y<sub>2</sub>O<sub>3</sub> Powder Mixtures with the Nanocrystalline Component*
- P1-10 Schneider, J.J.; Czap, N.; Hornyak, L.; Heben M.J.; Germany  
*Template Assisted Synthesis of Ultrafine (Nanosized) Iron Oxide Particles and Their Catalytic Utility in Carbon Nanotube Array Formation*
- P1-11 Kiraly, Z.; Mastalir, A.; Debreceni; Katalin; Szucs, A.; Dekany, I.; Hungary  
*Preparation of Palladium Organoclay Catalysts*
- P1-12 Latysh, V.; Raab, G.I.; Alexandrov I.V.; Russia  
*Development of Methods of Severe Plastic Deformation or Processing of Bulk Nanostructured Metals and Alloys*
- P1-13 Oshima, R.; Yamamoto, T.A.; MizUKoshi, Y.; Nagata, Y.; Japan  
*Electron Microscopy of Noble Metal Alloy Nanoparticles Prepared by Sonochemical Methods*
- P1-14 Eremeev, A.; Bykov, Yu.; Egorov, S.; Ivanov, V.; Kotov, Yu.; Khrustov, V.; Russia  
*Sintering of Nanostructural Titanium Oxide Using Millimeter-Wave Radiation*
- P1-15 Chernykh, L.V.; Skripkin, M.Yu.; Russia  
*Topological Correlation of Multicomponent Liquid and Solid Systems Containing Copper(I) Haloids*
- P1-16 Ivanov, V.; Paranin, S.; Khrustov, V.; Kotov., Y.; Beketov, I.; Murzakaev, A.; Medvedev, A.; Shtol'st, A.; Russia  
*Making Ceramics from Nanometer-Sized Al<sub>2</sub>O<sub>3</sub> Powders with Additions of MgO and TiO<sub>2</sub> by Dynamic Compaction and Sintering*

- P1-17 Kotov Y.A.; Samatov, O.M.; Russia  
*Production of Nanometer-Sized AlN Powders by the Exploding Wire Method*
- P1-18 Ivanov, V.; Nozdrin, A.; Russia  
*Dynamic Compression Adiabats of Nanometer-Sized Powders*
- P1-19 Tamou, Y.; Tanaka, S-I; Japan  
*Formation and Coalescence of Tungsten Nanoparticles Under Electron Beam Irradiation*
- P1-20 Schlorke, N.; Weib, B.; Schultz, L.; Germany  
*Properties of Mg-Y-Cu Glasses with Nanocrystalline Particles*
- P1-21 Tajika, M.; Matsubara, H.; Japan  
*Microstructural Development in AlN Composite Ceramics*
- P1-22 Niklasson, G.A.; Sotelo, J.A.; Sweden  
*Optical Properties of Quasifractal Metal Nanoparticle Aggregates*
- P1-23 Kulikov, L.M.; Semjonov-Kobzar, A.A.; Kartuzov, V.V.; Krasikov, I.V.; Efimova, E.A.; Grinkevych, K.E.; Odokienko, I.I.; Ukraine  
*Transition Metal Chalcogenides Nanopowders*
- P1-24 Tcherdyntsev, V.V.; Kaloshkin, S.D.; Tomilin, I.A.; Shelekhov, E.V.; Baldokhin, Yu.V.; Russia  
*Formation of Iron-Nickel Nanocrystalline Alloy by Mechanical Alloying*
- P1-25 Stoeva, S.; Stoimenov, P.; Dragieva, I.; Pavlikyanov, E.; Klabunde, K.; Bulgaria  
*Complex Formation in Solutions for Chemical Synthesis of Nanoscale Particles Prepared by Borohydride Reduction Process*
- P1-26 Jiang, J.S.; Yang, X.L.; Gao, L.; Guo, J.K.; Jiang, J.Z.; China  
*Synthesis and Characterization of Nanocrystalline Zinc Ferrite*
- P1-27 Janackovic, Dj.; Orlovic, A.; Skala, D.; Drmanjic, S.; Kostic-Gvozdenovic, Lj; Jokanovic, V.; Uskokovic, D.; Yugoslavia  
*Synthesis of Nanostructured Mullite from Xerogel and Aerogel Obtained by the Nonhidrolitic Sol-Gel Method*
- P1-28 Estournes, C.; Lutz, T.; Guille, J.L.; France  
*Metallic Iron Nanoparticles in Silica Gels*
- P1-29 Ravishankar, N; Varghese, V.; Abinandanan, T.A.; Chattopadhyay, K.; India  
*Kinetics of Solid Solution Formation During Mechanical Milling*
- P1-30 Nakahira, A.; Kijima, K.; Japan  
*Novel Synthesis Method of Nanograde Apatite Whisker by Hydrolysis of A-TCP*
- P1-31 Mehta, B.R.; Acharya, D.P.; Balamurugan, B.; Sharma, S.K.; India  
*Fabrication and Characterisation of Cd<sub>x</sub>Zn<sub>1-x</sub>S Nano Particles*
- P1-32 Lazar, K.; Beuer, H.K.; Onyestiyak, Gy.; Jönssson, B.J.; Varga, L.K.; Hungary  
*Iron Nanoparticles in X and Y Zeolites*
- P1-33 Jachimowicz, M.; Fadeeva, V.I.; Grabias, A.; Matyja, H.; Poland  
*Formation of Nanocrystalline Fe<sub>87</sub>B<sub>13</sub> and Co<sub>89</sub>B<sub>11</sub> Alloys by Mechanical Alloying*
- P1-34 Szewczak, E; Presz, A.; Witek, A.; Wyrzykowski, J.W.; Poland  
*Microstructure and Phase Composition of Mechanically Alloyed and Hotpressed Ti-Al Alloys*
- P1-35 Szewczak, E.; Wyrzykowski, J.W.; Poland  
*Influence of the Mechanical Alloying Parameters on Crystalline Size of Al-Ti Powders*

- P1-36 Kharlamov, A.; Kirillova, N.; KosoroUkov, P.; BordyyUK, E.; Ukraine  
*Synthesis of the Nanocrystalline Powder of the Titanium Hydride in the Process of the Mechanochemical Decomposition of the Water*
- P1-37 Kharlamov, A.; Kirillova, N.; Loychenko, S.V.; Kovalchuk, I.A.; Ukraine  
*Peculiarities of Synthesis of Nanodispersed Powder High Hardness Boron-Containing Aluminium and Oxygen Compounds*
- P1-38 Malic, B.; Kosec, M.; Draie, G.; Slovenia  
*Pb(Zr, Ti)O<sub>3</sub> Based Ceramics Prepared by Solution Processing*
- P1-39 Shabatina, T.I.; Vovk, E.V.; Morosov, Y.N.; Sergeev, G.B.; Russia  
*Cryosynthesis of Metal and Mesogens Nanostructures*
- P1-40 Scholz, S.M.; Carrot, G.; Plummer, C.; Hilborn, J.; Hofmann, H.; Switzerland  
*Size Control of Quantum Size CdS Particles Using Macroligands*
- P1-41 Valmalette, J-C.; Gavarri, J-R; France  
*Synthesis and Properties of Nanocrystalline VO<sub>2</sub>*
- P1-42 Valmalette, J-C; Lomello-Tafin, M.; Galez, P.; Jorda, J.L.; France  
*Spontaneous Formation of Nanopowders at Room Temperature by Oxidation of Zr<sub>x</sub>Au<sub>y</sub> Alloys*
- P1-43 Kakimoto, K.I.; Wakai F.; Bill, J; Aldinger, F.; Germany  
*Fabrication of Polycarbosilane-Derived SiC Bulk Ceramics by Carbothermic Reduction*
- P1-44 Klabunde, K.J.; Lucas, E.; USA  
*Nanocrystals as Destructive Adsorbents for Mimics of Chemical Warfare Agents*
- P1-45 Seip, Candace, T.; O'connor, C.J.; USA  
*The Fabrication and Organisation of Self -Assembled Metallic Nanoparticles Formed in Reverse Micelles*
- P1-46 Kim, B.K.; Lee, G.G.; Ha, G.H.; Lee, D.W.; Korea  
*Synthesis of High Density Ultrafine W/Cu Composite Alloy*
- P1-47 Liu, W; McCormick; Australia  
*Formation and Magnetic Properties of Nanosized Sm<sub>2</sub>Co<sub>17</sub> Magnetic Particles via Mechanochemical/Thermal Processing*
- P1-48 Valtchev, K.; Veith, M.; Lecerf, N.; Germany  
*Preparation and Characterisation of Nanostructured Ni/Al<sub>2</sub>O<sub>3</sub> and Cu/Al<sub>2</sub>O<sub>3</sub> Composites for Catalytic Application*
- P1-49 Mathur, S.; Veith, M.; Huch, V.; Germany  
*Novel Hetero (Bi-And Tri-)Metal Alkoxides as Single Source Precursors to Nano-Scaled Ceramics and Metal / Metal Oxide Composites*
- P1-50 Begin Colin, S.; Girot, T.; Caér, G.Le; Mocellin, A.; France  
*Kinetics of Formation of Nanocrystalline TiO<sub>2</sub> II by High Energy Ball-Milling of Anatase TiO<sub>2</sub>*
- P1-51 Yu, J.H.; Kim, S.Y.; Lee, J.S.; Ahn, K.H.; Korea  
*In-situ Observation of Formation of Nanosized TiO<sub>2</sub> Powder in Chemical, Vapor Condensation*
- P1-52 Okazaki, M.; Matsumoto, T.; Japan  
*Dispersed Nano-Structural Organic-Apatite Composite in Porous Apatite*
- P1-53 Hofmeister, H.; Ködderitzsch, P.; Germany  
*Nanosized Silicon Particles by Inert Gas Arc Evaporation*

- P1-54 Hofmeister, H.; Drost, W.-G.; Berger, A.; Germany  
*Oriented Prolate Silver Particles in Glass - Characteristics of Novel Dichroic Polarizers*
- P1-55 YelsUkov, E.P.; Mikhailik, O.M.; Konygin, G.N.; Mikhailova, S.S.; Povstugar, V.I.; Russia  
*Phase Composition Study of Bulk and Surface Layers of Stabilized Iron Powder*
- P1-56 Wu, X.; Tan G.-L.; China  
*Preparation of Nanophase WC Powders from the Reduction of Ammonium Metatungstate by C<sub>2</sub>H<sub>2</sub>-H<sub>2</sub> Mixtures*
- P1-57 El-Shall, M.S.; USA  
*Synthesis of Nanoparticles by a Laser Vaporization- Controlled Condensation Technique: Nanoparticles of Metal and Semiconductor Oxides and Carbides*
- P1-58 Wu, X.; Zhang, H.; Du, L.; Wang, Y.; Li, Z.; China  
*Synthesis and Mechanical Property of Nanocrystalline Metals Copper and Silver*
- P1-59 Macek, J.; Degen, A.; Slovenia  
*Preparation of Submicrometer Nickel Powders by the Reduction from Nonaqueous Media*
- P1-60 Schwitzgebel, G.; Heyer, M.; Koch, M.; Rullang, F.; Werkmeister, K.-St.; Germany  
*Nanocrystalline (Ni, Fe) Alloys, Preparation and Physico-Chemical Characterization*
- P1-61 Rozenberg, A.S.; Pomogailo, A.D; Russia  
*The Solid State Thermal Transformation of the Metal Carboxylates as a Source of the Formation of the Nanosized Stabilized Particles*
- P1-62 Bochkin, A.M.; Pomogailo, A.D.; Russia  
*Polymer-Supported Titanium-Magnesium Catalyst for Ethylene Polymerization*
- P1-63 Novakova, A.A.; Kiseleva, T.Yu.; Lyovina, V.V.; Dzidziguri, E.L.; Kuznetsov, D.V.; Russia  
*Influence of the Initial Concentration on Phase Formations During Chemical Processing of Nanocrystalline Fe-W Powders*
- P1-64 Leslie-Pelecky, D.L.; Bonder, M.; Kirkpatrick, E.; Kim, S.H.; Rieke, R.D.; USA  
*Structural and Magnetic Properties of Nickel/Nickel Carbide Nanostructures Fabricated by Chemical Reduction*
- P1-65 Jiang, J.Z.; Bender Koch, C.; Mörup, S.; Denmark  
*Mechanical Milling of Fe(Iii)-Si Oxides: Formation of an Amorphous Fe(Ii)-Containing Phase*
- P1-66 Sastry, S.M.L.; Kurihara, L.; Provenzano, V.; USA  
*Synthesis and Consolidation of Nanocrystalline Particles Produced by Polyol Process*
- P1-67 Monty, C.J.A.; Rouanet, A.; Sibieude, F.; France  
*Nanomaterials: Synthesis Using Solar Radiations-Nanostructural Characterization*
- P1-68 Iwama, S.; Fukaya, T.; Ohshita, K.; Sakai, Y.; Japan  
*Nanocomposite Powders of Fe-C System Produced by the Plowing Gas Plasma Processing*
- P1-69 Kamei, S-I; Yogo, K.; Ishikawa, M.; Kawasaki, K.; Odawara, O.; Japan  
*Study on TiO<sub>2</sub> Nano-Clusters Synthesized by Laser Ablation*
- P1-70 Tepper, F.; Ivanov, G.V.; Lerner, M.I.; Davidovich, V.I.; Katz, J.D.; USA  
*Metastable Nanosize Metal Produced by Electro-Explosion*

- P1-71 Valmalette, J.-C.; Turquat, Ch.; Roubin, M.; Nihoul, G.; France  
*Synthesis and Structural Investigation of V Substituted HfO<sub>2</sub> Nanocrystals*
- P1-72 Solomin, V.A.; Luapunov, V.V.; Lyakh, E.N.; Zhubanov, B.A.; Kazakstan  
*Synthesis of Nanostructurized Polyheterocycles*
- P1-73 Yoo, S.H.; Sudarshan, T.S.; Sethuram, K.; Subbash, G.; Dowding, R.J.; USA  
*Dynamic Compression Behavior of Nanocrystalline Tungsten Consolidated with a New Plasma Pressure Compaction(P<sup>2</sup>C) System*
- P1-74 Falk, L.K.L.; Carlstöm, E.; Sweden  
*In-situ Formation of Nanosized SiC Particles in an Al<sub>2</sub>O<sub>3</sub> Matrix*
- P1-75 Stopic, S.; Uskokovic, D.; Yugoslavia  
*Synthesis of WC-Co Powders from Soluble Tungsten Salts by Ultrasonic Spray Pyrolysis*
- P1-76 Karppinen, M.; Mizsei, J.; Pirttiaho, L.; Lantto, V.; Finland  
*Nanoparticle Catalysts by Agglomeration of Nanofilms*
- P1-77 Takacs, L.; Pogany, L.; Varga, L.K.; Horvath, M.P.; Bakhshai, A.; USA  
*ZnO-Fe Nanocomposites via Ball Milling and Annealing*
- P1-78 Tellkamp,V.L.; Lavernia, J.; USA  
*Processing and Mechanical Properties of Nanocrystalline 5083 Al Alloy*
- P1-79 Adhikari, S.; Gopinathan, C.; India  
*Pulse Radiolytically Induced Colloidal Metal Formation in Water and Water-in-Oil Microemulsion*
- P1-80 Wahlberg, S.; Grenthe, I.; Muhammed, M.; Sweden  
*Nanostructured Hard Material Composites by Molecular Engineering 2. Synthesis from Ammonium Paratungstate*
- P1-81 Gromov, V.; Koltsov, S.; Russia  
*Nanostructures Synthesis on the Surface of Semiconductors, Metals and Insulators and Ellipsometric Investigation of the Boundary Between the Substrate and Synthesized Layer*
- P1-82 Smirnov, E.P.; Russia  
*Formation and Growth of Oxide Nanoscale Structures on the Carbon Surface*
- P1-83 Turkki, T.; Muhammed, M.; Pirjamali, M.; Järås, S.; Dalmazio, L.; Julbe, A.; Guizard C.; Sweden  
*Nanophase Cerium Oxide Based Catalysts for Environmental Catalysis*
- P1-84 Wang, M.; Shourie, S.; Zhang, Yu; Muhammed, M; Sweden  
*Synthesis and Characterisation of Thermoelectric Skutterudite CoSb<sub>3</sub> via Solution Chemistry Route*
- P1-85 Voronkov, G.P.; Semenov, V.G.; Gitzovich, V.N.; Murin, I.V.; Smirnov, V.M.; Russia  
*Mössbauer Study of Structural-Chemical Transformations at Transport Reduction of Two-Dimensional Iron-Oxide Nanostructures*
- P1-86 Korznikov, A.V.; Idrisiva, S.; Noskova, N.I.; Russia  
*Structure and Thermal Stability of Nanocrystalline Mo*
- P1-87 Hahn, H.; Möller, A.; Germany  
*Synthesis and Characterization of Nanocrystalline Ni/RO<sub>2</sub>- and Ni/Al<sub>2</sub>O<sub>3</sub>-Composite Coatings*
- P1-88 Winterer, M.; Germany  
*A Simple Model for the Chemical Vapor Synthesis of Nanocrystalline Silicon Carbide*

- P1-89 Kapustin, M.G.; Astakhov, M.V.; Trushevsky, S.M.; StelmUKh, I.V.; Russia  
*Method of Producing Nanocrystals with the Use of Solution Microcapsulation at Thermodynamic Equilibrium*
- P1-90 Grigorieva, T.F.; Barinova, A.P.; Ivanov, E.Yu.; Lyakhov, N.Z.; Russia  
*Mechanochemically Synthesized Nanocrystalline Indium Oxide*
- P1-91 Grigorieva, T.F.; Barinova, A.P.; KryUkova, G.N.; Belykh, V.D.; Lyakhov, N.Z.; Russia  
*Nanocrystalline Complex Oxides Obtained by Mechanochemical Synthesis*
- P1-92 Tarasov, B.P.; Fokin, V.N.; Moravsky, A.P.; Shul'ga, Yu.M.; Yartys, V.A.; Schur, D.V.; Russia  
*Synthesis and Properties of Crystalline Fullerene Hydrides*
- P1-93 Tyunina, M.; Levoska, J.; KoivUSAari, J.; Leppävuori, S.; Finland  
*Agglomeration and Surface Morphology During Pulsed Laser Deposition of Pb-Zr-Ti-O*
- P1-94 Bhattacharya, P.; Chattopadhyay, K.; India  
*Nano Al<sub>2</sub>O<sub>3</sub>-Pb and SiO<sub>2</sub>-Pb Cermets by Sol-Gel Technique and the Phase Transformation Study of Embedded Pb Particles*
- P1-95 Skandan, G.; Glumac, N.; Chen, Y.-J.; Kear, B.H.; USA  
*Low Pressure Flame Deposition on Nanostructures Oxide Films*
- P1-96 Busmann, H-G; Günther, B.; Meyer, U.; Germany  
*Polymer Matrix Composites Filled with Nanoporous Metal Powders Preparation and Electrical Properties*
- P1-97 Dligatch, S.; Smith, G.B.; Australia  
*Ellipsometric Studies of Nanocomposite Cermets*
- P1-98 Christodoulides, J.A.; Shevchenko, N.B.; Hadjipanayis, G.C.; USA  
*Preparation of Dy and Mn Nanoparticles*
- P1-99 Li, G.H.; Zhang, L.D.; China  
*Sintering, Strengthening and Toughening of Nano-Alumina Composites*
- P1-100 Eckert, J.; Seidel, M.; Xing, L.Q; Börner, I.; Weib, B.; Germany  
*Nanophase Composites in Easy Glass Forming Systems*
- P1-101 Kübler, A.; Eckert, J.; Schultz, L.; Germany  
*Nanoparticles in an Amorphous Zr<sub>35</sub>Al<sub>10</sub>Cu<sub>30</sub>Ni<sub>5</sub>-Matrix- the Formation of Composites by Mechanical Alloying*
- P1-102 Simon, U.; Jockel, J.; Starrost, F.; Krasovskii, E.E.; Schattke, W.; Germany  
*Electronic and Optical Properties of Cetineites: Nanoporous Semiconductors with Zeolite-Like Channel Structure*
- P1-103 Berzhanova, S.K.; Stepanenko, N.B.; Zhubanov, B.A.; Kazakhstan  
*Modified Polyamide Structures*
- P1-104 Ferkel, H.; Naser, J.; Germany  
*Laser-Induced Synthesis of Al<sub>2</sub>O<sub>3</sub>-Cu Nanoparticle Mixtures*
- P1-105 Tzeng, S-J.; Tsai, W-L.; Lin, H-M; Hwu, Y.; Lee, P-Y.; Taiwan  
*Synthesis of TiN/Ni Nanocomposites*
- P1-106 Solntsev, V.P.; Fenouchka, B.V.; Semjonov-Kobzar, A.A.; Solntseva, T.A.; Ukraine  
*The Self-Dispersing and Nanostructure Formation Processes in Non-Equilibrium Diffusion-Kinetic Systems*

- P1-107 Chen, Y.; Australia  
*Nanoporous Powders Produced by High Energy Ball Milling*
- P1-108 Krasnowski, M.; Fadeeva, V.I.; Matyja, H.; Poland  
*Nanocomposites Produced by Mechanical Alloying of the Al<sub>50</sub>Fe<sub>25</sub>Ti<sub>25</sub> Powders Mixture*
- P1-109 Fernandez, A.; Sanchez-Lopez, J.C.; Reddy, E.P.; Rojas, T.C.; Sayagues, M.J.; Spain  
*Preparation and Characterisation of CdS and ZnS Nanosized Particles Obtained by the Inert Gas Evaporation Method*
- P1-110 Rusu, F.; Chiriac, H.; Lozovan, M.; Urse, M.; Romania  
*On Microstructure, Magnetic and Electric Properties of (NiFe)<sub>x</sub>-(SiO<sub>2</sub>)<sub>1-x</sub> Nanocomposite Films*
- P1-111 Klabunde, K.J.; Khaleel, A.; Li, Weifeng; USA  
*Nanocrystals as Stoichiometric Reagents with Unique Surface Chemistry: New Adsorbents for Air Purification*
- P1-112 Yang, D.; Westreich, P.; Frindt, R.F.; Canada  
*Transition Metal Dichalcogenide/Polymer Nanocomposites*
- P1-113 Kim, S.Y.; Yu, J.H.; Lee, J.S.; Korea  
*The Characteristics of Nanosized TiO<sub>2</sub> Powder Synthesized by Chemical Vapor Condensation*
- P1-114 Nam, J.G.; Lee, J.S.; Korea  
*Mechano-Chemical Synthesis of Nanosized Stainless Steel Powder*
- P1-115 Knorr, P.; Nam, J.G.; Lee, J.S.; Korea  
*Densification and Microstructural Development of Nanocrystalline Y-Ni-Fe Powders*
- P1-116 Yelsukov, E.P.; Lomayeva, S.F.; Konygin, G.N.; Dorofeev, G.A.; Povstugar, V.I.; Mikhailova, S.S.; Kadikova, A.H.; Russia  
*Structure, Phase Composition and Magnetic Characteristics of the Nanocrystalline Iron Powders Obtained by Mechanical Milling in Heptane*
- P1-117 Povstugar, V.I.; Pletnev, M.A.; Dorfman, A.M.; Mikhailik, O.M.; Russia  
*The Technique for Evaluating the Corrosion Resistance of Iron-Based Nanodispersive Materials*
- P1-118 Hagfeldt, A.; Keis, K.; Vayssieres, L.; Rensmo, H.; Lindquist, S.-E.; Sweden  
*Photoelectrochemical Properties of Nanostructured ZnO Electrodes with Different Morphologies*
- P1-119 Sakamoto, K.; Tsunawakit, Y.; Japan  
*Nano-Sized Layered Composite of Aluminium Tri-Hydrogen Bis (Orthophosphates) and Organic Compounds*
- P1-120 Moga, A.E.; Chiriac, H.; Urse, M.; Necula, F.; Romania  
*Structural and Magnetic Investigation of Mechanically Alloyed Fe<sub>70</sub>Co<sub>3.5</sub>Cu<sub>1</sub>Nb<sub>3</sub>B<sub>9</sub>Si<sub>13.5</sub> Powders*
- P1-121 Ragulya, A.V.; Andrievskaya, E.R.; Skorokhod, V.V.; Ukraine  
*On Rate-Controlled Sintering of Yttria- and Lanthana-Stabilized Zirconia Nano-Powders*
- P1-122 Macek, J.; Marinsek, M.; Slovenia  
*Formation of Nickel and Zirconia Nanocomposites by the Coprecipitation Method*
- P1-123 Gorodetskaya, T.A.; DanilyUK, A.F.; Kuznetsov, V.L.; Derevyankin, A.I.; Fenelonov, V.V.; Chesnokov; Zaikovskii, V.I.; Russia  
*Structural Characteristics of Composites Based on Silica Aerogels and Carbon*

- P1-124 Xing, L.Q.; Eckert, J.; Schultz, L.; Germany  
*Evolution of Nanocrystalline Quasicrystals from Bulk Zr-Cu-Ni-Al-Ti Amorphous Alloy and the Mechanical Property of the Alloy*
- P1-125 Ng, C.B.; Siegel, R.W.; Schadler, L.S.; USA  
*Synthesis and Mechanical Properties of TiO<sub>2</sub>-Epoxy Nanocomposites*
- P1-126 Trakhtenberg, L.I.; Gerasimov, G.N.; Grigor'ev, E.I.; Grigor'ev, A.E.; Vorontsov, P.S.; Zavjalov, S.A.; Russia  
*Mechanisms of Conductivity in Metal-Polymer Nanocomposites*
- P1-127 Ryu, S.-S.; Kim, J.-C.; Moon, I.-H.; Korea  
*Microstructural Changes of Mechanically Aligned W-Cu Composite Powders During Solid-State Sintering*
- P1-128 Khadar, M.A.; Potty, S.N.; India  
*Impedance Spectroscopy of Nano-Phase AgI and AgI-Al<sub>2</sub>O<sub>3</sub> Nano-Composites*
- P1-129 Kholmanov, I.N.; Aliev, A.E.; Uzbekistan  
*Study of Interaction of Surface Atoms in Pores and Some Dielectrics Embedded in Porous Glasses.*
- P1-130 Koshizaki, N.; Sasaki, T.; Koinuma, M.; Matsumoto, Y.; Japan  
*Preparation of M/TiO<sub>2</sub> (M=Au, Pt) Nanocomposite Films Using Co-Sputtering Method*
- P1-131 Michel, D.; Borisov, B.F.; Charnaya, E.V.; Hoffmann, W.D.; Plotnikov, P.G.; Germany  
*Solidification and Melting of Gallium and Mercury in Porous Glasses as Studied by NMR and Acoustic Techniques*
- P1-132 Krüger, J.K.; Holtwick, R.; Le Coutre, A.; Germany  
*On the Influence of Nano-Scaling on the Glass Transition of Molecular Liquids*
- P1-133 Yamamoto, T.A.; Nishimaki, K.; Harabe, T.; Shiomi, K.; Nakagava, T.; Katsura, M.; Japan  
*A Magnetic Composite Composed of Iron - Nitride Nanograins Dispersed in a Silver Matrix*
- P1-134 Nishimaki, K.; Ohmae, S.; Yamamoto, T.A.; Katsura, M.; Japan  
*Formation of Iron -Nitrides by Reaction of Iron Nanoparticles with a Stream of Ammonia*
- P1-135 Kapoor, S.; Salunke, H.G.; Pande, B.M.; Kulshreshtha, S.K.; Mittal, J.P.; India  
*Radiolytic Preparation of Nanophase Cubic Cobalt and Nickel Metal Particles*
- P1-136 Nakayama, T.; Yamamoto, T.A.; Choa, Y.H.; Niihara, K.; Japan  
*Structure and Magnetic Property of Iron-Oxide /Silver Nanocomposite*
- P1-137 Dearmitt, C.; Breese, K.; Sweden  
*Systematic Dispersant Selection Methodology Applied to Find Suitable Surface Treatment Additives for Mineral Fillers in Polymer Composites*
- P1-138 Zhang, Z.; Wahlberg, S.; Wang, M.; Muhammed, M.; Sweden  
*Processing of Nanostructured WC-Co Powder from Precursor Obtained by Co-Precipitation*
- P1-139 Piccaluga, G.; Cannas, C.; Musinu, A.; Italy  
*Effects of Mechanical Treatment of Fe<sub>2</sub>O<sub>3</sub>-SiO<sub>2</sub> Nanocomposites Prepared by a Sol-Gel Method*
- P1-140 Fitz-Gerald, J.; Singh, R.K.; Pennycook, S.J.; Gao, H.; USA  
*Z-Contrast Scanning Transmission Electron Microscopy of Nanofunctionalized Particulate Materials*

**Poster Session II**

- P2-1 Stietz, F.; Stuke, M.; Viereck, J.; Wenzel, T.; Träger, F.; Germany  
*Influence of Surface Roughness on Light Absorption by Metal Nanoparticles*
- P2-2 Dmitruk, N.; Lepeshkina, T.; Pavlovska, M.; Zabashta, L.; Ukraine  
*Polarizability of Gold Clusters on the Gaas Surface*
- P2-3 Pustovit, V.N.; Grechko, L.G.; Ukraine  
*Optical Properties of Disordered Cluster Systems*
- P2-4 Hou, M.; Azzaoui, M.E.; Belgium  
*Cobalt Clusters in Silver Studied by Means of Classical Molecular Dynamics, AB Initio Electronic Calculations Ad Mössbauer Spectroscopy*
- P2-5 Molochnikov, L.S.; Kovalyova, E.G.; Russia  
*Individual Complexes and Clusters of Copper(II) Ions in Ion-Exchangers*
- P2-6 Perez, A.; Negrier, M.; Tuailon, J.; Dupuis, V.; Melinon, P.; France  
*Magnetic Nanostructures Elaborated from Co-Sm Mixed Cluster Depositions*
- P2-7 Prevel, B.; Palpant, B.; Lerme, J.; Pellarin, M.; Treilleux, M.; Vialle, J.L.; Broyer, M.; France  
*Optical Properties of Nanostructured Thin Films Containing Noble Metal Clusters*
- P2-8 Billas, I.M.L.; Heinebrodt, M.; Malinowski, N.; Tast, F.; Branz, W.; Martin, T.P.; Germany  
*Layered Clusters Produced by Laser-Vaporization*
- P2-9 Xenoulis A; Tsouris P; Doukellis, G; Boukos, N; Tsakalakos, Th.; Greece  
*Ionisation and Coagulation of Metal Particles in Plasma*
- P2-10 Johansson, C.; Åklint, T.; Hanson, M.; Andersson, M.; Olsson, E.; Gustavsson, F.; Wäppling, R.; Rosen, A.; Sweden  
*Deposited Nano-Metre Sized Iron Clusters*
- P2-11 Andersson, M.; Iline, A.; Stietz, F.; Träger, F.; UK  
*Optical Extinction and Surface Morphology of Silicon Nanostructures Grown on Dielectric Substrates*
- P2-12 Il'chenko, V.V.; Bomk, O.I.; Il'chenko, L.G.; Kuznetsov, A.; Pinchuk, A.M.; Pinchuk, V.M.; Strikha, V.I.; Ukraine  
*Cluster Model of Gas Sensitivity Nanostructural Sensors of Ammonia*
- P2-13 Pomogailo, A.D.; Russia  
*Polymer-Immobilized Nanoscale and Cluster Metal Particles*
- P2-14 Dzhardimalieva, G.I.; Pomogailo, S.I.; Pomogailo, A.D.; Russia  
*Cluster-Containing Metal Monomers and Their (Co)Polymers*
- P2-15 Tillement, O.; Illy, S.; Dubois, J.M.; France  
*Size Dependent Structural Transition Correlated with Catalytic Activity in Nanosized Nickel Particles.*
- P2-16 Compagnini, G.; Pignataro, B; Puglisi, O; Italy  
*Vibrational Analysis of Ion Irradiated Self-Assembled Monolayers*
- P2-17 Jokanovic, V; Janackovic, Dj.; Spasic, P.; Uskokovic, D.; Yugoslavia  
*Modelling of Nanostructural Design of Ultrafine Mullite Powder Particles Obtained by Ultrasound Reactional Spraying*

- P2-18 Khait, Yu.L.; Israel  
*Nanoscopic Dynamic Fundamentals of Rate Processes in Solids and Applications to Nanosystems*
- P2-19 Smith, G.B.; Reuben, A.J.; Australia  
*Normal Mode Analysis of Optical Polarisation Response in Nanoparticle Clusters*
- P2-20 Lin, H.-M.; Lin, H.-M.; Hsu, S-L.; Taiwan  
*Molecular Simulation for Gas Adsorption on TiO<sub>2</sub> Rutile and Anatase Surfaces*
- P2-21 Petrunin, V.A.; Gromov, V.E.; Sosnin, O.V.; Ya, V.; Tsellermaer, Kuchumova, E.S.; Gromova, A.V.; Russia  
*Synergetics of Nanosizable Structures in Metals in Conditions of Electrostimulated Deformation*
- P2-22 Iskakova, Y.L.; Zubarev, A.Y.; Russia  
*Structure Transformation in Compositions of Colloidal Ferromagnetic Particles in Liquid Crystals*
- P2-23 Kolesnikova, A.L.; Mikaelyan, K.N.; Ovid'ko, I.A.; Romanov, A.E.; Russia  
*Energy and Stress Fields of Quasiperiodic Tilt and Interphase Boundaries in Nanostructured Materials*
- P2-24 Tomilin, I.A.; Kaloshkin, S.D.; Tcherdynsev, V.V.; Russia  
*Thermodynamic Basis of Formation of Nanocrystalline and Amorphous Structures by Mechanical Alloying*
- P2-25 Senet, P.; Hou, M.; Belgium  
*Computation of Capacitances of CuN Nanoclusters*
- P2-26 Brjezinskaya, M; Baytinger E.; Kormilets V.; Russia  
*The Density of Valence States of Small Diameter Carbon Nanotubes*
- P2-27 Alymov, M.I.; Shorshorov, M.Kh.; Russia  
*Surface Tension of Ultrafine Particles*
- P2-28 Nazarov, A.A.; MUSAlimov, R.Sh.; Russia  
*Recovery of the Excess Volume in Ultrafine-Grained Materials Produced by Severe Plastic Deformation*
- P2-29 Il'chenko, L.G.; Il'chenko, V.V.; Ukraine  
*Theoretical Investigation of the Microscopical Structure Semiconductor/Thin Metal Film Internal Interface with Nanometer Resolution*
- P2-30 Vayssieres, L.; Jolivet, J.P.; Livage, J.; Sweden  
*Water-Oxide Interfacial Tension Modelling & Growth Control of Spinel Iron Oxide Nanoparticles*
- P2-31 Menard, S.; Saul, A.; Bassani, F.; Arnaud D'avitaya, F.; France  
*Band Gap Calculation of Thin Si Polycrystalline Films.*
- P2-32 Schiotz, J.; Vegge, T.; Di Tolla, F.D.; Jacobsen, K.W.; Denmark  
*Atomic-Scale Simulations of Nanocrystalline Metals*
- P2-33 Jin Zhao-Hui; Lu, K.; China  
*To What Extent a Crystal Can Be Superheated*
- P2-34 Bugaev, A.S.; Korshunov, S.M.; Kuzmichev, S.D.; Sorokoumov, V.E.; Russia  
*The Simulation of Charge Transport in the Nanostructure "Camel" and Heterotransistors*
- P2-35 Sheka E.F.; Khavryutchenko, V.D.; Nikitina, E.A.; Russia  
*Quantum-Chemical Technology of Nanos*

- P2-36 Yao, Y.D.; Liou, Y; Lee, S.F.; Wu, C.Y; Chen, Y.Y.; Huang, G.Z; Shiang, H; Kang, W.T; Lin, J.J.; Taiwan  
*Magnetic Anisotropy Study in Nano-Sized Ni and Ni/Cu Films*
- P2-37 Weissbuch, I.; Lahav, M.; Leiserowitz, L.; Israel  
*Self-Assembly at the Air-Water Interface. In-situ Preparation of Thin Films of Metal Ion Grid Architectures*
- P2-38 Fogel, N.Y.; Mikhailov, M.Y.; Yuzephovich, O.I.; Bomze, Y.V.; Ukraine  
*Superconductivity Re-Entrance in Strong Magnetic Fields in Mo/Si Multilayers*
- P2-39 Venger, E.F.; Dmitruk, N.L.; Dvoynenko, M.M.; Goncharenko A.V.; Romaniuk V.R.; Ukraine  
*Optical Transmittance of Semicontinuous Gold Films*
- P2-40 Hedlund, J.; Sterte, J.; Sweden  
*Synthesis of Thin Molecular Sieve Films*
- P2-41 Kudaikulova, S.; Syzdykova, A.; Boiko, G.; Zhubanov, B.; Buranbaev, M.; Kazakstan  
*Silvered Polyamide Films with High Reflectivity*
- P2-42 Yuzephovich, O.I.; Buchstab, E.I.; Fogel, N.Y.; Mikhailov, M.Y.; Sidorenko, A.S.; Isreal  
*Interlayer Coupling in Mo/Si Multilayers*
- P2-43 Riera, R.; Martin, J.L.; Bergues, J.M.; Betancourt-Riera, R; Mexico  
*One Phonon Resonant Raman Scattering in Quantum Wires and Free Standing Wires*
- P2-44 Bobrysheva, N.; Osmolovski, M.; Smirnov, V.; Russia  
*Magnetic Ordering in Two-Dimensional Titanium- and Iron-Oxygen Nanostructures on Diamagnetic Matrix*
- P2-45 Nedeljkovic, J.M.; Dramicanin, M.; Rajh, T.; Thurnauer, M.C.; Yugoslavia  
*Optical Properties of Photocatalytically Deposited Nanocrystalline Silver on Thin TiO<sub>2</sub> Films*
- P2-46 Smirnov, V.M.; Menshcikova, S.V.; Bogdanova, L.P.; Russia  
*Reactivity of Two-Dimensional Oxide Nanostructures*
- P2-47 Mikhailov, M.Yu.; Cherkasova, V.G.; Dmitrenko, I.M.; Fogel, N.Ya.; Yuzephovich, O.I.; Stetzenko, A.N.; Ukraine  
*Critical Magnetic Fields and Crossover in V/Zr Quasiperiodic Multilayers*
- P2-48 Bomze, Yu.V.; Erenburg, A.I.; Fogel, N.Ya.; Sipatov, A.Yu.; Federenko, A.I.; Langer, V.; Ukraine  
*Structural Investigations of Superconducting Multilayers Consisting of Semiconducting Materials*
- P2-49 Borgohain, K.; Mahamuni, S.; India  
*Luminescence of Doped and Undoped ZnO Quantum Dots*
- P2-50 Kotov, N.A.; Diaz, D.; Ni, T.; USA  
*Electronic Conjugation Between Semiconductor Nanoparticles and Adsorbed pi-Systems*
- P2-51 Sergeev, I.A.; Gittsovich, V.N.; Semenov, V.G.; Russia  
*Mössbauer Study of Hyperfine Fields Distribution in Fe/Cr Superlattices*
- P2-52 Ikegami, T.; Yamazato, M.; Yamagata, Y.; Ebihara, K.; Alexander, G.; Japan  
*Nanocrystalline Oxide and Nitride Films Fabrication Using Laser and Plasma Process*

- P2-53 Kikineshi, A.; Mishak, A.; Palyok, V.; Shiplyak, M.; Ukraine  
*Nanolayered Chalcogenide Glass Structures for Optical Recording*
- P2-54 Gordeev, N.Yu.; Kopchatov, V.I.; Ustinov, V.M.; ZhUKov, A.E.; Egorov, A.Yu.; Kovsh, A.R.; Kop'ev, P.S.; Zaitsev, S.V.; Russia  
*Properties of Recombination Processes in Quantum Dot Laser Emitting at 1.9  $\mu$ m*
- P2-55 KovtyUKhova, N.; Ollivier, P.J.; Mallouk, T.E.; Ukraine  
*Self-Assembly of Surface Composite Inorganic/Organic Thin Films*
- P2-56 Rogachev, A.A.; Russia  
*Capture of Exciton Molecules by Quantum Dots and Isoelectronic Impurities in Multivalency Semiconductors*
- P2-57 Kurihara, L.K.; Chow, G.M.; USA  
*Modified Sol-Gel Processing of Nanostructured Thermal Barrier Coatings*
- P2-58 Kataby, G.; Ulman, Avi.; Prozorov, R.; Gedanken, A.; Israel  
*The Coating of Amorphous Iron Nanoparticles by Long-Chain Alcohols*
- P2-59 Gurin, V.S.; Prokopenko, V.B.; Alexeenko, A.A.; Melnichenko, I.M.; Belorussia  
*Sol-Gel Derived Silica Films Doped by CuS and CuInS<sub>2</sub> Small Particles*
- P2-60 Nanda, J.; Kuruvilla, B.A.; Sarma, D.D.; India  
*Photoemission Study of CdS Quantum Dots*
- P2-61 Zsebök, O.; Thordson, J.V.; Ilver, L.; Andersson, T.G.; Sweden  
*Surface Morphology and Compositional Variations in Molecular Beam Epitaxy Grown Ganxas1-X Alloys*
- P2-62 Petrov, V.A.; Sandomirsky, V.B.; Russia  
*Influence of the Strong Electromagnetic Wave on the Optic Properties of the Quantum Wells in the Quantum Confinement Stark Effect Condition*
- P2-63 Hanarp, P.; Sutherland, D.; Gold, J.; Sweden  
*Nanostructured Model Biomaterial Surfaces Prepared by Adsorption of Charged Polystyrene Particles on Titanium*
- P2-64 Bassani, F.; Ménard, S.; Ronda, A.; Arnaud D'avitaya, F.; France  
*Elaboration of Si Nanowires or Dots on CaF<sub>2</sub> V-Grooved Surfaces*
- P2-65 Scholl, M.; Becker, M.; Atteridge, D.; USA  
*Microstructure of Plasma Sprayed Nanoscale Tungsten Carbide-Cobalt Coatings*
- P2-66 Scholl, M.; USA  
*Properties of Plasma Sprayed Nanoscale Tungsten Carbide-Cobalt Coatings*
- P2-67 Kuruvilla, B.A.; Nanda, J.; Sarma, D.D.; India  
*Optical Properties of PbS-CdS Coated Semiconductor Nanoparticles*
- P2-68 Misra, S.; India  
*The Scanning Electron Microscopy of (Bi<sub>2</sub>S<sub>3</sub>)<sub>0.40</sub>(CdS)<sub>0.60</sub> Thin Film on Glass and Si <111> Substrates*
- P2-69 Seifried, S.; Winterer, M.; Hahn, H.; Germany  
*Nanocrystalline Silicon Carbide Films by Chemical Vapor Synthesis*
- P2-70 Noskova N.I.; Russia  
*Microstructure, Strength and Plasticity of Nanophase Materials*
- P2-71 Srinawasan, D; Chattopadhyay, K.; India  
*Mechanical Behaviour of Nanocomposite Al-X-Zr (X=Cu, Si, Ni) Alloys*
- P2-72 Li, J.; Su, Z.; Hahn, H.; Wei, F.L.; Yang, Z.; Wang, T.M.; Ge, S.H.; China  
*Structure and Magnetic Properties of Nanostructured Fe<sub>40</sub>Ni<sub>38</sub>Mo<sub>4</sub>B<sub>18</sub>*

- P2-73 Xu, B.; Tanaka, S; Japan  
*Behaviour and Bonding Mechanisms of Aluminium Nanoparticles by Electron Beam Irradiation*
- P2-74 Qi, Min; Sagel, A.; Fecht H.J.; Germany  
*The Crystallization of Amorphous and Formation of Bulk Nanocrystalline in Zr-Based Alloys*
- P2-75 Lin, H-M.; Tung, C-Y.; Tzeng, S.J.; Tsai, W.L.; Hwu, Y.; Yao, Y.D.; Lee, P-Y.; Taiwan  
*Structure and Magnetic Properties of Ag<sub>x</sub>-Co<sub>1-x</sub> Nanoparticles*
- P2-76 Qin, B.; Zhang, X.; Liu, G.; Tejada, J.; China  
*Magnetic Characterisation of Pure Nano-Iron*
- P2-77 Aizikovich S.M.; Krenev, L.I.; Serova, N.A.; Russia  
*Determination of Elastic Properties of Functional Graded Nanostructured Coatings*
- P2-78 Jin, Z.Q.; Tang, W.; Zhang, J.R.; Tang, S.L.; Lu, L.Y.; Du Y.W.; China  
*Synthesis and Magnetic Characterisation of Solid-Header PrFe<sub>10</sub>VMo<sub>y</sub> Nanocrystalline Alloys*
- P2-79 Shi, J.L.; Qian, Z.; China  
*Thermal Conducting Behavior of Nanostructured Y-TZP Compacts*
- P2-80 Stolyarov, V.V.; Gunderov, D.V.; Russia  
*Formation of Nanostructures and of Powder Consolidation of Nd(Pr)FeB Alloys by SPD-Method*
- P2-81 Islamgaliev R.K.; Kuzel, E.; R., Mikov; S., Obraztsova; Chmelik, F; Valiev, R.Z.; Russia  
*Structure and Optical Properties of Nanocrystalline Germanium and Silicon*
- P2-82 Stolyarov, V.V.; Valiev, R.Z.; Russia  
*Aging Effects in Metastable Nanostructured Alloys*
- P2-83 Jartych, E.; Zurawicz, J.K.; Oleszak, D.; Pekala, M.; Poland  
*Magnetic Properties and Structure of Nanocrystalline Fe-Al and Fe-Ni Alloys*
- P2-84 Girhardt, T.; Hesse, J.; Grabias, A.; Kopcewicz, M.; Ramin, D.; Riehmann, W.; Germany  
*Investigation of the Soft Magnetic Properties of FeCuNbB Alloys*
- P2-85 Hesse, J; Graf, T.; Kopcewicz, M.; Germany  
*Soft Magnetic Properties of Fe(Cu, Nb)SiB Alloys Evidenced by Mössbauer Experiments in Ratio Frequency Magnetic Fields*
- P2-86 Bobrysheva, N.; Mikhailova, M.; Chezhina, N.; Osmolovski, M.; Russia  
*Heterovalent Clusters of Copper Atoms in Layered Superconducting Oxides and Their Solutions*
- P2-87 Osmolovski, M.G.; Gittsovich, V.N.; Semenov, V.G.; Russia  
*Magnetite Nanoparticles: Formation under Hydrothermal Conditions*
- P2-88 Hernandez, J.M.; Del Barco, E.; Julia, A.; Ziolo, R.; Tejada, J.; Spain  
*Experiments on the Possible Use of Nanoscale Particles as Nanocompass*
- P2-89 Fiorani, D.; Suber, L.; Garcia, A.; Testa, A.M.; Imperatori, P.; Dormann, J.L.; Angiolini, M.; Italy  
*Size and Shape Effect on the Canted Antiferromagnetism in α-Fe<sub>2</sub>O<sub>3</sub> Particles*
- P2-90 Sarnatskii, V.M.; Charnaya, E.V.; Lin, K.J.; Tien, C.; Smirnov, V.M.; Russia  
*Anomalies in Magnetic Properties of Fe-O Two-Dimensional Nanostructures on the Surface of Diamagnetic Matrix*

- 
- P2-91 Wäckelgård, E; Niklasson, G.A.; Sweden  
*Magnetic Dipole Effects in the Optical Properties of Nanocomposites*
- P2-92 Hartmann, O.; Wäplling, R.; Ekström, M.; Sweden  
*Positive Muons in Nanocrystalline Transition Metals: Diffusion and Magnetic Nanostructure*
- P2-93 Kolobov, Y.R.; Russia  
*Diffusion - Induced Creep of Polycrystalline and Nanostructured Metals*
- P2-94 Ratochka, I.V.; Grabovetskaya, G.P.; Kolobov, G.P.; Ivanov, K.V.; Russia  
*Influence of Grain Boundary Diffusion Fluxes of Impurity on the Value of Creep Activation Energy of Nanostructured and Coarse-Grained Nickel.*
- P2-95 Ivanov, K.V.; Ratochka, I.V.; Kolobov, Y.R.; Russia  
*Investigation of Possibility to Get Superplastic State of Nanostructured Copper*
- P2-96 Dmitrev, A.I.; Lashkarev, G.V.; Kulikov, L.M.; Semyonov-Kobzar, A.A.; Ukraine  
*Magnetic Susceptibility of Nanocrystalline Particles of Diselenides of V(Nb) and Vi (Mo, W) Metals of Periodic System*
- P2-97 Chinnasamy, C.N.; Chinnasamy, C.N.; Chattopadhyay, K.; Ponpandian, N.; India  
*Magnetic Properties of Mechanically Alloyed Nanocrystalline Ni<sub>3</sub>Fe*
- P2-98 Lauer, St.; Guan, Z.; Wolf, H.; Natter, H.; Schmelzer, M.; Hempelmann, R.; Wichert, Th; Germany  
*Local Magnetic Properties of Nanocrystalline Ni and Pd-Fe*
- P2-99 Aliev, F.G.; Seynaeve, E.; Volodin, A.; Temst, K.; Van Haesendonck, C.; Bruynseraede, Y.; Belgium  
*Pinning of Magnetic Domain Walls at Line Crossings in Mesoscopic Co Structures*
- P2-100 Kopeliovich, A.I.; Gurzhi, R.N.; Kalinenko, A.N.; Yanovsky, A.V.; Ukraine  
*On Electron-Electron Scattering Mechanism in 2D Degenerated Systems*
- P2-101 Kopeliovich, A.I.; Kalinenko, A.N.; Yanovsky, A.V.; Ukraine  
*Response of 2d Electron Gas to a Nonstationary Injected Electron Beam*
- P2-102 Markushev, M.V.; Murashkin, M.Yu.; Prangnell, P.B.; Maiorova, O.A.; Russia  
*Structure and Mechanical Behaviour of a Commercial Al-Mg Alloy After Equi-Channel-Angular Extrusion*
- P2-103 Tsenev, N.K.; Shammazov, A.M.; Berdon, P.; Russia  
*Peculiarities of Mechanical Behaviour and Structural Changes in Commercial Al Alloys with Nanocrystalline Structure During High Rate Superplasticity*
- P2-104 Pakhomov, A.B.; Wang, S.K.; Yan, X.; Hong Kong  
*Electric Relaxation in Conducting Metal-Insulator Nanocomposites*
- P2-105 Jiang, J.Z.; Wu, G.Y.; Lin X.P.; Denmark  
*Low-Temperature Mössbauer Studies of Nanoglass Fe<sub>79</sub>B<sub>21</sub> Powder Prepared by Chemical Reduction*
- P2-106 Gerward, L.; Jiang, J.Z.; Olsen, J.S.; Morup, S.; Denmark  
*On the Behavior of Mechanically Milled Fe-Cu Materials under High Pressure and Temperature*
- P2-107 Tomut, M.; Chiriac, H.; Neagu, M.; Romania  
*Improving the Magnetic Properties of Nanocrystalline Fe<sub>73.5</sub>Cu<sub>1</sub>Nb<sub>3</sub>Si<sub>13.5</sub>B<sub>9</sub> by Heat Treatment of the Melt*
- P2-108 Mehta, B.R.; Acharya, D.P.; India  
*In-situ Characterisation of Capped Nano Particles Using Spectroscopic Ellipsometry Technique*

- P2-109 Fagnant, S.; Sauques, L.; Sainte Catherine, M.C.; Sella, C.; Berthier, S.; France  
*Ag/SiO<sub>2</sub> Cermets Made by Radio-Frequency Sputtering; Microstructure and Optical Properties*
- P2-110 Natter, H.; Schmelzer, M.; Hempelmann, R.; Krill,C.E.; Birringer, R.; Germany  
*Grain-Size Dependence of Magnetisation in Nanocrystalline Ni and Co*
- P2-111 Roth, M.; Hempelmann, R.; Borgmeier, O.; Eifert, T.; Lueken, H.; Germany  
*Nanocrystalline NH<sub>4</sub>MnF<sub>3</sub> with Controlled Grain -Size: Synthesis and Antiferromagnetism*
- P2-112 Mamiya, H.; Nakatani, I.; Japan  
*Spin-Glasslike Behavior of Iron -Nitride Nanoparticle Systems*
- P2-113 Löffler, J.F.; Braun, H-B.; Wagner, W.; Switzerland  
*Nanoscale Characterization and Modeling of the Magnetiza-Tion Behavior in Nanostructured Metals*
- P2-114 Petrov, A.; Belogurov, S.; Kudrenitskis, I.; Latvia  
*Exchange Anisotropy in Fine Cobalt Particles*
- P2-115 Sergeev, G.B.; Zagorskii, V.V.; Ivashko, S.V.; Bochenkov, V.E.; Russia  
*Cryochemical Synthesis and Physical-Chemical Properties of Nano-Dispersed Metallopolymers*
- P2-116 Rusu, F.; Chiriac, H.; Urse, M.; Lozovan, M.; Romania  
*Comparative Study on the Electrical and Magnetic Behaviour of Co-Sputtered and Multilayer Nanocomposite Ni<sub>x</sub>-(SiO<sub>2</sub>)<sub>1-x</sub> Thin Films,*
- P2-117 Ramin, D.; Riehemann, W; Germany  
*Magnetic Properties of Finemet in Dependence of Nanocrystallisation Conditions and Surface Treatment*
- P2-118 Vargas, W.; Niklasson, G.A.; Costa Rica  
*A Multiple Scattering Approach to Solve the Radiative Transfer Equation*
- P2-119 Andersson, M.; Grimaud, C-M; Siller, L.; Palmer, R.E.; UK  
*Electronic Structure of a Cluster-Assembled Nanocrystalline Silver Film Investigated with Heels*
- P2-120 Broßmann, U.; Södervall, U.; Würschum, R.; Schaefer, H-E; Germany  
*Oxygen Diffusion in Nanocrystalline Monoclinic ZrO<sub>2</sub>*
- P2-121 Soifer, Y.M.; Kobelev, N.P.; Brodiva, I.G.; ManUKhin, A.N.; Korin, E.; Soifer, L.; Russia  
*Internal Fronton and the Young's Modulus Change Associated with Amorphous to Nanocrystalline Phase Transition in Mg-Ni-Y Alloy*
- P2-122 Chuvil'deev, V.N.; Gryaznov, M.Y.; Kopylov, V.I.; Sysoev, A.N.; Russia  
*Internal Friction in Microcrystalline Metals*
- P2-123 Chuvil'deev, V.N.; Russia  
*Model of Nonequilibrium Grain-Boundary Diffusion in Microcrystalline Materials*
- P2-124 Alymov, M.I.; Russia  
*Pressure Sintering of Ultrafine Iron and Nickel Powder*
- P2-125 MulyUKov, R.R.; Pyshmintcev, I.Yu.; Khotinov, V.A.; Mikhailov, S.B.; Korznikov, V.A.; Russia  
*Mechanical Behavior of Fe-6Mn-2Ni-Mo-V with Ultra Fine-Grained Structure*

- P2-126 Wu, X.; Wang, Y.; China  
*Application of Nanopowders to High Temperature Single Crystal Fiber Sensor*
- P2-127 Dobatkin, S.V.; Valiev, R.Z.; Kaputkina, L.M.; Krasilnikov, N.A.; Kazakov, M.A.; SUKhostavskaya, O.V.; Russia  
*Microhardness and Submicrocrystalline Structure of Stainless Steels Obtained by Severe Plastic Deformation*
- P2-128 Crespo, D.; Garrido, V.; Garrido, V.; Spain  
*Characteristic Functions of Nanostructured Materials*
- P2-129 Winter, R.; Heitjans, P.; Germany  
*NMR Relaxation and Lineshape Study on Li<sup>+</sup> Diffusion in Nanocrystalline Layer-Structured Li<sub>x</sub>TiS<sub>2</sub>*
- P2-130 Kobiyama, M.; Inami, T.; Okuda, S.; Japan  
*Thermal Stability of Nanocrystalline Gold Film Prepared by Gas Deposition Method Studied by Bending Test*
- P2-131 Herr, U.; Friedrich, J.; Samwer, K.; Germany  
*Mechanical Crystallisation of Amorphous FeZrBCu Soft Magnetic Material*
- P2-132 Skorvanek, I.; Marcin, J.; Idzikowski, B.; Duhaj, P.; Kovac, J.; Kavecansky, V.; Slovakia  
*Influence of Microstructure on Magnetic Behaviour in Nanocrystalline Fe-Nb-B-(Cu) Alloys*
- P2-133 Leslie-Pelecky, D.L.; Schalek, R.; USA  
*Disorder-Enhanced Coercivity in Mechanically Milled Sm-Co Alloys*
- P2-134 Prozorov, T.; Prozorov, R.; Koltypin, Y.; Gedanken, A.; Israel  
*The Sonochemical Synthesis of Acicular Amorphous Nanoparticles in Magnetic Field*
- P2-135 Unruh, K.M.; Taylor, R.S.; Wilson, W.R.; Yu, R.H.; Xiao, J.Q.; USA  
*Structural and Magnetic Studies of Co-Containing Nanocrystalline Soft Magnets*
- P2-136 Del Bianco, L.; Bonetti, E.; Savini, L.; Tiberto, P.; Vinai, F.; Italy  
*Structural Configuration and Magnetic Properties of the Rapidly Solidified CuCo Alloy*
- P2-137 Bonetti, E.; Campari, E.G.; Pasquini, L.; Sampaolesi, E.; Scipione, G.; Italy  
*Mechanical Behaviour of Ni<sub>3</sub>Al<sub>12</sub> Ordered Compound Entering the Nano-Grain Size Regime*
- P2-138 Yu, S.C.; Kim, C.G.; Ryu, G.-H.; Rao, K.V.; Korea  
*Annealing Effects of Magnetic Properties in Fe<sub>8</sub>Zr<sub>7</sub>B<sub>8</sub>Cu<sub>2</sub>*
- P2-139 Shevchenko, S.I.; Terent'ev, S.V.; Verkin, B.I.; Ukraine  
*Superfluidity and Quantum Vortices in Systems with Pairing of Spatially Separated Electrons and Holes.*
- P2-140 Grabias, A.; Kopcewicz, M.; Idzikowski, B.; Poland  
*Mössbauer Study of Nanocrystalline Fe<sub>80</sub>Ti<sub>7</sub>B<sub>12</sub>Cu<sub>1</sub> Alloy*
- P2-141 Pekala, K.; Jaskiewicz, P.; Latuch, J.; Poland  
*Nanocrystallization Process in Alloys Al-Y-Ni-Fe*
- P2-142 Zaichenko S.G.; Glezer, A.M.; Russia  
*Anomaly of the Half - Petch Relation for Nanocrystalline Materials*
- P2-143 Lashkarev, G.V.; Dmitriev, A.I.; Kulikov, L.M.; Kobzar, Aa.S.; Ukraine  
*Magnetic Susceptibility of Nanocrystalline Particles of Diselenides of V(Nb) and V(Mo, W) Metals of Periodic System*

- P2-144 Bork, D.; Heijtjans, P.; Germany  
*Nmr Investigation on Ion Dynamics and Structure in Nanocrystalline and Polycrystalline LiNbO<sub>3</sub>*
- P2-145 Gvozdikov, V.M.; Gvozdikova, M.V.; Ukraine  
*Damping Factors of De Haas-Van Alphen Oscillations in the Vortex State of Superconducting Multilayers*
- P2-146 Kita, E.; Sasaki, Y.; Hyakkai, M.; Tanimoto, H.; Tasaki, A.; Japan  
*3D Transition Ferromagnetic Metal Nano-Crystals Prepared with Gas Deposition Method (GDM)*
- P2-147 Charnaya, E.V.; Lin, K.J.; Sarnatskii, V.M.; Tien, C.; Smirnov, V.M.; Russia  
*Anomalies in Magnetic Properties of Fe-O Two-Dimensional Nanostructures on the Surface of Diamagnetic Matrix*
- P2-148 Zakharenko, M.; Babich, M.; Tsvetkova, T.; Yurgelevych, I.; Ukraine  
*Paramagnetic Susceptibility of the Thermally Treated Co-Based Amorphous Alloys*
- P2-149 Betz, U; Hahn, H.; Germany  
*Ductility of Nanocrystalline Zirconia Based Ceramics at Low Temperatures*
- P2-150 Grishin, A.M.; Khartsev, S.I.; Johnsson, P.; Rao, K.V.; Sweden  
*Effect of High Hydrostatic Pressure on the Ferroelectric Properties of Epitaxial PbTiO<sub>3</sub>/YBa<sub>2</sub>Cu<sub>3</sub>O<sub>7-x</sub> Nanostructures*
- P2-151 Wittborn, J.; Rao, K.V.; Proksch, R.; Revenko, R.; Dan Dalberg, E.; Bazylinski, D.A.; Sweden  
*Magnetization Reversal Observation and Manipulation of Chains of Nanoscale Magnetic Particles Using the Magnetic Force Microscope*
- P2-152 Szabó, S.; Beke, D.L.; Kis-Varga, M.; Kerekes, Gy.; Hungary  
*Combined Effects of Grain Size and Residual Strain as Well as Iron Impurities on the Magnetic Properties of Ball Milled Nickel*

**Poster Session III**

- P3-1 Jang, L.Y.; Yao, Y.D.; Chen, Y.Y.; Taiwan  
*X-Ray Absorption Study in Nanocrystalline Fe, Co, Ni and Cu Metallic Powders*
- P3-2 Chaim, R.; Ravi, B.G.; Israel  
*Sintering of Bimodal Alumina Powder Mixtures with the Nanocrystalline Component*
- P3-3 Kir'janov, Y.V.; Abrosimova, G.E.; Aronin, A.S.; Gloriant T.; Greer, A.L.; Russia  
*Nanostructure and Microhardness of  $Al_{36}Ni_{11}Yb_3$  Nanocrystalline Alloy*
- P3-4 Aronin, A.S.; Abrosimova, G.E.; Kir'janov, Y.V.; Zver'kova, I.I.; Russia  
*Ni-Mo-B Alloys: Nanostructure Formation and Properties*
- P3-5 Gao, Y.; Li, Y.; Zhang, T.; China  
*Microstructure Study on Nanophase Powder of Indium TiN Oxide*
- P3-6 Yang, Z.; Li, Z.; Tang, K.; Ou, H.; Fu, Y.; China  
*Nanometer Sized ZnO with Novel Morphology and Its Metastable State Characteristics*
- P3-7 Ohnuma, M.; Hono, K.; Ping, D.H.; Onodera, H.; Japan  
*Cu Clustering and Si Partitioning in the Early Crystallisation Stage of a  $Fe_{73.5}Si_{13.5}B_9Nb_3Cu_1$  Amorphous Alloy*
- P3-8 Tang, S.L.; Jin, X.M.; Wang, B.W.; Jin, Z.Q.; Zhang, S.Y.; Du, Y.W.; China  
*Nonequilibrium Phase Transition of  $Nd_3(Fe, Ti)_{29}$  Compound During Mechanical Milling*
- P3-9 Alexandrov, I.V.; Valiev, R.Z.; Russia  
*Nanostructures from Severe Plastic Deformation and Mechanisms of Large-Strain Work Hardening*
- P3-10 Islamgaliev R.K.; Russia  
*Elastic Strain Distribution from Grain Boundaries in Ultrafine-Grained Copper*
- P3-11 Brodova, I.; Manukhin, A.; Russia  
*Phase Transformation in Rapidly Quenched and Annealed  $Mg_{80}Ni_{15}Y_5$  Alloy*
- P3-12 Li, Y.; Gao, Y.; Zhang, T.; China  
*Influence of Ion Thinning on the Microstructure of Nanophase Metal*
- P3-13 Hupe, O.; Bremers, H.; Afanas'ev, A.; Chuev, M.; Germany  
*Structural and Magnetic Information About a Nanostructured Ferromagnetic Fe-Cu-Nb-B Alloy by Novel Model Independent Evaluation of Mössbauer Spectra*
- P3-14 Girhardt, T.; Friedrichs, B.; Woldt, E.; Hesse, J.; Germany  
*Nanocrystallisation of Fecunbb Alloys*
- P3-15 Kotov Y.A.; Osipov, V.V.; Samatov, O.M.; Ivanov, M.G.; Russia  
*Characteristics of Nanometer-Sized Ysz Powders Produced by Evaporating the Target by a Pulsed CO<sub>2</sub>-Laser*
- P3-16 Chow, P.Y.; Gan, L.M.; Chew, C.H.; Quek, C.H.; Chong, P.F.; Singapore  
*Synthesis and Characterization of Polymer-Metallic Nanocomposites via Microemulsion Reaction/Polymerization*
- P3-17 Babanov, Yu.A.; Blaginina, L.A.; MulyUKov, R.R.; Russia  
*Local Atomic Structure of Nanocrystalline Pd and Submicrocrystalline Cu by EXAFS*
- P3-18 Bokhimi, X.; Morales, A.; Portilla, M.; García-Ruiz, A.; Mexico  
*Hydroxides as Precursors of Nanocrystalline Oxides*

- P3-19 Bokhimi, X.; Morales, A.; Novaro, O.; López, T.; Gómez, R.; Xiao, T.D.; Strutt, P.R.; Mexico  
*Nanocrystalline Tetragonal Zirconia Stabilized with Yttrium and Hydroxyl Ions*
- P3-20 Szabo, D.V.; Vollath, D.; Germany  
*Morphological Characterisation of Nanocrystals with Layered Structures*
- P3-21 Serventi, A.M.; Horrillo, M.C.; Rickerby, D.G.; Jacques, R.G.S.; Italy  
*Dependence of Microstructure on Deposition Conditions in r.f.Sputtered Tin Oxide Films for Gas Sensing Applications*
- P3-22 Wiedenmann, A.; Lembke, U.; Hoell, A.; Germany  
*Crystalline and Magnetic Nanostructures in a Glass Ceramic Characterized by Small Angle Neutron Scattering*
- P3-23 Wiedenmann, A.; Keiderling, U.; Gerold, U.; Macht, M-P; Germany  
*Neutron Scattering Investigations of Nanoscaled Microstructures in Bulk Amorphous Alloys*
- P3-24 Baró, M.D.; Petkov, V.; Spassov, T.; Suriñach, S.; Spain  
*New Gd-Al Nanophase Obtained by Crystallization of Gd<sub>4</sub>Al<sub>3</sub> Metallic Glass*
- P3-25 Mukoseev, A.G.; Shabashov, V.A.; Russia  
*Anomalous Accommodation Phenomena Taking Place During the Strain-Induced Formation of Superfine HCP Structure in Fe-Mn Alloys*
- P3-26 Dragieva, I.; Stoynov, Z.; Bulgaria  
*Boron-Containing Nanoparticles and Their Contribution to the Theory and Production of New Materials*
- P3-27 Koch, M.G.; Reetz, M.T.; Germany  
*Electrochemical Preparation of Water-Soluble Metallic Nanoparticles Stabilized by Surfactants*
- P3-28 Maase, M.; Tesche, B.; Reetz, M.T.; Germany  
*Size and Shape Selectivity in the Synthesis of Nanostructured Metal Colloids*
- P3-29 Estournes, C.; Keller, N.; Pham-Huu, C.; Ledoux, M.J.; France  
*Fe<sub>2</sub>O<sub>3</sub> Nanoparticles Supported on Silicon Carbide*
- P3-30 Cziraki, A.; Gerochs, I.; Varga, L.K.; Lovas, A.; Bakonyi, I.; Hungary  
*Structural Evolution of the Amorphous Matrix in Soft Magnetic Nanocrystalline Alloys*
- P3-31 Oleszak, D.; Portnoy, V.K.; Matyja, H.; Poland  
*Phase Transformations in Nanocrystalline Mechanically Alloyed Ni-Mo Powders*
- P3-32 Fadeeva, V.I.; Portnoy, V.K.; Kotchetov, G.A.; Matyja, H.; Russia  
*Nanocrystalline Bcc Solid Solution of Al-Fe-V System Prepared by Mechanical Alloying*
- P3-33 Costa, B.F.O.; Caer, G.Le; Campos, N.Ayres; Portugal  
*Comparison of Sigma Phase Formation on Coarse Grained and Nanocrystalline Fe-Cr-Sn Alloys*
- P3-34 Swygenhoven, H.Van; Spaczek, M.; Farkas, D.; Caro, A.; Switzerland  
*Characterisation of the Microstructure Of Nanophase Ni and Its Influence on Mechanical Properties: A Molecular Dynamics Computer Simulation*
- P3-35 Bonny, V.; Swygenhoven, H.Van; Wagner, W.; Segers, D.; Van Der Klink, J.; Switzerland  
*Structural Properties of Nanosize Ni<sub>3</sub>Al*

- P3-36 Sergeev, B.M.; Sergeev, G.B.; Prusov, A.N.; Russia  
*Cryochemical Synthesis of Bimetallic Nanoparticles in Silver - Lead - Methylacrylate System*
- P3-37 Zhou, F.; Luck, R.; Lu, K.; Germany  
*Characterisation of Al-Rich Al-Fe Alloys Prepared by Ball Milling*
- P3-38 Levi, S.; Van Veggel, F.C.J.M.; Huisman, B-H; Flink, S.; Friggeri, A.; Beulen, M.; Reinhoudt, D.N.; Netherlands  
*Functional Self-Assembled Monolayers on Gold for the Selective Recognition of Neutral Molecules and Cations from Aqueous Solutions*
- P3-39 Reimann, K.; Schaefer, H-E.; Germany  
*Ordering of Nanocrystalline FeAl Produced by Cluster Condensation*
- P3-40 Kim, B.K.; Lee, G.G.; Ha, G.H.; Lee, D.W.; Korea  
*Characteristics of Nanostructured TiO<sub>2</sub> Powders Synthesized by Combustion Flame-Chemical Vapor Condensation Process*
- P3-41 Begin Colin, S.; Millot, N.; Perriat, P.; Caér, G.Le; France  
*Characterization of Ferrites Synthesized by Mechanical Alloying and Soft Chemistry*
- P3-42 Petrunin, V.F.; Russia  
*Structural Characterization of Ultra Dispersed (Nano-) Materials as Middle Between Amorphic and Crystalline*
- P3-43 Yamaguchi, S.; Niihara, K.; Japan  
*Nano-Structural Polyacetylene-Layered Phosphate Composite*
- P3-44 Kemény, T.; Kaptas, D.; Balogh, J.; Kiss, L.F.; Varga, L.K.; Vincze, I.; Hungary  
*Magnetic Properties of the Residual Amorphous Phase in Nanocrystalline Fe-Zr-B-Cu Alloys*
- P3-45 Sternberg, A.; Shebanovs, L.; Antonova, M.; Livinsh, M.; Yamashita, J.Y.; Shorubalko, I.; Spule, A.; Latvia  
*New High Piezoelectric Coupling PluNT Binary System Ceramics*
- P3-46 Agladze, O.V.; Novakova, A.A.; Gvozdover, R.S.; Tarasov, B.P.; Russia  
*The Crystalline-To-Amorphous Transformations in the TiH<sub>2</sub>-Fe System During Ball Milling*
- P3-47 Garrido, V.; Crespo, D.; Pineda, E.; Pradell, T.; Capitán, M.; Spain  
*Nanostructured Precipitates: Experimental Versus Exact Theoretical Profiles*
- P3-48 Andreeva, M.A.; Chumakov, A.I.; Irkaev, S.M.; Prochorov, K.A.; Ruffer, R.; Salaschenko, N.N.; Semenov, V.G.; Russia  
*Anomalous Decreasing of the Hyperfine Magnetic Field in the Top Layer of Fe/Cr Multilayer Covered by Zr Observed by Mössbauer Reflectometry*
- P3-49 Martinez-Miranda, L.J.; Li, Y.; Kurihara, L.K.; Chow, G.M.; USA  
*A Depth Profile Study of the Structure and Strain Distribution in Chemically Grown Cu Films on AlN*
- P3-50 Inami, T.; Kobiyama, M.; Okuda, S.; Maeta, H.; OhtsUKa, H.; Japan  
*Grain Size Measurement of Nanocrystalline Gold by X-Ray Diffraction Method*
- P3-51 Okuda, S.; Kobiyama, M.; Inami, T.; Takamura, S.; Japan  
*On the Thermal Stability of Nanocrystalline Pure Metals*
- P3-52 Krill, C.E.; Meier, M.; Birringer, R.; Germany  
*Recovery Phenomena in Nanocrystalline Materials: Do Grain Boundaries Really Relax?*

- P3-53 Yao, Yimin; Thölen, A.R.; Sweden  
*Adhesion Between Nanoparticles*
- P3-54 Gervasyeva, I.V.; Bunge, H.J.; Helming, K.; Lukshima, V.A.; Alexandrov, I.V.; Russia  
*X-Ray Study of Nanocrystalline Ribbons FeCu NbSiB Subjected to the Thermomechanical Treatment*
- P3-55 Yu, S.C.; Yang, D.S.; Yoo, Y.G.; Kim, W.T.; Korea  
*Exafs Study on Nanocrystalline Fe<sub>40</sub>Co<sub>10</sub>Cu<sub>50</sub> Alloy Processed by Mechanical Alloying*
- P3-56 Keblinski, P.; Eastman, J.A.; USA  
*On the Structure of Nanocrystalline Pd by Molecular Dynamics Simulations and X-Ray Diffraction*
- P3-57 Prozorov, T.; Prozorov, R.; Shafi, K.V.P.M.; Gedanken, A.; Israel  
*Self-Organisation of Ferrofluids Prepared Using Sonochemical Irradiation*
- P3-58 Weins, W.N.; Makinson, J.D.; Deangelis, R.J.; USA  
*Characterization of Bulk Nanostructured Materials through the Use of Low-Frequency Internal Friction Studies*
- P3-59 Frattini, R.; Enzo, S.; Primavera, A.; Trovarelli, A.; Italy  
*Neutron Diffraction Studies of Ceria-Zirconia Catalysts Prepared by High-Energy Mechanical Milling*
- P3-60 Dzidzigury, A.L.; Lyovina, V.V.; Kuznetsov, D.V.; Ryzhonkov, D.I.; Russia  
*The Studying of Phase Composition, Characteristics of the Structure and Range of the Particle Dimensions of Nanostructured Iron by X-Ray Diffraction Method*
- P3-61 Siegbahn, H.; Södergren, S.; Rensmo, H.; Westermark, K.; Eriksson, G.; Henningsson, A.; Hagfeldt, A.; Sweden  
*Electron Spectroscopy of Nanostructured Liquid Interfaces*
- P3-62 Kristiakova, K.; Svec, P.; Slovakia  
*Distribution of Thermodynamic Processes Controlling (Nano) Crystallization of Metallic Glasses*
- P3-63 Baró, M.D.; Tonejc, A.M.; Ramsak, N.; Prodan, A.; Suriñach, M.D.; Tonejc, A.; Spain  
*Correlation Between Microstructure and Soft-Magnetic Properties of FeCuNbSiB Based Alloys*
- P3-64 Trudeau, M.L.; Turkki, T.; Muhammed, M.; El-Shall, M.S.; Canada  
*Surface Reactivity of Ce-Riched Nanophase Ce(Zr)O<sub>2</sub> Compounds*
- P3-65 Solis, J.L.; Lantto, V.; Frantti, J.; Häggström, L.; Wikner, M.; Finland  
*Identification of Nanostructures at Grain Surfaces in Stannous Tungstate Films*
- P3-66 Tanimoto Hisanori; Farber, P.; Würschum, R.; Schaefer, H.E.; Germany  
*Self-Diffusion in High -Density Nanocrystalline Fe*
- P3-67 Bonetti, E.; Del Dianco, L.; Pasquini, L.; Sampaolesi, E.; Italy  
*Thermal Evolution of Ball Milled Nanocrystalline Iron*
- P3-68 Betz, U.; Sturm, A.; Löffler, J.F.; Wagner, W.; Wiedenmann, A.; Hahn, H.; Germany  
*Low-Temperature Isothermal Sintering and Microstructural Characterization of Nanocrystalline Zirconia Ceramics Using Small Angle Neutron Scattering*
- P3-69 Winterer, M.; Srdic, V.V.; Germany  
*Local Structure in Nanocrystalline Zirconia*

- P3-70 Grishin, A.M.; Khartsev, S.I.; Johnsson, P.; Sweden  
*The Dominance of Stress Anisotropy on Giant Magnetoresistance in Nanostructured La<sub>0.7</sub>Mn<sub>1.3</sub>O<sub>3</sub> Films*
- P3-71 Warren, P.J.; Niu, F.; Gögebakan, M.; Weston, C.; Smith, G.D.W.; Cantor, B.; UK  
*High Resolution Studies of Metallic Nanocrystalline Materials*
- P3-72 Grigorieva, T.F.; Tsybulya, S.V.; Cherepanova, S.V.; KryUKova, G.N.; Boldyrev, V.V.; Russia  
*Microstructural Evolution During Mechanical Alloying of Supersaturated Solid Solutions*
- P3-73 Merkert, P.; Schneider, P.; Hahn, H.; Rödel, J.; Germany  
*Sintering Behaviour of Nanocrystalline Y<sub>2</sub>O<sub>3</sub>*
- P3-74 Xu, B.; Tanaka, S; Japan  
*Formation and Bonding of Platinum Nanoparticles Controlled by High Energy Beam Irradiation*
- P3-75 Qin, B.; Liu, G.; Gao D.; Pei, C.; China  
*On Microwave Absorption Property of Spherical Nano-Iron Powders*
- P3-76 Zhang, L.; China  
*Anomalous Optical and Electric Properties in Assemblies of Nanoporous Composites*
- P3-77 Mo, C.M.; Zhang, L.D.; China  
*Effect of Surface Coatings and Mesoporous Confinement on Photoluminescence of Nano-ZnO Particles*
- P3-78 Cai, W.P.; Zhang, L.D.; China  
*Photoluminescence of Dispersed Nano-Ce Doped Silica Particles*
- P3-79 Kumzerov, Yu., A.; Colla, E.V.; Fokin, A.V.; Koroleva, E.Yu.; Savenko, B.N.; Vakhrushev, S.B.; Russia  
*Ferroelectric Phase Transitions in Materials Embedded in Porous Media*
- P3-80 Yu, S.C.; Kim, K.S.; Korea  
*Magnetoimpedance Effect in Nanocrystalline Fe<sub>92-x</sub>Zr<sub>x</sub>B<sub>x</sub>Cu<sub>1</sub> (X = 6, 8, 10) Alloys*
- P3-81 Igo, A.I.; Gorelik, V.S.; Mikov, S.N.; Puzov, I.P.; Russia  
*Optical Spectra of Nanocrystalline Diamond*
- P3-82 Rogacheva, E.A.; Lushnikov, S.G.; Siny, I.G.; Katiyar, R.S.; Russia  
*Transition Dynamics in Nanoordered Relaxor Ferroelectrics*
- P3-83 Suzdalev, I.P.; Maksimov, Yu.V.; Buravtsev, V.N.; Russia  
*Novel Properties of Iron Oxide Nanosystems Affected by Interfacial Interactions*
- P3-84 Chiriac, H.; Ovari, T.-A.; Marinescu, C.S.; Romania  
*Comparative Study of the Giant Magneto-Impedance Effect in Amorphous and Nanocrystalline Glass-Covered Wires*
- P3-85 MulyUKov, R.R.; Zubairov, L.R.; Yumaguzin, Yu.M.; MUSAlimov, R.Sh.; Bakhtizin, R.Z.; Russia  
*Field Autoelectronic Emission from Submicrocrystalline Nickel*
- P3-86 Tetelbaum, D.I.; Gorshkov, O.N.; Stepikhova, M.V.; Trusin, S.A.; Markov, K.A.; Russia  
*The Phosphorous-Doping Effect on the Photoluminescence Spectra of Nanosystem SiO<sub>2</sub>:Si Fabricated by the Ion Implantation*
- P3-87 Wu, X.; Wang, Y.; Tan, G.; China  
*Fluorescence Study of Nanocrystalline Ysz:Eu<sup>3+</sup> Powders Tungsten Carbides Powders*

- P3-88 Semchuk, O.Yu.; Grechko, L.G.; Ogenko, V.M.; Ukraine  
*Optical Properties of the Ferromagnetic Semiconductors with the Periodic Nanostructures, Produced by Coherent Light Beams*
- P3-89 Barariu, F.; Chiriac, H.; Romania  
*Thermoelectromotive Force in Nanocrystalline Wires*
- P3-90 Koshizaki, N.; Yasumoto, K.; Sasaki, T.; Japan  
*A Gas-Sensing CoO/SiO<sub>2</sub> Nanocomposite*
- P3-91 Koshizaki, N.; Umehara, H.; Sasaki, T.; Pal, U.; Oyama, T.; Japan  
*Nanostructure and Photoluminescence Property of Si/MgO and Si/ZnO Co-Sputtered Films*
- P3-92 Wu, M.; Li, W.; Li, X.; Gu, W.; Wang, F.; China  
*Photoelectrochemical Behavior of ZnS Quantum Dots Materials with Guest/Host Structure*
- P3-93 Kumbhojkar, N.; Mahamuni, S.; Kshirsagar, A.; India  
*Studies of Cubic and Hexagonal ZnS Quantum Dots*
- P3-94 Tripathy, S.; Ghoshal, S.K.; Soni, R.K.; Jain, K.P.; India  
*Investigation of Optical Properties of Nano-Silicon Using Photoluminescence and Raman Scattering*
- P3-95 Weissmuller, J.; Lemier, C.; Germany  
*Differential Dilatometry Investigation of Hydrogen Solution in Nanocrystalline Palladium*
- P3-96 Zheng, W.; Friedman, J.R.; Averin, D; Han, S.; LUKens, J.E.; USA  
*Strong Coulomb Blockade in Resistively Isolated Tunnel Junction*
- P3-97 Jeunieau, L.; Nagy, J.B.; Belgium  
*Adsorption of Pseudoisocyanine and Two Thiacarbocyanine Dyes on Silver Halides Nanoparticles*
- P3-98 Bezrukova, A.G.; Russia  
*Characterization of Bioengineered Nanostructures by Multiparametric Optical Assay*
- P3-99 Galetich, I.K.; Shelkovsky, V.S.; Ukraine  
*Mass Spectrometric Study of Cluster Formation Between the Proteins and Nucleic Acids*
- P3-100 Zagorodni, A.A.; Zhang, Yu; Wang, L.; Muhammed, M.; Sweden  
*Synthesis and Scaling-Up of the Nanopowder Production by Chemical Co-Precipitation*
- P3-101 Lin, H-M.; Pan, S-F.; Taiwan  
*Combined Nanocrystalline Material with Piezoelectric Crystal Detector for Application in Gas Sensor*
- P3-102 Tzeng, S-J.; Hsiau, P-J.; Lin, H-M.; Tsai, W-L.; Taiwan  
*Detecting Co and NO<sub>2</sub> Gases by Nanophase ZnO Gas Sensors with Neural Network Technique*
- P3-103 Gleeson, D.; Burch, R.; Tsang, S.C.E.; UK  
*Structural and Catalytic Properties of MnO<sub>x</sub>O-Clusters Supported on Mesoporous Mcm-41*
- P3-104 Dugal, M.; Reetz, M.T.; Germany  
*Immobilization of Nanostructured Metal Colloids in Hydrophobic Sol-Gel Materials*
- P3-105 Yatsimirsky, V.K.; Zacharenko, M.I.; DiyUK, V.; Revo, S.; Ukraine  
*The Evidence of Ni Nanoparticles Catalytic Activity in Nio Reduction*

- P3-106 Andersson, M.; Ilinc, A.; Stietz, F.; Träger, F.; UK  
*Formation of Parallel Gold Nanowires by Scanning Force Microscopy*
- P3-107 Gerasimov, G.N.; Grigor'ev, E.I.; Grigor'ev, A.E.; Vorontsov, P.S.; Nikolaeva, E.V.; Zavjalov, S.A.; Trakhtenberg, L.I.; Russia  
*Metal- Polymer Nanocomposites as New Type of Chemical Sensors*
- P3-108 Barariu, F.; Chiriac, H.; Vinai, F.; Murgulescu, I.; Ferrara, E.; Romania  
*Structural and Magnetic Properties of  $(Fe_{100-x}Co_x)_{73.5}Cu_1Nb_3Si_{13.5}B_9$  Nanocrystalline Wires*
- P3-109 Zarur, Andrey J.; Hwu, Henry.H.; Ying, J.Y.; USA  
*Catalytic Combustion with Nanocrystalline Barium Hexa-Aluminate- Based Systems*
- P3-110 Tschöpe A.; Birringer, R.; Germany  
*Tailoring the Microstructure and Defect Chemistry in Nanostructured Cerium Oxide for Optimised Gas Sensor Properties*
- P3-111 Zharmagambetova, A.; MUkhamedzhanova, S.; Selenova, B.; Chanyshева, J.; Kazakhstan  
*Formation of Monodispersed Palladium Catalysts*
- P3-112 Pak, A.; Kartonozhkina, O.I.; Slepov, S.K.; Komashko, L.; Kazakhstan  
*Monodispersed Copper Catalysts for Stereoselective Hydrogenation of Acetylene Compound*
- P3-113 Garcia, N.; Krämer, J.L.C.; Zhao, Y.W.; Spain  
*Intensity -Voltage Characteristics of Metallic Nanowires*
- P3-114 Hjelm, S.; Turkki, T.; Muhammed, M.; Mussman, L.; Sweden  
*Synthesis and Characterisation of Cerium-Zirconium-Calcium Oxides and Their Application in Three Way Car Catalysts*
- P3-115 Chou, S.Y.; Kong, L.; Zhang, L.; Li, M.; Wu, W.; USA  
*Quantunized Magnetic Disks for Ultra-High Density Magnetic Storage*
- P3-116 Liu, J.P.; Liu, Y.; Sellmyer, D.J.; USA  
*High Energy Products and High Coercivity in Exchange Coupled Hard / Soft Nanocomposites*
- P3-117 Zhernakov, V.S.; Latysh, V.V.; Stolyarov, V.V; Valiev R.Z.; Russia  
*Engineering of Nanostructured Commercial Alloys for Structural Application*
- P3-118 Hellmig, R.J.; Ferkel, H.; Germany  
*Stability of Alumina Ceramics Bonded with Nanoscaled Alumina Powder*
- P3-119 Curtis, C.J.; Schulz, D.L.; Ginley, D.S.; Gandelsman, V.Z.; Tepper, F.; USA  
*Nano-Ag and Nano-Al (ALEX<sup>TM</sup>) Based Inks for Contacts to Silicon Solar Cells*
- P3-120 Sastry, S.M.L.; Provenzano, V.; USA  
*Intrinsic and Extrinsic Effects in Nanocrystalline Materials and Some Technological Challenges*
- P3-121 Yamamoto, T.A.; Seino, S.; Katsura, M.; Okitsu, K.; Oshima, R.; Nagata, Y.; Japan  
*Hydrogen Gas Evolution from Nanoparticles Dispersed in Water Irradiated with Gamma-Ray*
- P3-122 Miyahara, K.; Nagashima, N.; Ohmura, T.; Matsuoka, S.; Japan  
*Evaluation of Mechanical Properties in Nanometer Scale Using AFM-Based Nanoidentation Tester*

**NANOSTRUCTURES:  
IMMUNOLOGY, TISSUE CULTURE AND BIOSENSORS**

*Ivar Giaever*

Rensselaer Polytechnic Institute  
Troy, NY 12180-3590, USA <giaevi@rpi.edu>

In 1959 Richard Feynman gave a talk entitled: "There's plenty of room at the bottom".<sup>1</sup> In the talk he speculates on how information can be stored on a small scale, and he marvels at how nature has solved the problem by using about 30 atoms per bit in the DNA of genes. His prediction that there would be lots of fun for creative scientists in the micro-world is born out by this conference. This talk illustrates in simple terms how one can explore some problems in biotechnology using small structures.

In the first part I will describe how to design an immunological test for a disease. The test is based upon the optical properties of small, metallic particles of the order 100 nanometers. Somewhat surprisingly, single layers of adsorbed protein upon these particles are easily visible to the unaided eye. If these protein layers are exposed to specific antibody, double layers of protein forms and that results in another clearly visible change.

In the second part I will describe how morphology and motion of mammalian cells can be determined by electrical impedance measurements. In this approach the cells must be cultured on small gold electrodes. Because the 10 nanometer thick cell membranes are basically insulating, the attached cells will block the electrode area, and therefore the impedance will increase. With confluent cell layers about 50 cells can be accommodated on the electrode, but the system is capable of following the motion of even a single cell. This method has great potential as a biosensor, because the cells respond with morphological changes when challenged by virions, toxins, drugs or other chemical compounds.

1. Richard P. Feynman, Journal of Microelectromechanical Systems, Vol 1, No.1, March 1992.

**THE EVOLUTION OF NANOSCALE IN SEMICONDUCTOR PHYSICS**

*Leo Esaki*

Science and Technology Promotion Foundation of Ibaraki  
Tsukuba, Ibaraki 305 0047, Japan.

In the early twentieth century, encounters with physical phenomena which require detailed analyses at a nanoscale, such as electron motion, prompted the advent of quantum mechanics, since Newton mechanics could not possibly provide adequate explanation for them. Electron tunneling through nanoscale barriers is the most direct consequence of the law of quantum mechanics, for which the Esaki tunnel diode gave most convincing experimental evidence in 1957. Following the evolutionary path of nanoscience in semiconductor physics, significant milestones are presented, including resonant tunnel diodes, superlattices, quantum wires and dots.

**TRANSITION METAL (Pt, Ag) NANO-CLUSTER ARRAYS FABRICATED  
BY ELECTRON BEAM LITHOGRAPHY (2.5-50 nm RANGE):  
STRUCTURE, STABILITY AND CATALYTIC REACTION STUDIES**

*A. Eppler, A. Avoyan, and G.A. Somorjai*

Materials Science Division, Lawrence Berkeley National Laboratory,  
Chemistry Department, University of California, Berkeley, USA

Supported metal nanoparticles (platinum and silver) have been fabricated using electron beam lithography (EBL). EBL produced ordered two-dimensional arrays with particle diameters of  $10 \pm 0.5$  nm, uniform interparticle distances ( $230 \pm 2$  nm), and uniform height ( $20 \pm 0.5$  nm). Due to the narrow size distribution and the long-range ( $\text{cm}^2$ ) order, the arrays produced using EBL were applied as models for supported metal catalysts. The nanoparticles have been characterized using TEM, AFM, and SEM. Different oxides,  $\text{SiO}_x$ ,  $\text{AlO}_x$ , and  $\text{TiO}_x$ , were used as supports for the metal particles. Temperature programmed desorption was used to determine the metal surface area. Reaction studies included ethylene hydrogenation and oxidation, and n-hexane conversion. Thermal stability of the metal particles was investigated in the 200 to 700°C range under both oxidizing and reducing conditions. The results of these studies will be reviewed, and the unique chemical behavior of metal nano-clusters as compared to single crystal surfaces of the same metals will be discussed.

**HIGH ENERGY DENSITY RECHARGEABLE LITHIUM-ION BATTERY  
PREPARED BY THE SELF-ASSEMBLY OF GRAPHITE OXIDE  
NANOPLATELETS AND POLYELECTROLYTES NANOLAYERS**

*Thierry Cassagneau and Janos H. Fendler*

Department of Chemistry and Center for Advanced Materials Processing,  
Clarkson University, Box 5814, Potsdam, New York 13699, USA

Using our general method for the preparation of ultrathin films by the layer-by-layer self-assembly of polyelectrolytes, nanoparticles and nanoplatelets we have constructed a high-energy lithium ion battery. The working electrode consisted a transparent indium tin oxide, ITO, substrate onto which nanoplatelets of graphite oxide (GO), and nanolayers of poly (diallyldimethyl-ammonium) chloride, PDDA and polyethylene oxide, PEO, were self-assembled. Positively charged PDDA has been chosen as the "building-polymer" since it is known to interact strongly with negatively charged GO nanoplatelets by electrostatic forces and thus it facilitates the quantitative self-assembly of these nanolayers onto a conductive substrate. PEO, an ion-conducting polymer, have synergized the "building" function of the polyelectrolyte by allowing further layer-by-layer growth of the films. The structure of the working electrode was characterized by a large variety of techniques. Lithium wires have served as the anode and the counter electrode. The cell has contained LiASF<sub>6</sub> as a supporting electrolyte and methyl formate and ethylene carbonate as solvent. The specific capacity of this cell (1232 mAh per gram of graphitic carbon) is substantially greater than that currently available

## ON MELTING CRITERIA OF 2D SYSTEMS

*S.I. Shevchenko<sup>1</sup> and E.B. Alyab'eva<sup>2</sup>*

<sup>1</sup> B.I. Verkin Institute for Low Temperature Physics and Engineering,

Lenin Ave. 47, Kharkov 310164, UKRAINE <shevchenko@ilt.kharkov.ua>

<sup>2</sup> Kharkov State Polytechnical University, Frunze St. 21, Kharkov 310002, UKRAINE

The dislocation theory of melting by Kosterlitz-Thouless (KT) gives a satisfactory description of melting for a wide class of 2D systems. This theory does not take into account quantum effects. Such effects can become important at crystallization of 2D electron or hole gases. By the famous Lindeman criterion of melting  $\langle u^2(l) \rangle = \gamma a^2$  it is impossible to obtain a melting temperature since in the 2D case a thermodynamic mean-square of deviation of atoms from the equilibrium position of  $T \neq 0$  diverges logarithmically. The consequences following from the generalized criterion of melting  $\langle [u(l+a) - u(l)]^2 \rangle = \tilde{\gamma} a^2$  have been studied in present work. The equation obtained for a melting temperature which is true in a general case has been analysed for a dipole crystal assuming that a distance  $d$  between positive and negative charges in dipole is small than the average distance between dipoles.

The main results consist in the following. The behaviour of melting temperature  $T_m$  as a function of density of dipoles  $n$  is determined by the relationship between the average energy of interaction of dipoles  $(ed)^2 n^{3/2}$  and the quantum-mechanical energy  $h^2 n / M$ . If the first energy exceeds essentially the second one, then the melting temperature obtained by means of the generalized criterion is equal to  $T_m \approx 4.3 \tilde{\gamma} (ed)^2 n^{3/2}$ . At all reasonable values of  $\tilde{\gamma}$  this magnitude exceeds the melting temperature  $T_m \approx 0.14 (ed)^2 n^{3/2}$  which follows the KT theory. Therefore, in this case the melting of crystal will take place through the KT mechanism, i.e. through dissociation dislocation pairs.

At  $n < n_c$  where a critical density  $n_c$  is determined from the relationship  $h^2 n / M = 7.7 \tilde{\gamma}^2 (ed)^2 n^{3/2}$  the quantum effects are so large that the system of dipoles remains liquid even at  $T = 0$ . At  $n_c >> n - n_c > 0$  a crystallization of dipoles takes place and  $T_m = 10.8 \left( \frac{h^2 n}{M} (ed)^2 n^{3/2} \right)^{1/2} \left( \frac{n - n_c}{n_c} \right)^{1/3}$  the obtained temperature is below than the melting temperature following from the KT theory. As a result, in this density range dislocations do not affect the melting temperature and the melting take place due to quantum effects. At  $M \approx 10^{-27} g$ ,  $d \approx 10^{-6} cm$ , and  $\tilde{\gamma} = 1/16$  (as in Lindeman criterion case) the critical density of dipoles  $10^{10} cm^{-2}$ .

---

**FABRICATION OF NANOSCALE HETEROJUNCTION OF Si/Au AND Si/Ag  
BY SURFACE DROPLET EPITAXY**

*Yutaka Wakayama and Shun-Ichiro Tanaka*

Tanaka Solid Junction Project, ERATO, Japan Science and Technology Corporation  
1-1-1 Fukuura, Kanazawa-ku, Yokohama, 236, JAPAN <waka@tanaka.jst.go.jp>

Because of the increasing demand for downsizing of the elemental scale of VLSIs and the development of quantum-functional devices, investigations of an alternative technique of the nanoscale processing to conventional lithography have been extensively carried out for recent years. The purpose of this study is to establish a new technique of a material design on a nanometer scale. Particularly, the fabrication of the nanometer-scaled metal/semiconductor heterojunction is the main object, because that is one of the most fundamental constitutions of the semiconductor devices.

In this study, the metal/semiconductor heterojunction was successfully fabricated on a nanometer scale by employing metal nanoparticles for transport media of liquid phase epitaxy (LPE). The nanoparticles of the metals were produced by a gas-condensation method in argon atmosphere and deposited on single-crystalline silicon substrates. Following thermal annealing resulted in the bilayered dot formation on the flat silicon substrates. On the basis of a structural and elemental analysis by a transmission electron microscope and an energy-dispersive X-ray spectroscopy, the kinetics was revealed as follows. First, surface-diffusing Si atoms are dissolved into the metal particles to form molten alloy at the elevated temperature. Second, during cooling down, the Si atoms are precipitated from the molten alloy to grow epitaxial Si dot on the surface leaving the metal particle on it. Finally, Si and the metal separate out to form the bilayer dot. This process is called "surface droplet epitaxy (SDE)". The treatment required for SDE is only the thermal annealing in ultra high vacuum and do not involves in any conventional patterning techniques. In this sense, SDE can be regarded as a kind of a self-assembly process. SDE can take place in any semiconductor-metal binary systems, which undergo endothermic and eutectic reaction, for example, the combination between Si or Ge for the semiconductors and Au, Ag or Al for the metals. In this study, we demonstrate the fabrication of the Si/Au and Si/Ag bilayer dots.

**PANEL ON MECHANICAL ALLOYING PROCESS:  
THEORETICAL FRAMEWORK AND EXPERIMENTAL SUPPORTS**

*M. Magini, A. Iasonna and F. Padella*

ENEA-INN-NUMA, C.R. Casaccia, Via Anguillarese, Rome, ITALY  
<Magini@casaccia.enea.it>

Mechanical Alloying (MA) has been widely employed in the last decade as a preparative tool able to synthesise materials, both equilibrium and metastable materials, often having a nanocrystalline structure. In order to establish a *predictive* capability for the MA process, so that a wanted final product can be planned as a function of the milling conditions, it is essential to understand in which way and how much energy is transferred from the milling tools to the powder under processing.

We have developed a model for mechanical alloying based on a detailed kinetic analysis of the ball collisions inside a planetary ball mill. The model enables calculating both the energy transferred per impact and per unit of mass and the total energy consumption due to the process itself.

Such a power consumption, electrical and mechanical, have been experimentally measured during milling. The experimental results are perfectly in line with the prediction of the collision model and comparison between experimental and theoretical power absorptions is quite satisfactory. The dependence of the power consumption on the rotation speed of the planetary mill and the effect of the filling of the milling device on the energy transfer and power consumption have clearly been established.

The model and the "in-situ" power measurements are the guidelines in planning the experimentally proper milling conditions in order to obtain a final wanted product.

**SONOCHEMICAL APPROACH FOR THE PREPARATION  
OF NANOSTRUCTURED FERRITE PARTICLES**

*Kurikka.V. P. M. Shafi, and Aharon Gedanken\**

Department of Chemistry, Bar-Ilan University, Ramat-Gan 52900, ISRAEL  
<muhamms@mail.biu.ac.il>

A new method, via the sonochemical decomposition of the solutions of organic precursors, for the synthesis of nanostructured crystalline Ferrite particles is proposed. Nanosized amorphous Ferrite powders ( $\text{NiFe}_2\text{O}_4$ ,  $\text{CoFe}_2\text{O}_4$  and  $\text{BaFe}_{12}\text{O}_{19}$ ) powders were prepared by high intensity ultrasound irradiation of the solutions of  $\text{Fe}(\text{CO})_5$ ,  $\text{Ni}(\text{CO})_4$ ,  $\text{Ba}[\text{OOCCH}(\text{C}_2\text{H}_5)\text{C}_4\text{H}_9]_2$  in decane or decalin at 273 K, under oxygen pressure of 100 to 150 kPa or under air. The amorphous nature of these particles was confirmed by various techniques, such as SEM, TEM, electron microdiffraction, and X-ray diffractograms. Magnetic measurements, Mössbauer, and EPR spectral studies indicated that the as-prepared amorphous ferrite particles were superparamagnetic. The amorphous as prepared particles were heated at low enough temperatures (500-700°C) to get the final single phase nanocrystalline ferrite particles. Mössbauer parameters and the magnetization data ie. hyperfine field value and the saturation magnetization of the annealed samples were significantly lower than that for the reported multidomain bulk particles, reflecting the ultrafine nature of the sample. Differential scanning calorimetry (DSC) was used to find the crystallization temperatures of the amorphous forms and the thermogravimetric measurements with a permanent magnet gave Curie temperatures for the crystallized ones.

**NANOSTRUCTURED MATERIALS PROCESSED  
BY SEVERE PLASTIC DEFORMATION**

*Ruslan Z. Valiev*

Institute of Physics of Advanced Materials, Ufa State Aviation Technical University,  
K. Markska 12, 450000 Ufa, RUSSIA

Recent studies have demonstrated that ultrafine-grained nanostructured metals and alloys can be prepared by severe plastic deformation, i.e. intense plastic straining under high imposed pressure [1, 2].

The results obtained from TEM/HREM and X-ray show that processed nanostructures are of a granular type and posses high angle grain boundaries. A special attention is given to a defect structure of these grain boundaries and it is shown that they are in non-equilibrium state because content a high density of extrinsic dislocations and disclinations.

The second part of the paper deals with enhanced properties of nanostructured materials such as a very high strength, fatigue, superplasticity. The origin of these unusual properties is considered and discussed on the basis of features of the processed nanostructures. Several examples of applications of these advanced materials are given.

- [1] R.Z. Valiev, A.V. Korznikov and R.R. Mulyukov, Mater. Sci. Eng., A168 (1993) 141.
- [2] Ultrafine-grained Materials Produced by Severe Plastic Deformation, the thematical issue, ed. By R.Z. Valiev, Ann. Chim. Fr., 21 (1996) 369-450.

**NANOSTRUCTURED OXIDE FILMS BY FERRITE PLATING  
WITH SONOCHEMISTRY**

*Yoshitaka KITAMOTO and Masanori ABE*

Department of Physical Electronics, Tokyo Institute of Technology,  
O-okayama, Meguro-ku, Tokyo, 152-8552, JAPAN <kitamoto@pe.titech.ac.jp>

Sonochemistry, the use of power ultrasound to stimulate chemical processes in liquids, is currently the focus in a wide range of chemical materials science and technology, since it causes novel chemical and physical reactions, which do not occur unless sonically stimulated [1]. This paper reports that combining sonochemistry with ferrite plating, a chemical ferrite film synthesis [2], broke the limitation inherent in the ferrite plating. The powder ultrasound generates in the liquids localized "hot spots" of extremely high temperatures (~3000 K) and high pressures (~1000 atm) due to collapse of cavitation bubbles, which activates not only chemical reactions but also dynamics of ions [1] during the plating. Because the hot spots are localized, the average temperature of the solution is kept below 100°C, which allows us to use non-heat-resistant substrates, as well as in the conventional ferrite plating without applying ultrasound.

Applying power ultrasound waves (19.5 kHz, 600W) to 300 ml of FeCl<sub>2</sub> aqueous solution (pH=7.0) at 70°C, we successfully encapsulated polyacrylate spheres of two sizes, 250 nm and 4.5 μm in average diameter, with magnetite ferrite coatings. This broke the previous lower limit (300 nm) of the size of the particles to be encapsulated; without application of the ultrasound waves, the ferrite coating became discontinuous or insular. From TEM observation of the cross section, the polymer spheres were covered with uniform crystallites of around 30 nm in size. The ultrasound waves produce on the polymer surfaces OH groups which work as ferrite nucleation sites and activate the migration of ions near the surface; these are responsible for the improvement obtained in the quality of the ferrite coatings. The ferrite-encapsulated particles will greatly improve the performance of the enzyme immunoassay, which has been put to clinical use as a cancer test reagent with insular-ferrite-coated particles.

- [1] T.J. Mason, Chem. Industry, 18 January (1993) 47-50.  
[2] M. Abe, T. Itoh and Y. Tamura, Thin Solid Films, 216 (1992) 155-161.

**SIZE-SELECTED GOLD NANOPARTICLES BY AEROSOL TECHNOLOGY**

*Knut Deppert, Martin H. Magnusson, Jan-Olle Malm<sup>1</sup>, Jan-Olov Bovin<sup>1</sup> and  
Lars Samuelson*

Solid State Physics and <sup>1</sup>Inorganic Chemistry,  
Lund University, Box 118, 221 00 Lund, SWEDEN <Knut.Deppert@ftf.lth.se>

The use of very small particles as building blocks in electronic circuits and nanostructured materials demands that these particles be produced with high efficiency and purity. For many applications, e.g., where coulomb blockade or quantum size effects are studied, it is important that the particles have a narrow size distribution. A common means for producing particles with a narrow size distribution is colloid chemistry, which can give good results. A problem with colloids is that the particles must be coated with a surfactant if they are not to coalesce, which will inevitably introduce some contaminants. Also, wet chemical methods are, in general, less clean than gas-phase methods.

We present an approach toward producing nanometer-sized, size-selected gold particles, with high purity and high yield, through a physical synthesis method based on aerosol technology. In the process, gold is heated to approximately 1650°C in a tube furnace, through which nitrogen is flowing. As the gold vapor leaves the furnace, it quickly becomes supersaturated, and will condense into particles. These particles coalesce into larger aggregates, which have a fractal-like shape, and the resulting size distribution will be quite broad. The aerosol is passed through a charging device, and the particles are classified by means of a Differential Mobility Analyzer (DMA). In the DMA, an electric field forces the charged particles to move toward a sampling slit, and only the particles with a certain aerodynamic size will be collected. In order to obtain spherical particles, the aerosol is then passed through a second furnace, where the particles are sintered. The sintering can be monitored by a second DMA, and, finally, the particles can be deposited onto a substrate by an electric field. In addition to the characterization of the process itself, we will present TEM studies of the produced particles.

**GAS PHASE SYNTHESIS AND CHARACTERIZATION  
OF EQUAL-SIZED NANOSCALE SEMICONDUCTOR PARTICLES**

*F.E. Kruis<sup>1</sup>, B.Rellinghaus<sup>2</sup>, F.Otten<sup>1</sup>, H.Fissan<sup>1</sup>, and E.F.Wassermann<sup>2</sup>*

<sup>1</sup> Process- and Aerosol Measurement Technology, <sup>2</sup> Experimental Low-temperature Physics, Gerhard-Mercator-University Duisburg, D-47048 Duisburg, GERMANY  
*<h.fissan@uni-duisburg.de>*

We report on low-cost aerosol synthesis of size-classified PbS nanocrystals. The experimental apparatus consists of (i) particle generation by evaporation and subsequent coagulation, (ii) charging the particles and selection in size by a Differential Mobility Analyser (DMA), (iii) sintering and crystallisation in an annealing step, and finally (iv) deposition of particles. The DMA (NANO-DMA, TSI) was specially developed and characterised for nanoparticles (3-50 nm). The sublimation temperature employed is under the stoichiometric evaporation temperature, thus enabling direct and simple synthesis by sublimation. The irregularly shaped and amorphous agglomerate particles necessitate the sintering in a second furnace, resulting in the formation of monocrystalline and quasi-spherical particles with sizes adjustable between 3 and 20 nm and having a geometric standard deviation of 1.13. The nanometer-sized PbS particles are deposited in a newly developed electrostatic precipitator at atmospheric pressure on planar substrates with a rate of about  $10^{11} \text{ cm}^2\text{h}^{-1}$ . TEM and XRD show the development of amorphous agglomerates into monocrystalline quasi-spherical particles by sintering.

## NANOPARTICLES OF MICROPOROUS MATERIALS

*B. J. Schoeman\*, K. Higberg and J. Sterte*

Division of Chemical Technology, Luleå University of Technology,  
S-971 87 Luleå, SWEDEN

\* Central & New Businesses R&D, The Dow Chemical Company,  
Midland, MI 48674, USA <bschoeman@dow.com>

Microporous materials, in particular zeolites, have played a significant role within the field of catalysis. However, in certain catalytic applications, diffusional limitations demand smaller crystal sizes. The conventional crystallite size is, broadly speaking, within the micron range. There are now several reports in the literature describing methods to prepare smaller crystals in the colloid size range 30 to 200 nm[1]. A major advance within this area was made when it was very recently recognised that the silicate precursor solutions used for the synthesis of colloidal zeolite contained sub-colloidal particles with sizes smaller than 5 nm[2].

A typical precursor preparation entails the hydrolysis of tetraethoxy silane (TES) in the presence of a dilute solution of a tetraalkylammonium (TAA) hydroxide where the alkyl group may be methyl (TMA), ethyl (TEA), propyl (TPA) or butyl (TBA). Typical molar compositions of the precursor solutions are

$x \text{ TAAOH } 25 \text{ SiO}_2 \text{ } y \text{ H}_2\text{O } 100 \text{ EtOH}$  (EtOH = ethanol - a hydrolysis product)

where  $3 \leq x \leq 9$  and  $480 \leq y \leq 1500$ . The particles in these solutions have an average particle size in the range 2 to 5 nm, the size being a function of the solution composition. Furthermore, the extensive experimental data collected (TG/DTA, MAS NMR, FT-i.r., FT-Raman,  $\text{N}_2$  adsorption, cryo-TEM, etc) shows that the nanoparticles do possess an ordered microporous structure. Under controlled conditions, partial removal of the organic base renders the outer pore region accessible to probe molecules and hence, the possibility of preparing a catalytically active material is made possible. Further modifications may be made to the properties of the resulting hydrolysis product by the introduction of trace amounts of alumina and / or titania. Trace amounts of the latter present in the microporous structure yield a nano-sized material that is active in phenol hydroxylation and 1-hexene epoxidation using  $\text{H}_2\text{O}_2$  as an oxidant [3].

Recognising the fact that the nanoparticles are the product of a base-catalysed hydrolysis allows for the tailoring of the particles properties. This important fact will be discussed with close reference to sol-gel chemistry.

- [1] Schoeman, B. J., Sterte, J., Otterstedt, J.-E., *Zeolites* 14, 110-116 (1994).
- [2] Schoeman, B. J., in "Progress in Zeolites and Microporous Materials" (Eds.) H. Chon, S.-K. Ihm and Y. S. Uh, Elsevier, Amsterdam, 1996, p. 647.
- [3] Ravishankar, R, Schoeman, B, et. al., To be presented at the 12th IZA Conference, Baltimore, 1998.

**SYNTHESIS OF MESOPOROUS TiO<sub>2</sub> AND TiN***T.V. Anuradha and S. Ranganathan*

Department of Metallurgy, Indian Institute of Science, Bangalore 560 012 INDIA

Mesoporous materials based on alumino silicate(MCM-41) were first reported by Mobil in the year 1992. Only recently, this class of materials has been extended to include transition metal oxides. These materials can be synthesized using the template based approach.

The synthesis of titanium oxide based mesoporous materials at room temperature was tried by templating TiO<sub>2</sub> onto a self-assembled liquid crystal mesostructure formed from dodecylamine, but this resulted in the formation of amorphous and non-mesoporous titania which was confirmed by small angle XRD. The particle morphology of the product obtained was also studied using SEM and TEM which indicated the particles to be nanostructured with spherical morphology. There are earlier reports which say that TiO<sub>2</sub> particles with diameter less than 100 Å can be produced by controlled hydrolysis of Ti(O<sub>2</sub>C<sub>3</sub>H<sub>7</sub>)<sub>4</sub> in the reverse micelles of Aerosol OT produced in an Aerosol OT- hexane - H<sub>2</sub>O solution (water/oil emulsion) whereas in our case, we are assuming that nano particles of TiO<sub>2</sub> particles are getting formed by the controlled hydrolysis of titanium isopropoxide in the reverse micelles of dodecylamine produced from dodecylamine - isopropanol- H<sub>2</sub>O solution (water/oil emulsion). The order of addition of the precursor materials was found to vary the particle morphology of the product thus obtained. Mesoporous materials based on TiN have been synthesized at 800°C by templating TiN onto the cationic surfactant namely, cetyltrimethylammonium bromide and by the suitable adjustment of the reaction conditions. Many samples have been synthesized by using different reaction parameters, for which the characterization has been carried out using XRD and SEM wherein some satisfactory results were obtained.

**CONTROL OVER THE FILM STRUCTURE  
IN LAYER-BY-LAYER SELF-ASSEMBLED FILMS**

*N. A. Kotov<sup>1</sup>; S. Magonov<sup>2</sup> and Y. Tropsha<sup>3</sup>*

<sup>1</sup> Department of Chemistry, Oklahoma State University, Stillwater, OK 74078, USA

<sup>2</sup> Digital Instruments, Santa Barbara, CA, USA

<sup>3</sup> Becton-Dickinson, Research Triangle Park, NC, USA

Layer-by-layer self-assembly is a convenient method for the preparation of composite films where an inorganic material (M) is interlaced with layers of polymer (P). The structure and possible applications of sandwich assemblies of magnetic nanoparticles, semiconductor nanocrystallites and aluminosilicate sheets are discussed. Due to the slow rate of conformational transitions the structure of clay-polymer films can be also regulated by applying an external voltage. For montmorillonite-polyelectrolyte films the effect of self-healing of defects has been observed.

On the basis of XRD, AFM, SPS, TEM data, and synthetic methods various models of M/P self-assembled films are considered. The deviation from an ideal multilayer structure is attributed to the agglomeration of inorganic particles catalysed by loose loops and ends of adsorbed polyelectrolyte layer. The interlayer roughness of M/P films can be controlled by (1) rigidity of a polymer, (2) crosslinking, and (3) introduction of hydrophobic groups. Account of all these factors affords preparations of exceptionally smooth M/P films. First results on gas permeation properties of layer-by-layer self-assembled films will be presented. Finer ordering of multilayers resulted in improved gas selectivity.

Laser irradiation or microwave treatment of the polymer films yields well ordered layers of magnetite nanoparticles. The effect is attributed to effective crosslinking of the polyelectrolyte chains. Such composite magnetic films were found to possess exceptional mechanical and environmental resilience.

**THE MODERN SYNTHETIC POSSIBILITIES FOR TOPOLOGICAL  
ORGANIZATION OF OXIDE NANOSTRUCTURES AND  
NANOSTRUCTURED MATERIALS**

V. M. Smirnov

Department of Chemistry, St.Petersburg State University,  
St.Petersburg 198904 RUSSIA <smirnov@moss.pu.ru>

In this communication the possibility is discussed to construct highly organized nanostructured materials on the basis of precision inorganic synthesis, which allows us to reach the principally new level of controlling the materials structure and properties.

The modern synthetic methods for spatial atom distribution in the bulk oxide structure (i.e. topology of the structure) are considered. Introduction of a topology term for the solid chemical compounds is due to variety of spatial atom distribution in a compound synthesized by the beforehand given synthetic program.

Chemical principles, lying in the basis of the method, are considered with the example of two-dimensional oxide nanostructures formation (5-100 Å).

The simplest topological organization is an inhomogeneous atom distribution alongside one of the spatial coordinates (layered, i.e. consisting of a great number of nanolayers), including the structures with periodic (Fig. 1) and aperiodic (Fig. 2) unhomegeneity in the chemical composition and the structure. The examples are given on how to control the properties of highly organized nanostructures and nanostructured materials.

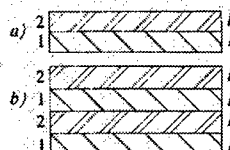


Fig. 1. Periodic distribution (along z axis) of E-O layers consisting of certain numbers of nanolayers; for example, according to the scheme: E-O layers (1), E<sub>x</sub>O layers (2); a - two-layers structure,  $l_1=l_2$ , b - four-layers structure,  $l_1=l_2=l_3=l_4$ , c - four-layers structure  $l_1 \neq l_2, l_3 \neq l_4$ .

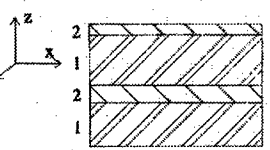
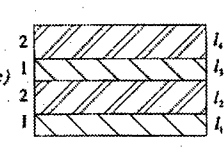


Fig. 2. Aperiodic distribution along z axis (four-layers structure  $l_1 \neq l_2 \neq l_3 \neq l_4$ ).

This work has been funded by RFBR grant 96-03-33990.

**NANOCRYSTALLINE Fe AND Fe-RICHED Fe-Ni  
THROUGH ELECTRODEPOSITION***Michel L. Trudeau*

Emerging Technologies, Hydro-Quebec, 1800 Boul. Lionel-Boulet,  
Varennes, Quebec, J3X 1S1, CANADA <trudeau@ireq.ca>

There is a constant need for new softer magnetic materials. Since the early 90's, a large number of studies have shown that, by decreasing the average crystal size of a magnetic material in the nanometer regime, it is possible to reduce drastically its magnetic losses. This was clearly demonstrated in nanostructured magnetic alloys based on the thermal crystallization of amorphous ribbons. However, the quest for obtaining dense single phase soft magnetic materials using different powder processing has always been hindered by the difficulty of producing fully dense and relax samples without grain growth. Moreover, in powder processes, such as gas phase evaporation/condensation and ball milling, crystalline surface contamination is also found to be a major difficulty as well as a major cause in the deterioration of the magnetic properties. The purpose of this study is to present results on synthesis aspects and properties of nanostructured magnetic materials produced by pulsed electrodeposition. It was shown in recent years that by controlling the current profile during electrodeposition, e.g. by applying a high current density for a short period of time followed by longer time period with no applied current, it is possible to control the nucleation and growth of the deposited materials. It follows those samples with a crystalline size as low as 5 to 7 nm can be synthesized. Surprisingly, compared to other technique, pulse-electrodeposition has received little attention as a synthesis method for producing large quantities of fully dense nanostructured materials. In this work we present results for Fe and Fe-riched Fe-Ni alloys obtained by controlling different electrodeposition parameters: composition of the solution, peak current density, pulsation profile, temperature, pH. Structural analysis was performed using x-ray diffraction and TEM. The magnetic properties were analyzed using a vibrating sample as well as a SQUID magnetometer. Finally, we will also describe some of the technological possibilities that are offered by this process and compare them to other synthesis methods. It is possible to demonstrate that pulse electrodeposition is probably the only technique that offers the technical as well as the commercial advantages for large scale technological application in soft nanostructured magnetic materials.

**PREPARATION AND CHARACTERISATION  
OF COBALT OXIDE NANOSIZED PARTICLES  
OBTAINED BY AN ELECTROCHEMICAL METHOD**

*E.P. Reddy<sup>1</sup>, T.C. Rojas<sup>1</sup>, J.C. Sánchez López<sup>1</sup>, M. Domínguez<sup>2</sup>, E.Roldan<sup>2</sup>, J.Campora<sup>3</sup>,  
P. Palma<sup>3</sup> and A. Fernández<sup>1</sup>*

<sup>1</sup>Instituto de Ciencia de Materiales de Sevilla, Centro de Investigaciones Científicas "Isla de la Cartuja", Avda. Americo Vespucio s/n, 41092-Sevilla, SPAIN <asuncion@cica.es>

<sup>2</sup>Depto. de Química-Física, Universidad de Sevilla, c/Prof.García González s/n,  
41012-Sevilla, SPAIN

<sup>3</sup>Instituto de Investigaciones Químicas, Centro de Investigaciones Científicas "Isla de la Cartuja", Avda. Americo Vespucio s/n, 41092-Sevilla, SPAIN

The preparation and characterisation of nanometric particles of antiferromagnetic materials is interesting due to the apparition of superparamagnetic behaviour, resulting from an imperfect compensation of the magnetic sublattices at the particle surface. Recently, an electrochemical process has been described,<sup>1</sup> that metal foils are anodically dissolved and that the metal salts formed as intermediates are cathodically reduced with quantitative formation of metal clusters stabilised by tetra-alkylammonium salts. In the present communication we have studied such process for the preparation of nanosized Co clusters and their ulterior oxidation to cobalt oxide nanosized particles, stable in air.

Co and Pt foils have been used as anode and cathode respectively. Tetra-n-octylammonium bromide and tetra-n-butylammonium acetate (0.1M) in THF have been used simultaneously as supporting electrolyte and stabiliser for the clusters. During electrolysis under N<sub>2</sub> atmosphere the transparent electrolyte solution become dark brown and a black precipitate formed under certain conditions. This precipitate was separated and dried under nitrogen flux and finally exposed to air. The characterisation of the resulting powder was carried out by Transmission Electron Microscopy (TEM), Electron Diffraction, X-ray Absorption Spectroscopy (XAS), Electron Energy Loss Spectroscopy (EELS) and X-Ray Photoelectron Spectroscopy (XPS).

The TEM analysis shows the formation of homogeneously nanosized dark particles (2-4 nm in diameter) embedded in a surfactant protective matrix. Electron diffraction shows broad but clear peaks corresponding to the formation of small CoO crystalline nanoparticles. This result has been confirmed by XAS, XPS and EELS. The application of the different available techniques to the characterisation of such nanometric systems will be emphasised.

A mechanism is proposed for the formation of CoO nanoparticles that involves the oxidation of metallic Co clusters by residual oxygen pressure. Removal of the surfactant produces the formation of large CoO crystals due to the high surface energy of the very small nanometric particles

1. Reetz, W. Helbig, J. Am. Chem. Soc. 116, 7401 (1994).
2. Reetz, W. Helbig, S.A. Quaiser, Chem. Mater. 7, 2227 (1995).

**SYNTHESIS AND REACTIVITY OF NANOPHASE FERRITES  
IN REVERSE MICELLAR SOLUTIONS**

*Charles J. O'Connor, Candace T. Seip, Everett E. Carpenter, Sichu Li, and Vijay T. John*

Advanced Materials Research Institute, University of New Orleans,  
New Orleans, LA 70148, USA <AMRI@uno.edu>

Self assembly preparative techniques in confined media that lead to magnetic materials with nanometer dimensions will be described. Synthesis of nanoparticles using the restricted environments offered by surfactant systems such as water-in-oil microemulsions (reverse micelles) provide excellent control over particle size, inter-particle spacing, and particle shape. These environments have been used in the synthesis of  $\gamma$ -Fe<sub>2</sub>O<sub>3</sub>, Fe<sub>3</sub>O<sub>4</sub>, MnFe<sub>2</sub>O<sub>4</sub>, and CoFe<sub>2</sub>O<sub>4</sub> with particle sizes ranging from 10-20 nm. In the fluid reversed micelle system, particle growth is restricted by the size of the water droplets. The controlled environment of the reverse micelle also allows sequential synthesis, which can produce a core-shell type structure. Interest in GMR type nanoparticles has invoked fabrication of core-shell type materials consisting of ferromagnetic Fe<sub>3</sub>O<sub>4</sub> nanoparticles with antiferromagnetic MnO coatings. Because the lattice match between the ferrite and MnO is similar, a thin manganese oxide layer can coat the ferrite center.

Lyotropic liquid crystal media also offer template effects for the synthesis of magnetic nanostructures. The lyotropic liquid crystal gels contain microstructured organic and aqueous phases. The nanoscale ordering of magnetic particles when synthesized in these systems is characterized through electron microscopy. The gel phase also offers an opportunity to synthesize polymer-nanoparticle composites with unique structural and morphological characteristics, where the polymer synthesized in the organic microphase locks in the ferrite nanostructure morphology. The correlation of magnetic properties to supramolecular structure is explored in these composites.

The structures, theory and modeling concepts and novel physical properties of these materials are discussed with emphasis given to the differences between coarse and fine grained magnetic materials.

**SIZE-CONTROLLED SYNTHESIS OF NANOSCALE ALUMINATE SPINELS  
VIA W/O MICROEMULSIONS USING HETEROBIMETALLIC ALKOXIDE  
PRECURSORS**

*F. Meyer<sup>1,3</sup>, A. Dierstein<sup>1,3</sup>, Ch. Beck<sup>1,3</sup>, J. Wagner<sup>1,3</sup>, W. Härtl<sup>1,3</sup>, R. Hempelmann<sup>1,3</sup>,  
S. Mathur<sup>2,3</sup> and M. Veith<sup>2,3</sup>*

<sup>1</sup> Physikalische Chemie, <sup>2</sup> Anorganische Chemie, <sup>3</sup> Sonderforschungsbereich 277  
Universität Saarbrücken, D-66123 Saarbrücken, GERMANY

Nanosized spinels,  $MAl_2O_4$  ( $M = Mg, Co, Ni, Cu$ ) were prepared by a sol-gel type hydrolysis of alkoxides in the inverse micelles of w/o-microemulsions [1,2].

As single source precursors we have used heterobimetallic alkoxides such as  $Co[Al(O-ipr)_4]_2$  which were prepared by the salt elimination reaction including anhydrous metal halides and alkali metal isopropoxo-aluminate ( $[MAl(O-ipr)_4]$ ,  $M = Li, Na, K$ ). The products obtained were characterised by single crystal X-ray diffraction analysis. Alternatively, appropriate mixtures of single metal alkoxides like  $Al(O-ipr)_3$  and  $Co$ -di(triphenylcarbinolate) were used.

The microemulsions contain cyclohexane or n-heptane as outer phase, nonyl-phenol-poly(n)-glycol ether as nonionic surfactant and 1-octanol as cosurfactant. By variation of the length of the hydrophilic part of the surfactant molecules the diameter of the water droplets could be tuned to values between 8 and 55 nm as determined by dynamic light scattering. The size of the resulting nano-spinels ( $6 \text{ nm} \leq \langle D \rangle_{vol} \leq 33 \text{ nm}$ ) was evaluated from X-ray diffraction peak profile analysis and correlates to the droplet size. Small angle X-ray scattering yields the same particle size like X-ray diffraction, which indicates non-agglomerated particles. The resulting particle size distribution is very narrow.

- [1] H. Herrig und R. Hempelmann, *A Colloidal Approach to Nanometre-Sized Mixed Oxide Ceramic Powders*, Materials Letters 27, 287-292 (1996)
- [2] Ch. Beck, W. Härtl und R. Hempelmann, *Size-Controlled Synthesis of Nanocrystalline BaTiO<sub>3</sub> by a Sol-Gel-Type Hydrolysis in Microemulsion-provided Nanoreactors*, J. Mater. Research (1998), in print

**MECHANOCHEMICAL SYNTHESIS OF  
METAL SULPHIDES NANOPARTICLES**

*Takuya Tsuzuki and Paul G. McCormick*

Special Research Centre for Advanced Mineral and Materials Processing,  
The University of Western Australia, Nedlands, Perth, WA 6907, AUSTRALIA  
[<takuya@mech.uwa.edu.au>](mailto:<takuya@mech.uwa.edu.au>)

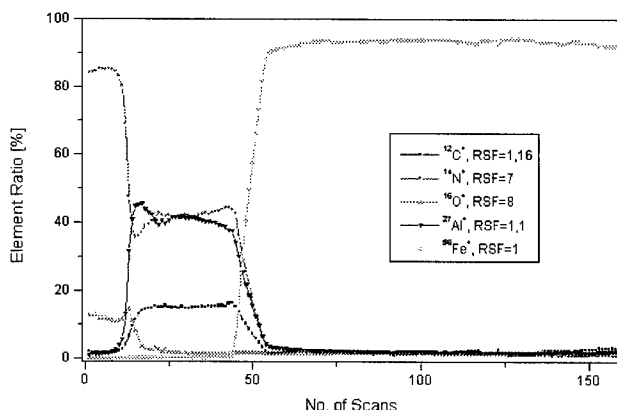
Metal sulphides have been recognised as advanced materials for many applications including phosphors, pigments and magnetic materials. In this study, the synthesis of ZnS, CdS and Ce<sub>2</sub>S<sub>3</sub> nanoparticles by mechanochemical reaction has been investigated using X-ray diffraction, transmission electron microscopy and BET surface area analysis. During mechanical milling, solid-state displacement reactions between the respective metal chloride and alkali sulphide or alkaline earth sulphide were induced in a steady-state manner. The chloride by-products were removed by a simple washing process, leaving ultrafine sulphide powder. When the volume ratio of by-products to sulphide particles was low, large aggregates of nano-crystallites were formed. However, the addition of inert diluent into the starting reactants led to the formation of separated nanoparticles; ZnS, CdS and Ce<sub>2</sub>S<sub>3</sub> nanoparticles of ~7 nm, <8 nm and ~20 nm, respectively, were obtained. The average size of CdS nanoparticles was controlled within the range of 4 to 8 nm by varying the size of the grinding media. The onset energy of optical absorption showed a blue shift with decreasing particle size due to the quantum confinement effect. Those sulphide nanoparticles had cubic structures, and as the particle size increases, they showed structural transformation into thermally stable phases.

**GLOW DISCHARGE MASS SPECTROMETRY (GDMS)**  
**- A POWERFUL TOOL IN THE ANALYSIS OF NANO-SCALED MATERIALS**

*M.Veith,\*<sup>†</sup> K.Bartz, A.Altherr, J. Blin, M. Heintz and F.Pillong*

Institute of Inorganic Chemistry, University of Saarland, D-66041 Saarbrücken, GERMANY

Nano-composite thin layers, prepared by either CVD- or Sol-Gel Processes, are a challenge to conventional analytical methods. In this regard, GDMS is a simple-to-use but powerful analytical tool. In this method a low-pressure Argon-Glow-Discharge with the sample as cathode is used as an ion-source for mass-spectrometric investigations. The surface of the sample is sputtered with argon-ions and sample-atoms are emitted into the glow-discharge, where they are ionised before passing to the quadrupole mass spectrometer. There the ions are separated to obtain a qualitative and quantitative analysis of the sample composition. The technique combines the advantages of a low selectivity difference between many elements with a high dynamic range concerning calibration linearity. As the method continuously produces ion-intensity by burning the sample layer by layer, it is also possible to record depth-profiles. This gives access to information about homogeneity and thickness of thin-film samples. Using GDMS, thin-layers of nitrides, oxides and composites (e.g., metal/metaloxide) deposited on different substrates (e.g., glass, silicon or metals) were analysed to determine composition, homogeneity and layer thickness. We have optimised the method for the analysis of even non-conductive film-materials, by using a secondary-cathode-technique. The technique was applied to nano-sized samples of magnesium aluminium spinel ( $MgAl_2O_4$ ) thin films as well as to layers containing group 13 and 14 nitrides (AlN, SiN). For the first time, nano-composites such as M/ $Al_2O_3$  have also been analysed by this method.



The depth profile of an Al-N-C containing thin film on steel

**FORMATION OF IRON-CONTAINING NANOPARTICLES BY LASER-ASSISTED PHOTOLYTICAL DISSOCIATION OF FERROCENE.**

*Karine Elihn, Frank Otten\*, Mats Boman, F. Einar Kruis\*, Heinz Fissan\* and Jan-Otto Carlsson.*

Inorganic Chemistry, The Ångström laboratory, Box 538, Uppsala University,  
751 21 Uppsala, SWEDEN <karine.elihn@kemi.uu.se>

\*Process and Aerosol Measurement Technology, Gerhard-Mercator University,  
Duisburg, 470 57 Duisburg, GERMANY <frank.otten@uni-duisburg.de>

Laser-assisted formation of iron-containing nanoparticles has been performed by photolytical dissociation of ferrocene vapour by a pulsed ArF excimer laser at 193 nm. Reactions were performed at atmospheric pressure, either in inert gas of argon or in a reactive gas mixture of argon and oxygen. Differential Mobility Analysers, DMA:s, were used for determination of the size distribution. By changing laser parameters like repetition rate (Hz), pulse energy (J) and beam size ( $\text{mm}^2$ ), different particle sizes, ranging from 3 to 100 nm, were generated. Morphology and size of the nanoparticles were studied by Transmission Electron Microscopy, TEM, and structural information was obtained from electron diffraction. Chemical composition was analysed by X-ray Photoelectron Spectroscopy, XPS, and Energy Dispersive X-ray Spectroscopy, EDS.

---

**MAGNETIC ANISOTROPY OF ULTRATHIN Co FILMS AND  
Co-BASED SANDWICH STRUCTURES**

*Akihiro Murayama, Kyoko Hyomi, James Eickmann, and Charles M. Falco*

Optical Sciences Center and Surface Science Division of Arizona Research  
Laboratories, University of Arizona, Tucson, AZ 85721-0077, USA  
<falco@u.arizona.edu>

The fundamental mechanism underlying the phenomena of surface and interface magnetic anisotropy remains an interesting and important unresolved problem in modern magnetism. This strong anisotropy appears at either a free surface or at the interface between two different materials, and for thin film systems it is often the dominant anisotropy energy determining the overall easy-direction of the magnetization. However, the magnetic anisotropy is particularly sensitive to the perfection of interfaces in ultrathin films and multilayer structures, and thus is strongly dependant upon the quality of the deposition process.

For some time we have been studying the magnetic interface anisotropy of MBE-grown multilayers and ultra-thin films. Recently, we have focussed on X/Co/Y sandwich structures, where X and Y are each one of the non-magnetic metals Ag, Au, Cu or Pd. Using *in situ* polar Kerr effect measurements, we reported an anomalous magnetic behavior in the monolayer coverage regime, finding that the magnitude of the perpendicular magnetic anisotropy is strongly peaked at ~1 atomic monolayer (ML) non-magnetic overlayer coverage. Very recently we have succeeded in applying sensitive spinwave Brillouin light scattering techniques to these materials, with *in situ* studies to be underway shortly. As one example of the sensitivity of this technique, we used MBE to grow ultra-thin Co films with thickness in the range 1-7 ML on 1 ML Au-underlayers. For samples as thin as 1 ML of Co we are able to clearly observe spin-wave excitations. We find the magnetic field dependence of the spin-wave energy can be quantitatively explained by a calculation that includes out-of-plane magnetization due to uniaxial perpendicular magnetic anisotropy. Also, with Co thickness 2 ML, we observe significant broadening of the spin-wave spectrum as well as degradation of the perpendicular anisotropy. Although we believe this latter effect is the result of magnetic inhomogeneities due to structural imperfections, future work is planned with an atomic-resolution UHV AFM/STM to observe the structure directly. The physical origin of the thickness dependence of the perpendicular anisotropy in these ultra-thin films and sandwiches will be discussed in this talk.

Research supported in part by U.S. DOE grant DE-FG02-93ER45488.

**STRUCTURE AND PROPERTIES OF NANOSCALE MULTILAYERS**

*Th. Tsakalakos<sup>1</sup>, M. Croft<sup>1</sup>, A. Simopoulos<sup>2</sup>, E. Devlin<sup>2</sup>, A. Jankowski<sup>3</sup> and N. Kioussis<sup>4</sup>*

<sup>1</sup> Rutgers University, Piscataway, NJ 08855-0909, USA

<sup>2</sup> National Center for Scientific Research, Demokritos, GREECE

<sup>3</sup> LLNL, Livermore, CA, USA

<sup>4</sup> California State University, Northridge, CA, USA

The fabrication and use of nanoscale multilayered thin films have generated a great deal of studies worldwide, because of the unusual and often superior properties that they exhibit with respect to their bulk counterparts.

Examples of such systems will be presented which include Fe-fcc high spin magnetic phase in near-monolayer thin films, giant magnetoresistance and magnetostrictive ultra thin films and nanoparticulate composites. The oscillating indirect magnetic coupling and spin dependent transport properties will be reviewed.

Nanomultilayers such as Fe/Au, Fe/Cu and Fe/Pt prepared by magnetron sputtering and characterized by XRD, SQUID magnetometry and Mössbauer spectroscopy will be discussed. In these samples, Hyperfine fields larger than the bulk Fe were observed and displayed an oscillatory dependence on the distance of the corresponding Fe monolayer from the interface.

The parameters determining the enhancement of the magnetization will be discussed in relation with theoretical predictions. Using ab-initio calculations (FLAPN) it will be shown that the valence contribution changes from negative near the interior to positive at the interface. Some applications of Nanomultilayers to exchange coupling recording will be also presented.

---

**ARRAYS OF SUBMICRON MAGNETIC DOTS:  
HYSTERESIS AND FLUX PINNING***Ivan K. Schuller*

Physics Department 0319, University of California-San Diego, La Jolla,  
CA 92093-0319, USA <ischuller@ucsd.edu>

Electron beam lithography is a powerful technique that allows the preparation and control of arrays of small magnetic dots. In this way, we have fabricated, triangular and square lattices, lines etc. of submicrometer magnetic dots (Ni, Co and Fe). We have studied the magnetic and transport properties of these arrays using a variety of techniques including magnetotransport, magnetization, Magnetic Force Microscopy and light scattering.

The interaction between an ordered array of small magnetic particles and a superconducting thin film can lead to important pinning effects due to the synchronized interaction with the vortex lattice. Using electron beam lithography we have fabricated and studied the influence of artificial lattices of small magnetic particles on the superconducting properties of Niobium films.

The resistivity vs. magnetic field curves present sharp minima close to the transition temperature, whereas the transport critical currents exhibit pronounced maxima. These minima and maxima appear at constant field intervals, clearly related with the lattice parameter of the vortex lattice array. The angular dependence reveals that this interval increases with the angle between the field and the film normal showing that only the perpendicular component of the magnetic field is relevant for this synchronized pinning effect. I will describe a series of experiments and comparisons to address many of the aspects of this interesting collective matching phenomenon.

**SIMULATION OF THE MAGNETIC PROPERTIES  
DURING THE NANOSTRUCTURAL GROWTH OF ULTRATHIN FILMS**

*R. Brinznik<sup>1</sup>, P.J. Jensen<sup>2</sup>, and K.H. Bennemann<sup>1</sup>*

<sup>1</sup> Institut für Theoretische Physik, Freie Universität Berlin  
Arnimallee 14, D-14 195 Berlin, GERMANY

<sup>2</sup> Hahn-Meitner Institute, D-14 109 Berlin, GERMANY

The interaction of the atomic and the magnetic structure is especially strong for very thin magnetic films. A small change of the preparation conditions may change the magnetic properties markedly. Due to the recent progress of experimental methods (MFM, SNOM, Kerr-microscope, etc.) the atomic as well as the magnetic structure of surfaces and thin films can be investigated into greater detail. For example, it was found that the domain structure of thin films and its relaxation into the single domain state depends on the direction of magnetization. In this study we have investigated the development of the magnetization and the domain structure in the early states of film growth. We apply a relatively simple growth model ('Erlen-model'). Each atom is added randomly to already existing islands and stays immovable afterwards. This model is valid for a fast surface diffusion and a negligible step diffusion, which is the case for many thin film metal systems at room temperature. We consider the exchange coupling, the uniaxial lattice anisotropy, the dipole coupling, and an applied magnetic field. During the growth each island may change the direction of its magnetization. The magnetic easy axes are possibly separated by energy barriers, which might be surmounted by thermal excitation (Arrhenius type model). These energy barriers are subjected to competing surface and volume interactions, namely the exchange coupling at the edge between neighboring islands, and the magnetic anisotropy and field proportional to the island volume. Generally, an influence of the growth velocity is observed: for small velocities the islands have more time to align themselves and to create larger domains or an uniform state. On the other hand, for a fast growth the islands become too fast too big to overcome the energy barriers, and the resulting domains are expected to be smaller.

Furthermore, we have investigated the effect of the temperature and the lattice anisotropy on the long range magnetization. To simulate experiment, the magnetic film is fully aligned by an applied magnetic field after each growth step. After removal of the field the film starts to relax to its equilibrium state, the remanent magnetization is monitored after a certain time. In the case of a vanishing long range equilibrium magnetization, an increasing anisotropy impedes the relaxation towards equilibrium, resulting in a finite remanent magnetization. In addition, we have calculated the hysteresis loop and the resulting coercive field for different temperatures and anisotropies at different states of film growth. The qualitative behavior of the coercive field agrees with the experimental findings.

**PROPERTIES OF SILICON AND SILICON-CARBON CLUSTER ASSEMBLED FILMS**

*P. Keghelian, P.Melinon and A. Perez*

Département de Physique des Matériaux, Université Claude Bernard Lyon 1,  
69622 Villeurbanne, FRANCE

Since the two past decades, the physics of free clusters and nanostructured materials obtained from cluster deposition opened a large field of potential applications. In this paper we focused on covalent cluster films especially silicon and silicon-carbon compounds. Such materials are prepared using the Low Energy Cluster Beam Deposition Technique (LECBD). In the low energy regime ("soft landing" process), free incident clusters are not fragmented upon impact onto the substrate leading to a film growth by a ballistic process. In some defined conditions, no rearrangement into the clusters or coalescence between adjacent clusters occur, and novel nanostructured phases exhibiting a memory effect of the free cluster properties are obtained. In terms of structure, these materials could be classified in between amorphous and crystalline materials. In terms of properties, they are governed by the intrinsic properties of the nanograins (*i.e.* the supported clusters) and the interaction between adjacent grains.

Pure Si-clusters and Si-C mixed clusters are produced in a laser vaporization source in a wide range of size from a few atoms up to one thousand of atoms, typically. Clusters grow in non-equilibrium conditions allowing the formation of a large collection of isomers (*i.e.* cluster shapes) which are controlled in a time of flight mass spectrometer after photoionization. Neutral clusters are deposited in UHV conditions onto various substrates to form films of about 100 nm thickness which are analyzed by several complementary techniques including electron microscopy observations and Raman, Infrared, Auger and X-Ray photoemission spectroscopies.. In the case of silicon, the existence of five-fold rings in the small size range (<100 atoms per cluster) is evidenced. The presence of odd-membered rings could be justified from the minimization of the surface/volume ratio which strongly decreases the number of dangling bonds at the surface. Because of the so called « frustration effect » which takes place in the odd-membered rings, the electronic properties of our films strongly differ from amorphous, crystalline, or other nano-porous silicon forms. Moreover, a photoluminescence effect in the red is observed in pure silicon cluster films which cannot be correlated to a classical confinement effect. In the case of Si-C mixed cluster deposition, we observe the formation of amorphous SiC films at low temperature ( $T < 300$  K), and the growth process seems independent on the nature of the substrate. Furthermore, a partial chemical ordering is observed. The electronic structure is understood from the competition between the chemical ordering which favors the presence of even-membered rings in the network, the surface reconstruction process which favors the presence of odd-membered rings, and the constraint relaxations within the film which favor the phase separation between carbon and silicon.

**ULTRATHIN DIBLOCK COPOLYMER FILMS:  
A TOOL FOR NANOLITHOGRAPHY**

*Peter Eibeck<sup>1</sup>, Joachim P. Spatz<sup>1</sup>, Martin Möller<sup>1</sup>, Thomas Herzog<sup>2</sup> and Paul Ziemann<sup>2</sup>*

<sup>1</sup>Universität Ulm, Organische Chemie III-Makromolekulare Chemie,  
D-89081 Ulm, GERMANY <peter.eibeck@chemie.uni-ulm.de>

<sup>2</sup>Universität Ulm, Abteilung Festkörperphysik, D-89081 Ulm, GERMANY

Diblock copolymers of polystyrene, PS, and polyvinylpyridine, PVP, were adsorbed on an ionic, high surface energy substrate (mica). The resulting ultra thin films showed spontaneous formation of regular, chemically heterogeneous surface structures consisting of separated polystyrene domains which dewet a strongly adsorbed PVP layer of 1nm height below. So far PS patterns of hexagonally arranged clusters and parallel oriented stripes were observed. The morphology of the PS surface pattern depends on several factors e.g. the blocklength ratio, the grafting density and the chemical nature of the polar block (P2VP or P4VP). The periodicity as well as the size of the PS structures are controlled by the molecular weight of the diblock copolymers. The degree of polymerisation of the PS block determines the number of PS chains per cluster and therefore influences both cluster size and periodicity. In contrast a variation of the PVP block length has only a minor effect and mainly influences the periodicity of the PS structures. The observed range for the PS structure size varies from 30 to 200 nm and the periodicity is within 50 to 400 nm. Decreasing the absolute molecular weight of the dewetting PS block below a certain threshold results in an order to disorder transition of the laterally segregated domains.

In a second step these polymer films are modified by vapour deposition of a metal film (titanium). The growth of titanium occurs preferentially on the less polar polystyrene islands resulting in titanium films with regular thickness variations corresponding to the pattern of the laterally segregated PS-b-PVP film. The treatment of these titanium films with oxygen plasma allows the conversion of Ti into TiO<sub>2</sub> providing a higher sputter resistance against argon ions. Etching the surface by oriented argon ion plasma allows the transfer of the PS/TiO<sub>2</sub> pattern into the substrate with high aspect ratios since the sputtering paths of the PS/TiO<sub>2</sub> domains are greater than the sputtering path between these domains. This procedure easily facilitates the parallel preparation of periodic patterns into an inorganic substrate where the range can be modified from 50 to 400 nm.

1. Spatz, S. Sheiko, M. Möller Adv. Mater. **8**, 513 (1996)
2. Spatz, M. Noeske, J. Behm, M. Pietralla, M. Möller Macromolecules **30**, 3874 (1997)

**STABILITY OF MULTILAYER STRUCTURES: CAPILLARY EFFECTS**

*D. Josell and W.C. Carter*

National Institute of Standards and Technology, Gaithersburg, MD, USA  
<Daniel.Josell@nist.gov>

When multilayer materials are composed of nonreactive, immiscible materials, their long-term stability is related to the equilibrium shapes of the individual grains within the layers. These shapes are, in turn, determined by the free energies of the interfaces within the multilayer (grain boundaries as well as interlayer boundaries) and the dimensions of the grains.

We first summarize experimental techniques that study the creep of multilayer structures to measure the free energies associated with the internal interfaces. All of the techniques utilize the fact that multilayer materials exhibit "zero creep" at nonzero loads: under tensile loads larger than the zero creep load the multilayers stretch, under a tensile load equal to the zero creep load the films are in equilibrium (static), and under loads lighter than the zero creep load the films shrink. For example, silver/nickel multilayers 1 cm wide and less than 25  $\mu\text{m}$  thick [1] steadily (though slowly) lift applied loads of 20 g at 700 °C, while applied loads of 30 g slowly descend, stretching the multilayer. Reduction of the interfacial free energy, the films have 43 layers, is competing with the pull of gravity.

We then present structural models based on thermodynamic equilibrium to predict which structures will be stable against the formation of pinholes at the junctions where grain boundaries meet. Materials properties required by the models include the interfacial free energies, as well as in-plane grain dimensions and grain volumes. These models determine the conditions for structural stability in terms of the biaxial in-plane forces that are associated with equilibrium. In this manner, we link the experimentally measured equilibrating forces, accompanied by grain dimensions obtained using electron microscopy, with the interfacial free energies.

[1] D. Josell and F. Spaepen, *Acta Metallurgica et Materialia* **41**, 3017 (1993).

**EPITAXIAL SILICON NITRIDE THIN FILMS GROWN  
BY PULSED YAG LASER DEPOSITION**

*Y. Suda<sup>1</sup>, K. Ebihara<sup>2</sup>, K. Baba<sup>3</sup>, H. Abe<sup>4</sup> and A. M. Grishin<sup>5</sup>*

<sup>1</sup> Department of Electrical Engineering, Sasebo National College of Technology,  
1-1 Okishin-machi, Sasebo, Nagasaki 857-11, JAPAN  
*<y-suda@post.cc.sasebo.ac.jp>*

<sup>2</sup> Department of Electrical and Computer Engineering, Kumamoto University,  
2-39-1 Kurokami, Kumamoto 860, JAPAN

<sup>3</sup> Technology Center of Nagasaki, 2-1303-8 Ikeda, Omura, Nagasaki 856, JAPAN

<sup>4</sup> Ceramic Research Center of Nagasaki, 605-2 Hasami-cho, Nagasaki 859-37, JAPAN

<sup>5</sup> Department of Condensed Matter Physics, Royal Institute of Technology,  
S-100 44 Stockholm, SWEDEN

Epitaxial silicon nitride (SiN) thin films have been obtained on Si (100) substrates by using a pulsed Nd:YAG laser ( $\bullet = 532$  nm). The laser beam is incident on the  $\text{Si}_3\text{N}_4$  targets. The films are grown using the energy density  $3.8 \text{ J/cm}^2$  at a laser repetition rate of 10 Hz. The nitrogen gas pressure in the chamber is 10.0 Pa. The experiments have been done at different substrate temperatures. The SiN films have been characterized by Fourier transform infrared spectroscopy (FT-IR), energy dispersive spectroscopy (EDS), glancing angle X-ray diffraction (GXRD) and field-emission secondary electron microscopy (FE-SEM). FT-IR absorption spectra show that the peaks near  $900 \text{ cm}^{-1}$  are for the SiN stretching modes and  $460 \text{ cm}^{-1}$  for its breathing modes, respectively. GXRD indicates that the crystalline  $\text{Si}_3\text{N}_4$  thin films are obtained. FE-SEM shows that the film consists of many particles of which sizes are about 200-800 nm.

**ENERGY SHIFT AND DAMPING OF DIPOLE-EXCHANGE SPIN WAVES  
IN ULTRATHIN FERROMAGNETIC FILMS**

*R. N. Costa Filho<sup>1,2</sup> and M. G. Cottam<sup>1</sup>*

<sup>1</sup> Dept. of Physics and Astronomy, University of Western Ontario,  
London, Ontario N6A 3K7, CANADA <mgc@uwovax.uwo.ca>

<sup>2</sup> Dept. de Fisica, Universidade Federal do Ceara, 60455-760 Fortaleza-Ce, BRAZIL

A finite-temperature perturbation formalism is developed to study the processes of spin-wave interactions in ultrathin ferromagnetic films, including the effects of both the long-range magnetic dipole-dipole interactions and the short-range exchange interactions. By contrast with previous macroscopic methods for evaluating spin-wave interactions, the dipolar terms are treated here within a Hamiltonian method, together with exchange and anisotropy terms, to obtain a theory applicable to ultrathin films at temperatures below the Curie temperature. This is accomplished by generalizing a previous perturbation formalism for Heisenberg ferromagnetic films<sup>1</sup> to include a microscopic evaluation of magnetic dipole-dipole sums<sup>2</sup>. The contributions to the energy shift and the damping (or reciprocal lifetime) of the dipole-exchange spin waves due to three-magnon and four magnon processes are calculated. Numerical examples are presented applicable to EuO and to iron.

This research was supported by the agencies NSERC (of Canada) and CAPES (of Brazil).

1. D. Kontos and M.G. Cottam, J. Phys. C **19**, 1189 and 1203 (1986).
2. P. Erickson and D.L. Mills, Phys. Rev. B **43**, 10715 (1991).

**CRYSTALLIZATION AND REACTION BEHAVIOR  
OF NANO-SIZED AMORPHOUS SILICON POWDERS**

*H. Hofmann<sup>1</sup>, R. Houriet<sup>1</sup>, H. Hofmeister<sup>2</sup> and J. Dutta<sup>3</sup>*

<sup>1</sup> Swiss Federal Institute of Technology, Materials Science and Engineering,  
Lausanne, SWITZERLAND

<sup>2</sup> Max Planck Institute of Microstructure Physics, Halle, GERMANY

<sup>3</sup> Balzers AG, Balzers Liechtenstein

Amorphous silicon powders prepared by plasma-enhanced chemical vapor deposition, of 8 - 24 nm sized particles agglomerated into larger aggregates were annealed in a reducing atmosphere to study the phase transformation behavior of these particles. Upon 1h annealing at temperatures between 300 and 600 °C circular contrast features, 1,5 - 2,5 nm in size, are observed in the amorphous particles, hinting to the formation of medium-range order or the formation of clusters. A distinct onset of crystallization is achieved at 700 °C. The particles are covered by a 1 - 2 nm thick amorphous oxide layer, which is found to develop with the onset of crystallization.

The sintering behavior was observed of these powder by heating in the TEM. Si-cluster which are formed during the synthesis as well the first heating step acts as seeds for the crystallisation of polycrystalline particles. Classical sintering theories are insufficient to explain the sintering behaviour but hard core/sinterable coating or model of particle sliding can explain the sintering rate of this powder. Even at 900°C only a sintering of the agglomerates could be observed whereas the macroscopic effect of sintering was negligible.

The reaction behavior, especially the formation of silicon nitride, was studied with and without catalytic additives. Iron, which is well known for his catalytic effect for the formation of silicon nitride from silicon by a gas-solid reaction, was add in different forms. The results show very clearly, that the composition of the iron salt have a strong influence on the reaction kinetic as well as on the amount of crystalline, nanosized silicon nitride powder.

**THREE-DIMENSIONALLY PERIODIC NANOSTRUCTURED FOAMS AND HYBRID MATERIALS FROM OPALS**

*R. H. Baughman<sup>1</sup>, A. A. Zakhidov<sup>1</sup>, C. Cui<sup>1</sup>, I. Khairullin<sup>1</sup>, L. M. Liu<sup>1</sup>,  
Z. Iqbal<sup>1</sup>, S. O. Dantas<sup>2</sup>, and V. G. Ralchenko<sup>3</sup>*

<sup>1</sup> AlliedSignal, Research and Technology, Morristown,  
NJ 07962-102, USA <ray.baughman@alliedsignal.com>

<sup>2</sup> Dept. de Fisica, UFJF, CEP 36036-330, Juiz de Fora, BRAZIL

<sup>3</sup> Russian Academy of Sciences, ul. Vavilova 38, 117942 Moscow, RUSSIA

Double-step and multiple-step templating process is demonstrated for the fabrication of nanostructures materials with cubic superlattice symmetry and lattice parameters at optical wavelengths. Monodispersed nanospheres (such as SiO<sub>2</sub>) are first self-assembled into a face-centered-cubic lattice, and then made mechanically robust by thermal annealing. This lattice serve as the template for obtaining a three-dimensionally periodic assembly of a second material by melt phase, chemical, electrochemical, or vapor phase processes. The SiO<sub>2</sub> balls are then chemically removed, and one or more other materials are optionally infiltrated into the resulting inverse-opal lattice.

We have used this approach to make a variety of materials that Bragg diffract at optical frequencies. By using plasma-assisted chemical deposition to template diamond-seeded opals, novel forms of carbon were produced. These include diamond foams which consist of assemblies of tetrahedrally and octahedrally shaped motifs (with concave sides and maximum dimensions of about 56 nm and 104 nm, respectively, for a templated opal with lattice parameter  $a = 353$  nm).

The same route also produces low density (0.03 gm/cm<sup>3</sup>) periodic foams which are similar to theoretically proposed carbon phases based on the tiling of periodic minimal surfaces. About nine nested layers of graphite in 200 nm multi-wall carbon "onions" (containing small concentration of non-six-fold rings) form substantially continuous three-dimensional surfaces having cubic symmetry. Other inverse-opal lattices that we have made include periodically nanostructured phenolic, phenolic-derived carbon (which remains periodic up to at least 2000 °C), polystyrene, and poly(methyl methacrylate).

We have extended this process to making hybrid structures via multiple templating and filling processes. One such material is a nano-structured cubic phase obtained by the filling of a phenolic inverse opal with polystyrene. Related methods can be used to conveniently fabricate complex electronic devices having device separations of order a hundred nanometers. For example, a plate of inverse opal comprising a redox material can be contacted on one plate side with a metal coating, coated internally with a polymer electrolyte, filled with a second redox polymer from the reverse side, and then contacted on this plate side with a second metal coating. The anticipated result is a battery or super-capacitor that has extremely high rate performance, since it consists of over 10<sup>14</sup> per cm<sup>3</sup> of in-parallel redox devices

### SYNTHESIS AND PROPERTIES OF CERAMIC - POLYMER COMPOSITS

*D. Vollath, D. V. Szabo, and J. Fuchs*

Forschungszentrum Karlsruhe, Institut für Materialforschung III  
P.O. Box 3640, D-76021 Karlsruhe, GERMANY <dieter.vollath@imf.fzk.de>

The microwave plasma process is suitable to synthesize a broad range of oxide, nitride, sulphide, etc. nanomaterials. The particle size of the material can be adjusted in the range from 3 to 20 nm. Most preferable is the range from 5 to 10 nm. Additionally, it is possible to coat these particles with a layer of a second ceramic. This coating is [1]

- to avoid grain growth during sintering,
- to keep active particles at a certain distance minimizing their interaction, and
- to change the surface chemistry of the particles.

In many cases the high strength and temperature stability of a ceramic part are not necessary. In these cases a polymer coating of the ceramic particles is desired. Therefore a process to produce this type of material was developed [2]. The ceramic core of the particles is produced by the microwave plasma process using a precursor evaporating at a relatively low temperature. The reaction temperature can be kept at a temperature less than 150°C. Therefore, it is possible to introduce a vaporized monomer directly after the microwave plasma reaction zone, where the ceramic particles are formed. This monomer condenses on the surface of the ceramic nanoparticles in the gas. Forced by temperature and UV radiation of the plasma properly selected monomers will polymerize. The ceramic particles with the polymer coating are precipitated on cold surfaces. For oxides of the main group elements like Al<sub>2</sub>O<sub>3</sub>, this process works without major problems. It is more difficult with the oxides of the transition elements, such as TiO<sub>2</sub> or Fe<sub>2</sub>O<sub>3</sub> because these oxides may act as catalysts. In these cases the monomers are catalytically dissociated before the polymerisation starts. The most versatile precursors are methacrylic (MA) acid and methylmethacrylate (MMA). In the case of alumina, isobutylmethacrylate (i-BMA) gave excellent results.

The mechanical properties of alumina containing composites pressed at a temperature of 100°C are given in the following table. The mechanical properties were determined at a load of 100 mN.

Polymer	Polymer content	Hardness [Nmm <sup>-2</sup> ]	Young's Modulus [GPa]
PMMA, Standard	100 wt%	230 ± 4	5.01 ± 0.04
PMA	14.1 wt%	424 ± 18	10.01 ± 0.22
Pi-BMA	13.1 wt%	361 ± 30	7.67 ± 1.01

Pressed bodies of γ-Fe<sub>2</sub>O<sub>3</sub> and Cr<sub>2</sub>O<sub>3</sub> with PMA with particle sizes of 5 nm for the oxide are superparamagnetic. In the case of Cr<sub>2</sub>O<sub>3</sub> superparamagnetic behaviour can be observed down to a temperature of 2 K. The electron spin resonance frequencies without external field are above 1 GHz.

[1] D. Vollath, D. V. Szabo, J. HauQelt, J. Europ. Ceram. Soc. 17(1997)1317-1324

[2] [2] D. Vollath, D. V. Szabo, B. Seith, German Patent 196 38 601.2-43 (1997)

**ENCAPSULATED IRON, COBALT, AND NICKEL NANOCRYSTALS:  
EFFECT OF COATING MATERIAL ( $Mg$ ,  $MgF_2$ )  
ON MAGNETIC PROPERTIES**

*Kenneth J. Klabunde, Dajie Zhang, and Christopher Sorensen*

Department of Chemistry and Department of Physics, Kansas State University,  
Manhattan, KS 66506, USA <KENJK@KSU.EDU>

A metal vapor-low temperature matrix method has been employed for the preparation of metastable alloys and intimate mixtures of Mg metal with Fe metal, and  $MgF_2$  with Fe, Co, or Ni metals. Controlled heating caused phase segregation to yield encapsulated Fe, Co, or Ni with Mg or  $MgF_2$  outer coatings. The magnetic metal crystallite sizes could be controlled by the ratio of Mg:M or  $MgF_2$ :M and by the heat treatment temperature/time. The core/shell particles were stable in air, the core ranged in size from 3 to 20 nm.

Detailed magnetic studies (SQUID magnetometry) have revealed interesting particle size effects on saturation magnetization and coercivity. However, the Mg and  $MgF_2$  coatings exhibit different effects, which is especially evident in the temperature dependence of the magnetic moment per Fe, Co, or Ni atom. In the case of  $MgF_2$  coated particles, magnetic moments are depressed most for Ni, then Co, and least for Fe, and are equally depressed as temperature rises. However, for Mg coated Fe, strong temperature dependence is observed with the smaller crystallites, but is much less noticeable with larger (10-20 nm) crystallites. It is evident that the smaller crystallites are significantly altered in their magnetic properties by surface effects, and these surface effects are related to d-shell occupational levels that are dependent on the shell material.

**PRACTICAL APPLICATIONS FOR ELECTRODEPOSITED  
NANOCRYSTALLINE MATERIALS**

*A. Robertson<sup>1</sup>, U. Erb<sup>2</sup> and G. Palumbo<sup>1</sup>*

<sup>1</sup> Microengineered Materials Dept., Ontario Hydro  
800 Kipling Ave, Toronto, M8Z 5S4, CANADA

<sup>2</sup> Dept. Of Metallurgy and Materials Science, University of Toronto  
Toronto, M5S 3E4, CANADA

Electrodeposition provides a cost-effective means of producing fully dense nanocrystalline (10nm-100nm avg. grain size) metals, alloys and metal-matrix composites as coatings or freestanding forms (foil, sheet, wire, complex shapes). The electrosynthesis approach is highly adaptable to conventional industrial material processes, yielding significant material and process improvements from relatively small capital equipment and process modifications. In this presentation, several examples of current and emerging commercial applications for this technology (NanoPlate<sup>TM</sup>) are presented, including (1) the in-situ structural repair of nuclear steam generators (Electrosleeve<sup>TM</sup> process), (2) production of sheet, foil and wire products of nanocrystalline Ni-Fe and Co alloys for high performance ferromagnetic applications (e.g., high efficiency transformers, motors, amplifiers, field sensors etc.), (3) electroforming of high purity nanocrystalline Cu foil for ultra-fine line etchability in high density printed circuit boards (PCB's), and (4) catalytic coatings on battery and fuel cell electrodes.

**PLASTIC DEFORMATION OF PURE SILICON NANOCRYSTALS  
BY MOLECULAR DYNAMICS**

*Masao DOYAMA<sup>1</sup>, Tadatoshi NOZAKI<sup>1</sup>, Yoshiaki KOGURE<sup>1</sup> and  
Tatsuo YOKOTSUKA<sup>2</sup>,*

<sup>1</sup> Teikyo University of Science & Technology, Uenohara,  
Yamanashi 409-0193, JAPAN <doyama@ntu.ac.jp>

<sup>2</sup> Matsushita Research Institute Tokyo, Inc. 3-10-1 Higashimita,  
Tamaku, Kawasaki-City, Kanagawa 214 JAPAN

Micromachining is becoming a quite important process of electronic industries. This paper is the results of high speed deformations of pure silicon nano crystals using the molecular dynamics. The paper suggests that plastic deformation may be possible for the silicon with a high speed deformation even at room temperature. The potential used was three body Stillinger-Weber potential.

The size of a crystal is 6(X) X 16(Y) X 2 (Z)[nm]. x, y and z axes are taken in {110}, {112} and [111] direction, respectively. [110]direction is the cutting direction. (111) is the cutting plane and a slip plane. A sharp vertical solid edge was advanced in the x direction with a speed of 10 m/s. Surfaces are free and periodic boundary condition was not used. The time step interval was  $10^{-16}$  sec. The simulation was extended up to 400,000 steps.

In front of the cutting edge, atoms are pushed up. The chip becomes amorphous. The cut surface is (111) plane and paralleled to the cutting direction. The creation of dislocations was not clearly observed, instead the amorphous region extended on the surface of cutting when the cutting speed was high. At lower cutting speed, the cut surface was not amorphous.

Another nano size single crystal was compressed using molecular dynamic method. The surfaces are (111), (110) and (112). The compressed direction was [111]. It was found that silicon crystals are possible to be compressed with a high speed deformation. This may suggest that silicone may be plastically deformed with high speed deformation. Stress-strain curves were also obtained. The results are compared with those of copper.

At the conference we will report other high speed plastic deformations of nano silicon crystals which are in progress.

### MAGNETISM AT THE NANOSCALE

*P. Jena, S.K. Nayak, B.V. Reddy, S.N. Khanna and B.K. Rao*

Department of Physics, Virginia Commonwealth University  
Richmond, VA 23284-2000, USA <jena@gems.vcu.edu>

Materials at the nanoscale possess many unique structural, electronic, and magnetic properties. This is brought about by their reduced size, unique geometry, low coordination and large surface-to volume ratio. Atomic clusters constitute the ultimate nanostructured materials. The ability of researchers to synthesize and characterize atomic clusters and nanoparticles with precise size and composition has given rise to the possibility that a new class of materials with tailored properties could be made by assembling these particles in ordered arrays. We will provide a brief overview of the salient parameters that govern magnetism at the nanoscale. We will illustrate not only how magnetic moments of clusters of ferromagnetic transition metal elements get enhanced over their bulk value, but also how otherwise paramagnetic and antiferromagnetic systems exhibit ferromagnetism in the cluster phase. Examples will include clusters of V, Mn, Fe, Co, and Ni as well as oxides of Mn and Ni. We will also demonstrate that interaction of clusters and multilayers with hydrogen, nitrogen, and substrate can influence their ambient magnetic order. All our results are based on first principles state-of-the-cart calculations that have predictive capability. It is argued that an in-depth understanding of the evolution of magnetism from clusters to crystals can lead to the synthesis of new nanoscale magnetic materials. This can have potential impact on the technology of the future as man strives to build smaller and faster electronic, magnetic, and optical devices.

**CARBON NANOTUBES-SCIENCE AND APPLICATIONS**

*Peter C. Eklund*

Dept. of Physics & Astronomy Associate Director, Carbon Materials,  
Center for Applied Energy Research University of Kentucky, USA

Single wall carbon nanotubes (SWNT) can be envisioned as a graphene sheet rolled into a very long seamless tube. They shortly will be commercially available in gram quantities. Born in a hot, catalyzed carbon plasma, SWNTs have approximately the same diameter as that of DNA and lengths longer than several microns. On the one hand, they are expected to exhibit unusually high tensile strength and are envisioned as important new additives in polymer composites for aerospace and military applications. On the other hand, they have been found to exhibit one-dimensional quantum confinement effects, coulomb blockade, etc., and they are the current playground for quantum transport physicists. After introductory remarks, and background material, I will discuss recent results from our group dealing with some of the physical properties of pristine and chemically doped SWNTs.

**TEMPLATE SYNTHESIS OF CARBON NANOTUBES**

*G.L. Hornyák<sup>1</sup>, J.J. Schneider<sup>2</sup>, N. Czap<sup>2</sup>, K.M. Jones<sup>1</sup>, F.S. Hasoon<sup>1</sup> and M.J. Heben<sup>1</sup>*

<sup>1</sup>National Renewable Energy Laboratory, 1617 Cole Blvd.,  
Golden, CO 80401, USA <mikeh@nrel.nrel.gov>

<sup>2</sup>Institut für Anorganische Chemie, Universität-GH Essen,  
Universitätsstrasse 5-7, 45117 Essen, GERMANY

Amorphous carbon nanotubes and concentric carbon nanotubes with various degrees of graphitic character have been synthesized via chemical vapor deposition (CVD) methods within the pore channels of anodically formed alumina template membranes.<sup>1-3</sup> The template material consists of parallel hexagonal close-packed pore channels that traverse the thickness of the membrane. Parameters such as pore diameter (< 2 nm to > 500 nm), thickness (< 50 nm to > 500 nm), and pore density (< 10<sup>7</sup> to ca. 10<sup>12</sup> cm<sup>-2</sup>) can be controlled by manipulation of anodize conditions. The dimensions, orientation, and number of carbon nanotubes formed via CVD in alumina membranes adhere to the physical constraints imposed by the host template material. The alumina membranes are solvent resistant (dissolve only in strong acids or bases), optically transparent (> 95% transmission in the visible range), thermally stable (to > 1000°C, undergoing phase changes without compromising the porous structure), and derivatizable (via active surface hydroxyl groups).

Carbon nanotubes were formed by the CVD pyrolytic decomposition of propylene (2.5% in nitrogen) or acetylene (9.0% in nitrogen) gases in a quartz tube furnace at the temperature range from 720°C to higher than 900°C. Nanoparticle catalysts consisting of iron, cobalt or nickel was introduced into the pore channels of the alumina by one of three methods: aqueous incipient wetness impregnation, low-temperature decomposition of organometallic precursor, and ac electro-deposition through the barrier layer of the alumina. The nanoparticles ranged in size from a few nm to about 10 nm in diameter. High temperatures (> 900°C) and the presence of nanocatalysts during synthesis increased the degree of graphitization. Samples were analyzed by x-ray and electron diffraction, Raman spectroscopy, and transmission and scanning electron microscopy. Composite transverse electrical conductivity was determined by several methods.

We are currently exploring the *in situ* synthesis of fullerenes and graphitic nanotubes using the well-defined porous alumina template materials. The objectives, synthetic strategies, and experimental results of research into graphitic nanotube / alumina composite material fabrication for diverse and important applications such as hydrogen storage (for vehicle fuel) intercalation behavior and recyclability with lithium species (battery applications), and selective gas separations, e.g. purification of natural gas are presented.

1. C.R.Martin, Science 266, 1961 (1994).
2. W.Z. Li, S.S.Xie, L.X.Qian, B.H.Chang, B.S.Zhou, R.A.Zhao, G.Wang, *Science* 274, 1701 (1996).
3. T. Kyotani, L-F.Tsai, A. Tomita *Chem. Mater.* 8, 2109 (1996).

### EXPERIMENTAL AND COMPUTATIONAL STUDIES OF HETEROFULLERENES

*I.M.L. Billas, W. Branz, N. Malinowski, F. Tast, M. Heinebrodt, T.P. Martin,  
C. Massobrio\*, M. Boero and M. Parrinello.*

Max-Planck Institut für Festkörperphysik,  
Heisenbergstr. 1, 70569 Stuttgart, GERMANY

\*Institut de Physique et de Chimie des Matériaux de Strasbourg,  
23 rue de Loess, 67037 Strasbourg, FRANCE

Heterofullerenes are obtained by modifying the fullerene geometry by means of a small number of atoms other than carbon. The motivation for doping fullerenes is the possibility of altering their insulating electronic properties and enhancing their chemical reactivity. Particularly fascinating are substitutionally doped fullerenes where one or more carbon atoms of the fullerene cage are replaced by heteroatoms. Several experimental groups have demonstrated the existence of boron-, nitrogen-, silicon-, and niobium-substitutionally doped fullerenes [1-5]. The two principal methods used to fabricate these species comprise laser vaporisation and arc discharge by starting either a) with carbon- or graphite rods doped with some percentage of heteromaterial or b) with pure carbon- or graphite rods in an inert gas atmosphere containing some fraction of gaseous heteromaterial.

Here we report on mass spectrometric evidence of the existence of fullerenes substitutionally doped with an atom of the late transition metals Fe, Co, Ni, Rh and Ir as well as with one or more Si atoms. The heterofullerenes are produced in the gas phase starting with metal-coated C<sub>60</sub> and C<sub>70</sub> molecules. These transform upon irradiation with high laser fluences to heterofullerenes of the composition C<sub>n-1</sub>M, where n=60 and 70 and M= Fe, Co, Ni, Rh, Ir and Si. Furthermore, smaller heterofullerenes of the composition C<sub>59.2k</sub>M (k=0,...10), resp. C<sub>69.2k</sub>M(k=0,...15) are observed with prominence of the heterofullerenes having a total number of atoms equal to 70, 60, 50 and 44, just as observed for pure fullerenes. These observations complemented by detailed photofragmentation studies give strong support to the assumption of the in-cage substitution of the fullerene molecules. Calculations performed within the framework of the *ab-initio* molecular dynamics (MD) method introduced by Car and Parrinello [6] complement our experimental study on these heterofullerenes. In particular, ground state electronic and geometric structures of selected substitutionally doped fullerenes are presented.

- [1] T. Guo, C. Jin and R. E. Smalley, J. Phys. Chem. **95**, 4948 (1991).
- [2] H.-J. Muhr, R. Nesper, B. Schnyder, R. Kötz, Chem. Phys. Lett. **249**, 399 (1996).
- [3] W. Krätschmer, L.D. Lamb, K. Fostiropoulos, D. Huffman, Nature **347**, 354 (1990).
- [4] J.L. Fye, M.F. Jarrold, J. Phys. Chem. **A101**, 1836 (1997); K.B. Shelimov, D.E. Clemmer, M.F. Jarrold, J. Chem. Soc. Dalton Trans., 567 (1997).
- [5] M. Pellarin, C. Ray, P. Melinon, J.L. Vialle, P. Keghelian, A. Perez, M. Broyer, Chem. Phys. Lett. **277**, 96 (1997).
- [6] R. Car and M. Parrinello, Phys. Rev. Lett. **55**, 2471 (1985).

**FORMATION OF CARBON NANOCAPSULES WITH CLUSTERS**

*Takeo Oku, Günter Schmid\*, Koichi Niihara, and Katsuaki Saganuma*

Institute of Scientific and Industrial Research, Osaka University, Mihogaoka 8-1,  
Ibaraki, Osaka 567-0047, JAPAN <Oku@sanken.osaka-u.ac.jp>

\* Institut für Anorganische Chemie, Universität Essen, D-4300 Essen 1, GERMANY

Carbon has various hollow-cage-structures such as C<sub>60</sub>, giant fullerene, nanocapsule, Bucky-onion, nanopolyhedra, cones and nanotubes. Nanoclusters encapsulated with these carbon hollow-cage-structures are intriguing for both scientific researches and future device application. The purpose of the present work is to prepare the carbon nanocapsules with nanoclusters at low temperatures without using the arc discharge method. SiC nanoparticles with polyvinyl alcohol and Pd clusters with carbon support were selected for the nanocapsule formation. To understand the formation mechanism of the nanocapsules, high-resolution electron microscopy (HREM) was carried out for microstructure analysis. These studies will give us a guideline for designing and synthesis of the carbon nanocapsules, which are expected as the future nanoscale devices.

Carbon nanocapsules with SiC nanoparticles were produced by thermal decomposition of polyvinyl alcohol with SiC clusters at 500°C in Ar gas atmosphere. High-resolution electron microscopy also showed the formation of carbon hollow-structure such as nanoparticles, polyhedra, and clusters.

Pd clusters with carbon onions were also produced in an electron microscope by electron irradiation. Under the beam current of 150 pA/cm<sup>2</sup> at 200 kV for 60 min, Pd clusters combined to form Pd nanoparticles with the size of 47 nm, and the amorphous carbon support formed onion-like structure. Pd atoms would be intercalated between the graphite onion sheets.

The present work indicates that the pyrolysis of polymer materials with clusters is a useful fabrication method for the mass-production of carbon nanocapsules at low temperatures compared to the ordinary arc discharge method. It is also believed that the Pd clusters would have effective driving force for the formation of onions by catalytic effect.

### **NATURE OF GRAIN BOUNDARIES IN NANOCRYSTALLINE DIAMOND BY ATOMISTIC SIMULATIONS**

*P. Kebinski<sup>1,2</sup>, D. Wolf<sup>1</sup>, S. R. Phillpot<sup>1</sup>, and H. Gleiter<sup>2</sup>*

<sup>1</sup> Materials Science Division, Argonne National Laboratory, Argonne, IL, USA

<sup>2</sup> Forschungszentrum Karlsruhe, Karlsruhe, GERMANY

Using atomistic simulation we found that most grain boundaries in nanocrystalline diamond are highly disordered and contain up to 80% of the atoms exhibiting local sp<sup>2</sup>-bonding. This is consistent with the results of Raman spectra of nanocrystalline diamond films showing the presence of 1-2% of sp<sup>2</sup>-bonded carbon that can be assigned to the atoms residing at the grain boundaries. We find that despite the large fraction of carbon atoms in the grain boundaries being three coordinated they are poorly connected to each-other, therefore graphite-like electrical conduction through the grain boundaries is unlikely without "bridging" impurities. Surprisingly, based on their fracture energies, the *high-energy*, large-unit-cell boundaries are more stable against brittle decohesion into free surfaces than low-energy ones and perhaps even the perfect crystal.

This work was supported by the U.S. Department of Energy BES-Materials Science under Contract No. W-31-109-Eng-38. P. K. gratefully acknowledges support from the Alexander von Humboldt Foundation.

**SYNTHESIS OF  $\beta$ -SiC NANOWIRES WITH  $\text{SiO}_2$  WRAPPERS**

*G.W. Meng and L.D. Zhang*

Institute of Solid State Physics, Chinese Academy of Science, Hefei 230031, CHINA

Since the discovery of carbon nanotubes in 1991, efforts have been made on the synthesis of one dimensional nanoscale materials because of their potential uses in mesoscopic research and nanostructured composite materials, as well as the development of nanodevices. Up to now, the syntheses of nanoscale one dimensional structures can be mainly divided into two catalogues: (a) synthesis of nanotubes, such as  $\text{WS}_2$ ,  $\text{MoS}_2$ , BN,  $\text{BC}_2\text{N}$ , lipid, tubules-within-a-tubule in MCM-41, peptide and nanotube aggregates of  $\beta$ - and  $\gamma$ -cyclodextrins; (b) synthesis of nanoscale one dimensional solid structures including nanorods, nanowires and nanofibers, such as carbides,  $\text{MgO}$ ,  $\text{GaN}$ ,  $\text{Si}_3\text{N}_4$ , silicon and  $\text{KMn}_8\text{O}_{16}$ .

As far as the synthesis of nanoscale one dimensional solid structures is concerned, a carbon nanotube-confined reaction method is generally used. In this paper we report an alternative approach to synthesising a new kind of one dimensional nanoscale structures  $\beta$ -SiC nanowires with uniform amorphous  $\text{SiO}_2$  wrappers on the outer.

Silica xerogels containing carbon nanoparticles were obtained by sol-gel technique based on the hydrolysis of TEOS and the dissolving of saccharose ( $\text{C}_{11}\text{H}_{22}\text{O}_{11}$ ) in aqueous solution.

$\beta$ -SiC nanowires with uniform amorphous  $\text{SiO}_2$  wrappers were synthesised by the combination of a low temperature ( $1650^\circ\text{C}$ ) carbothermal reduction and a high temperature ( $1800^\circ\text{C}$ ) heating of sol-gel derived silica xerogels containing carbon nanoparticles. The as-synthesised product was characterised by XRD, TEM, HREM, XPS and IR. The nanostructures are more than  $20 \mu\text{m}$  in length. The diameters of the center thinner  $\beta$ -SiC nanowires are typically in the range  $10 \sim 30 \text{ nm}$ , while the outer diameters of the corresponding amorphous  $\text{SiO}_2$  wrappers are between  $20$  and  $70 \text{ nm}$ . The high nucleation density of SiC and the nanometer-sized nucleus sites on carbon nanoparticles are both favourable to the formation of much thinner  $\beta$ -SiC nanowires.

**A NOVEL STRUCTURE OBSERVED IN NANOPARTICLES OF GOLD**

*M. Jose-Yacaman, J.A. Ascencio and M. Perez-Alvarez*

Instituto Nacional de Investigaciones Nucleares, Amsterdam No.46-202, Hipodromo  
Condesa, 06100 Mexico, D. F., MEXICO <yacaman@fenix.ifsicacu.unam.mx>

The structure of nanoparticles of metals has been come increasingly important due to the fact that the single electron tunneling devices, which will be the basis of future nanoelectronics, are based on arrays of such particles. It is well known that small gold particles can show structures with five-fold symmetry such as the decahedron or the icosahedron. In the present paper we report a new structure which is an intermediate between decahedra and icosahedra with appears to correspond to a minimum energy configuration and therefore to an stable structure and is the icosahedral equivalent to Marks decahedra. The particle, as predicted by theoretical calculations, was found experimentally. We show that this particle generates a new family of metallic nanostructures.

**NANOCLUSTERED SILICON-BASED  
ARTIFICIAL DIELECTRICS AND SUPERLATTICES:  
FABRICATION, CHARACTERIZATION AND PHOTOPHYSICS**

*Zafar Iqbal<sup>1</sup>, S. Vijayalakshmi<sup>2</sup>, C.W. White<sup>3</sup>, John C. Federici<sup>4</sup> and  
Haim Grebel<sup>2</sup>*

<sup>1</sup> Research and Technology, AlliedSignal Inc, Morristown, NJ 07962, USA

<sup>2</sup> Optical Waveguide Laboratory and <sup>4</sup> Department of Physics,

New Jersey Institute of Technology, Newark, NJ 07102, USA

<sup>3</sup> Oak Ridge National Laboratory, Oak Ridge, Tennessee 37831, USA

Quantum confinement effects in silicon contain new physics as well as technological applications. In the nanometer-size range three-dimensional quantum confinement increases the band gap and excited electronic states become discrete with high oscillator strength. This could lead to enhancement in band gap luminescence - possibly enough to enable laser or display applications, and the emergence of non-linear optical properties. Silicon nanoclusters have been assembled on quartz in the form of micron-sized droplets using KrF excimer laser ablation to form an artificial dielectric and by ion implantation on ordered superlattices of silica spheres. In addition, disordered superstructures of silicon nanocrystals were formed by electrochemical etching of silicon in hydrofluoric acid-ethanol solution. Detailed characterisation of the crystallinity, cluster size distribution and phonon localisation in the samples were carried out with micro-Raman spectroscopy in combination with scanning and high resolution transmission electron microscopy and atomic force microscopy. Observed Raman lineshapes and frequency shifts have been correlated with cluster size, cluster-cluster interactions and the cluster assembly process, which differs in key aspects from plasma CVD growth of silicon nanocrystals [1]. The linear and non-linear optical responses at 355 nm using the Z-scan technique and at 532 nm using both Z-scan and pump probe methods, and photoluminescence of the silicon clusters in the various samples, have been measured. Nanoclusters that were laser-ablated on quartz showed  $\chi(3)$  values up to  $2.28 \times 10^{-5}$  esu at 355 nm with a lifetime of 143 nm, and a negative value of  $1.33 \times 10^{-3}$  esu at 532 nm with a response time as low as 3.5 ns, limited by the laser pulse duration [2]. The optical non-linearities observed were found to be strongly correlated with the size of the clusters. Mechanisms for the observed non-linearities and photoluminescence are proposed, where the difference between the non-linearity of the laser-ablated clusters and that of the ordered and disordered superlattices are attributed to photoactivated coupling between adjacent clusters.

- [1] S. Veprek, F.-A. Sarott and Z. Iqbal, Phys. Rev. B36, 3344 (1987) and references therein.
- [2] S. Vijayalakshmi, F. Shen and H. Grebel, Appl. Phys. Lett. 71, 3332, (1997) and references therein

**THE NATURE OF FERROELECTRIC ORDER IN FINITE SYSTEMS**

*Pushan Ayyub, Soma Chattopadhyay, K. Sheshadri and Rangan Lahiri*

Tata Institute of Fundamental Research, Homi Bhabha Road,  
Mumbai 400 005, INDIA <pushan@tifrvax.tif.res.in>

Though the experimental study of finite size effects in ferroelectric materials has a long history (which we briefly review), the rapid development of advanced synthetic techniques has now made it possible to study different compounds in the form of phase-pure, ultrafine particles with a narrow size distribution. There is also a strong motivation for studying size-limited ferroelectric systems in view of their current and potential applications as sensors, memory elements, nano-robotic and micro-electromechanical devices. Recent studies on chemically synthesized nanophase ferroelectric<sup>1</sup> and antiferroelectric<sup>2</sup> oxides have shown that a decrease in particle size is accompanied by: (a) monotonic reductions in the Curie temperature ( $T_c$ ) and the ferroelectric distortion of the lattice, (b) a decrease in the peak dielectric constant and a broadening of the dielectric and thermal response peaks. The size-induced diffuse phase transition can be understood in terms of local structural fluctuations from the high-symmetry paraelectric phase.

We have developed a simple theory<sup>3</sup> for structural transitions in quasi-free ferroelectric nanoparticles. In typical "displacive" ferroelectrics, a dipole moment is created in each unit cell - below the  $T_c$  - by the static displacement of the ion at the center of each cell. In our model, the competition, between the elastic energy cost for the displacement of the homopolar ion from a centrosymmetric position and the energy gain due to the ferroelectric ordering of the dipoles formed thereby, leads naturally to a first order transition from the paraelectric to a ferroelectric phase. The transition takes place at a certain temperature  $T_c(L)$  as the temperature is decreased, and at a certain size  $L_c(L)$  as the system size ( $L$ ) is increased. The transition temperature,  $T_c(L)$ , is suppressed as the sample size is reduced, and vanishes for samples below a certain size.

Finally, we discuss the recent observation<sup>4</sup> of an interesting size effect in polycrystalline thin films deposited on semiconducting substrates. When a typically anti-ferroelectric material such as PbZrO<sub>3</sub> or BiNbO<sub>4</sub> is deposited on Si, it displays ferroelectric behavior below a critical film thickness. Since the grain size was found to be roughly proportional to the film thickness, we believe that the ferroelectricity is produced in single domain grains (in the thinner films) due to an intrinsic electric field at the semiconductor-insulator interface,

1. S. Chattopadhyay, P. Ayyub, V.R. Palkar and M.S. Multani, Phys. Rev. B 52, 13177(1995)
2. S. Chattopadhyay, P. Ayyub, V.R. Palkar, A.V. Gurjar, R.M. Wankar and M.S. Multani, J. Phys.: Condensed Matter 9, 8135 (1997).
3. K. Sheshadri, R. Lahiri, P. Ayyub and S. Bhattacharya, Phys. Rev. B (submitted).
4. P. Ayyub, S. Chattopadhyay, R. Pinto and M.S. Multani, Phys. Rev. B (in press),

**HEAVY-FERMION BEHAVIOR IN CeAl<sub>2</sub> NANOPARTICLES***Y.Y. Chen, Y.D. Yao, T.K. Lee and W.C. Liu*

Institute of Physics, Academia Sinica, Taipei, Taiwan

*H.C. Chang, K.Y. Lin and Y.S. Lin*

Department of Physics, Fu-Jen University, Taipei, Taiwan

*Z.C. Wang and W.H. Li*

Department of Physics, National Central University, Taipei, Taiwan

In order to examine the quantum size effects on the heavy-fermion behavior in CeAl<sub>2</sub>, we have performed measurements of the low-temperature specific heats for CeAl<sub>2</sub> nanoparticles with average particle size 80 Å and 120 Å for temperature down to 80 mK and magnetic field up to 4 teslas. For 80 Å - nanoparticles the magnitude of  $\gamma$  of CeAl<sub>2</sub> can be as high as 350 mJ/K<sup>2</sup> f.u. at T = 80 mK with T<sub>K</sub> ≈ 0.4 K. Compared with the sharp anti-ferromagnetic order (T<sub>N</sub> = 3.8 K) in bulk CeAl<sub>2</sub> only a blurred peak at same temperatures is observed in CeAl<sub>2</sub> nanoparticles. The enhanced heavy-fermion (Kondo) behavior and the disappearance of magnetic order in CeAl<sub>2</sub> nanoparticles are closely related to the quantum size effects in nanoparticles. Due to the suppression of the long-range magnetic order by the limited geometric size and the small degeneracy of the density of states of conduction electrons D( $\epsilon_F$ ), the existing heavy-fermion behavior in bulk CeAl<sub>2</sub> is entirely revealed in nanoparticles. Both magnitudes of the entropy integrated from Kondo anomaly and the experimental g are less than theoretical values Rln2 and 1100 mJ/ K<sup>2</sup> f.u. for ground state J =1/2 and Kondo temperature T<sub>K</sub>= 0.4 K respectively. The inconsistency in entropy and  $\gamma$  implies incomplete Kondo interactions or only a partial of Ce ions involved in the heavy-fermion behavior. As compared to T<sub>K</sub> = 5 K in the bulk, the smaller value of T<sub>K</sub> ≈ JD( $\epsilon_F$ ) exp(-1/JD( $\epsilon_F$ )) of nanoparticles is conceptually reasonable since D( $\epsilon_F$ ) is smaller in nanoparticles. A conclusion is made that CeAl<sub>2</sub> can become a very heavy fermion compound if its magnetic order can be properly suppressed by such quantum size effects.

### **OPTICAL PROPERTIES OF SQUARE LATTICES OF GOLD NANOPARTICLES**

*G.A. Niklasson<sup>1</sup>, P.A. Bobbert<sup>2</sup> and H.G. Craighead<sup>3</sup>*

<sup>1</sup> Department of Materials Science, Uppsala University,  
P.O. Box 534, S-75121 Uppsala, SWEDEN

<sup>2</sup> Department of Applied Physics, Eindhoven University of Technology,  
P.O. Box 513, NL-5600 MB Eindhoven, THE NETHERLANDS

<sup>3</sup> Department of Physics, Cornell University, Ithaca, NY 14853, USA

We reanalyse optical measurements on two-dimensional lattices of ultrafine gold particles and demonstrate good agreement between theory and experiments. The samples were produced by electron beam lithography and consisted of 15x15 mm square arrays of gold particles with diameters in the range of 15 to 35 nm and center-to-center spacing of 50 nm. Electron microscopy showed that the particles were flattened in the direction orthogonal to the substrate, with an axial ratio of 1.5±0.2. The optical transmittance was measured in the wavelength range 400-750 nm by a diode array spectrometer. The spectra exhibit a distinct absorption peak due to the localized plasma resonance of the conduction electrons in the particles.

The theoretical modelling used rigorous solutions, in the long-wavelength limit, for the polarizability of oblate spheroids and truncated spheres on a substrate. The dipole-dipole interactions between the particles in the square lattice were also taken into account. We find good agreement between experimental and theoretical absorption peak positions for the case of oblate spheroids, but not for truncated spheres. Peak widths and minimum transmittances also show satisfactory agreement with theory. Previous attempts at reconciling theory and experiments yielded less satisfactory results, because (a) it was not realized that particle sizes were probably overestimated by electron microscopy and (b) only approximate relations for the electron relaxation time were used.

**SYNTHESIS AND CHARACTERIZATION OF SILICON NANOCRYSTALS  
AND INCORPORATION IN POLYMER FILMS**

*Shoutian Li, Igor Germanenko and M. Samy El-Shall*

Department of Chemistry, Virginia Commonwealth University  
Richmond, VA 23284-2006, USA <selshall@gems.vcu.edu>

Weblike aggregates of coalesced Si nanocrystals are produced by laser vaporization - controlled condensation technique. SEM micrographs show particles with ~ 10 nm diameters but the Raman shift suggests the presence of particles as small as ~ 4 nm. The particles show luminescence properties that are similar to those of porous Si and Si nanoparticles produced by other techniques. The nanoparticles do not luminesce unless, by exposure to air, they acquire the  $\text{SiO}_x$  passivated coating. They show a short-lived blue emission characteristic of the  $\text{SiO}_2$  coating and a biexponential longer-lived red emission. The short lifetime component of the red emission, about 12  $\mu\text{s}$ , does not depend on emission wavelength. The longer-lived component has a lifetime that ranges from 90 to over 130  $\mu\text{s}$  (at 300 K), increasing with emission wavelength. Different methods to incorporate the Si nanocrystals in polymeric films of polystyrene and polyvinyl acetate will be discussed. The quenching effect of different organic molecules such as nitrobenzenes and benzonitriles on the photoluminescence of the nanoparticles have been investigated. The quenching effect results in decreasing both the intensity and the lifetime of the red emission. The results suggest an electron transfer mechanism for the photoluminescence quenching. The results from the measurements of the Si nanocrystals will be compared to similar measurements on porous Si.

**OPTICAL PROPERTIES OF METAL NANOPARTICLES:  
ADSORBATE INDUCED MODIFICATIONS***A. Iline, M. Simon, F. Stietz, and F. Träger*Fachbereich Physik, Universität Kassel, Heinrich-Plett Str. 40,  
D-34132 Kassel, GERMANY <stietz@physik.uni-kassel.de>

Research on metal nanoparticles with size dependent optical, chemical and electronic properties is motivated by potential applications which include for example novel optical components or catalytic converters with enhanced performance. For a variety of scientific and practical reasons characterization of reactions between metal particles and adsorbate molecules is of great value.

Here we report studies with the objective to clarify if and how the optical spectra of small metal particles are changed by adsorption reactions on their surface. The goal of this work is to distinguish between the different physical processes contributing to adsorbate induced modifications. Understanding of these effects would open the door to exploit the optical spectra to study chemical interface reactions on their surface and, furthermore, to predict possible variations of their electronic and optical properties caused by adsorption. In our experiments sodium and potassium clusters ( $R = 30 \text{ nm}$ ) grown on quartz substrates served as model systems. Their optical transmission spectra were measured with s- and p-polarized incident light and photon energies ranging from  $E = 1.0$  to  $4.7 \text{ eV}$ . The spectra are dominated by two maxima brought about by the excitation of surface plasmon resonances in the direction of the long and short axis of the oblate particles. The energetic position of the resonances is determined by the shape, i.e. the axial ratio, of the metal clusters. By recording the spectra under ultrahigh vacuum conditions and, subsequently, after exposure to gases like  $\text{O}_2$ ,  $\text{N}_2\text{O}$ ,  $\text{CO}_2$ ,  $\text{H}_2$  or  $\text{N}_2$  changes of the optical spectra can be identified if the clusters are covered by as little as half a molecular monolayer. Depending on the adsorbed molecules different modifications of the maximum position, the width and the amplitude of the surface plasmon resonances are observed. The results of a series of measurements together with calculations performed with the quasi static approximation indicate that the variations allow one to distinguish between physisorption and chemisorption, i.e. to characterize the strength of the chemical bond. In addition, diffusion of molecules into the interior of the clusters and transformation into compound particles can be detected. Particular interesting is the observation that the clusters can experience a change of their shape if gases like  $\text{O}_2$  or  $\text{CO}_2$  react with their surface.

**CORRELATION BETWEEN STRUCTURAL AND OPTICAL PROPERTIES OF  
NANOCRYSTAL PARTICLES PREPARED AT LOW TEMPERATURE BY  
PLASMA-ENHANCED CHEMICAL VAPOR DEPOSITION**

*D. Milovzorov\*, T. Inokuma, Y. Kurata, and S. Hasegawa*

Department of Electronics, Faculty of Technology, Kanazawa University,  
2-40-20 Kodatsuno, Kanazawa 920, JAPAN

<e-mail:demil@ec.t.kanazawa-u.ac.jp>

\* The Institute of Physical and Chemical Research (RIKEN),  
2-1 Hirosawa, Wako, Saitama, 351-01, JAPAN

Silicon nanocrystallites produced by low temperature plasma-enhanced chemical vapor deposition (PECVD) technique have been shown size-dependent photoluminescent (PL) response. For deposition the gas mixture SiF<sub>4</sub>/SiH<sub>4</sub>/H<sub>2</sub> was used. Crystalline volume fraction was characterized by Raman scattering measurements. The average grain sizes of crystallites were estimated by using x-ray diffraction. The structural chemical properties of poly-Si films with nanocrystallites were studied by means of Fourier-transformed infra red spectroscopy. Furthermore, the surface morphology of the films was investigated by means of atomic force microscopy. The PL properties were studied by different deposition conditions: deposition temperature, hydrogen and SiF<sub>4</sub> flow rate. The PL response of poly-Si films is result of the presence of nanocrystallites and quantum-size effect in them. There is strong correlation between size distribution of nanocrystallites and PL characteristics such as PL peak energy, integrated PL intensity and FWHM of PL spectra. Also, the luminescent properties of nanocrystallites depend on hydrogen termination of their surface. We deposited the poly-Si films with controlled size distribution of hydrogenated nanocrystals and sufficient luminescent properties.

**CAN BALL-MILLING YIELD SUPERIOR SOFT MAGNETIC MATERIALS?***A. S. Arrott*

Simon Fraser University, Burnaby, BC, V5A 1S6, CANADA <arrott@sfu.ca>  
Virginia State University, Petersburg, VA 23804, USA

The ideal soft magnetic material would have the highest possible saturation magnetization, zero anisotropy, zero magnetostriction, zero conductivity and be made of something as cheap as iron, which historically costs less per unit weight than potatoes. All of these properties should be insensitive to temperature. Barring the possible emergence of  $\text{Fe}_{16}\text{N}_2$  from the realm of mysteries, Fe(Co) alloys have the highest saturation magnetization, remaining near  $\mu_0\text{M}_s = 2.45 \text{ T}$  from 27 to 52 percent cobalt. The anisotropy constant  $K_1$  changes sign near 50 percent cobalt, the exact composition depending upon the state of atomic order. The effective Curie temperature is well above the ferritic to austenitic phase change near 1260 K. That is the good news. The bad news is that the magnetostriction is very large, greater than  $160 \times 10^{-6}$  near 50 percent Co, the resistivity at ambient temperature is lower than that of iron, and the price of cobalt is high. The obstacle that iron-cobalt alloys are brittle was overcome by metallurgical tricks a long time ago. The commercial alloys Supermendur (Hiperco 50) have a nominal composition of 49 Co and 2 V with some additives that enhance the response to the heat treatment cycles. These alloys are used in aircraft applications with lamination 0.1 mm or less in thickness; V increases the resistivity. The knee of the magnetization curve is above  $\mu_0\text{M}_s = 2.2 \text{ T}$ . The initial challenge to nanotechnology is whether it is possible to reproduce Supermendur starting with ball-milled material with nanocrystalline grain size. The well-established argument is that coercivity goes through a maximum as the grain size becomes comparable to the exchange length  $d_{ex}(A_{ex}/K_1)$ , decreasing toward zero in the limit of amorphous materials. This should remove the restrictions of staying near the composition where the anisotropy changes sign, allowing the move to lower cobalt concentrations, with rapid decrease in magnetostriction, rapid increase in resistivity and lower materials cost. The basic idea of ball milling is to hit the material with a hammer hard enough to produce shear and to hit it often enough to move atoms again before there is much relaxation. It appears that 15 Hz is rapid enough at temperatures below 500 K. As ball milled materials can have as much as 30 percent of the material in the region of the grain boundaries, these are effectively two phase materials. The grain boundaries may have different composition than the grains. Some additives will go preferentially to the boundaries and others to the grains. This can be used to stabilize the nanostructure. The magnetostriction of the grains and the grain boundaries should be different, possibly some compensation could be achieved. That is the hype, what is the reality? This is being investigated both experimentally and theoretically. The experiments use a saucer-and-puck mill to produce kilograms of material. The theoretical challenge is to predict the magnetostriction.

**FULL-DENSITY *in situ* Cu-Fe NANOCOMPOSITES CONSOLIDATED FROM MECHANICALLY ALLOYED SOLID SOLUTION PRECURSORS**

*L. He<sup>1</sup>, L. F. Allard, Jr.<sup>2</sup> and E. Ma<sup>1</sup>*

<sup>1</sup> Department of Mechanical Engineering, Louisiana State University,  
Baton Rouge, LA 70803, USA <memma@me.lsu.edu>

<sup>2</sup> Oak Ridge National Laboratory, P.O. Box 2008, Oak Ridge, TN 37831, USA

A new route has been developed to produce full-density, bulk, two-phase nanocomposites in the Cu<sub>100-x</sub>Fe<sub>x</sub> system across the entire composition range (x = 0 to 100). Nanocrystalline, single-phase, fcc (e.g., Cu<sub>60</sub>Fe<sub>40</sub>) and bcc (e.g., Cu<sub>15</sub>Fe<sub>85</sub>) precursors were obtained by mechanical alloying of Cu and Fe at room temperature or liquid nitrogen temperature. These supersaturated solid solutions were decomposed on nanoscale *in situ* upon hot consolidation, forming Cu-Fe two-phase nanocomposites. Fully dense composite specimens have been obtained using either unconstrained or constrained sinter forging for the entire composition range. The microstructures of the consolidated nanocomposites at representative second-phase volume fractions were characterized using transmission electron microscopy. The Cu and Fe phase domains and their distributions were analyzed using energy dispersive X-ray spectroscopy with a focused electron beam. The average domain/grain sizes of Cu and Fe observed were well below 100 nm, confirming the formation of nanocomposites. Alloying on the atomic scale to ensure uniform mixing of the two elements in the precursor was found to be important for obtaining homogeneous microstructure and nanophase grain/domain size in the consolidated product. The full density nanocomposites exhibit enhanced microhardness as compared with the rule-of-mixtures predictions obtained using nanophase Cu and Fe as constituent phases. This enhancement is explained in terms of additional microstructural strengthening due to interphase boundaries and dislocation structures unique to these fcc-bcc two-phase nanocomposites. Other possible contributions due to solid solution hardening, precipitation hardening, and dispersion hardening are also discussed.

**A STUDY OF Al-Mo ALLOYS SYNTHETIZED  
BY MECHANICAL TREATMENT AND ANNEALED IN-SITU**

*S. Enzo<sup>1</sup>, R. Frattini<sup>2</sup>, P. Canton<sup>3</sup>, G. Mulas<sup>1</sup> and P. Radaelli<sup>4</sup>*

<sup>1</sup> Istituto Nazionale di Fisica della Materia e Dipartimento di Chimica dell'Università di  
Sassari, via Vienna 2, 07100 Sassari, ITALY <enzo@micromat.dipchim.uniss.it>

<sup>2</sup> Istituto Nazionale di Fisica della Materia e Dipartimento di Chimica Fisica dell'  
Università di Venezia, Dorsoduro 2137, 30123 Venezia, ITALY <frattini@unive.it>

<sup>3</sup> Dipartimento di Chimica Fisica dell'Università di Venezia, ITALY  
# ILL B.P. 156, f-38042 Grenoble Cedex 9, FRANCE

There is an interest in material science for the structural characterization of aluminium-based nanocrystalline alloys owing to their enhanced physical, electrocatalytic and mechanical properties. We have previously studied extensively the structural behaviour and thermal stability of Al-Fe alloys, as a function of mechanical alloying (MA) treatment time and of annealing temperature. We have extended the study further replacing Fe with Mo to get more insight into the structural transformation of initial phases and the formation of nanostructured solid solution and/or intermetallic phases. This is because, contrary to the iron case, first, the diffraction peaks of Mo are not superimposed to those of Al and second, the peak broadening due to mechanical damage is expected isotropic for Mo phase. These facts permit a better analysis of size and strain effects. Therefore the structural behaviour of Al<sub>75</sub>Mo<sub>25</sub> alloys, produced by mechanical alloying of pure elemental powders in a SPEX mixer/mill model 8000 was studied as a function of treatment time and in-situ annealing temperature by means of the constant wavelength neutron diffraction instrument D20 at ILL laboratory of Grenoble (France). The diffraction data were analysed with the Rietveld method. A progressive reduction of Al integral intensity was observed as a function of treatment time, suggesting that this element dissolves in the remaining bcc Mo-based phase. However, during the mechanical treatment, the Mo phase does not seem to change the lattice parameter value. In fact, after 78 h of MA, peaks of fcc Al still persist in the pattern dominated by the bcc Mo-based phase. This allows us to note that no single solid solution nor an amorphous phase can be achieved within the experimental parameters employed.

The specimens MA 4 h, 32 h and 78 h were placed in the furnace and subjected to an increasing temperature (the velocity of the ramp varied from 50 to 100°C/h) until 750°C. For the specimen MA 4 h a transformation was observed at about 600 °C, while the data referring to specimen 32 h MA show the presence of two different transformations, the first at about 400°C, the second at about 500°C. Furthermore, the specimen 78 h MA shows just one transformation at a temperature near to 390°C. Concerning the nature of products, after annealing of the specimen milled 4 h mainly the Al<sub>8</sub>Mo<sub>3</sub> phase is present, with a minor quantity of AlMo<sub>3</sub>. The same products seem to precipitate after annealing at 700°C of the specimens 32 h and 78 h MA, though the relative content seems to vary as a function of the treatment time. This confirms that the nature of the transformed phases is related to the quantity of mechanical energy (dose) transferred to the system during the treatment.

**STRUCTURE AND PLASTIC FLOW MECHANISMS  
OF MELT-QUENCHED NANOCRYSTALS***A.M.Glezer*

Institute for Physical Metallurgy, I.P.Bardin State Science Center of Ferrous Metallurgy,  
107005 Moscow, RUSSIA <mogutnov@imph.msk.ru>

It has been reviewed structure, phase transformations (diffusional and martensitic type) and mechanical properties of Fe-based nanocrystalline alloys obtained by melt quenching. Three types of structure states are considered: nanocrystals formed by the complete crystallization of the melt at quenching; nanocrystals formed in the melt quenching with the critical rates which suppress the complete crystallization and nanocrystals formed by primary crystallization of melt-quenched amorphous precursors. In the nanocrystals of the first type significant peculiarities of phase and structural transformations have been observed. As a consequence, the clear tendency to the strengthening and plasticity increase of the alloys is observed. For second type of nanocrystals the melt quenching forms in the amorphous matrix nanocrystallites which have a degree of crystallinity decreasing from the centre to the periphery. This nanocrystalline state leads to a very high strength of nanocrystals. The presence of the amorphous interlayers at certain crystallization stages is typical of the third type of nanocrystals.

The theoretical and experimental study of mechanical properties and plastic flow features in melt-quenched nanocrystals with amorphous intergranular layers has been carried out. It was shown that the yield stress increases linearly with a rise of both the amorphous phase yield stress and the nanocrystal size. The amorphous interlayer sliding mechanism and the triple junction disinclination mechanism of plastic flow of nanocrystals were proposed for explaining the Hall-Petch anomaly.

**MAGNETIC STRUCTURE EVOLUTION IN MECHANICALLY MILLED  
NANOSTRUCTURED ZnFe<sub>2</sub>O<sub>4</sub> PARTICLES**

*J.Z. Jiang<sup>1</sup>, P. Wynn<sup>2</sup>, S. Mørup<sup>1</sup>, T. Okada<sup>3</sup>, and F.J. Berry<sup>2</sup>*

<sup>1</sup>Department of Physics, Building 307, Technical University of Denmark,  
DK-2800 Lyngby, DENMARK

<sup>2</sup> Department of Chemistry, The Open University, Milton Keynes, MK7 6AA, UK.

<sup>3</sup> Magnetic Materials Lab, The Institute of Physical and Chemical Research,  
Riken 351-01 Wako, Saitama, JAPAN

Zinc ferrite (ZnFe<sub>2</sub>O<sub>4</sub>) is usually considered to be a normal spinel structure having zinc cations in the tetrahedral, A, sites and iron cations in the octahedral, B, sites. It is antiferromagnetic with a Néel temperature of approximately 10 K. However, the magnetic structure can be altered by developing a non-equilibrium state with iron cations in the A-sites. This inversion can be achieved by several methods including the sol-gel, quenching, and co-precipitation methods. It seems, however, that the most effective method is high-energy ball milling. Here we report a detailed study of nanometer-sized ZnFe<sub>2</sub>O<sub>4</sub> particles during milling by x-ray diffraction, TEM, and Mössbauer spectroscopy. We observed a magnetic transition temperature above 295 K in ball-milled ZnFe<sub>2</sub>O<sub>4</sub> particles. Especially, the evolution of the magnetic structure, from anti- to ferri-magnetic structures, in milled samples will be discussed on the basis of our low-temperature and in-field Mössbauer measurements.

### CRYOSYNTHESIS AND PROPERTIES OF METAL-ORGANIC NANOMATERIALS

*G.B. Sergeev, A.V. Nemukhin, B.M. Sergeev, T.I. Shabaiina and V.V. Zagorskii*

Department of Chemistry, Moscow State University, 119899 Moscow, RUSSIA  
*<gbs@cryo.chem.msu.su>*

Encapsulation and isolation of nanosize metal particles in solid and liquid organic media and polymers allow us to obtain materials with novel and unique properties. Materials with metal nanoparticles have been obtained by co-condensation of metal and organic compounds at the surfaces cooled at 77 K. The size of particles has been estimated by transmission electron microscopy (TEM).

Codeposition of metal vapours (Ag, Mg, Cd, Zn, Pb, Sm, Mn, etc) with the reactive monomer p-xylylene, which is able to polymerize at low temperatures and thereby to restrict the growth of metal aggregates, has been used. Globular particles of different metals of 5-8 nm size encapsulated in polymer films have been obtained. The new method to encapsulate of mesogenic cyanobiphenyls and metal nanoparticles in polymer matrices using co-condensation of metal, liquid crystal and reactive p-xylylene monomer has been also developed.

By codeposition of metal (Ag, Pb, Zn) vapours with acetone, alcohol's, acrylic acid, methylacrylate different cryoorganic dispersions have been prepared. Bimetallic Ag/Pb cryo organodispersions with particles of 5 nm size also have been obtained.

To predict the properties of the bi-metallic systems the mixed clusters  $M_nM'_m$  ( $M, M' = Ag, Cd, Cu, Mg, Na, Pb, Sm, Sn, Zn, n+m=5$ ) have been computed by using ab initio quantum chemistry techniques. The bimetallic system Ag/Pb have been suggested as one of the most stable. The binding energies and ionization potentials of the clusters have been estimated. The electron spectra of  $Ag_2, Pb_2$  and  $AgPb$  have been evaluated.

UV-Vis, IR-spectroscopy and gas chromatography techniques was used to control the processes of preparing nanomaterials. The method of electric conductivity measuring during the sample condensation has been developed.

Series of chemical transformations in low temperature co-condensates including nanoparticles has been performed. It was shown that the materials possess catalytic and sensor activity.

**Acknowledgements.** The work was partially supported by RFBR grant N 96-0333970a

**ELECTROCHEMISTRY OF NANOCRYSTALLINE COPPER***U. Heim and G. Schwitzgebel*

FB 11.3, Physical Chemistry, Universität des Saarlandes, Postfach 151150,  
D-66041 Saarbrücken, GERMANY <g.schwitzgebel.rz.uni-sb.de>

In a few cases it has been shown that nanocrystalline (nc) electrode materials (e.g.[1]) exhibit, on account of their interfacial energy, a shift of the electrode potential  $\Delta E^{\text{ex}}$  compared with the microcrystalline (mc) electrode. As a good candidate for systematic electrochemical characterisations of the nanostate because of its high exchange current density and its not too low recrystallisation temperature,  $\text{Cu}_{\text{nc}}$  was prepared by inert-gas condensation, pulse electrodeposition and ball-milling, and characterised by XRD (mean grain size  $d$  and its distribution, microstrain). For the electrochemical investigation we used cells, in which the electrodes could be immersed into the aqueous solution (0.1 m  $\text{CuSO}_4$ , 0.05 m  $\text{H}_2\text{SO}_4$ ) by a mere tilting of the cell.

Only under total exclusion of  $\text{O}_2$  the potential of  $\text{Cu}_{\text{mc}}$  could be determined reproducibly ( $-384.5 \pm 0.1$  mV versus  $\text{Hg}/\text{Hg}_2\text{SO}_4$  in the cell solution, at  $25.00^\circ\text{C}$ ). Its potential served for calculating  $\Delta E_{\text{ex}}$  of  $\text{Cu}_{\text{nc}}$  electrodes. The values range from 0.5 mV for  $d = 24$  nm to 12.8 mV for  $d = 8$  nm, and they are inversely proportional to  $d$ , according to a modified Gibbs-Thomson equation, when the deformation energy (from microstrain) is taken into account. The equilibrium concentration of  $\text{Cu}^+$  in the solution, measured with a Pt-electrode, is three times higher in contact with  $\text{Cu}_{\text{nc}}$  than with  $\text{Cu}_{\text{mc}}$ . Therefore, corrosion by  $\text{O}_2$  changes the  $\text{Cu}_{\text{nc}}$  potential less than that of  $\text{Cu}_{\text{mc}}$ . For both electrodes, the kinetics of the corrosion and the potential shifts are in good agreement with a three step mechanism, in which  $\text{Cu}^+$  is oxidised by OH radicals and formed by oxidation of Cu by  $\text{Cu}^{2+}$ .

Very interesting information could be taken from impedance spectra. In corrosion-free solutions the electrode kinetics is dominated by diffusion processes. At slightly corroded surfaces an unusual diffusion type was observed, whose Nyquist plot contained a straight line with a  $25^\circ$  slope, not depending on stirring. This phenomenon could be attributed to diffusion in channels and pores, which were detected in the electrode surfaces by REM.

[1] S. Villain, P. Knauth, G.Schwitzgebel, J. Phys. Chem. B 101 (1997) 7452

**SYNTHESIS AND PROPERTIES OF  
NANOFUNCTIONALIZED PARTICULATE MATERIALS**

*Rajiv K. Singh and James M. Fitz-Gerald*

Department of Materials Science and Engineering  
University of Florida, Gainesville, FL 32611, USA

A wide range of advanced technology based on existing and emerging products such as high temperature metal - ceramic composites used in aircrafts, cutting tools, lithium-ion based rechargeable batteries, superconductors, field emission based flat-panel displays, etc. employ micro to submicron sized (0.1-10 microns) particulate precursors for synthesis and fabrication. Although there has been significant emphasis given to control of the particle characteristics (shape, size, surface chemistry, adsorption, etc.), relatively little or no attention has been paid to designing the desirable properties at the particulate level, which can ultimately lead to enhanced properties of the product. By attaching atomic to nano-sized inorganic, multi-elemental clusters either in discrete or continuous form onto the surface of the core particles, i.e. nano-functionalization of the particulate surface, materials and products with significantly enhanced properties can be obtained. In this paper, we demonstrate for the first time the synthesis of artificially structured, nano-functionalized particulate materials with unique optical, cathodoluminescent, superconducting and magnetic properties. This paper will also talk about this class of particulate materials for various applications and the methods to characterize nano-functionalized materials will also be discussed.

The authors gratefully acknowledge funding for this research by the Engineering Research Center for Particle Science and Technology at the University of Florida under NSF grant No. 94-02989.

**HIGH-MECHANICAL STRENGTH OF BULK NANOSTRUCTURE ALLOYS  
CONSISTING OF COMPOUND AND AMORPHOUS PHASES***Akihisa Inoue*

Institute for Materials Research, Tohoku University, Sendai 980-8577, JAPAN

The dispersion of nanoscale metallic particles into an amorphous matrix has been found to cause an increase in tensile fracture strength ( $s_f$ ) in the maintenance of good ductility. However, the improvement of  $s_f$  had been limited to melt-spun ribbons. There had been no data on the formation and high  $s_f$  of nanostructure alloys in a bulk form. Recently, bulk amorphous alloys with thickness of 1 to 8 mm were produced in Mg-, lanthanide-, Zr-, Fe-, Pd- and Co-based systems. The use of the bulk amorphous alloys is expected to enable the synthesis of bulk nanostructure alloys with good mechanical properties. We have found that the addition of Ag, Pd, Au or Pt, leading to the increase in the degree of structural inhomogeneity for the Zr-based amorphous alloys, is effective for formation of a nanostructure consisting of nanoscale compound particles embedded in an amorphous matrix by annealing in the supercooled liquid region. The nanostructure alloys keep good ductility at volume fractions up to 70 % for the ribbon and 30 % for the bulk cylinder of 3 mm in diameter and the  $s_f$  increases by 15 to 25 %. The formation of the nanostructure is due to the ease of nucleation of a crystalline phase and the difficulty of growth reaction by the enrichment of Al in the amorphous phase. The maintenance of the good ductility leading to the high  $s_f$  is due to the reentrance of a number of free volumes by water quenching from the annealing temperature. The synthesis of the nanostructure alloys with good mechanical properties is promising for future development of a new type of high-strength materials.

**MICROSTRUCTURAL REFINEMENT AND MECHANICAL PROPERTY  
IMPROVEMENT OF COPPER AND COPPER-Al<sub>2</sub>O<sub>3</sub> SPECIMENS  
PROCESSED BY EQUAL CHANNEL ANGULAR EXTRUSION (ECAE)**

*Shankar M.L. Sastry, William Klein and Mark Favre*

Washington University, Campus Box 1185, One Brookings Drive,  
St. Louis, MO 63130, USA <smls@mecf.wustl.edu>

Equal Channel Angular Extrusion (ECAE) extrusion is a proven method for producing large strains in materials which in turn can be used to produce strain hardening, fine grain strengthening, grain size control, and high temperature superplasticity. In the present investigation, pure copper and copper alloys containing different volume fractions of nanosize Al<sub>2</sub>O<sub>3</sub> dispersoids were processed by ECAE at 25-250°C, annealed at 25-500°C, and microstructural refinement and mechanical property improvement were studied. In samples processed by ECAE to strains of 5, hardness values increased by 100% in copper specimens and 40-50% in Cu-Al<sub>2</sub>O<sub>3</sub> specimens. A drastic increase in hardness was observed after a strain of 1, and hardness values levelled off beyond a strain of 2. Samples were annealed at 25-500°C, to determine the extent of recovery of hardness values. In CAE processed copper samples, significant reduction in hardness occurs between 100-200°C, and higher temperature annealing results in hardness values close to the values before ECAE processing. However, in Cu-Al<sub>2</sub>O<sub>3</sub> specimens, the increased hardness is maintained in samples annealed at 500°C. Strength and ductility values determined from 3 point bend tests showed strength values of 150-200 MPa for copper and 650-800 MPa for Cu-Al<sub>2</sub>O<sub>3</sub> samples with excellent ductility in copper as well as Cu-Al<sub>2</sub>O<sub>3</sub> samples. The observed results were analyzed in terms of the magnitudes of strengthening contributions from dislocation substructure, fine grains, and incoherent dispersoids.

**MECHANICAL PROPERTIES OF HIGH DENSITY NANOCRYSTALLINE  
GOLD PREPARED BY GAS DEPOSITION METHOD**

*S. Sakai, H. Tanimoto\* and H. Mizubayashi*

Institute of Materials Science, University of Tsukuba,  
Tsukuba, Ibaraki 305, JAPAN <sakai@mat.ims.tsukuba.ac.jp>

\*Now at : Universität Stuttgart, Institut für Theoretische und Angewandte  
Physik, Pfaffenwaldring 57, 70550 Stuttgart, GERMANY

The atomic structure in the grain boundary (GB) regions in nanocrystalline (n-) materials may, in general, differ much from those found in conventional polycrystalline materials, and a volume fraction of the GB regions increases with decreasing grain size. Thus the properties of n-materials are expected to reflect those of the GB regions. In n-materials, the mechanical property may be sensitive to that of the GB regions as well as grain size. However, the present knowledge on the mechanical property of n-materials is very limited, because the inherent mechanical property can be spoiled by pores and flaws contained in n-material specimens as well as the contamination of the GB regions. The gas deposition method (GDM) for the preparation of n-materials has an advantage to minimize the defects and the contamination. We prepared the high-quality n-gold specimens by means of the GDM, where the density of the n-gold specimens was about 98 % of the theoretical density, and the thermal desorption spectra measured in a high vacuum indicated no detectable desorption of gas atoms (molecules) from the specimens. The average-grain-size of the present n-gold specimens is in the range between 20 and 60 nm. We carried out the tensile tests as well as the vibrating reed measurements. In the tensile test at 300 K, the n-gold specimens show a fracture strain of 1.5 – 3 %, and the yield stress and the tensile strength are about three times higher than those found in annealed conventional coarse-grained gold specimens (cg-gold specimen, hereafter). At 77K, the n-gold specimens show the tensile strength as high as about five times of that in the cg-gold specimens and then fail at a strain less than 1 % exhibiting no yielding. The Young's modulus evaluated from the linear elasticity found in a low strain range in tensile tests is higher than 90 % of that reported for a cg-gold specimen in the temperature range between 77 and 200 K. At higher temperature, the Young's modulus shows a decrease due to the increasing anelastic strain with elevating temperature, e.g., the Young's modulus of the n-gold specimens decreases to about 85 % of that reported in a cg-gold specimen at 300 K. The observed results of the vibrating reed measurements show good agreement with those found in the tensile tests. The Young's modulus found at low temperatures in the present high-quality n-gold specimens suggests that the Young's modulus in the GB-regions is not much lower than the bulk value. The results of creep and internal friction will be given too.

---

**PHYSICAL PROPERTIES AND STRUCTURE  
OF NANOSTRUCTURED HIGH-MELTING POINT COMPOUNDS**

*R.A. Andrievski*

Institute for New Chemical Problems, Russian Academy of Sciences  
Chernogolovka, Moscow Region 142432, RUSSIA <ara@incp.ac.ru>

High-melting point compounds (HMPC) are carbides, borides, nitrides, oxides and other compounds with the melting point above 2000°C. These compounds such as TiC, TiN, TiB<sub>2</sub>, WC, AlN, Al<sub>2</sub>O<sub>3</sub>, SiC, Si<sub>3</sub>N<sub>4</sub>, ZrO<sub>2</sub>, CeO<sub>2</sub> and some others may be described as advanced ceramics and their promising properties and wide application are well known. Clearly there is the interest to HMPC in the nanocrystalline (nc) state. In this paper, we have attempted to review the progress in our knowledge of physical properties of nanostructured HMPC.

The main preparation methods of nanostructured materials (NM) such as powder technology, controlled crystallization from amorphous state, severe plastic deformation and film/coating technology are considered in brief. Regarding to HMPC only powder technology and film/coating one seem to be the more important. In this connection the structure features of NM produced by these methods are discussed and classified.

Hardness, fracture toughness, electrical, optical and some other physical properties of NM based on HMPC are generalized and discussed in detail. The special attention is also taken to the structure, porosity, and composition features of these subjects. We emphasize that in the case of nc metals (copper, palladium, silver, titanium, etc.) the hardness increased on average, by four to six times, as a result of the transition to the nc state. However, in the case of HMPC both in the particulate form and filmy one such increase is not so large and equal to only two times. The nature of such difference is to be further clarified and it is desirable to study the availability of Hall-Petch-like behaviour for nc HMPC in the wide range of the grain size. The effect of porosity, stoichiometry, and admixtures on both hardness and other physical-mechanical properties are also considered.

Attention has been also focused on both bulk and surface physical-mechanical properties of nanostructured films. Interpretation of their properties must be based not only on conventional examination by TEM, SAED, and XRD to estimate the phase composition and crystallites sizes but also on characterization by AES, XPS, and AFM to state deviations from the stoichiometry, reveal the availability of structural vacancies, and study topography and composition features of surface layers. The importance of such investigations is illustrated on the results of nanoindentation test.

Two types of nanostructured films fracture under Vickers indentor connected with homogeneous and inhomogeneous deformation have been described.

**FINE STRUCTURE OF NANOSTRUCTURED SPOTS CRYSTALLIZED IN  
THIN AMORPHOUS IRON OXIDE FILMS BY AN ELECTRON BEAM**

*V.Yu.Kolosov\* and A.R.Thölén*

Dept. of Experimental Physics, Chalmers University of Technology  
412 96 Göteborg, SWEDEN <tholen@fy.chalmers.se>

\*Ural State Economic University, 8 March St. 62,  
Ekaterinburg 620219, RUSSIA <postmaster@uinh.rcipi.e-burg.su>

Laser and electron beam annealing are powerful methods for locally modifying and crystallizing thin amorphous films, and the obtained structures are also interesting for information storage. The structures produced can carry unusual features and this paper reports on the fine structure of spots crystallized in amorphous iron oxide films. Thin films (~ 40 - 50 nm) prepared by pyrolysis and separated from the substrate were studied mainly using the bend contour technique and high resolution electron microscopy in a Philips CM200 FEG. Crystallization initiated by electron beam focusing can be stopped or resumed at any moment by change of the beam intensity in the electron microscope, thus different circled areas ranging in diameter from 1 - 50  $\mu\text{m}$  can be produced. As reported earlier [1] thin crystallized areas often resemble a target board having regularly alternating annular zones of different lattice orientation and imperfection with a width of about 1  $\mu\text{m}$ . The main structural feature is a strong (up to 100°/ $\mu\text{m}$ ) permanent internal rotation of the lattice orientation round the axes lying in the film plane.

These crystallised spots correspond in some features to spherulites but have a much more complicated texture with no radially elongated grains and they do not follow the traditional scheme of spherulite formation. Actually the change from perfect single-crystalline zones with a [001] normal to imperfect fine-grained zones with a [100] normal is gradual. Owing to the presence of numerous bend contours conical dark field images made it possible to visualize the grain boundaries (more than one thousand for a crystallised spot of middle size) in the imperfect zones. Graphs have been produced on the distribution of the length of grain boundaries and the width of crescent-like and ribbon-like grains.

Qualitatively the influence of grain boundary origin, number and nonequiaxial features upon change in lattice orientation is clear. Because of the anisotropy of the elastic properties, for some lattice orientations large deformations (caused by the action of internal lattice bending) exceed the elastic limit and plastic deformation with grain boundary formation starts. High resolution electron microscopy studies of the grain boundaries support this idea.

This work is partially supported by RSAS grant 1557 and RFBR grant 97-02-17784

1. Kolosov V.Yu. and Thölén A.R., *NanoStructured Materials*, **9**, 323 (1997).

**CHARACTERIZATION OF COMPOSITE AEROGELS  
BY CONTRAST-MATCHED SMALL-ANGLE NEUTRON SCATTERING**

*C.I. Merzbacher<sup>1</sup>, J.G. Barker<sup>2</sup>, M.L. Anderson<sup>3</sup>, J.W. Long<sup>3</sup> and D.R. Rolison<sup>3</sup>*

<sup>1</sup> Optical Sciences Division, Naval Research Laboratory,  
Washington, DC 20375, USA <merzbacher@nrl.navy.mil>

<sup>2</sup> Center for Neutron Research, NIST, Gaithersburg, MD 20899, USA

<sup>3</sup> Chemistry Division, Naval Research Laboratory, Washington, DC 20375, USA

Contrast-matched small-angle neutron scattering (SANS) has been used to characterize various aerogels consisting of two solid phases. Aerogels are a class of nanostructured materials with extremely low densities, high porosities and high surface areas. They are typically prepared by synthesizing a sol-gel with a large liquid fraction and then removing the liquid from the pores under supercritical conditions to prevent pore collapse. By filling the pores that are probed by SANS (2 nm – 100 nm) with a D<sub>2</sub>O+H<sub>2</sub>O mixture that matches the neutron scattering length density of one phase, it is possible to observe scattering solely from the second phase. The structure of each solid phase can thereby be independently determined.

We used contrast-matched SANS to investigate metal oxides deposited on the surfaces of silica aerogel. Ruthenium oxide/silica composite aerogels were formed by either vapor-phase deposition of ruthenocene or impregnation from a Ru(III)acetylacetone acetone solution, followed by oxidation in air at 400°C. Iron oxide/silica composites were formed by vapor-phase infiltration of ferrocene, reduction at 400°C and exposure to ambient air. The deposited ruthenium oxide forms particles several tens of nanometers in diameter, whereas the iron oxide conforms to the morphology of the silica aerogel support. The variation in structure of the deposited oxides may arise from the differences in post-depositional treatment.

Contrast-matched SANS has also been used to study composites of silica aerogel and gold colloids which range from 5 nm to 100 nm in diameter. The gold colloidal sol was mixed with the silica sol, prior to gelation. The structure of the two phases in the aerogel can be readily isolated by the contrast-matching technique. These data are used to gauge the location of colloidal gold in the silica network.

This work was supported in part by ONR, DARPA and the NSF under Agreement No. DMR-943101.

**Fe DIFFUSION IN NANOCRYSTALLINE ALLOYS AND THE INFLUENCE  
OF AMORPHOUS INTERCRYSTALLINE LAYERS**

R. Wiirschum<sup>1</sup>, T. Michel<sup>1</sup>, P. Scharwaechter<sup>2</sup>, W. Frank<sup>2</sup> and H.-E. Schaefer<sup>1</sup>

<sup>1</sup>Institut für Theoretische und Angewandte Physik, Universität Stuttgart,  
70550 Stuttgart, GERMANY

<sup>2</sup> Max-Planck-Institut für Metallforschung, Heisenbergstr. 1,  
70569 Stuttgart, GERMANY

Atomic transport in nanocrystalline solids represents a key issue since it controls both the physical properties, as e.g. plasticity, and the structural stability of these materials. On the other hand, tracer diffusion may serve as highly structure-sensitive probe of interfaces. According to recent studies the diffusion in relaxed interfaces of nanocrystalline pure metals is similarly fast as in conventional grain boundaries [1].

The present work aims at <sup>59</sup>Fe tracer diffusion studies of crystallization-prepared nanocrystalline alloys, the interfaces of which differ from those in pure metals due to amorphous intercrystalline layers. The Fe self-diffusivity in the interfaces of nanocrystalline Fe<sub>73.5</sub>Si<sub>13.5</sub>B<sub>9</sub>Nb<sub>3</sub>Cu<sub>1</sub> (Finemet) is much lower than in nanocrystalline pure metals. This arises from an intergranular amorphous phase and densely packed interfaces between these interlayers and the DO<sub>3</sub>-Fe<sub>80</sub>Si<sub>20</sub> nanocrystallites of the Finemet alloy. The Fe self-diffusivity increases upon transition from the amorphous to the nanocrystalline state due to a rapid vacancy-mediated self-diffusion in the DO<sub>3</sub>-Fe<sub>80</sub>Si<sub>20</sub> nanocrystallites [2]. In nanocrystalline Fe<sub>90</sub>Zr<sub>10</sub>, on the other hand, where self-diffusion in nanocrystallites is negligible, the diffusivity decreases upon the amorphous-to-nanocrystalline transition. Analyses of the <sup>59</sup>Fe-penetration profiles indicate the existence of different types of interfaces with a low diffusion in interfaces with amorphous interlayers and fast diffusion paths as characteristic of conventional grain boundaries. On the basis of these studies and earlier results obtained from positron annihilation and hydrogen-site spectroscopy the interfacial structure of nanocrystalline Fe<sub>90</sub>Zr<sub>10</sub> is discussed.

[1] R. Wiirschum, K. Reimann, S. GruB, A. Käßler, P. Scharwaechter, W. Frank, O. Kruse, H.-D. Carstanjen, and H.-E. Schaefer, Phil. Mag. B 76, 407 (1997).

[2] R. Wiirschum, P. Farber, R. Dittmar, P. Scharwaechter, W. Frank, and H.E.Schaefer, Phys. Rev. Letters 79, 4918 (1997).

**EXPERIMENTAL EVIDENCES OF LATTICE DISTORTION  
IN NANOCRYSTALLINE MATERIALS***K. Lu*

State Key Laboratory for Rapidly Solidified Non-equilibrium Alloys (RSA)  
Institute of Metal Research, Chinese Academy of Sciences, Shenyang, CHINA  
<kelu@imr.ac.cn>

The property enhancements in nanocrystalline (nc) materials are frequently attributed to either the numerous amount of grain boundaries or the specific grain boundary structure that was claimed to differ fundamentally from that of the conventional grain boundary. While many structure investigations on the nc grain boundary structure yield rather controversial results, the structure characteristics of the nm-sized crystallites, which still constitute a major part of nc materials, has seldom received attention.

In recent years, a series of experimental investigations have been carried out on the microstructure and properties of the nm-sized crystallites in nc materials. It shows that the lattice structure parameters in nc materials differ evidently from those in their conventional coarse-grained polycrystalline counterparts. In this work, experimental evidences of the lattice distortion in nc samples will be summarized and discussed with an emphasis on nc Se and Cu samples processed by means of different techniques. Quantitative x-ray diffraction analysis indicated that for the nc samples the unit cell is dilated with an enhanced static Debye-Waller parameter and a depressed Debye temperature. The thermal expansion behavior of the nc lattice is much altered relative to the conventional polycrystals. These structure parameters are found to be sensitive to grain size and the sample processing procedures. The observed lattice distortion may contribute significantly to the property changes in nc materials. In other words, the property enhancement of nc materials should be attributed not only to the numerous non-equilibrium grain boundaries, but to the distorted crystallites as well.

**POSITRON ANNIHILATION STUDY OF NANOCRYSTALLINE IRON.**

*D. Segers<sup>1</sup>, S. Van Petteghem<sup>1</sup>, J. F. Löffler<sup>2</sup>, H. Van Swygenhoven<sup>2</sup>, W. Wagner<sup>2</sup> and  
C. Dauwe<sup>1</sup>,*

<sup>1</sup>RUG, Department of Subatomic and Radiation Physics, NUMAT,  
Proeftuinstraat 86, B-9000 Gent, BELGIUM

<sup>2</sup>Paul Scherrer Institute, CH-5232 Villigen PSI, SWITZERLAND

Positron annihilation lifetime measurements are performed on different nanocrystalline iron samples synthesised by the inert-gas condensation technique. The differences in free volume distribution are studied in terms of compaction parameters and annealing treatments after compaction. The mean grain size of the samples is measured by X-ray diffraction and Small Angle Neutron Scattering. The grain boundary structure is studied in the electron microscope.

The lifetime spectra are first analysed in terms of three discrete components. A short lifetime is measured in the range of 160 to 190 ps indicating the presence of atomic interfacial free volume in the order of a mono-vacancy. In all samples a microvoid lifetime ranging from 370 up to 450 ps with intensities from 16 to 45% is observed. These microvoids are located at the intersection of several interfaces. A long lifetime in the nanosecond range is also present in all the samples. This component is due to the formation of ortho-positronium in larger free volumes, probably of the size of a missing grain.

When the grain size is of the order of 100 nm or more a fourth lifetime is observed. This very short lifetime (smaller than the free lifetime of pure iron) is in agreement with the trapping model. This indicates that the positron diffusion length is of the order of 100 nm.

High statistical measurements are in progress, in order to analyse the data with lifetime distributions instead of discrete lifetime components as discussed above.

**METALLIC NANOWIRES: THEORY AND EXPERIMENTS***N. García*

Laboratorio de Física de Sistemas Pequeños y Nanotecnología  
Consejo Superior de Investigaciones Científicas, Serrano 144, Madrid 28006, SPAIN

Metallic nanowires or nanocontacts have been a field of large activity recently. The reason is that this object of nanometric size present quantum effects in the conductivity because the Fermi wavelength is of the order of 1 nm. The conductance behaves step-like with jumps of the quantum of conductance. This phenomena can be observed at room temperature due to the fact that the energy levels at the contact are separated by eV and therefore the smeared out due to temperature is small.

In this presentation we will discuss:

- 1) the production and realization of the nanowires,
- 2) electrical properties (conductance and IV characteristics),
- 3) mechanical and thermal properties,
- 4) microscopy and visualization of the nanowires and
- 5) the realization of the first nano-optoelectronic-transistor gated by LASER illumination of the nanowire.

**NANOIMPRINT LITHOGRAPHY  
--A NEW LOW-COST HIGH-THROUGHPUT SUB-10-NM LITHOGRAPHY**

*Stephen Y. Chou, Wei Zhang, Lei Zhuang, and Lingjie Guo*

NanoStructure Laboratory, Department of Electrical Engineering  
Princeton University, Princeton, NJ 08544, USA

Nanoimprint lithography (NIL), a new breakthrough in nanopatterning, is presented [1]. NIL patterns a resist by deforming the resist shape through embossing (with a mold), rather than by altering resist chemical structure through radiation (with particle beams). NIL can pattern sub-10 nm features over a large area with high throughput and low cost—a feat that might be impossible with current conventional lithography. Presently, we have achieved 10 nm diameter holes of 40 nm pitch in PMMA cast on either semiconductor or metal substrates with an excellent uniformity over an area of 1 square-inch. We have investigated other aspects of NIL, such as ultimate resolution, maximum imprint area, uniformity, mold durability, process repeatability, non-flat surfaces, and alignment. Furthermore, we have fabricated silicon quantum dot, wire, and ring transistors using NIL and observed the same device performances as those fabricated using e-beam lithography. Finally, we will discuss the challenges for future development of NIL.

[1] S.Y. Chou, P.R. Krauss, and P.J. Renstrom, *Appl. Phys. Lett.*, 67, 3114 (1995), and *Science*, Vol. 272, 85-87 (1996).

**MAGNETIC NANOPARTICLES , HENKEL PLOTS , AND PREISACH MODELS: INTERACTIONS AND DYNAMICS***R.M. Roshko, P.D. Mitchler*

Dept. of Physics, University of Manitoba, Winnipeg, Manitoba, R3T 2N2, CANADA

*E. Wesseling, and E. Dan Dahlberg*School of Physics and Astronomy, University of Minnesota,  
Minneapolis, MN 55455, USA

Through the history of magnetic nanoparticle research, workers have made magnetic measurements on collections of particles to understand the magnetic properties of individual particles. Interactions between the particles are seldom, if ever, taken into consideration in the interpretation of the results. However interactions are often important and may dominate hysteresis loop measurements, dynamics studies such as done on collections of nanoparticles in macroscopic quantum tunneling investigations and so forth. In part, this ignoring of interactions and their effects arises from the difficulty of even determining their presence. In a series of papers, summarized in this talk, we have used Henkel plots, parametric plots of the demagnetizing remanence vs. the magnetizing remanence in concert with Preisach modeling to determine the presence, magnitude, and effects of interparticle interactions and have developed a model for the dynamics which focuses on the effects of the interactions. Although Henkel plots have been previously criticized because the zero magnetization state was not statistical in nature, much of our work focused on systems which could be thermally demagnetized, thereby obtaining a truly statistically randomized state. The systems investigated include CrO<sub>2</sub> recording tape, spin glasses (Ag and Cu:Mn), CoCr, and magnetoferitin. The broad range of systems studied in this investigation have provided a sufficient range in physical parameters that a rather general picture of the effects of interactions have been determined. This includes the effects of interactions on both magnetization measurements and dynamics. These results impact and can be used by researchers studying particulate systems for fundamental physics, magnetic recording technology, and MQT.

**COLLECTIVE GLASS STATE IN MAGNETIC NANOPARTICLES SYSTEMS**

*J.L. Dormann<sup>1</sup>, D. Fiorani<sup>2</sup>, R. Cherkaoui<sup>1</sup>, L. Spinu<sup>1</sup>, F. Lucari<sup>3</sup>, F. D'Orazio<sup>3</sup>,  
M. Nogues<sup>1</sup>, E. Tronc<sup>4</sup>, J.P. Jolivet<sup>4</sup> and A. Garcia<sup>2</sup>*

<sup>1</sup> LMOV, CNRS, Université de Versailles, 78035 Versailles-Cedex, FRANCE

<sup>2</sup> ICMAT, CNR, C.P. 10, 00016 Monterotondo Stazione, Roma, ITALY

<sup>3</sup> Dip. di Fisica, Università, 67100 L'Aquila, ITALY

<sup>4</sup> LCMC, Université P. et M. Curie, 75252 Paris-Cedex 05, Paris, FRANCE

The dynamic and static properties of  $\gamma\text{-Fe}_2\text{O}_3$  nanoparticle ( $\langle f \rangle = 5$  nm) assemblies with interparticle interactions of varying strength have been investigated by ac and dc susceptibility and magnetic relaxation measurements. The frequency dependence of the temperature of the maximum of the ac susceptibility ( $T_{\max}$ ), the temperature variation of the non linear dc susceptibility and the ageing effect on the relaxation of the magnetisation have been analysed.

The results give evidence of the existence of three magnetic regimes with increasing strength of interparticle interactions:

- Pure superparamagnetism, for very weak dipolar interactions in a dilute dispersion of particles in a polymer (polyvinilic alcohol): the frequency dependence of  $T_{\max}$ , related the average blocking temperature, is described by the Néel-Brown model;
- Superparamagnetism modified by interactions, for dipolar interactions of intermediate strength in a concentrated dispersion of particles in a polymer: the dynamical properties can still be described by superparamagnetic laws, accounting for the contribution of the interparticle interaction energy to the energy barrier of individual particles and for the number of particle neighbours;
- Collective state, for strong dipolar or (and) exchange interparticle interactions in a nanoparticles powder sample: it is no longer possible to describe the dynamic and static properties in terms of individual blocking processes.  $T_{\max}$ , very weakly frequency dependent, signals a cooperative phase transition.

The latter regime has the characteristics of a cooperative glass magnetic state, with some analogies with the spin glass one:

- Critical slowing down of the relaxation time according to a power law;
- Ageing effect on the relaxation of the magnetisation;
- Increase of the non linear susceptibility approaching  $T_{\max}$  with decreasing temperature.

**NANOSCALE MAGNETIC CHARACTERIZATION OF NANOPARTICLES***Sara Majetich*

Department of Physics, Carnegie Mellon University, Pittsburgh, PA15213, USA  
[<sm70@andrew.cmu.edu>](mailto:<sm70@andrew.cmu.edu>)

The ability to characterize magnetization on a nanometer length scale leads to new insights about magnetization reversal in individual SmCo<sub>5</sub> nanoparticles and interactions between particles in self-assembled arrays of g-Fe<sub>2</sub>O<sub>3</sub> nanorods. Both of these systems are characterized using the Foucault method of Lorentz microscopy. While this technique is standard for studying domain patterns in thin films, the image interpretation is more complex in nanoparticles. Following an explanation of the Foucault method, its application in these two nanoparticle case studies will be described. Magnetization reversal results in individual SmCo<sub>5</sub> nanoparticles will be compared with coercivity data for assemblies of particles. SmCo<sub>5</sub> is an interesting material for fine particles because its high magnetocrystalline anisotropy leads to a very large monodomain threshold of 2 microns. The coercivity as a function of average particle size shows a rise with increasing average particle diameter until d<sub>avg</sub> is on the order of 15 nm, followed by a slow decrease. This decrease is proportional to d<sub>avg</sub><sup>-1/3</sup>, where the average diameter is determined from TEM. However, the decay of the coercivity is also proportional to the inverse of the average grain size found from Scherrer analysis of the x-ray diffraction peaks. Neither of these results agrees with the theoretical prediction that the coercivity should be constant up to an average particle size of 2 microns. Two possibilities for this discrepancy are investigated using Lorentz microscopy: 1) some of the particles are not monodomain, and 2) grain boundaries and other structural defects or irregularities serve as low energy nucleation sites for magnetization reversal. Lorentz microscopy is also used to demonstrate how particle interactions affect the switching field. For more quantitative experiments on interparticle coupling, this technique is applied to self-assembled arrays of g-Fe<sub>2</sub>O<sub>3</sub> nanorods, where the exact interparticle spacing is known, and not just its projection onto the sample plane. The self-assembled arrays have a smectic liquid crystal structure which has been embedded in a silica matrix. Following an explanation of the array preparation and characterization by TEM, electron diffraction, and SQUID magnetometry, Lorentz microscopy is used to show the coupling between neighboring particles both within a single plane, and between planes of particles.

**ANOMALOUS PROPERTIES OF MAGNETIC NANOPARTICLES**

*A. E. Berkowitz<sup>1</sup>, R. H. Kodama<sup>1</sup>, K. Takano<sup>1</sup>, S. Foner<sup>2</sup>, E. J. McNiff<sup>2</sup>,  
S. H. Makhlof<sup>d,3</sup> and F. T. Parker<sup>1</sup>*

<sup>1</sup> University of California, San Diego, M.S. 0401,  
La Jolla, CA 92093, USA <aberk@ucsd.edu>

<sup>2</sup> Francis Bitter Magnet Laboratory, MIT, Cambridge, MA 02139, USA

<sup>3</sup> Permanent address: Assiut University, Assiut 71516, EGYPT

Magnetic surface properties can differ significantly from those in the bulk. This is principally a result of the lower coordination of the surface atoms, but it is also influenced by surface roughness, and by modified exchange bonds when surface impurity atoms are present. These effects are most clearly evident for magnetic materials with localized exchange interactions, such as are found in ferrimagnetic (FIM) and antiferromagnetic (AFM) systems in which superexchange *via* an oxygen atom occurs. When these materials are prepared as nanoparticles (NP), with large surface/volume ratios, surface magnetic properties or surface-driven spin rearrangements can dominate the net magnetic behavior, with some remarkable results.

We will discuss two such examples of magnetic nanoparticles: FIM NiFe<sub>2</sub>O<sub>4</sub> (nickel ferrite)<sup>1</sup> and AFM NiO.<sup>2</sup> The NiFe<sub>2</sub>O<sub>4</sub> - NP exhibit anomalies such as low magnetization (without a 'dead layer'), huge coercive forces, shifted hysteresis loops, increasing magnetization with time in fields of 7 tesla, and a constant decay rate of magnetization at low temperatures. By numerical atomic modeling of the spin configurations in these NP, we have shown that all these anomalies arise from the presence of surface spin states with spin directions deviating randomly from the collinear spin directions in the NP's cores. NiO - NP have surprisingly large magnetizations, enormous coexisting coercive forces and hysteresis loop shifts, and they also show magnetization increases with time in large fields. In this case, the numerical modeling showed that the number of spin sublattices of these AFM - NP changed from two to as many as eight at small enough diameters. The near-degeneracy of these spin configurations are responsible for the unusual properties.

1. R. H. Kodama, A. E. Berkowitz, E. J. McNiff, Jr, and S. Foner. *Phys. Rev. Lett.*, **77**, 394 (1996).
2. R. H. Kodama, S.A. Makhlof, and A. E. Berkowitz, *Phys. Rev. Lett.*, **79**, 1393 (1997).

**FERROMAGNETIC / ANTIFERROMAGNETIC STRUCTURES  
WITH FERROMAGNETIC INTERLAYER COUPLING**

*A.S. Edelstein<sup>1</sup> R.H. Kodama<sup>1</sup> M.M. Miller<sup>1</sup>, V. Browning<sup>1</sup>, P. Lubitz<sup>1</sup> and H. Sieber<sup>2</sup>*

<sup>1</sup> Naval Research Laboratory, Washington DC 20375, USA  
[<edelstein@anvil.nrl.navy.mil>](mailto:edelstein@anvil.nrl.navy.mil)

<sup>2</sup> Dept. of Materials Science and Engineering, Univ. of Wisconsin-Madison,  
WI 53705, USA

Structures composed of NiO(d)/Co(2.5 nm)/NiO(d)/Permalloy(2.5 nm)/NiO(d) with d=5 and 10 nm were investigated. It was found that the magnetization curves for both structures at 400 K show the separate contributions of Co and permalloy and the coercivities of both ferromagnets are small. With decreasing temperature, the coercivities of Co and permalloy increase. The increases are larger for the d=10 nm structure. Of more importance, for both structures the difference between the smaller coercivity of permalloy and the larger coercivity of Co decreases until the two contributions can not be distinguished. The two contributions can not be distinguished for d=5 nm, 250°T<sup>2</sup>300 K and for d=10 nm, 360°T<sup>2</sup>380 K. These results indicate that there is a sufficiently strong ferromagnetic coupling between the Co and permalloy layers in these temperature ranges to overcome the difference in anisotropy energies between the Co and permalloy films. It is surprising that the interlayer coupling prevails over the anisotropy at higher temperatures for the structure with the larger separation between the layers. A possible explanation is that antiferromagnetism is strengthened at higher temperatures, i.e., 360°T<sup>2</sup>T<sub>N</sub>, by the increase in the thickness of the NiO layer and that this strengthening is more important than the greater distance over which the spins must be correlated. Ferromagnetic resonance measurements on the d=5 nm sample show that the permalloy resonance lines shift strongly with temperature for T>300 K. The behavior supports the result that the Co and permalloy layers are coupled at approximately 300 K and become uncoupled above 360 K. SAXS and AFM measurements on the d=5 nm structure and on multilayer films show the films are very smooth, having rms roughness less than 1 nm. The smoothness of these films and results on samples that were made purposely rougher by first depositing a Mg/MgO multilayer, indicate that the ferromagnetic coupling observed is not due to roughness. Instead we believe it is due to a canted spin arrangement of the spins of the intervening antiferromagnetic layer. The coupling decreases with increasing temperature as T@T<sub>N</sub>, the Néel temperature of NiO. Using a phenomenological model for the magnetization, we estimate that the ferromagnetic coupling between the layers must be greater than 0.02 ergs/cm<sup>2</sup> in order that one can not distinguish the separate Co and permalloy contributions to the magnetization. Extensive results on multilayers will also be presented.

---

**GRAIN SIZE DEPENDENCE OF REMANENCE ENHANCEMENT  
OF NANOCRYSTALLINE Nd-Fe-B POWDERS**

*V. Neu, L. Schultz, and H.-D. Bauer*

Institut für Festkörper- und Werkstoffforschung Dresden, Institut für Metallische Werkstoffe, Helmholtzstr. 20, 01069 Dresden, GERMANY <l.schultz@ifw-dresden.de>

Single-phase, isotropic Nd-Fe-B powders exhibit remanence values above 0.8 T (which is the Stoner-Wohlfarth-limit) when exchange coupling between adjacent grains contribute to a considerable amount to the total magnetization. This effect of an increasing remanence with decreasing average grain size is already known for melt-spun Nd-Fe-B and will be presented for intensively milled, nanocrystalline Nd-Fe-B powders.

A homogenized, arc-melted  $\text{Nd}_2\text{Fe}_{14}\text{B}$  pre-alloy and a Co-containing  $\text{Nd}_2(\text{FeCoNbGa})_{14}\text{B}$  composition have been milled on a Spex mill and nanocrystalline 2:14:1 powders were obtained after subsequent annealing under vacuum. The average grain size has been evaluated by TEM investigations and Rietveld analysis of X-ray data, with good agreement between both methods for grain sizes in the range of 20 to 50 nm. These investigations show an increase in remanence with decreasing grain size in accordance with existing micromagnetic calculations and a coercive field  $H_c$  that is more or less unaffected by the grain size. Concerning the dependency of  $H_c$  there are still discrepancies in the predictions of different models and in different experimental results.

Co-containing samples with optimum microstructure exhibit improved hard magnetic properties (remanence  $J_r = 0.95$  T, coercive field  $\mu_0 H_c = 0.96$  T, energy density  $(BH)_{\max} = 140$  kJ/m<sup>3</sup>) together with a high Curie temperature of  $T_c = 470^\circ\text{C}$ .

**THERMOMAGNETIC STUDY OF METASTABLE NANOGRAINS  
IN SOFT MAGNETIC NANOCRYSTALLINE ALLOYS**

*L.K. Varga<sup>1</sup> and K.V. Rao<sup>2</sup>*

<sup>1</sup> Research Institute for Solid State Physics,  
1525 Budapest P.O.B. 49, HUNGARY

<sup>2</sup> Department of Condensed Matter Physics  
The Royal Institute of Technology, Stockholm, SWEDEN

The magnetic decoupling and the transformation temperatures of metastable nanophases have been investigated as a function of annealing temperature in partially crystallized Finemet and  $\text{Fe}_{92-x}\text{B}_x\text{Zr}_{7-y}\text{Nb}_y\text{Cu}_1$  (with  $x = 2, 4, 6, 8, 10, 12$  and  $y = 0, 3.5$  at%) type nanostructured soft magnetic alloys. By comparative initial permeability ( $\mu_i$ ) and low field dc magnetization ( $M_s$ ) measurements it is demonstrated that the nanograins shows a superparamagnetic transition at high temperatures, between the Curie points belonging to the starting amorphous and equilibrium bcc phases respectively, in both type of nanocrystalline alloys. We find that the superparamagnetic transition temperature depends on the volume fraction of the nanograins. The gradually decoupling of the monodomain nanograins with increasing temperature is responsible for the broad distribution of  $\mu_i$  and  $M_s$  thermograms.

**ANOMALOUS ELECTRON TRANSPORT IN MAGNETIC MULTILAYERS  
TUNED BY ELECTRIC AND MAGNETIC FIELDS**

*F.G.Aliev, V.V.Moshchalkov and Y. Bruynseraede*

Laboratorium voor Vaste-Stoffysica en Magnetisme, Katholieke Universiteit Leuven  
Celestijnenlaan 200D, K.U. Leuven, B-3001, Leuven, BELGIUM  
<Aliev.Farkhad@fys.kuleuven.ac.be>

We have recently observed a strong variation of the magnetoresistance and electron-electron interactions in magnetic trilayers which may be induced by resonant tuning of the structural disorder inside the double spacer [1]. Here we demonstrate that these films may be used to reveal the ground state of the disordered two-dimensional metal. The asymptotic electron transport, studied in the limit of the vanishing applied electrical fields, at temperatures down to 20mK and in the magnetic fields up to 13Tesla shows a transition from logarithmic ( $\Delta\rho \sim \log T$ ) to square root of temperature ( $\Delta\rho \sim \sqrt{T}$ ) dependences which are both insensitive to the magnetic field. We explain this crossover as an evidence for a possible cut-off of the electron-electron interactions by the electron scattering on symmetrical two-level systems. We have also shown that the classical magnetic multilayers may be used as model systems to study quantum magnetic phase transition phenomena. That transition has been tuned in  $[Fe/Cr]_{10}$  multilayers and has been investigated by measuring the temperature variation of the spin dependent part of the electrical resistivity in different applied magnetic fields. We determined this contribution,  $\rho_s(T)$ , for different applied magnetic fields in a wide temperature interval below 300K . We observed that below 100K  $\rho_s$  varies as a power of temperature  $\Delta \rho_s \sim T^\alpha$  with  $\alpha$  being a function of magnetic field. The electron scattering by the antiferromagnetic fluctuations is shown to be anomalous near quantum magnetic phase transition resulting in a linear variation of  $\rho_s(T)$  as function of temperature.

This work has been supported by the Fund for Scientific Research - Flanders (FWO) as well as by the Flemish Concerted Action (GOA) and the Belgian Inter-University Attraction Poles (IUAP) research programs.

1. F.G.Aliev, E.Kunnen, K.Temst, K.Mae, G.Verbanck, J.Barnas, V.V.Moshchalkov, and Y.Bruynseraede, Phys. Rev. Lett., **78**, 134 (1997).

**NANOSTRUCTURED LASER ABLATED CuCo THIN FILMS:  
MAGNETIC AND MAGNETORESISTIVE PROPERTIES**

*V. Madurga<sup>1</sup>, J. Vergara<sup>1</sup>, I. Pérez de Landazábal<sup>1</sup>, R.J. Ortega<sup>1</sup>, and K.V.Rao<sup>2</sup>*

<sup>1</sup> Department of Physics, Universidad Pública de Navarra,  
E-31006 Pamplona, SPAIN

<sup>2</sup> Department of Condensed Matter Physics, Royal Institute of Technology,  
S-10044 Stockholm, SWEDEN

The possibility to produce nanostructured thin films formed by a ferromagnetic non-miscible element in a non-magnetic conductor matrix, by Pulsed Laser Ablation, will be examined.

We have studied the magnetoresistive properties of the CuCo thin films prepared by PLA. From the X-ray diffractogram, SEM and AFM we have found a homogeneous Co cluster distribution in the Cu matrix and a close to atom-to atom deposition for these elements: a surface roughness no higher than 0.5 nm has been found for the as deposited films and no magnetoresistive character. After thermal treatments the GMR are present and the surface roughness of these films take values between 5 and 10 nm.

In particular, we have studied the influence of the thickness samples in the GMR. For samples 60 to 120 nm thick we have found an isotropic behaviour of the GMR. Contrary, the samples 30 nm thick have anisotropy GMR. A clearly in plane easy direction for the magnetization is found in these samples: the magnetization measurements show also this anisotropy.

Furthermore, for these 30 nm thick samples we have studied the influence of the target speed rotation in the magnitude of this anisotropic GMR character. The films obtained at low target speed rotation present a higher anisotropy than the samples prepared at high target speed rotation. The surface roughness from the low target speed rotation samples, ~ 9.5 nm, are higher than the corresponding to the high target speed rotation films, ~ 6.0 nm.

These anisotropic magnetization and magnetoresistive behavior and their dependence with the target speed rotation is explained by the different size anisotropy corresponding to the different nanoclusters present in the films, which origin is the different surface morphology of the target, produced by the laser impact and plasma generation, which is different for the corresponding different target sped rotation.

**FIELD ION MICROSCOPY AND MAGNETIC PROPERTIES  
OF THE Cu<sub>80</sub>Co<sub>20</sub> NANOPHASE COMPOUNDS BY MECHANICAL MILLING**

V.A. Ivchenko<sup>1</sup>, M.A. Uimin<sup>2</sup>, A.Ye. Yermakov<sup>2</sup> and A.Yu. Korobeinikov<sup>2</sup>

<sup>1</sup> Institute of Electrophysics, Ural Branch of Russian Academy of Sciences,  
Komsomolskaya St. 34, Ekaterinburg 620049, RUSSIA <ivchenko@ief.intec.ru>

<sup>2</sup> Institute of Metal Physics, Ural Branch of Russian Academy of Sciences,  
S.Kovalevskaya St. 18, Ekaterinburg 620219, RUSSIA

A direct observation of the atomic structure of the mechanically milled Cu<sub>80</sub>Co<sub>20</sub> compounds is made with the field-ion microscope (FIM). The advantages of FIM consist in the possibility of precision analysis of real surface structure at atomic level. This analysis is achieved by the examination of subsurface volume during the sequential controlled evaporation of surface atoms by an electric field at cryogenic temperatures. Atomically clean surface is constantly observed and registered (at atomic scale) during this process.

The microstructure analysis of Cu<sub>80</sub>Co<sub>20</sub> samples in a volume (up to 0.2  $\mu$  m in depth and up to 0.2  $\mu$ m in diameter of total ionic image) allowed us to determine that compounds under investigation are ultradisperse mixture of particles of two FCC phases, i.e. Cu-Co diluted solid solution and pure cobalt. The size of solid solution particles is ~ 80 nm, the size of cobalt particles is up to 15 nm. Cu-Co solid solution is heterogeneous: in a copper matrix alongside with single cobalt atoms Co clusters of 1-2 nm are available. Vacancy pores (~ 6-8 nm in diameter) are observed at the interface surfaces. The boundary surfaces between particles, both of different phases and those of one phase, have been established to vary in sizes and structure compared to the conventional intergrain and interphase boundaries in metals and alloys. The structure variations of Cu-Co compounds upon annealing have been analysed.

The peculiarities of magnetic properties of the studied compounds, i.e. superparamagnetism at room temperature and a magnetization deficit (its value is ~ 1/4 of the initial mixture magnetization) at 4.2 K as well as a giant magnetoresistance effect are discussed on the basis of the above-mentioned structural data.

**GIANT MAGNETO-IMPEDANCE EFFECT  
IN NANOCRYSTALLINE RIBBONS**

*H. Chiriac, T.-A. Ovari, and C.S. Marinescu*

Natl. Inst. of R&D for Technical Physics, 47 Mangeron Blvd., 6600 Iași 3, ROMANIA

The most sensitive giant magneto-impedance (GMI) effect – large changes in the high frequency impedance  $Z$  of a magnetic conductor with small variations of a dc magnetic field  $H_{dc}$  – has been reported in low magnetostrictive  $\text{Co}_{68.15}\text{Fe}_{4.35}\text{Si}_{12.5}\text{B}_{15}$  amorphous wires and ribbons [1].

In this paper we study the GMI response of  $\text{Fe}_{73.5}\text{Cu}_1\text{Nb}_3\text{Si}_{13.5}\text{B}_9$ ,  $\text{Fe}_{90}\text{Hf}_7\text{B}_3$ , and  $\text{Fe}_{90}\text{Zr}_7\text{B}_3$  nanocrystalline ribbon shaped samples. The GMI measurements have been performed at frequencies of the driving ac current up to 1 MHz, on samples with similar cross section areas. The results on the GMI effect in nanocrystalline ribbons are compared with those obtained for CoFeSiB amorphous ones, using the MI ratio, defined as  $DZ/Z = [Z(H_{dc} = 0) - Z(H_{dc} = 1 \text{ kA/m})]/Z(H_{dc} = 0)$ .

The most sensitive GMI response is given by the  $\text{Fe}_{90}\text{Zr}_7\text{B}_3$  nanocrystalline ribbon – about 30%, which is comparable to that of the CoFeSiB amorphous one. A sensitivity of about 25% has been observed for the  $\text{Fe}_{90}\text{Hf}_7\text{B}_3$  nanocrystalline ribbon, while for the  $\text{Fe}_{73.5}\text{Cu}_1\text{Nb}_3\text{Si}_{13.5}\text{B}_9$  one, the maximum MI ratio reaches only 10%.

The results are discussed and explained in terms of differences in the electrical resistivities of the investigated samples, as well as by taking into account the local anisotropy distributions in each case. One of the main goals of this paper is to elucidate the role of good soft magnetic properties on the magnitude and sensitivity of the GMI effect.

Our study is directly related to the practical interest presented by nanocrystalline magnetic materials in general, and particularly to the criteria for the choice of an appropriate material for GMI-based applications.

[1] L. V. Panina, K. Mohri, T. Uchiyama, K. Bushida, and M. Noda, in *Nanostructured and Non-Crystalline Materials*, Eds. M. Vázquez and A. Hernando, World Scientific, Singapore, 1995, p. 461.

## INFLUENCE OF OXIDATION TIME ON THE MAGNETOTRANSPORT PROPERTIES OF MAGNETIC TUNNEL JUNCTIONS

*R.J.M. van de Veerdonk<sup>1,2</sup>, N.C.W. Kuijpers<sup>1</sup>, H.J.M. Swagten<sup>1</sup>, J.S. Moodera<sup>2</sup>,  
and W.J.M. de Jonge<sup>1</sup>*

<sup>1</sup> Department of Physics and COBRA, Eindhoven University of Technology,  
P.O. box 513, 5600 MB Eindhoven, THE NETHERLANDS <swagten@phys.tue.nl>

<sup>2</sup> Francis Bitter Magnet Laboratory, Massachusetts Institute of Technology,  
170 Albany Street, Cambridge, Massachusetts 02139, USA

In the last few years progress in the fabrication of devices consisting of two ferromagnetic electrodes separated by a 1-2 nm insulator has led to large and reproducible magnetoresistance ratios at room temperature.<sup>1</sup> It is believed that the magnetotunneling effect exploits the asymmetry in density of states of the majority and minority energy bands of the ferromagnetic electrodes. Potentially, these spin tunnelling devices are applicable as strongly miniaturised magnetic field sensors or non-volatile memory cells.

In this presentation we will focus on the control of the oxidation stage of the junction barrier, which crucially determines the magnetotransport properties of a ferromagnet-insulator-ferromagnet tunnel structure. In our preparation scheme the interface between the bottom magnetic electrode and the insulator is formed during the glow discharge oxidation of an Al overlayer. If the oxidation time is too short, a thin metallic Al layer will be left, while a too long oxidation time will lead to partial oxidation of the bottom electrode. Both effects tend to degrade the magnetoresistance of the junctions.

To investigate the effect of the (glow discharge) oxidation time in more detail we have prepared Si/Co Al<sub>2</sub>O<sub>3</sub>/Ni<sub>80</sub>Fe<sub>20</sub> tunnel junctions in which both the Al thickness prior to oxidation (1.0 nm, 1.2 nm, and 1.4 nm) and the oxidation time (between 30 s and 500 s) were varied. We will correlate the magnetotransport and magnetic properties of these junctions with the preparation conditions.

1. J.S. Moodera *et al.*, Phys. Rev. Lett. 74, 3273 (1995)

## MAGNETIC DOMAINS IN NANOCRYSTALLINE AND NANOCOMPOSITE MATERIALS

*R.D. Shull<sup>1</sup>, A.J. Shapiro<sup>1</sup>, H.D. Chopra<sup>2</sup>, V. Nikitenko<sup>3</sup>, V. Gornakov<sup>3</sup>, A. Khapikov<sup>3</sup>,  
L.M. Dedukh<sup>3</sup>, and A. Chaiken<sup>4</sup>*

<sup>1</sup> National Institute of Standards and Technology, Gaithersburg,  
MD 20899, USA <shull@nist.gov>

<sup>2</sup>Mechanical & Aerospace Engineering Department, SUNY at Buffalo,  
Buffalo, NY 14260, USA <hchopra@eng.buffalo.edu>

<sup>3</sup>Institute of Solid State Physics, RAS, 14232 Chernogolovka, RUSSIA

<sup>4</sup>Hewlett-Packard Laboratory, Palo Alto, CA 94304, USA

Large grain-sized crystalline ferromagnets possess a magnetic domain structure because magnetic alignment along certain orientations, called "easy" directions, is energetically favored. Even in a single crystal, a domain structure will result since there will be several choices of equivalent directions in the crystal with the same "easy" direction indices. As the grain size of a ferromagnet is reduced, however, the net polarization of the moments inside any single grain increasingly feels the influence of the magnetic polarization of neighboring grains. Consequently, the total magnetic anisotropy averages closer to zero with smaller grain size as each grain becomes surrounded by increasingly more neighboring grains. Consequently, it is not obvious what kind of domain wall structure is present in nanocrystalline or nanocomposite ferromagnets. In this presentation Bitter patterns of domains in 20 nm grain-sized Ni and magneto-optic images (via the magneto-optic indicator film, MOIF, technique) of domains in granular Ag-Co nanocomposites will be shown evidencing that such phenomena do occur in nanometer-scale materials. In addition, magnetic domain structure will be shown in an antiferromagnet (AF) - ferromagnet (FM) bilayer possessing unidirectional magnetic anisotropy. In this latter nanocomposite, magnetization reversal upon application of a reversed magnetic field was found to occur by domain nucleation and growth. For the first time, however, different domain nucleation sites were observed in such an AF/FM sandwich for the remagnetization processes in opposite directions while cycling the field, as in the measurement of a magnetic hysteresis loop. These findings indicate that the nucleation of domains in such a material is intimately connected with the magnetic bias imposed on the material, as well as on the sample's microstructure. This has important ramifications for magnetic recording devices.

---

**NANOCRYSTALLINE Sm-(Co, Cu, Ni) THIN FILMS  
WITH GIANT COERCIVITY***G.C. Hadjipanayis*

Department of Physics and Astronomy, University of Delaware,  
Newark, DE 19716, USA

*C. Prados*

Instituto de Magnetismo Aplicado, Carretera de la Coruna km 22.500,  
30230 Las Rozas, Madrid, SPAIN

Nanocrystalline Sm(Co, Ni, Cu) / Cr bilayers were fabricated by dc sputtering deposition. The as-made films are initially amorphous and relatively soft. A nanocrystalline structure is developed after annealing giving rise to a huge enhancement of coercivity. The room temperature coercivity increases from less than 100 Oe in the amorphous state to 42 kOe in a Sm<sub>2</sub>Co<sub>17</sub> sample annealed for 30 min. at 550°C. Structural data in the optimum samples suggest a particle size around 10 nm. Magnetic viscosity measurements indicate that the switching volume is of the same order as the crystallite size. Remanence measurements show that interparticulate interactions are magnetizing and rather independent of the crystallization stage. A correlation of the structural and magnetic data indicates domain wall pinning at the high anisotropy precipitates as the origin of the giant coercivity. The possibility of tuning the coercivity along more than two orders of magnitude through the annealing conditions makes this type of thin films suitable for a wide variety of applications, from longitudinal recording media to thin film permanent magnets.

**STUDIES OF TRIBOLOGY AND LIQUID STRUCTURES  
AT A NANOMETER SCALE USING SPM***Miquel Salmeron*

Lawrence Berkeley National Laboratory, University of California,  
Berkeley, CA 94720 <salmeron@stm.lbl.gov>

In the first part, a review of nontribology studies using proximal probes will be presented. Because of its high spatial resolution, the atomic force microscope (AFM) has made it possible to study various contributions to the energy dissipation occurring during friction: phonon (heating) and electronic excitations, atomic scale wear (creation of surface vacancies and interstitials), and larger scale wear that involves the removal of atomic layers of material. In organic layers of lubricants, viscoelastic effects play a special role. In the second part of the talk, a brief review will be presented of the novel use of AFM to study liquid films and capillary phenomena at the nanometer scale.

**MEASUREMENT OF MECHANICAL PROPERTIES OF  
NANOSCALED FERRITES USING ATOMIC FORCE  
MICROSCOPY AT ULTRASONIC FREQUENCIES**

*E. Kester, U. Rabe, and W. Arnold*

Fraunhofer Institut for Nondestructive Testing (IZFP), Bldg. 37, University,  
D-66123 Saarbrücken, GERMANY <kester@izfp.fhg.de>

Thanks to their particular physical properties, thin films of nanoscaled ferrites with spinel or hexagonal structure, and garnets can be used in different recording systems. These materials exhibit high magneto-optic effects, a reduced optical absorption at wavelengths between 400 - 500 nm, and a high coercivity that allows magnetic stabilizing of small-sized bits. They are also chemically stable and have a high mechanical hardness. Thus, in magneto-optic and magnetic recording systems, or in more future oriented systems, such as near-field magneto-optic recording systems, these materials are good candidates for applications. Their technological future depends largely on the control of their preparation and their structure.

Previous researches have shown that the coercivity is not only correlated with the chemical composition, but also with the grain size and the chemical gradients from the bulk into the grain boundary. On the one hand, it has been shown that the coercivity is maximal when the grain size is about 40 nm. On the other hand, the coercivity depends on the cation distribution and the point defects in the two sublattices of the spinel structure whose evolutions are related for a given grain size with the quenching temperature under oxygen pressure. Up to now, researchers using theoretical simulations, XPS spectroscopy and X-ray diffraction demonstrated that the coercivity is related with the ferrite nanostructure. To understand the coercivity as a function of the nanostructure, the chemical gradients induced by the thermal evolution have to be interpreted in terms of mechanical gradients, tensile stresses on the grain boundary and compressive ones in the bulk. In the absence of local mechanical measurements, this assumption is not yet verified.

In order to measure the elastic properties locally; a new near-field acoustic Atomic Force Microscope is employed. The sample placed in a commercial AFM is insonified by ultrasonic waves in the frequency range between 75 kHz and 5 MHz. In contact with the specimen, the cantilever-tip system vibrates out of plane and its resonance frequencies depend on the tip-sample force. A quantitative model based on linear tip-sample forces shows that the stiffness of the specimen can be derived from the shift of the resonance frequencies. With this near-field acoustic AFM the local elasticity in nanoscaled ferrite thin films are measured in order to understand the influence of the grain size, and the chemical and mechanical gradients on the coercivity. The instrument has been applied to thin films of magnetite  $\text{Fe}_3\text{O}_4$  and magnemite  $\gamma\text{-Fe}_2\text{O}_3$ , with different grain sizes in the nanoscaled range 10-200 nm, and with different controlled chemical gradients.

**GRAIN SIZE DEPENDENCE OF INTERGRANULAR MAGNETIC CORRELATIONS IN NANOSTRUCTURED METALS**

*J.F. Löffler<sup>1</sup>, W. Wagner<sup>1</sup>, H.-B. Braun<sup>1</sup>, G. Kostorz<sup>2</sup> and A. Wiedenmann<sup>3</sup>*

<sup>1</sup>Paul Scherrer Institut, CH-5232 Villigen PSI, SWITZERLAND <joerg.loeffler@psi.ch>

<sup>2</sup>ETH Zürich, Institut für Angewandte Physik, CH-8093 Zürich, SWITZERLAND

<sup>3</sup>Hahn-Meitner-Institut, D-14109 Berlin, GERMANY

We produced nanostructured Fe, Co and Ni by inert-gas condensation and investigated the magnetic properties as a function of grain size. In magnetization measurements on Fe and Ni we observed a distinct crossover of the coercivity when the grain size is of the order of the domain wall width. For grain sizes smaller than a critical length scale  $L_{\text{crit}}$  (which e.g. in Fe is about 35 nm), the coercivity increases with increasing grain size to a maximum at grain sizes near  $L_{\text{crit}}$ , and subsequently decreases. The increase of the coercivity is in qualitative agreement with the random-anisotropy model, while the decrease of the coercivity beyond  $L_{\text{crit}}$  can be understood by the formation of domain walls within one grain.

However, based on magnetization measurements alone, a quantitative comparison with theoretical models on principle has limitations. The random-anisotropy model for example predicts a coercivity  $H_c \sim D^{-6}$ . Such an exponent is difficult to be verified owing to a limited range in grain size which can be attained in the experiment. On the other hand, based on the same theory, the zero-field intergranular magnetic correlations are expected to scale with  $1/D^3$ , which is easier to detect. Therefore, we performed small-angle neutron scattering measurements on Fe, Co and Ni to analyze the grain size dependence of the magnetic correlations on the nanometer scale.

As expected from theory, we generally observed a decrease of the correlation length with increasing grain size up to  $D \approx L_{\text{crit}}$ , followed by a moderate increase. In particular in Fe, the decrease of the correlation length follows the  $D^{-3}$  behavior predicted by the random-anisotropy model. The increase of the correlation length for larger grain sizes is attributed to grains being in a single-domain state. Furthermore, for all materials investigated the magnetic correlation length is observed to be always larger than  $L_{\text{crit}}$ . This is consistent with theoretical arguments which show that nonuniform magnetization configurations can only exist for grains with  $D > L_{\text{crit}}$  with  $L_{\text{crit}} = \pi\sqrt{A/K}$ , where  $A$  and  $K$  are exchange and anisotropy constants, respectively.

**UNUSUAL LOW-ENERGY COLLECTIVE EXCITATIONS  
IN NANoclUSTERS AND NANoclUSTER COMPOUNDS**

*Vladimir Z. Kresin<sup>1</sup> and Vitaly V. Kresin<sup>2\*</sup>*

<sup>1</sup> Lawrence Berkeley Laboratory, University of California, 1 Cyclotron Road  
Berkeley, California 94720, USA <vzkresin@lbl.gov>

<sup>2</sup> Department of Physics and Astronomy, University of Southern California  
Los Angeles, California 90089-0484, USA <kresin@usc.edu>

Excitation spectra of small nanoclusters, quantum dots, and their assemblies can display unusual features which are peculiar to the small-particle size range and do not appear in bulk materials. We will describe two types of low-energy collective states which are predicted to occur in cluster systems.

1. We consider collective excitations in metal nanoclusters containing two overlapping sets of electrons of different effective masses (e.g., *s* and *d* electrons in transition metal compounds). We show that such particles will exhibit a new type of low-frequency electron collective mode. In the bulk limit this mode develops into an acoustic plasmon ("demon"). In small particles it acquires dipole oscillator strength and gives rise to a photoabsorption band. This effect is unique to finite systems. Consequently, the demon-like collective states can be detected by optical spectroscopy of individual nanoclusters or nanocluster assemblies.
2. We analyze collective excitations of carriers in two-dimensional arrays made up of cluster-type units: quantum dots, passivated metal nanoclusters, etc. Such networks are unique in that they combine two degrees of electron delocalization. First, within each unit cell the electrons are distributed throughout the cluster and are strongly bound to it. Secondly, if the electrons are able to tunnel between cells, the array will become conducting. We show that in such arrays the dispersion law of conduction-band plasmons will be strongly modified from the case of bulk surfaces: it becomes measurably steeper and can acquire a downward slope. (The same effect also has a strong influence on the plasmon dispersion in doped fullerides.)

It would be interesting to verify the existence of such unconventional excitations experimentally.

In addition, we will discuss the possibility of superconducting-type pair correlations in finite systems and their experimental manifestations, e.g., odd-even effects in excitation spectra.

\* Work supported by the US National Science Foundation.

**MOLECULAR DYNAMICS SIMULATIONS OF  
NANOCRYSTALLINE GLASS FORMING ALLOYS***Ulrich Herr*

Institute of Physics, University of Augsburg, Memminger Str. 6,  
86135 Augsburg, GERMANY <ulrich.herr@physik.uni-augsburg.de>

We report about molecular dynamics simulations of model nanocrystalline binary alloys. The alloy systems of interest here are characterized by a size mismatch of the constituent atoms. It has been demonstrated [1] that in such systems a crystal-to-glass transition associated with a mechanical instability may occur at a critical solute concentration. The size mismatch of the constituents is the main parameter which destabilizes the crystalline phase. We study the effect of atomic size mismatch on the stability of nanocrystalline model materials. The main subjects of the study are:

- (a) the elastic properties of the nanocrystalline alloys depending on the parameters grain size, solute concentration and size mismatch.
- (b) the structure of the grain boundaries in the nanocrystalline alloys.

It has been proposed recently that in nanocrystalline glass forming alloys the formation of an amorphous phase at high energy grain boundaries may lead to the reduction of the free energy [2]. The phase formation does not require diffusion of the constituents. The molecular dynamics study can provide insight into the atomistic details of the grain boundary structure in these alloys and the validity of the continuum concepts used in [2] on the atomistic scale.

[1] M.Li and W.L.Johnson, Phys. Rev. Lett. 79 (1993) 1120

[2] P.Desre, Phil Mag. A 74 (1996) 103

**OPTICAL ABSORPTION BY AN ENSEMBLE  
OF SEMICONDUCTING NANOPARTICLES***Dirk Uwe Saenger*

Institut für Neue Materialien, Im Stadtwald, 66123 Saarbruecken, GERMANY  
*<saenger@inm-gmbh.de>*

Optical absorption by an ensemble of semiconducting nanoparticles embedded in a dielectric matrix is theoretically studied, taking into account the microscopic disorder, which produces a broadening and a redshift of the absorption spectra. It is shown<sup>1</sup> that microscopic disorder generates a significant broadening and redshift of all resonances in the regime where the fluctuations of the transitions induced by disorder exceed the electron-electron correlation energy. Lowering the impurity concentration, the electron-electron correlation energy can narrow effectively the resonance lines close to the band gap. In the latter regime the absorption spectra looks like the absorption spectra of a high-quality bulk semiconductor with the difference, that the level spacing between resonances is enlarged due to quantum-size effects. This spectral feature is measured in a system consisting of GaAs nanoparticles in an AlAs matrix as grown by molecular beam epitaxy<sup>2</sup>, while in the former regime also the lowest resonance is strongly broadened. Such a spectral feature is observed in systems containing CdSe particles embedded in an organic matrix as produced by wet chemical methods<sup>3</sup>. Similar effects as in the GaAs/AlAs-system are postulated for the III-V-Nitrides.

1. D. U. Saenger, Phys. Rev. B 54, 14604 (1996)
2. R. Noetzel and K. H. Ploog, Adv. Mater. 5, 22 (1993)
3. C.R. Kagan et al., Phys. Rev. Lett. 76, 1517 (1996)

**A MATHEMATICAL MODEL TO TRACE THE GENESIS OF  
NANOCRYSTALLINITY IN COATINGS OBTAINED VIA HIGH VELOCITY  
OXYGEN FUEL THERMAL SPRAY (HVOF/TS)**

*Vikas V. Gupta, Maggy L. Lau, and Enrique J. Lavernia*

Dept. of Chemical and Biochemical Engineering and Materials Science, University of California, Irvine, CA-92697, USA <vgupta@stress.eng.uci.edu>

The High Velocity Oxygen Fuel Thermal Spray (HVOF/TS) process is currently being investigated for obtaining nano-crystalline coatings. Thermal spraying of nanocrystalline agglomerates obtained via ball-milling has resulted in nanocrystalline coatings. These coatings show better bonding and hardness properties as a result of the nanostructure.

An important unanswered question is the origin of the nanocrystallinity of the coatings. Is the nanostructure of the coatings a result of the nanostructure of the starting ball-milled powders? The answer to this question rests on what happens to the agglomerates during the thermal spray process. This can be investigated by developing appropriate mathematical models.

Previous models of the HVOF/TS process assumed a spherical particle shape. However, the ball-milled particles have irregular shapes and high aspect ratios. We have developed a model of the heat transfer process in the gun barrel during HVOF thermal spraying which accounts for the irregular shape of the ball-milled particles. Furthermore, most previous models neglect radiative heat transfer, assume Newtonian heat flow inside the particle, and follow equilibrium melting and solidification paths. We have developed a new model without making any of these assumptions. Using this model we have delineated the regimes where these assumptions are valid.

Our results show that fractions of the ball-milled powders will maintain their nanocrystallinity through the thermal spraying process and that the remaining fraction will melt completely and lose its nanostructure. These results are in agreement with the experimental results which show the existence of elongated nanocrystalline grains in the coatings. The elongated structure can be linked to the development of the nanostructure during the ball-milling which is based on mechanical deformation. Hence, these grains are evidence that some of the ball-milled powders did not melt. The experimental results also show the existence of nanocrystalline grains even smaller than the grains in the ball-milled powders. These probably originate from the complete melting and subsequent nucleation of a fraction of the ball-milled powders.

An important conclusion of our investigation is that the nanocrystallinity of the starting powders might not be a prerequisite to obtaining nanocrystalline coatings. However, the important factor might be the shape and size of the starting powders and the processing conditions.

(This work was supported by the Office of Naval Research.)

**THE ROLE OF THE GRAIN SIZE AND THE PRESENCE OF LOW AND HIGH ANGLE GRAIN BOUNDARIES IN THE DEFORMATION MECHANISM OF NANOPHASE Ni: A MOLECULAR DYNAMICS COMPUTER SIMULATION**

*H. Van Swygenhoven<sup>1</sup>, M. Spaczer<sup>1</sup>, D. Farkas<sup>2</sup> and A. Caro<sup>3</sup>*

<sup>1</sup> Paul Scherrer Institute, CH-5232 Villigen PSI, SWITZERLAND <helena.vs@psi.ch>

<sup>2</sup> Virginia Polytechnic Institute, 213 Holden Hall, Blacksburg, VA, USA

<sup>3</sup> Centro Atomico Bariloche, 8400 Bariloche, ARGENTINA

The microstructure of computer generated Ni nanophase samples prior to and after uniaxial constant stress deformation is studied by means of pair distribution functions, coordination number, atom energetics, and local crystalline order in terms of a bond analysis technique.

Two types of samples are considered: those with random crystallographic orientation, representing samples with mainly high angle grain boundaries, and those originated from the same seeds as before, but with a limited misorientation, representing samples with mainly low angle grain boundaries. The mean grain size of the samples vary between 3 and 12 nm, each containing at least 15 grains. A full characterization of the microstructure of the samples is given in another contribution "Characterisation of the Microstructure of Nanophase Ni and Its Influence on Mechanical Properties: A Molecular Dynamics Computer Simulation".

The samples are loaded with uniaxial stress and elastic and plastic deformation are studied. At the smallest grain sizes a reduction in Young's modulus is observed, but from 10 nm on the value equals that of a coarse grain sample. It is shown that there is an increased plastic deformation when grain size is reduced.

The role of the low-angle and high angle grain boundaries in the mechanism for plastic deformation is discussed and analyzed on atomic level. The structure of the interface determines the nature of the mechanism contributing to plastic deformation, eventually activating deformation processes inside grains. In samples with mainly low angle grain boundaries deformation induces stacking faults inside the nano grain, even in a 5 nm grain size, whereas in samples with only high angle grain boundaries plastic deformation is accommodated in the grain boundaries only. The nature of the stacking faults is studied by visual inspection of slices and by projection of the sample in a 3D simulator using the cave at Virginia Tech. A short movie of the creation of stacking faults inside the grains is shown.

## NANOSINTERING

*J. R. Groza*

Chemical Engineering/Materials Science Department  
UC Davis, One Shields Ave, Davis, CA 95616, USA <jrgroza@ucdavis.edu>

In many circumstances, to take advantage of the unique properties of nanocrystalline materials, the powders have to be densified into bulk parts of well controlled properties, geometry and size. Key to the nanopowder consolidation process is to achieve densification with minimal microstructural coarsening and/or undesirable microstructural transformations in functional nanostructures. Thermodynamically, nanopowders are highly unstable due to large surface area. Kinetically, nanosintering is significantly enhanced due to the large available surface area and strong thermodynamic driving force for the sintering process. Thus, densification of nanopowders without increase in grain size presents considerable challenges.

The main problems in nanosintering will be presented: powder agglomeration, high surface reactivity and contamination, grain coarsening and inability to fabricate large and dense parts. A parallel between the nanosintering and densification of regular powders will be analyzed in order to understand the similarities and detect the specifics.

**PRODUCING NANO- AND MICROCRYSTALLINE MATERIALS  
BY ECAP-PROCESS***V.I. Kopylov*

Physico-Technical Institute, Belorussian Academy of Sciences, Zhodinskaya 4,  
220730 Minsk, BELORUSSIA <phti@ns.igs.ac.by>

The equal-channel angular pressing (ECAP) is a pressing the blank through the intersecting channels of same section. In our monograph [1], the mechanics, producing technology of ECAP-process and the properties of materials produced by ECAP, were described very detailed. Application of ECAP-process for producing nano and microcrystalline (NMC) materials was described for the first time in our article [2]. As shown in [1] for producing of NMC-materials a multi-cycle ECAP-process is applied in such conditions which provide large homogeneous plastic deformation. In this case ECAP causes effective refinement of the grains down to the nanometer range. The final size of the microstructure depends on the parameters of the deformation process (temperature, strain rate, intensity and route of repeated deformation) and the nature of the material (crystal symmetry, number of slip systems, stacking fault energy, impurities, phase composition, etc.).

The main advantage of ECAP-process in comparison with other methods of plastic deformation is as follows:

- 1) Nowadays ECAP is the only method, which provides producing of NMC-structures in massive samples. (Now we have an experience of ECAP-processing of Mo and its alloys in massive samples with cross-section 150x150 mm<sup>2</sup>).
- 2) Nowadays ECAP is the best method of plastic refinement, which provides homogeneous plastic deformation, and, as result homogeneous structure with ultrafine grains.

It is necessary to underline that homogeneity of deformation is an obligatory condition for creating NMC-structures. It means, that not any realisation of "a pressing the blank through the intersecting channels" provides the formation of NMC-structure. Our investigation shows that in case of non-homogeneous deformation state the plasticity of material is soon over and good NMC-structure are not formed. The ECAP - process which provides realisation of homogeneous deformation we named clear ECAP. Beside high mechanical properties, NMC-materials produced by clear ECAP show extremely perspective physical properties. ECAP-technology opens up great possibilities for solution of various applied problems related to plastic structure formation, treatment of massive metal products, and obtaining materials with unique properties.

1. Segal V.M., Reznikov V.I., Kopylov V.I., Pavlik D.A., Malyshev V.F. Processes of Plastic Structural Formation of Metals, Nauka i Technika, Minsk, 1994 (in Russian)
2. Akhmadeev N.A., Valiev R.Z., Kopylov V.I., Mulyukov R.R. Metally, 5, 96, 1992 (in Russian)

**CONSOLIDATION AND HIGH RATE MECHANICAL BEHAVIOR  
OF NANOCRYSTALLINE TANTALUM POWDERS**

Sang H. Yoo<sup>1</sup>, T.S. Sudarshan<sup>1</sup>, Krupa Sethuram<sup>1</sup>, Raja Kalyanaraman<sup>1</sup>,  
Ghatu Subhash<sup>2</sup>, R.J. Dowding<sup>3</sup>

<sup>1</sup> Materials Modification Inc, 2929-P1 Eskridge Rd, Fairfax, VA 22031, USA

<sup>2</sup> Michigan Technological University, Houghton, MI 49931, USA

<sup>3</sup> Army Research Laboratory, AMSRL-WM-MD, Aberdeen Proving Ground,  
MD 21005, USA

The high strain rate response of the nanocrystalline tantalum is discussed in this paper. Nanocrystalline tantalum was investigated since high ductility and strength exhibited in nanograined materials can potentially be exploited in the explosively formed penetrator liner applications. The nanocrystalline tantalum powder was synthesized using Plasma Chemical Synthesis (PSC) technique, and rapidly consolidated by Plasma Pressure Compaction (P<sup>2</sup>C) system to retain its initial microstructure. Systematic experiments were conducted to find the optimum consolidation conditions for nanocrystalline tantalum powders. The effect of temperature, pressure, isothermal holding time, and electrical discharge on densification and grain growth of the nanocrystalline tantalum powder was determined. The consolidated specimens were cut by Electric Discharge Machining (EDM) and polished to study the dynamic compression behavior of the nanocrystalline tantalum using Kolsky apparatus. The effect of grain size and oxygen content on yield stress and strain was investigated at the various strain rates.

**THE REAL ORIGIN OF LOGNORMAL SIZE DISTRIBUTION  
OF NANOPARTICLES AR VAPOUR GROWTH PROCESSES**

*J. Soderlund, L. B. Kiss, G. A. Niklasson, and C. G. Granqvist*

Uppsala University, Materials Science Department, The Angstrom Laboratory,  
Box 534, Uppsala, S-75121, SWEDEN.

In nanoscience, the growth and the usual lognormal size distribution of nanoparticles are commonly explained by coagulation models. However, by surveying these models, it becomes obvious that the origin of the lognormal size distribution of particles has not really been explained. In fact, the lognormality has artificially been put into the available models, or the models are physically unacceptable. We had the opportunity to introduce a new way of thinking by focusing onto the time spent for growth by the particles, an issue, which has not really been addressed by others. In this fashion, a new model is proposed to explain lognormal particle size distributions found in vapour growth processes such as gas evaporation, without invoking coagulation. In the model, particles are moving by diffusion and drift through a finite growth region. The particle size is assumed to be a power function of growth time, and the final size distribution is determined by the first passage times. By computer simulation, lognormal size distributions and scaling laws interrelating the distribution parameters, the size of the growth region and the drift speed were found.

1. J. Soderlund, L. B. Kiss, G. A. Niklasson, and C. G. Granqvist, "Lognormal size distributions in particle growth processes without coagulation", Physical Review Letters, accepted for publication

**NANOSTRUCTURE PROCESSING OF ADVANCED CATALYTIC MATERIALS***Jackie Y. Ying*

Department of Chemical Engineering, Massachusetts Institute of Technology  
Cambridge, MA 02139-4307, USA

Nanostructured materials are of interest for a variety of catalytic and chemical applications. This talk describes the synthesis and properties of two classes of nanostructured materials: nanocrystalline materials and nanoporous materials. Nanocrystalline materials are made up of crystallites with dimensions of 5-15 nm. They may be generated by various physical and chemical approaches. As ultrahigh surface area materials, they are of great interest in catalytic applications. In our laboratory, we have used the gas condensation method to produce Cu/cerium oxide nanocrystallites with excellent dispersion and nonstoichiometry to promote catalytic reduction of sulfur dioxide, and oxidation of carbon monoxide and methane. With sol-gel processing followed by hydrothermal treatment, we have obtained quantum-confined titania nanoparticles which display excellent activity in photocatalytic decomposition of chlorinated organic compounds. The ultrahigh surface area transition metal oxide nanocrystalline materials we recently derived via chemical precipitation demonstrated the highest activity for NO reduction by methane for a non-zeolitic catalytic system. These examples illustrate the uniqueness of nanocrystalline materials, enabling us to design and tailor microstructure, surface reactivity, defect chemistry, and electronic structure for catalytic applications.

The other class of nanostructured materials investigated by us are known as molecular sieves or nanoporous materials. We have recently found that sol-gel processing can be combined with supramolecular templating agents in deriving well-defined porous structures. Through ligand interaction between alkoxide precursors and surfactant head groups, we were able to derive mesoporous and microporous transition metal oxide molecular sieves (termed TMS) with hexagonally-packed cylindrical pore structures analogous to mesoporous MCM-41 silicate materials. The compositional flexibility and pore size tailoring of the TMS system open new possibilities for catalytic applications beyond the traditional silicate-based zeolitic materials.

**APPLICATIONS OF METAL AND SEMICONDUCTOR NANOCLUSTERS  
AS THERMAL AND PHOTO-CATALYSTS**

*J.P. Wilcoxon, T.R. Thurston and J.E. Martin*

Organization 1152, Sandia National Labs, Albuquerque,  
NM 87185-1421, USA <jpwilco@sandia.gov>

In addition to their large specific surface areas, nanoclusters may have unusual surface morphologies and bonding arrangements, which make them particularly effective catalysts. We first discuss inverse micelle synthesis and surface modification of nanoclusters to produce size selected materials. After purification of the nanoclusters using high-pressure liquid chromatography and/or extraction the nanoclusters can be used as catalysts. We discuss studies of photo and thermal catalysis reactions, which illustrate the unique features of nanoclusters which may be of great technical use. In the area of photocatalysis we discuss the photo-oxidation of organic pollutants using such nanoclusters MoS<sub>2</sub> and WS<sub>2</sub>. We have been able to demonstrate improved destruction of organics such as phenol compared to traditional materials such as TiO<sub>2</sub> or ZnO, but with the advantage of tunable bandgaps, which allow destruction using only visible light. Thermal catalysis using both dispersed and supported nanoclusters of Rh, Pt, Pd, MoS<sub>2</sub>, Fe, and FeS<sub>2</sub> is illustrated with studies of pyrene hydrogenation and direct coal liquefaction and hydrogenolysis. We discuss the use of nanoclusters dispersed in solution and supported on traditional metal oxide supports in these reactions and comment on the effect of size and material type on the catalytic activity and final product distribution. The product selectivity possible with nanosize materials appears to be significantly greater than with conventional catalysts. This feature may be of great significance to the fuel refining industry. Some nanoclusters can be used to directly produce hydrocarbon fuels by simple deposition on coal powders. We find that even base metal catalysts (eg. MoS<sub>2</sub>, Fe, and FeS<sub>2</sub>) can be quite effective in nanosize form for these reactions. The effect of selective doping of the nanosize catalysts is also discussed.

**AN OVERVIEW ON NANOPHASE MATERIALS  
AND MAGNETIC APPLICATIONS**

*A. Hernando, L. Del Bianco, J. M. Rojo and C. Ballesteros*

IMA-UCM-RENFE-CSIC, P. O. Box 155, Las Rozas, 28230 Madrid, SPAIN

Soft to hard magnetic anisotropy in nanostructured magnets as a function of the typical scale lengths is reviewed. In particular, emphasis is focussed on the exchange through interphases. The following example of nanocrystalline Fe is described. Pure Fe powders, milled down to 10 nm crystallite size, have been analyzed by a combination of Mössbauer spectroscopy, high resolution transmission electron microscopy and magnetization measurements. After annealing the as-milled powders at 570 K for 1 hour, a new phase is identified with a hyperfine field of 21 T, a lower magnetic moment than bulk Fe, a magnetic order-disorder transition temperature of about 500 K and fcc crystal structure. It is tentatively interpreted as a new magnetically-ordered phase of Fe.

**THIN FILM DEPOSITIONS IN MESOPOROUS CHANNELS AS NOVEL  
SENSOR AND CATALYST MATERIALS**

*S.C.E. Tsang, R. Burch and D. Gleeson*

The Catalysis Research Centre, Department of Chemistry, University of Reading,  
Whitenights, Reading, RG6 6AD, UK <s.c.e.tsang@reading.ac.uk>

The physical and chemical properties of nanocrystallites whose dimensions are sufficiently small that deviations from bulk behaviour are observed is one of the most exciting areas of modern research. Recently, there has been much work on studying microporous supports (less than 20 Å) such as zeolites and related structures, (AlPOs and SAPOs) as hosts for dispersing 3-D arrays of metal or semiconductor nanoparticles. At Reading, we are interested in studying mesoporous materials (of pore sizes between 20-100 Å) as hosts for guest compound deposition, which may allow the formation of long range nano-thin films or reactive linings of chemical species because of their extended internal surface. Two mesoporous materials namely, *MCM-41* (1-2) and *carbon nanotubes* (3) as hosts for guest material entraptments have therefore been studied.

The MCM-41 silicas are produced by the co-operative assembly of silica and surfactants, which are characterized by large pores and large internal surface areas, greater than any known molecular sieves. The elongated hexagonally arranged channels are structurally well defined with a large number of surface hydroxyl groups which can provide reaction or nucleation sites for the entrapment of a wide variety of metal complexes. It thus provides a stable and reproducible environment for a thin film formation.

Carbon nanotubes are made by an arc evaporation of graphite. They are composed of multilayers of graphite-like concentric tubes with a central hollow internal cavity within the mesoporous range. Under typical arcing conditions, the synthesized tubes have internal diameters of 30-50 Å and 100 - 500 nm in length.

Through the reactions of their surface functional groups with various tin containing species followed by heat treatments in air , we have recently synthesized thin films of tin oxides anchored on the mesoporous silica MCM-41 or the carbon nanotubes using wet impregnation and CVD methods. It was shown that the encapsulated tin oxide films display unusual behaviors in chemical sensing and catalysis as compared to bulk tin oxide. In this talk, we will present some of our work (TEM, EXAFS, etc) on the characterization of the ultrathin tin oxide layers encapsulated within the mesoporous hosts. It is intended to correlate these structures with the sensing and catalytic properties.

1. R. Burch, N.A. Cruise, D. Gleeson, S.C. Tsang, J. Mater. Chem., (1998) 8, 227.
2. R. Burch, N.A. Cruise, D. Gleeson, S.C. Tsang, J. Chem. Soc., Chem. Comm., (1996) 951.
3. S.C. Tsang, Y.K. Chen, P.J. Harris, M.L.H. Green, Nature, (1994) 372, 159.

**WC/Co/DIAMOND NANOCOMPOSITES**

*R.K. Sadangi<sup>1</sup>, O.A. Voronov<sup>1</sup>, and B.H. Kear<sup>2</sup>*

<sup>1</sup> Diamond Materials Inc., 120 Centennial Ave., Piscataway, NJ 08854, USA

<sup>2</sup> Dept. of Ceramic and Materials Engineering, Rutgers University,  
Piscataway, NJ 08854-8065, USA

Nanophase WC-Co powder compacts are routinely consolidated by liquid phase sintering at 1350°C in vacuum. Solid state sintering of the same powder compacts at temperatures of 1050-1200°C gives partially sintered material, in which the degree of densification increases with temperature. An important characteristic of these partially sintered materials is that the pores are interconnected in three dimensions. Furthermore, by varying the hold time at the lowest sintering temperatures, where solid state diffusion predominates, the interconnected pore structure can be coarsened without significant reduction in compact dimensions. Thus, materials with precisely controlled pore connectivity and scale can easily be produced. Using a gas phase infiltration technique, we have infiltrated such nanoporous structures with graphitic carbon. After infiltration, the graphite-infiltrated WC-Co preform is transformed to WC-Co-Diamond by a high pressure/high temperature treatment. The resulting superhard material has a characteristic tricontinuous structure, which may or may not be functionally graded, depending on the infiltration treatment used. Results on structural characterization and wear testing of these novel triphasic superhard materials will be discussed.

**PERIODIC NANOCOMPOSITES AND NANOPOROUS STRUCTURES  
FOR PHOTONIC CRYSTALS AND ADVANCED THERMOELECTRICS**

*A.A. Zakhidov<sup>1</sup>, R.H. Baughman<sup>1</sup>, C. Cui<sup>1</sup>, I. Khairullin<sup>1</sup>, M. Shkunov<sup>2</sup> and  
V. Z. Vardeny<sup>2</sup>*

<sup>1</sup> AlliedSignal Inc., Morristown, NJ 07962, USA <anvar.zakhidov@alliedsignal.com>

<sup>2</sup> Dept. of Physics, University of Utah, Salt Lake City, Utah 84112, USA

Photonic crystals (PC) have attracted considerable interest, due to a number of exciting predicted phenomena that can result from photonic band gaps (PBG) - including suppression of spontaneous emission, thresholdless lasing, and the ability to precisely mold the flow of light. However the fabrication of photonic crystals in the optical domain requires the assembly of periodic 3-dimensional nanocomposites with lattice constants on the scale of optical wavelengths (200-400 nm), which remains a major synthetic problem.

We describe the structure and optical and electronic properties for synthesized photonic crystals, and for periodic nanocomposite structures that are of interest for advanced electronic applications. The synthetic method starts with the templating of porous SiO<sub>2</sub> lattices (synthetic opals) with various materials. The removal of the original SiO<sub>2</sub> matrix by chemical means yields opal-replicas. Surprisingly, the structure of the original opal lattice (having a typical cubic lattice dimension of 150-350 nm) is reliably replicated down to the nanometer scale. By either the complete filling or coating-type filling of the voids in a host matrix, the replicas may have either one or two sets of independent channels. We fill these channels with semiconductors, metals, or polymers to provide electronic and optical materials with novel properties dependent on the nanoscale periodicity. Some of these opal replicas are "air type" photonic crystals (where air replaces silica spheres), which are most favorable for photonic bandgap formation. The optical properties of these photonic crystals are reported, emphasizing the observed lasing effect of the infiltrated dye molecules, which shows unexpected spectral features. The graphitic opal replicas obtained by chemical vapor deposition are highly electrically conductive, and thus provide the first example of a network type metallic photonic crystal for the optical domain. Large photonic bandgaps are expected below the cut-off frequency, in the infrared region, for these materials.

The nanocomposite structures made of thermoelectric semiconductors are expected to have superior thermoelectric figures of merit due to several effects. A suppressed thermal conductivity is predicted due to an increased interfacial thermal resistance and the opening of a phononic band gap (which becomes important at low temperatures). The use of this approach for creating advanced thermoelectrics is demonstrated. This involves the opal infiltration of semiconductors and semimetals (Bi, Pb, Te, Bi<sub>2</sub>Te<sub>3</sub>) by high pressure melt phase, chemical, electrochemical, and vapor phase processes. The creation of 10<sup>14</sup> per cm<sup>3</sup> of in-parallel n-p junctions is theoretically described as a method for obtaining high thermoelectric power. Another described approach uses low work function materials as separated thermionic nanoscale plates within the nanospace of replicas and opals.

**MECHANICAL PROPERTIES OF NANOSTRUCTURED CHROMIUM-BASED ALLOYS***V. Provenzano<sup>1</sup>, R. Valiev<sup>3</sup>, D.G. Rickerby<sup>2</sup>, and G. Valdre<sup>4</sup>*<sup>1</sup> Naval Research Laboratory, Washington DC 20375-5343, USA<sup>2</sup> Ufa Technical University, Institute of Materials Physics, Ufa, RUSSIA<sup>3</sup> JRC, Institute of Advanced Materials, I-21020 Ispra (VA), ITALY<sup>4</sup> University of Bologna, Department of Physics, Bologna, ITALY

Due to their elevated temperature properties such as high strength, oxidation resistance, and high melting temperature, the chromium-based alloys are potentially very attractive for variety of structural applications. However, when compared to the structural steels or the nickel-based superalloys, the major drawback of the high chromium alloys is their low ductility and fracture toughness, and the unacceptably high ductile-to-brittle transition temperature. During past thirty years, limited studies both theoretical and experimental have indicated that the ductility and fracture toughness properties of these alloys can be significantly improved by refining the microstructure to nanoscale dimensions. In this paper we will present initial mechanical property results of pure chromium and of Cr5Fe and Cr45Fe alloys whose grain structure was refined by two different processing techniques: severe plastic deformation and high vacuum ball-milling. These results are part of a larger collaborative effort involving our laboratories whose basic objective is the enhancement of the mechanical properties of high-chromium alloys through grain refinement. Besides the mechanical property results, we also present and discuss the results of the microstructural analysis both on the unstained and strained materials and the corresponding fractographic features of the fractured samples together with structure-property correlations. The possible mechanisms for the improved mechanical properties resulting from the nanoscale structure will be discussed.

---

**FACTORIAL ENHANCEMENT IN THERMOELECTRIC FIGURE  
OF MERIT WITH Si/Ge SUPERLATTICE STRUCTURES**

*R. Venkatasubramanian and E. Siivola*

Research Triangle Institute, Research Triangle Park, NC 27709, USA

Freestanding, thin-film, Si/Ge superlattice (SL) structures over a wide range of periods, from  $\sim 300\text{\AA}$  to  $\sim 10\text{\AA}$ , have been experimentally investigated for their thermoelectric properties in the plane of the SL interfaces. We have observed a several-fold enhancement in the power factor at 300K in these Si/Ge SL structures, compared to thin-film SiGe and bulk SiGe alloys. The thermoelectric power factor and Hall-effect measurements, with model calculations for effective conduction-band density of states, have been used to understand the mechanism behind the strong enhancement in power factor in these apparently weakly-quantum confined SL structures. AC calorimetry measurements have also been completed to determine the in-plane thermal diffusivity of these Si/Ge SL thin-films. The variation of thermal conductivity ( $k$ ) with the SL period appears complex, with reduction in  $k$  coming apparently from both short-period and lattice-mismatch effects. Finally, we will present the first experimental demonstration of a *factorial* improvement in the three-dimensional figure-of-merit ( $ZT_{3D}$ ) of Si/Ge SL structures with respect to comparable bulk SiGe alloys, with all the properties measured in the same direction, suggesting a proof-of-concept validation for thin-film SL structures. The implications of the ZT enhancement with Si/Ge SL structures would be significant for a variety of applications.

**MOLECULAR SHUTTLES AND NANOTRACKS**

*John R. Dennis<sup>1</sup>, Jonathan Howard<sup>2</sup> and Viola Vogel<sup>1</sup>*

<sup>1</sup> Department of Bioengineering and <sup>2</sup> Department of Physiology and Biophysics,  
University of Washington, Seattle, WA 98195, USA

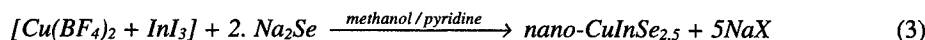
Nature has evolved specialized molecules, namely motor proteins, to actively transport molecules over long distances and against concentration gradients. Our goal is to develop molecular shuttles that can operate on surfaces under ex-vivo conditions. This includes creating nano-engineered surfaces across which molecular motors move materials, under user control, and between user-specified locations. We have used polymers to create surface textures that act as tracks for the movement of microtubules on kinesin functionalized surfaces.

### NANO-Cu-In-Se AS A PRECURSOR TO CIS SOLAR CELLS

*Douglas L. Schulz, Calvin J. Curtis and David S. Ginley*

National Renewable Energy Laboratory, 1617 Cole Blvd., Golden,  
CO 80401-3393, USA <dginley@nrel.nrel.gov>

The use of nanoparticle colloids for spray deposition of Cu-In-Se precursor films and subsequent thermal treatment to form CuInSe<sub>2</sub> (CIS) films has been investigated. In the present study, the metathesis reaction between Na<sub>2</sub>Se in methanol at -78 °C and metal salts (i.e., Cu(BF<sub>4</sub>)<sub>2</sub> and/or InI<sub>3</sub>) in pyridine at -40 °C under inert atmosphere produced CuSe (Eq. 1), In<sub>2</sub>Se<sub>3</sub> (Eq. 2), and CuInSe<sub>2.5</sub> (Eq. 3) nanoparticle colloids in high yield.



Purified colloid was sprayed onto heated molybdenum-coated sodalime glass substrates to form CuInSe<sub>2.5</sub>/Mo and CuSe/In<sub>2</sub>Se<sub>3</sub>/Mo precursor films. These precursor films were subjected to various thermal treatments in an effort to produce large-grained CIS films from the nano-sized precursors. The annealed CIS films were characterized by scanning electron microscopy (SEM) and x-ray diffraction. Three different approaches were employed including annealing a CuInSe<sub>2.5</sub>/Mo film (Fig. 1a), annealing a composite CuSe/In<sub>2</sub>Se<sub>3</sub>/Mo film (Fig. 1b), and annealing both these types of films with Se in a sealed tube. In all instances, very little evidence of liquid-assisted growth was observed and small-grained CIS films were the products. Results of initial grain boundary engineering experiment, with a goal of affecting the grain boundary defects in such a way as to produce electronic grade materials from particulate-based precursors, will be discussed.

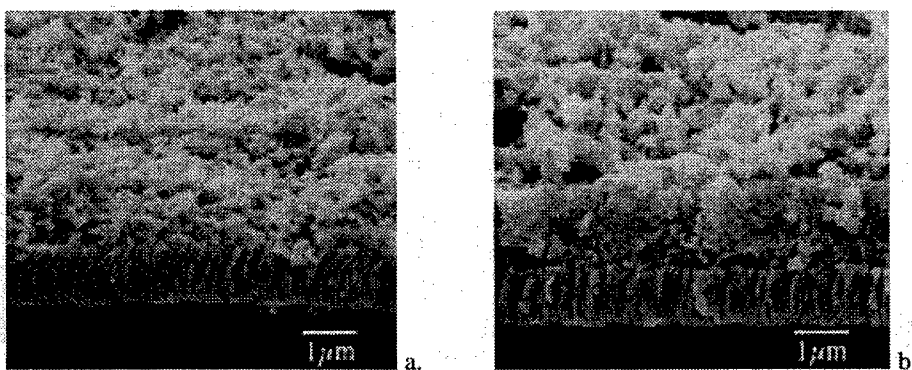


Figure 1. SEM photographs of (a) CuInSe<sub>2.5</sub>/Mo and (b) CuSe/In<sub>2</sub>Se<sub>3</sub>/Mo films annealed at 600 °C for 20 min under static Ar.

### NANOFABRICATED SUBSTRATES FOR PROBING SINGLE BIOMOLECULES BY SURFACE ENHANCED RAMAN SCATTERING

*Linda Hedberg<sup>1</sup>, Sarunas Petronis<sup>1</sup>, Bengt Kasemo<sup>1</sup>, Hongxing Xu<sup>2</sup>, Mikael Käll<sup>2</sup> and Lars Börjesson<sup>2</sup>*

<sup>1</sup>Chemical Physics Group and <sup>2</sup>Condensed Matter Physics Group,  
Chalmers University of Technology, 412 96 Göteborg, SWEDEN  
<linda@fy.chalmers.se>

The effect of Raman scattering enhancement when coherent laser light interacts with molecules attached to rough surfaces and microscopic metal domains has been known for more than two decades and is called Surface Enhanced Raman Scattering (SERS). The intensity of the Raman signals for such molecules is frequently enhanced by a factor  $10^5$ - $10^6$  at best [1, 2]. However recently much larger enhancement factors, in the range  $10^{14}$ - $10^{15}$ , have been observed for molecules adsorbed on colloidal silver particles of specific dimensions [3, 4]. This giant enhancement allows the recording of vibrational spectra from a *single* molecule for the first time, instead of the ensemble averaged spectra from many molecules, which are normally obtained in optical spectroscopies.

Here we report on an attempt to use nanolithography to fabricate structures of silver in the size range 100 - 200 nm and having different shapes in order to explore the size and geometry dependence of the SERS effect. Microfabricated structures which give the highest enhancement could be used for probing different biomolecules and perhaps designing a biosensor. SERS active substrates were prepared as arrays of silver particles on a Si wafer. Within each array the silver particles had a constant shape, size and separation. Three particle shapes (circular, triangular and square), two particle sizes (100 nm and 200 nm), and five different particle separations (10, 50, 100, 150 and 200 nm) were produced by electron beam lithography with a double-layer resist system and "lift-off" procedure. A reference area of uniformly deposited Ag film mimicked an infinite silver surface. The final structures and the chemical composition of the silver particles were characterized by Scanning Electron Microscopy (SEM) and Auger electron spectroscopy (AES), respectively.

Preliminary Raman scattering experiments have been performed on the dye-molecule Rhodamin 6G adsorbed on the nanofabricated substrates. A giant enhancement of the Raman signal was observed on all patterns, but not on the Ag film or the Si surface. There was, however, a very high fluorescence background compared with spectra obtained from the uniform Ag film. This suggests the necessity of a metal film shield under the patterns for depressing the fluorescence level in future experiments.

- 1) M.Moskovits, *Rev. of Mod. Phys.*, vol. 57, No 3, 1985, pp 783-826;
- 2) A.G.Mal'shukov, *Phys. Rep.*, vol 194, Nos 5&6, 1990, pp 343-349;
- 3) K.Kneip et al., *Phys. Rev. Lett.*, vol. 78, No 9, 1997, pp1667-1670;
- 4) S.Nie, S.R. Emory, *Science*, vol. 275, No 21, 1997, pp 1102-1106.

**OSTEOBLAST FUNCTION ON NANOPHASE ALUMINA**

*Thomas J. Webster, Richard W. Siegel\* and Rena Bizios*

Departments of Biomedical Engineering and \* Materials Science and Engineering  
Rensselaer Polytechnic Institute, Troy, NY 12180-3590, USA <webstt2@rpi.edu>

The function (such as adhesion and proliferation) of osteoblasts (the bone forming cells) on the surface of nanophase alumina was investigated *in vitro*. Circular alumina ( $\gamma$ - $\text{Al}_2\text{O}_3$ ) samples (10 mm in diameter; 2 mm in thickness) were prepared by compacting nanophase (20-67 nm grain size) alumina powder (Nanophase Technologies Corp.) in a tool-steel die *via* a uniaxial pressing cycle (0.2 GPa to 1 GPa over a 10 minutes period). Nanophase compacts were sintered (in air at 10°C/min) from room temperature to a final temperature of 1000°C to obtain grain sizes in the range of 20 - 100 nm. Conventional alumina compacts (controls) were sintered (in air at 10 °C/min) from room temperature to a final temperature of 1200°C to obtain grain sizes greater than 100 nm. All compacts were degreased, ultrasonically cleaned and sterilized. Borosilicate glass coverslips (reference material) were etched in 1N NaOH and prepared for cell culture experiments. For adhesion studies, osteoblasts (3500 cells/cm<sup>2</sup>) were seeded in Dulbecco's Modified Eagle Medium (DMEM; in the presence and absence of 10% fetal bovine serum) for 0.5, 1, 2, and 4 hours. For proliferation studies, osteoblasts (2000 cells/cm<sup>2</sup>) were seeded in DMEM (in the presence of 10% fetal bovine serum) for 1, 3, and 5 days. All experiments were conducted in a 37°C, humidified, 5% CO<sub>2</sub>/95% air environment. At the end of the prescribed times, the cells were fixed, stained and counted *in situ*. All experiments were run in triplicate and repeated at three different times. Numerical data were analyzed statistically using student t-tests.

Osteoblasts did not adhere on alumina in the absence of serum. In the presence of 10% serum, however, osteoblast adhesion on nanophase alumina was significantly ( $p < 0.01$ ) greater than on borosilicate glass for all time periods tested in the present study; when compared to borosilicate glass, osteoblast adhesion on nanophase alumina increased by more than 50% for all time periods tested. Since proteins mediate cell adhesion on substrates, the present data imply that nanophase materials may promote interaction(s) (such as adsorption, configuration, bioactivity, *etc.*) of select serum protein(s) and, thus, enhance subsequent osteoblast adhesion.

**CERAMIQUE-COPPER METAL-MATRIX NANOCOMPOSITES  
PREPARED BY REACTIVE MILLING.**

*K. Tousimi, and A.R. Yavari*

LTCPCM-CNRS, BP75, Institut National Polytechnique de Grenoble  
Domaine Universitaire, ST. Martin-d'Hères 38402, FRANCE  
[<euronano@ltpcm.inpg.fr>](mailto:<euronano@ltpcm.inpg.fr>)

We report on the preparation of ceramique-copper matrix nanocomposites of selected compositions. The new method consists of milling a copper alloy containing a second element with a stable oxide, in a reactor mill under controlled oxygen atmosphere, in such a way as to oxidize only and all the added element and not the copper matrix. Such selective oxidation of various alloys has been achieved by introducing in the milling atmosphere the exact quantity of oxygen needed for obtaining a ceramique-Cu matrix composite.

This method of controlled reactive milling has been successfully applied to systems such as CuTi, CuZr, and CuHf, so as to prepare Cu-TiO<sub>2</sub>, Cu-Zr O<sub>2</sub> and Cu-Hf O<sub>2</sub> nanocomposites which can have interesting applications due to their nanostructures, mechanical and electrical properties. Results on TEM, X-rays and DSC characterization will be presented.

**THE MOLECULAR CLUSTERS-MATERIALS FOR NANOELECTRONICS**

*V.V. Kislov<sup>1</sup>, V.V. Kolesov<sup>1</sup>, S.P. Gubin<sup>2</sup>, E.S. Soldatov<sup>3</sup> and A.S. Trifonov<sup>3</sup>*

<sup>1</sup> Institute of Radioengineering&Electronics, Russian Academy of Sciences, RUSSIA  
*<kvv@mail.cplire.ru>*

<sup>2</sup> Institute of General and Inorganic Chemistry, Russian Academy of Sciences, RUSSIA  
<sup>3</sup> Physics Department, Moscow State University, RUSSIA

This is known that in molecular tunnel nanostructures already under room temperatures can be appear different quantum-dimensioned effects, for instance, correlated single-electronic tunnelling. One of the perspective ways of making the tunnel junction with small dimensions is the using a metallofullerens and the carbon-containing atomic clusters. Syntheses of cluster materials are already well developing area of chemical technology. Metallic cluster is a good candidate on the role elementary unit for making the single-electronic devices with the small scattering of parameters, since features and parameters of tunnel transport through cluster are defined by only its chemical composition. In this work the clusters  $Pd_3(CO)_3[P(C_6H_5)_3]_4$ ,  $Pt_5(CO)_6[P(C_2H_5)_3]_4$ ,  $Pd_{10}(CO)_{12}[P(C_4H_7)_3]_6$  were used.

Planar nanostructures were formed on surfaces highoriented pyrolytic graphite. On first stage the monomolecular layer of stearic acid was deposited on the surface of substrate by the Langmuir-Shaefer method. Then on the monolayer stearic acid was formed monolayer of corresponding clusters material.

The study of tunnel transport in the created nanostructure was produced by STM/STS methods. The topographical STM-images of the planar ordered molecular cluster structures are received. The I-V curves were measured under the topographical study. Curves had practically symmetrical form. The distinctive particularity nearly beginning of co-ordinates was observed on all I-V curves. This particularity caused by so called the Coulomb blockade, when alongside with background tunnel current begin to observe effects of correlated tunneling the separate electrons. The I-V curves of Langmuir layers from metallic cluster molecules without dielectric sublayer nearly zero had approximately line form. The value of the Coulomb blockade potential can be estimated by extrapolations linear branch a I-V curve from the area with the large tunnel current before intersection with the axis of ordinates. For clusters  $Pd_3(CO)_3(PPh_3)_4$ ,  $Pt_5(CO)_6(PEt_3)_4$ ,  $Pd_{10}(CO)_{12}(PBu_3)_6$  value of the Coulomb blockade potential lies within the range of accordingly 460-470 mV, 230-240 mV, 270-290 mV. Differential tunnel conductivity curves  $dI/dV$  also show a suppression of conductivity in the area of small voltages. Evaluation of the Coulomb blockade energy  $\Delta_\pi = e^2/2C$  on the base known geometric dimensions of single clusters gives qualitative same results.

**NANOTECHNOLOGY: A DATA STORAGE PERSPECTIVE**

*Arik Menon*

Read-Rite Corporation Miliptas, CA, USA

The exponential increase in a real density of recording of magnetic storage devices has reduced the recorded bit size to nano length scale. This has profound implications on all aspects of the storage system including recording device modeling, materials, fabrication, metrology, characterization, and tribology of the head-disk interface. In this paper, the impact of nanotechnology in extending the data storage device storage systems is explored with an emphasis on the fabrication and characterization of nanolayers and structures.

**NANOSTRUCTURED FILMS  
FOR EXTREMELY HIGH DENSITY MAGNETIC RECORDING**

*D.J. Sellmyer, M. Yu, C.P. Luo, R. Thomas and Y. Liu*

Center for Materials Research and Analysis University of Nebraska, Lincoln, NE, USA

We report results on the growth and magnetic properties of nanocrystalline magnetic films with high anisotropy and relatively high coercivity (5-10 kOe). Emphasis is on Co-rich films including Co-R where R = Pr, Sm, Fe-Pt and related alloys. An important issue addressed is that of thermal stability as the grain size decreases below 10 nm, which is required as the areal density exceeds about 20 Gbits/in<sup>2</sup>. Measurements of activation volumes and derived magnetic cluster dimensions are presented and compared with the nanostructure of the films. Likely ultimate limits for the areal density of longitudinal continuous film media are discussed.

\* Research supported by NSF, NSIC and CMRA.

**SUPERPARAMAGNETISM AND DYNAMIC COERCIVITY  
IN MAGNETIC RECORDING MEDIA**

*D. Weller, A. Moser, M. Best, M. Doerner L. Folks, B. Jones and J. Kaufman*

IBM Almaden Research Center, K11B, 650 Harry Rd., San Jose, CA 95120, USA

Superparamagnetic effects may pose a serious limitation to the achievable real density in magnetic recording. If conventional head and media scaling approaches prevail, such a limit may be reached in about 5 years at densities near  $40 \text{ Gb/in}^2$  [1].

The present talk will discuss basic physical models underlying the above superparamagnetic limit prediction. We will emphasize that there is a time and grain size dependence of coercivity and retentivity. This has been observed in artificially thinned media of thickness  $< 10 \text{ nm}$ . A particularly elegant way of characterizing media decay is to examine the time dependence of the remanent coercivity. We will discuss such an experiment, which allows measurements in the  $10 \text{ ns}$  to  $10 \text{ s}$  range, i.e. over 9 decades in time [2]. The accuracy is sufficient to test the data against available models and to extract parameters like the intrinsic switching / anisotropy field and the stability ratio  $KV/kT$ . These data will be compared with a recent experiment that was performed at a much shorter, picosecond, timescale [3]. Under such conditions the switching is dominated by dynamic processes, i.e. initial fast precession followed by damped relaxation.

- [1] S.H. Charap, Pu-Ling Lu, Yanjun He, *Thermal Stability of Recorded Information at High Densities*, IEEE Trans. Mag., Vol. 33, 978 (1997).
- [2] A. Moser, D. Weller, M. Best and M. Doerner, MRS Spring Meeting, San Francisco, April 13-17, 1998
- [3] Ch. Back et al. (submitted to Physical Review Letters, 1998)

**GIGABIT NANOSCALE BISMUTH OXIDE ELECTRODE  
SELF-PATTERNING FERROELECTRIC THIN FILMS  
FOR MEMORY APPLICATION**

*J. F. Scott, M. Alexe, C. Curran, A. Pignolet, D. Hesse, and N. D. Zakharov*

Max Planck Institute for Microstructural Physics, Halle (Saale), GERMANY

A fundamental limitation on the recent development of ferroelectric thin-film memories in the 64 Mbit - 4 Gbit density regime has been the ability to scale capacitor cell sizes below 1 sq. micron. Until now the smallest cells reported were 0.7 x 0.7 microns for the NEC memory and 1.0 x 1.0 microns from Mitsubishi. Here we report self-assembling bismuth nano-electrode cells of ferroelectric thin films of bismuth titanate and strontium bismuth tantalate which are 50x smaller than the previous NEC record.

We have produced rectangular planar arrays of crystalline conducting delta-phase bismuth oxide ( $\text{Bi}_2\text{O}_3$ ) on ferroelectric thin-film capacitors of bismuth-containing layer-structure perovskites. The nano-electrodes are rather uniform in size -- depending upon processing conditions the maximum sizes are ca. 125 x 125 nm, and the nano-electrodes are well separated from each other with no overlap or terraces, yielding ca. 1 Gbit of accessible cells per chip. Under sol-gel, metal-organic decomposition (MOD), or pulsed laser deposition (PLD), bismuth titanate (BiT) and strontium bismuth tantalate (SBT) films segregate out metallic elemental bismuth at the surface (Hartmann, Scott, et al., IMF-9, Seoul, in press). Previous XPS data showed that about 30% of the surface Bi in SBT is metallic and 70% is oxidised  $\text{Bi}^{3+}$ . Angular dependence revealed that the metallic Bi is confined to the surface. Our new SEM, TEM, and AFM studies of epitaxial PLD films shows that an ordered array of crystalline, mesa-like bismuth islands, 45 nm high, grows on the surface during cooling (crystalline Bi results in vacuum; in air, the conducting delta-phase of bismuth oxide crystallises). These have a well-defined nearest neighbour separation of 150 nm and a strong rectangular angular correlation function peaking every 90 degrees. We have measured switching with these nanoelectrodes and leakage currents through them. The latter are ohmic up to 0.6 V and quadratic in V (space charge limited) above that.

**LIQUID CHROMATOGRAPHY USED TO SIZE-SEPARATE THE  
AMPHIPHILIC-MOLECULES STABILIZED NANO-PARTICLES  
OF CdS IN THE 1-10 nm RANGE**

*R. Sivamohan<sup>1</sup>, H. Takahashi<sup>2</sup>, A. Kasuya<sup>1</sup>, S. Tsunekawa<sup>1</sup>, S. Ito<sup>1</sup>, K. Tohji<sup>2</sup> and  
B. Jeyadevan<sup>3</sup>*

<sup>1</sup> Institute for Materials Research, Tohoku University, Sendai, 980-77, JAPAN

<sup>2</sup> Dept. of Geosciences and Technology, Tohoku University, Sendai, 980-77, JAPAN

<sup>3</sup> Mining College, Akita University, Akita, 010, JAPAN

The making of nano-particles in the 1-10 nm range in micro-emulsions, the surface coating of these by the amphiphilic-molecules in the same microemulsion and the subsequent treatment of the oil-phase based particles in the liquid chromatography (HPLC) is the focus of this work.

A reverse phase preparative column using a bonded phase was used. Silica (5  $\mu$ m diameter, 120 Å pore size) with C<sub>18</sub> (ODS) bonded phase is the stationary phase. Toluene is used as the mobile phase. The CdS nanoparticles in the mobile phase was continuously monitored by UV spectroscopy. The CdS products were collected at different time intervals.

For a relatively coarse feed, in 5.7 nm range, a rich product with a sharp size distribution can be obtained. HRTEM micrograph shows that the product is well crystallized.

The eluted products from the HPLC were treated separately in a Size Exclusion Chromatography. SEC elution times show that the different HPLC products come out in different time intervals suggesting the possibility of nano particle size separation by SEC.

The tendency of the surfactant coated nano-particles to aggregate in the polar solvent severely limits the possibility of separating the nano-particles by HPLC using the solvophobic mechanism of the HPLC. We are in the process of experimentally characterizing the aggregation tendency of the surfactant coated nano-particles.

**MECHANICAL PROPERTIES OF MULTILAYER MATERIALS**

*D. Josell<sup>1</sup>, D. van Heerden<sup>2</sup>, D. Shechtman<sup>3</sup>, and D. Read<sup>4</sup>*

<sup>1</sup> National Institute of Standards and Technology, Gaithersburg, MD, USA  
<Daniel.Josell@nist.gov>

<sup>2</sup> The Johns Hopkins University, Baltimore, MD, USA  
<sup>3</sup> Technion, Haifa, ISRAEL

<sup>4</sup> National Institute of Standards and Technology, Boulder, MD, USA

Nanoindentation studies have shown that the hardness of metal/metal multilayers increases as the individual metal layers are made thinner. We conducted uniaxial tensile tests on free standing aluminum/titanium multilayer thin films in order to determine whether the yield stresses and ultimate tensile strengths of these materials are similarly affected. The aluminum/titanium system was selected for its low density.

We observed a distinct transition from elastic to plastic behavior at a value of stress which increased with decreasing layer thickness. The yield stress increased from approximately 450 MPa to more than 700 MPa as we reduced the bilayer thickness from 90 nm to 13 nm. The multilayers possessed higher specific strengths (fracture stress divided by material density) than other multilayer materials described in the literature. They also possessed higher specific strengths than high strength aluminum alloys, with values approaching those of high strength steels.

A controversy exists concerning the crystal structure of the titanium phase in titanium/aluminum multilayers; the equilibrium bulk structure is hexagonal close packed at room temperature, but face centered cubic titanium has been seen by transmission electron microscopy (TEM) of cross-sectioned multilayer specimens. We address this issue with reflection and transmission geometry x-ray studies of the as-deposited multilayer films and TEM of cross-sectioned specimens.

**PREPARATION, SOME PROPERTIES AND APPLICATIONS OF ULTRAFINE AEROSOL PARTICLES OF METALS, THEIR ALLOYS AND COMPOUNDS***Yu.I. Petrov*

Semenov Institute of Chemical Physics, Russian Academy of Sciences,  
Kosygin str.4, 117977 GSP-1, Moscow, RUSSIA <shafr@chph.ras.ru>

Distinctions of preparing ultrafine particles of substances by "gas condensation" method are discussed. The main results of thermal, magnetic, electronic and optical investigations of prepared particles are given. Some aspects of their application are considered. The report summarize the author experience of long-term (more than 40 years) work in the nanoscale material science.

1. M.Ya. Guen, M.S. Ziskin and Yu.I. Petrov. The dependence of the Al aerosol dispersivity on conditions of their formation. Dokl. Akad. Nauk (in Russian), 1959, Vol.127, p.366-368.
2. M.Ya. Guen and Yu.I. Petrov. The dispersed condensate of metal vapours. Uspekhi Khimii (Advances in Chemistry), 1969, Vol.38, p2249-2278 (in Russian)
3. Yu.I. Petrov and V.A. Kotelnikov. Lattice contractions in microcrystals of metals in the range of overheating. Phys. Stat. Sol.,1969, Vol.34, K123-K127.
4. Yu.I. Petrov. Physics of small particles. Moscow: Nauka, 1982, 359 p.(in Russian).
5. Yu.I. Petrov. Clusters and small particles. Moscow: Nauka, 1986,367 p.(in Russian)
6. Yu.I. Petrov. Surface pressure in clusters and small particles - Is it real ? Phase Transitions, 1990, Vol.24-26, p. 407-417.
7. Yu.V. Baldokhin and Yu.I. Petrov. Two states of the face-centered-cubic structure in iron discovered while investigating the Mössbauer spectra and the thermal expansion of small particles. Dokl. Akad. Nauk, 1992, Vol.327, p.87-91. Translated in Sov. Phys. Dokl. Vol.37(11), November 1992, 563-565, American Institute of Physics.
8. Yu.I. Petrov. A new view on the surface stresses in condensed media. Phase Transition, 1993, Vol.45, p.221-250.
9. Yu.V. Baldokhin, P.Ya. Kolotyrkin Yu.I. Petrov, and E.A. Shafranovsky. Some specific features of fine Fe and Fe-Ni particles. J.Appl.Phys.,1994, Vol.76, p.6496-6498.
10. Yu.I. Petrov and G.A. Lontsova. Photoconductivity of a high-dispersed CdSe films. Doklady Akademii Nauk (in Russian), 1995, Vol.343, p. 345-349.
11. Yu.V. Baldokhin, P.Ya. Kolotyrkin Yu.I. Petrov, and E.A. Shafranovsky. Comparative study of the structure and local magnetic order in bulk and ultrafine particles of Fe-Mn(32%-35%) and Fe<sub>3</sub>Pt. J.Appl.Phys.,1997, Vol.82, p.3042-3047.

**MICROSTRUCTURE OF SPUTTER-DEPOSITED  
Co-Al-O GRANULAR THIN FILMS**

*M. Ohnuma<sup>1</sup>, K. Hono<sup>1</sup>, H. Onodera<sup>1</sup>, S. Mitani<sup>2</sup> and H. Fujmori<sup>2</sup>*

<sup>1</sup> National Research Institute for Metals, Tsukuba 305, JAPAN <oh-numa@nrim.go.jp>

<sup>2</sup> Tohoku University, Sendai 980-77, JAPAN

Recent findings of giant magnetoresistance (GMR) in metal oxide granular thin films such as Co-Al-O receive much research interest, because the mechanism of the GMR is different from that observed in metallic granular films. The high electrical resistivity and its negative temperature dependence suggest that the electrical conduction occurs by tunneling among metallic particles which are embedded in the insulating matrix. In this work, we have studied microstructures of  $\text{Co}_{72}\text{Al}_{28}\text{-O}$  films with different oxygen concentrations by means of x-ray and electron diffraction, transmission electron microscopy (TEM), high resolution electron microscopy (HREM) and small-angle x-ray scattering (SAXS), in order to clarify the correlation between the microstructures and the electron transport behaviors.

The specific resistivity of  $\text{Co}_{72}\text{Al}_{28}\text{-O}$  films under zero field increases abruptly when oxygen content in the film exceeds 20 at.%. GMR also appears above this concentration. The microstructures of the films are composed of extremely fine grains of approximately 2-3 nm in diameter and are embedded in the amorphous oxide matrix. Figure 1 shows a typical HREM image of the film exhibiting the largest MR ratio. Lattice fringes are clearly observed from the particle, and the stacking of the fringes imply that planar faults exist. For example, the stacking of the planes in the upper part consists of three types of planes, like A, B, C, A, B, C ...., and corresponds to the fcc structure, but the lower part exhibits the feature of the hcp stacking consisting of two types of planes, like A,B,A,B..... In the energy dispersive X-ray spectra measured from the center of the granular particles, no Al spectrum is observed, suggesting that the granular particles are essentially pure Co. No fringes are observed from the matrix phase between the metallic particles, suggesting that the matrix is amorphous aluminum. In order to evaluate the difference in the microstructures more quantitatively, SAXS has been measured for these films. All specimens except for the  $\text{Co}_{71}\text{Al}_{29}$  film show clear peaks which are attributed to inter-particle interference. From the analysis of these peak positions, we have found that a maximum MR appears when the interparticle distance is minimum. These observations are consistent with the electron tunneling mechanism as the origin of magnetoresistance.

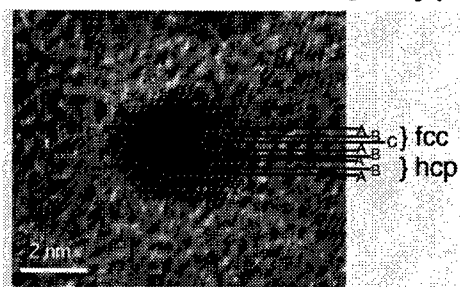


Fig. 1 High-resolution transmission electron micrograph of  $\text{Co}_{52}\text{Al}_{20}\text{O}_{28}$  films. The upper part of the particle exhibits the feature of fcc stacking and the lower part shows hcp stacking.

**SYNTHESIS AND CHARACTERIZATION  
OF NANOCRYSTALLINE WC-Co COATINGS**

*M.L. Lau, B. Huang and E.J. Lavernia*

Department of Chemical and Biochemical Engineering and Materials Science,  
University of California, Irvine, CA 92697-2575, USA <maggylau@uci.edu>

The present paper describes the synthesis and characterisation of nanocrystalline WC-Co coatings. The feedstock powders were prepared by mechanical milling which micron-sized powders were milled in either hexane environment to produce agglomerates with an average grain size of less than 100 nm. The powders were introduced into the high velocity oxy-fuel (HVOF) process to produce nanocrystalline coatings. X-ray diffraction analysis and transmission electron microscopy were used to determine the average grain size of the milled powders. Furthermore, scanning electron microscopy and transmission electron microscopy were used to examine the particle morphology as well as the microstructure of the as-sprayed coatings. In addition, coating properties were characterised by hardness and abrasion wear measurements. The properties of the nanocrystalline coatings are compared to those of the micron-sized conventional WC-Co coatings.

### NANOSTRUCTURING OF POLYMER SURFACES BY GAS PLASMA TREATMENT

*M.B. Olde Riekerink, J.G.A. Terlingen, G.H.M. Engbers, and J. Feijen*

Department of Chemical Technology, University of Twente, P.O. Box 217, 7500 AE  
Enschede, THE NETHERLANDS <m.b.olderiekerink@ct.utwente.nl>

Plasma treatment processes are extensively used for the modification of the surface chemistry of polymeric materials. However, the use of plasma treatments for tailoring the surface morphology has found far less applications. Structuring of a polymer surface on the nanoscale level is of interest for several areas such as biomedical technology, membrane technology and the microchips industry. The aim of this study is to develop nanostructured polymer surfaces by selective plasma etching of semi-crystalline polymers. In this case, preferential etching of the amorphous phase is expected. The etching behaviour and surface structural changes of a range of commercial poly(ethylene) (PE) grades (14-59% crystallinity) were studied using a tetrafluoromethane ( $\text{CF}_4$ ) radio-frequency plasma (48-49W, 0.06-0.07 mbar, continuous vs. pulsed treatment). With increasing crystallinity a significant and almost linear decrease of the etching rate was found, ranging from 50 Å/min for LLDPE to 35 Å/min for HDPE. This indicates that the amorphous phase of PE was etched faster than the crystalline phase. XPS analysis revealed that during  $\text{CF}_4$  plasma treatment the PE surfaces were highly fluorinated up to F/C ratios of 1.6. Moreover,  $\text{CF}_4$  plasma treatment of PE resulted in extremely hydrophobic surfaces as was found by water contact angle measurements. Advancing angles up to 150° were measured for treated LDPE films. Both SEM and AFM analysis revealed that pronounced surface restructuring took place during prolonged continuous plasma treatment ( $\geq 15$  minutes). The lamellar surface structure of LDPE changed into a nanoporous-like structure (figure 1). However, pulsed plasma treatment did not result in any surface structural changes. Therefore, the restructuring of continuously plasma treated surfaces was attributed to a combined effect of etching and an increase of surface temperature, resulting in phase separation of PE-like and PTFE-like material of which the latter is surface oriented.

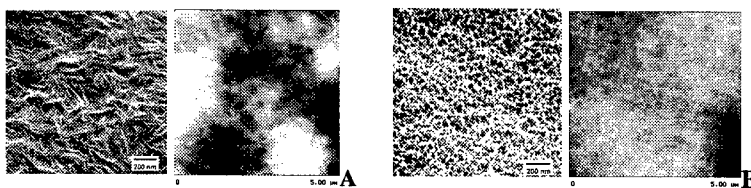


Figure 1. SEM (left) and AFM (right) images of untreated (A) and plasma treated (B) LDPE surfaces.

This study showed that prolonged  $\text{CF}_4$  plasma treatment of PE resulted in a selective etching process. During this treatment the PE films were highly fluorinated and extremely hydrophobic surfaces were formed. Moreover, a change of surface structure was observed leading to uniform pores and grains in the order of tens of nanometers.

**TEM AND HREM STUDY OF THE 3D SUPERLATTICE CONSISTING  
OF NANOCLUSTERS IN SYNTHETIC OPAL MATRIX**

*L.M.Sorokin, J.L.Hutchison\*, V.N.Bogomolov and T.N.Zaslavskaya*

A.F.Ioffe Physico-technical Institute of the Russian Academy of Sciences  
Polytechnicheskaya str. 26, 194021 St.-Petersburg, RUSSIA

\*Department of Materials, Oxford University, Oxford, Parks Road, OX1 3PH, U.K.

Fabrication of various types of nanostructures is a major objective in present-day electronics technology. Nanostructures in the form of one-dimensional superlattices produced by MBE or MOCVD enjoy currently wide-spread use. Further progress in electronics requires development of structures with still higher degree of device integration, a goal which, in principle, can be achieved by reducing device size and using the third dimension. In principle obtaining structures with up to  $10^{14}$  devices per unit volume is possible already with elements (clusters) submicron size. A number of publications deal with the engineering of such structures using the matrix method [1-3].

The dielectric matrix (for example, synthetic opal) with inserted a semiconductor or metal material in its regularly distributed voids can serve as a novel type of nanocomposites.

Thus so-called 3D superlattices or cluster lattices are produced in opal matrix. Unusual bulk properties of these nanostructures are compiled from the properties of individual clusters either through united energy system or by means of the proximity effects of both sublattices if the specific lengths of material (free length for "quasiparticle", coherency length for superconductor) are comparable with the dimension of structural elements of system under study. They are also due to the high concentration of similar clusters and depend on the properties of the interconnections (channels) between neighbouring clusters.

The synthetic opal, similarly to natural one, consists of closed-packed amorphous silica ( $\text{SiO}_2$ ) spheres fairly uniform in size (200-250 nm in diameter). The regularly distributed the octa- and tetrahedral voids amount to 22-26% of the total volume of opal matrix. As determined from geometrical considerations the dimensions of the voids (i.e. the diameters of inscribed spheres) are in the ranges of ~ 45-55 and 85-105 nm, respectively).

It thus appears essential to study by TEM the structural state of the cluster material, the possibility of crystallization of a substance in microscopic volumes, the effect of channels between voids on the crystallographic orientation of a given crystallizing cluster relative to its neighbors, as well as the void filling pattern dependence on the method used to impregnate the guest materials (Te, GaAs, InSb, In).

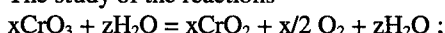
**ULTRAFINE CHROMIUM DIOXIDE POWDERS**

*M.G. Osmolovski and L.Yu.Ivanova*

St Petersburg State University, Universitetskii pr.2, St.Petersburg,  
Petrodvorets 198904, RUSSIA <chezhina@nc2490.spb.edu>

Ultrafine powders of CrO<sub>2</sub> , are known for rather a long time, they are applied in magnetic recording. However, a realistic description of the chemical processes of their obtaining is still absent .

The study of the reactions



$x\text{CrO}_3 + (y_1 + y_2) \text{Cr}_2\text{O}_3 + z\text{H}_2\text{O} = (x + 2y_1) \text{CrO}_2 + y_2\text{Cr}_2\text{O}_3 + (x/2 - y/2) \text{O}_2 + z\text{H}_2\text{O}$  resulted in the conclusion that in both cases the hydrothermal synthesis amounts to crystallization of CrO<sub>2</sub> from the aqueous solution wth the ratio Cr<sup>VI</sup>/Cr<sup>III</sup> = 7: 2.

In all the cases during the hydrothermal synthesis one, two or more of the modifying additions are used. The formation of the compounds with the rutile-type structure, which further act as nanosize nuclei during the crystallization of ultrafine CrO<sub>2</sub> is the first aim of applying modifying agents.

The increase in. the coercive force H<sub>c</sub> , as the result of the increase in the magnetic anisotropy constant k<sub>2</sub> at the formation of the solid solutions (e.g., (Cr,Fe)O<sub>2</sub> ) is the second aim.

The precursor of the formation of nuclei can bc nanofragments of the modifying agent (e.g., SnO<sub>2</sub> ·nH<sub>2</sub>O), resulting from its peptization. The nuclei can result also from the spontaneous crystallization from the solution (for example CrSbO<sub>4</sub>). The formation of nuclei can be a multistage heteroepitaxial process.

The temperature of the beginning of CrO<sub>2</sub> crystallization depends on the size of the nanoparticles, being the potential nuclei, and on their crystal parameters. The maximum H<sub>c</sub> of the needle-shaped CrO<sub>2</sub> crystals is achieved when their thickness (diameter d) is rather close to 30 nm. In this case H<sub>c</sub> = f( d ) + nC , where C is the molar concentration of iron, and n is close to 40 Oe/mol % Fe.

A sensible combination of the selection of optimal components, their relationships, and the relationship of temperature-time-pressure allows us to ensure a high homogeneity of CrO<sub>2</sub> particles by the sizes and a desired complex of magnetic properties. The selection of optimal variants of the stabilization of the particle surface results in the improvement in the quality of magnetic tapes.

**HIGH STRENGTH AL-ALLOYS WITH NANO-QUASICRYSTALLINE PHASE AS MAIN COMPONENT**

*F. Schurack, J. Eckert and L. Schultz*

Institut für Festkörper- und Werkstoffforschung Dresden, Postfach 270016,  
01171 Dresden, GERMANY, <f.schurack@ifw-dresden.de>

The design of a new kind of Al-alloys based on the coexistence of aperiodic particles and fcc-matrix on a nanoscale is subject of the present investigation. The underlying microstructural concept has been investigated for  $\text{Al}_{92}\text{Mn}_6\text{Ce}_2$  and  $\text{Al}_{91}\text{Mn}_7\text{Fe}_2$  alloys with emphasis on the investigation of the formation of quasicrystalline or amorphous phases for different processing techniques. For that reason arc-melted prealloyed ingots as well as powder mixtures of pure elements were milled in a planetary ball mill at different intensity under various atmospheres ( $\text{O}_2, \text{N}_2, \text{H}_2$ ). For comparison, thin ribbons of the same alloys were produced by rapid solidification.

Due to the high Al content, mechanical alloying of mixtures of pure elements has to be supported by a process-control agent or by an excess amount of Al to prevent a significant change in the overall Al content due to sticking to the milling tools. In contrast, milling of prealloyed samples succeeded using alternating milling conditions. We found a more difficult formation of quasicrystalline phases upon milling than for rapid quenching assuming same nominal compositions. Whereas, depending on the cooling conditions, volume fractions of quasicrystalline particles of about 20-60Vol.% can be obtained for the melt-spun ribbons, there is an amorphization of initially existing intermetallic phases during milling. This will be discussed with respect to different kinetic conditions of these processes and their influence on the composition dependence and the effect of milling conditions on the phase formation. However, subsequent milling of the melt-spun ribbons leads to complete amorphization of the quasicrystalline as well as of the remaining intermetallic phases. Extended milling of these samples induces secondary crystallization. The grain size of the quasicrystalline particles and of the surrounding fcc-matrix amounts to less than 50 nm after rapid quenching and to less than 20 nm already after short milling.

The thermal stability of the material was analyzed by DSC-measurements yielding crystallization of quasicrystalline regions at about 733 K. Microhardness measurements of the ribbons as well as first results of CERT-compression tests reveal promising mechanical properties compared to conventional Al-based alloys concerning the combination of strength and ductility.

**NANOSTRUCTURAL STATE AND MAGNETISM OF RFe<sub>2</sub>H<sub>X</sub> HYDRIDES  
OBTAINED BY HYDROGEN-INDUCED AMORPHYZATION**

*A.Ye. Yermakov, N.K. Zajkov, N.V. Mushnikov, V.S. Gaviko, V.V. Serikov and  
N.M. Kleinerman*

Institute for Metal Physics, Ural Branch of the Russia Academy of Sciences,  
S.Kovalevskaya Str.18, GSP-170, Yekaterinburg 620219, RUSSIA  
[yermakov@hotmail.com](mailto:yermakov@hotmail.com)

Amorphous hydrides obtained by alloy treatment in hydrogen under special conditions (hydrogen-induced amorphization) belong to a new and scarcely studied class. Amorphous hydrides on the base of RFe<sub>2</sub> (R- rare earth element) which had a crystal MgCu<sub>2</sub> type structure and being two-sublattice ferrimagnets have been studied in this work. Thermally activated deterioration of the long-range crystallographic order and variation of the amorphous matrix parameters (a width and position of the amorphous diffraction halo) are shown to take place under change of hydrogen treatment regimes. During amorphization process weakening of the intersublattice exchange interaction and strengthening of Fe-Fe exchange interaction occur.

Both due to the crystall field symmetry distortion inducing a local uniaxial anisotropy and nonuniform exchange interaction a canted magnetic structure is realized in a magnetic sublattices, which results in a considerable magnetic structure deformation in the field, which, in turn influences on magnetization curves (no ferrimagnetic saturation) and a great volume magnetostriction appears.

Magnetic data and studies of hyperfine fields on Fe<sup>57</sup> nuclei by the Mössbauer method make it possible to consider amorphous hydrides as chemically heterogeneous, cluster-like objects. They are characterized by two parameters of intersublattice exchange R-Fe interaction differing in an order of magnitude and, most likely, consist of structurally and chemically heterogeneous regions of nanocrystalline size. One of these parameters, the larger in value characterizes exchange inside the particles, the other, the smaller, is determined by the exchange at the boundary between them or interfaces properties. At high-temperature hydrogen treatment the diffusion of metal atoms between clusters takes place and then a rare-earth hydride and α-Fe are formed in final state.

**GREEN DENSITY EFFECTS IN THE SINTERING OF NANOCRYSTALLINE  
AND NEAR-NANOCRYSTALLINE CERAMICS**

S.M. Sweeney and M.J. Mayo

Department of Materials Science & Engineering, The Pennsylvania State University,  
University Park, PA 16802 USA <sms24@psu.edu, mayo@ems.psu.edu>

The manufacture of nanocrystalline ceramics has often required that samples be prepared under enormous (1-9 GPa) compaction pressures to achieve "suitable" green densities that lead to superior sintering behavior. Exactly how higher green density accelerates densification is, however, unclear. The present study examines the isothermal densification rates of a nanocrystalline and near-nanocrystalline ceramic (yttria-stabilized tetragonal zirconia and titania, respectively) compacted to a series of green densities between 45 and 66%; the corresponding compaction pressures are between 70 MPa and 1.1 GPa. Though different density-time curves are obtained for each green density, the different sets of data converge to a common master curve when plotted as normalized densification rate vs. inverse grain size (to the third or fourth power, depending on the system) times the inverse pore size. Since the grain size and grain growth kinetics for a given starting powder are the same for all green densities, these results suggest that differences in pore size are the root cause of the green density effect.

**INVESTIGATION OF NANOSIZED CERAMIC POWDERS  
PRODUCED BY MECHANOCHEMISTRY**

*Ying Chen*

Department of Engineering, FEIT & EME, RSPHYSSE,  
The Australian National University, Canberra, ACT 0200, AUSTRALIA  
<ying.chen@anu.edu.au>

This study demonstrates mechanochemical synthesis of metal nitride and carbide materials with both nanocrystalline structure and nanometre-sized particles. Ultrafine particles of metal carbides and nitrides with the particle size below 100 nm were formed in the course of ball milling at room temperature, during which chemical reactions (carburisation and nitridation) were realised by high energy ball impacts (collisions). The nanophase formation has been investigated as a function of different milling conditions. Nanosized structures were analysed using X-ray diffraction, scanning electron microscopy, high-resolution microscopy and surface area measurement, etc. Based on the observed structural changes in the milled materials, the nanophase formation seems to be due to a local reaction process whereby carburisation and nitridation reactions occur progressively during collision events. The low reaction temperature limits the grain growth of newly formed phases. The relationships between the formation of nanophases and the milling conditions will be discussed in details.

**DESIGNING ATOMIC CLUSTERS AS SUPER ATOMS**

*B. K. Rao, S. N. Khanna and P. Jena*

Department of Physics, Virginia Commonwealth University  
Richmond, VA 23284-2000, USA <[brao@saturn.vcu.edu](mailto:brao@saturn.vcu.edu)>

Using *ab initio* quantum mechanical calculations, we show that the size, composition, and charge of atomic clusters can be manipulated such that they can mimic different elements of the periodic table. This allows the possibility of using these clusters as building blocks for a new class of cluster-assembled materials with uncommon electronic, magnetic, and structural properties. We demonstrate this by carrying out a systematic study of the stability, atomic and electronic structure of  $KAl_n$  ( $n \leq 14$ ) clusters. We show that  $Al_{13}$  can be viewed as a super halogen atom (Cl) and the bonding between K and  $Al_{13}$ , in analogy with that of KCl, is ionic. We have identified two nearly degenerate structures for  $KAl_{13}$  clusters. One is a regular icosahedron of  $Al_{13}$  with the K positioned at a three-fold symmetry site on one of the triangular faces. In the second one (0.35 eV lower in energy), the two pentagons of the icosahedron are rotated relative to each other and the K is bonded to the four-fold site of a resulting square face. This preference of the K atom to bind to four Al atoms is evident from the study of smaller  $KAl_n$  clusters. The binding energy of K with  $Al_4$  is larger compared to that with  $Al_3$  or  $Al_5$ . Equilibrium geometries, binding energies, ionization potentials, and electron affinities of  $KAl_n$  clusters have been calculated systematically to establish if the electron affinity bears the signature of ionic bonding in  $KAl_{13}$ . Stability of crystals made of  $KAl_{13}$  units as building blocks has also been examined. Such crystals are found to be metastable and metallic even though  $KAl_{13}$  cluster is bound by ionic interactions. The results will be compared with most recent experimental data.

**ORDER-DISORDER TRANSITIONS  
IN A NANOCRYSTALLINE BALL MILLED Fe-40Al at% ALLOY**

*X. Amils<sup>1</sup>, J. Nogués<sup>1</sup>, S. Suriñach<sup>1</sup>, J.S. Muñoz<sup>1</sup>, S. Galianella<sup>2</sup> and M. D. Baró<sup>1</sup>*

<sup>1</sup> Labmater, Departament de Física, Universitat Autònoma de Barcelona,  
Bellaterra, E-08193 (Barcelona), SPAIN <baro@cc.uab.es>

<sup>2</sup> Dipartimento di Ingegneria dei Materiali, Università degli Studi di Trento,  
Mesiano, I-38050 (Trento), ITALY <Stefano.Galianella@ing.unitn.it>

It is well known that different metastable states with nanocrystalline microstructures can be induced to intermetallic powders by ball milling [1]. These non-equilibrium structures can potentially overcome some of the typical shortcomings of intermetallic compounds. In particular FeAl alloys have been proposed as high temperature structural materials [2]. Moreover, FeAl alloys exhibit interesting magnetic properties [3]. Ordered B2 Fe-40Al at% is paramagnetic at room temperature, however it becomes ferromagnetic when disordered.

In the present work the order-disorder-order transitions induced in Fe-40Al at.% powders by mechanical milling (disordering) and the posterior annealing (reordering) have been investigated. Their structural, mechanical, magnetic and calorimetric properties were studied by means of X-ray diffraction, Vicker's microhardness, vibrating sample magnetometer, Mössbauer spectroscopy and differential scanning calorimetry measurements.

Increasing the milling time in Fe-Al powders causes an increase in plastic strains and a reduction in the mean crystallite size (nanometric scale) and in the long-range order (disordered). A fully recovered alloy is obtained after an annealing for 1 hour at 700°C [4]. Ball milling also hardens the alloy, the microhardness values increase up to 900 HV after 72 hours of milling.

A high increase in magnetic moment of the alloys is induced during ball milling. These changes in magnetic moment are related to long range order and lattice parameter variations.

- [1] C.C. Koch, Materials Science Technology, eds. R.W. Cahn, P. Haasen and E.J. Kramer (VCH Weinheim), 15 (1991), p. 193.
- [2] N.S. Stoloff, Mat. Res. Soc. Symp. Proc., 39 (1985), p. 3.
- [3] P.A. Beck, Metall. Trans., 2 (1971), p. 2015.
- [4] S.Suriñach, S.Galianella, X.Amils, L.Lutterotti and M.D.Baró, Mat. Sci. For., 225-227 (1996), p. 395.

**HARDNESS OF COMPOSITIONALLY NANO-MODULATED TiN FILMS**

*E.Kusano, M.Kitagawa, A.Satoh, T.Kobayashi, H.Nanto, and A.Kinbara*

Kanazawa Institute of Technology, AMS R&D Center, Yatsukaho, Matsutou, Ishikawa,  
JAPAN <kusano@neptune.kanazawa-it.ac.jp>

It has been reported that the hardness of coatings can be enhanced by using nano-laminated multilayer structures. The mechanisms involved in the hardness enhancement have been described by the effects based on the difference in mechanical properties of two alternatively laminated films. Since the interface seems to play an important role in an enhancement of the properties, it is expected that the films with stronger lamination, with a large number of repeated layers, provide better tribological properties. A compositionally modulated multilayer film without any abrupt interfaces is one of the films of this type. In this study, hardness enhancement for compositionally nano-modulated TiN multilayer coatings has been studied.

Compositionally nano-modulated films have been deposited by a reactive gas flow rate modulation sputtering using a Ti target and N<sub>2</sub> gas. The modulation periods explored in this study ranged from 6.7 nm to 80 nm. The thickness of the modulated layer was 400 nm. A TiO<sub>2</sub>/Ti underlayer with a thickness of 100 nm was deposited for the entire sample films. The film structure was analysed by X-ray diffraction (XRD). The film composition depth profiles was obtained by X-ray photoelectron spectroscopy (XPS). The film hardness was measured by nanoindentation. The energy dissipated during a load/unload process of the indentation was also estimated.

By the XRD measurements, it was found that films consisted of polycrystalline Ti and TiN mixtures for modulation periods longer than 10 nm and of monolithic TiN for modulation periods of 6.7 nm and 8 nm. The XPS results for the film with a modulation period of 80nm showed that the N concentration in metallic layers was about 45% and that of the nitride layers was about 30%. The maximum hardness of 11.2 GPa was obtained at a modulation period of 10nm for an indenter load of 2.9 mN. This value is larger than that obtained for a monolithic TiN film (8.4 GPa). The ratio of the dissipated energy to the applied energy during the indentation showed a minimum of 26% for the film with a modulation period of 8nm and was about 40% for the films with modulation periods longer than 30 nm.

It is concluded that, for compositionally nano-modulated TiN films, the film hardness as well as the energy dissipated during a load/unload process of the indentation depends on modulation period. The maximum hardness of 11.2 GPa was obtained for the film with a modulation period of 10 nm.

**PHONON CONFINEMENT IN NANOCRYSTALLINE Y<sub>2</sub>O<sub>3</sub>  
STUDIED BY RAMAN LIGHT SCATTERING**

*Ch. Beck<sup>1,3</sup>, R. Hempelmann<sup>1,3</sup> Ch. Bruch<sup>2,3</sup> and H.-G. Unruh<sup>2,3</sup>*

<sup>1</sup>Physikalische Chemie, <sup>2</sup>Experimentalphysik, <sup>3</sup>Sonderforschungsbereich 277  
Universität Saarbrücken, D-66123 Saarbrücken, GERMANY

Nanocrystalline Y<sub>2</sub>O<sub>3</sub> was prepared by a sol-gel type hydrolysis in the inverse micelles of w/o-microemulsions [1,2] with controlled particles sizes between 7 and 20 nm and with very narrow particle size distribution. The material exhibits the cubic high temperature structure and was studied by means of X-ray powder diffraction and micro-Raman scattering.

With decreasing crystallite size the characteristic Raman lines shift to lower frequencies and exhibit an increasing line broadening, in qualitative agreement with the phonon-confinement model of Richter et al. [3]. Quantitatively, however, discrepancies are observed which we attribute to the lattice expansion with decreasing particle size, evident from the significant increase of the lattice constant, which also contributes to the softening of the vibrations. A model that combines both effects is under construction.

- [1] H. Herrig and R. Hempelmann, *A Colloidal Approach to Nanometre-Sized Mixed Oxide Ceramic Powders*, Materials Letters **27**, 287-292 (1996)
- [2] Ch. Beck, W. Härtl and R. Hempelmann, *Size-Controlled Synthesis of Nanocrystalline BaTiO<sub>3</sub> by a Sol-Gel-Type Hydrolysis in Microemulsion-provided Nanoreactors*, J. Mater. Res. (1997) in print
- [3] H. Richter, Z. P. Wang and L. Ley, *The one Phonon Raman Spectrum in Microcrystalline Silicon*, Solid State Commun. **39**, 625 (1981)

## CHARACTERISATION OF VANADIUM OXIDE AND NEW V/Ce OXIDE FILMS PREPARED BY SOL GEL PROCESS

*Zorica Crnjak Orel<sup>1</sup> and Igor Muševc<sup>2</sup>*

<sup>1</sup> National Institute of Chemistry, Hajdrihova 19, 1001 Ljubljana, SLOVENIA

<sup>2</sup> Faculty of Mathematics and Physics, University of Ljubljana, Jadranska 29, Ljubljana  
and J.Stefan Institute, Jamova 39, Ljubljana, SLOVENIA

The preparation of vanadium oxide and new mixed V/Ce oxide thin films as intercalation compound for lithium ions (at 78, 55, 38 and 32 atomic % of V) started from aqueous inorganic precursors. Thin films were prepared as only one dip-coated layer via the sol gel process on glass substrate covered with SnO<sub>2</sub>:F.

The influence of added cerium precursors on the electrochemical, structural, and optical properties of thin films was studied by cycling voltammetry (CV), IR spectroscopy, X-ray analysis and atomic force microscopy (AFM). The addition of CeO<sub>2</sub> improved the poor stability of vanadium oxide films and enhanced their ion-charge capacity up to 30 mC/cm<sup>2</sup>. In all films the process of intercalation of lithium ions was followed by FT-IR spectroscopy performed at near-grazing incidence angle. The intercalation of Li<sup>+</sup> ions was confirmed by the observed shifts of V-O<sub>v</sub> vibrations in the IR spectra.

X-ray diffraction (XRD) was performed at reflectance mode for only one dip-coated layer which was heated at 400° C for 5 and 15 minutes, respectively. The results indicated that the film was amorphous due to the absence of any diffraction line except for the presence of the SnO<sub>2</sub> diffraction line from the substrate. The surface of the films was also characterised by the AFM imaging of the surfaces of all samples before and after cycling in 1 M LiClO<sub>4</sub> in propylene carbonate electrolyte. Typically, we observe amorphous grains of the size of 50-100 nm on the surface of V oxide and V/Ce oxide (at 55 at % of V) films before and after cycling. The results clearly indicate that the surface roughness of both films decreases after cycling. The RMS surface roughness of these films decreases from 11 nm to 6 nm in V oxide films and from 40 nm to 30 nm in V/Ce oxide (at 55 at % of V) films. On the contrary, pristine V/Ce oxide (at 38 at % of V) films are extremely flat, with a typical RMS surface roughness of only 2 nm and no observable grain structure. However, after cycling, these films show an increased RMS surface roughness of 8 nm and a grain structure with a typical grain size of 100 nm.

---

**MEASUREMENT OF ELASTIC AND ANELASTIC PROPERTIES OF  
NANOCRYSTALLINE METALS**

*M. Lang and W. Arnold*

Fraunhofer Institut for Nondestructive Testing (IZFP) and Sonderforschungsbereich  
277, Bldg. 37, University, D-66123 Saarbrücken, GERMANY <matlang@izfp.fhg.de>

Due to their high content in nanocrystalline materials, the grain boundaries are expected to contribute significantly to the elastic and anelastic properties of the bulk material. Thus nanocrystalline materials lend themselves to the study of absorption and dispersion effects that may otherwise be hidden behind those effects more prominent in polycrystalline materials.

The absorption and dispersion of high frequency ultrasound in nanocrystalline Palladium, Copper, and Nickel was examined. The specimens were prepared by pulsed electrodeposition and inert gas condensation. Parameters varied were frequency, temperature, and amplitude. The ultrasonic absorption and velocity were evaluated using contact and immersion techniques using both time and frequency domain signal processing. The frequencies and temperature of our measurement extended from 20 to 150 MHz, and 10 - 300 K, respectively. In addition, an acoustic microscope was used to determine Rayleigh wave velocities between 0.1 and 2 GHz at room temperature.

Within the given frequency range the absorption depends linearly on frequency, with a coefficient about twice as large as that of polycrystalline reference materials. For both nanocrystalline and polycrystalline specimen absorption increases with increasing intensity of the ultrasonic waves, the increase being much more pronounced with nanocrystalline material. No temperature dependency of anelastic properties was apparent. This behaviour is considered to be caused by a thermal hysteretic damping mechanisms present in the grain boundaries or agglomerates of grains.

**PbSe, PbS QUANTUM DOTS: SYNTHESIS AND PHYSICAL PROPERTIES***A.A. Lipovskii, E.V. Kolobkova and V.D. Petrikov<sup>1</sup>*

St.-Petersburg State Technical University, <sup>1</sup>A.F.Ioffe Physico-Technical Institute  
Polytechnicheskaja 29, St.-Petersburg, 195251 RUSSIA <lipovskii@phtf.stu.neva.ru>

The synthesis and theoretical studies of the glasses embedded with narrow-band IV-VI SQD have recently been performed [1-4]. The interest for these materials is due to their applicability in infrared optoelectronics, particularly in 1.3 and 1.5 micron range, and up to 3.5 microns. We used  $P_2O_5-Na_2O-ZnO-AlF_3-Ga_2O_3$  [3-4] and new  $P_2O_5-Na_2O-ZnO-PbO-AlF_3-Ga_2O_3$  glass systems for the formation of PbSe and PbS SQD. The glasses were synthesized at  $\sim 1100^{\circ}C$ , the glass transition temperature  $T_G=365-380\ ^{\circ}C$ . The technique of raw batch has been applied. The closed crucible was used to prevent the decreasing of sulfur concentration through the volatility during synthesis. Thermal treatment of the glasses at  $390-440^{\circ}C$  led to their coloring to brown and black depending of the duration and the temperature of the annealing. X-ray diffraction of longer annealed glass samples proved existence of PbSe, PbS SQD with NaCl cubic structure in the glasses. Transmission electron microscopy (TEM) of the glass samples has demonstrated existence of spherical grains within the annealed glass. Size of the grains varied between ~2 and 15 nm depending on the duration and temperature of annealing. The measured spectrum of the secondary X-rays indicated presence of lead and sulfur in the grains. The optical absorption spectra of the annealed glass samples with PbS and PbSe SQD were measured in the spectral range 350-3500 nm at several temperatures. Sets of optical absorption peaks corresponded to different quantum transitions were clearly observed in the spectra measured at room temperature, and the measurements at He temperature indicated narrow absorption peaks corresponding to the narrow size distribution of the SQD. Evaluated width of the size distribution of the SQD is ~5-7%. This narrow distribution is a unique one for SQD formed in glasses, and it is more close to the distributions typical for SQD formed with chemical techniques. The optical absorption data (position of the first quantum transition) and the TEM data show that time dependence of the size is close to  $t^{1/2}$  that is typical for the independent growth of nuclei. This coincides with the narrow size distribution observed.

We compare theoretical k•p model accounting anisotropy and non-parabolicity of the bands [2] with the observed optical transitions of complicated structure (up to 6 separate transitions). The optical transitions corresponded to the predicted positions as well as to the position of the first forbidden transition were observed. To explain the last phenomenon it is necessary to account Coulomb interaction that permits the transition. We also discuss another observed phenomenon concerning the dependence of the value and the sign of the thermal shift on the SQD size.

1. N.F.Borrelli, D.W.Smith. J. Non. Cryst. Solids, **80**, 25 (1994).
2. I.Kang, F.W.Wise. J. Opt. Soc. Amer. B, **14**, 1632 (1997).
3. A.A.Lipovskii, E.V.Kolobkova, V.D.Petrikov. Electron. Lett., **33**, 101 (1997).
4. A.Lipovskii, E.Kolobkova, V.Petrikov, I.Kang, A.Olkhovets, T.Krauss, M.Thomas, J.Silcox, F.Wise, Q.Shen, S.Kycia. Appl. Phys. Lett., **71**, 3406 (1997).

---

**MECHANICAL EXPLOSION SYNTHESIS OF  
NANOCRYSTALLINE TUNGSTEN CARBIDES POWDERS**

*Guo-long TAN, Xi-jun WU, Yan-qi WANG and Zong-quan LI*

Department of Materials Science and Engineering, Zhejiang University,  
Hangzhou 310027, CHINA <mse\_xjwu@ema.zju.edu.cn>

The nanocrystalline powders of tungsten carbides were prepared by a mechanical explosion synthesis (MES) method, a process of reactive high ball milling of  $\text{WO}_3+\text{Mg}$  mixtures containing graphite as a source of carbon for W phase. The microstructure of these nanocrystalline tungsten carbide powders has been analyzed by TEM and HREM respectively. The synthesis processing was completed in two steps, namely the explosive reactive synthesis of alpha-W by reductive reaction of Mg with  $\text{WO}_3$  and the diffusion reaction of high activity alpha-W with C. The chemical regularities of the mechanical explosion synthesis of the refractory compound and alloy were analysed. The products of the process mainly depend on composition ratio of the raw materials and the atmosphere in the vial. A thermodynamic metastable phase of h.c.p  $\text{W}_2\text{C}$  was produced while in a W rich environment, and the cubic phase of  $\text{WC}_{1-z}$  was formed while in a C rich environment. If the raw materials were milled at a  $\text{H}_2$  gas atmosphere, the mixture of WC,  $\text{W}_2\text{C}$  and  $\text{WC}_{1-z}$  was fabricated. The final product of the single phase tungsten carbides with an average grain size ranged from 4 to 20 nm were obtained after  $\text{MgO}$  was removed by HCl solution. The reason for the phase transition of WC to  $\text{W}_2\text{C}$  in a W rich environment and  $\text{W}_2\text{C}$  to  $\text{WC}_{1-z}$  during the milling was elucidated.

**THE LOW TEMPERATURE DEPENDENCE OF MAGNETIZATION  
OF AS-DEPOSITED Fe-Hf-N NANOCRYSTALLINE THIN FILMS**

*K.S. Kim<sup>1</sup>, S.C. Yu<sup>1</sup>, I.Y. Song<sup>2</sup> and H.J. Kim<sup>2</sup>*

<sup>1</sup> Department of Physics, Chungbuk National University,  
Cheongju 361-763, KOREA <scyu@cbucc.chungbuk.ac.kr>

<sup>2</sup> Thin Film Technology Research Center, Korea Institute of Science  
and Technology, P.O Box 131, Seoul 130-650, KOREA

We have carried out the low temperature dependence of magnetization of as-deposited Fe-Hf-N nanocrystalline thin films with good soft magnetic properties. As-deposited thin films have been prepared by a reactive magnetron sputtering method in a nitrogen atmosphere. The Fe-Hf-N thin films are fully nanocrystallized during deposition by controlling the composition and sputtering condition. Our films show the good soft magnetic properties of saturation magnetization of about 17 kG and coercivity of 0.5 Oe. Especially, the films show the excellent frequency dependence of high permeability of about 3000 up to 100 MHz without any loss till several 10 MHz. As-deposited Fe-Hf-N thin films are composed of finely dispersed Fe (~ 5 nm) and smaller Hf precipitates. It seems that the exceptionally small grains and precipitates enhance the soft magnetic properties. In order to investigate the intrinsic magnetic properties, we analyzed the temperature dependence of magnetization. The variation of the magnetic properties are discussed and compared with the composition of materials.

**NANOSTRUCTURAL CHARACTERIZATION OF SOLID CLUSTERS AND OXIDE BY HREM WITH RESIDUAL INDICES**

*Takeo Oku, Jan-Olov Bovin<sup>1</sup>, Satoru Nakajima<sup>2</sup>, Hiroshi Kubota<sup>3</sup>, Takeshi Ohgami<sup>3</sup>, and Katsuaki Saganuma*

Institute of Scientific and Industrial Research, Osaka University, Mihogaoka 8-1,  
Ibaraki, Osaka 567-0047, JAPAN <Oku@sanken.osaka-u.ac.jp>

<sup>1</sup>National Center for HREM, Inorganic Chemistry 2, Chemical Center, Lund University,  
P. O. Box 124, S-221 00 Lund, SWEDEN

<sup>2</sup>Department of Chemistry, Tohoku University, Aramaki, Aoba-ku,  
Sendai 980-77, JAPAN

<sup>3</sup>Department of Electrical Engineering and Computer Science, Kumamoto University,  
Kumamoto 860, JAPAN

It is difficult to determine the atomic arrangement of B, C, and O in the solid clusters and oxides because of their low atomic number. However, it is believed that the high-resolution images should have "some" information for disordering, ordering, and doping atomic positions in these materials. In the present work, we obtained the information for disordering, ordering, and doping in YB<sub>56</sub>, HgTlBa<sub>2</sub>CuO<sub>x</sub>, and N@C<sub>60</sub> from digital HREM images. Residual indices ( $R_{HREM} = \sum I_{obs} - I_{cal} / \sum I_{obs}$ ) were used for image analysis. Based on the crystal thickness and defocus value, which show the minimum  $R_{HREM}$  value, difference images between observed and simulated images were calculated.

Disordering of both yttrium and boron atoms in YB<sub>56</sub> was observed in difference HREM images. Averaged HREM images recorded at thin regions (5 nm) along the [100], [110] and [111] directions of the YB<sub>56</sub> were compared to calculated images based on the x-ray data. The difference images showed the disordered atomic positions, which are yttrium positions and boron clusters around the yttrium atoms.

The structure model for HgTlBa<sub>2</sub>CuO<sub>x</sub> was proposed from high-resolution electron microscopy using residual indices. Digital HREM image of the HgTlBa<sub>2</sub>CuO<sub>x</sub> showed the existence of separated Hg layers and oxygen vacancies in the double (Hg,Tl) layers. Image calculations based on the proposed structure model of HgTlBa<sub>2</sub>CuO<sub>5</sub> agreed well with the observation, and showed low  $R_{HREM}$  values.

Possibility of direct detection of N atoms inside the C<sub>60</sub> clusters by HREM was also discussed. The calculated difference image between C<sub>60</sub> and N@C<sub>60</sub> showed the  $R_{HREM}$  value of 0.03, which could be detected by digital HREM. This approach is useful for evaluation of local atomic positions in the crystal.

## COULOMB BLOCKADE NANOTHERMOMETER

*J.J. Toppari, J.P. Kauppinen, K.P. Hirvi, K.M. Kinnunen, and J.P. Pekola*

Department of Physics, University of Jyväskylä, P.O. box 35  
40351 Jyväskylä, FINLAND <jajuto@kanto.cc.jyu.fi>

The Coulomb blockade based primary nanothermometer, CBT, invented in Jyväskylä in 1994, is the first practical application of the Coulomb blockade phenomenon. It is based on arrays of nanoscale tunnel junctions which exhibit properties very suitable for primary and secondary thermometry.

The CBT operates in the weak Coulomb blockade regime where the thermal energy  $k_B T$  is larger than the electrostatic charging energy  $E_c$  and electric current is not totally prohibited at low bias voltage across an array but depends on the ratio of these two energies. In this limit the dynamic conductance of a junction array has nearly a bell shaped minimum around zero bias voltage. The width of the conductance minimum in bias voltage scales linearly and universally with  $T$  and  $N$  [1], the number of junctions, and qualifies as a primary thermometer. The zero bias drop in the conductance is proportional to  $T^{-1}$  and it can be used as a secondary thermometer.

Coulomb blockade thermometers are fabricated on a silicon substrate by electron beam lithography and two angle evaporation of aluminium with oxidation in between. Temperature range is lithographically adjustable and it extends over about two decades. At low temperatures the hot electron effect due to poor electron phonon coupling ultimately takes over at  $T \ll 1$  K. By optimizing the geometry of the junction array we have pressed the minimum temperature down to 20 mK. At high temperatures,  $T > 50$  K, the barrier suppression limits the use of  $\text{AlO}_x$  based junctions.

The CBT is now a product whose fundamental characteristics are already mapped out to a large extent [2]. It is remarkably insensitive to nonuniformities in the actual pattern and to even strong magnetic fields [3]. Currently the long term stability of the sensors is under testing. Control electronics and sensor packaging are also being developed.

- [1] J.P. Pekola, K.P. Hirvi, J.P. Kauppinen, and M.A. Paalanen, *Phys. Rev. Lett.* **73**, 2903 (1994), K.P. Hirvi, J.P. Kauppinen, A.N. Korotkov, M.A. Paalanen, and J.P. Pekola, *Appl. Phys. Lett.* **67**, 2096 (1995).
- [2] Sh. Farhangfar, K.P. Hirvi, J.P. Kauppinen, J.P. Pekola, J.J. Toppari, D.V. Averin, and A.N. Korotkov, *J. Low Temp. Phys.* **108**, 191 (1997).
- [3] J.P. Pekola, J.J. Toppari, J.P. Kauppinen, K.M. Kinnunen, A.J. Manninen, and A.G.M. Jansen, "Coulomb Blockade Based Nanothermometry in Strong Magnetic Fields", Submitted for publication (1997).

**MAGNETOELASTICITY AND INTERNAL STRAINS IN  
NANOCRYSTALLINE NICKEL**

*E. Bonetti, E.G. Campari, L. Pasquini, E. Sampaolesi and G. Scipione*

Dipartimento di Fisica, Università di Bologna and Istituto Nazionale per la Fisica della Materia, viale Berti-Pichat 6/2, 40127 Bologna, ITALY <pasquini@df.unibo.it>

The microstructure of nanocrystalline materials, mainly the grain size and the internal strains, has been widely investigated by a number of experimental methods, in particular transmission electron microscopy and diffraction techniques. For magnetic materials with appreciable magnetostriction, information on the distribution and entity of the internal stresses can be also obtained studying the magnetic or the magneto-mechanical behaviour. Nanocrystalline nickel prepared by ball milling is the subject of the present research. The milling was carried out in a vacuum of  $10^{-6}$  mbar, for times selected in order to obtain materials with different microstructures. Thin bar-shaped samples were prepared by consolidation of the milled powder under uniaxial pressure of 2 GPa at room temperature. In addition, the sample with the smallest grain size (15 nm) was subjected to several annealing steps, up to 400°C. All these samples have been fully characterised by X-ray diffraction to determine the grain size and the internal strains distribution. The thermal evolution of the microstructure was also studied by calorimetric measurements. The elastic modulus and the internal friction of the samples were measured by the vibrating reed technique, as a function of the applied magnetic field and temperature. From the variation of the elastic modulus with the magnetic field (known as DE effect), the internal stresses in the samples can be evaluated, giving values which agree with those obtained by standard X-ray diffraction procedures. The evolution of the internal stresses upon annealing was studied in a comparative way by X-ray diffraction and magnetoelectric measurements: it is shown that, at annealing temperatures where practically no strain is detected by X-ray, marked increases in the DE effect are still observed. The temperature dependence of the DE effect indicates that the magnetoelastic behaviour is dominated by the internal stresses, rather than by magnetocrystalline anisotropy. The results show that magnetoelastic measurements are more sensible than X-ray to the presence of small internal strains. These strains are likely localised in the boundary regions, and act as pinning points against magnetic domain mobility, thereby reducing the measured DE effect. This interpretation is also supported by the increase of the DE effect which follows grain growth at high annealing temperatures (> 300°C).

**RAMAN AND PHOTOLUMINESCENCE STUDIES OF  
NANOCRYSTALLINE SILICON PROCESSED BY CW – LASER ANNEALING**

*Puspashree Mishra<sup>1</sup> and K.P. Jain<sup>2</sup>*

Department of Physics, Indian Institute of Technology, Delhi, Hauz Khas, New Delhi – 110016, INDIA <sup>1</sup><puspashr@physics.iitd.ernet.in>, <sup>2</sup><kpjain@physics.iitd.ernet.in>

The fundamental properties of reduced dimension semiconductor systems have attracted tremendous interest worldwide for their potential applications in electronics and optoelectronics. We present detailed Raman and Photoluminescence studies on nanocrystalline silicon prepared by CW laser annealing of a-Si:H samples on quartz substrates. This laser initiated bulk-induced solid phase crystallization process produced stable nanocrystals of sizes 2.5 nm to 8 nm embedded in amorphous matrix . An argon – ion laser and a microprocessor controlled X -Y scanning system were employed to obtain uniform annealing. The optimum parameters for controlling the size of the nanocrystals were the incident power density of the laser and the scan speed of the microcontrol. The first order Raman spectra showed downshift, broadening and asymmetry as compared to bulk silicon. The average particle size was estimated by analyzing the line shape and correlating with the phonon confinement model according to which there is a relaxation of  $q=0$  selection rule due to confinement of phonons in finite dimension materials. The nanoparticles were found to be bigger in size with increasing power and exposure time of the laser. In order to fully explain the spectra, contribution from the amorphous component was separated and the correction due to strain effects arising from the difference in the thermal expansion coefficient of quartz and silicon was incorporated. We have also observed and analyzed red shifted, rather weak and broad higher order modes. Photoluminescence from these nanoparticles was in the orange region of the visible spectrum and was broad indicating large size distribution of the nanoparticles. It showed a two peak behavior and a strong dependence on temperature and the annealing condition.

**WC(0001)-Co and WC(0001)-CoO<sub>x</sub> STUDIED BY STM AND AES**

*M. Göthelid<sup>1</sup>, S. Haglund<sup>2</sup> and J. Ågren<sup>2</sup>*

<sup>1</sup> Materials Physics, KTH, 10044 Stockholm, SWEDEN <gothelid@matphys.kth.se>

<sup>2</sup> Materials Science, KTH, 10044 Stockholm, SWEDEN

Wetting of Co on WC surfaces is one of the most important properties during sintering of cemented carbide powders in the hard materials industry. For a pure WC-Co powder mixture wetting starts below 800 °C, however with presence of oxides or low levels of impurities the wetting may be hindered. In order to gain a more fundamental understanding of the early stages of wetting the WC(0001)-Co and WC(0001)-CoO<sub>x</sub> surfaces have been studied using scanning tunneling microscopy (STM) and Auger electron spectroscopy (AES). Deposition of Co on the sputter cleaned WC(0001) surface and subsequent annealing at 650 °C results in a surface with large flat areas exhibiting a 2x2 “precursor” structure with approximately 0.25 ML Co coverage. On top of the 2x2 structure excess Co grows in islands of ordered Co clusters. The islands are loosely bound to the underlying substrate, and can be moved with the STM tip. Annealing at 800-850°C removes all the excess Co and leaves only the 2x2 surface. Oxidation of the ordered WC(0001)-Co structure results in fine CoO<sub>x</sub> particles on the surface. On annealing their size increases to reach a maximum around 600-700°C. Higher temperatures breaks the oxide and the ordered WC(0001)-Co structure is restored.

### MECHANICAL PROPERTIES OF NANOCRYSTALLINE METALS IN COMPRESSION

*C.J. Youngdahl<sup>1,2</sup>, S.R. Agnew<sup>1</sup>, B.R. Elliott<sup>1</sup>, P.G. Sanders<sup>1,2,3</sup>, J.R. Weertman<sup>1</sup>, and  
J.A. Eastman<sup>2</sup>*

<sup>1</sup>Department of Materials Science & Engineering, Northwestern University,  
Evanston, IL 60201, USA

<sup>2</sup>Materials Science Division, Argonne National Laboratory, Argonne, IL 60439, USA

<sup>3</sup>now at Department of Engineering and Applied Sciences, Harvard University,  
Cambridge, MA 02138, USA

Compression tests have been performed on bulk nanocrystalline Cu, Ni, and Pd samples produced by inert gas condensation followed by compaction. These dense samples exhibit high compressive strengths. For example, the compressive strength of 98% dense Cu with a 20 nm nominal grain size (based on x-ray peak broadening measurements), is on the order of 800 MPa. Specimens tested in tension exhibit apparent strengths 30-50% lower than the compression results. Larger strains-to-failure are also observed when samples are tested in compression rather than tension. A possible explanation for these differences in behavior is that tensile tests are more susceptible to flaws. Recent microscopic studies of samples sectioned parallel and perpendicular to the compaction direction show that many have a wide grain size distribution, regions that have probably recrystallized, and a number of other morphological features that are likely to impact the mechanical behavior.

This work was supported by the U.S. Department of Energy, Grant DE-FG02-86ER45229 at Northwestern University, and by the U.S. Department of Energy, Basic Energy Sciences-Materials Sciences, under contract #W-31-109-ENG-38 at Argonne National Laboratory.

---

**MOLECULAR DYNAMICS SIMULATIONS OF METAL CLUSTER COOLING  
AND HEATING IN NOBLE GAS ATMOSPHERE**

*Jan Westergren, Henrik Grönbeck and Arne Rosén*

Department of Physics, Chalmers University of Technology and Göteborg University  
S-412 96 Göteborg, SWEDEN

Sture Nordholm, Department of Physical Chemistry, Göteborg University  
S-412 96 Göteborg, SWEDEN

Metal cluster properties such as ionization potential, magnetic moment and reactivity strongly depend on the temperature of the cluster. Using molecular dynamics simulations we have investigated how much energy is transferred from noble gas atoms to unsupported Pd<sub>13</sub> clusters in collisions. Series of collisions were simulated with various noble gas masses and parameters of the potential between gas and cluster and the potential between cluster atoms. The heavier the gas mass and the softer the Pd-Pd-potential, the more efficient is the energy transfer. However, the potential between Pd and a noble gas atom influences the energy transfer only for cold gas. We have also seen that energy is more easily transferred for melted clusters than for solid ones.

Knowing the heat capacity of the cluster, the energy transfer can be translated into increase of cluster temperature per collision. Thus, we have used the energy transfer data and a statistical theory to predict the cluster cooling and heating processes in a noble gas atmosphere of constant temperature. The prediction fitted well to simulated cooling and heating processes.

## MEASURING MAGNETIC MICROSTRUCTURE BY SPIN-POLARIZED SMALL-ANGLE NEUTRON SCATTERING

*J. Weissmüller<sup>1</sup>, A. Michels<sup>1</sup>, J. Barker<sup>2</sup>, R.D. Shull<sup>2</sup>, R.D. McMichael<sup>2</sup> and U. Erb<sup>3</sup>*

<sup>1</sup> Universitat des Saarlandes, Saarbrücken, GERMANY

<sup>2</sup> National Institute of Standards and Technology, Gaithersburg, USA

<sup>3</sup> University of Toronto, Toronto, Ontario, CANADA

In nanocrystalline ferromagnets, magnetocrystalline and magnetostrictive anisotropy fields suffer random jumps at grain boundaries, that result in nonuniformity of the magnetization. The detailed nature of this nonuniformity, in other words the magnetic microstructure on a length scale of nm to  $\mu\text{m}$ , is not yet understood in detail, nor is its importance, relative to that of magnetic domains, in magnetization reversal. In addition to this effect of magnetic anisotropy, the modified atomic short range order in the core of grain boundaries may or may not result in local variations of an effective atomic moment and of the strength and sign of the exchange coupling at grain boundaries.

Small-Angle Neutron Scattering (SANS) probes the magnetic microstructure of ferromagnets on length-scales between 2 nm and 200 nm, and is thus one of the few techniques that can provide information on magnetic structure in bulk. We combine SANS experiment with a model based on the theory of micromagnetics, a phenomenological approach that applies to the range of length-scales of interest. Based on quite general assumptions, we have derived closed form expressions for the variation of scattering cross section with applied magnetic field, scattering vector, and their relative orientation, that show excellent agreement with experiment on nanocrystalline Ni [1] and Co. This proves that the magnetic microstructure in the relevant length scales, in agreement with theory, is the convolution product of an anisotropy field microstructure and of a response function with a correlation length  $l_H$  that depends on the applied field  $H_a$ . The agreement of experiment with theory indicates that the changes in the magnetic microstructure with  $H_a$  are not from displacements of domain walls, but from changes in  $l_H$  and hence in the magnetic response to an entirely stationary anisotropy field microstructure.

Combining theory and experiment, we are able to measure quantitatively the Fourier components of the anisotropy field at saturation, the field-depended exchange length, and the value of an effective exchange constant in nanocrystalline ferromagnets. Spin-polarized SANS data support the separation of micromagnetic structure due to anisotropy fields from the influence of regions of reduced atomic density at pores or grain boundaries, that we find negligible in the electrodeposited samples.

1. J. Weissmüller, R.D. McMichael, J. Barker, H.J. Brown, U. Erb, R.D. Shull, "Magnetic Microstructure of a Nanocrystalline Ferromagnet - Micromagnetic Model and Small-Angle Neutron Scattering", MRS Symp. Proc. 457, (Eds.) S Komarneni, J. Parker, H. Wollenberger, 231 - 236 (1997)

**SOL-GEL DERIVED YSTZ-Al<sub>2</sub>O<sub>3</sub> AND YSTZ-Al<sub>2</sub>O<sub>3</sub>-SiO<sub>2</sub> NANOCOMPOSITES**

*R.N, Viswanath and S. Ramasamy*

Department of Nuclear Physics, University of Madras,  
Guindy Campus, Chennai 600 025, INDIA

Yttria stabilized tetragonal zirconia (YSTZ)-alumina nanocomposite system has been synthesized by sol-gel process. The synthesized products were studied using the techniques XRD, TGA, DSC, FT-IR, FT-Raman and SEM. Our investigations reveal that the grains and grain boundary regions are crystallised independently at two different temperatures. The bulk grains are crystallized into tetragonal symmetry above 750°C with an average crystallite size of 10 nm. The crystallisation temperature increases with alumina contents. The specimens underwent to structural phase transition from tetragonal to monoclinic at 1300°C or below for low concentration of alumina (less than 10 wt %). But, with the addition of 15 wt% of alumina the system retains its tetragonal symmetry up to its processing temperature 1300°C. The size of the crystallites does not exceed 45 nm at this temperature. The high temperature stable composition YSTZ-15 wt% Al<sub>2</sub>O<sub>3</sub> was dispersed into TEOS solution and the product was condensed into a solid dense mass. Temperature dependent dielectric behaviour of the specimens with and without silica matrix has been studied in the frequency region between 10 MHz and 10Hz using the 1impedance analyser. The results will be discussed in this paper. The technological importance of these materials will also be discussed.

**SELF-ASSEMBLED SINGLE ELECTRON TUNNELING DEVICES.**

*S.H.M. Persson<sup>1,3</sup>, L. Olofsson<sup>1</sup> and L. Hedberg<sup>2</sup>*

<sup>1</sup>Department of Microelectronics and Nanoscience

<sup>2</sup>Department of Applied Physics

<sup>3</sup>Department of Microwave technology

Chalmers University of Technology and University of Göteborg  
S-412 96 Göteborg, SWEDEN <persson@ep.chalmers.se>

Single electron tunneling devices were made by self-assembly of colloidal ligand-stabilized gold clusters in the small gap between two gold electrodes. With this method we control the size of the active part of the device, that is smaller than the traditional lithographic resolution, with chemical methods and leave the positioning of the particle to the weak forces between the substrate and the particle. The current voltage characteristic of the devices exhibit a Coulomb staircase at 4.2 K and a prominent Coulomb blockade at room temperature. A modulation is observed at 4.2 K as a function of a voltage applied to a gate electrode.

**ULTRATHIN  $A_2^{V}B_3^{VI}$  THERMOELECTRIC FILMS CONFINE  
CHARGE CARRIERS TO MOVE IN TWO DIMENSIONS**

*Yu.A. Boikov<sup>1,2</sup>, V.A. Danilov<sup>2</sup>, T. Claeson<sup>1</sup> and D. Ertz<sup>1</sup>*

<sup>1</sup> Physics and Engineering Physics, Chalmers University of Technology and University of Göteborg, S-41296 Göteborg, SWEDEN <boikov@fy.chalmers.se>

<sup>2</sup> Ioffe Physico-Technical Institute RAS, 194021 St. Petersburg, RUSSIA

$Bi_2Te_3$  -  $Sb_2Te_3$  layered thermoelectric materials posses the highest values of the figure of merit  $Z = (\alpha^2\sigma/\kappa)$  at  $T = 300K$  for the thermoelectrics ( $\alpha$  - Seebeck coefficient,  $\sigma$  - electrical conductivity,  $\kappa$  - thermal conductivity).  $Z$  for ultrathin ( $d < 10$  nm) thermoelectric films may be improved even further due to a modification of the density of states, if electrons are confined to move in two dimensions. Selective scattering of phonons and charge carriers at the interfaces may influence  $Z$  for a thin films as well. There are lots of problems, however, with the growth of ultrathin epitaxial multicomponent thermoelectric films with desirable orientations and charge carrier concentrations.

We used hot wall epitaxy and laser ablation to grow stoichiometric (0001)( $Bi,Sb$ )<sub>2</sub> $Te_3$  thin films with electron (n-type) and hole (p-type) conductance on freshly cut (0001)mica. To promote layer-by-layer growth, the difference in temperature between the substrate and the ( $Bi,Sb$ )<sub>2</sub> $Te_3$  powder was decreased down to 10% during the film growth by hot wall epitaxy. To decrease the density of antisite defects, ( $Bi,Sb$ )<sub>2</sub> $Te_3$  films grown by laser ablation were heat treated at 400°C in a specially designed chamber, formed from bulk polycrystalline material with corresponding composition.

The density of stable nuclei at the substrate surface was less than  $10^5$  cm<sup>2</sup>, due to low supersaturation of the vapour phase in the case of hot wall epitaxy. A system of well in-plane oriented, triangular (0001) ( $Bi,Sb$ )<sub>2</sub> $Te_3$  islands were observed by atomic force microscopy AFM at the surface of the mica during the initial stage of the film growth. The island thickness was about two order of magnitude less than its typical extensions in the axb plane (~10 μm). A system of equidistant steps (1 nm height) was observed at the surface of the island by AFM. Due to a high supersaturation of the vapour phase, the density of stable ( $Bi,Sb$ )<sub>2</sub> $Te_3$  nuclei was  $10^5$  times larger in the case of laser ablation than that for films grown by hot wall epitaxy. ( $Bi,Sb$ )<sub>2</sub> $Te_3$  films with a thickness larger than 1 nm (1/3 of the unit cell along the c-axis) were continues. The( $Bi,Sb$ )<sub>2</sub> $Te_3$  films ( $d = 3 - 10$  nm) grown by laser ablation consist of c-axis oriented grains with size - 10 nm.

Temperature dependencies of the  $\sigma$  for the ultrathin( $Bi,Sb$ )<sub>2</sub> $Te_3$  films ( $d = 1-10$  nm) grown by laser ablation were weaker than those for the epitaxial films grown by hot wall epitaxy ( $\sigma \sim T^{-\beta}$ ,  $\beta = 1.8 - 2.3$ ).  $\alpha^2\sigma$  products for the n - and p-( $Bi,Sb$ )<sub>2</sub> $Te_3$  epitaxial films were higher than those for corresponding bulk single crystals at  $T < 300$  K. The thermoelectric parameters for ultrathin ( $Bi,Sb$ )<sub>2</sub> $Te_3$  films depended crucially on processing conditions, because of deviation of the stoichiometry at the interfaces.

**NANOPHASE PLATINUM PARTICLES  
ON Na ZEOLITE A SURFACE BY  $\gamma$ -RADIOLYSIS**

*R. Vijayalakshmi, S. Kapoor, S.K. Kulshreshtha and J.P. Mittal*

Chemistry division , Bhabha Atomic Research Centre , Mumbai - 400 085, INDIA

Nanosized platinum particles supported on Na zeolite A surface have been prepared the radiolytic reduction of  $H_2PtCl_6$ . The sodium aluminosilicate gel containing appropriate amount of  $H_2PtCl_6$ , was  $\gamma$  - irradiated with a dose of 22 KGy and hydrothermally heated at 100 K for 9 hours, to obtain the platinum metal particles dispersed, crystalline zeolite A samples. The powder X-ray diffraction studies revealed an average Pt crystallite size of 8-10 nm. These Pt agglomerates formed over the zeolite surface have been studied by SEM and an average particle size of approximately 100nm was observed .The Pt particles have been found to be highly active for catalytic processes as revealed by temperature programmed desorption of chemisorbed hydrogen and the room temperature hydrogenation of ethylene. The catalytic results obtained for the radiolytically reduced Platinum particles have been compared with those obtained for the samples prepared by the conventional method of hydrogen reduction of zeolite samples containing  $H_2PtCl_6$  at ~ 500K.

**THE DEFORMATION AND PECULIARITIES  
OF THE DESTRUCTION OF NANOPHASE MATERIALS**

*N.I.Noskova, and E.G.Volkova*

Institute of Metal Physics, Ural Division of Russian Academy of Sciences  
18 Kovalevskaya Str., GSP-170, Ekaterinburg 620219, RUSSIA

The deformation (uniaxial tension, creep, indenting) and destruction of nanophase materials produced by crystallisation of amorphous state in the temperature range 273-573 K were investigated. The data of the electron microscopy research into the nature of deformation defects are given, and the level of the corresponding strength and plastic characteristics investigated materials is shown.

**SYNTHESIS OF CARBON NANOTUBES  
ON POROUS ANODIC ALUMINA BY ECR/CVD**

*H.C. Shih, S.H. Tsai and T.G. Tsai*

Department of Materials Science and Engineering, National Tsing Hua University,  
Hsinchu300, Taiwan <hcshih@mse.nthu.edu.tw>

The synthesis of carbon nanotubes on porous anodic alumina could first be achieved by electron cyclotron resonance chemical vapor deposition (ECR/CVD) in this laboratory. The composite film of the aligned carbon nanotubes embedding in the porous anodic alumina was robust and a large area can be prepared because of the advantages of ECR/CVD, e.g. low temperature, low ion damage, contamination-free, etc. Through adjusting the pore size of the anodic alumina, various carbon nanotube diameters can be obtained in a range of 30 to 230 nm. Precursor gas of ethyne and argon was used in ECR/CVD for synthesizing carbon nanotubes. The carbon nanotubes on anodic alumina as a whole were analyzed by FESEM and FTIR. TEM was used to characterize the individual carbon nanotube, which was extracted from the composite film. Results indicated that the carbon made of nanotubes are diamond-like carbon (DLC) instead of graphite, and extreme short synthesis time (1~5 minutes).

1. S. Lijima, *Nature* 354, 56 (1991).
2. W. Z. Li, S. S. Xie, L. X. Qian, B. H. Chang, B. S. Zou, W. Y. Zhou, R. A. Zhao, G. Wang, *Science* 274, 1701 (1996).

---

**MODIFICATION OF CHEMICAL VAPOR SYNTHESIS PROCESS FOR  
DIFFERENT ZIRCONIA-ALUMINA NANOPARTICLES**

*V.V. Srdic, M. Winterer and H. Hahn*

Darmstadt University of Technology, Materials Science Department, Thin Films  
Division, Petersenstr.23, D-64287 Darmstadt, GERMANY

Different types of nanocrystalline zirconia-alumina powders with up to 50 mol% Al<sub>2</sub>O<sub>3</sub> have been prepared by chemical vapour synthesis, CVS (a modified chemical vapour deposition). Composite powders are synthesized by mixing of zirconia and alumina particles separately formed by decomposition of precursor/helium gas flows in parallel hot wall reactors. Single-phase solid solutions of alumina in zirconia are produced when the precursor vapour flows are first mixed and then introduced into the hot wall reactor. Coated powders are obtained in two reactors connected in series. The core is produced in the first reactor by CVS and the shell is produced in the second by heterogeneous nucleation of a film on the core particles. Powders characteristics are strongly dependent on the processing conditions, such as: temperature and pressure in the reactor, helium and oxygen flow rates, bubbling temperatures and CVS modifications described above. Synthesized zirconia-alumina nanopowders are nonagglomerated, mostly crystalline with crystallite size 4 to 6 nm, and specific surface area ranging from 200 to 300 m<sup>2</sup>/g.

### STRUCTURAL MEASUREMENTS FOR SINGLE-WALL CARBON NANOTUBES BY RAMAN SCATTERING TECHNIQUE

*E.D. Obraztsova<sup>1</sup>, J.-M. Bonard<sup>2</sup>, V.L. Kuznetsov<sup>3</sup>, V.I. Zaikovskii<sup>3</sup>, S.M. Pimenov<sup>1</sup>,  
A.S. Pozarov<sup>1</sup>, S.V. Terekhov<sup>1</sup>, V.I. Konov<sup>1</sup>, A.N. Obraztsov<sup>4</sup> and A.P. Volkov<sup>4</sup>*

<sup>1</sup>General Physics Institute, RAS, 38 Vavilov street,  
117942 Moscow, RUSSIA <elobr@kapella.gpi.ru>

<sup>2</sup>Institute de Physique Exp., EPFL, CH-1015, Lausanne, SWITZERLAND

<sup>3</sup>Boreskov Inst. of Catalysis, Lavrentieva 5, 630090, Novosibirsk, RUSSIA

<sup>4</sup>Physics Department of M.V. Lomonosov MSU, 119899, Moscow, RUSSIA

A pure carbon exists in nature in many modifications differing from each other at the "macro"-level. Moreover last few years have shown that this chemical element gave a birth to a big family of materials having a different geometry at the "nano"-level: *carbon nanotubes, nanospheres, nanocones*. The Raman scattering appeared to be among the most informative techniques being able to measure the structural parameters of such new materials. Though the Raman technique doesn't possess a direct high spatial resolution (as HRTEM or STM), the dynamics of a photon-phonon interactions appears to be very sensitive to the atomic-scale variations of the structure characteristic size. This allows to estimate correctly the average sizes of nanostructures. In case of single-wall carbon nanotubes moreover the diameter-selective resonance enhancement of the Raman scattering intensity takes place depending on the excitation energy. This allows to get information about the nanotube distribution over the fractions having the different diameters. The resonance behavior is a consequence of a discrete character of an electron density of states for a single-wall nanotube.

In this work single-wall carbon nanotubes grown by different techniques have been investigated by the Raman scattering with a scanned excitation energy. The size, geometry and distribution of nanotubes over diameter estimated from the Raman spectra have been compared with the direct measurements by the high resolution electron microscopy (HRTEM). The temperature-induced additional resonances have been observed.

The low-field electron emission parameters have been measured for the different nanotube fractions. The threshold fields were of 1-2 V/ $\mu$ m, the emission current reached the value 15 mA/cm<sup>2</sup> at fields of 10 V/ $\mu$ m. These data allows to consider the single-wall carbon nanotubes as a promising material for vacuum electronics.

*The work is supported in part by the grant N97-02-17282 of the Russian Foundation for Fundamental Research and by the grant NK1129 of the Russian Federal Program "Integration".*

**LASER ABLATION DEPOSITION OF SILICON NANOSTRUCTURES**

*J. Levoska, M. Tyunina<sup>\*</sup> and S. Leppävuori*

Microelectronics and Materials Physics Laboratories and EMPART Research Group of  
Infotech Oulu, University of Oulu, PL 444, FIN-90571 Oulu, FINLAND  
<juhani.levoska@ee.oulu.fi>

\*Permanent address: Institute of Solid State Physics, Latvian University,  
8 Kengaraga, LV-1063, Riga, LATVIA

Nowadays, considerable attention is paid to study silicon nanostructures of different types, where quantum size effects modify the band gap and make luminescence possible. In this study, pulsed laser deposition in low-pressure argon ambient was used to produce films of nanosized silicon clusters or crystallites. The films were deposited in off-axis geometry using a XeCl excimer laser, n-type silicon wafer target and MgO and Si single crystal substrates at room temperature. The Ar gas pressure was varied in the range 0...2 mbar. The local film structure and luminescence properties of the films were studied as a function of the distance from the target using a triple micro-Raman spectrometer and Ar<sup>+</sup> laser excitation. Synchrotron radiation photoemission and photoabsorption spectroscopy was used to study electron structure and bonding.

At low Ar pressures (< 0.2 mbar) the films were amorphous, and their Raman spectrum consisted of a broad band centred near 480 cm<sup>-1</sup>. In the pressure range 0.4...2 mbar nanocrystalline films were obtained. In the Raman spectra, the line of crystalline silicon at 521 cm<sup>-1</sup> was moved to lower wavelengths, due to relaxation of the selection rule q~0 in small crystals. Using relationships between Raman shift and crystal size, it was found that the nanocrystal size varied in the range 1...5 nm, increasing with increasing distance from the target. This could be explained by the collision geometry. Room temperature photoluminescence of the samples was rather weak. Synchrotron radiation studies showed the existence of a silicon dioxide layer on the surface of the nanoparticles.

**INTERFACES IN NANOSTRUCTURES:  
OPTICAL INVESTIGATIONS ON CLUSTER-MATTER**

*U. Kreibig, M. Gartz, A. Hilger and R. Neuendorf*

Physikalisches Institut der RWTH, Aachen, BRD, GERMANY

Interface layers, being basic topological constituents of nanostructured systems, have strong impact upon their structural and electronic properties.

Due to the extremely wide range and variability of topological structures in nanostructured matter, the general role of such interfaces has not yet found the consideration it deserves.

We present a study on the simple model-system of metal-clusters embedded in a wide range of embedding materials like oxides, semiconductors and fullerite. The optical Mie resonance served as a highly sensitive sensor to evaluate cluster-matrix interface properties. In particular, static and dynamic charge transfer processes were regarded and quantitative comparisons with the theory of B. PERSSON could be achieved by including experiments on the free cluster beam in UHV.

Static charge transfer may exhibit strong effects on the electronic properties of, both, the clusters and the surrounding matrix. Dynamic charge transfer, inducing phase relaxation of the cluster plasmon resonance, enables information about electronic adsorbate states. The obtained phase relaxation frequencies correspond well to recent results of femtosecond-spectroscopy on clusters.

The results of the present study yield, beyond the inspected cluster-matrix systems, information about the role and importance of interface layers of nanostructured matter in general.

**NANOCRYSTALLINE SOFT MAGNETIC Fe-M-B(M=Zr, Hf, Nb),  
Fe-M-O(M=Zr, Hf, RARE EARTH) ALLOYS AND THEIR APPLICATIONS**

*A. Makino<sup>1</sup>, A. Inoue<sup>2</sup> and T. Masumoto<sup>3</sup>*

<sup>1</sup> Central Research Laboratory, Alps Electric, 1-3-5 Higashitakami,  
Nagaoka 940-8572, JAPAN

<sup>2</sup> Institute for Materials Research , Tohoku University, 2-1-1 Katahia, Aoba-ku,  
Sendai 980-8577, JAPAN

<sup>3</sup> The Research Institute of Electric and Magnetic Materials, 2-1-1 Yagiyamaminami,  
Taihaku-ku, Sendai 982-0807, JAPAN

New soft magnetic nanocrystalline materials in Fe-M-B (M=Zr,Hf,Nb) and Fe-M-O (M=Zr,Hf,rare earth) systems have been fabricated by use of partial crystallization of melt-spun amorphous phase and sputtering-induced partial crystallization, respectively. These alloys have a mixed structure of nano-scale bcc-Fe grains and an amorphous phase containing a large amount of M, B and O, respectively. These structural properties should be a dominant factor for achieving good soft magnetic property in both alloys. The Fe-M-B ribbons with high Fe content about 90% exhibit the high magnetic flux density of 1.5 to 1.7T as well as the high permeability of 30000 to 100000 at 1kHz and very low core losses at low frequency. On the other hand, the soft magnetic Fe-M-O films with high O content of 20 to 30 at% show high permeability at the high frequency above 100MHz because of their electrical resistivity of 4 to 23 micro ohm meter much higher than those of the other conventional soft magnetic alloy films.

The Fe-M-B ribbons should be more suitable for low frequency applications such as power transformers and choke coils for active filters for power supplies and so on. The Fe-M-O films should be useful for high frequency applications such as thin-film inductors and transformers for micro switching converters for portable electric equipment and others.

**NET CoPt/Ag GRANULAR FILMS FOR  
HIGH DENSITY RECORDING MEDIA.***S. Stavroyiannis, I. Panagiotopoulos and D. Niarchos*

IMS, NCSR "Democritus", Ag. Paraskevi Attiki 153 10, GREECE

*J.A. Christodoulides and G.C. Hadjipanayis*Department of Physics and Astronomy, University of Delaware,  
Newark, DE 19716, USA

The drive for higher magnetic recording density imposes the need for particle sizes below 10 nm. This puts the current recording materials in their limit of performance because of their low  $H_c$  and thermal effects. Current studies have been focused on nanocrystalline rare earth compounds with high anisotropy [1,2]. We have recently started a project on CoPt/M (M=Ag,C) thin films consisting of highly anisotropic fct CoPt nanoparticles embedded in Ag and C matrices. Multilayer CoPt/Ag films were made by magnetron sputtering from CoPt and Ag targets in the tandem mode. Laser ablation using a KrF excimer laser was used to prepare the CoPt/C multilayer films. Samples with different CoPt and Ag(C) thickness were made and their structural and magnetic properties were measured after different annealing in the temperature range 500-700°C. All the as-made films are soft with  $H_c < 100$  Oe. In CoPt/Ag, annealing at 500°C and above leads to a granular structure consisting of highly anisotropic fct CoPt particles in the Ag matrix with a corresponding increase in  $H_c$ . The size and spatial distribution of the particles and therefore their coercivity was found to change significantly with annealing temperature and time. Particles with size in the range of 5-50 nm have been obtained with coercivities up to 15 kOe. Larger particle sizes and higher  $H_c$  were obtained by annealing at higher temperatures. In CoPt/C the optimum microstructure and  $H_c$  were obtained much more slowly and only after annealing at 700°C. The evolution of microstructure in samples with different composition and at different heat treatments will be reported and compared with the magnetic properties.

- [1] Y. Liu et al., IEEE Trans. Magn., MAG 31, 2740 (1995)
- [2] D. Lambeth, in "Magnetic Hysteresis in Novel Magnetic Materials", NATO ASI Series E, 338, 767 (1997) Ed. G, C Hadjipanayis.

**APPLICATION OF SPECIFIC METALLOTHERMIC METHOD  
IN VOLFRAM POWDER OBTAINING FROM SCHEELITE**

*R. Curcic<sup>1</sup>, P.Zivanovic<sup>2</sup>, G. Djurkovic<sup>1</sup>, V. Jokanovic<sup>1</sup>*

<sup>1</sup> Institute for Technology of Nuclear and Other Mineral Raw Materials,  
Franche dÆEpere 86, 11000 Belgrade, YUGOSLAVIA

<sup>2</sup> Institute of Technical Sciences of the Serbian Academy of Sciences and Arts,  
Knez Mihailova 35/IV, 11000 Belgrade, YUGOSLAVIA

A fine, high purity wolfram powder was produced by a method of self-propagating combustion wave (SHS) from the mixture of scheelite powder ( $\text{CaO}, \text{WO}_3$ ) and reducing agent powder-magnesium, in one case, and aluminium, in the other. Microstructural investigation of obtained powder by the X-ray diffraction and scanning microscopy methods showed that it is composed of spheroidal particles of fine and uniform coarseness.

Chemical analysis confirmed that impurity content is negligible. Chemical, morphological and microstructural characteristics of so obtained wolfram powder recommend it as ideal starting base for use in powder metallurgy. The principle of the self-propagating combustion wave reduction method was analyzed as one of the methods that promise significant rationalization of wolfram obtaining technologies and some other technologies for obtaining powders from their oxide concentrates.

**PRELIMINARY STUDIES ON WEAR RESISTANCE  
OF BULK AlN<sub>p</sub>/AL NANOCOMPOSITE MATERIALS**

*Sun Xiangcheng<sup>1,2</sup>, Bi Hongyun<sup>2</sup>, Sun Xiukui<sup>2</sup>, Wei Wenduo<sup>2</sup> and M. José-Yacamán<sup>1</sup>*

<sup>1</sup> Instituto Nacional de Investigaciones Nucleares,  
Carretera México-Toluca Km.36.5, 52045 Salazar, MÉXICO

<sup>2</sup> National Key Lab for RSA, Institute of Metal Research,  
Chinese Academy of Science, 72 Wenhua Road, Shenyang, 110015, CHINA

Bulk AlN<sub>p</sub>/Al nanocomposite materials have been synthesized by sintering the compacts consist of Al and AlN nanoparticles, which were produced by an active plasma-metal reaction method. The excellent dry-sliding wear resistance of this AlN<sub>p</sub>/Al nanocomposite with diamond couterfaces in the laboratory air has been found. The wear resistance of AlN<sub>p</sub>/Al nanocomposite materials with most AlN ratio is 20 times higher than that of pure Al materials, and the wear coefficient have been found to fluctuate in the different friction times.

Interestingly, the uniform Al<sub>2</sub>O<sub>3</sub> film formation has been found on the friction surface in all kinds of conditions. The results showed that the possible mechanism of dry-sliding wear can be controlled by both fatigue wear and oxidation wear.

**STUDY ON THERMAL OXIDATION BEHAVIOR AND PRODUCTS  
OF BULK AlN<sub>p</sub>/Al NANOCOMPOSITE MATERIALS**

*Sun Xiangcheng<sup>1,2</sup>, Sun Xiukui<sup>2</sup>, Wei Wenduo<sup>2</sup> and M. José-Yacamán<sup>1</sup>*

<sup>1</sup> Instituto Nacional de Investigaciones Nucleares,  
Carretera México-Toluca Km. 36.5, 52045 Salazar, MÉXICO

<sup>2</sup> National Key Laboratory of RSA, Institute of Metal Research,  
Chinese Academy of Sciences, Shenyang 110015, CHINA

Thermal oxidation behavior and products of bulk AlN<sub>p</sub>/Al nanocomposite and pure Al(15μm) materials have been investigated in 0.1MPa pure oxygen atmosphere at temperature range from 20°C to 1000°C. TG, XRD SEM experiment have shown that the oxidation behavor of bulk AlN<sub>p</sub>/Al nanocomposite was complicated because nanometer AlN grain will play vital role in oxidation process, and the oxidation products consisted of α, β, δ, γ, η, κ, θ-Al<sub>2</sub>O<sub>3</sub>, AlON and AlN compounds. However, in comparison with, the oxidation behavior for pure Al(15μm) material was simple and completed, the oxidation products were composed of α, β, δ, γ, η, κ, θ, ε-Al<sub>2</sub>O<sub>3</sub> compounds.

It is suggested that the antioxidation of AlN<sub>p</sub>/Al nanocomposite materials were more higher than that of pure Al(15μm) materials. This is proved that the AlN<sub>p</sub>/Al nanocomposite materials will be promising in higher temperature conditions.

**SYNTHESIS OF CARBON/OXIDE NANOCOMPOSITES BY  
INTERCALATION/DEINTERCALATION  
OF NANOSTRUCTURED CARBONS**

*V.Z. Mordkovich*

ICMR, East 601, KSP, Sakado 3-2-1, Takatsu-ku, Kawasaki 213, JAPAN  
<vladimir@icmr.co.jp>

A new chemical route for producing carbon/oxide nanocomposite by intercalation/deintercalation of nanostructured carbons has been explored. Nanostructured carbons such as carbon nanotubes, soots and submicrofibers enter the intercalation reaction with various metal chlorides such as  $\text{FeCl}_3$ ,  $\text{AlCl}_3$ ,  $\text{ZnCl}_2$  and others. The intercalation compounds formed are subject to easy deintercalation in air at the temperatures up to 400°C. Chlorine is displaced with oxygen during deintercalation. The result of deintercalation is a nanocomposite where nanoparticle of carbon play a role of carriers for newly formed oxide nanoparticles. By oxidation of carbon nanoparticles it is also possible to obtain fine powder of the oxide. Synthesis results on several systems and the results of STM and TEM studies of the nanocomposites are described in the paper.

**SYNTHESIS OF  $\text{Al}_2\text{O}_3$  NANOPOWDERS USING INORGANIC SALT  
AND ITS THERMODYNAMICS***Wenming Zeng, Linhua Gui, Jun Wang, and Jinkun Guo*

The State Key Lab .of High Performance Ceramics and Superfine Microstructure,  
Shanghai Institute of Ceramics, Chinese Academy of Sciences, Shanghai, CHINA

Boehmite ( $\gamma$ - $\text{AlOOH}$ ) powder was first prepared by Sol-Freeze Drying method using cheap  $\text{AlCl}_3 \cdot 6\text{H}_2\text{O}$  as raw materials, and then  $\gamma$ - $\text{Al}_2\text{O}_3$  nanopowder with the average diameter of 5nm and  $\alpha$ - $\text{Al}_2\text{O}_3$  nanopowder with the mean diameter of 27nm were obtained by the calcination of the above  $\gamma$ - $\text{AlOOH}$  powder at  $500^\circ\text{C}$  and  $1100^\circ\text{C}$ , respectively. The potential-pH diagrams of Al-H<sub>2</sub>O system at  $25^\circ\text{C}$  and  $90^\circ\text{C}$  were presented, separately. Thermodynamic analysis of the main reactions in the process of thermal decomposition of  $\text{Al}(\text{OH})_3$  was also made using Temkin-Schwarzman's method and by means of regression analysis. Investigations of the potential-pH diagrams of Al-H<sub>2</sub>O system and the thermodynamic analysis of thermal decomposition of  $\text{Al}(\text{OH})_3$  provide a certain guide for the formation of boehmite sol and the heat treatment of boehmite powder, respectively.

The characterization results of calcined powders are summarized in table 1.

**TABLE 1. Characterization Results of Calcined Powders**

Powder	Specific surface area ( $\text{m}^2/\text{g}$ )	$d_{\text{BET}}$ nm	$d_{50}$ nm	$d_{\text{TEM}}$ nm	$d_{50} / d_{\text{BET}}$
$\gamma$ - $\text{Al}_2\text{O}_3$	291.95	6	537	4	89.5
$\alpha$ - $\text{Al}_2\text{O}_3$	51.21	29	755	25	26.0

**SYNTHESIS OF HIGH ACTIVE-SITE DENSITY NANOFIBROUS  
MnO<sub>2</sub>-BASE MATERIALS WITH ENHANCED PERMEABILITIES***T.D. Xiao<sup>1</sup>, P.R. Strutt<sup>1</sup>, and B.H. Kear<sup>2</sup>*<sup>1</sup> Inframet Corporation, 29 Washington Avenue, North Haven, CT 06473, USA<sup>2</sup> Department of Ceramic and Materials Engineering, College of Engineering,  
Rutgers University, Piscataway, NJ 08855, USA

High surface area powders are widely used to promote chemical reactions. A limitation of such nanoscale powders is their tendency to form agglomerates, in which the pore size is of comparable dimensions. This has the adverse effect of restricting the passage of gaseous or liquid reactants through the material, particularly when in the form of a flat bed. A potential solution to this problem is to develop a nanofibrous structure, which combines high active site density with enhanced permeability. Here, we report on the chemical synthesis of such a structure in MnO<sub>2</sub>-base materials. A critical step in the synthesis is an extended period of solution refluxing, which induces the gradual transformation of an initial nanoparticle agglomerated mass into a random-weave nanofibrous structure. Partial transformation of the material realizes a mixed nanoparticle/nanofibrous structure, which enables relatively easy flow of the reactant gases or liquids through the powder bed, while exposing them to the high density of active sites associated with the nanoparticle agglomerates. Considerable flexibility in morphological design is afforded by the fact that relatively small changes in synthesis procedure and/or chemical doping give rise to large variations in size, shape and distribution of both the original nanoparticle agglomerates and the resulting nanofibrous structures. Potential applications for such morphologically designed MnO<sub>2</sub>-base materials include battery electrodes, fuel cell membranes, pollution control devices, and catalytic converters.

**HIGH PRESSURE/LOW TEMPERATURE SINTERING  
OF BULK NANOCRYSTALLINE ALUMINA**

*S.-C. Liao, Y.-J. Chen, B.H. Kear, and W.E. Mayo*

Dept. of Ceramic and Materials Engineering, Rutgers University,  
Piscataway, NJ 08854, USA

Bulk n-Al<sub>2</sub>O<sub>3</sub> samples with relative density > 95% and grain size < 60 nm have been fabricated at temperatures as low as 0.35 T<sub>m</sub> at pressures up to 8.0 GPa, using a high pressure apparatus of novel design. Nanocrystalline  $\gamma$ -alumina powder was used as the starting material. During sintering, the metastable  $\gamma$  phase transformed to the stable  $\alpha$  phase. We believe that this phase transformation enhanced the diffusion rate, thus promoting the densification process. Grain growth was limited by the low sintering temperature. In addition, the limited grain growth of the transformed phase was related to multiple nucleation events in the parent phase during sintering at very high pressure. The average grain size of n-Al<sub>2</sub>O<sub>3</sub> increased from 12 nm in the original powder to only 60 nm in the sintered compact.

Due to its high surface area, the n-Al<sub>2</sub>O<sub>3</sub> powder reacts with chemical species in the environment. Aluminum hydrates, formed by reaction of n-Al<sub>2</sub>O<sub>3</sub> with absorbed OH<sup>-</sup> species, had a profound influence on the sintering behavior and transformation kinetics. The effect of high pressure on nucleation and growth of the transformed phase will be discussed.

**PARTICLE SIZE CONTROL DURING FLAT-FLAME SYNTHESIS  
OF NANOPHASE OXIDE POWDERS**

*Y.-J. Chen, N. Glumac<sup>1</sup>, B.H. Kearn and G. Skandan<sup>2</sup>*

Dept. of Ceramic and Materials Engineering, Rutgers University,  
Piscataway, NJ 08854 USA

<sup>1</sup>Dept. of Mechanical and Aerospace Engineering, Rutgers University,  
Piscataway, NJ 08854, USA

<sup>2</sup>Nanopowder Enterprises Inc., 120 Centennial Ave., Piscataway, NJ 08854-3908, USA

Low pressure combustion synthesis has been used to generate oxide nanopowders of narrow particle size distribution. However, little is known about their formation mechanism in the uniformly flat combustion zone. Detailed understanding of the mechanism is required in order to more effectively control the particle size and to avoid particle agglomeration. In this research, reactor pressure, precursor feed rate, burner-to-substrate distance, and fuel feed rate were systematically varied in order to obtain a better understanding of their effect on particle size and agglomeration. SiO<sub>2</sub> nanopowder was chosen as the target material; it was produced in the flat-flame combustor by pyrolysis of HMDS. Powder was collected from the chamber wall as well as from the substrate below the burner. In situ diagnostics using laser induced fluorescence provided information on the temperature profile, the extent of reaction, and the particle size distribution in the combustion zone. Preliminary results show that (1) particle size decreases as precursor feed rate increases, (2) particle size decreases as the gap distance increases, and (3) particle size increases with pressure up to a maximum of about 25 mbar. SiO\* emission was also monitored, and the intensity was found to increase with the precursor feed rate. For a fixed precursor feed rate, the SiO\* emission intensity decreased with distance along the gap and was close to zero at about half of the gap distance. When normalizing the intensity profiles, all the plots fall onto the same curve, which indicate that the reaction behavior varies little along the gap, irrespective of precursor feed rate over the range of interest. An interpretation of these findings will be presented.

**SINTERING OF BIMODAL ZrO<sub>2</sub> - 4 WT% Y<sub>2</sub>O<sub>3</sub> POWDER MIXTURES  
WITH THE NANOCRYSTALLINE COMPONENT**

*M. Moskovits, B. G. Ravi and R. Chaim*

Department of Materials Engineering,  
Technion - Israel Institute of Technology, Haifa 32000, ISRAEL

ZrO<sub>2</sub> - 4 wt% Y<sub>2</sub>O<sub>3</sub> powders with four different particle sizes in the range of 10 to 500 nm were used to prepare bimodal powder mixtures by ultrasonic and ball milling techniques. The effects of powder composition, solvent, polymer additives, mixing technique and compaction pressure on homogeneity and green density of the green compacts were investigated. The shrinkage characteristics of the powders were determined by dilatometry. The compacts were sintered within the temperature range of 1050-1400°C and duration of 1 to 10 hrs. The microstructure of the powders as well as the sintered compacts were characterized by x-ray diffraction, scanning (SEM) and transmission (TEM) electron microscopy. The composition for the maximum green packing depended on the coarse to fine size ratio. German's packing model was used to describe the observed green as well as sintered density and homogeneity of the compacts.

**TEMPLATE ASSISTED SYNTHESIS OF ULTRAFINE (NANOSIZED)  
IRONOXIDE PARTICLES AND THEIR CATALYTIC UTILITY  
IN CARBON NANOTUBE ARRAY FORMATION**

*Jorg J. Schneider<sup>1</sup>, Norbert Czap<sup>1</sup>, Gabor L. Hornyak<sup>2</sup> and Michael J. Heben<sup>2</sup>*

<sup>1</sup> Institut fur Anorganische Chemie der Universität-GH Essen, Universitätsstraße 5-7,  
45117 Essen, GERMANY <joerg.schneider@uni-essen.de>

<sup>2</sup> National Renewable Energy Laboratory, NREL, Golden, 80401 Colorado, USA

Nanosized late transition metal oxide particles are of growing interest in material science due to their unique properties, and may have potential applications in photonics<sup>(1)</sup>, magnetics ferrofluids, imaging and recording devices<sup>(2)</sup> (e.g. Fe<sub>3</sub>O<sub>4</sub>, Fe<sub>2</sub>O<sub>3</sub>). Such magnetic nanoclusters have been produced in a variety of matrix materials like silicon oxides<sup>(3)</sup>, porous glass<sup>(4)</sup>, vesicles<sup>(5)</sup>, and polymers<sup>(6)</sup>. Typical ways to prepare ultrafine (nanosized) transition metal oxide particles use incipient wetness techniques<sup>(7)</sup>, sol gel techniques<sup>(8)</sup>, thermal decomposition of organometallics<sup>(4)</sup>, or arrested hydrolysis of metal halides<sup>(9)</sup>.

Herein we report on our studies using a new unique low temperature molecular approach to synthesize nanosized Fe<sub>2</sub>O<sub>3</sub> particles within the mesoporous channels of anodically formed alumina membranes. The ultrafine particles prepared show a relatively narrow particle size distribution and exhibit a pronounced quantum size effect. The synthesis is accomplished via a "ship in the bottle" type approach employing mesoporous alumina as the host material. The template is loaded with a labile organo-iron compound. Impregnation of the oxide is accomplished at -78°C which present the mildest conditions ever reported for the synthesis of nanosized oxide particles. We have found that hydrogen reduction of such nanoscale Fe<sub>2</sub>O<sub>3</sub> particles can lead to ultrafine Fe particles which are catalytically active in the formation of carbon nanotube arrays formation within the channels of the mesoporous alumina host.

- [1] H. Miyoshi, H. Yoneyama, *J. Chem. Soc. Faraday Trans. 1*, (1989) 85, 1873
- [2] a) Q.A. Pankhurst, R.J. Pollard, *J. Phys.: Condens. Mater.* (1993) 5, 8487,  
b) H.E. Jones, P.R. Bisell, R.W. Chantrell, *J. Magn. Magn. Mater.* (1995) 149, 14,  
c) S.B. Oseroff, D. Clark, S. Schulz, S. Shtrikman, *IEEE Trans. Magn.* (1986) 21, 1495;
- [3] R.D. Shull, J.J. Ritter, L.J. Swartzendruder, *J. A@pl. Phys.* (1991) 69, 5414
- [4] E.A. Mendoza, E. Wolkow, D. Sunil, P. Wong, J. Sokolov, M.H. Rafailovich, M. den Boer, H.D. Gafney, *Langmuir*, (1991) 7, 3046
- [5] S. Mann, J.P. Hannington, *J. Colloid Interface Sci.* (1988) 22, 326
- [6] B.H. Sohn, R.E. Cohen, *Chem. Mater.* 1997, 9, 264
- [7] T. Abe, Y. Tachibana, T. Uematsu, M. Iwamoto, *Chem. Commun.* (1995) 1617
- [8] see various articles in special issue on sol-gel derived materials, *Chem. Materials* (1997) 9, no. 11 (November)
- [9] C. Kormann, D.W. Bahnemann, M.R. Hoffmann, *J. Phys. Chem.* (1988) 92, 5196

**PREPARATION OF PALLADIUM-ORGANOCLAY CATALYSTS**

*Zoltán Király, Ágnes Mastalir\*, Katalin Debreceni, Anna Szücs and Imre Dékány*

Department of Colloid Chemistry and \*Department of Organic Chemistry, University of Szeged, Aradi Vt. 1, H-6720 Szeged, HUNGARY <zkiraly@chem.u-szeged.hu>

Liquid sorption and X-ray diffraction measurements on various alcohol-hydrocarbon/hexadecylammonium montmorillonite dispersions indicated that a hydrocarbon-rich bulk liquid phase was equilibrated with a swollen, ethanol-rich interlamellar phase. The adsorption layer, where ethanol functioned as both a solvent and a reducing agent for organic palladium complexes, provided a suitable environment for the reduction of  $\text{Pd}^{2+}$  cations to  $\text{Pd}^0$  clusters in the clay host. Accordingly, introduction of  $\text{Pd}(\text{II})$ -acetate into the organoclay suspension led to the generation and deposition of finely divided (2 to 14 nm) metallic Pd dispersions in the interlamellar space. Alternatively, Pd-organoclays have been prepared by direct deposition of monodispersed Pd particles (1 to 4 nm) via adsorption of the particles from a separately prepared Pd sol. For both methods, the size of nanoparticles and the extent of particle loading were controlled by the experimental conditions. A number of samples were synthesized and subjected to instrumental investigations (BET surface area analysis, TEM, ICP and UV spectroscopies, XRD and SAXS measurements, low-shear rheology). The Pd-organoclay samples proved to be catalytically active in liquid phase olefin hydrogenation reactions.

**DEVELOPMENT OF METHODS OF SEVERE PLASTIC DEFORMATION  
FOR PROCESSING OF BULK NANOSTRUCTURED METALS AND ALLOYS.**

*V.V. Latysh, G.I. Raab and I.V. Alexandrov*

Institute of Physics of Advanced Materials, Ufa State Aviation Technical University,  
K.Marksa 12, 450000 Ufa, RUSSIA <igor@ippm.rb.ru>

Bulk nanostructured metals and alloys can be processed using different methods of severe plastic deformation (SPD), in particular, torsion under high pressure, equal channel angular (ECA) pressing and others [1]. The results of development of SPD methods for processing of hard-to-deform materials and low ductile metals and alloys, such as titanium and quenched aluminium alloys, high melting metals, metalloceramic compounds, are presented in the given work.

On the basis of the analysis of mechanics of SPD processing of model materials (copper) the main parameters restricting technological deformability and nanostructured formation in the process of ECA pressing were investigated.

Development of ECA pressing includes modification of the die (choice of angle between channels, tribology characteristics, etc), as well as optimal temperature-strain rate conditions of processing for forming required samples without damages and having homogeneous structure. Examples of fabrication of massive samples-rod, 100-150 mm in length, out of aluminium and titanium alloys and metalloceramic compound are presented.

1. R.Z. Valiev. Structure and Mechanical Properties of Ultrafine-Grained Metals. Mater. Sci. Eng., 1997, Vol. A234-236, p. 59-66.

**ELECTRON MICROSCOPY OF NOBLE METAL ALLOY NANOPARTICLES  
PREPARED BY SONOCHEMICAL METHODS**

*R.Oshima, T.A.Yamamoto\*, Y.Mizukoshi and Y.Nagata*

Research Institute for Advanced Science and Technology, Osaka Prefecture University,  
1-2 Gakuencho, Sakai, Osaka 599-8570, JAPAN <oshima@riast.osakafu-u.ac.jp>

\* Department of Nuclear Engineering, Osaka University, 2-1 Yamadaoka, Suita,  
Osaka 565-0781, JAPAN

It was reported that Au, Pd and Pt nanoparticles are successfully produced by reduction of argon-saturated aqueous solutions of  $\text{NaAuC}_{14}$ ,  $\text{PdCl}_{22}\text{NaCl}$  and  $\text{K}_2\text{PtC}_{14}$  by ultrasound irradiation, respectively. In the present study, the procedure has been developed to prepare binary noble metal alloy nanoparticles directly by reducing mixture of aqueous solutions with various concentrations of Au, Pd or Pt metal ions by sonochemical methods. Sample solutions of 60mL were charged in cylindrical glass vessels, and were irradiated with an ultrasonic wave of 200kHz with an input power of 200W. During the irradiation, the whole system was water-cooled. Droplets of obtained colloidal dispersion were recovered on carbon-supported copper grids, and were dried in vacuum, and their characterisation was carried out using transmission electron microscopy (TEM), high resolution electron microscopy (HRTEM) and nano area energy dispersive X-ray spectroscopy (EDX). Comparing with size distribution of sonochemically prepared Au or Pd nanoparticles from 3 to 20 nm, equiautomic AuPd alloy nanoparticles exhibited a rather monodispersive distribution with a size of 8 nm. Sizes of Au-Pd alloy nanoparticles with different compositions were also monodispersive. It is known that the Au-Pd binary alloy system forms a continuous solid solution, while the sonochemically prepared Au-Pd nanoparticles were found to have a core-shell structure by HRTEM. Nano area EDX showed that the core is composed of gold, and the shell Pd. Au-Pt alloy nanopartilcles have not been obtained by this method, and mixtures of Au and Pt nanoparticles were formed. The present results clearly indicate characteristic differences in chemical and metallurgical properties between Au-Pd and Au-Pt systems, as suggested by marked change in the phase diagrams.

### SINTERING OF NANOSTRUCTURAL TITANIUM OXIDE USING MILLIMETER-WAVE RADIATION

*Yu. Bykov<sup>1</sup>, A. Eremeev<sup>1</sup>, S. Egorov<sup>1</sup>, V. Ivanov<sup>2</sup>, Yu. Kotov<sup>2</sup>, V. Khrustov<sup>2</sup> and  
A. Sorokin<sup>1</sup>*

<sup>1</sup> Institute of Applied Physics Russian Academy of Sciences, 46 Ulyanov str.,  
603600 Nizhny Novgorod, RUSSIA <byk@sci-nnov.ru>

<sup>2</sup> Institute of Electrophysics Ural Division of the Russian Academy of Sciences,  
Komsomolskaya str. 34, 620049 Ekaterinburg, RUSSIA <iwanov@ief.intec.ru>

The search of an adequate method of densification is of paramount importance for fabrication of nanostructured ceramic materials. The use of microwave sintering is one of the methods of great potential for densification of nano-sized powder compacts to the near theoretical density. Fast volumetric microwave heating opens the possibility to produce dense ceramic material while retaining the grain size on the nanometric scale.

The study was undertaken to compare microwave sintering of the green samples fabricated of the TiO<sub>2</sub> powder synthesised by two methods - wire electrical explosion and gas condensation. Both of these powders were compacted using two techniques - cold isostatic pressuring and magnetic dynamic compacting. The latter technique allows to achieve much higher density of the green samples and to overcome, to some extent, the problem of powder agglomeration within samples.

Results on the kinetics of sintering, as well as kinetics of grain growth will be presented. Comparative analysis of the kinetic data for both powders will be discussed. Comparison between the results of microwave and fast conventional sintering will be made and specific features pertinent to microwave processing be considered.

**TOPOLOGICAL CORRELATIONS OF MULTICOMPONENT LIQUID AND SOLID SYSTEMS CONTAINING COPPER (I) HALOIDS**

*Chernykh L.V. and Skripkin M.Yu.*

Dept. of Chemistry, Sankt-Petersburg State University, 198904,  
Sankt-Petersburg, RUSSIA <kburkov@kb1954.spb.edu>

Many kinds of optic materials ( photochromic, non-linear glasses etc. ) contain copper (I) complex haloids as nano-phase in inorganic matrix. The concentration of copper (I) compounds, their stability and the size of crystalline phase determine the properties of the glasses. These parameters are strongly dependent on the presence and concentration of other components, first of all, alkaline haloids. Experimental investigation of these regularities in solids is rather complicated but it was shown that there are some topological correlation between liquid and solid systems.

Therefore, we have undertaken the thermodynamic study of the systems CuX " MX " H<sub>2</sub>O (M<sup>+</sup> = Li<sup>+</sup>, Cs<sup>+</sup>, NH<sub>4</sub><sup>+</sup>; X<sup>-</sup> = Cl<sup>-</sup>, Br<sup>-</sup>). The solubility, activities of components and (Gf 0 of complex salts were determined. As the result: the influence of chemical nature of M<sup>+</sup> on the CuX solubility, forms and stability of complex salts was revealed and analysed; the considerable increasing of CuX solubility in the presence of alkaline haloids (up to 105 times) was found; the topological isomorphism of the diagrams "composition of fusion melting point" and composition of solution activity of water was established; the correlation between the fields of crystallisation of compounds in fusion and corresponding aqueous systems were observed; some correlation between the stability of complex compounds and the properties of corresponding glasses were established.

The results obtained may be utilised in any technologies if the concentration of CuX in liquid phase should be increased. They can lead to the new ways to change the properties of copper (I) haloids containing materials.

This work was supported by the Russian Fund of Fundamental Investigations under Grant 97-03-32095.

**MAKING CERAMICS FROM NANOMETER-SIZED  $\text{Al}_2\text{O}_3$   
POWDERS WITH ADDITIONS OF  $\text{MgO}$  AND  $\text{TiO}_2$   
BY DYNAMIC COMPACTION AND SINTERING**

*V. Ivanov<sup>1</sup>, S. Paranin<sup>1</sup>, V. Khrustov<sup>1</sup>, Y. Kotov<sup>1</sup>, I. Beketov<sup>1</sup>,  
A. Murzakaev<sup>1</sup>, A. Medvedev<sup>2</sup> and A. Shtol'ts<sup>2</sup>*

<sup>1</sup> Institute of Electrophysics, Ural Division of the Russian Academy of Sciences

Komsomolskaya Str. 34, 620049 Ekaterinburg, RUSSIA <razrad@ief.intec.ru>

<sup>2</sup> Ural State Technical University, Mira Str.19, Ekaterinburg 620002, RUSSIA

The influence of  $\text{MgO}$  and  $\text{TiO}_2$  additions on the properties of nanostructured  $\text{Al}_2\text{O}_3$  ceramics has been investigated. Nanometer-sized  $\text{Al}_2\text{O}_3$ ,  $\text{Al}_2\text{O}_3 + 1.3$  wt%  $\text{MgO}$ ,  $\text{TiO}_2$  powders with the mean particle size of 20 to 30 nm were produced by electrical explosion of Al, Ti and Al + Mg, alloy wires in an oxygen-containing atmosphere. Mixtures of powders, which contained 0.3, 0.6 wt%  $\text{MgO}$  and 0.3, 0.6, 1.0 wt%  $\text{TiO}_2$ , were prepared by mixing in the required proportion the initial powders in ethyl alcohol after removing by sedimentation the coarse fraction with particles over 0.2-0.5  $\mu\text{m}$  in size.

The powders were compacted dynamically by the magnetic pulsed method to a density of 0.70-0.74 relative to X-ray density. Further, the compacts were sintered in controlled-rate-of-shrinkage regimes by heating to temperatures of 1360-1400°C. It is shown that additions of  $\text{MgO}$  increase the rate of densification of compacts in the course of sintering and lead to the production of ceramics with a relative density of over 0.98 and with a hardness of 22 GPa. We present results of X-ray and electron microscope studies of these ceramic materials and also results of tests of their mechanical properties. ceramic materials and also results of tests of their mechanical properties.

**PRODUCTION OF NANOMETER-SIZED AlN POWDERS  
BY THE EXPLODING WIRE METHOD**

*Y.A. Kotov and O.M. Samatov*

Institute of Electrophysics, Ural Division of the Russian Academy of Sciences  
Komsomolskaya Str. 34, 620049 Ekaterinburg, RUSSIA <razrad@ief.intec.ru>

We have performed experiments to explore the possibility of making pure nanometer-sized AlN powders by electrical explosion of aluminum wire in an atmosphere of nitrogen-containing gases.

It is shown that raising the density of the energy injected into the metal, applying increased pressures, and a high working-gas flow rate help assure the production of AlN powders with a specific surface up to  $50 \text{ m}^2/\text{g}$ ,  $d_{\text{BET}} = 40 \text{ nm}$ . Particle shape ranges from nearly spherical to rigorous-cut particles. The yield of such powder accounts for 40% of the total mass of powder. The powder thus produced contains no more than 0.5 wt. % of impurities, including oxygen.

**DYNAMIC COMPRESSION ADIABATS OF NANOMETER-SIZED POWDERS**

*V. Ivanov and A. Nozdrin*

Institute of Electrophysics Russian Academy of Sciences, Ural Division,  
Komsomolskaya Str. 34, Ekaterinburg 620049, RUSSIA <ivanov@ief.intec.ru>

The dynamic compressibility of  $TiO_2$ ,  $Al_2O_3$  and  $ZrO_2$ , nanometer-sized powders of various agglomeration states has been investigated by the new method. It rests on measurements of pulsed pressure during the magnetic pulsed compaction of powder, on a physical model of the process, and on a specially devised computer program for the numerical processing of experimental data by spectral analysis means. This method permits us to extract from pulsed powder-compaction-pressure measurements all possible information, including, aside from pressure, the current density and the compression work of the powder. In the processes under study, the powder is exposed to soft pulsed compressing waves with smooth nonimpact loading and unloading fronts. Pulsed pressure in the powder is generated as a result of the press tool being accelerated by a strong pulsed magnetic field and subsequently retarded by the powder target and typically has rise and fall times on the order of 100  $\mu s$ . In this case, pulse shape and pulse amplitude are determined by three factors: accelerating force, elastic properties of the press tool, and powder compressibility. Using the experimentally measured compacting pressure pulse, the elastic properties of the press tool that are known from the calibration, and the accelerating magnetic force, the method permits calculation of the current powder density.

**FORMATION AND COALESCENCE OF TUNGSTEN NANOPARTICLES  
UNDER ELECTRON BEAM IRRADIATION**

*Yoshitaka Tamou and Shun-ichiro Tanaka*

Tanaka Solid Junction Project, Japan Science and Technology Corporation  
1-1-1 Fukuura, Kanazawa-ku, Yokohama 236-0004, JAPAN <tamo@tanaka.jst.go.jp>

Nanofabrication is a key technology for designing and assembling of semiconductor devices. In this paper, an electron microscope was applied to investigate the possibility of electron beam technology for creating nanostructured materials.

Powder particles of tungsten oxide ( $\text{WO}_3$ ) were irradiated by electron beam with 200 keV energy in a transmission electron microscope. A single crystal powder particle was irradiated with the probe current of  $6 \times 10^4 \text{ A/cm}^2$  under room temperature. A number of nanocrystals were induced in the powder particle as a result of the irradiation damage. Although the oxide phase is stable under the experimental conditions, EELS analysis exhibited the decrease of oxygen content in the powder particle which suggested the decomposition of the tungsten oxide.

In the vicinity of irradiated powder particles, a number of ultrafine particles of nm size were observed on a carbon film substrate. These nanoparticles were spherical and have the diameter of 2-6 nm with sharp distribution of the particle size. EDX and EELS analyses revealed these nanoparticles oxide free tungsten nanoparticles. These nanoparticles migrated under the subsequent electron beam irradiation. A few nanoparticles which came into contact were observed to coalesce each other to form a single crystal particle.

Electron beam technique has a possibility of assembling nanoparticles into nanostructured materials as a non-equilibrium fabrication process.

**PROPERTIES OF Mg-Y-Cu GLASSES  
WITH NANOCRYSTALLINE PARTICLES**

*N. Schlorke, B. Weiß, J. Eckert and L. Schultz*

Institut für Festkörper- und Werkstoffsorschung Dresden, Institut für Metallische  
Werkstoffe, Postfach 27 00 16, 01171 Dresden, GERMANY  
[<n.schlörke@ifw-dresden.de>](mailto:<n.schlörke@ifw-dresden.de>)

Nanocrystals embedded in an amorphous Mg-Y-Cu phase can lead to an increase in yield stress and fracture stress compared to the homogeneous amorphous alloy. Therefore, mechanical alloying of elemental Mg, Y and Cu powders with Si-, Ce- and  $\text{Y}_2\text{O}_3$ - additives was used to prepare amorphous/nanocrystalline phase mixtures. The crystallization behaviour and crystallization kinetics of the powders were compared with results for rapidly quenched ribbons and powders produced by ball milling of pieces of melt-spun ribbons. Despite the existence of nanocrystalline particles in the amorphous matrix, all samples exhibit a temperature difference  $\Delta T_x$  ( $=T_x - T_g$ ) of about 50 - 60 K between the glass transition temperature  $T_g$  and the crystallization temperature  $T_x$  and a decrease of viscosity above the glass transition temperature. Additions of 2.5-10 vol.% Si during mechanical alloying enhance the thermal stability of the amorphous Mg-Y-Cu phase. Bulk amorphous/nanocrystalline samples can be prepared via consolidation and subsequent hot working in the viscous state above  $T_g$ . The different crystallization behaviour of the samples provides the possibility to specifically tailor the microstructure during consolidation. Finally, first results on the mechanical properties of the samples are presented.

**MICROSTRUCTURAL DEVELOPMENT IN AlN COMPOSITE CERAMICS**

*Masahiko Tajika and Hideaki Matsubara*

Synergy Ceramics Laboratory Fine Ceramics Research Association,  
2-4-1, Mutsuno, Atsuta-ku, Nagoya, 456-8587 JAPAN <tajika@mxa.mesh.ne.jp>

Since aluminum nitride (AlN) has high thermal conductivity and good electrical properties, it is often considered as one of the candidate materials for heat management of semiconductor devices with high power. Recently AlN-BN composite ceramics have been developed with excellent properties such as good machinability and high heat shock resistance, and they are expected to find application in various fields. The purpose of this study was to understand microstructural development in the AlN-BN composite ceramic system. In particular, this study focused on microstructure change during heat treatment of sintered AlN-BN composites. AlN-BN composite ceramics were fabricated by sintering a mixture of fine AlN and BN powders containing  $\text{Y}_2\text{O}_3$  as a sintering aid at 2123 K in nitrogen atmosphere. BN content was set up to 10 vol%. The heat treatment of sintered AlN-BN composite was performed at 2073 K in nitrogen atmosphere. The microstructures of composite samples were observed using a scanning electron microscope, and thermal diffusivity and mechanical properties were evaluated using laser flash and IF (indentation fracture) methods, respectively. BN particles in the composite showed large anisotropic grain growth during sintering, and the shape of grown BN particles appeared to be plate-like. Moreover, the heat treatment gave very interesting microstructures of the composite, in which many more interfaces between AlN grains were observed and most of the secondary phase was located at triple points of AlN grains. The resultant microstructure change is thought to be due to the change in the ratio of interfacial energy (between grain and liquid) and grain boundary energy (between grains).

**OPTICAL PROPERTIES OF QUASIFRACTAL METAL  
NANOPARTICLE AGGREGATES**

*J.A. Sotelo<sup>1</sup> and G.A. Niklasson<sup>2</sup>*

<sup>1</sup> Dpto. de Fisica y Matematicas, Universidad Peruana Cayetano Heredia,  
Apto. 5045, Lima, PERU

<sup>2</sup> Department of Materials Science, Uppsala University, P.O. Box 534,  
S-75121 Uppsala, SWEDEN

We calculate the optical extinction efficiency of two-dimensional small quasifractal aggregates consisting of metal nanoparticles. The aggregates were taken to have the structure of a finite size fractal "snowflake". Computations were carried out by the theory of Gérardy and Ausloos in the octupolar approximation for aggregates of up to 25 particles. Some calculations for 125 particles in the dipole approximation have also been carried out. Computations for gold particles much smaller than the wavelength of light showed two major peaks in the extinction in the visible wavelength range. These are due to the localized plasma resonance of the conduction electrons in a single particle and in the whole cluster, respectively. Additional peaks due to the fractal structure and the quadrupole and octupole terms are also observed.

For particles with a radius of 30 Å the octupolar solution is well approximated by including interactions up to the third nearest neighbour particles only. Hence calculations for larger clusters may be possible to simplify. However, the approximation becomes worse as the particle size is increased. On the other hand a simple renormalization scheme earlier proposed by us does not give good results at low frequencies. Going to larger aggregate sizes, or including higher multipoles shifts the low frequency peak towards still lower frequencies.

**TRANSITION METAL DICHALCOGENIDES NANOPOWDERS**

*L.M. Kulikov<sup>1</sup>, A.A. Semjonov-Kobzar<sup>1</sup>, V.V. Kartuzov<sup>1</sup>, I.V. Krasikov, E.A. Efimova<sup>1</sup>,  
K.E. Grinkevych<sup>1</sup>, I.I. Odokienko<sup>1</sup>, L.G. Akselrud<sup>2</sup> and L.P. Romaka<sup>2</sup>*

<sup>1</sup> National Acad.Sci. of Ukraine, Kiev, UKRAINE <semkob@ipms.kiev.ua>

<sup>2</sup> L'viv State University, L'viv, UKRAINE

On account of peculiarity of the crystal structure the layered Transition Metal Dichalcogenides (TMD) are the objects of the great attention of the materials scientists. The initial anisotropy of their mechanical, physico-chemical and physical properties may be essentially enhanced as a result of topochemical reaction of their intercalation. The active motion of the intercalate fronts and appearance of mechanical stresses can initiate crystal dispersion and is possible to use this process as a direct method for production of dichalcogenide nanopowders. The realization of crystal structures activated due to their intercalation and transfer into nanostate will promote obtaining of such new physical properties that aren't available in coarse grained powders or single crystals.

The possibilities of nanocrystal materials on the basis of initial TMD and their intercalates (2H-NbSe<sub>2</sub>, 2H-MoSe<sub>2</sub>, 2H-WSe<sub>2</sub>, Cu<sub>x</sub>NbSe<sub>2</sub>, Cu<sub>x</sub>WSe<sub>2</sub>, Ti<sub>x</sub>WSe<sub>2</sub> etc.) produced by means of high power ultrasonic actions were studied. It was established that powders crystal structure and composition do not undergo essential changes during their dispersing in absence of intercalation by components of liquid dispersed media (acetone, water, ethanol, industrial oil, solutions of different salts). The universal set of programs for solving crystal structure parameters and average size of anisotropic dispersing particles has been developed (method of X-ray lines broadening). For different conditions of production, for example, average sizes of 2H-NbSe<sub>2</sub> particles are 23-28 nm (direction [013]) and 60-130 nm (direction [110]); 2H-WSe<sub>2</sub> – 16-46 nm, 90-94 nm; 2H-MoSe<sub>2</sub> -(44,8±1,5) nm only for [013]; 2H-MoS<sub>2</sub> -(110,4±7,0) nm, (13,0±7,2) nm; Ti<sub>0,67</sub>WSe<sub>2</sub> - (9,7±0,9) nm, (29,0±2,0) nm; Cu<sub>0,85</sub>WSe<sub>2</sub> – 98-134 nm, 140-148 nm; Cu<sub>0,2</sub>NbSe<sub>2</sub> - (5,0±1,0) nm only for [013] ; Cu<sub>0,75</sub>NbSe<sub>2</sub> - (56,9±1,9) nm, (87,0±3,1) nm.

On the basis of random walk method have been developed the computer imitation model that gave the possibility to describe the movement of intercalate front into crystal in significantly nonequilibrium conditions during the dispersing of particles.

The effect of addition of different nanophase TMD and their intercalates on lubricating capacity of different lubricants was studied. It was determined that dynamic loading, intensifying the wear in specific cases, causes formation of self-organizing films, decreasing wear and losses by friction. Nanophase TMD and their intercalates are prospective materials to form such coatings under dynamic (non-stationary) friction. They are much effective than the natural MoS<sub>2</sub>.

**FORMATION OF IRON-NICKEL NANOCRYSTALLINE ALLOY  
BY MECHANICAL ALLOYING**

*V.V. Tcherdyntsev<sup>1</sup>, S.D. Kaloshkin<sup>1</sup>, I.A. Tomilin<sup>1</sup>, E.V. Shelekhov<sup>1</sup>, and  
Yu.V. Baldokhin<sup>2</sup>*

<sup>1</sup> Department of Physical Chemistry, Moscow Steel and Alloys Institute,  
Leninsky prosp., 4, Moscow, 117936, RUSSIA <vvch@phch.misa.ac.ru>

<sup>2</sup> Institute of Chemical Physics Academy of Science,  
Kosygina str. 4, Moscow 117334, RUSSIA

Fe-Ni alloys were prepared by mechanical alloying of elemental powders in high-energy planetary ball mill in a wide concentration range of components. The intensity of milling process estimated by different methods was 10-15 W/g. The structure was studied by X-ray diffractometry, Mössbauer spectroscopy and SEM. The phases composition of mechanically alloyed (MA) samples show strong extending of single-phase solid solutions concentration ranges. Character of X-ray peaks indicates that there is a high density of crystalline lattice defects including stacking faults. According to the broadening of X-ray reflexes MA samples had grain size 10-20 nm. Formation of stacking faults in f.c.c. structure is typical for mechanically alloyed materials, especially for systems, which tend to form h.c.p. structure (Fe-Mn, Fe-Co, etc.). As Fe-Ni system do not tend to form h.c.p. structure, the concentration of stacking faults in MA samples were found to be lower (< 6 %) than in e.g. Fe<sub>80</sub>Mn<sub>20</sub> and Fe<sub>10</sub>Co<sub>90</sub> compositions (about 10 %). The concentration of stacking faults increases with increase of Fe content in  $\gamma$ -Ni(Fe) phase.

Kinetics of structure transformations at mechanical treatment was investigated for the Fe70Ni30 alloy. The ratio between the phase amounts changes linearly with milling time. This shows that the degree of transformation at milling is proportional to input energy. Single-phase f.c.c. alloy was formed after 30 min of milling. SEM micrographs show the increase of particles size with milling time.

The results were discussed on the basis of assumption that the rate of MA transformation is proportional to the work of grain boundary slipping at deformation.

**COMPLEX FORMATION IN SOLUTIONS FOR CHEMICAL SYNTHESIS  
OF NANOSCALE PARTICLES PREPARED  
BY BOROHYDRIDE REDUCTION PROCESS**

*Savka Stoeva<sup>1</sup>, Peter Stoimenov<sup>1</sup>, Iovka Dragieva<sup>2</sup>, Emil Pavlikyanov<sup>3</sup> and  
Kenneth Klabunde<sup>4</sup>*

<sup>1</sup> State University of Sofia, Dept. Chemistry, 1126 Sofia, BULGARIA

<sup>2</sup> Bulgarian Academy of Sciences, CLEPS, 1113 Sofia, BULGARIA

<banchem@bgearn.acad.bg; banchem@bgcict.acad.bg; iovka@cleps.acad.bg>

<sup>3</sup> Technical University, Russe, BULGARIA

<sup>4</sup> Kansas State Univ., Dept. Chemistry, KS 66506, USA

Complex forming agents are often used in chemical synthesis of nanoscale particles by means of a borohydride reduction process [1]. Their influence on the rate of nucleation and a growth of particles without oxide/hydroxides shell are estimated earlier. In this paper experimental data are presented about the synthesis of  $\text{Fe}_x\text{Nd}_{1-x}$  ( $\text{B}_y\text{H}_z$ ) particles from chloride water solutions by reduction with sodium borohydride , as well as a synthesis of  $\text{Fe}_{x_1}\text{Si}_{x_2}\text{Nd}_{1-(x_1+x_2)}$  ( $\text{B}_y\text{H}_z$ ) particles, containing silicon, by using iron (II) hexafluorosilicate.

According to the estimated influence of the aqua-complex structures on the synthesis of amorphous or nanocrystalline particles [2], synthesis of initial complex salts - precursors *trans*-[bis(ethylenediamine)dichlorocobalt(III)] chloride and *cis*-[bis(ethylenediamine) dichlorocobalt(III)] chloride is carried out.

The influence of the metal complex used in water solutions by a reduction with sodium borohydride on the composition, the structure and specific surface area of prepared nanoscale particles is investigated.

- [1] I. Dragieva, M. Slavcheva, D. Buchkov, *J. Less Common. Metals*, **117** (1986) 311.
- [2] V. Krastev, M. Stoycheva, E. Lefterova, I. Dragieva, Z. Stoynov, *J. Alloys and Compounds*, **240**, 1/2 (1996) 186.

**SYNTHESIS AND CHARACTERIZATION  
OF NANOCRYSTALLINE ZINC FERRITE**

J.S. Jiang<sup>1</sup>, X.L. Yang<sup>1</sup>, L. Gao<sup>2</sup>, J.K. Guo<sup>2</sup>, and J.Z. Jiang<sup>3</sup>

<sup>1</sup> Department of Chemistry and Physics, East China Normal University,  
Shanghai 200062, CHINA

<sup>2</sup> The state Key Lab on High Performance Ceramics and Superfine Microstructure,  
Shanghai Institute of Ceramics, Chinese Academy of Sciences, Shanghai, CHINA

<sup>3</sup> Department of Physics, Building 307, Technical University of Denmark,  
DK-2800 Lyngby, DENMARK

Nanocrystalline zinc ferrite powders,  $ZnFe_2O_4$ , have been successfully synthesised by high-energy ball milling at ambient temperature from a mixture of  $\alpha\text{-Fe}_2O_3$  and  $ZnO$  crystalline powders in equimolar ration. The phase evolution in samples during milling was investigated by X-ray diffraction, transmission electron microscopy, and Mössbauer spectroscopy. From the X-ray diffraction patterns it is found that after a milling time of 70 h,  $\alpha\text{-Fe}_2O_3$  and  $ZnO$  phases disappear while a new phase with a spinel structure,  $ZnFe_2O_4$ , is formed. The average crystallite size and the morphology of the  $ZnFe_2O_4$  powders prepared are found to be about 10 nm and a spherical shape, respectively. From low-temperature and in-field Mössbauer measurements it is revealed that  $ZnFe_2O_4$  particles prepared are in superparamagnetic state at ambient temperature, although the magnetic transition temperature of bulk  $ZnFe_2O_4$  is about 10 K. Furthermore, a superparamagnetic doublet with a quadrupole splitting of 0.75 mm/s is observed for the as-milled sample at 295 K, which is much larger than that for bulk  $ZnFe_2O_4$  (0.33 mm/s) and that for ultrafine  $ZnFe_2O_4$  particles (0.57 mm/s) prepared by the coprecipitation method. This indicates larger structural defects in the nanometer-sized  $ZnFe_2O_4$  particles prepared by high-energy ball milling.

**SYNTHESIS OF NANOSTRUCTURED MULLITE FROM XEROGEL AND AEROGEL OBTAINED BY THE NONHIDROLITIC SOL-GEL METHOD**

*Dj. Janackovic<sup>1</sup>, A. Orlović<sup>1</sup>, D. Skala<sup>1</sup>, S. Drmanjić<sup>1</sup>, Lj. Kostić-Gvozdenović<sup>1</sup>, V. Jokanović<sup>2</sup> and D. Uskoković<sup>3</sup>*

<sup>1</sup> Faculty of Technology and Metallurgy, Karnegijeva 4,  
11000 Belgrade, YUGOSLAVIA <nht@elab.tmf.bg.ac.yu>

<sup>2</sup> Institute for Nuclear and Other Mineral Raw Materials, Belgrade, YUGOSLAVIA

<sup>3</sup> Institute of Technical Science of Serbian Academy of Sciences and Arts,  
Belgrade, YUGOSLAVIA

In this paper, the synthesis of nanosized mullite by the nonhidrolitic sol-gel method is presented. Synthesis of gel was performed by mixing AlCl<sub>3</sub> and TEOS in stoichiometric mullite composition. In order to obtain xerogels and aerogels, synthesised gels were dried in oven under the vacuum at elevated temperature, as well as under supercritical conditions of CO<sub>2</sub>, which is used for solvent extraction.

The influences of drying and synthesis conditions on the structure of obtained xerogels and aerogels are investigated by the DT, TG, IR and SEM analyses, as well as with the BET and pore size distribution, performed with N<sub>2</sub> absorption at the temperature of liquid N<sub>2</sub>. The influence of structure on the phase transformation of xero- and aero-gels during heating is examined by IR and X-ray analyses. The shrinkage of specimens during heating is observed by thermomicroscope.

These results show that:

- High homogeneity mullite gels were synthesized by the nonhidrolitic sol-gel method. After drying under the N<sub>2</sub> atmosphere and under the supercritical condition for CO<sub>2</sub>, the xero- and aero-gels were obtained.
- Mullite phase was obtained after heating xero and aero gels below 900°C.
- The crystallite size of xero- and aero-gel heated at 900, 1000, 1100 and 1400°C was followed by X-ray method. It is observed that in the case of aerogels, the crystallite size is from 12 to 20 nm, while in the case of xerogels, the crystallite size is from 32 to 100 nm, respectively.
- Difference in shrinkage during heating between xero- and aero-gels is a consequence of phase separation: the enhanced shrinkage of aerogels compared to xerogels in the temperature range between 900 and 1000°C is probably due to viscous flow phenomenon provoked by amorphous silica.

**METALLIC IRON NANOPARTICLES IN SILICA GELS**

*C. Estournès, T. Lutz and J.L. Guille*

I.P.C.M.S. Groupe des Matériaux Inorganiques UMR 46 CNRS, ULP, ECPM.  
23, rue du Loess B.P. 20/CR 67037 Strasbourg Cedex, FRANCE

Silica gels containing metallic iron particles are prepared from a mixture of tetraethyl orthosilicate, ethanol, 0.1N nitric acid and formamide in the proportion 1:4:4.5:1 in which iron is added in the form of nitrate. The range of Fe/Si molar ratio is varied from 0.01 to 0.2. After drying, the xerogels are thermally treated under hydrogen in the temperature range 600 to 1000°C. The changes occurring during these treatments are followed by X-ray diffraction, Mössbauer spectroscopy, Transmission Electron Microscopy (TEM) and static magnetic measurements.

X-ray patterns and Mössbauer spectra show that the non ferromagnetic phase  $\text{Fe}_2\text{SiO}_4$  (Fayalite) is formed, whatever iron concentration, in the temperature range 700 to 850°C. In addition, some metal particles are also formed by partial reduction. For treatment at lower temperatures, in-situ magnetic measurements show that no metallic iron is formed which is confirmed by Mössbauer spectroscopy. A nearly total reduction of the metal is only obtained at high temperatures ( $\geq 1000^\circ\text{C}$ ). Furthermore, TEM shows the presence of a layer at the interface metallic particles-silica. This is confirmed by Mössbauer spectra, which suggest the existence of a thin layer resulting from the onset of hybridisation of O with superficial Fe atoms. Indeed, one observes on Mössbauer spectra a second magnetic component which exhibits a significant increase of isomer shift; in addition, the magnetic moments assigned to this component are weakly canted in presence of an external field, consistent with the presence of antiferromagnetic interactions

**KINETICS OF SOLID SOLUTION FORMATION  
DURING MECHANICAL MILLING**

*N. Ravishankar, V. Varghese, T.A. Abinandanan and K. Chattopadhyay*

Department of Metallurgy, Indian Institute of Science, Bangalore 560 012, INDIA

It is well known that solid solution forms by mechanical alloying even in systems, which exhibit solid state immiscibility under equilibrium conditions. The formation of solid solution proceeds through several stages starting from a pure metal mixture initially to a complete solid solution at long times. At any intermediate instance, the system is comprised of a mixture of solid solutions of various compositions. This composition distribution varies with time and it is important to obtain this distribution as a function of time to understand the kinetics of solid solution formation. X-ray diffraction is the technique that is typically used to follow the phase evolution as a function of time. However, it is not possible to obtain direct information of all the compositions present from conventional XRD analysis. We present an elegant method by which this information can be obtained from XRD measurements. This method is applied to the study of the kinetics of solid solution formation in the Cu-Ni system processed by mechanical alloying.

**NOVEL SYNTHESIS METHOD OF NANOGRADE APATITE WHISKER  
BY HYDROLYSIS OF  $\alpha$ -TCP***A. Nakahira and K. Kijima*

Faculty of Engineering and Design, Kyoto Institute of Technology,  
Matsugasaki, Sakyō-ku, Kyoto 606, JAPAN <nakahira@ipc.kit.ac.jp>

A novel simple method for synthesis of nanograde hydroxyapatite whisker was developed for the biomaterials with excellent biocompatibility and bioactivity using the alpha-tricalcium phosphate ( $\alpha$ -TCP) as a starting material. Especially the hydroxyapatite whisker is greatly expected to be utilised as reinforcements of bone and teeth, because of its good mechanical properties, such as Young's modulus and strength and so on. Generally hydroxyapatite whisker was synthesised under the sever condition, such as hydrothermal synthesis. In this work, nanograde hydroxyapatite whisker was synthesised under the relatively mild processing condition by the hydrolysis of  $\alpha$ -TCP at 70°C and atmospheric pressure. The effect of organic solvent on the transformation of  $\alpha$ -TCP to hydroxyapatite was mainly examined in the present paper. The characterisation of nanograde hydroxyapatite whisker was analysed by XRD and FTIR. Its microstructure was observed by transmission electron microscopy. It was found that the morphology, size and aspect ratio of nanograde hydroxyapatite whisker could be controlled with using the organic solvent during the hydrolysis reaction of  $\alpha$ -TCP. Also other effects of temperature, NH<sub>4</sub>OH, pH, and reaction time on hydrolysis of  $\alpha$ -TCP to hydroxyapatite were discussed.

**FABRICATION AND CHARACTERIZATION  
OF Cd<sub>x</sub>Zn<sub>1-x</sub>S NANO PARTICLES**

*D.P. Acharya, B. Balamurugan, S.K. Sharmaa and B.R. Mehta.*

Thin Film Laboratory, Physics Department, Indian Institute of Technology,  
N. Delhi 110016, INDIA <brmehta @physics.iitd.ernet.in>  
Electron Microscopy Division, National Physical Laboratory, Delhi 110052, INDIA

Chemical Capping method is a simple, inexpensive and effective method for preparing semiconductor nano particles. In the present study, nano particles of Cd<sub>x</sub>Zn<sub>1-x</sub>S have been grown by chemical capping method using thiophenol as the capping agent. The size of the nano particles is controlled by varying the relative composition of the reactants and the capping agent. One of the highlights of the present work is the preparation of Cd<sub>x</sub>Zn<sub>1-x</sub>S nano particles having varying composition (x). Optical absorption spectroscopy, glancing angle x-ray diffraction, transmission electron microscopy and electron diffraction techniques have been used to characterise these nano particle. Results of x-ray and electron diffraction techniques confirm the formation Cd<sub>x</sub>Zn<sub>1-x</sub>S solid solution in the nano particle samples. The size dependence of the absorption edge has been studied for Cd<sub>x</sub>Zn<sub>1-x</sub>S nano particle samples having different values of x. It was observed that the absorption edge of the Cd<sub>x</sub>Zn<sub>1-x</sub>S nano particles was closer to the absorption edge of CdS than what is predicted from the bulk value of Cd<sub>x</sub>Zn<sub>1-x</sub>S at the same value of x. Size of the nano particles has been obtained from the shift in the optical absorption edge and the width of the x-ray diffraction peaks and these values have been compared with the transmission electron microscopy results.

**IRON NANOPARTICLES IN X AND Y ZEOLITES**

*H.K. Beyer<sup>1</sup>, K. Lázár<sup>2</sup>, Gy. Onyestyák<sup>1</sup>, B.J. Jönsson<sup>3</sup> and L.K. Varga<sup>4</sup>*

<sup>1</sup> Institute for Chemistry, H-1525 Budapest P.O.B.17, HUNGARY

<sup>2</sup> Institute for Isotope and Surf. Chem., H-1525 Budapest P.O.B. 77, HUNGARY

<sup>3</sup> Dept. Cond. Mat. Phys. Royal Inst. of Tech. S-10044 Stockholm, SWEDEN

<sup>4</sup> Res. Inst. for Solid State Physics, 1525 Budapest P.O.B. 49, HUNGARY

Iron nanoparticles less than 6 nm have been prepared by reduction of iron ions in X and Y zeolites. The reduction has been accomplished by sodium vapour generated in-situ through thermal decomposition of sodium azide. The process was studied by thermogravimetry. The ultrafine particles gave no observable X-ray pattern. Presence of zero valence iron could be detected in significant amounts by Mössbauer spectroscopy, although this component does not display the magnetic splitting characteristic for iron particles larger than a threshold size (c.a 6 nm at 300 K). These small particles have shown no clear superparamagnetic feature: the frequency dependence of the AC susceptibility was modest and the temperature dependence shows a characteristic break at about 120 K similar to the oxidised iron nanoparticles prepared by laser evaporation<sup>1</sup>. The catalytic activity of these iron particles have been characterised by the amount of the metallic surface sites available for CO chemisorption.

<sup>1</sup>T. Turkki, B.J. Jönsson, V. Ström, H. Medellius, M.S. El-Shall, K.V. Rao, Journal of Korean Magn. Soc. vol.5 (1995) 745-748.

**FORMATION OF NANOCRYSTALLINE Fe<sub>87</sub>B<sub>13</sub> AND Co<sub>89</sub>B<sub>11</sub> ALLOYS  
BY MECHANICAL ALLOYING**

*M. Jachimowicz<sup>1</sup>, V.I. Fadeeva<sup>1</sup>, A. Grabias<sup>2</sup> and H. Matyja*

Department of Materials Science and Engineering, Warsaw University of Technology,  
Narbutta 85, 02-524 Warsaw, POLAND

<sup>1</sup> Department of Chemistry, Moscow State University, Moscow, RUSSIA

<sup>2</sup> Institute of Electronic Materials Technology,  
Wolczynska 133, 01-919 Warsaw, POLAND

Nanocrystalline Fe<sub>87</sub>B<sub>13</sub> and Co<sub>89</sub>B<sub>11</sub> alloys were prepared by mechanical alloying of elemental powders. The phase formation and the microstructure of the milled powders were characterized by X-ray diffraction (XRD), differential scanning calorimetry (DSC) and Mossbauer spectroscopy (for the Fe containing alloy).

Mechanical alloying of Fe<sub>87</sub>B<sub>13</sub> powder mixture leads to the formation of supersaturated bcc solid solution with grain sizes of 10-14 nm. The lattice parameter of the Fe(B) phase decreases for the short milling times (up to 60 h), then increases after longer processing reaching a value of 0.2866 nm. This indicates that at different milling stages the boron atoms can occupy various positions in the  $\alpha$ -Fe crystalline lattice forming nanocrystalline Fe(B) solid solution. This fact was also confirmed by Mossbauer spectroscopy. Heating of as-milled Fe-B powders up to 700°C results in the appearing of metastable boride phases with various crystalline structures.

The ball milling of the Co<sub>89</sub>B<sub>11</sub> powder mixture leads to the following phase transformations: fcc+hcp  $\xrightarrow{20h}$  hcp  $\xrightarrow{40h}$  fcc+hcp  $\xrightarrow{50h}$  amorphous  $\xrightarrow{80h}$  fcc +amorphous  $\xrightarrow{150h}$  hcp. It can be assumed that amorphous phase formation is due to the allotrophic phase transformations in Co and dissolution of boron in the cobalt crystalline lattice.

**MICROSTRUCTURE AND PHASE COMPOSITION OF  
MECHANICALLY ALLOYED AND HOT PRESSEd Ti-Al ALLOYS**

*E. Szewczak<sup>1</sup>, A. Presz<sup>2</sup>, A. Witek<sup>2</sup> and J.W. Wyrzykowski<sup>1</sup>*

<sup>1</sup> Department of Materials Science and Engineering, Warsaw University of Technology, Narbutta 55, 02-524 Warsaw, POLAND

<sup>2</sup> High Pressure Research Center "UNIPRESS", Polish Academy of Science, Sokolowska 29/37, 01-142 Warsaw, POLAND

Elemental mixtures of  $Ti_xA_{100-x}$  ( $x=75, 50, 35$  at.%) were mechanically alloyed in a vibratory ball mill and then hot pressed. This permitted us to obtain fully dense bulk samples of Ti-Al intermetallics with a grain size of the order of  $10^2$  nm. The microhardness of the samples was about 500-900 HV 0,2 according to the composition and no brittle cracking was observed during the microhardness measurements. Scanning electron microscopy linked with energy dispersive spectroscopy was used for the structural and compositional analysis.

**INFLUENCE OF THE MECHANICALL ALLOYING PARAMETERS  
ON CRYSTALITE SIZE OF Al-Ti POWDERS**

*E. Szewczak and J.W. Wyrzykowsk*

Department of Materials Science and Engineering, Warsaw University of  
Technology Narbutta 85, 02-524 Warsaw, POLAND

Nanocrystalline  $Ti_xAl_{100-x}$  ( $x=75, 50, 40, 35$  at.%) alloys were prepared by mechanical alloying. The influence of milling parameters (the milling equipment, milling time and energy) on the crystallite size of the alloys obtained as well as on the thermal stability of the crystallite size was examined. The powders were characterised by X-ray diffraction, scanning differential calorimetry and transmission electron microscopy. Attention was also paid to the influence of the phase transformations during annealing of milled powders upon the crystallite size of the product.

**SYNTHESIS OF THE NANOCRYSTALLIC POWDERS  
OF THE TITANIUM HYDRID IN THE PROCESS OF THE  
MECHANOCHEMICAL DECOMPOSITION OF THE WATER**

*A. Kharlamov<sup>1</sup>, N. Kirillova<sup>2</sup>, P. Kosoroukov<sup>1</sup> and E. Bordyuk<sup>1</sup>*

<sup>1</sup> Frantsevich Institute for Problems Materials Science, 3 Krjijanoyski str.  
252680 Kiev, UKRAINE <dep73@ipms.kiev.ua>

<sup>2</sup> Shevchenko National University, Department of Chemistry, Kiev, UKRAINE

As it was earlier [1] established by us that the products of the mechanical treatment of V<sub>2</sub>O<sub>5</sub> powder at the presence of water were vanadium dioxide and peroxide. It was supposed that discoverent processes of the oxidation and the reduction due to hydrogen and hydrogen peroxide, whose are generated from water during its decomposition in the conditions of the mechanical activation. In the present work the results of the hydrogenation transition metal's especially titanium investigation in the conditions their mechanical treatment at the presence of water are representing. Mechanical treatment of metallic powders at the presence of water was carried out in the high speed (3000 turns/min) planetary ball mill.

First of all, the experiments were carried out on the mechanical treatment of water at the absence of any solid in the mill's drum. The fact of the water decomposition was established according to the detection of H<sub>2</sub> and H<sub>2</sub>O<sub>2</sub> in the gassy medium and water respectively. It was shown that the quantity of H<sub>2</sub>O<sub>2</sub> in the mechanically activated H<sub>2</sub>O the more increases the longer is treatment duration. Experiments on the metallic powder dispergation at the presence water were shown that metals are saturating by hydrogen and hydrogen peroxide is concentrating into water.

The quantity of hydrogen in dispergated metallic powder depended from the mechanical activation duration, metal/H<sub>2</sub>O ratio into the drum and reached about 250sm<sup>3</sup>/g of titanium. Moreover, metal also enriched by iron (from mill drum and balls) with the forming of TiFe phase. Obtained powder dispersions of the hydrogen material depend from hydrogen contends in it and the particles reach nano-crystal dimensions to composition TiH<sub>0.8</sub> and higher. Synthesised powders tested by chemical and X-ray analyses and also electron microscopy are investigated on the stability in the different media by the help of DTA.

- [1] A.Kharlamov, V.Zazhigalov. Peculiarities of Properties of Mechanically Activated in Various Media Oxide Vanadium. NATO ASI Advances and Challenges in the Catalytic Activation and Functionalisation of light Alkanes May 25- June7.,Faro Portugal, 1997.P43-45.

**PECULIARITIES OF SYNTHESIS OF NANODISPERSED  
POWDERS HIGH HARDNESS BORON-CONTAINING  
ALUMINUM AND OXYGEN COMPOUNDS**

*A.I. Kharlamov<sup>1</sup>, N.V. Kirillova<sup>2</sup>, S.V. Loychenko<sup>1</sup> and I.A. Kovalchuk<sup>1</sup>*

<sup>1</sup> Frantsevich Institute for Problems Materials Science, 3 Krjijanoyski str.  
252680 Kiev, UKRAINE <dep73@ipms.kiev.ua>

<sup>2</sup> Shevchenko National University, Department of Chemistry, Kiev, UKRAINE

The boron-containing aluminum compounds are least investigated of all known boride phases because of absence of a simple synthesis method. Notwithstanding that the interaction between boron and metals including aluminum is thermodynamically a very profitable process, the boron-containing aluminum phases were not synthesised from simple substances up to present time as against the boride phases of the most metals. This fact is a bright evidence of a prevailing role of the kinetic factor in proceeding of a chemical reaction, which is conditioned by an anomalous interaction between boron and aluminum. In the present report, the reasons of the anomalous proceeding of Al+B reaction are described and a mechanism for the boride phase forming. An obligatory initial stage of a reaction of interaction between boron and a transition metal is the stage of boron intrusion into the metal lattice with forming the intrusion phase of the composition with a lower boron contents (of TiB type). This stage intends scission of B-B bonds in the boron structure and forming Me-B bonds in the metal lattice. In the subsequent metal lattice saturation with boron (borating), new B-B bonds arise being and Me-Me bonds disappear (or weaken) with the result that a new, different from metal, structure (of TiB type) is formed. According to Hagg's rule, the intrusion stage are not characteristic for aluminum and boron solubility in solid aluminum is not fixed. We propose, in principle, a new mechanism triggering off arise and formation of a boride phase consisting not in the metal borating but in the metallising (by intrusion of the metal atoms) of the boron lattice. Heat effect from again formed bonds at similar mechanism of forming compounds is spending on the atomisation process activation, for example aluminum and consequently on the increasing it is aluminising reaction that rate. Spasmodity of the temperature increasing do not occur as it be observed at the metal-similar borides synthesis; the produce particles do not sinter and therefore succeed the particles form of the initial boron powder. Aluminum borides and borocarbides and boron suboxide powders was synthesised from boron with particles of spherical form and its dimension ~ 0.1 mkm, formed in the process boranes pyrolytic decomposition. The properties of aluminum borides ( $\text{AlB}_2$ ,  $\text{AlB}_{12}$ , and  $\text{AlB}_{18-31}$ ), aluminum borocarbides ( $\text{Al}_3\text{B}_{48}\text{C}_2$ ,  $\text{AlB}_{24}\text{C}_4$  and  $\text{Al}_8\text{B}_4\text{C}_7$ ) and boron suboxide  $\text{B}_{13}\text{O}_2$  was investigated by chemical, crystallooptical and X-ray methods as well as with the help of electronmicroscopy, mercury porosimetry and optical spectroscopy.

**Pb(Zr,Ti)O<sub>3</sub> BASED CERAMICS PREPARED BY SOLUTION PROCESSING**

*Barbara Malič, Marija Kosec and Goran Dracič*

Josef Stefan Institute, Jamova 39, P.O.B. 3000, 1000 Ljubljana, SLOVENIA  
<barbara.malic@ijs.si>

Solution processing of multicomponent materials, such as Pb(Zr,Ti)O<sub>3</sub> (PZT), should yield better homogeneity, chemical purity and lower processing temperatures as a consequence of sub-micron particle size in comparison to solid state synthesis. It has been shown that although molecular homogeneity may be obtained in solution, it is in some instances lost upon thermal processing.

Pb(Zr<sub>0.53</sub>Ti<sub>0.47</sub>)O<sub>3</sub> ceramic precursors were prepared by hydrolysis of the reaction product of anhydrous lead acetate, zirconium and titanium n-butoxides in n-butanol. The dopants were introduced as niobium ethoxide or iron 2,4 pentanedionate. Stoichiometric materials and those with an excess of lead oxide were prepared. Crystalline products were obtained by annealing above 500°C. Ceramic samples were annealed up to 1200°C. Thermal analysis, X-ray diffraction, scanning and transmission electron microscopy with microanalysis and piezoelectric measurements were used to characterise the ceramic materials.

In the present contribution the phase composition and microstructural features of undoped, acceptor (Fe) and donor (Nb) doped PZT ceramic materials prepared in solution, are correlated with synthesis and thermal processing.

**CRYOSYNTHESIS OF METAL AND MESOGENS NANOSTRUCTURES**

*T.I. Shabatina, E.V. Vovk, Yu.N. Morosov and G.B. Sergeev*

Department of Chemistry, Moscow State University, 119899 Moscow, RUSSIA  
<tsh@cryo.chem.msu.su>

In present work the possibilities of metal-organic nanostructures formation have been studied via low temperature codeposition of metal and organic component vapours using a new class of organic ligands - mesogenic alkyl(alkoxy)cyanobiphenils (CB) and some of their derivatives:  $C_nH_{2n+1}-C_6H_5-C_6H_5-CN$ , where n=5 (5 CB), 7 (7 CB), and 8 (8 CB).

At the first stage we have made the IR-spectroscopic study of silver/cyanobiphenyl co-condensates of different metal-to-ligand ratio (from 1:1 to 1:100) in temperature range 80-300 K.. The IR-study of Ag/5 CB and Ag/5CB/decane (iso-octane) systems of different components ratio varied from 1:1 to 1:50 and from 1:1:10 upto 1:1:100 at low temperatures shows the existence of Ag-5 CB complexes due to Ag interaction with  $\pi$ -electrons of C≡N-bond of CB. It was indicated by the appearance of two new bands in the field of CN-stretching vibrations at 2030 and 2130 (2080)  $cm^{-1}$ . The shift of about 100  $cm^{-1}$  to lower frequencies is similar to  $\pi$ -complexes of zero-valent transition metal complexes with  $\pi$ -donating ligands. We also registered the appearance of a new band at 650-660  $cm^{-1}$  and considered it as metal-ligand vibrations. Similar results were obtained for higher CB homologies. It was shown that Ag-CB complexes are stable only at low temperatures and degrade upon heating.

UV-vis spectroscopic study of Ag/5CB and Ag/5CB/decane at 80 K showed the appearance of new wide absorbance band at 370-400 due to pale-yellow color of co-condensate. The new band disappeared by heating up to 200 K confirming the nonstability of Ag-5CB  $\pi$ -complexes at room temperatures. The dissolution of Ag/5 CB system by co-condensed hydrocarbon (decane) led to the increase of complexes yield at 80 K due to increasing of the general mobility of the system.

Silver - 5 CB samples were encapsulated in poly-p-xylylene polymeric films under vacuum conditions using special cryostate with inlet for xylylene-monomer injection into the system. Two kinds of Ag particles were stabilized in CB matrix: globes of about 15-30 nm and anisotropic rod-like particles more than 100 nm in length. UV-vis spectra show the broad absorption in the range of 450-600 nm. IR-spectra at room temperature indicate no difference with the spectra of pure 5 CB condensate films. Thus Ag atoms/small clusters stabilized at low temperatures by  $\pi$ -donating interactions with CB molecules can aggregate at higher temperatures in anisotropic matrix.

**Acknowledgements.** The work was partially supported by INTAS grant 94-4299 and International OMMEL programme.

**SIZE CONTROL OF QUANTUM SIZE CdS PARTICLES  
USING MACROLIGANDS**

*G. Carrot<sup>1</sup>, S.M. Scholz<sup>2</sup>, C. Plummer<sup>1</sup>, J. Hilborn<sup>1</sup> and H. Hofmann<sup>2</sup>*

<sup>1</sup> Polymer Laboratory and <sup>2</sup>Powder Technology Laboratory,  
Department of Materials Science, Swiss Federal Institute of Technology,  
Lausanne, SWITZERLAND <Stefan.Scholz@epfl.ch>

CdS nanoparticles are recently studied intensely, because they show a wide range of variations of their optical properties as a function of particle size. This is leading to a broadened range of possible applications, especially for optoelectronic purposes. The photoluminescence wavelength, for example, can be tuned over the whole visible range of the optical spectrum depending on the size of the particles.

Size control and colloid stability constitute an important point in the synthesis of CdS nanoparticles. We present results of a study on the kinetics of the growth of nanoparticles under the presence of ligand polymers with a thiol functional group. These nanometer-sized molecular entities are formed through the competitive reactions between the CdS core cluster growth and surface capping by macroligands. This is leading to small clusters whose reactive surface has been passivated by covalently attached polymers.

CdS particle formation has been carried out in both aqueous and organic media. In water, Na<sub>2</sub>S is used as the sulfurizing agent and mercapto-poly(oxyethylene) as stabilizer. In DMF, thiourea and mercapto-poly(caprolactone) were used, respectively. Particle sizes are characterized *in-situ* from optical transmission and photoluminescence spectroscopy as well as *ex-situ* by transmission electron microscopy. Reaction mechanisms are currently subject to further investigations.

The capabilities of different thiopolymers to stabilize particle sizes in the low nanometer range between 2 and 10 nm are presented. Influence of ligand concentrations and polymer chain lengths on the process are discussed.

**SYNTHESIS AND PROPERTIES OF NANOCRYSTALLINE VO<sub>2</sub>**

*J.-C. Valmalette and J.-R. Gavarri*

Laboratoire des Matériaux Multiphasés et Interfaces Université de Toulon et du Var,  
F-83957 La Garde, FRANCE <valmalette@univ-tln.fr>

Vanadium dioxide VO<sub>2</sub> (rutile) exhibits a reversible Insulator-Metal phase transition at T<sub>c</sub>=68°C associated with strong changes in electrical, magnetic and optical properties. Both scientific investigations and technological applications are of great interest due to the temperature range of this structural transition. The contrast of this transition strongly depends on stoichiometry, microstructure and surrounding medium of the oxide.

The reported work describe the first successful synthesis of nanocrystalline vanadium dioxide achieved trough a novel approach using the low temperature irreversible structural transformation of metastable VO<sub>2</sub>(B). This monoclinic VO<sub>2</sub>(B) phase is obtained at low temperature from V<sub>2</sub>O<sub>5</sub> by formation of oxygen vacancies. During this oxygen diffusion process, we shown that intermediate compounds of the homologous series V<sub>n</sub>O<sub>2n+1</sub> are formed and with n → ∞ for VO<sub>2</sub>(B). At this step, thermal energy transforms the metastable VO<sub>2</sub>(B) onto nanocrystalline VO<sub>2</sub> resulting from a total rearrangement of VO<sub>6</sub> octahedra in the rutile type structure associated with strong increase of density and formation of well faceted nanoparticles.

Modification of thermodynamical and physical properties with modifying particle size are discussed. The contrast of the optical transition in the near-infrared is remarkably increased with decreasing size of thermochromic VO<sub>2</sub> particles and can be tailored through the control of the ratio 2R /l in nanocomposites such as polymer films.

**SPONTANEOUS FORMATION OF NANOPOWDERS  
AT ROOM TEMPERATURE BY OXIDATION OF ZR<sub>x</sub>AU<sub>y</sub> ALLOYS**

*J.-C. Valmalette<sup>1</sup>, M. Lomello-Tafin<sup>2,3</sup>, P. Galez<sup>2</sup> and J. L. Jorda<sup>2</sup>*

<sup>1</sup> Laboratoire des Matériaux Multiphasés et Interfaces, Université de Toulon et du Var,  
F-83957 La Garde, FRANCE <valmalette@univ-tln.fr>

<sup>2</sup> Laboratoire d'Instrumentation et des Matériaux d'Annecy, Université de Savoie,  
F-74942 Annecy-Le-Vieux, FRANCE

<sup>3</sup> Institut de Chimie Minérale et Analytique, Université de Lausanne,  
CH-1015 Lausanne, SWITZERLAND

Since many important catalytic properties as activity, selectivity or poisoning effect can be affected by microstructure features, it is important to understand mechanisms involved in the interaction between two solid phases as noble metal and metal oxide, and one gas phase. The oxidation of alloys at high temperature has been shown to be an interesting route for obtaining high surface catalyst.

This work focuses on the mechanism that leads to formation of nano-Au particles and zirconia powder starting from Zr<sub>x</sub>Au<sub>y</sub> alloys. Samples were obtained by mixing Zr and Au powders (25 mm) and heating at 1100°C. Massive alloys are well crystallized with grain size of a few microns. After one day at 25°C (in air) samples with a composition of 40 at.% Au transform spontaneously into dark grey submicronic powder showing an amorphous-like pattern when submitted to X-ray diffraction. After one month, diffraction peaks of Au and ZrO<sub>2</sub> appear and TEM micrographs reveal the presence of gold nanoparticles at the surface of zirconia grains.

This transformation leads to zirconia supported nano-Au particles appearing spontaneously at room temperature for well defined initial composition and morphology of crystallised Zr<sub>x</sub>Au<sub>y</sub> alloy. Current knowledge of the Zr-Au equilibrium phase diagram, particularly the solid state transitions (eutectoid and peritectoid) occurring in the central part, allows us to prepare metallic sample holding the expected properties. A mechanism is proposed based on diffusion of Au through alloys grains associated with oxidation of Zr. This unexpected ionic exchange occurring at room temperature is of great interest for a better understanding of catalytic processes at the triple interface gas/noble metal/metal oxide.

### **ULTRATHIN DIBLOCK COPOLYMER FILMS: A TOOL FOR NANOLITHOGRAPHY**

*Peter Eibeck<sup>1</sup>, Joachim P. Spatz<sup>1</sup>, Martin Möller<sup>1</sup>, Thomas Herzog<sup>2</sup> and Paul Ziemann<sup>2</sup>*

<sup>1</sup> Universität Ulm, Organische Chemie III-Makromolekulare Chemie,  
D-89081 Ulm, GERMANY <peter.eibeck@chemie.uni-ulm.de>

<sup>2</sup> Universität Ulm, Abteilung Festkörperphysik, D-89081 Ulm, GERMANY

Diblock copolymers of polystyrene, PS, and polyvinylpyridine, PVP, were adsorbed on an ionic, high surface energy substrate (mica). The resulting ultra thin films showed spontaneous formation of regular, chemically heterogeneous surface structures consisting of separated polystyrene domains which dewet a strongly adsorbed PVP layer of 1nm height below. So far PS patterns of hexagonally arranged clusters and parallel oriented stripes were observed. The morphology of the PS surface pattern depends on several factors e.g. the blocklength ratio, the grafting density and the chemical nature of the polar block (P2VP or P4VP). The periodicity as well as the size of the PS structures are controlled by the molecular weight of the diblock copolymers. The degree of polymerisation of the PS block determines the number of PS chains per cluster and therefore influences both cluster size and periodicity. In contrast a variation of the PVP block length has only a minor effect and mainly influences the periodicity of the PS structures. The observed range for the PS structure size varies from 30 to 200 nm and the periodicity is within 50 to 400 nm. Decreasing the absolute molecular weight of the dewetting PS block below a certain threshold results in an order to disorder transition of the laterally segregated domains.

In a second step these polymer films are modified by vapour deposition of a metal film (titanium). The growth of titanium occurs preferentially on the less polar polystyrene islands resulting in titanium films with regular thickness variations corresponding to the pattern of the laterally segregated PS-b-PVP film. The treatment of these titanium films with oxygen plasma allows the conversion of Ti into TiO<sub>2</sub> providing a higher sputter resistance against argon ions. Etching the surface by oriented argon ion plasma allows the transfer of the PS/TiO<sub>2</sub> pattern into the substrate with high aspect ratios since the sputtering paths of the PS/TiO<sub>2</sub> domains are greater than the sputtering path between these domains. This procedure easily facilitates the parallel preparation of periodic patterns into an inorganic substrate where the range can be modified from 50 to 400 nm.

1. Spatz, S. Sheiko, M. Möller Adv. Mater. **8**, 513 (1996)
2. Spatz, M. Noeske, J. Behm, M. Pietrala, M. Möller Macromolecules **30**, 3874 (1997)

**NANOCRYSTALS AS DESTRUCTIVE ADSORBENTS FOR MIMICS OF CHEMICAL WARFARE AGENTS***Kenneth J. Klabunde and Erik Lucas*

Department of Chemistry, Kansas State University,  
Manhattan, KS 66506, USA <KENJK@KSU.EDU>

A modified aerogel-hypercritical drying procedure has been developed for the synthesis of nanaocrystals of common metal oxides such as MgO, CaO, ZnO, and ZrO<sub>2</sub>, as well as core/shell nanoparticles with monolayer coatings of transition metal oxides, such as [Fe<sub>2</sub>O<sub>3</sub>]MgO. These nanocrystals possess intrinsically higher surface reactivities than normal sized crystals due to unusual morphologies of the particles, with high concentration of edge/corner sites. This, coupled with very high surface areas (nanocrystalline MgO = 400 m<sup>2</sup>/g), and the basic character of the oxides allows them to serve as high capacity destructive adsorbents for a variety of toxic chemicals. We have studied mimics of two chemical warfare agents: CH<sub>3</sub>CH<sub>2</sub>SCH<sub>2</sub>CH<sub>2</sub>Cl and CF<sub>3</sub>CF=CF<sub>2</sub>. Several metal oxide fine particles have been compared in rate and capacity for destructive adsorption. Over nanocrystalline MgO the sulfur compound suffers dehydrohalogenation with the partial release of CH<sub>3</sub>CH<sub>2</sub>SCH=CH<sub>2</sub> at room temperature. In the case of CF<sub>3</sub>CF=CF<sub>2</sub> adsorption occurs at room temperature, and increases at elevated temperature. In addition to rate and adsorption capacity studies, FT-IR analysis of adsorbed species will be discussed.

**THE FABRICATION AND ORGANIZATION OF SELF-ASSEMBLED METALLIC NANOPARTICLES FORMED IN REVERSE MICELLES**

*Candace T. Seip and Charles J. O'Connor*

Advanced Materials Research Institute, University of New Orleans,  
New Orleans, LA 70148, USA <AMRI@uno.edu>

The demand for smaller materials for use in high density storage media is one of the fundamental motivations for the fabrication of nanoscale magnetic materials. Development of a high-density magnetic memory device may be achieved by patterning these magnetic nanoparticles into organized arrays onto the surface of a substrate. The preparation and properties of thin films of this type are discussed. An increasingly popular method of yielding nanoparticles takes advantage of molecular self-assembly. Fabrication of particles in water-in-oil microemulsions (reverse micelles) affords great control over the size and shape of the particles and results in highly uniform morphologies. We employ the reverse micelle method to synthesize metallic nanoparticles and subsequently use the reverse micelle as a 'nano reactor' to form specialized nonmagnetic coatings on the metallic particles. The purpose of the nonmagnetic coating is to direct the ferromagnetic nanoparticles into an ordered array on the surface of a substrate such as silicon or glass to produce a thin film. Multilayers can be formed by additional self-assembly reactions.

Metallic iron nanoparticles are synthesized in reverse micelles of cetyltrimethyl-ammonium bromide (CTAB). Iron(II) is incorporated into the water pools of a reverse micellar solution formed by using CTAB as the surfactant, butanol as a cosurfactant, and octane as the oil phase. Hydrazine is injected into the solution reducing Fe(II) to Fe(0). The metallic iron particles grow to fill the centers of the micelle and minimal aggregation of iron centers occurs since the organic portions of the micelle keep particles separate. After complete reaction, an aqueous solution of gold is added to the iron/CTAB mixture. Addition of the aqueous gold solution increases the size of the reverse micelle and the Au(III) is reduced to Au(0) via excess hydrazine. Since gold and iron grow with complementary crystal structures, the metallic gold forms a coating on the outer surface of the iron particles. The gold shells on the iron particles provide the functionality required forming organized arrays. Thin films of the gold coated particles have been made by self-assembly reactions between the gold surface of the particle and thiol functionalised substrates.

**SYNTHESIS OF HIGH DENSITY ULTRAFINE W/Cu COMPOSITE ALLOY**

*G.G.Lee, B.K.Kim, G.H.Ha and D.W.Lee*

Korea Institute of Machinery & Materials, KOREA

A new manufacturing process has been developed to obtain high density ultrafine W/Cu composite alloy by mechano-chemical process. Nanostructure W-/Cu-oxide and W-/Cu-metal mixed powders which are loosely agglomerated by homogeneous clusters of nanoscale size particles can be synthesised by chemical process using metallic salt precursors as the starting material. These powders are retreated by thermo-mechanical process to obtain high density ultrafine W/Cu composite. Liquid phase sintered W/Cu composite by W-/Cu-oxide mixed powder with passing through reduction steps has shown the higher density than that by W-/Cu-metal mixed powder. The effect of thermo-mechanical treatment, milling and reduction steps on sintering behaviour are discussed.

**FORMATION AND MAGNETIC PROPERTIES  
OF NANOSIZED Sm<sub>2</sub>Co<sub>17</sub> MAGNETIC PARTICLES  
VIA MECHANOCHEMICAL/THERMAL PROCESSING**

*W. Liu and P.G. McCormick*

Special Research Centre for Advanced Mineral and Materials Processing  
The University of Western Australia, Nedlands, WA 6907, AUSTRALIA

Nano-sized Sm<sub>2</sub>Co<sub>17</sub> magnetic particles have been prepared by mechanical milling and subsequent heat treatment of a mixture of Sm<sub>2</sub>O<sub>3</sub>, CoO and Ca with a suitable amount of CaO as diluent. The mechanical milling produced a nanostructured composite consisting of a nanocrystalline CaO supersaturated with Ca, CoO and Sm<sub>2</sub>O<sub>3</sub>, nano-sized Co particles and a small amount of free CoO. Heat treatment of as-milled powders at temperatures above 300 °C resulted in the formation of ultrafine Sm<sub>2</sub>Co<sub>17</sub> particles of 10-100 nm in size embedded in a CaO matrix. TEM studies showed that the particles size of Sm<sub>2</sub>Co<sub>17</sub> grew larger and the size distribution became wider with increasing heat treatment temperatures. The nano-sized Sm<sub>2</sub>Co<sub>17</sub> particles embedded in the CaO matrix were characterised by a high coercivity of 10-14 kOe. The by-product CaO could be removed by a carefully controlled washing process without serious oxidation of the ultrafine alloy particles. The formation mechanism of the magnetic nanoparticles was discussed based on the microstructure and magnetic measurements.

**PREPARATION AND CHARACTERISATION OF NANOSTRUCTURED  
NI/AL<sub>2</sub>O<sub>3</sub> AND CU/AL<sub>2</sub>O<sub>3</sub> COMPOSITES FOR CATALYTIC APPLICATIONS***Michael Veith\*<sup>†</sup> Kroum Valtchev and Nicolas Lecerf*Institute of Inorganic Chemistry, University of Saarland,  
D-66041 Saarbrücken, GERMANY

Alumina supported transition metals are widely used as catalysts in technical processes. By the chemical vapour deposition of the precursor compound [<sup>t</sup>BuOAlH<sub>2</sub>]<sub>2</sub> over NiO powder a reduction of the nickel oxide to metal takes place and a composite system of Ni/NiO/Al<sub>2</sub>O<sub>3</sub> is obtained. The catalytic properties of this composite powder have been investigated in hydrogenation experiments of organic compounds containing an unsaturated C-C double bond (e.g., styrene, maleic acid) and it has been found that such composites retain their high catalytic activity, even after many reaction cycles. Using bimetallic alkoxyaluminates of the transition metals e.g., Ni{Al(O*i*Pr)<sub>4</sub>}<sub>2</sub> and Cu{Al(O*i*Pr)<sub>4</sub>}<sub>2</sub> as molecular precursors in MOCVD processes, we have deposited nanocomposites of composition M.MAl<sub>2</sub>O<sub>4</sub>.Al<sub>2</sub>O<sub>3</sub> (M = Ni, Cu). The analysis of the reaction gases during the thermolysis by a mass spectrometer coupled to the CVD apparatus reveals isopropanol, acetone, propene and hydrogen as volatile decomposition products. The formation of acetone could be explained with the reduction process of Ni(II) or Cu(II) by isopropanol. Using transition metal stannates such as Ni<sub>2</sub>Sn<sub>2</sub>(OBu<sup>t</sup>)<sub>8</sub> in a single source chemical vapour deposition process has resulted in the formation of Ni<sub>2</sub>Sn<sub>4</sub> alloy dispersed in an SnO<sub>2</sub> matrix. These findings have been confirmed by ESCA measurements.

The obtained solid materials are composed of highly dispersed metals in an amorphous matrix. Electron microscopy studies of the thin solid films on steel show a structure of globular particles. In the case of Ni-Al and Cu-Al systems, energy dispersive X-ray analysis (EDX) reveals a homogeneous distribution of nickel and aluminium or copper and aluminium. Elemental analysis of the nickel containing composite is in agreement with the composition: Ni.NiAl<sub>2</sub>O<sub>4</sub>.Al<sub>2</sub>O<sub>3</sub>. X-ray diffraction of the composites reveals elemental nickel or copper to be the only nanocrystalline phase.

**NOVEL HETERO(BI- AND TRI-)METAL ALKOXIDES  
AS SINGLE SOURCE PRECURSORS TO NANO-SCALED  
CERAMICS AND METAL / METAL OXIDE COMPOSITES**

*Michael Veith, Sanjay Mathur and Volker Huch*

Institute of Inorganic Chemistry, University of Saarland,  
D-66041 Saarbrücken, GERMANY

Using specially designed molecules as tailor-made precursors, we are exploring new and effective routes to nano-scaled ceramics and metal/metal oxide composites *via* MOCVD and sol-gel processes. A considerable amount of progress in the materials chemistry has been built upon novel molecular precursors and their reaction chemistry [1,2]. The chemical synthesis route provides better control over purity, composition, homogeneity and microstructure, which are crucial parameters for high performance materials. In addition, the precursors used are generally readily purifiable and the possibility of variable atomic ratios in the precursors allows for novel compositions not easily available by other conventional routes. Whereas mono-metallic alkoxides are easily synthesised as well as available commercially, the synthesis of heterometal alkoxides with metal stoichiometry corresponding to that of targeted ceramic material (e.g., BaZr(OR)<sub>6</sub> for BaZrO<sub>3</sub> or YBa<sub>2</sub>Cu<sub>3</sub>(OR)<sub>13</sub> for YBa<sub>2</sub>Cu<sub>3</sub>O<sub>7-8</sub>) continues to be a synthetic challenge. We have synthesised and structurally characterised a Ba-Zr mixed-metal alkoxide based on 1:1 stoichiometry of the metals which has proved to be an excellent precursor for clean and selective synthesis (sol-gel) of BaZrO<sub>3</sub> ceramic at much lowering sintering temperatures than usually required for the solid state synthesis. The thermal decomposition of heterometal tert-butoxy zirconates [MZr(OBu<sup>t</sup>)<sub>6</sub>] (M = Ge<sup>II</sup>, Sn<sup>II</sup>, Pb<sup>II</sup>) in a CVD process offered mixed-metal composites of composition M/MO<sub>3</sub>/ZrO<sub>2</sub>. Similarly, well-characterised lanthanide aluminates of general formula [Ln{Al(OPr<sup>t</sup>)<sub>4</sub>}<sub>3</sub>] (Ln = Pr, Nd) have been used to deposit nano-scaled Ln-Al binary oxides, *via* chemical vapour deposition technique.

The single-source approach becomes more challenging when molecular precursors [3,4] to heterotrimetallic oxides are sought. For the first time, we have been able to construct a **volatile heterotrimetallic** alkoxide [{Al(OPr<sup>t</sup>)<sub>4</sub>}Ba{Zr<sub>2</sub>(OPr<sup>t</sup>)<sub>9</sub>}] which has been employed as a single source precursor in an MOCVD process to deposit Ba-Zr-Al oxides on a variety of substrates. The nano-composites obtained have been characterised using X-ray diffraction, electron spectroscopy, energy dispersive X-ray analysis (EDX), photoelectron spectroscopy (XPS), FTIR and glow discharge mass spectrometry (GDMS). An account of the above along with the single crystal X-ray diffraction analysis of representative precursors will be presented.

- [1] M. Veith, S. J. Kneip, A. Jungmann, S. Hüfner *Z. Anorg. allg. Chem.* **623**, 1507 (1997).
- [2] M. Veith, S. Faber, R. Hempelman, S. Janssen, J. Prewo, H. Eckerle *J. Mater. Sci.* **31**, 2009 (1996).
- [3] M. Veith, S. Mathur, V. Huch *J. Am. Chem. Soc.* **118**, 903 (1996).
- [4] M. Veith, S. Mathur, V. Huch *Inorg. Chem.* **36**, 2391 (1997).

**KINETICS OF FORMATION OF NANOCRYSTALLINE  $TiO_2$  II BY HIGH ENERGY BALL-MILLING OF ANATASE  $TiO_2$** *S. Begin-Colin, T. Girot, G. Le Caér and A. Mocellin*

Laboratoire de Science et Génie des Matériaux Métalliques, UMR CNRS 7584,  
Ecole des Mines, 54042 Nancy Cedex, FRANCE <begin@mines.u-nancy.fr>

Mechanical alloying is a dry and high energy ball milling process. Various materials from metallic to ionic can be prepared by ball-milling mixtures of elemental powders. The synthesised materials, often with non equilibrium structures, include among others, crystalline materials with nanometer sized grains. Besides materials synthesis, high energy ball-milling is moreover a way of inducing chemical reaction, of changing the reactivity of solids and a way of inducing phase transformations in solids. Polymorphic transformations may take place during dry milling in various oxides. Various polymorphs may further appear transiently even for very short milling times. Many oxides formed in such conditions are metastable at ambient temperature and pressure and exist at equilibrium only at high temperature or/and at high pressure. Mechanical alloying and grinding of materials are thus complex processes which depend on many factors, for instance, on the type of mills, on physical and chemical parameters such as the precise dynamical conditions, temperature, nature of the atmosphere, chemical composition of the powder mixtures, chemical nature of grinding tools.

We have investigated the influence of some milling parameters on the polymorphic transformations induced by grinding in anatase  $TiO_2$ . Anatase  $TiO_2$  is transformed by high energy ball-milling into rutile via the a- $PbO_2$  type high pressure modification of  $TiO_2$ :  $TiO_2$ II whatever the materials constituting the milling tools. In this study, are presented the influences of the nature of grinding media, of the powder to ball weight ratio and of the ball diameter on the kinetics of transformation of anatase  $TiO_2$  in  $TiO_2$  II and of  $TiO_2$  II in rutile.

**MOLECULAR DYNAMICS SIMULATIONS OF METAL CLUSTER COOLING  
AND HEATING IN NOBLE GAS ATMOSPHERE**

*Jan Westergren, Henrik Grönbeck and Arne Rosén*

Department of Physics, Chalmers University of Technology and Göteborg University  
S-412 96 Göteborg, SWEDEN

Sture Nordholm, Department of Physical Chemistry, Göteborg University  
S-412 96 Göteborg, SWEDEN

Metal cluster properties such as ionization potential, magnetic moment and reactivity strongly depend on the temperature of the cluster. Using molecular dynamics simulations we have investigated how much energy is transferred from noble gas atoms to unsupported Pd<sub>13</sub> clusters in collisions. Series of collisions were simulated with various noble gas masses and parameters of the potential between gas and cluster and the potential between cluster atoms. The heavier the gas mass and the softer the Pd-Pd-potential, the more efficient is the energy transfer. However, the potential between Pd and a noble gas atom influences the energy transfer only for cold gas. We have also seen that energy is more easily transferred for melted clusters than for solid ones.

Knowing the heat capacity of the cluster, the energy transfer can be translated into increase of cluster temperature per collision. Thus, we have used the energy transfer data and a statistical theory to predict the cluster cooling and heating processes in a noble gas atmosphere of constant temperature. The prediction fitted well to simulated cooling and heating processes.

**DISPERSED NANO-STRUCTURAL ORGANIC-APATITE COMPOSITE  
IN POROUS APATITE**

*M. Okazaki and T. Matsumoto*

Osaka University Faculty of Dentistry 1-8 Yamadaoka, Suita, Osaka 565, JAPAN  
[<okazaki@dent.osaka-u.ac.jp>](mailto:<okazaki@dent.osaka-u.ac.jp>)

Many efforts have been made for advanced artificial bone based on apatite. Especially, organic - apatite hybrid material is a potent bioactive bioceramics. We have developed the novel process of bioactive bioceramics including bioactive organic compounds. Principle idea of the process is to utilise the difference of reaction rate between reactants and apatite precursors. It should be noticed that this approach enables thermally unstable bioactive organic compounds to be incorporated in apatite perform under nano-size control. We present the detail of the novel process and structure of nano-structural composite.

**NANOSIZED SILICON PARTICLES BY INERT GAS ARC EVAPORATION**

*H. Hofmeister and P. Ködderitzsch*

Max Planck Institute of Microstructure Physics, Weinberg 2,  
D-06120 Halle, GERMANY,

Silicon based materials having structural characteristics on the nanometer scale exhibit interesting optoelectronic properties that result from size-induced quantum confinement effects as well as the presence of Si-O bonds at the surface. While erosive surface techniques are widely used to process bulk silicon, there is growing interest in the fabrication of particulate silicon showing comparable properties. Such materials are designed to achieve, by embedding in a passivating matrix, stability against influences of the ambient. Various methods of synthesis are reported ranging from co-sputtering of Si and silica, ion implantation of Si into silica, laser ablation and gas phase evaporation of silicon, to plasma-assisted decomposition of silane.

We have explored the possibilities of inert gas arc evaporation of silicon for producing nanosized Si particles of high crystallinity and perfection. Aggregation and condensation in inert gas atmosphere of the highly supersaturated vapour originating from arc discharges ignited at solid Si electrodes should best be suited for this aim. Arc evaporation of silicon was achieved by indirectly preheated Si electrodes powered with short pulses of 60 - 100 A in an Ar gas atmosphere of about 2 mbar pressure. Carbon coated microgrids placed at appropriate distance above the arc evaporator served to collect particles from the gas stream. Investigation of the Si particulates high resolution electron microscopy revealed structural characteristics related to the peculiarities of the particle synthesis. Under the conditions mentioned above, inert gas arc evaporation yields spherical particles of about 3 to 16 nm diameter completely covered by amorphous oxide layers. The thickness of these layers linearly decrease from about 1.5 to 0.5 nm with decreasing particle size. The particles, loosely adhering to each other by their oxide shells, are considerably agglomerated into chain-like and tangle-like structures. There is no indication of particle coalescence or sintering, which points to the fact that oxidation is already starting before deposition of the particles. They are single crystalline and completely free of lattice defects. The lattice of diamond cubic type, however, exhibits distinctly reduced spacing as compared to the bulk value. This lattice compression is observed to diminish for decreasing particle size. With the formation of oxide at the particle surface compressive stresses arise at the Si/oxide interface that may attain values of several Gpa, hence enabling lattice contractions of the observed extent. Since the oxide layer thickness is inversely proportional with particle size, its effect on the state of stress appears to be reduced accordingly. From the size dependence of the lattice contraction an effective interface stress of -1.17 N/m indicating a strong interaction is determined. This behaviour may be influenced also by considerable melting point suppression with decreasing particle size and by changes in oxygen content with decreasing oxide thickness.

**ORIENTED PROLATE SILVER PARTICLES  
IN GLASS-CHARACTERISTICS OF NOVEL DICHROIC POLARIZERS**

*H. Hofmeister\*, W.-G. Drost and A. Berger*

\*Max Planck Institute of Microstructure Physics, Weinberg 2,  
D-06120 Halle, GERMANY

Farbige Optoelektronische Bauelemente GmbH, Weinbergweg 23,  
D-06120 Halle, GERMANY

Nanosized metal particles in glass cause a coloration depending on the material of matrix and inclusions as well as on size and shape of the particles. Spherical Ag particles of various sizes and number density in soda-lime glasses are readily obtained by Na/Ag ion exchange and subsequent reduction treatment. Stretching at elevated temperatures of such modified glasses results in elongated particles uniformly oriented along the direction of deformation. Consequently, the optical absorption of the spherical particles splits into two bands according to the long and short axes of the now ellipsoidal shaped particles. The position of these absorption bands may be tuned by varying the initial size of the spherical particles as well as by changing the degree of glass deformation that determines the aspect ratio of the prolate particles [1]. Basing on this procedure, novel dichroic polarisers are produced which not only exhibit advanced mechanical, chemical and thermal durability as compared to common dichroic, dye-doped sheet polarisers, but also have some additionally interesting features like the wide range of dichroic colours accessible and the possibility to apply microstructuration with strip or pixel dimensions less than 10 µm. The latter procedure utilizes thermally induced shape relaxation of deformed Ag particles to a well-defined extent within sharply bounded areas [2]. Spherical Ag particles of 4 to 40 nm size have been formed in commercial soda-lime glasses by ion exchange in a NaNO<sub>3</sub>/AgNO<sub>3</sub> melt mixture and subsequent annealing at 560 °C. Stretching of the coloured glasses was done at 650 °C by pulling at constant stress of 50 to 150 N/mm<sup>2</sup> so to obtain elongated particles (mean aspect ratio 2.5 to 5.5). Microstructuration is achieved by patterned laser light or scanned electron beam illumination. Characterisation of the dichroic glass polarisers by optical absorption spectroscopy is mainly done to demonstrate the influence of the deformation and shape relaxation on their polarising and spectral properties. Structural characterisation of these interesting materials is aimed at monitoring the uniformity of the particle deformation that mainly influences their spectral properties, and at exploring the relations between size, degree of deformation and shape of the particles. High resolution electron microscopy enabled to detect in the elongated particles lattice inhomogeneities with respect to the direction of deformation. A lattice contraction opposed to the stretching direction of the glass is found which indicates frozen-in compressive strains within the glass matrix. This finding explains the shape relaxation of deformed particles by local heating of small areas of the coloured and stretched glass.

[1] A. Berger, J. Non-Crystalline Solids **163** (1993) 185.

[2] M. Wahl, G. Gleske, W.-G. Drost and H.-J. Cornelius, Proc. 12. Electronic Displays '97 Conf., Chemnitz 1997, p. 104.

**PHASE COMPOSITION STUDY OF BULK AND SURFACE LAYERS  
OF STABILIZED IRON POWDER**

*E.P. Yelsukov, O.M. Mikhailik\*, G.N. Konygin, S.S. Mikhailova and V.I. Povstugar*

Physical -Technical Institute UrB RAS, 132 Kirov str,  
426001 Izhevsk, RUSSIA <povst@uds.fti.udmurtia.su>

\* SRC Sonar NAS of Ukraine, Kiev, UKRAINE

Finely dispersed ferromagnetic materials are applied as magnetic liquid bases, fillers for metal-polymer composites, and microcarriers of biologically active substances. Preparation of such materials requires the knowledge of their structure and phase composition both in bulk and on particle surfaces.

Mössbauer spectroscopy was used to study iron powders in process of their preparation by high temperature reduction of  $\alpha$ -FeOOH in hydrogen. The powders formed were stabilised by oleic acid.

It is seen from the Mössbauer spectra that on initial stages of reduction the particles represented mostly  $\alpha$ -FeOOH with a slight quantity of disordered  $Fe_3O_4$ . Increase of reduction time results in predominance of  $Fe_3O_4$  phase with traces of  $\alpha$ -Fe. Post-reduction powders represented  $\alpha$ -Fe. Thus, the following conversions occur in process of reduction of  $\alpha$ -FeOOH up to  $\alpha$ -Fe:  $\alpha$ -FeOOH  $\rightarrow$   $Fe_3O_4$   $\rightarrow$   $\alpha$ -Fe.

To study surface layers by means of Mössbauer spectroscopy we propose the original two-step technique of preparing finely dispersed iron powders with the particle "nuclei" from  $^{56}Fe$  and with particle surface layer 4-5 nm thick, enriched in  $^{57}Fe$ . It allowed registering high-quality Mössbauer spectra, informative of structural and chemical changes in surface layer on different reduction stages.

The resulting finely dispersed iron powders were subjected to corrosion in isotonic solution (0.85% aqueous solution NaCl). The Mössbauer spectra indicate the presence of a considerable quantity of  $\gamma$ -FeOOH and the disordered  $Fe_3O_4$  phase after corrosion.

**PREPARATION OF NANOPHASE WC POWDERS FROM THE REDUCTION  
OF AMMONIUM METATUNGSTATE BY C<sub>2</sub>H<sub>2</sub>-H<sub>2</sub> MIXTURES**

*Guo-Long Tan and Xi-Jun Wu*

Department of Materials Science and Engineering, Zhejiang University,  
Hangzhou 310027, CHINA <mse\_xjwu@ema.zju.edu.cn>

The synthesis of nanophase tungsten carbide powders from the reduction of ammonium metatungstate by C<sub>2</sub>H<sub>2</sub>-H<sub>2</sub> mixtures was investigated. Under most experimental conditions, The single phase WC powders with the grain size of 8-20 nm were produced. The formation of metastable W<sub>2</sub>C, which is the usual product of the reduction and carburization of tungsten oxides, is avoided. The effect of the process parameters, such as temperature and gas pressure, on the final phase of tungsten carbides was determined. The microstructural morphology of the product prepared under various reaction conditions which was studied by scanning electron microscopy (SEM) and transmission electron microscopy (TEM) will be discussed.

---

**SYNTHESIS OF NANOPARTICLES BY A LASER VAPORIZATION-CONTROLLED CONDENSATION TECHNIQUE: NANOPARTICLES OF METAL AND SEMICONDUCTOR OXIDES AND CARBIDES**

*M. Samy El-Shall*

Department of Chemistry, Virginia Commonwealth University  
Richmond, VA 23284-2006, USA <selshall@gems.vcu.edu>

A method which combines laser vaporization of metal targets with controlled condensation from the vapour phase is used to synthesize nanoscale metal and semiconductor oxide, carbide and nitride particles (5 - 10 nm) of well - defined composition. The metal vapor is generated by pulsed laser vaporization using the second harmonic (532 nm) of a Nd-YAG laser. Following the laser pulse, the ejected atoms react with the reactive gas within the ambient atmosphere and condense to form nanoparticles. The role of convection in the experiments is to remove the small particles away from the nucleation zone (once condensed out of the vapor phase) before they can grow into larger particles. Several examples of nanoparticles will be discussed including ZnO, FeO, MoO<sub>3</sub>, MoC<sub>3</sub>, WO<sub>3</sub>, CeO<sub>2</sub>, ZrO<sub>2</sub> and Ga<sub>2</sub>O<sub>3</sub>. The effects of solvents and temperature on the morphology of the nanoparticles will be presented and discussed. We also present evidence for a novel photoreduction of the white WO<sub>3</sub> nanoparticles into the blue W<sub>2</sub>O<sub>5</sub> following the irradiation of the particles with the second harmonic of the Nd:YAG laser at 532 nm in air. Finally, we report the observation of efficient blue photoluminescence from Ga oxide nanoparticles. These examples demonstrate the potential of nanoparticles in the design of optical and photonic devices

**SYNTHESIS AND MECHANICAL PROPERTY OF  
NANOCRYSTALLINE METALS COPPER AND SILVER**

*Hong-fei ZHANG, Xi-jun WU, Li-guang DU, Yan-qi WANG and Zong-quan LI*

Department of Materials Science and Engineering, Zhejiang University,  
Hangzhou 310027, CHINA <mse\_xjwu@ema.zju.edu.cn>

The larger disk-shaped specimens of nanocrystalline metals copper and silver, with a diameter 80 mm and the thickness 5 up to 10 mm, were synthesized by means of an inert gas condensation and in-situ warm compacting technique. The grain size of the specimens was controlled in the range of 15 to 100 nm by changing the compacting temperatures from RT to 700 K. The density of the specimens was controlled in the range of 90% to 97% by controlling the compacting pressures ranged from 0.5 to 1.0 GPa and the compacting temperatures. In this way, the larger bulk specimens of nano-Cu and nano-Ag with ultrafine grain size and full density have been prepared. The tensile and fatigue properties of nano-Cu and nano-Ag were studied by using the samples cut from the larger specimens. The primary results showed that the tensile strength of nano-Cu and nano-Ag increases obviously for about two up to four times, comparing with that of the coarse-grained counterparts. The deformation mechanism is dependent upon temperature and strain rate. The analysis of the fatigue property of nano-Cu and nano-Ag is in progress.

**PREPARATION OF SUBMICROMETER NICKEL POWDERS BY THE  
REDUCTION FROM NONAQUEOUS MEDIA**

*Andrej Degen and Jadran Macek*

University of Ljubljana, Faculty of Chemistry and Chemical Technology,  
1000 Ljubljana, Askerceva 5, SLOVENIA <jadran.macek@uni-lj.si>

Nickel powders can be prepared by a variety of processes. One of the possible preparation methods is the reduction of nickel cations from the solutions of nickel salts by a powerful reducing agent. The rate and yield of the reaction are both enhanced at higher reaction temperatures. Reaction temperatures in aqueous media are limited by the relatively low boiling point of water unless the experiments are carried out at higher pressures in the autoclaves. High pressure work can be avoided if the reactions are performed in nonaqueous media.

Nickel acetate and chloride were used as the nickel precursors, hydrazine was the reducing agent and ethylene glycol, di- and tri-ethanolamine were used as the reaction media. These organic media enable reactions at temperatures of 180°C and higher and the later two favor the reduction also by their basic nature. By the selection of the reaction conditions and media the particle size, size distribution and other characteristics of the nickel powders were influenced. The reduction/precipitation reaction and the properties of the final products were also influenced by the changes in the concentration of the reactant, the reaction temperature and the selection of nickel precursor. The nickel powders with the mean particle sizes from 0.1 to 1 µm and up to 99.8% purity were obtained. The mean particle size of the nickel powders was lowered also by changing the homogenous nucleation into heterogeneous one by the addition of traces of palladium.

### **NANOCRYSTALLINE (Ni,Fe) ALLOYS, PREPARATION AND PHYSICO-CHEMICAL CHARACTERIZATION**

*M. Heyer, M. Koch, F. Rullang, K.-St. Werkmeister and G. Schwitzgebel*

FB 11.3, Physical Chemistry, Universität des Saarlandes, Postfach 151150,  
D-66041 Saarbrücken, GERMANY <g.schwitzgebel@rz.uni-sb.de>

It is well known, that microcrystalline alloys of nickel and iron  $(\text{Ni},\text{Fe})_{mc}$  can be prepared by electrodeposition[1] and it has been shown, that in order to obtain the nanocrystalline materials  $(\text{Ni}_{nc}, \text{Fe}_{nc})$  and  $(\text{Ni}, \text{Fe})_{nc}$ [2], this preparation modified by applying pulsed current can be transferred to the pure compounds as well as to the alloy system. For this purpose, ball-milling, the most universal method, is also appropriate.

In our work both methods led to single-phased  $\gamma$ - $(\text{Ni},\text{Fe})_{nc}$  for atom fractions  $x_{\text{Ni}} > 0.5$ , but, in contrast to  $(\text{Ni},\text{Fe})_{nc}$  conventionally prepared from the melt, only two-phase alloys ( $\gamma$ - $(\text{Ni},\text{Fe})_{nc}$  and Fe-rich  $\alpha$ - $(\text{Ni},\text{Fe})_{nc}$ ) could be prepared for  $x_{\text{Ni}} < 0.5$ . This means that homogeneous Fe-rich alloys (e.g. Invar), which according to the phase diagram are metastable at low temperatures, do not form in the nanostate.

The alloys were investigated using XRD, DSC, solution calorimetry, AFM, electrochemical impedance spectroscopy and potentiometry. Comparison of the energetic results for the micro- and nanocrystalline materials of different grain diameters and stored strains leads to specific values of the interfacial energy, but also to some apparent inconsistencies, especially between excess energies from DSC and from solution calorimetry. Even for the microcrystalline state, we obtained new findings: By the help of EMF values from high temperature cells of the solid electrolyte or of the salt melt type, parts of the free enthalpy curve in the metastable region of the phase diagram could be traced.

[1] S.S. Djokic et al., Modern Aspects of Electrochemistry 22 (1991) 417

[2] H. Natter et al., Ber. Bunsenges. Phys. Chem. 100 (1996) 55

---

**THE SOLID STATE THERMAL TRANSFORMATION OF  
THE METAL CARBOXYLATES AS A SOURCE OF THE FORMATION OF  
THE NANOSIZED STABILIZED PARTICLES**

*A.S. Rozenberg, and A.D. Pomogailo*

Institute of Chemical Physics in Chernogolovka Russian Academy of Sciences,  
142432 Chernogolovka, Moscow Region, RUSSIA <rozenberg@icp.ac.ru>

The energy saturated nanosized particles synthesised in strongly non-equilibrium conditions are the chemical reactivity extremely. Therefore, the effective ways of the nanosized particles chemical passivation search are the active problem highly. The solid state thermal transformations of the transition and heavy metal carboxylates are one of the perspective ways of this direction. These problems are discussed here on the example of the thermolysis of simple and cluster salts of the saturated (formiates, oxalates) and unsaturated (acrylates, maleates) acids.

In the self-generated atmosphere the kinetics, topography and compositions of the thermal transformations products of the formiates Fe(2+,3+), Ni(2+), Pb(2+), Cu(2+), oxalate Fe(3+), metal containing monomers: acrylates Co(2+), Ni(2+), Cu(2+), Fe(3+), maleate Co(2+) as well as (co)crystallizes of acrylates Fe(3+) and Co(2+) (1:1, 2:1) have been studied. The ample information, concerning different influence factors both for the thermolysis kinetics and for the formed products dispersity have been received.

The solid phase metal containing products of the thermolysis of formiates and oxalates are the compact sphere-like particles (metal and (or) metal oxide) with a narrow distribution of their size (electron microscopic and the specific surface data observation). The average particle size is 20-35 nm. In the transformation course this particles are preserved. The correlation between the thickness of the polymer passivating cover, the formed products dispersity and thermolysis process conditions are ascertained.

The thermal transformations of the metal containing monomers consist of the temperature separated macro stages: dehydration, solid state radical polymerisation of the dehydrated monomer with formation of macromolecular metal complexes and the decarboxylation with the formation of metal containing products. The solid state products of this thermal transformation are the sphere-like compact particles (metal and (or) metal oxide or cobalt ferrite  $\text{CoFe}_2\text{O}_4$  for the (co)crystallizes) also with a narrow distribution of their size and the average particle size of 5.0-8.0 nm which are uniformly distributed in the decarboxylating matrix with a distance of 8.0-10.0 nm.

**POLYMER-SUPPORTED TITANIUM-MAGNESIUM  
CATALYST FOR ETHYLENE POLYMERIZATION**

*A.M. Bochkin and A.D. Pomogailo*

Institute of Chemical Physics in Chernogolovka, Russian Academy of Sciences,  
142432 Chernogolovka, Moscow, RUSSIA <bochkin@icp.ac.ru>

A new method for synthesis of polymer supported organometallic titanium-magnesium catalysts was developed. Polyethylene with grafted polydiallilamine (PE-gr-PDAA), polyacrylic acid (PE-gr-PAA), poly(allyl alcohol) (PE-gr-PAAl), and poly(methyl vinyl ketone) (PE-gr-PMVK) were used as polymer support. The grafting of appropriate monomers to the polyethylene surface was carried out by gas-phase graft polymerization initiated by  $^{60}\text{Co}$   $\gamma$ -irradiation. Polymer-analogous reaction were used to fix Mg(II) to the surface of the PE-gr-PDAA, PE-gr-PAA, PE-gr-PAAl and PE-gr-PMVK. The amount of fixed Mg(II) depends on the temperature, the nature of functional groups, reactant ratios and consist 0.13-1.12 mmol/g Mg. Interaction between  $\text{TiCl}_4$  and the Mg- containing polymer support proceeds via formation of an alkyltitanium derivative, followed by the reduction  $\text{Ti(IV)} \rightarrow \text{Ti(III)}$ . Characteristics of polymer-supported titanium-magnesium catalysts are summarized in table:

Type of polymer support	Loading mmol/g Mg	mmol/g Ti	$[\text{Ti(III)}]/[\text{Ti}]$	$\Delta H_{1/2}$ (%)	g-factor	Crystalline size (nm)
ESR						
PE-gr-PAAl	0.28	0.58	0.8	120	1.929	-
PE-gr-PDAA	0.41	0.096	19	183	1.886	4.5
PE-gr-PMVK	0.92	0.38	9.6	190	1.897	7.5
PE-gr-PAAl	0.57	0.042	55	190	1.899	4.5
PE-gr-PAAl	0.32	0.054	2.7	175	1.915	4.5
PE-gr-PAAl	0.17	0.038	1.0	140	1.923	-
PE-gr-PAAl	0.13	0.092	0.8	134	1.918	-

The catalysts contain up to 55% of total fixed Ti in the form of isolated Ti(III) ions. G-factors of the T1(III) ion signals change within the range of 1.886-1.929. Ti(III) is assumed to coordinate to the polymer support moieties at low Ti(III) content, and to form layers at high Ti(III) content in the catalysts. The crystallite sizes were estimated according to the width of these peaks. Table show that crystallites appear only at a total Mg-Ti content exceeding 0.3 mmol/g. No aggregation was observed for samples with low Ti-Mg content. The absence some of an X-ray diffraction peak in spectra of the polymer-supported catalysts, characteristic for Ti-Mg catalysts on an inorganic support, may point to a considerable dispersion of the crystallites caused by mixed  $\text{TiCl}_3\text{-MgCl}_2$ , aggregation, complexation with the functional groups of the grafting layer and, probably, by predominant orientation of crystallite growth (along the macromolecular chain). A correlation between catalyst activity and isolated Ti(III) ion content was found. The polymer-supported catalysts have the activity up to 550 kg PE/g Ti MPa h.

**INFLUENCE OF THE INITIAL CONCENTRATION ON  
PHASE FORMATIONS DURING CHEMICAL PROCESSING  
OF NANOCRYSTALLINE Fe-W POWDERS**

*A.A. Novakova<sup>1</sup>, T. Yu. Kiseleva<sup>1</sup>, V.V. Lyovina<sup>2</sup>, E.L. Dzidziguri<sup>2</sup> and  
D.V. Kuznetsov<sup>2</sup>*

<sup>1</sup> Department of Physics, Moscow M.V.Lomonosov State University,  
117234 Moscow, RUSSIA <aan@runar.phys.msu.su>

<sup>2</sup> Department of Theory of Metallurgical Processes, Moscow State Steel and Alloys  
Institute, 117936 Moscow, RUSSIA

We studied in detail nanocrystalline Fe-W powders, obtained by common reduction in hydrogen of oxygen containing iron and tungsten compounds mechanical mixture in wide concentrations range.

The formations of Fe-rich and W-rich solid solutions and intermetallic compounds with different compositions were investigated by means of Mössbauer spectroscopy and X-ray diffraction.

It was found that the different metallization velocities of Fe and W compounds and their initial concentrations in mixture affect the type of reaction during chemical processing and the morphology of nano-scaled heterogeneous final products.

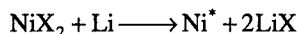
**STRUCTURAL AND MAGNETIC PROPERTIES OF NICKEL/NICKEL CARBIDE NANOSTRUCTURES FABRICATED BY CHEMICAL REDUCTION**

*Diandra L. Leslie-Pelecky<sup>1</sup>, M. Bonder<sup>1</sup>, E. Kirkpatrick<sup>1</sup>, S.H. Kim<sup>2</sup> and  
Reuben D. Rieke<sup>2</sup>*

<sup>1</sup> Department of Physics & Astronomy and Center for Materials Research,  
University of Nebraska, Lincoln, NE 68588-0111, USA <diandra@unlinfo.unl.edu>

<sup>2</sup> Department of Chemistry and Center for Materials Research,  
University of Nebraska, Lincoln, NE 68588-0111, USA

Chemical synthesis offers a direct route to fabricating multiphase nanocomposites. A reduction technique that produces highly reactive metals has been used to fabricate nickel-based nanostructures via



where X is Cl or Br. The reaction takes place in a hydrocarbon solvent, with the assistance of an electron carrier to facilitate electron transfer. The technique produces particulate materials with nickel grain sizes on the order of 5 nm. X-Ray diffraction and transmission electron microscopy indicate that disordered (turbostratic) graphite is introduced as a result of interactions between the highly reactive nickel clusters and the solvent molecules. Annealing produces micron-sized particles with grain sizes from 10-75 nm. The metastable Ni<sub>3</sub>C phase is formed upon annealing between 200°C and 400°C. The magnetic properties of the resulting materials depend primarily on the nickel and Ni<sub>3</sub>C grain sizes, with coercivities ranging from 0 to 200 Oe at room temperature. The linear dependence of the coercivity on temperature indicates strong interactions between magnetic grains. Analysis using a model by Krommüller indicates that magnetization reversal proceeds via nucleation. The magnetic properties of Ni<sub>3</sub>C have been determined by synthesizing the pure material by mechanical alloying and will be used to explain the role of the metastable carbide phase in the magnetic properties of the nanocomposite.

**MECHANICAL MILLING OF Fe(III)-Si OXIDES:  
FORMATION OF AN AMORPHOUS Fe(II)-CONTAINING PHASE**

*C. Bender Koch<sup>1</sup>, J.Z. Jiang<sup>2</sup> and S. Mørup<sup>2</sup>*

<sup>1</sup> Chemistry Department, The Royal Veterinary and Agricultural University,  
Thorvaldsensvej 40, DK-1871 Frederiksberg C, DENMARK <cbk@kvl.dk>

<sup>2</sup>Department of Physics, Building 307, Technical University of Denmark,  
DK-2800 Lyngby, DENMARK. <jiang@fysik.tu.dk>

A number of different phases exists in the Fe(II)-Fe(III)-Si-O system. In the present study, we have investigated the changes induced by high-energy mechanical ball milling of a mixture of 25 % mol Fe(III)<sub>2</sub>O<sub>3</sub> in amorphous SiO<sub>2</sub> in closed and open containers. In the open containers, all the iron remains in the ferric state in a hematite of nanocrystalline size and no indication of mixing was found. Contrasting behaviour was observed in the closed container experiment, where substantial mixing of Fe(II) into an amorphous silica was found. The contrasting behaviour is discussed with respect to the active state during the ball milling reaction.

**SYNTHESIS AND CONSOLIDATION OF NANOCRYSTALLINE PARTICLES PRODUCED BY POLYOL PROCESS**

Shankar M.L. Sastry<sup>1</sup>, Lynn Kurihara<sup>2</sup> and Virgil Provenzano<sup>2</sup>

<sup>1</sup> Washington University, Campus Box 1185, One Brookings Drive,  
St. Louis, MO 63130, USA <smls@mecf.wustl.edu>

<sup>2</sup> Naval Research Laboratory, Code 6320, 4555 Overlook Ave.,  
SW, Washington, DC 20375, USA

Nanocrystalline copper and nickel particles were produced by POLYOL synthesis, consolidated by vacuum hot pressing, and characterized by thermogravimetric analysis (TGA), combustometric chemical analysis, X-ray diffraction, microhardness measurements, and bend strength and ductility evaluation. In the POLYOL process, a powdered inorganic metallic compound is suspended in a liquid polyol (such as ethylene glycol and diethyleneglycol). The suspension is stirred and heated to 140-190°C to produce a complete reduction of the compound to finely divided metallic powder in 2-4 hours. 20-50 g quantities of nanocrystalline particles were produced. TGA of as synthesized particulate indicated that the organic solvents can be removed by heating the samples in vacuum at temperatures of 100-130°C (well below the temperatures required for consolidation to full densification).

Nanocrystalline particulates were consolidated by two routes: (1) cold pressing to 70 % density followed by vacuum hot pressing to near theoretical density and (ii) direct vacuum hot pressing to near theoretical density. Copper samples were consolidated at 250, 350, and 350°C, and nickel samples were consolidated at 450, 650, and 750°C. The chemistry of vacuum hot pressed samples determined by combustometric analyses indicated carbon concentrations of 0.03 wt% and oxygen concentration of 0.088 wt%. These levels are considerably lower than those found in nanocrystalline samples prepared by other methods. Vicker's Microhardness values of 75-99 kg/mm<sup>2</sup> for copper and 330kg/mm<sup>2</sup> for nickel were observed. However, the specimens failed without exhibiting any plastic deformation in 3-point bend tests. The fracture surfaces indicated inter agglomeration separation. With the objective of improving the inter particle and inter agglomerate bonding, the vacuum hot pressed samples were processed by equichannel angular extrusion (ECA) and strength and ductility were determined from 3 point bend tests.

## NANOMATERIALS: SYNTHESIS USING SOLAR RADIATIONS - NANOSTRUCTURAL CHARACTERIZATION

*Claude J.A. Monty, Alain Rouanet and François Sibieude*

CNRS, IMP-Odeillo, 66125-cedex Font Romeu, FRANCE <monty@imp-odeillo.fr>

Oxide nanomaterials<sup>1</sup> have been prepared by two processes using solar furnaces (specially useful when the melting point of the material is high): vaporization-condensation in solar reactors leading to nanophases and splat-cooling from the melt leading to nanostuctured materials.

The first method is efficient when the vapour pressure of the material is high.<sup>2</sup> Oxide nanophases have been prepared by this way and characterized by X-ray diffraction and High Resolution Electron Microscopy: the cases of ZnO,  $\gamma$ -Fe<sub>2</sub>O<sub>3</sub>, SnO<sub>2</sub>, Zr<sub>1-x</sub>Y<sub>x</sub>O<sub>2- $\delta$</sub>  and (Nd or La)<sub>1-x</sub>Sr<sub>x</sub>MnO<sub>3- $\delta$</sub>  have been considered.<sup>3</sup> The giant magneto-resistant perovskite like (Nd or La)<sub>1-x</sub>Sr<sub>x</sub>MnO<sub>3- $\delta$</sub>  were obtained according to the well known condensation process of a complex vapour system. A mixture of starting oxides (La<sub>2</sub>O<sub>3</sub>, SrO and MnO<sub>2</sub>) was melted at temperatures above 2000°C in air and vaporized as a complex gas mixture of (M)<sub>g</sub> and (MO)<sub>g</sub> species whose global composition depends mainly on the oxygen partial pressure. Some experiments were carried out in air using different mixtures of oxide powders, specially the compositions related to the following cationic ratios: Mn / La+Sr = 1/4 and 4/6, and the ratio La/Sr = 1/1 and 2/1. Among them only the composition: {La (or Nd)<sub>2/3</sub> Sr<sub>1/3</sub>}<sub>4</sub> MnO<sub>x</sub> led to the formation of a crystallized condensed phase exhibiting a cubic or pseudo-cubic Perovskite-like structure. The x-ray diffraction peaks of this product are homogeneously wide as expected in the case of nanosize crystallite diffraction spectrum.

The splat cooling method<sup>4</sup> leads to nanomaterials (ribbons or rough powders depending on the viscosity and on the thermal conductivity of the melt) which can be amorphous or nanostructured (depending on the composition). Nanosize powders can be obtained from it by ball-milling. Bulk nanomaterials can be prepared by sintering the powders. This method is specially well adapted to prepare yttria-doped zirconia/alumina nanocomposites but it has also been applied to prepare (Nd or La)<sub>1-x</sub>Sr<sub>x</sub>MnO<sub>3- $\delta$</sub>  nanomaterials exhibiting giant magnetoresistance

1. C. Monty, "Nanomaterials: the state of the art", *High Temperature Chem. Processes* **3** (1994) 467-480.
2. G. Pichelin, A. Rouanet, "Predictive modelling of high temperature chemical system vaporization under atmospheric pressure", *Chem. Eng. Sci.* **7** (1991) 1635.
3. A. Rouanet, H. Solmon, G. Pichelin, C. Rouau, F. Sibieude and C. Monty, "Synthesis by vaporization-condensation and characterization of  $\gamma$ -Fe<sub>2</sub>O<sub>3</sub>, In<sub>2</sub>O<sub>3</sub>, SnO<sub>2</sub>, ZnO, and Zr<sub>1-x</sub>Y<sub>x</sub>O<sub>2- $\delta$</sub>  nanophases", *Nanostructured Materials*, **6** (1995) 283-286.
4. A. Rouanet, F. Sibieude and M. Faure, *J. of Physics E., Sc. Instruments*, **8** (1975) 389.

**NANOCOMPOSITE POWDERS OF Fe-C SYSTEM PRODUCED  
BY THE FLOWING GAS PLASMA PROCESSING**

*S. Iwama<sup>1</sup>, T. Fukaya<sup>1</sup>, K. Ohshita<sup>2</sup> and Y. Sakai<sup>2</sup>*

<sup>1</sup> Department of Applied Electronics, Daido Institute of Technology

<sup>2</sup> Department of Chemistry, Daido Institute of Technology

2-21 Daido-cho, Minami-ku, Nagoya 457-0811, JAPAN

Nanometer-sized  $\alpha$ -Fe particles formed by the gas evaporation method were transferred into the microwave plasma region with a carrier gas of Ar. When small amount of CH<sub>4</sub> was included in the carrier gas, particles collected after the plasma region were found to show a composite phase of Fe-C system consisted of  $\alpha$ -Fe,  $\gamma$ -Fe(Austenite, including solid solution of carbon) and Fe<sub>3</sub>C. The relative amount of these three phases depended on mainly two factors ; CH<sub>4</sub> content in Ar gas and a microwave power.

Mössbauer spectroscopy was used to estimate the relative amount of three phases. An increase of  $\gamma$ -Fe followed by the decrease of  $\alpha$ -Fe with increasing CH<sub>4</sub> content. Formation of Fe<sub>3</sub>C was recognized at 0.5 vol.% of CH<sub>4</sub> in Ar gas and became more remarkable when the CH<sub>4</sub> content was increased.

Electron microscopic observations of the powder and plasma characteristics in the present set-up will be presented at the conference.

**STUDY ON TiO<sub>2</sub> NANO-CLUSTERS SYNTHESIZED BY LASER ABLATION**

*Shin-ichi Kamei<sup>1</sup>, Katsunori Yogo<sup>1</sup>, Masamichi Ishikawa<sup>1</sup>,  
Kiichiro Kawasaki<sup>2</sup>, and Osamu Odawara<sup>2</sup>*

<sup>1</sup> Mitsubishi Research Institute, Inc. 2-3-6 Otemachi Chiyoda-ku,  
Tokyo 100, JAPAN <MXH03166@niftyserve.or.jp>

<sup>2</sup> Tokyo Institute of Technology 4259 Nagatsuta, Midori-ku, Yokohama 226, JAPAN

Since titanium dioxide (TiO<sub>2</sub>) has the ability to synthesize hydrogen through the photo electrolysis of water, and also the capability to decompose nitrogen oxides, high capability is placed on it as a promising future material. In this study, Laser ablation was carried out on the target of a TiO<sub>2</sub> rod prepared by pressing TiO<sub>2</sub> powders and sintering at 1700 K for 2 hours. The apparatus was a combination molecular beam generation part and ablation part. The TiO<sub>2</sub> target was irradiated by a Q-switched Nd:YAG laser. The wavelength of irradiating light was changed by second and forth harmonic of Nd:YAG laser, so that 266 nm, 532 nm, and 1064 nm were used. Ar and O<sub>2</sub> gas mixture with high pressure was injected into this plume to cool it. Injection was synchronized with the laser pulse. The cluster ions of the plume were analyzed by a Q-mass analyzer. Synthesized materials were analyzed by TEM and ED, XPS, and photoluminescence (PL). They showed that 532 nm wavelength laser and high pressure gas mixture injection were required for formation of small and uniform TiO<sub>2</sub> particles, and that O<sub>2</sub> concentration of the injected gas mixture was the parameter to control particle size. The obtained material was ultra small anatase particles with a characteristic properties.

**METASTABLE NANOSIZE METAL PRODUCED BY ELECTRO- EXPLOSION**

*G.V. Ivanov<sup>1</sup>, M.I. Lerner<sup>2</sup>, V.I. Davidovich<sup>2</sup>, J.D. Katz<sup>3</sup> and F. Tepper<sup>4</sup>*

<sup>1</sup> Instit. Petroleum Chemistry, Russ. Acad. of Sciences (RAS), 634055 Tomsk, RUSSIA  
<canc@ihn.tomsk.su>

<sup>2</sup> Republican Research Inst. of Design Engr., RAS, Tomsk, RUSSIA

<sup>3</sup> Los Alamos National Laboratory, MS G 770, Los Alamos, NM, USA

<sup>4</sup> Argonide Corporation, Sanford, Florida, USA <fred@argonide.com>

Metastable nanosize metal powders are being manufactured by the electroexplosion (Elex process) of metal wire. The history of the process can be traced back to 1777 when Narne and Faraday both aerosolized a conductor with an electric current to produce oxide smoke. The process involves superheating a metal wire with a very large electrical pulse during a brief (microseconds) duration to cause the wire to explode into metallic clusters. Extraordinary rapid adiabatic quenching occurs from peak temperatures of 15,000+ Kelvin. Any metal which can be obtained in the form of ductile wire can be used as a starting material, and the Elex process has produced 18 different nanosize metals so far. The process is semi-continuous, with wire continuously being fed into an argon-filled reactor producing kilogram size batches of powder. The powder is either used in dry form or is submerged under hexane to prevent oxidation.

The particles may be as small as 10 nanometers, but most experience to date has been with 100 nm size particles, which are less prone to self-ignition. High resolution transmission electron microscopy shows a high density of crystalline defects. They are metastable in that they have a source of internal energy that is released at threshold temperatures well below the melting point. Data gathered at Los Alamos confirmed earlier Russian DTA data that showed Elex silver powder exotherms at 220°C without evidence of any weight change. Data are given for DTA and DSC of several of the Elex powders.

The powders are highly reactive and have unusual physical and chemical properties. They exhibit reduced melting points and heats of fusion. Elex aluminum and copper exotherm at about 400°C, often emitting light and releasing enough heat to self sinter and sometimes self melt if the powders are consolidated into a pellet. Elex aluminum when combined with water in a gel can be ignited and will burn to form hydrogen at about 3000°C. Binary intermetallic alloys of two of the metal powders can be formed by igniting a pelletized mixture with a hot wire. Elex aluminum will burn in pressurized nitrogen to form aluminum nitride.

Applications include powder metallurgical alloying, bonding and coating of metals to other metals, ceramics and semiconductors, synthesis of metallorganic compounds, as catalysts, as lubricating agents and as additives to propellants, explosives and pyrotechnics.

**SYNTHESIS AND STRUCTURAL INVESTIGATION  
OF V SUBSTITUTED HfO<sub>2</sub> NANOCRYSTALS**

*Ch. Turquat, Ch. Leroux, M. Roubin\*, G. Nihoul and J.-C. Valmalette*

Matériaux Multiphasés et Interfaces, UPRES 2135,

\*Physico-Chimie des Matériaux et Milieux Marins, UPRES 1356,  
Université de Toulon-Var, B.P.132, 83957 La Garde Cedex, FRANCE  
<valmalette@univ-tln.fr>

Hafnia is commonly produced in nuclear industry as a residue in the purification of zirconia. These two oxides HfO<sub>2</sub> and ZrO<sub>2</sub> have great structural similarities, but physical and chemical properties of HfO<sub>2</sub> have only been scarcely investigated so far. Modification of structural properties of hafnia with size of particles are also expected. This work describes the influence of substitution of hafnium by vanadium. Indeed, modulation of the oxidation state and size of V<sup>4+</sup> cations by controlling oxygen pressure is of great interest for both structural and transport properties.

Nanocrystals of Hf<sub>1-x</sub>V<sub>x</sub>O<sub>2</sub> were elaborated by decomposition of oxalic complexes. Pyrolysis under controlled atmosphere 700°C leads to well faceted nanocrystals of Hf<sub>1-x</sub>V<sub>x</sub>O<sub>2</sub> with size ranging from 10 to 50 nm. Samples heated in air yield monoclinic structure and slight expansion of cell parameters compared with pure HfO<sub>2</sub>, whereas samples heated in inert atmosphere have a cubic structure. Solubility limit of vanadium also depends on atmosphere (from 7 to 20 at.%).

The control of microstructure and crystallographic structure of powder with substitution is discussed involving formation of ordered vacancies on the cationic sites. These results are promising for applications as ionic conductivity, high refractive index materials or thermal barrier coatings (TBCs).

**SYNTHESIS OF NANOSTRUCTURIZED POLYHETEROCYCLES**

*V.A. Solomin, V.V. Luapunov, E.N. Lyakh and B.A. Zhubanov*

Institute of Chemical Sciences Ministry of Sciences - Academy of Sciences,  
106 Sh. Ualikhanov Str., Almaty, 480100, KAZAKSTAN  
<adm@chem.academ.alma.su>

The new approach to the synthesis of nanostructurized condensation cyclochain polymers on the basis of alicyclic dianhydrides has been developed. Under conditions of thermodynamically unstable (metastable) reaction media (mixed water-organic solvents) the structurization of oligomer polyimidoamic acid solutions took place by means of formation the one - dimension ordered associates of reagents. By the light scattering study the structurization processes in reaction solutions have been investigated. It has been shown that the formation of nanostructures with dimensions from 5 till 300 nm can results in the shift of polycondensation equilibrium to the formation of high molecular weight polymer products and to spontaneous growth of condensation cyclochain macromolecules. Upon standing of the oligomeric solutions at the points that form boundary curves of methastable nanostructurized areas, an increase in reduced viscosity and also in polymerization degree from 7 up to 120 was observed. The later increase in polymerization degree led to the gradual precipitation of the polyheterocycles due to the loss of solubility. Polymeric glasses of non-crystalline polyheterocycles obtained under such conditions show double refraction properties. This testifies of the conservation of the nanosize macromolecule aggregates under the conditions of heterophase. X-ray analysis of such polymeric glasses at small deflection angles  $4^\circ < 2\theta < 11^\circ$  allowed to estimate the dimensions of the supermolecular formation as close to 20-50 nm. The molecular weight distribution tends to narrow in comparison with the most probable one.

**DYNAMIC COMPRESSION BEHAVIOR OF  
NANOCRYSTALLINE TUNGSTEN CONSOLIDATED  
WITH A NEW PLASMA PRESSURE COMPACTION (P<sup>2</sup>C) SYSTEM**

*Sang H. Yoo<sup>1</sup>, T.S. Sudarshan<sup>1</sup>, Krupa Sethuram<sup>1</sup>, Ghatu Subhash<sup>2</sup> and R.J. Dowding<sup>3</sup>*

<sup>1</sup> Materials Modification Inc, 2929-P1 Eskridge Rd, Fairfax, VA 22031, USA

<sup>2</sup> Michigan Technological University, Houghton, MI 49931, USA

<sup>3</sup> Army Research Laboratory, AMSRL-WM-MD, Aberdeen Proving Ground,  
MD 21005, USA

The mechanical behavior of nanocrystalline tungsten was investigated using the compression Kolsky bar. The performance of pure tungsten in high loading rate application has been poor due to its brittleness. Efforts have been initiated to increase the ductility of tungsten by decreasing the grain size to the nanometer range (<100 nm) using novel synthesis and consolidation process. Pure nanocrystalline tungsten powder was produced by a DC plasma synthesis technique, and consolidated using the rapid consolidation technique, Plasma Pressure Compaction, to minimize grain growth. The consolidation experiments were conducted systematically to optimize the parameters that yielded high density, nanocrystalline, tungsten compacts. The densities of the consolidated specimens were measured using Archimedes' method and the grain sizes were measured using scanning electron microscope and X-ray diffraction techniques. The high strain rate mechanical properties were examined using the consolidated specimens with the highest density and the small grain size. The effect of grain size and oxygen content on yield stress and strain was investigated at the various strain rates.

**IN-SITU FORMATION OF NANOSIZED SiC PARTICLES  
IN AN Al<sub>2</sub>O<sub>3</sub> MATRIX**

*Lena K.L. Falk and Elis Carlström\**

Department of Experimental Physics, Chalmers University of Technology,  
S-412 96 Göteborg, SWEDEN <lklfalk@fy.chalmers.se>

\*Swedish Ceramic Institute, Box 5403, S-402 29 Göteborg, SWEDEN <ec@sci.se>

Composite materials containing a dispersion of nanosized inter- and intra-granular SiC particles in an Al<sub>2</sub>O<sub>3</sub> matrix have been fabricated by sol-gel technology and *in-situ* reaction during densification. Nanosized SiO<sub>2</sub> sol particles (diameter 15 nm) and saccharose as the carbon precursor were homogeneously dispersed in a suspension of Al<sub>2</sub>O<sub>3</sub> powder. The homogeneous dispersion was retained in the green bodies through freeze granulation followed by calcination, and the saccharose was transformed to carbon during heat treatment at temperatures up to 500°C in N<sub>2</sub> atmosphere. The green bodies were subsequently pressureless sintered or hot-pressed in Ar atmosphere at temperatures up to 1910°C. Reaction between SiO<sub>2</sub> and carbon during densification resulted in the formation of SiC particles. The particle size was typically in the range 40 to 100 nm. Transmission electron microscopy showed also that the Al<sub>2</sub>O<sub>3</sub> grains had a comparatively high dislocation density after densification, and the dislocations were frequently locked by intragranular SiC particles. Dislocation networks had locally resulted in the development of cell structures and subgrain boundaries. The development of this type of intragranular structure, brought about by the SiC particles, would promote fabrication of tough and creep resistant nanocomposite ceramics.

**SYNTHESIS OF WC-Co POWDERS FROM SOLUBLE TUNGSTEN SALTS  
BY ULTRASONIC SPRAY PYROLYSIS**

*S. Stopić<sup>1</sup> and D. Uskoković<sup>2</sup>*

<sup>1</sup> Faculty of Technology and Metallurgy, Belgrade, YUGOSLAVIA

<sup>2</sup> Institute of Technical Sciences, Serbian Academy of Sciences and Arts,  
Belgrade, YUGOSLAVIA

Hard alloys based on WC-Co have a wide application in industry; and the properties of these materials depend, to a great extent, on the microstructure, composition and purity of the component metal powders. Especially good results have been obtained for WC-Co nano-phase during reduction, carburisation and sintering performed separately.

The aim of our work was to obtain WC-Co powders of high uniformity using soluble tungsten (ammonium-metatungstate and sodium-tungstate) and cobalt (cobalt-nitrate hexahydrate) in the presence of saccharose in a reduction atmosphere of hydrogen in static and dynamic conditions of continuous process. The reduction of tungstate was performed in temperature range from 700-900°C. As a grain growth inhibitor 0.1 mass. percent VC in the form ammonium-metavanadate was used. To intensify the starting components reduction 0.1 mass percent of PdCl<sub>2</sub> was added and the hydrogen spillover effect caused acceleration of the transformation. X-ray diffraction and thermalgravimetric methods were used to determine the degree of transformation of the starting compounds in static conditions, and a positive effect of the increased temperature on the reduction intensity was confirmed. Using aqueous solutions of tungsten and cobalt salts a WC-Co nano-phase was obtained by reduction in hydrogen and nitrogen atmosphere in dynamic conditions of ultrasonic spray pyrolysis. SEM and stereological semi-automatic analyses revealed the shape and size of particles obtained. As confirmed non-agglomerated spherical nanostructured particles of WC-Co powders were obtained.

**NANOPARTICLE CATALYSTS BY AGGLOMERATION OF NANOFILMS**

*Janos Mizsei\*, Mikko Karppinen, Lauri Pirttiaho and Vilho Lantto*

Microelectronics and Materials Physics Laboratories, University of Oulu,  
Linnanmaa, FIN-90570 Oulu, FINLAND <mk@ee.oulu.fi>

\* Department of Electron Devices, Technical University of Budapest,  
Goldman Gy. ter 3., 1521 Budapest, HUNGARY <mizsei@eet.bme.hu>

A simple technique is developed to produce noble metal nanocatalysts on oxide surfaces by annealing ultra-thin metal films in suitable atmospheres. These catalytically active additives are used, e.g., to increase selectivity and sensitivity of metal-oxide semiconductor gas sensors.

This study considers formation of palladium and silver nanoparticles (clusters) from 1–15 nm thick Pd and Ag films deposited by r.f. sputtering on oxidized silicon slices and glass substrates. During agglomeration the smooth metal layer becomes discontinuous forming a surface coverage of nanoparticles. Ag layers agglomerate in air at 300°C without noticeable oxidation. Pd layers agglomerate at 500°C if hydrogen is present in the ambient air, but Pd also oxidizes at that temperature. The PdO is reduced to Pd nanoparticles by another H<sub>2</sub> treatment at 300°C.

The agglomeration processes were monitored by *in situ* conductivity measurements. The morphologies and compositions of the layers were studied by atomic force microscopy (AFM) and x-ray diffraction (XRD).

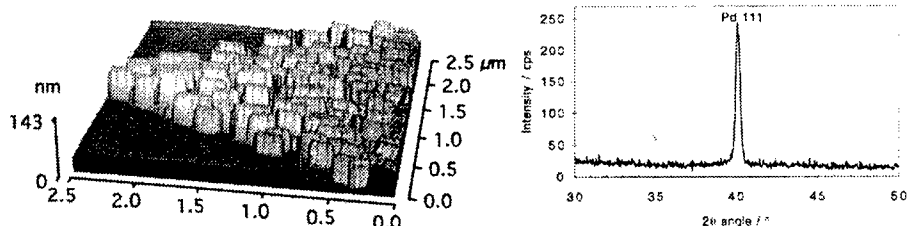


Figure 1. AFM picture and XRD pattern measured from an ultra-thin Pd layer agglomerated and reduced by successive H<sub>2</sub> treatments at 500°C and at 300°C, respectively.

**ZnO- Fe NANOCOMPOSITES VIA BALL MILLING AND ANNEALING**

*L. Takacs<sup>1</sup>, L. Pogany<sup>2</sup>, L.K. Varga<sup>2</sup>, M. Pardavi-Horvath<sup>3</sup> and A. Bakhshai<sup>4</sup>*

<sup>1</sup> University of Maryland, Baltimore County, Department of Physics, Baltimore,  
MD 21250, USA <takacs@umbc.edu>

<sup>2</sup> Research Institute for Solid State Physics of the Hungarian Academy of Sciences,  
H-1525, Budapest, P.O.B. 49, HUNGARY <pogany or varga@power,szflki,kfki.hu>

<sup>3</sup> The George Washington University, Institute for Magnetics Research, Washington,  
D.C. 20052, USA <pardavi@seas.gwu.edu>

<sup>4</sup> Goucher College, Department of Physics, Towson, MD 21204, USA  
<abakhsha@goucher.edu>

When a metal oxide,  $M_xO_y$  is ball milled with a more reactive metal,  $N$ , a mechano-chemical reaction takes place. Ideally, the product is a nanocomposite, containing grains of  $M$  and  $N_xO_y$ . As earlier investigations have shown, the mechanism of the reaction is more complicated than a single-step displacement of oxygen from the less reactive to the more reactive metal. For example, when  $Fe_3O_4$  is milled with Zn, the first product is an intermediate Fe-Zn oxide, which constitutes more than 50% of the sample after about 100 min. of milling. This intermediate phase decomposes into Fe metal and ZnO upon continued milling. The freshly formed iron particles are highly supersaturated in Zn; the Zn concentration decreases with increasing milling time. Some Fe remains in the oxide phase. The final product is a semihard magnetic material, its saturation magnetization is well below the value based on the ideal stoichiometry.

In the present investigation of the  $Fe_3O_4$ -Zn system, milling is used only to prepare the intermediate mixed oxide. The final product is obtained via annealing at relatively low temperatures (200 - 300°C.) Several questions are addressed, some related to understanding the mechanism of the preparation process, others aimed at preparing a useful magnetic material with controlled properties. (i) The effects of milling and annealing on the intermediate phase are compared. Milling maintains high defect concentration and a broad particle size distribution, while annealing results in fewer defects and a decreasing fraction of the finest particles. Different phases may form as a result of milling and annealing. (ii) The X-ray characterization of the intermediate phase is very difficult, as its broadened diffraction lines overlap with lines from other phases. Low temperature annealing may decrease particle size and strain broadening without changing the phase composition of the sample, thereby making the evaluation of X-ray diffraction data more straightforward. (iii) The magnetic properties of the material are studied as a function of milling time and the time and temperature of annealing. The possibility of obtaining useful properties is explored. (iv) The microstructure of the samples is investigated by SEM and related to the preparation process and the magnetic properties.

**PROCESSING AND MECHANICAL PROPERTIES  
OF NANOCRYSTALLINE 5083 AL ALLOY**

*V.L. Tellkamp and E. J. Lavernia*

Materials Science and Engineering, University of California,  
916 Engineering Tower, Irvine, California, USA

A commercial aluminum alloy, 5083, was processed using a cryomilling operation to produce a bulk nanocrystalline extrusion. This paper presents the processing techniques utilized including; the details of the cryomilling operation, the method of degassing the powders, hot isostatic pressing to produce a bulk material, and extrusion for complete densification. The grain size at each processing step was measured utilizing both x-ray diffraction and transmission electron microscopy. The mechanical properties of this extruded material were measured utilizing ASTM E 8-93, Standard Test Methods for Tension Testing of Metallic Materials. The fracture surfaces of the tensile specimens are presented to discuss possible failure mechanisms.

---

**PULSE RADIOLYTICALLY INDUCED COLLOIDAL METAL  
FORMATION IN WATER AND WATER -IN-OIL MICROEMULSION**

*S. Adhikari and C. Gopinathan*

Chemistry Division, Bhabha Atomic Research Centre,  
Trombay, Mumbai 400085, INDIA

The nanocluster of metals is a highly dispersed state of matter. These are useful for studying the "neglected dimensions" in material research, the nanometer and subnanometer size regime, where a transition from bulk to molecular properties takes place. The possibility of use of gold and silver as condensers for electron storage in artificial photosynthesis has promoted the interests in this area of research. Several methods have been developed for synthesizing these clusters which include radiation chemical reduction of metal ions from solution.

In the present study the pulse radiolytic technique has been employed to investigate the reduction of metal ions including gold ion in water and water-in-oil microemulsion. The bimolecular rate constants for the reduction reactions have been determined. The formation kinetics, stability and characterization of the metal particles will be presented. Formation of copper and cadmium colloids by reduction of a metal-bio complex will also be covered.

**NANOSTRUCTURED HARD MATERIAL COMPOSITES  
BY MOLECULAR ENGINEERING:  
2. SYNTHESIS FROM AMMONIUM PARATUNGSTATE**

*Sverker Wahlberg<sup>1</sup>, Ingmar Grenthe<sup>2</sup> and Mamoun Muhammed<sup>1</sup>*

<sup>1</sup>Department of Materials Science and Engineering, Materials Chemistry

<sup>2</sup>Department of Chemistry, Inorganic Chemistry,  
Royal Institute of Technology (KTH), S-100 44 Stockholm, SWEDEN

Several new techniques to produce nanophase WC-Co powders have been presented during the last decade. A nanostructured mixture of WC and Co can be prepared by reduction and carburisation of uniform cobalt tungstate precursors prepared by e.g. spray-drying, co-precipitation or gel-formation. In a previous communication we reported the synthesis via co-precipitation starting from sodium tungstate or ammonium metatungstate and soluble cobalt salts. In this paper we report the preparation of precursors starting from ammonium paratungstate (APT) and different cobalt salts. The overall reaction can be described as a solvent mediated process in which paratungstate clusters ( $H_2W_{12}O_{42}^{10-}$ ), released by dissolution of APT in the aqueous phase, reacts with cobalt and ammonium ions and precipitates as a cobalt ammonium paratungstate salt. The aqueous chemistry is determined both by thermodynamic and kinetic factors. The speciation of tungsten is to a large extent controlled by slow condensation or hydrolysis reactions between different polytungstate clusters.

**NANOSTRUCTURES SYNTHESIS ON THE SURFACE OF  
SEMICONDUCTORS, METALS AND INSULATORS AND  
ELLIPSOMETRIC INVESTIGATION OF THE BOUNDARY  
BETWEEN THE SUBSTRATE AND SYNTHESIZED LAYER**

*V. Gromov and S. Koltsov*

State Institute of Technology, St.-Petersburg, RUSSIA <cespero@mail.marinform.ru>

The results of the ellipsometric investigation of the boundary between a substrate and a nanolayer (0-10.0 nm) for the substances of different nature are presented. As substrates there were chosen monocrystal silicon, polycrystal copper and quartz. As nanostructures synthesized on the surface of the substrates there were chosen titanium dioxide nanolayers.

The ellipsometric parameters of the surface were measured *in situ* in the process of synthesis and in various immersion media. Anomalous changes of the ellipsometric parameters  $\Psi$ ,  $\Delta$  with the growth of the thickness of the nanolayers was detected, that was connected to change of optical parameters of the substance in the near-boundary area during the synthesis of nanolayers.

The evaluation of the experimental data obtained during measurement of ellipsometric parameters  $\Psi$ ,  $\Delta$  has shown that the optical parameters of the substance in the near-boundary area are changing exponentially with the growth of the thickness of the nanolayers. This was explained by the structure accommodation of the substances of different nature in the near-boundary area: the substrate - the synthesized nanolayer.

**FORMATION AND GROWTH OF OXIDE NANOSCALE  
STRUCTURES ON THE CARBON SURFACE***E.P. Smirnov*State Institute of Technology, St.-Petersburg, RUSSIA <[diamond@infopro.spb.su](mailto:diamond@infopro.spb.su)>

Synthesis of oxide (titanium, vanadium, chromium) nanostructures on the surface of carbon (diamond, graphite and carbon films) has been carried out using method of chemical designing from molecular structural units of halogenides metals and water in cyclic reactions of replacement.

Kinetic regularities of nanostructure synthesis reactions are described by the equation  $-ln(1-q) = kt$ . The activation energy ranges from 10 to 20  $kJ/mol$ . It has been established that the quantity of primary element-haloid complex is determined by concentration of proton-containing oxy-centers which can be in the range from 0.05 to 3.0  $complex/nm^2$ .

The theoretical model was suggested. The feasibility of controlled formation and growth of nano-crystals and nano-films based on involving into reactions the functional centers of different activity and concentration was demonstrated. Electronic microscopy showed dynamics of the formation and growth of nanocrystals beginning with 5 nm. The region of electron interplay between substrate and film was evaluated by X-ray photoelectron spectroscopy using the ionization values of the inner  $2P^{3/2}$  states of titanium ions. For diamond surface it extends to the thickness up to 500 nm and its presence was completely unnoticed in the case of growing nanolayers on graphite surface.

### NANOPHASE CERIUM OXIDE BASED CATALYSTS FOR ENVIRONMENTAL CATALYSIS

*Tarja Turkki<sup>1</sup>, Mamoun Muhammed<sup>1</sup>, Massoud Pirjamali<sup>2</sup>, Sven Järås<sup>2</sup>,  
Laetitia Dalmazio<sup>3</sup>, Anne Julbe<sup>3</sup>, Christian Guizard<sup>3</sup>*

<sup>1</sup> Materials Chemistry Division and <sup>2</sup> Chemical Technology Division,  
Royal Institute of Technology, SE-100 44 Stockholm, SWEDEN

<sup>3</sup> Laboratoire des Matériaux et Procédés Membranaires (UMR 5635 CNRS)- ENSCM-  
8 rue de l'Ecole Normale, 34 296 Montpellier cedex 5, FRANCE

This work concerns the development of nanophase CeO<sub>2</sub> based catalysts for car exhaust emission control. The doping of nanophase CeO<sub>2</sub> has been shown to greatly enhance the ceria oxygen storage capacity and consequently their interest for use in environmental catalysis. In this work two synthesis methods have been investigated for the synthesis of the doped CeO<sub>2</sub> catalyst: the co-precipitation and the sol-gel methods.

Several doped cerium oxides (Ce<sub>1-x</sub>Nd<sub>x</sub>O<sub>2-y</sub>, Ce<sub>1-x-y</sub>Nd<sub>y</sub>Zr<sub>x</sub>O<sub>2</sub> and Ce<sub>1-x</sub>Ca<sub>x</sub>O<sub>2</sub>) and spinels (Nd<sub>2-x</sub>Ce<sub>x</sub>CuO<sub>4</sub>) have been synthesized using co-precipitation. Physical and chemical characterizations have been performed. Both the combustion of methane and the conversion of CO and SO<sub>2</sub> to respectively CO<sub>2</sub> and elementary sulfur have been investigated. The reduction of NO to N<sub>2</sub> and the oxidation of CO and hydrocarbons to CO<sub>2</sub> have been also studied. Detailed ESCA studies for microstructure correlation to the catalytic activities will be presented.

Both aqueous and organic media were investigated for the synthesis of CeO<sub>2</sub> based materials (molar composition YCeO<sub>2</sub>-(0.98-YAl<sub>2</sub>O<sub>3</sub>)-0.02CaO with Y=0 to 0.98) by the sol-gel process from either cerium chloride or cerium acetylacetone. The methods led to homogeneous sols which can produce homogeneous powders or which can be directly cast on honeycomb supports. The evolution of the characteristics (XRD, SEM, N<sub>2</sub> adsorption-desorption) of the powders heat-treated in air at 700°C or 1000°C has been studied as a function of Y. TPD measurements of oxygen adsorption capacity of the powders showed that the presence of alumina can positively influence the oxygen storage capacity of the powders. The TPD results have been correlated with the powder textural characteristics (namely the specific surface area and ceria crystallite size) which are greatly influenced by the CeO<sub>2</sub>/Al<sub>2</sub>O<sub>3</sub> molar ratio.

This work is supported from Brite EuRam Program (BRPR-CT96-0290)

**SYNTHESIS AND CHARACTERISATION OF THERMOELECTRIC  
SKUTTERUDITE  $\text{CoSb}_3$  VIA SOLUTION CHEMISTRY ROUTE**

*M. Wang, S. Shourie, Yu Zhang, and M. Muhammed*

Materials Chemistry Division, Royal Institute of Technology,  
SE-100 44 Stockholm, SWEDEN

Some Skutterudite alloys have been recently reported as a new group of the advanced thermoelectric materials. It has been generally recognized that Skutterudite structure is difficult to prepare in pure phase via conventional metallurgical routes. A chemical coprecipitation route has been developed for synthesis of nanophase precursor of Skutterudite  $\text{CoSb}_3$ . Computer-assisted thermodynamic modelling approach has been applied to guide the coprecipitation experiments. The optimum conditions, pH range and oxalate addition ratio, have been evaluated for oxalate/oxide coprecipitation. The predicted results from modelling have been verified experimentally. A nanophase powder of Co and Sb composite has been prepared by coprecipitation under controlled pH. The coprecipitated powder has been found to be a good precursor for further thermal treatments. The thermal processing of as-precipitated precursor is simple and straightforward, including calcination and reduction in sequence. These two steps of processing have been optimized to require relatively low temperature (400-500°C) and short time (3-4 hours in total). The calcined oxides have been found much more stable in maintaining constant mole ratio of Co:Sb = 1:3 than the mechanical mixture of pure oxides during the treatments. Heating the calcined oxides in  $\text{H}_2$  can directly produce the Skutterudite  $\text{CoSb}_3$  without further treatment such as annealing. The materials produced at various processing steps have been characterized by AAS, TGA, XRD and SEM. The thermoelectric properties of the materials have been also evaluated.

**MÖSSBAUER STUDY OF STRUCTURAL-CHEMICAL  
TRANSFORMATIONS AT TRANSPORT REDUCTION OF  
TWO-DIMENSIONAL IRON-OXIDE NANOSTRUCTURES**

*G.P. Voronkov, V.G. Semenov, V.N. Gitzovich, I.V. Murin and V.M. Smirnov*

Chemistry Department, St.-Petersburg State University,  
Petrodvorez, St.-Petersburg 198904, RUSSIA

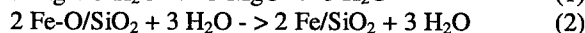
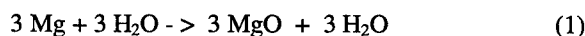
Generalised results of NGR-investigations of two-dimensional iron-oxide two-dimensional iron-oxide nanostructures (in thickness 0.3-2 nm) on surface of silica and products their transport reduction (TR) are presented in this report.

The synthesis of Fe-O groups and Fe-O monolayers (1-4 monolayers) on surface of silica ( $S=275 \text{ m}^2/\text{g}$ , and a mean porous diameter of 10-14 nm) realised by the molecular layering (ML) method.

The method ML is based on conducting several step-by-step nonreversible surface reactions between functional groups of silica (Si-OH) and low-molecular compounds ( $\text{FeCl}_3$ , then  $\text{H}_2\text{O}$ -one cycle).

As a result of reaction cycle on silica the monolayer Fe-O group is arisen, quantity such cycles determines a number of build up monolayers.

TR takes place in the system of space divided Fe-O nanostructures [ $\text{Fe-O/SiO}_2$ ] and of Mg, being closed ampoule at the presence of several millilitre of water, needed for beginning of reaction. TR may be described as:



Peculiarity of these reactions is they make possible precise regulation  $\text{O}_2$  percentage at the all range of resulting oxygen nanostructures, up to its dicipating (metallic state).

Application of NGR- spectroscopy made possible to receive date about sequence of structural-chemical transformations of two-dimensional iron-oxide substance in comparing with reducing of  $\alpha\text{-Fe}_2\text{O}_3$  (hematite).

The work has been funded by RFBR grants N 96-03-33342 and N 96-03-33990.

**STRUCTURE AND THERMAL STABILITY OF NANOCRYSTALLINE Mo**

*A.V.Korznikov\*, S.Idrisiva\*, and N.I.Noskova*

\*Institute of Problems of Metal Superplasticity, Russian Academy of Sciences,

39 St.Khalturina Str., Ufa, 450001 Bashkortostan, RUSSIA

Institute of Metal Physics, Ural Division of Russian Academy of Sciences

18 Kovalevskaya Str., GSP-170, Ekaterinburg 620219, RUSSIA

The structure and thermal stability of nanocrystalline Mo produced by severe torsional plastic deformation under a quasi-hydrostatic pressure were studied. The structure with a grain size of 20-100 nm formed upon the deformation is characterised by strong lattice distortions. The hardness of nanocrystalline molybdenum is equal to 5.8 GPa. The heating in a temperature range of 1000-1100°C leads to an abrupt increase in the grain size and a decrease in the hardness (to 2 GPa).

**SYNTHESIS AND CHARACTERIZATION OF NANOCRYSTALLINE  
NI/ZrO<sub>2</sub>- AND NI/ Al<sub>2</sub>O<sub>3</sub> -COMPOSITE COATINGS**

*A. Möller and H. Hahn*

Darmstadt University of Technology, Department of Materials Science,  
Thin Films Division, Petersenstr. 23, 64287 Darmstadt, GERMANY  
<hhahn@hrzpub.tu-darmstadt.de>

Nanocrystalline Ni/ZrO<sub>2</sub>- and Ni/Al<sub>2</sub>O<sub>3</sub>-composite coatings were produced by codeposition of ZrO<sub>2</sub>- and Al<sub>2</sub>O<sub>3</sub>-particles during pulsed electroplating of Ni. In this process nanocrystalline ceramic powders with grain sizes below 10 nm were suspended in the plating solution and the ceramic particles co-deposit with the metal to produce nanocrystalline metal matrix composite coatings. The influence of the plating parameters like pulse height, pulse time, pulse form, pH etc. on content and dispersion of the co-deposited ceramic particles were investigated. Additionally, the microstructure of the deposited coating was examined and the experimental results were correlated with the mechanical properties of the coatings. Selected samples were thermally treated to evaluate the grain growth behavior and the thermal stability of the synthesized coatings. Composites were also produced under nonpulsed conditions and examined as described above. The results are compared with the experiments for samples produced by pulsed plating. The comparison of coatings deposited under pulsed and nonpulsed conditions shows that the properties of the deposited metal matrix composites are different.

**A SIMPLE MODEL FOR THE CHEMICAL VAPOR SYNTHESIS  
OF NANOCRYSTALLINE SILICON CARBIDE***Markus Winterer*

Thin Films Division, Materials Science Department, Darmstadt University of Technology, Petersenstr. 23, D-64287 Darmstadt, GERMANY

Chemical vapor synthesis (CVS) is a modified CVD process where the process parameters are chosen to limit film growth on a substrate and promote the nano-particle formation in the gas phase. This process provides nanocrystalline powders of very small grain size, narrow size distribution, weak agglomeration, high purity at high production rates and yields and the possibility for scale up. It is desirable for the optimization of this process to have a simple model available describing the grain size as a function of process parameters, namely decomposition temperature, reactor pressure, precursor material and partial pressure.

A simple model will be presented describing the formation of nanocrystalline silicon carbide from tetramethylsilane (TMS) in the CVS process. The model fits the grain size as a function of process parameters with a single parameter, an effective residence time. It is based on chemical reaction kinetics and kinetic gas theory. Evidently, the formation of nanograins in the CVS process can not be described by classical homogeneous nucleation but by diffusion limited growth.

Agglomeration is described by Brownian coagulation and a method is suggested to determine which process mode, film (CVD) or particle formation (CVS) is favoured. An extension of this model to other materials should be straight forward, provided the formation reaction can be described by first order kinetics.

**METHOD OF PRODUCING NANOCRYSTALS  
WITH THE USE OF SOLUTION MICROCAPSULATION  
AT THERMODYNAMICAL EQUILIBRIUM.**

*M.V. Astakhov, M.G. Kapustin, S.M. Trushevsky and I.V. Stelmukh*

Department of Physical Chemistry, State Steel and Alloys Institute Leninsky pr.4,  
Moscow 117936, RUSSIA <[astahov@phch.misa.ac.ru](mailto:astahov@phch.misa.ac.ru)>

Usual methods for producing ultra fine particles (UFP) of different materials do not allow to change the particle size during physico-chemical investigations. In many cases, the phase composition of nanoparticles depends on the method of producing. Then it can not be used for studying of size effect. That is why it is very important to produce the nanoparticles in equilibrium state.

We have developed a method of UFP production with the use of microcapsulating of salt aqueous solution. The method is based on the compound solubility dependence on temperature. The size of crystallite can be changed by change of temperature. In this case, the particle size can be estimated by the formula of solubility temperature dependence.

This method has following advantages:

1. The opportunity to receive a salt crystal, in thermodynamic balance with the solution.
2. The possibility of changing the particles size of the same sample, using a change of temperature.
3. It minimizes the influence of the matrix on the properties of crystallized nanoparticles.

Using this technique, we was produced microcapsules containing saturated at 20°C solution of  $\text{FeNH}_4(\text{SO}_4)_2 \cdot 12\text{H}_2\text{O}$  and  $\text{K}_4[\text{Fe}(\text{CN})_6] \cdot 3\text{H}_2\text{O}$  and we investigated them by Mössbauer spectroscopy. It is known that Mossbauer spectroscopy is sensitive to the size of ferroelectric crystals. The doublet-line was observed in spectrum of  $\text{FeNH}_4(\text{SO}_4)_2 \cdot 12\text{H}_2\text{O}$ . The analysis of the spectrum has shown combination of several doublet-lines, that was connected with the size distribution of the microcapsules.

For  $\text{K}_4[\text{Fe}(\text{CN})_6] \cdot 3\text{H}_2\text{O}$ , the singlet-line was observed in the spectrum obtained at 20°C. Increase of experiment temperature up to 40°C transforms the singlet-line to a doublet-line. That proves the appearance of a ferroelectric phase, as a result of the change of salt solubility and the decrease of the crystal size. Changes in the spectrum are reversible.

Thus, the present studies have shown that the technique, mentioned above, for producing nanoparticles of soluble compounds with the use of microcapsulating method has essential advantages in comparison with other techniques and allows to study systems of any soluble compounds at thermodynamic equilibrium with a master solution.

**MECHANOCHEMICALLY SYNTHESIZED  
NANOCRYSTALLINE INDIUM OXIDE**

*T.F.Grigorieva<sup>1</sup>, A.P.Barinova<sup>1</sup>, E.Yu.Ivanov<sup>2</sup>, N.Z.Lyakhov<sup>1</sup>*

<sup>1</sup> Institute of Solid State Chemistry, Kutateladze 18, 630128 Novosibirsk, RUSSIA

<sup>2</sup> Tosoh SMD Inc., 3600 Gantz Road, Grove City, Ohio 43123, USA

Indium oxide was mechanochemically synthesized in planetary ball mill. The analysis of X-ray data lets to assume the nanometric size of particle and high defect structure. HRTEM researches of formed  $\text{In}_2\text{O}_3$  were conducted on transparent electron microscope JEM-2010X (resolution 0.14 nm, accelerating voltage 200 kV). Study showed that the particle of indium oxide had the round shape of diameter from 30 to 70 nm. These particles consist of more small-sized particles of the round shape diameter 1-3 nm. Microdiffraction of particle confirmed the developed microblock structure.

**NANOCRYSTALLINE COMPLEX OXIDES OBTAINED  
BY MECHANOCHEMICAL SYNTHESIS**

*T.F.Grigeova<sup>1</sup>, A.P.Barinova<sup>1</sup>, G.N.Kryukova<sup>2</sup>, V.D.Belykh<sup>2</sup>, N.Z.Lyakhov<sup>1</sup>*

<sup>1</sup> Institute of Solid State Chemistry, Kutateladze 18, 630128 Novosibirsk, RUSSIA

<sup>2</sup> Boreskov Institute of Catalysts, Lavrentiev avenue 5, 630090 Novosibirsk, RUSSIA

The production of nanocrystalline powder complex oxides is one of main problems of modern technology of segneto-, piezo- and magnetic ceramics. The conventional technology of obtaining of ceramics on the basis of complex oxides is based on high-temperature synthesis from simple oxides or from their mixtures with carbonates. This diffusion limiting process requires high temperatures, high degree of dispersion of initial powders. The complex oxides obtained by these methods represent particles measuring 1-5  $\mu\text{m}$ . Complex oxides may be produced by self-propagating high-temperature synthesis, however these processes are attended with high temperature in reaction zone. Temperature of combustion zone for reaction alkali earth metal with metal (titanium, zirconium, and aluminium) ranges up to 2500-3000K and size of particle in this case comprises 5-10  $\mu\text{m}$ .

The mechanochemical synthesis in constantly cooling drums of planetary ball mill allow to reduce the temperature at the reaction mixture, because the balls and reaction mix are in continuous contact with surface of constantly cooling drums. It is hoped that the reduction of this temperature is able to change the size of particles at mechanochemical synthesis.

The purpose of this work is mechanochemical synthesis of nanocrystalline complex oxides.

It is shown that the interaction of peroxides of alkaline and alkali-earth metals with pure metals gives significant reduction of free Gibbs energy. Mechanochemical synthesis in systems  $\text{BaO}_2 + \text{Me}$  ( $\text{Me} = \text{Ti}, \text{Zr}, \text{Mo}, \text{Al}, \text{Sn}, \text{Si}, \text{Fe}$ ) is performed in planetary ball mill. X-ray and IR-spectroscopy prove the formation of complex oxides  $\text{BaMe}_x\text{O}_y$ . HRTEM investigation of products of mechanochemical synthesis in  $\text{BaO}_2 - \text{Me}$  ( $\text{Me} = \text{Ti}, \text{Zr}, \text{Al}$ ) showed that particle of complex oxides consisted of nanocrystalline blocks (6-12 nm). Microblocks are turned relative to each other at an angle 3-5°, the interfacing regions between microblocks are highly disordered.

### SYNTHESIS AND PROPERTIES OF CRYSTALLINE FULLERENE HYDRIDES

*B.P. Tarasov<sup>1</sup>, V.N. Fokin<sup>1</sup>, A.P. Moravsky<sup>2</sup>, Yu.M. Shul'ga<sup>2</sup>, V.A. Yartys<sup>3</sup>, and  
D.V. Schur<sup>4</sup>*

<sup>1</sup> Institute of New Chemical Problems, Russian Academy of Sciences,  
142432 Chernogolovka, RUSSIA <ara@incp.ac.ru>

<sup>2</sup> Institute of Chemical Physics in Chernogolovka, Russian Academy of Sciences;  
142432, Chernogolovka, RUSSIA <moralex@icp.ac.ru>

<sup>3</sup> Karpenko Physico-Mechanical Institute, The National Academy of Sciences of  
Ukraine, 5 Naukova Str., L'viv 290601, UKRAINE <yartys@ah.ipm.lviv.ua>

<sup>4</sup> Institute for Problems of Materials Sciences, The National Academy of Sciences of  
Ukraine, 252150 Kiev, UKRAINE <shurzag@ipms.kiev.ua>

Recent intensive studies on fullerenes are inspired by their probable applications in different fields of science and technology prospected by the unique physical and chemical properties of fullerene-based materials. Hydrogenation of double C-C bonds in the fullerene molecules substantially modifies their properties and is useful in many applications.

Thus, the interest in fullerene hydrides, containing up to about 7.7 wt.% of hydrogen, is caused by their possible use as catalysts, electrodes in electrochemical cells, additives to lubricants and active media in the systems of hydrogen accumulation and storage. A direct hydrogenation of fullerene C<sub>60</sub> is inconvenient, since it proceeds under rather high hydrogen pressures (50-85 MPa) and temperatures (573-623 K).

In this work we studied in details the process of formation of crystalline fullerene hydrides and deuterides under relatively mild conditions, at low hydrogen pressures (1-2.5 MPa) and temperatures (300-673 K). This direct hydrogenation of solid fullerenes involved use of hydrogen evolved from intermetallic hydrides, thus substantially reducing level of contamination in hydrogen gas. The resulting crystalline fullerene hydrides contain 10 to 30 hydrogen atoms per fullerene molecule. They were characterized by IR and XRD techniques. DTA studies revealed that fullerene hydrides decompose liberating hydrogen gas at 800 K. Upon dehydrogenation the fullerene cage remains intact and can be subjected to next hydrogenation.

The mechanism of hydrogenation of fullerenes by hydrogen evolved from rare earth intermetallic hydrides is discussed.

The work was supported through Grant 96-03-33586 from RFBR and Grant 96125 from Russian Program «Fullerenes & Atomic Clusters».

**AGGLOMERATION AND SURFACE MORPHOLOGY  
DURING PULSED LASER DEPOSITION OF Pb-Zr-Ti-O**

*M. Tyunina\*, J. Levoska, J. Koivusaari and S. Leppävuori*

Microelectronics and Materials Physics Laboratories and EMPART Research Group of  
Infotech Oulu, University of Oulu, PL 444, FIN-90571 Oulu, FINLAND  
[<juhani.levoska@ee.oulu.fi>](mailto:<juhani.levoska@ee.oulu.fi>)

\*Permanent address: Institute of Solid State Physics, Latvian University,  
8 Kengaraga, LV-1063, Riga, LATVIA

The agglomeration/clustering process in the pulsed laser induced plume and the nanometer scale surface morphology of the deposited amorphous lead zirconate titanate films were studied using scanning electron microscopy and atomic force microscopy. The surface roughening of the deposit depended on the pressure and nature of ambient gas, as well as on the duration of deposition. The development of surface features was discussed in terms of agglomeration in the plume and the adsorption of species and surface diffusion. The power law dependence of surface roughness on the number of laser shots, observed in oxygen and in argon, was explained by the assumption of non-thermal mobility with adatom -cluster barriers formed due to cluster generation in the plume.

**NANO  $\text{Al}_2\text{O}_3$ -Pb AND  $\text{SiO}_2$ -Pb CERMETS BY SOL-GEL TECHNIQUE AND THE PHASE TRANSFORMATION STUDY OF EMBEDDED Pb PARTICLES**

*P. Bhattacharya and K. Chattopadhyay*

Department of Metallurgy, Indian Institute of Science, Bangalore 560 012, INDIA

Nanosized Pb is dispersed in ultrafine nanograined  $\gamma$   $\text{Al}_2\text{O}_3$  and amorphous  $\text{SiO}_2$  matrices using sol-gel method. Lead nitrate is used as a precursor for Pb. Reduction of the nitrate to Pb has been carried out by flowing high purity  $\text{H}_2$  at different temperatures. Phase identification and particle size determination is done using XRD and TEM. Particle size is observed to increase with higher reduction temperatures. TEM observation exhibit the faceted morphology of Pb particles. Phase transformation of these nanodispersed Pb has been studied using DSC. Although sharp melting peak is observed during heating, no solidification exotherm is obtained. Occurrence of solidification is detected indirectly using melting experiments. Solidification event is simulated and the role of different catalytic nucleation sites in influencing the variation of surface energy to yield the possible broad undetectable solidification has been discussed.

**LOW PRESSURE FLAME DEPOSITION  
OF NANOSTRUCTURED OXIDE FILMS**

*G. Skandan<sup>1</sup>, N. Glumac, Y.-J. Chen and B.H. Kear*

<sup>1</sup> Nanopowder Enterprises Inc., 120 Centennial Ave., Piscataway, NJ 08854, USA  
Rutgers University, College of Engineering, 98 Brett Road,  
Piscataway, NJ 08854-8058, USA

A novel process, called Low Pressure Flame Deposition (LPFD), designed to deposit nanostructured oxide films at high rates, will be described. The process involves pyrolysis of chemical precursors in a flat flame combustor and deposition of an adherent film on suitable substrates. Films with thickness between 0.5 and 10.0  $\mu\text{m}$  are formed at rates in excess of 1  $\mu\text{m}/\text{min}$ . by condensing nanoparticles from the gas phase and allowing the "superheated" particles to sinter on a substrate. Either porous or dense films, with nanoscale features in both cases, are formed by altering the processing parameters such as substrate temperature and flame temperature profile. Processing parameters and structures of  $\text{SiO}_2$ ,  $\text{SnO}_2$  and  $\text{Al}_2\text{O}_3$  coatings will be described.

**POLYMER MATRIX COMPOSITES FILLED WITH NANOPOROUS METAL POWDERS: PREPARATION ELECTRICAL PROPERTIES**

*Hans-Gerd Busmann, Bernd Gunther and Udo Meyer*

Fraunhofer-Institut for Applied Materials Research (IFAM)  
Lesumer Heerstrasse 36, D-28717 Bremen, GERMANY <bu@ifam.fhg.de>

The electrical properties of composite materials of metallic filler particles embedded in polymer matrices strongly depend on the concentration, morphology and degree of agglomeration of the filler particles. Generally, the electrical conductivity or equivalent to this the dielectric properties shift from dielectric to metallic behavior with increasing metal content. Due to percolation and depending on the morphology of the particles, this transition can be highly non-linear with an abrupt increase of the conductivity around the percolation threshold. Properties of the composites regarding their durability normally deteriorate with increasing metal content. Therefore, filler systems with a low percolation threshold are preferred in applications like isotropically conductive adhesives (ICA's) and injection molding feedstocks. Commercially available ICA's for uses in electronics are almost exclusively filled with flakes of high aspect ratios and thresholds of around 25 Vol% of filler material.

Recently, a novel nanoscale metal / polymer composite made by the dispersion of a nanoporous silver powder into a polymer matrix has led to a reduction of the percolation threshold to less than 7 Vol%. This talk addresses the preparation of both the nanoporous filler and the composite material: In a modified inert gas condensation apparatus, the silver is evaporated into a forced helium gas flow to form agglomerated nanoparticles. These agglomerates are separated from the gas down stream by means of a Biter, where they form a nanoporous deposit. This filter is periodically blown off to collect the deposit at the bottom of the vacuum chamber. The final powder is obtained by sieving/classifying the nanoporous deposit and dispersed into polymer matrices by commercial technologies.

Depending on the conditions employed in the individual steps of the preparation of the composite, filler structures of different morphologies can be produced. The influence of the concentration and morphology of the filler as well as thermal treatments of the composites on the electrical conductivity will be discussed.

**ELLIPSOMETRIC STUDIES OF NANOCOMPOSITE CERMETS**

*S. Dligatch and G B Smith*

Applied Physics Department, University of Technology, Sydney, PO Box 123,  
Broadway NSW 2007, AUSTRALIA <G.Smith@uts.edu.au>

A bi-axial metal insulator composite in which the nanoscale metal inclusion is distributed anisotropically has an interesting complex optical response. Independent optical constants (3 pairs of complex refractive indices) are needed to completely describe this optical system. They also give insights into how nano-size particle properties change relative to the bulk, when effective medium theories are used to interpret results. In principle optical characterisation can be done with a combination of spectroscopic ellipsometry and spectrophotometry using various angles of incidence. However, to be assured that the result that is obtained is the one that is physically relevant, we have found that a particular approach is needed in setting up the initial search conditions to find the appropriate local minimum in the least squares minimisation routine.

These issues will be demonstrated in the context of analysis of the thin film optical constants for a silver/Al<sub>2</sub>O<sub>3</sub> composite in which the silver deposits as fine nano-size particulates in reasonably well defined positions in the oxide matrix structure .

**PREPARATION OF Dy AND Mn NANOPARTICLES**

*J.A. Christodoulides, N.B. Shevchenko and G.C. Hadjipanayis*

Department of Physics and Astronomy, University of Delaware,  
Newark, DE 19716, USA

Recent studies on transition metal (Fe, Co, Ni) nanoparticles have shown unique and interesting magnetic properties, which are different than those in bulk. We have extended these studies to rare earth and Mn particles. Strong size effects are expected in the rare earth particles, which show several magnetic transitions at low temperatures and in Mn where a strong ferromagnetic behavior is predicted. The nanometer scale Dy particles have been prepared using a new technique involving a particle gun. By this method particles are first formed from high purity constituent materials in an inert gas atmosphere and then embedded into a matrix by planar magnetron sputtering. Unlike other techniques, our method allows for the synthesis of a wider variety of materials by reducing the problems of miscibility and reactivity between the particles and the matrix material. A transmission electron microscope was used to measure the size and structure of the nanoparticles. The Dy-containing samples consisted of particles with diameters on the order of 10 nm, which were separated by the matrix material. Magnetic hysteresis measurements revealed coercivity higher than in the bulk material. A strong relationship was observed between the particle size and the magnetic ordering temperature through the thermomagnetic data. A description of the preparation technique will be presented along with a correlation of structural and magnetic data.

**SINTERING, STRENGTHENING AND TOUGHENING  
OF NANO-ALUMINA COMPOSITES**

*Guanghai Li and L.D. Zhang*

Institute of Solid State Physics, Chinese Academy of Sciences, Hefei 230031, CHINA

Nano-Al<sub>2</sub>O<sub>3</sub> powders processed by the hydrolysis technique of pure Al sheet after activation were added into conventional large-grain Al<sub>2</sub>O<sub>3</sub> (c-Al<sub>2</sub>O<sub>3</sub>) ceramics. It is found that the nano-Al<sub>2</sub>O<sub>3</sub> addition can increase not only the sinterability of the c-Al<sub>2</sub>O<sub>3</sub> ceramics, in which the ultra-fine particle size of nano-Al<sub>2</sub>O<sub>3</sub> allows it to fill into grain boundaries and the voids between large alumina particles, improving the packing, lowering required sintering temperature, increasing the density and decreasing the grain size of sintered bodies, but the fracture toughness, bending strength and thermal shock resistance as well, and this kind of increase can be obtained only when the grain size of nano-Al<sub>2</sub>O<sub>3</sub> is small enough. Both the fracture toughness and bending strength can increase by 50% with 10% addition. It is interesting that, on the fracture surface of nano-alumina composites under AFM, there still exist some nanoparticles after sintering. The reasons and mechanisms of the strengthening and toughness were discussed.

**NANOPHASE COMPOSITES IN EASY GLASS FORMING SYSTEMS**

*J. Eckert, M. Seidel, L.Q. Xing, I. Börner and B. Weiß*

IFW Dresden, Institut für Metallische Werkstoffe, Postfach 270016,  
D-01171 Dresden, GERMANY <j.eckert@ifw-dresden.de>

The discovery of ultra-high strength, good ductility and excellent wear resistance for nanophase composite materials prepared by devitrification of easy glass forming alloys has stimulated considerable interest in crystallization of metallic glasses as a way of obtaining new materials with very uniform microstructure and interesting properties. Alternatively, such amorphous/nanophase microstructures can also be prepared directly by solid state processing utilizing mechanical alloying techniques with or without subsequent annealing.

This contribution reports on the formation and the properties of mechanically alloyed, rapidly quenched and slowly cooled multicomponent Zr-, Al- and Mg-based glassy alloys containing nanoscale metallic precipitates or oxide particles for mechanical strengthening. Various experimental methods such as x-ray diffraction, thermal analysis, viscosity measurements, scanning and transmission electron microscopy and mechanical testing were applied to investigate the microstructure and the properties of the materials. Partial devitrification of initially fully amorphous samples leads to ultra-fine quasicrystalline or crystalline precipitates with high stability against grain growth. This will be discussed with respect to the thermodynamics and kinetics of nucleation and growth processes in such multicomponent systems. Several of these alloys exhibit a wide supercooled liquid region before crystallization, even in the presence of a large volume fraction of second phase particles. This allows an easy consolidation of powders or shaping of bulk samples due to viscous flow. Room temperature mechanical properties will be presented and potential applications will be critically assessed.

**NANOPARTICLES IN AN AMORPHOUS  $Zr_{55}Al_{10}Cu_{30}Ni_5$ -MATRIX - THE FORMATION OF COMPOSITES BY MECHANICAL ALLOYING**

*A. Kübler, J. Eckert, and L. Schultz*

Institut für Festkörper- und Werkstoffforschung Dresden, Institut für Metallische Werkstoffe, Postfach 27 00 16, D-01171 Dresden, GERMANY  
[<a.kuebler@ifw-dresden.de>](mailto:a.kuebler@ifw-dresden.de)

Bulk amorphous materials exhibit interesting properties such as high processability in the supercooled liquid state, high strength combined with perfect elastic behaviour and high corrosion resistance. Homogeneous dispersion of nanoparticles in an amorphous matrix by mechanical alloying promises to further improve the strength and hardness of the material. The samples were prepared by mechanical alloying of pure elemental powders blended with W, WC and  $SiO_2$  particles. The powders are characterized by x-ray diffraction, wavelength dispersive x-ray analysis, calorimetric measurements and thermal mechanical analysis. We find that amorphous nanoscaled composites can be synthesized by mechanical alloying while maintaining an extended supercooled liquid region before crystallization  $DT_x = T_x - T_g$  ( $T_g$ : glass transition temperature,  $T_x$ : crystallization temperature). The addition of W does not reduce the supercooled liquid region compared to samples without additions and comparable oxygen content. Only for more than 10 at.% W, we find a slight reduction in  $DT_x$  which might be the result of some alloying of tungsten in the amorphous matrix. Similarly, WC additions up to 5 at.% do not affect  $DT_x$ . In contrast, there is no supercooled liquid region for the sample containing 10 at.% WC. The addition of  $SiO_2$  slightly reduces  $DT_x$ . W and WC additions have no significant effect on the viscosity of the material. However, the addition of  $SiO_2$  increases the viscosity remarkably. Consolidation of the mechanically alloyed powders was done in a uniaxial hot press at temperatures above  $T_g$  utilizing the viscous flow in this temperature range. This leads to dense bulk samples.

**ELECTRONIC AND OPTICAL PROPERTIES OF CETINEITES:  
NANOPOROUS SEMICONDUCTORS  
WITH ZEOLITE-LIKE CHANNEL STRUCTURE**

*U. Simon<sup>1</sup> J. Jockel<sup>1</sup> F. Starrost<sup>2</sup> E. E. Krasovskii<sup>2</sup> W. Schattke<sup>2</sup>*

<sup>1</sup> Institut für Anorganische Chemie, Universität GH Essen, Schützenbahn 70,  
D-45127 Essen, GERMANY <u.simon@uni-essen.de>

<sup>2</sup> Institut für Theoretische Physik, Universität Kiel,  
Leibnizstr. 15, D-24118 Kiel, GERMANY

Cetineites are oxoselenoantimonates with zeolite-like channel structure, the synthesis of which was described by Wang and Liebau.<sup>1</sup> In contrast to zeolites and related metal oxides, which are electrical insulators, cetineites have shown to be the first crystalline nanoporous material with a photo-semiconducting host lattice.<sup>2</sup> This made the material attractive for further detailed experimental and theoretical investigations of the electronic structure of this novel class of nanomaterials.

The general composition of cetineites is  $A_6(Sb_{12}O_{18})(SbX_3)_2 \cdot (6-mx-y)H_2Ox(B^{m+}(OH)_m)_m$  with  $A = Na^+, K^+, Rb^+, Sr^{2+}, Ba^{2+}$ ;  $X = S^{2-}, Se^{2-}$  and  $B = Na^+, Sb^{3+}, CO_3^{2-}$  the phases with  $A = Na, K$  and  $X = S, Se$  being discussed in the present work. The preparation of these phases results from hydrothermal reaction<sup>1,2</sup>, from which single crystals with a maximum length of 2 mm and a hexagonal cross section of  $3.1 \times 10^{-2} \text{ mm}^2$  could be obtained. All these phases are photosemiconductors at room temperature and the optical band gaps correspond to the onset energy of photoconduction. The calculation of the electronic structure has been done by means of the LAPW method on an ab-initio basis.<sup>3</sup> The electronic potential was determined self-consistently for the elementary cell of the host structure which consists of 44 atoms. To take into account a lower charge density inside the tubes, an empty sphere was added there. From the potential, the partial and total densities of states, band structure, dielectric function and extinction coefficient were obtained. From the theoretical extinction coefficient two energy values have been derived, which represent the characteristics of each compound, i.e., (i) a fundamental band gap, which is the onset of the extinction coefficient, and (ii) the energy of maximum absorption, which dominates the optical excitation of charge carriers. While the fundamental gap is typically in the range of 0.5-0.8 eV the energy of maximum absorption is in the range of 1.6-2.1 eV. Comparison of the experimentally obtained values from optical absorption, photoconductivity and temperature dependent conductivity measurements and their theoretical counterparts reveals an excellent agreement with respect to the chemical trend.

- [1] X. Wang, Z. Kristallogr. 210, **1995**, 693; F. Liebau, X. Wang, Beih. z. Eur. J. Mineral. 7, **1995**, 152
- [2] U. Simon, F. Schüth, S. Schunk, X. Wang, F. Liebau, Angew. Chem. Intern. Ed. Engl. 36, **1997**, 1121
- [3] F. Starrost, E. Krasovskii, W. Schattke, J. Jockel, U. Simon, X. Wang, F. Liebau, Phys. Rev. Lett. 80(15), **1998**, 3313

**LASER-INDUCED SYNTHESIS OF Al<sub>2</sub>O<sub>3</sub>/CU-NANOPARTICLE MIXTURES**

*J. Naser and H. Ferkel*

Institut für Werkstoffkunde und Werkstofftechnik, Technische Universität Clausthal,  
Agricolastrasse 6, D-38678 Clausthal-Zellerfeld, GERMANY

Nanoscaled powder mixtures of the binary system Al<sub>2</sub>O<sub>3</sub> and Cu are produced by laser ablation from pressed Al<sub>2</sub>O<sub>3</sub> and CuO micro powder mixtures of various compositions with the pulsed radiation of a 1000W Nd:YAG-laser followed by condensation of the induced vapour in argon and hydrogen. The generated nanoparticles are analyzed regarding their grain size, crystalline structure and phase distribution in the powder by X-ray diffraction and transmission electron microscopy. The results reveal that any powder composition can be produced and that the different nanoparticle components are homogeneously distributed in the powder.

**SYNTHESIS OF TiN/Ni NANOCOMPOSITES**

*Wen-Li Tsai<sup>1</sup>, Hong-Ming Lin<sup>1</sup>, Shah-Jye Tzeng<sup>1</sup>, and Y. Hwu<sup>2</sup> and Pee-Yew Lee<sup>3</sup>*

<sup>1</sup> Dept. of Materials Engineering, Tatung Institute of Technology, Taipei, 104, Taiwan  
*<sjtzeng@alpha.cc.ntut.edu.tw>*

<sup>2</sup>Institute of Physics, Academia Sinica, Nankang, Taipei 115, Taiwan

<sup>3</sup>Institute of Materials Eng., National Taiwan Ocean University, Keelung, Taiwan

Gas condensation method is employed to synthesize titanium nitride (TiN) nanocrystalline (NC) under different helium and ammonia partial pressures in this study. By controlling the ammonia partial pressures, TiN is synthesized under the reaction between Ti vapor and ammonia molecules. The particle size distribution and the microstructure of NC TiN are examined by TEM. According to previous experiments, the results show that nano-sized TiN particles have excellent sinterability, but because of its tremendous amount of shrinkage under sintering, the dense sintered TiN bodies are not easy to achieve. To lower the sintering temperature and to enhance the toughness of sintered TiN bodies, nano-sized Ni particles prepared by gas condensation method are introduced to form mixed TiN/Ni nanoparticles. The sinterability of TiN/Ni nanoparticle mixtures and their hardness after sintering are examined. The results indicate that nano-sized TiN/Ni mixtures have excellent sintering activity, and the low-temperature sintering process below 1000 °C for dense TiN/Ni bodies is feasible.

---

**THE SELF-DISPERSING AND NANOSTRUCTURE FORMATION  
PROCESSES IN NON-EQUILIBRIUM DIFFUSION-KINETIC SYSTEMS**

*V.P. Solntsev, B.V. Fenochka, A.A. Semjonov-Kobzar and T.A. Solntseva*

Institute for Materials Science problems, Natl.Acad.Sci. of Ukraine,  
Krzhyzhanovsky St. 3, 252680 Kiev, UKRAINE <semkob@ipms.kiev.ua>

Reaction-diffusion kinetic systems are of special interest for developing self-oscillating process which bring the systems to dynamic steady state peculiar to living matter.

The same behaviour was experimentally found in complex physico-chemical systems on transition metals' base containing components with significantly different thermodynamic properties. In such systems the concentration waves are brought about by originating oscillatory reactions and diffuse convection concurrence.

Concentration waves' interaction may result in homogeneous medium separating into layers (phase change) and formation of cellular structure. Reaction process is located within the cell. So far as reaction volatile component does not dissolve in refractory matrix the process recurs in the smaller volume.

By this means self-dispersing of refractory matrix and component take place and nano-structures are formed. The interaction processes at nanolevel are interlinked and it stimulates mesoscopic and macroscopic behaviour of the composition upon the whole.

On such systems' base there have been worked up the materials able to scatter effectively the concentrated flows of different kinds' energy and capable of self-healing.

**NANOPOROUS POWDERS PRODUCED BY HIGH ENERGY BALL MILLING***Ying Chen*

Department of Engineering, FEIT

Department of Electronic Materials and Engineering, RSPHYSSE  
The Australian National University, Canberra, ACT 0200, AUSTRALIA  
<ying.chen@anu.edu.au>

Nanostructured carbon and boron powders have been prepared by high energy ball milling at room temperature. Interesting phase transformations from graphite to disordered, turbostratic and amorphous structures have been observed during milling processes and the structures were characterized using X-ray diffraction, thermal analysis and transmission electron microscopy. Milling conditions (milling intensity, energy and time) have strong influence on the formation of different phases. Furthermore, the milled carbon and boron powders have nanoporous structures as discovered by both field-emission scanning electron microscopy and the surface area measurement. It has been found that the nanoporous structures are related to the metastable phases induced by high energy ball milling. The powders with nanoporous structures have significantly high chemical reactivity.

**NANOCOMPOSITES PRODUCED BY MECHANICAL ALLOYING  
OF THE  $Al_{50}Fe_{25}Ti_{25}$  POWDERS MIXTURE.**

*M. Krasnowski, V.I. Fadeeva and H. Matyja*

Department of Materials Science and Engineering, Warsaw University of Technology,  
Narbutta 85, 02-524 Warsaw, POLAND <makr@inmat.pw.edu.pl>

Nanocomposite powders were produced by high energy ball milling of the  $Al_{50}Fe_{25}Ti_{25}$  (at%) powder mixture added with ethanol ( $C_2H_5OH$ ) and ammonium carbonate ( $(NH_4)_2CO_3$ ). The phase transformations occurring in the material during the process were monitored by X-ray diffractometry; the thermal stability of the powders after various milling times was examined using differential scanning calorimetry and the structures of the milled samples by transmission electron microscopy. The nanocrystalline composite powder, consisting of titanium carbide distributed in the Fe(Al) matrix was obtained as the final product of the milling with participation of ethanol whereas the process performed with an addition of ammonium carbonate led to the formation of TiN-Fe(Al) nanocomposite.

**PREPARATION AND CHATACTERISATION OF CdS AND ZnS NANOSIZED PARTICLES OBTAINED BY THE INERT GAS EVAPORATION METHOD**

*J.C. Sánchez-López, E.P. Reddy, T.C. Rojas, M.J. Sayagués and A. Fernández*

Instituto de Ciencia de Materiales de Sevilla, Avda. Americo Vespucio s/n,  
41092 Sevilla, SPAIN <asuncion@cica.es>

Research focused upon semiconductor nanostructured materials has become wide spread over the last years. In particular ZnS, CdS and also telluride compounds are some of the materials more widely investigated for the fabrication of optoelectronic devices. In addition zinc and cadmium sulphide have been investigated as photocatalysts and for solar cell devices. Although the preparation of nanosized particles of ZnS and CdS has been widely studied by precipitation and stabilisation in micelles, to our knowledge there is no a previous study of the application of the inert gas evaporation method to the preparation of sulphide ultrafine powders. In the present communication we describe how this method leads in the case of ZnS and CdS to the formation of ultrafine powders formed by a very homogeneous distribution of spherical nanoparticles.

Evaporation in 1 Torr He of commercial zinc sulphide platelets at 1373 K produces powders with a mean particle diameter of 8 nm. In the case of cadmium sulphide the evaporation at 1073 K in 1 Torr He produces a mean particle size of 15 nm. The materials are constituted in both cases by spherical particles most of them being a single crystallite as stated by High Resolution TEM images. Several preparations have been carried out by changing the inert gas pressure.

The materials have been characterised by X-ray diffraction (XRD) and Transmission electron Microscopy (TEM). Special attention has been paid to the presence of cubic or hexagonal phases and also to the UV-vis absorption characteristics of the samples. Relative band gap values have also been determined for the different materials.

**ON MICROSTRUCTURE, MAGNETIC AND ELECTRIC PROPERTIES  
OF  $(\text{NiFe})_x(\text{SiO}_2)_{1-x}$  NANOCOMPOSITE FILMS**

*Horia Chiriac, Florin Rusu, Mihai Lozovan and Maria Urse*

National Institute of R&D for Technical Physics,  
47 Mangeron Blvd., 6600 Iasi 3, Romania <lozovan@uaic.ro>

Granular metal films are composite materials consisting of a thin film matrix embedded with nanometer-size metal particles. This class of materials with ultra fine microstructure displays unusual transport and magnetic properties for values of the metal content in film near a critical value  $x_c$ , usually called "percolation threshold". Their electrical and magnetic properties are also strongly dependent on composition and microstructure. This fact allows the optimisation of the characteristics required for different kind of sensors based on cermet films [1-3].

This paper presents some results concerning the thermoelectric properties and electrical conductivity of  $(\text{NiFe})_x(\text{SiO}_2)_{1-x}$  granular thin films, where  $x$  is the metal percentage of metal in films. These properties were investigated for  $x$  values between 40% and 60% and they reflect the metal-insulator transition at about 50% of metal content. The films were prepared by r.f. sputtering in Ar atmosphere ( $p \sim 1\text{Pa}$ ), using composed targets. Their microstructure and composition have been investigated by X-ray diffractometry and transmission electron microscopy (TEM) respectively. The samples were thermally treated at  $400^\circ\text{C}$ , in order to stabilise their electrical properties. We measured the resistivity of the samples, before and after the thermal treatment, using the standard four-point probes method. For thermoelectric power measurements, we realised thin film thermocouples ( $\text{Pt}/(\text{NiFe})_x(\text{SiO}_2)_{1-x}$ ), on alumina substrates. We also made Hall and saturation magnetisation measurements which confirm the percolation threshold at about 50 % of metal content in films. The transport and magnetic behaviour of the metallic and non-metallic components highly disordered systems shows specific dependencies on the microstructure length scale. The physical properties of such films may be tailored for specific applications by changing the preparing conditions. The  $(\text{NiFe})_x(\text{SiO}_2)_{1-x}$  thin films can be suitable for temperature and /or magnetic field miniature sensors.

1. P.Sheng, J.Klafter, Phys. Rev. B, 27(1983), 2583-2586
2. P.Sheng, Philosophical Magazine B, 65(1992), 357-384
3. A.Heinrich, J.Schumann, H.Vinzelberg, U.Brustel, C.Gladun, Thin Solid Films, 223(1993), 311-319.

**NANOCRYSTALS AS STOICHIOMETRIC REAGENTS WITH UNIQUE SURFACE CHEMISTRY: NEW ADSORBENTS FOR AIR PURIFICATION**

*Kenneth J. Klabunde, Abbas Khaleel and Weifeng Li*

Department of Chemistry, Kansas State University,  
Manhattan, KS 66506, USA <KENJK@KSU.EDU>

In our laboratory, using an aerogel procedure, we have synthesized nanoscale particles of metal oxides of magnesium, calcium, zinc, zirconium and other metals. These materials have exhibited a remarkable capacity to adsorb, and in some cases react with, a number of organic and inorganic molecules that present environmental hazards. Due to the unusual morphological features, the nanocrystals exhibit intrinsically higher surface reactivities per unit surface area than normal sized crystals. This enhanced surface reactivity, coupled with very large surface areas (e.g. nanocrystals MgO surface area = 400 m<sup>2</sup>/g), adsorption capacities often are much greater than for the best commercially available activated carbon adsorbents. Furthermore, the nanocrystals can be compressed at moderate pressures to yield pellets that retain these high surface areas due to their porous structure.

A series of experiments with the following adsorbates in the presence of air and the absence of air have been carried out: acetaldehyde, methanol, acetonitrile, acetone, methylethyl ketone, benzene, toluene, ammonia, diethylamine, propionaldehyde, and sulfur dioxide. Comparisons with activated carbon have shown that nanocrystalline MgO is superior in capacity and usually rate of absorption. Other nanocrystals have also been studied including CaO and Fe<sub>2</sub>O<sub>3</sub> coated MgO.

Polar molecules adsorb very strongly to MgO nanocrystals, and in the case of acetaldehyde an exothermic process takes place that yields oligomerised molecules on the surface. Fourier transform infra red studies have revealed molecular structure of adsorbates at various temperatures, and molecular details of several adsorption processes will be discussed.

**TRANSITION METAL DICHALCOGENIDE/POLYMER**

*Yang, D., Westreich, P., Frindt, R.F.*

Simon Fraser, Dept. of Physics, B.C. - V5A 1S6, Burnaby, CANADA

Single molecular layers of transition metal dichalcogenides (TMDs) such as MoS<sub>2</sub>, MoSe<sub>2</sub> and WS<sub>2</sub>, have been formed in suspension in water by lithium intercalation of crystalline powders and then exfoliation in water. The two-dimensionality of such systems is readily identified using powder X-ray diffraction, where the strong asymmetric shape of the (hk0) peaks and the absence of (00l) peaks and mixed (hkl) peaks are observed. Water-soluble polymers, such as poly(ethylene oxide), poly(ethylene glycol) and poly(vinylpyrrolidone), can be encapsulated in TMD layers to form TMD/polymer lamellar nanocomposites. TMD/polymer nanocomposites are turbostratically restocked with the TMD layers parallel to each other with an expanded interlayer spacing due to the polymer insertion. The expansion of interlayer spacing varies from 8 to 22 and can be remarkably uniform. Highly oriented TMD/polymer films can be formed on glass substrates. Possible applications of TMD/polymer nanocomposites are discussed.

**THE CHARACTERISTICS OF NANOSIZED TiO<sub>2</sub> POWDER  
SYNTHESIZED BY CHEMICAL VAPOR CONDENSATION**

*S.Y. Kim, J.H. Yu and J.S. Lee*

Department of Metallurgy and Materials Science, Hanyang University  
Ansan 425-791, KOREA <jslee@email.hanyang.ac.kr>

The characteristics of nanoscale TiO<sub>2</sub> powders synthesised by chemical vapour condensation method using metalorganic precursor were investigated under various oxygen flow rate conditions. TiO<sub>2</sub> powders for study were sampled from the air-cooling zone in the tubular furnace and the powder size, size distribution, crystalline size, degree of agglomeration, and the phase formation of the powders were investigated by TEM, LPA, BET, and XRD. With increasing oxygen flow rate the powder- and crystalline size decreased to less than 10 nm and the size distribution became uniform, followed by decrease in degree of agglomeration. Phase identification revealed that the amount of rutile phase also decreased with increasing oxygen flow rate. Based on the results the effect of oxygen flow rate on the kinetics of chemical vapour condensation process relating to the nucleation/growth of nanosized powder was discussed in terms of supersaturation, collision rate and residence time.

**MECHANO-CHEMICAL SYNTHESIS OF  
NANOSIZED STAINLESS STEEL POWDER***J.G. Nam and J.S. Lee*

Department of Metallurgy and Materials Science, Hanyang University  
Ansan 425-791, KOREA <jslee@email.hanyang.ac.kr>

The present investigation has attempted to fabricate nanosized stainless steel powder of Fe-18Cr-8Ni (wt%) by mechano-chemical synthesis. The synthesis process was conducted by hydrogen reduction of high energy ball milled mixture of  $\text{Fe}_2\text{O}_3$ -NiO- $\text{Cr}(\text{NO}_3)_3 \cdot 9\text{H}_2\text{O}$ . In-situ alloying of Ni-Fe-Cr nanophase simultaneously occurring during reduction process is presumably responsible for the formation of nanophase stainless steel powders. The powder characteristics were examined by laser particle size analysis, BET, XRD and SEM observation. The kinetic phenomena in association with the oxide reduction and the alloying process were investigated by thermogravimetry, hygrometry and X-ray diffractometry, and discussed in relation to powder characteristics.

**DENSIFICATION AND MICROSTRUCTURAL DEVELOPMENT OF  
NANOCRYSTALLINE  $\gamma$ -Ni-Fe POWDERS**

*P. Knorr, J.G. Nam and J.S. Lee*

Department of Metallurgy and Materials Science, Hanyang University  
Ansan 425-791, KOREA <jslee@email.hanyang.ac.kr>

Nanocrystalline  $\gamma$ -Ni-Fe powders were synthesised by subsequent ball milling and hydrogen reduction of metal oxide mixtures. The sintering behaviour of the  $\gamma$ -Ni-Fe powders was investigated by laser-photo-dilatometry. Experimentally observed shrinkage rates exhibit two densification maxima at the onset and the end of densification. The sinterability of nanocrystalline  $\gamma$ -Ni-Fe powders was found to depend crucially on the state of agglomeration. The results are discussed on the basis of the microstructural evolution during densification, which was followed by optical microscopy, BET specific surface area measurements and XRD.

**STRUCTURE, PHASE COMPOSITION AND MAGNETIC  
CHARACTERISTICS OF THE NANOCRYSTALLINE IRON POWDERS  
OBTAINED BY MECHANICAL MILLING IN HEPTANE**

*S.F. Lomayeva, E.P. Yelsukov, G.N. Konygin, G.A. Dorofeev, V.I. Povstugar,  
S.S. Mikhailova and A.H. Kadikova*

Physical -Technical Institute UrB RAS, 132 Kirov str, 426001 Izhevsk, RUSSIA  
[<povst@uds.fti.udmurtia.su>](mailto:<povst@uds.fti.udmurtia.su>)

X-ray diffraction, Mössbauer spectroscopy, Auger spectroscopy and magnetic measurements have been used to investigate the particle sizes, structural state, phase composition and magnetic behaviour of powders, obtained by milling of carbonyl iron in a planetary ball mill in liquid hydrocarbon environment (heptane).

It has been stated that the increase of milling time (from 1 h to 47 h) results in the decrease of particle sizes from 300  $\mu\text{m}$  to 5-10  $\mu\text{m}$ , and grain sizes decrease from 50 nm to 4 nm. The surface layers ( $\approx$ 40 nm) of the particles formed in all milling stages are, as the Auger-spectroscopy data show, enriched in carbon (up to 40%).

The X-ray pattern and Mössbauer spectrum demonstrate the formation of a metastable Fe-C - phase with the Curie point of 600-620 K. The quantity of this phase grows with milling time. On reaching 800 K the phase turns into iron carbide,  $\text{Fe}_3\text{C}$ . Based on the Mössbauer spectrum, the bulk C content at  $t_{\text{mil}} = 47$  h was found to be 6 -7%. Saturation of particles with carbon in process of milling results in variation of magnetic characteristics of the iron powders formed. Thus, specific magnetisation of saturation decreases from  $220 \text{ A}\cdot\text{m}^2/\text{kg}$  to  $207 \text{ A}\cdot\text{m}^2/\text{kg}$  (47 h), coercivity rises from 6 Oe to 25 Oe (1 h milling) with the following drop to 12 Oe (47 h milling) .

**THE TECHNIQUE FOR EVALUATING THE CORROSION RESISTANCE OF  
IRON-BASED NANODISPERSIVE MATERIALS**

*M.A. Pletnev, A.M. Dorfman, V.I. Povstugar, and O.M. Mikhailik*

Physical -Technical Institute UrB RAS, 132 Kirov str,  
426001 Izhevsk, RUSSIA <povst@uds.fti.udmurtia.su>

The wide use of nanodispersive materials in many practical applications (magnetic carriers, catalysts, sorbents, etc.) often requires estimation of their corrosion resistance. To estimate the corrosion losses for the massive metal samples in practice there is a popular gravimetric technique requiring cleansing of the sample surface from the corrosion products by acid etching or by mechanical or electrochemical treatment. Due to a number of reasons this method is not valid for the nanodispersed metals with particle sizes 1-10<sup>2</sup> nm. Namely, for a highly developed sample surface the dissolution of the unoxidized iron even for low depth may result in a gross error in corrosion resistance estimation. Furthermore, it is technically difficult or even impossible to separate and remove the corrosion products from the finely dispersed particles of the uncorroded iron.

To evaluate the corrosion resistance of iron-based nanodispersive materials (powders, wires, and fibers), including those with modified coatings, here we suggest a method that allows determining the quantity of the uncorroded iron.

The procedure consists in measuring the quantity of the hydrogen evolved in process of the dissolution of the control sample ( $V_c$ ) and the sample exposed to the selected corrosive environment for the predetermined time  $\tau$  (V). The corrosive losses (C) are calculated according to the formula  $C = (1 - V_m/V_c) m \cdot 100 / \tau$ , where  $m_c$  - the mass of the control sample and  $m$  - the mass of the sample to be exposed in corrosive environment.

The corrosion resistance of finely dispersed powders (obtained by high-temperature reduction of  $\alpha$ -FeOOH in hydrogen flow) after 2 hr exposure at 37°C in 0.85% solution of NaCl was measured. The value of C calculated according to the above method was shown to be 7.35% while a traditional gravimetric analysis demonstrated the overestimated value of C equal to 62.1%. Similar results concerning C were obtained for finely dispersed powders of iron produced by electrochemical reduction (0% and 76% for a 6 hr test).

**PHOTOELECTROCHEMICAL PROPERTIES OF NANOSTRUCTURED  
ZnO ELECTRODES WITH DIFFERENT MORPHOLOGIES.**

*Karin Keis, Lionel Vayssières, Håkan Rensmo, Sten-Eric Lindquist and  
Anders Hagfeldt.*

Department of Physical Chemistry, Uppsala University.Box 532,  
S-75121 Uppsala, SWEDEN <hagfeldt@fki.uu.se>

Nanostructured ZnO electrodes with varied particle size and morphologies have been fabricated. By producing the ZnO films from different colloidal solutions we are trying to understand the relation between the morphology and photoelectrochemical properties. The experiments are performed with bare ZnO electrodes in the UV region to study the electron transport properties of these films. Using a ruthenium-dye as a sensitizer, monochromatic photon to current conversion efficiencies were measured in visible region. The high efficiencies obtained show the possibility to use ZnO as the nanostructured material in efficient photoconverting applications. The results also indicate that the morphology of a nanostructured electrode (size and shape of colloidal particles, porosity, etc.) plays an essential role in the photoelectrochemical characteristics of these films. Controlling and varying the morphology will thus be of great importance in order to optimise devices and for a fundamental understanding of the photoelectrochemical properties of nanostructured electrodes.

**NANO-SIZED LAYERED COMPOSITE OF ALUMINIUM TRI-HYDROGEN BIS (ORTHOPHOSPHATES) AND ORGANIC COMPOUNDS**

*Kiyoko Sakamoto and Yoshiaki Tsunawakit*

Osaka Sangyo University, 3-1-1 Nakagaito, Daito-shi, Osaka 574, JAPAN  
<kasei@las.osaka-sandai.ac.jp>

The novel crystalline aluminum orthophosphate such as molecular sieves denoted AlPO-n and VPI-5 were well studied recently. These molecular sieves, which have pore and channels, have been widely used for adsorbent and catalyst. Aluminium tri-Hydrogen Bis (orthophosphates);  $\text{AlH}_3(\text{PO}_4)_2(\text{JH}_2\text{O})$  is known to possess layered structure, however, it is difficult to prepare a pure single phases of  $\text{AlH}_3(\text{PO}_4)_2(\text{JH}_2\text{O})$ . Recently, we found the preparation method of pure  $\text{AlH}_3(\text{PO}_4)_2(\text{JH}_2\text{O})$  in solvothermal reaction. Aluminium tri-hydrogen bis(orthophosphates)  $\text{AlH}_3(\text{PO}_4)_2(\text{JH}_2\text{O})$  is a potent precursor for functional nano-composite because of layered structure and acidic protons.

In this work, we examined the inclusion property of  $\text{AlH}_3(\text{PO}_4)_2(\text{JH}_2\text{O})$  with organic compounds. Nano-sized layered organic-inorganic hybrid material was confirmed by XRD, and TEM. Further transformation of the layered nano-composite to nano porous material in solvothermal reaction were performed. We present the properties and the detail of the transformation process of the nano-structural organic-inorganic hybrid material.

**STRUCTURAL AND MAGNETIC INVESTIGATION OF  
MECHANICALLY ALLOYED  $\text{Fe}_{70}\text{Co}_{3.5}\text{Cu}_1\text{Nb}_3\text{B}_9\text{Si}_{13.5}$  POWDERS**

*H. Chiriac, A.E. Moga, M. Urse and F. Necula*

National Institute of Research & Development for Technical Physics  
47 Mangeron Blvd. 6600 Iasi 3, ROMANIA <felicia@phys-iasi.ro>

The synthesis of metastable phases by ball milling has been studied intensively in the last several years since it can be used as a non-equilibrium processing tool [1].

Nanocrystalline iron alloys have been of great interest due to their excellent soft magnetic properties. In this work we present the experimental results obtained on the preparation of  $\text{Fe}_{70}\text{Co}_{3.5}\text{Cu}_1\text{Nb}_3\text{B}_9\text{Si}_{13.5}$  powders by mechanical alloying and their structural and magnetic properties. The obtained products were analyzed by X-ray diffraction and differential thermal analysis and magnetically tested in as-milling state and after annealing at different temperatures. The initially sharp diffraction lines corresponding to unmilled  $\text{Fe}_{70}\text{Co}_{3.5}\text{Cu}_1\text{Nb}_3\text{B}_9\text{Si}_{13.5}$  powders are considerably broadened after ball milling due to refinement of the crystal size and increase of the internal strain. From X-ray diffraction patterns it follows that the powders with the above mentioned composition obtained after 250 hours of milling are nanocrystalline, with the final alloy crystallite size of about 12.3 nm. After a prolonged milling of 350 hours, an increase of the crystallite size up to 32 nm can be observed due to recovery and crystallization.

An improvement in magnetic properties of mechanically alloyed powders (coercivity and saturation magnetization) occurs during heat treatments at temperatures between 200 and 300°C, for 10-90 minutes, because of the grain growth and strain relaxation.

A comparison between the magnetic properties of the  $\text{Fe}_{70}\text{Co}_{3.5}\text{Cu}_1\text{Nb}_3\text{B}_9\text{Si}_{13.5}$  and  $\text{Fe}_{73.5}\text{Cu}_1\text{Nb}_3\text{B}_9\text{Si}_{13.5}$  (FINEMET) mechanically alloyed powders it is also reported.

1. R.W. Siegel, *Processing and Properties of Nanocrystalline Materials*, edited by C. Suryanarayana, J. Singh and F.H. Froes, (1996), 3-10

**ON RATE-CONTROLLED SINTERING OF YTTRIA- AND  
LANTHANA-STABILIZED ZIRCONIA NANO-POWDERS**

*A.V. Ragulya, E.R. Andrievskaya and V.V. Skorokhod*

Frantzevich Institute for Problems of Materials Science NAS of Ukraine,  
Krzhizhanovsky Str. 3, 252142 Kiev, UKRAINE <ragulya@ipms.kiev.ua>

Rate-controlled sintering, the optimal sintering mode, is directed to homogenization and achievement the nano-grained structure in fully dense sintered materials. We are going to present our results on synthesis of binary-doped nanocrystalline zirconia powders and their sintering under rate-controlled conditions. The additives of the yttria, are known, affect some orders increase the high-temperature ion conductivity compared to other dopants. In ternary alloys based on zirconia it is shown to be possible the retaining the nano-grained structure of material in which grains of pyrochlore phase which strengthen the matrix, and prevent grain growth.

**FORMATION OF NICKEL AND ZIRCONIA NANOCOMPOSITES  
BY THE COPRECIPITATION METHOD**

*Jadran Macek and Marjan Marinsek*

University of Ljubljana, Faculty of Chemistry and Chemical Technology,  
1000 Ljubljana, Askerceva 5, SLOVENIA <jadran.macek@uni-lj.si>

Nickel/yttria-stabilised zirconia (Ni/YSZ) cermets are commonly used as the anode materials in the solid oxide fuel cells (SOFC). The reactions on the electrode are complex and the electrochemical performance of the anode is affected predominantly by the anode microstructural and morphological properties, which are strongly dependent on the preparation process. The preparation method for anode cermets should be oriented toward developing active contact area between electrocatalyst (nickel particles) and ionic conductor (YSZ framework), good porosity and activity.

Gel-coprecipitation is one of the possible wet chemistry preparation procedures and it is an attractive process for the preparation of composite materials with a high degree of homogeneity. Precursor solution was a solution of nickel, zirconium and yttrium chlorides. The coprecipitation was started by lowering the pH of the solution by the introduction of gaseous ammonia into it and a mixture of hydrated oxides and hydroxides was obtained that were subsequently dried, calcined and thermally treated.

Gel-coprecipitation from solution has one major benefit over many other preparation techniques for composite materials because it enables mixing of the precursors already in the starting solution theoretically on the molecular level. Although, the area of the dominance of one or the other phase in the composite during further thermal treatment of the mixed gel-precipitates rises, very fine dispersions of nickel particles in YSZ matrix can be preserved to a high degree. The one phase dominance after calcination at 950°C and reduction of nickel oxide to nickel at 1000°C is no larger than 50-100 nm. Thus, gel-coprecipitation method is a promising method for preparation of sub-micro Ni/YSZ dispersions.

**STRUCTURAL CHARACTERISTICS OF COMPOSITES  
BASED ON SILICA AEROGELS AND CARBON**

*T.A. Gorodetskaya, A.F. Danilyuk, V.L. Kuznetsov, A.Iu. Derevyankin,  
V.B. Fenelonov, V.V. Chesnokov and V.I. Zaikovskii*

Boreskov Institute of Catalysis, pr. Akademika Lavrentieva 5,  
Novosibirsk 630090, RUSSIA < sandra@catalysis.nsk.su>

Aerogels are three-dimensional open networks, consisting of nanodimensional oxide particles, which hold promise in designing the novel materials. In particular, silica based aerogels exhibit a number of unique structural, thermal and optical properties, and are widely used as the Cherenkov's detectors, insulators, precursors for monolithic glasses, catalysts, etc. [1].

We have studied the conditions of formation and the structure of two types of porous nanocomposites based on the silica aerogels and carbon.

In the first case, we have prepared aerogel-carbon composites where carbon was supported from the gas phase via thermal divinyl decomposition at 750-800°C on the preliminary formed silica aerogel. Aerogel was prepared from tetraethoxysilane (TEOS) by the sol-gel method associated with the high temperature supercritical drying procedure. Such silica aerogel has the specific surface above 1000 m<sup>2</sup>/g, average particle sizes 3-6 nm, pore volume up to 28 cm<sup>3</sup>/g, and volume density ρ = 0.025-0.06 cm<sup>3</sup>/g.

In the second case, silica-carbon composites were synthesized using the filamentary carbon with filament diameter equal to 50 nm prepared via hydrocarbon catalytic decomposition [2]. Filamentary carbon as a powder was added to the TEOS sol just before alcogel formation. The final composite was obtained via the supercritical drying.

A complex of physical methods (the low temperature sorption of argon and nitrogen, TEM, FTIR, SAXS and the differential-thermal analysis) was used to study the surface state and analyze textures of nanocomposites regarding their formation conditions.

The perspectives to use the nanocomposites are discussed.

1. Materials of the 5th Intern. Symp. on Aerogels, September 8-10, 1997, Montpellier-France
2. V.V.Chesnokov , V.I.Zaikovskii, R.A.Buyanov, V.V.Molchanov, L.M.Plyasova Kinet.Katal. 35, 146-151 (1994).

**EVOLUTION OF NANOCRYSTALLINE QUASICRYSTALS  
FROM BULK Zr-Cu-Ni-Al-Ti AMORPHOUS ALLOY AND  
THE MECHANICAL PROPERTY OF THE ALLOY**

*L.Q. Xing, J. Eckert and L. Schultz*

IFW Dresden, Institut für Metallische werkstoffe, Postfach 270016,  
D-01171 Dresden, GERMANY <L.Xing@ifw-dresden.de>

The  $Zr_{57}Cu_{20}Al_{10}Ni_8Ti_5$  alloy was solidified into an amorphous phase upon casting at low cooling rates. The bulk amorphous alloy was crystallized via precipitation of a nanocrystalline icosahedral quasicrystalline phase in the first crystallization step, leading to a composite microstructure of nanocrystalline quasicrystals of 2-10 nm embedded in an amorphous matrix. The nanocrystalline precipitates exhibit a high stability against grain growth during annealing in the supercooled liquid region. The fine precipitates increase the yield stress and fracture stress of the alloy without decreasing the ductility of the alloy significantly when the volume fraction of the precipitates is within about 50%. Quasicrystals have many interesting properties, but bulk quasicrystals produced by solidification are very brittle. Evolution of quasicrystalline phase from bulk amorphous alloys provides a way to produce composite quasicrystalline alloys of high strength and good ductility.

**SYNTHESIS AND MECHANICAL PROPERTIES  
OF TiO<sub>2</sub>-EPOXY NANOCOMPOSITES**

*Chek Beng Ng, Richard W. Siegel and Linda S. Schadler*

Rensselaer Polytechnic Institute, Troy, NY 12180, USA <ngc@rpi.edu>

New developments in the synthesis of nanometer scale TiO<sub>2</sub> particles (30 - 40 nm diameter) prompted exciting possibilities of incorporating these particles in a polymer composite system. Homogeneously dispersed TiO<sub>2</sub>-epoxy nanocomposites were prepared by an ultrasonication technique. This technique eliminated the need for solvent incorporation without sacrificing the ease of processability. Electron microscopy showed that the particles are uniformly dispersed. Preliminary tests, such as the tensile test, weight and volume changes, and the scratch test, showed significant improvement in the properties of the nanocomposites over pure epoxy. For example, the tensile modulus of the nanocomposites were higher than the theoretically predicted values. The relationship between structure and properties will be discussed. The relatively easy processing technique combined with the enhanced properties of the nanocomposites make them a promising material for commercial applications.

### MECHANISMS OF CONDUCTIVITY IN METAL-POLYMER NANOCOMPOSITES

*L.I. Trakhtenberg, G.N. Gerasimov, E.I. Grigor`ev, A.E. Grigor`ev, P.S. Vorontsov and  
S.A. Zavjalov*

Karpov Institute of Physical Chemistry, Vorontsovo Pole 10,  
103064 Moscow RUSSIA <trakh@cc.nifhi.ac.ru>

This contribution is aimed at studying the dark and photoconductivity of poly-p-xylylene (PPX) films containing metal nanoparticles. The films were produced by co-condensation of p-xylylene monomer and metal vapors at 77 K followed by thermal solid-state polymerization of obtained co-condensate. P-xylylene monomers were prepared by pyrolysis of corresponding p-cyclophanes. Pb, Ag and Pd were chosen as metals. X-ray measurements showed such procedure allows to stabilize in PPX metal particles of size 3-10 nm depending on metal content ( $X_m$ ). In the investigated systems at  $X_m$  less than 5 vol%, metal particles do not practically participate in conductivity which is determined by the charge carrier transfer across a polymer matrix. At  $X_m$  more than 10 vol%, the infinite metal nanoparticle cluster resulted in percolation threshold to metallic conductivity. In both cases the ohmic law is obeyed. The characteristic features of the stabilized metal nanoparticle system is the non-linear voltage - current relationship in the intermediate range from 5 to 10 vol%. In this range the logarithm of current is proportional to square root of voltage; that is the conductivity is governed by tunnel charge transfer processes between metal nanoparticles in polymer media. The activation energy of the tunnel conductivity is  $10^{-1}$ - $10^{-2}$  eV.

On air Pb-nanoparticles in PPX-film oxidizes to semiconductor PbO-nanoparticles. The resulting PPX-PbO composite films are characterized by high photosensitivity: the photo-to-dark current ratio  $I_{ph}/I_d$  reaches  $10^3$ - $10^5$ . In the wave length(L) range 250-350 nm  $I_{ph}$  remains constant but sharply decreases by further increase of L. At  $L > 400$  nm  $I_{ph}$  reduces to zero; the critical value of L corresponds to the lower edge of the electronic absorption in obtained PbO-nanoparticles. PPX-films containing nanoparticles of PbS were also prepared. These films showed high photosensitivity ( $I_{ph}/I_d$  reaches  $10^3$ - $10^4$ ) at  $L > 600$  nm because of the low width of the forbidden energy band (F) in PbS-particles. The voltage dependence of  $I_{ph}$  is characteristic for tunnel current. Therefore, the photoconductivity of obtained nanocomposites results from the electronic excitation of semiconductor nanoparticles followed by electron tunnel transfer between particles. Evidently, in this case the barrier of tunnel transfer decreases. The diminution of particle size leads to the increase of F, but at the same time, causes the increase of the tunnel transfer probability at fixed value of  $X_m$ .

The results of this work show the tunnel processes play the decisive role in the conductivity of metal containing nanocomposites and strongly influence the percolation transition in these systems.

**MICROSTRUCTURAL CHANGES OF MECHANICALLY ALLOYED  
W-Cu COMPOSITE POWDERS DURING SOLID-STATE SINTERING**

*Jin-Chun Kim, Sung-Soo Ryu and In-Hyung Moon*

Department of Materials Engineering, Hanyang University,  
Seoul 133-791, KOREA <moon215@hyunp1.hanyang.ac.kr>

W and Cu system are insoluble in each other, so its composite has been produced by the conventional liquid-phase sintering or Cu-infiltration process. These processes have some limitation on homogeneity of W-grains in Cu-matrix, and the high sintering temperature above 1350°C are required for full densification. However, it has been found recently that the full densification of nanocrystalline W-Cu composite powders was attainable, even at the sintering temperature below 1100°C. The densification of nanostructured W-Cu composite powders prepared by mechanical alloying (MA) was enhanced by the double rearrangement process and nanosintering phenomenon of the MA powders. In the present study, the such enhanced densification process of MA W-Cu composite powders was analyzed and discussed on the basis of the nanostructural changes of the composite powders during solid-state sintering.

Mechanical alloying of elemental W and Cu powders was performed by the high-energy ball milling. The microstructure changes of as-milled W-Cu composite powders were investigated by the transmission electron microscopy and X-ray diffractometer after annealing treatment from 200 to 900°C. The thermal properties of MA W-Cu powders were analyzed by differential scanning calorimeter. Microstructure of some sintered part was observed by field-emission scanning electron microscopy.

The mean particle size of MA W-Cu powders was 3~4 μm, and its grain size was 20~30 nm. The recovery and recrystallization of W and Cu phase of MA powders occurred at 200 and 700°C respectively. The shape of nanosized W-crystalline was changed from irregular to round shape by annealing treatment, and significant W-grain growth took place over 700°C. The Cu-phase in the MA powders was found to act like liquid melt near 900°C. The enhanced densification of MA W-Cu composite powders at sintering temperature below Cu melting point (1083°C) should be attributable to the presence of liquid-like Cu phase.

**IMPEDANCE SPECTROSCOPY OF NANO-PHASE AgI AND  
AgI-Al<sub>2</sub>O<sub>3</sub> NANO-COMPOSITES**

*S.N. Potty<sup>1</sup> and M.Abdul Khadar<sup>2</sup>*

<sup>1</sup> School of Pure and Applied Physics, Mahatma Gandhi University,  
Priyadarsini Hills-P.O, Kottayam-686 560, Kerala, INDIA

<sup>2</sup> Department of Physics,University of Kerala, Kariavattom-P.O,  
Thiruvananthapuram 695 581 Kerala, INDIA <dlcampus@md 2.vsnl.net.in>

The properties of nano-phase materials have been a subject of current interest. Also of importance are nano-composites possessing several key properties. The electrical properties of these materials are observed to be conspicuously different from those of the bulk phase. A few reports on the effects of finite size on the electrical properties of ionic conductors have appeared. The present work was undertaken to investigate in detail the electrical properties of nano-phase AgI and AgI-Al<sub>2</sub>O<sub>3</sub> nano-composites. Nano-particles of AgI and Al<sub>2</sub>O<sub>3</sub> were prepared by chemical methods, and their sizes were characterised by X-ray diffraction. Pellets of AgI and AgI mixed with different concentrations of Al<sub>2</sub>O<sub>3</sub> were used for measurements. The impedance spectra of the samples were studied using HIOKI Hitester over a frequency range 40 Hz to 5 MHz and at different temperatures covering the stability range of beta phase of AgI and well beyond the beta to alpha transition temperature. The variations of the electrical properties with temperature and frequency were studied in detail.

**STUDY OF INTERACTION OF SURFACE ATOMS IN PORES AND  
SOME DIELECTRICS EMBEDDED IN POROUS GLASSES**

*A.E. Aliev and I.N. Kholmanov.*

Heat Physics Department, Uzbek Academy of Sciences  
Katartal str. 28, 700135 Tashkent, UZBEKISTAN <holisk@saturn.silk.org>

This paper will present results of dielectric constant measurements on some dielectrics embedded in porous borosilicate glass.

The porous matrix was made from a phase-separated soda borosilicate glass with pore structure produced by acid leaching. The average pore size is 4 nm and a volume fraction of pores is about 22% of the whole volume. According to our experimental results, the dielectric constant of pure porous glass equals 4.5, but when saturated by water it becomes temperature dependent. Moreover, an anomalous increase of  $\epsilon(T)$  has been observed within some narrow temperature range which can be explained by taking into account the interaction between water molecules embedded within the porous glass and the surface atoms of the pores. In another experiment, we have measured the dielectric constant for NaCl embedded in porous glass when a pressure gradient applied over the sample, at 363 K. By comparison of the differences of the dielectric constants, we can evaluate the reaction ability of the surface of the pores. Our experimental results, together with a theoretical description and a characterization of the interaction between the atoms of the surface of pores and embedded materials will be presented.

**PREPARATION OF M/TiO<sub>2</sub> (M=Au, Pt) NANOCOMPOSITE FILMS  
USING CO-SPUTTERING METHOD**

*Takeshi Sasaki<sup>1</sup>, Naoto Koshizaki<sup>1</sup>, Michio Koinuma<sup>2</sup> and Yasumichi Matsumoto<sup>2</sup>*

<sup>1</sup> National Institute of Materials and Chemical Research (NIMC), 1-1 Higashi,  
Tsukuba, Ibaraki 305-8565, JAPAN <tsasaki@nimc.go.jp>

<sup>2</sup> Department Applied Chemistry and Biochemistry, Faculty of Engineering,  
Kumamoto University, 2-39-2 Kurokami, Kumamoto 860-8555, JAPAN

Au/TiO<sub>2</sub> and Pt/TiO<sub>2</sub> nanocomposite films were deposited on quartz glass substrates by the co-sputtering method using a r.f. sputtering apparatus. Gold and/or platinum wires of 0.5 mm in diameter were placed symmetrically on a hot-pressed rutile titanium dioxide target. The length of the wires on the TiO<sub>2</sub> target was changed to obtain nanocomposite films with various noble metal content. All the samples were post annealed in air at 300 - 700°C. The structures of the films were examined by XRD and TEM. The chemical states of Ti and M, and the M/Ti (M=Au, Pt) atomic ratio in the nanocomposites were examined by XPS. The content of Au and Pt in the films was dependent on the amount of the wires placed on the TiO<sub>2</sub> target. The contents of Pt and Au in the films and the thickness of the nanocomposite films increased with an increase in the length of the wires on the TiO<sub>2</sub> target. Au in the as-deposited Au/TiO<sub>2</sub> nanocomposite films were crystallized, whereas Pt in the as-deposited Pt/TiO<sub>2</sub> nanocomposite films were amorphous. The TiO<sub>2</sub> matrices of both composite films were amorphous. The chemical states of Au and Pt in as-deposited nanocomposites were metallic and oxide like such, respectively. The crystallization of TiO<sub>2</sub> matrix in the nanocomposite films was observed after the post annealing at 400°C and above for both films. It was revealed from TEM, XPS and XRD measurements that heated nanocomposite films consist of noble metal nanoparticles in the matrix of rutile type TiO<sub>2</sub> Matrix. The size of noble metal nanoparticles in the composite films increased with the heat-treatment temperature. We also report optical and photoelectrochemical properties of these nanocomposite films.

**SOLIDIFICATION AND MELTING OF GALLIUM AND MERCURY IN  
POROUS GLASSES AS STUDIED BY NMR AND ACOUSTIC TECHNIQUES**

*B.F. Borisov<sup>1</sup>, E.V. Charnaya<sup>1</sup>, W.-D. Hoffmann<sup>2</sup>, D. Michel<sup>2</sup>, P.G. Plotnikov<sup>1</sup> and  
Yu.A. Kumzerov<sup>3</sup>*

<sup>1</sup> Institute of Physics, St.Petersburg State University, St.Petersburg 198904, RUSSIA

<sup>2</sup> Faculty of Physics and Geosciences, University of Leipzig,  
D-04103 Leipzig, GERMANY <michel@rz.uni-leipzig.de>

<sup>3</sup> A.F.Ioffe Physico-Technical Institute RAN, St.Petersburg 194021, RUSSIA

Phase transitions in materials confined within porous glasses are the object of continuing interest. They differ significantly from those in corresponding bulk samples and depend on many factors such as pore size and geometry, wetting, interactions with the inner surface and so on. Size and surface effects for particles in voids as well as the common behaviour of the ensemble of particles which form a thoroughly interconnected network within the porous matrix can dominate in particular cases. Among different phase transitions, the melting and freezing phase transitions are of particular interest because they are purely first order and well studied for bulk samples. Here we present results of studies of the melting and freezing phase transitions for gallium in porous glasses with various pore sizes from 3.5 to 200 nm and for mercury in a porous glass with pores of 7 nm in diameter using NMR and acoustic techniques. The NMR measurements provided direct information on a total amount of liquid metals versus temperature. Acoustic measurements provided information about changes in elastic moduli and relaxation phenomena. A depression of the phase transition temperatures and pronounced hysteresis between melting and freezing were found. However, for gallium there was no direct correlation between pore size and lowering of the transition temperatures. Such behavior was explained by different gallium structure within pores. Acoustic measurements for confined mercury shown that the freezing process was irreversible while the melting process consisted of reversible and irreversible temperature ranges. The use of longitudinal and transverse acoustic waves made it possible to obtain new information about the origin of reversible and irreversible behavior upon melting and to suggest that a liquid layer was formed on the mercury solid surface upon melting, freezing was driven by the pore geometry with no visible precursor effects.

---

### ON THE INFLUENCE OF NANO-SCALING ON THE GLASS TRANSITION OF MOLECULAR LIQUIDS

*J. K. Krüger, R. Holtwick and A. le Coute*

Fachbereich 10.2, Experimentalphysik, Universität des Saarlandes, Bau 38,  
Postfach 151150, 66041 Saarbrücken, GERMANY <ph12hujk@rz.uni-sb.de>

The nature of the glass transition is still a matter of debate. Recent investigations of the freezing behaviour of canonical glasses suggest that the formation and the consecutive coagulation of nano-clusters are responsible for the existence of an ideal glass transition. In order to get more insight into the nature of these clusters (size, morphology, dynamics, etc.) and their impact on the transition process we have performed extended calorimetric and Brillouin-spectroscopic work on molecular glass-forming liquids (di-n-butyl-phthalate (DBP), salol, ortho-terphenyl (OTP) and glycerol) confined in controlled pore glasses (CPG) with pore diameters between 2.5 nm and 70 nm. Elastic and inelastic light scattering results indicate, that already well above the thermal glass transition a super-structure on a length scale between 600 nm and 1000 nm is created. However, the formation of this super-structure seems not to affect the position of the glass transition temperature  $T_g$ . It turns out that even for pore diameters as small as 2.5 nm  $T_g$  is shifted only slightly to lower temperatures with respect to  $T_g$  of the bulk material. Specific heat capacity measurements using temperature modulated DSC (TMDSC) on the other hand show a significant influence of the pore size on the temperature dependence of the complex excess specific heat capacity. These results will be discussed in terms of the existence of an underlying ideal glass transition which seems to become more apparent in the nano-confined state.

**A MAGNETIC COMPOSITE COMPOSED OF IRON-NITRIDE  
NANOGRAINS DISPERSED IN A SILVER MATRIX**

*T.A. Yamamoto, K. Nishimaki, T. Harabe, K. Shiomi, T. Nakagawa and M. Katsura*

Department of Nuclear Engineering, Osaka University, 2-1 Yamadaoka,  
Suita, Osaka 565-0781, JAMPAN <takao@nucl.eng.osaka-u.ac.jp>

We tried to synthesise a magnetic nanocomposite in which iron nitride nanograins are dispersed in a silver matrix by intruding iron-oxide nanograins in the matrix. Ammonia gas stream with various flow conditions was employed to control the intruding potential to form selectively a ferromagnetic iron nitride of  $\gamma\text{-Fe}_4\text{N}$  or  $\epsilon\text{-Fe}_2\text{N}$ , the former of which is a stoichiometric compound in fcc structure while the later a nonstoichiometric in hcp. The iron nitride nanocomposite, on which much attention has not been paid yet, is regarded as a promising material system, since iron nitride family has various kinds of magnetism with large magnetic moments comparable to that of metallic iron and better chemical stability relative to those of metallic nanoparticle. We have found that 10-30 nm oxide grains have been converted into nitride phases after a reaction at 450°C. The nanocomposites are characterised with XRD, TEM, SEM and XANES, and the magnetic properties are studied by a SQUID magnetometer.

---

**FORMATION OF IRON-NITRIDES BY REACTION  
OF IRON NANOPARTICLES WITH A STREAM OF AMMONIA**

*K. Nishimaki, S. Ohmae, T.A. Yamamoto and M. Katsura*

Department of Nuclear Engineering, Osaka University, 2-1 Yamadaoka,  
Suita, Osaka 565-0781, JAPAN <knishi@nucl.eng.osaka-u.ac.jp>

Iron-nitride foundation by reaction of iron nanoparticles of about 10 nm or coarse particles of about 150  $\mu\text{m}$  with an ammonia stream was investigated with respect to correlation between nitrogen contents in the product and dissociation extent of the ammonia. Both of the reactions were performed in the same conditions, mass of reactant, flow rate, temperature ( $650^\circ\text{C}$ ) else other than the grain size. It was found that the nanoparticles much more enhance the ammonia dissociation and the product thereby was of lower nitrogen contents than the coarse particles,  $\alpha$ - Fe +  $\gamma$  -  $\text{Fe}_4\text{N}$  with the nano and  $\gamma$  -  $\text{Fe}_4\text{N} + \epsilon$  -  $\text{Fe}_{2-4}\text{N}$  with the coarse. Since the ammonia dissociation should occur on the particle surfaces in parallel with the nitridation, the larger specific surface area of the nanoparticles have enhanced the dissociation and then reduced the chemical potential of nitrogen in the product in equilibrium with the gas phase. The iron nanoparticles thus have a high reactivity due to the high Specific surface area but were less nitrided. These reactions would be understood by our thermodynamic analysis taking account of the reaction directly with ammonia molecules.

**RADIOLYTIC PREPARATION OF NANOPHASE CUBIC COBALT AND NICKEL METAL PARTICLES**

*S Kapoor<sup>1</sup>, H.G. Salunke<sup>2</sup>, B.M. Pande<sup>1</sup>, S.K. Kulshreshtha<sup>1</sup> and J.P. Mittal<sup>1</sup>*

<sup>1</sup>Chemistry Division and <sup>2</sup>Technical and Prototype Engineering Division,  
Bhabha Atomic Research Centre, Mumbai - 400 085, INDIA

Nanosized cobalt and nickel particles have been prepared by  $\gamma$ -radiolysis of  $\text{CoSO}_4$  and  $\text{NiSO}_4$  solutions in three different forms namely aqueous sol, self supporting powder and dispersed over  $\text{Al}_2\text{O}_3$  surface. The samples have been characterised for the particle size distribution and metallic characteristics by using powder X-ray diffraction, SEM, TEM and magnetisation measurements. Both metals showed face centred cubic structure and the average size of the crystallites is found to be in the range of 5 - 6 nm as estimated from the width of X-ray diffraction peaks. In See form these crystallites agglomerate to produce metal particles with wide distribution of size as revealed by SEM studies. The metal particles with 5-6 nm size were found. To be ferromagnetically ordered at low temperatures as revealed by magnetic hysteresis measurements carried out down to 5 K.

---

**STRUCTURE AND MAGNETIC PROPERTY  
OF IRON-OXIDE/SILVER NANOCOMPOSITE**

*T. Nakayama, T. A. Yamamoto<sup>1</sup>, Y. H. Choa and K. Niihara*

ISIR, Osaka University, 8-1 Mihogaoka, Ibaraki, Osaka 567-0047, JAPAN

<sup>1</sup>Department of Nuclear Engineering, Osaka University, 2-1 Yamadaoka,  
Suita, Osaka 565-0781, JAPAN <nky15@sanken.osaka-u.ac.jp>

In recent years, much interest has been paid on magnetic nanostructured materials because of attractive scientific aspects and application targets such as the giant magnetoresistance and advanced working substance for the magnetic refrigeration. We have synthesized a nanocomposite composed of magnetic iron-oxide and silver by the inert gas condensation method combined with *in-situ* coevaporation, oxidation and compaction techniques, and found its magnetism sensitive to conditions in the processing and post heat treatment. To study the correlation amongst processing conditions, material structures and magnetic properties, in this work, we synthesized nanocomposite samples with various conditions, performed heat treatments and characterized them with TEM, SEM, XRD, XANES (x-ray absorption near edge spectroscopy) and SQUID magnetometer. The smallest average size of grains, 10 nm, was obtained by optimizing evaporation rate and helium gas pressure in the evaporation, 0.5 Torr. At temperatures higher than 150 K the samples were basically of superparamagnetism evidencing existence of single domain grains magnetically isolated. This magnetic isolation seems to be achieved not only by the random arrangement of silver grains and iron-containing ones but also by incursion of iron clusters in the silver grains. TEM observation assisted with EDX indeed showed some silver grains embrace iron-containing clusters of a few nanometer.

**SYSTEMATIC DISPERSANT SELECTION METHODOLOGY  
APPLIED TO FIND SUITABLE SURFACE TREATMENT ADDITIVES  
FOR MINERAL FILLERS IN POLYMER COMPOSITES**

*Chris DeArmitt and Kevin Breese*

Institute for Surface Chemistry, P.O. Box 5607, SE-114 86 Stockholm, SWEDEN

Mineral fillers are used in many polymers in order to save cost, aid processing and improve the mechanical properties of the resultant polymer composite. The use of mineral fillers is therefore very widespread and is increasing steadily. The properties of the composite are known to be dependant on the dispersion of the mineral particles and the adhesion between the polymer matrix and the mineral. For this reason some organic surface treatment is commonly applied to the minerals to aid dispersion and to tune the adhesion, stearic acid is very often used as well as a range of organosilanes. Even though much research has been devoted to the development of better surface treatments there has been limited progress due to the absence of an effective, systematic methodology for selection and testing of possible new treatments.

We have developed a systematic rheological screening test that allows the selection of appropriate dispersants, not just for mineral filled composites but for a variety of applications. A dispersant molecule is composed of a "head" which (hopefully) attaches the dispersant to the particle, and a "tail" which must be tuned for the liquid. In our work, each of these two parts has been designed separately. Thus we have identified suitable chemistry to attach dispersants to nine commonly used mineral fillers; calcium carbonate, talc, dolomite, silica, wollastonite, magnesium hydroxide, titanium dioxide, mica and mineral fibres. Then we have chosen the appropriate "tail" structure for a dispersant which has to be used in a polypropylene matrix. Our chosen additives were applied to the minerals and composites were made followed by full mechanical and oxidative stability testing. By comparison with the untreated minerals and the commercially available treatments for the minerals we have shown the effectiveness of our methods for selecting dispersants which make better composites.

**PROCESSING OF NANOSTRUCTURED WC-Co POWDER  
FROM PRECURSOR OBTAINED BY CO-PRECIPITION**

*Zongyin Zhang, Sverker Wahlberg, Mingsheng Wang and Mamoun Muhammed*

Materials Chemistry Division, Royal Institute of Technology (KTH),  
S-100 44 Stockholm, SWEDEN <zongyinz@inorgchem.kth.se>

The mechanical properties of WC-Co composites are strongly influenced by the carbide grain size, i.e. decreasing grain size increases hardness, transverse rupture strength and wear resistance. Nanostructured WC-Co powder can be prepared by reduction and carburisation of homogeneous precursors containing W and Co mixed on the atomic scale. The precursor prepared by co-precipitation starting from ammonium paratungstate and cobalt hydroxide was used as raw material in present paper. The reduction and carburisation of the precursor without calcination were investigated to obtain a well-dispersed nanophase powder of WC-Co. Different processing parameters such as reduction- and carburisation-temperature and time, and processing composition of carburisation gas were studied. The reduced and carburised powders were evaluated using SEM, TEM, XRD and BET techniques. W-Co powders were obtained after the reduction at 600°C, 650°C and 700°C in hydrogen for different times. Decreasing the reduction temperature increased the specific surface area of W-Co powders. The carburization was carried out at 700°C for 3 hours using 70CO/30CO<sub>2</sub> and 80CO/20CO<sub>2</sub> gas compositions, the powders consisting of the mixture of different phases were obtained. WC-Co powder of nano-scale (20 nm) in micro-scale agglomeration was also obtained after carburisation under 90CO/10CO<sub>2</sub> gas.

**EFFECTS OF MECHANICAL TREATMENT OF  $\text{Fe}_2\text{O}_3\text{-SiO}_2$  NANOCOMPOSITES PREPARED BY A SOL-GEL METHOD***C. Cannas, A. Musinu and G. Piccaluga*

Dipartimento di Scienze Chimiche, Via Ospedale 72, 09124 Cagliari, ITALY

$\gamma\text{-Fe}_2\text{O}_3$  (maghaemite) has attracted technological interest on account of its magnetic and catalytic properties. Interest has increased following the observation that properties are strongly dependent on the size of the particles, with dramatic changes when nanometric sizes are reached. The preparation of nanophased  $\gamma\text{-Fe}_2\text{O}_3$  presents some difficulties. In the pure iron oxide,  $\gamma\text{-Fe}_2\text{O}_3$  transforms in  $\alpha\text{-Fe}_2\text{O}_3$  phase at rather low temperature ( $<380^\circ\text{C}$ ). Moreover,  $\gamma\text{-Fe}_2\text{O}_3$  nanoparticles tend to aggregate with a consequent increase of particle size, which makes easier the  $\text{g}$  to  $\text{a}$  transition. Various attempts have been made in order to stabilize nanometric  $\gamma\text{-Fe}_2\text{O}_3$  particles by dispersing maghemite in a polimeric, glassy or ceramic matrix.

We used a sol-gel method for the preparation of a series of  $\gamma\text{-Fe}_2\text{O}_3\text{-SiO}_2$  nanocomposites, exploring a wide range of compositions (9-33 wt% of  $\gamma\text{-Fe}_2\text{O}_3$ ). The effect of thermal treatment in the range 300-900°C of the various nanocomposites has been investigated through XRD and TEM. This induces the formation of  $\gamma\text{-Fe}_2\text{O}_3$  nanoparticles of 3-5 nm, which appear at lower temperatures depending on the increase of iron oxide content. A further increase of the temperature results in a slight increase of particle size together with an increase of the amount of  $\gamma\text{-Fe}_2\text{O}_3$  phase. These treatments however also induce the partial transformation of  $\gamma$ - to  $\alpha\text{-Fe}_2\text{O}_3$  phase. In order to overcome this problem, several attempts have been made of varying the starting conditions of preparation method (materials, pH etc.), without reaching more satisfactory results.

In order to obtain composites in which the nanosized microstructure is better controlled. To this end, we started with the ball milling of 28 wt%  $\text{Fe}_2\text{O}_3$  nanocomposite treated at 300°C. The XRD analysis evidenced that the four adopted milling times (3, 5, 10 and 20 h) result in a progressive increase of the amount of  $\text{g}$  phase up to the limit imposed by the iron oxide concentration. The good homogeneity of the particle size distribution in the samples is also preserved, as confirmed by TEM micrographs

---

**Z-CONTRAST SCANNING TRANSMISSION ELECTRON MICROSCOPY  
OF NANOFUNCTIONALIZED PARTICULATE MATERIALS**

*J. Fitz-Gerald<sup>1</sup>, R.K. Singh<sup>1</sup>, S.J. Pennycook<sup>2</sup> and H. Gao<sup>1</sup>*

<sup>1</sup> Department of Materials Science and Engineering

<sup>2</sup> Oak Ridge National Labs, Solid State Division,  
University of Florida, Gainesville, FL 32611, USA

Particulate materials with unique functional properties have been the focus of much attention in recent years. This new class of materials have greatly stimulated interest for their novel structure and properties in many applications such as flat-panel display materials, sintering of advanced ceramics, rechargeable batteries, drug delivery systems, etc... Consequently, imaging of the atomic structures at the interfaces can provide deep understanding of the relationship between the nanofunctionalized particulate and the corresponding properties. Z-contrast scanning transmission electron microscope (STEM-Z) provides a new view of materials on the atomic scale, a direct image of atomic structure composition which can be interpreted without the need for any preconceived model structure. Very few techniques are presently available to extract simultaneous chemical and spatial information at an atomic scale from the interface. Although high resolution transmission electron microscopy (HRTEM) provides information on the interface commensurability, not much atomic chemical information can be obtained. An important advancement in the area of simultaneous chemical and atomic imaging has been the development of scanning transmission electron microscopy with atomic number contrast (STEM-Z). The Z-contrast technique provides an incoherent image combining direct atomic resolution with "column by column" sensitivity. The objective lens of the microscope is located before the specimen and used to form a finely focused probe which is scanned over the sample. The resolution of the image depends on the probe size, which is approximately 1.8 Å for a 300 KeV beam. The contrast in this instrument is proportional to the square of the atomic number, thus all types of atoms in the materials can be distinguished from each other. Therefore it is a powerful tool in the study of particulate materials. In this paper, we will present the structures of 18 micron diameter alumina particles coated with Ag nanoparticles.

**CATALYTIC COMBUSTION WITH NANOCRYSTALLINE  
BARIUM HEXAALUMINATE-BASED SYSTEMS**

*Andrey Zarur J., Henry H. Hwu and Jackie Y. Ying.*

Massachusetts Institute of Technology, Dept. of Chemical Engineering,  
Cambridge, MA 02139, USA

Catalytic combustion of methane has been widely studied as an alternative to gas phase homogeneous combustion. It allows combustion to occur at high levels of excess air, leading to more complete reaction and reduced hydrocarbon emissions. Furthermore, it enables combustion to proceed at lower temperatures, significantly reducing the NO<sub>x</sub> production. Traditionally, noble metal systems, such as platinum and palladium, have been used as combustion catalysts. However, noble metal clusters tend to sinter or vaporize at the high combustion temperatures of >1000°C. Our research objective is to develop complex metal oxide systems that offer superior thermal resistance and high catalytic activity simultaneously. To achieve this, we have successfully synthesized nanocrystalline barium hexaaluminate (BHA) materials using a novel reverse micelle-mediated sol-gel technique. In this novel approach, a nanoemulsion is used to effectively confine the hydrolysis and polycondensation reactions to nanometer-sized aqueous domains. The resulting controlled nanostructured morphology and improved chemical uniformity enable nanocrystalline BHA to maintain surface areas in excess of 100 m<sup>2</sup>/g even upon extended exposure at 1300°C. We have also significantly improved the low-temperature catalytic activity of BHA through the introduction of transition metal oxide dopants. The ultrahigh dispersion of dopants on the surface of BHA nanocrystals enables light-off at temperatures as low as 430 °C, while sustaining complete methane conversion at 1000 °C, even under hydrothermal conditions. This novel nanocrystalline BHA-based system offers exciting potential applications in not only catalytic combustion, but also in methane reforming, due to its high surface reactivity and thermal stability.

### INFLUENCE OF SURFACE ROUGHNESS ON LIGHT ABSORPTION BY METAL NANOPARTICLES

*F. Stietz, M. Stuke\*, J. Viereck, T. Wenzel, and F. Träger*

Fachbereich Physik, Universität Kassel, Heinrich-Plett Str. 40,  
D-34132 Kassel, GERMANY <stietz@physik.uni-kassel.de>

\* Max-Planck-Institut für biophysikalische Chemie,  
P.O. Box 2841, D-37018 Göttingen, GERMANY

The size dependent optical properties of metal nanoparticles have long been the subject of extended experimental and theoretical investigations. Their optical spectra are characterized by strong resonances brought about by the excitation of plasmon polaritons, i.e. collective oscillations of the free electron gas driven by the electromagnetic field. The amplitude, width and energetic position of these resonances vary strongly as a function of the size and shape of the particles, their electronic structure and the chemical surrounding. For technical applications it is very attractive to exploit the size dependent optical properties of such systems with reduced dimensions to develop and fabricate new optical devices based on their tailor-made absorbance.

In contrast to the role of collective oscillations, details regarding the influence of *localized* electronic excitations on the optical properties of small particles has not been studied systematically in the past. However, the knowledge of such additional channels for absorption of light is of great relevance to fundamental science and applications as well.

Here we report on experiments which demonstrate that localized single electron excitations brought about by surface roughness, *i.e.* atoms located at binding sites with low coordination number, can be very essential for light absorption by metal nanoparticles. In addition, a method for separating experimentally the roughness induced contribution from absorption due to plasmon polaritons is presented. In our investigations large Na clusters served as a model system. They were prepared on quartz (100) single crystals by deposition of Na atoms evaporated from a Knudsen cell, subsequent surface diffusion and nucleation. The particles were irradiated with pulsed laser light of  $\lambda = 532$  nm and their temperature rise was derived from measurements of the kinetic energy distribution of thermally desorbed Na dimers. From the temperature increase the heat generated in the nanoparticles during the decay of both localized electronic excitations and plasmon resonances was calculated and taken as a measure of the total absorption cross section. Separation of the roughness and the plasmon polariton contribution was achieved by repeating the experiments after removal of the surface roughness by annealing. We find the surprising result that absorption due to localized electronic excitations contributes as much as 32% to the total optical absorption at  $\lambda = 532$  nm for Na particles of a mean radius R of 21 nm.

**POLARIZABILITY OF GOLD CLUSTERS ON THE GaAs SURFACE**

N.Dmitruk<sup>1</sup>, T.Lepeshkina<sup>1</sup>, M.Pavlovska<sup>2</sup>, L.Zabashta<sup>3</sup>

<sup>1</sup> Institute for Physics of Semiconductors of NASU, Prospect Nauki 45,  
252650 Kiev, UKRAINE <nicola@dep39.semicond.kiev.ua>

<sup>2</sup> Taras Shevchenko Kiev National University, Kiev, UKRAINE

<sup>3</sup> Sumy State University, Sumy, UKRAINE

In this paper the technology of electrochemical deposition of discontinuous metallic films on the semiconductor surface was used. The electrodynamic properties of small metallic clusters containing hundreds of atoms or less are investigated by ellipsometric measuring at multiple angles of incidence (MAI)  $\varphi=45^\circ\text{-}85^\circ$  and by spectroscopic ellipsometry at three incident angles in the range of wave length  $\lambda=0.27\text{-}1.15 \mu\text{m}$ . These allow to determine the polarizability of metallic nanocrystals in the dependence on their sizes (in the range of diameters  $d=2\text{-}50 \text{ nm}$  in the case of gold clusters on GaAs single crystal surface). Well isolated Au clusters on GaAs surface have been prepared by electrochemical deposition of metal from aqueous solution of  $\text{AuCl}_3$  with the  $\text{Au}^{3+}\text{-ions}$  concentration of  $(1\text{-}16)\cdot10^{-5} \text{ gram-ion/l}$ . Morphology of metallic coating and clusters sizes have been studied with electron microscopy using a carbon replica. The optical parameters  $n$  and  $k$  of effective absorbing film on GaAs substrate were obtained by solving the inverse problem in MAI-ellipsometry using Tikhonov's regularization method. The spectroscopic behaviour of both  $n(\lambda)$  and  $k(\lambda)$  depend on clusters dimensions and in the vicinity of  $\lambda=0.48 \mu\text{m}$  the equality of  $n$  and  $k$  is observed at  $d\approx10 \text{ nm}$ . After this point  $n(\lambda)$  is increased and  $k(\lambda)$  is decreased for less clusters and vice versa for more ones. Then modified Bruggeman's symmetrical theory of effective medium approximation have been used for calculation of the specific polarizability of Au clusters. The physical analysis of the size dependencies of polarizability is carried out with taking into account peculiarities of both surface plasmons and interband transitions in small clusters.

**OPTICAL PROPERTIES OF DISORDERED CLUSTER SYSTEMS**

*Leonid G.Grechko and Vitaly N.Pustovit*

Institute of Surface Chemistry,National Academy of Sciences, 31 Nauki ave,  
Kiev 252022, UKRAINE <vit@surfchem.freenet.kiev.ua>

The physical properties of small particles have been the subject of much recent interest. In particular the effect of shape and environment has been studied through their response to an electromagnetic excitation. The first influences the polarizability and the second the local field each particle is in. In particular we treat the case of a particle in the presence of one or more excitation whose wavelength is much larger than the particle diameter and interparticle separation. Shape and bulk properties are introduced through the particle polarizabilities.

A satisfactory solution to this problem is not necessarily simple since it must be self-consistent in the sense that the effect of environment on a given particle changes the response of the environment itself. Also there is the question of convergence in the multipole coupling between particle and environment that occur. The validity of the usual dipole approximation has been questioned by several authors when the particles are very close. We have provided calculations including higher multipole interactions between particles, and develop here a theory that yields a straightforward computational scheme for obtaining the normal modes of the system to an arbitrary pole order assuming only that polarizabilities are known. While studying resonances spectrum it is noted that with volume fraction increasing the pair multipole interactions between particles become significant.

**COBALT CLUSTERS IN SILVER STUDIED BY MEANS OF CLASSICAL MOLECULAR DYNAMICS, AB INITIO ELECTRONIC CALCULATIONS AND MÖSSBAUER SPECTROSCOPY***M. El Azaoui and M. Hou*Physique des Solides Irradiés, CP 234, Université Libre de Bruxelles,  
Bd du Triomphe, B-1050 Bruxelles, BELGIUM <mhou@ulb.ac.be>*Joris Verheyden, Guilin Zhang, Wim Deweerdt, Gerhard Koops, and Hugo Pattyn*Institute for Nuclear and radiation Physics, Physics Department, K.U. Leuven  
Celestijnenlaan 200D, B-3001 Leuven, BELGIUM <Hugo.Pattyn@fys.kuleuven.ac.be>

A method is developed in for the study of cobalt nanoclusters embedded in monocrystalline silver, which combines Mössbauer spectroscopy, classical molecular dynamics (MD) and ab initio electronic calculations. The MD is achieved in the NPT ensemble by means of the Rahman Parinello technique which accounts for the temporal fluctuations of all the components of the stress tensor. Atomic interactions are described within an empirical embedded atom model. The method suggested by Johnson [1] to describe the mixed component of the configuration energy in fcc systems is extended to the combination of cobalt and noble metals. It is applied to the Ag-Co system and it is assessed by means of comparisons with the few available experimental data.

The mean squared thermal vibration amplitude of substitutional Co is calculated and found the compare closely to the experimental value extracted from Mössbauer spectroscopy. As a next step towards the investigation of larger clusters, we predict the most stable relaxed cobalt dimer configurations in order to initiate an ab initio calculation of the local electric field gradient which, in turn, is then compared to the value obtained from Mössbauer spectroscopy on samples with 0.5 to 1 at.% Co in Ag [2]. Overall, this is to form a consistency check with the MD results. Finally, we model embedded cobalt clusters and present our first results of their local dynamic properties and compare these with Mössbauer spectroscopy data on the characteristic Mössbauer temperature of interior and interface Co atoms.

[1] R.A. Johnson, Phys. Rev. B41, 14 (1990) 9717

[2] J. Verheyden et al., Journal of Physics D: Applied Physics 29 (1996) 1316-1320

**INDIVIDUAL COMPLEXES AND CLUSTERS OF COPPER(II) IONS IN ION-EXCHANGERS**

*L.S. Molochnikov and E.G. Kovalyova*

Department of Chemistry, Urals State Wood Technology Academy  
37 Siberian Highway, 620032 Ekaterinburg, RUSSIA <L.Molochnikov@usfea.ru>

The character of distribution of metal complexes on the polymeric supports surface varies with the conditions of sorption and sorbent pretreatment. Different clusters with a high local concentration ( $\langle c_{loc} \rangle$ ) of attaching complexes were found to be formed in the phase of the studied ion-exchangers along with the individual complexes whereby copper ions do not interact with each other.

The structure and character of distribution of copper (II) complexes of different nature have been studied by the ESR method. The influence of sorbent matrices nature (polyacrylate for the cation-exchanger KB-2 and polyethylenepolyamine for the anion-exchangers AN-31 and AN-31a), degree of functional groups protonation, matrices reology, sorbent preadjustment to copper(II) ions and copper(II) content in ion-exchangers on the clusters formation on the cross-linked polyelectrolytes surface, is discussed here.

It was found that four types of different structures are formed in KB-2. They are following: I - individual complexes of copper (II) ions; II - binuclear copper (II) complexes; III - clusters-like aggregates of copper (II) wherein copper complexes are not bound together by chemical bonds; IV - clusters with a strong exchange interaction between copper ions which results from formation of bonds of copper ions with each other. The ways and conditions of forming predominantly one or other of cluster structure were found. In particular, it was found that acidity inside a sorbent grain effects on the formation of different structures in a sorbent.

It has been proved that structure and uniformity of distributing metal ions complexes in a sorbent matrices depend on the procedure of the adjusted sorbent AN-31a synthesis. The structural changes in metal-polymeric complexes under conditions of catalytic oxidation of hydrocarbons and sulfur-containing compounds with molecular oxygen were found during the research.

The calculations of local concentrations of copper (II) ions in an ion-exchanger phase ( $\langle c_{loc} \rangle$ ) and distances between them ( $\langle r \rangle$ ) in different cluster structures were conducted.

The authors are grateful to INTAS (Grant #96-0911) for the financial support.

**MAGNETIC NANOSTRUCTURES ELABORATED FROM Co-Sm MIXED CLUSTER DEPOSITIONS M***M. Negrier, J. Tuailon, V. Dupuis, P. Melinon and A. Perez*Département de Physique des Matériaux-UMR CNRS n°5586  
Université Claude Bernard - Lyon 1, 69622 Villeurbanne, FRANCE

The transition metals with a 3d-band (i.e. Fe, Co, Ni) exhibit a quite large magnetic moment at room temperature, but a relatively weak magnetocrystalline anisotropy. In the form of nanocrystallized clusters, we could expect an increase of the magnetic moment (Stoner's criterion) and of the surface anisotropy compared to the bulk phase. However, for such low particle size a superparamagnetic behaviour appears at temperatures higher than the blocking temperature  $T_B$  which is of the order of 20 to 30 K. To use these magnetic nanostructures in dense memory device applications, it is then necessary to increase the local anisotropy, and consequently the blocking temperature. One way to reach such objective could be the introduction of rare earth elements which are known to induce an increase of the magnetocrystalline anisotropy in some defined conditions. Among the bulk phases, SmCo<sub>5</sub> is a good example of a hard magnetic material.

Using a cluster source based on laser vaporization of a SmCo<sub>5</sub> target associated with a high pressure inert gas condensation we have produced intense supersonic jets of mixed Co-Sm clusters in a wide range of size up to thousands of atoms. Mass abundance spectra of photoionized clusters are studied in a high resolution time of flight mass spectrometer mounted at the exit of the source. Neutral clusters having the very low energy gained in the supersonic expansion are deposited on various substrates in an ultra high vacuum chamber on line with the source. In such deposition conditions (LECBD:Low Energy Cluster Beam Deposition), clusters are not fragmented upon impact onto the substrate leading to the growth of nanostructured films with a global composition SmCo<sub>5</sub> as those of the target in the source, and a mean grain size around 5 nm. Also, films of isolated mixed Sm-Co clusters embedded in a co-deposited silver matrix are prepared for magnetization measurements. Supported cluster size distributions and crystallographic structure are studied by transmission electron microscopy. X-ray photoemission spectroscopy measurements seems to evidence a segregation effect of samarium at the cluster surface in agreement with the results of the free cluster studies. This effect could be at the origin of the lower measured values of the magnetization and coercive field compared to the bulk phase ones. TEM, X-ray diffraction - absorption (EXAFS), and magnetic measurements are in progress to systematically study the influences of the source and deposition conditions on the structure, size, and composition of the mixed clusters in view to obtain an optimum anisotropy nanostructured system exhibiting a rather high blocking temperature.

### OPTICAL PROPERTIES OF NANOSTRUCTURED THIN FILMS CONTAINING NOBLE METAL CLUSTERS

*B. Prével<sup>1</sup>, B. Palpant<sup>2</sup>, J. Lermé<sup>2</sup>, M. Pellarin<sup>2</sup>, M. Treilleux<sup>1</sup>, J.L. Vialle<sup>2</sup>,  
M. Broyer<sup>2</sup> and A. Perez<sup>1</sup>*

<sup>1</sup> Département de Physique des Matériaux,

<sup>2</sup> Laboratoire de Spectrométrie Ionique et Moléculaire

CNRS - Université Claude Bernard, Lyon 1 , 69622 Villeurbanne cedex, FRANCE  
*<prevel@dpm.univ-lyon1.fr>*

Noble metal nanoparticles exhibit specific optical properties mainly due to the Mie surface plasmon resonance. Therefore, nanocomposite films consisting of such clusters embedded in a dielectric matrix open very interesting outlook for new optical devices. We report both experimental and theoretical results on alumina-embedded gold or silver cluster materials.

Clusters are produced in a laser vaporization source, analyzed in the gas-phase in a time-of-flight mass spectrometer, and deposited on a substrate under vacuum (Low Energy Cluster Beam Deposition technique). Simultaneously, the alumina matrix evaporated by an electron gun, embeds the metallic particles, leading to the growth of nanocomposite thin films. The morphology, thickness, porosity, crystallographic structure, composition and size distribution are determined for each film through RBS, Grazing-Incidence Small-Angle X-ray Scattering, X-ray diffraction and TEM . Optical absorption spectra are provided by spectrophotometric measurements. Finally, the effective dielectric function of these nanostructured materials is obtained from ellipsometry analysis.

The size effects experienced by the Mie plasmon resonance band are compared with the bulk properties within the classical Maxwell-Garnett effective medium theory . For gold clusters the Mie resonance band is clearly blue-shifted, broadened, and damped with decreasing cluster radius R. In the size range investigated, the Mie frequency is shown to follow a 1/R-dependence.

Quantum TDLDA calculations are performed for a better understanding of these size effects. The observed features can be understood through the study of the core d-electrons influence, as well as dielectric effects due to the matrix index and porosity. The experimental findings are then well reproduced by our calculations .

Moreover, the interband absorption threshold is also shown to experience a size effect: indeed, a fine analysis of the absorption spectra reveals its shift to higher energies with decreasing particle radius.

**LAYERED CLUSTERS PRODUCED BY LASER-VAPORIZATION**

*I.M.L. Billas, M. Heinebrodt, N. Malinowski, F. Tast, W. Branz and T.P. Martin.*

Max-Planck Institut für Festkörperphysik,  
Heisenbergstr. 1, 70569 Stuttgart, GERMANY

We report on the synthesis of heterogeneous layered clusters in the gas-phase and on their characterisation by means of transmission electron microscopy (TEM) and high resolution TEM (HRTEM). The heterogeneous clusters are composed of two materials (Au and Si, or Pb and Si). The evaporation of the materials has been achieved by laser vaporisation, with the 2nd harmonic of a pulsed Nd:YAG laser, of a target situated in a low-pressure inert gas condensation cell. Various evaporation arrangements have been tested and their influence on the cluster composition has been investigated. The evaporation was carried out with one single laser. The target was composed either of both materials in close contact or of an alloy compound. On the other hand, we have also performed experiments in which the two materials close to each other were evaporated by two laser pulses with various time delays between them. In the case of optimal experimental conditions, TEM studies indicate that the heterogeneous clusters are composed of a metallic core encapsulated by a thin layer of Si.

**IONIZATION AND COAGULATION OF METAL PARTICLES IN PLASMA**

*A.C. Xenoulis<sup>1</sup>, D.S. Vlachos<sup>1</sup>, G. Doukellis<sup>1</sup>, N. Boukos<sup>1</sup> and Th. Tsakalakos<sup>2</sup>*

<sup>1</sup> National Center for Scientific Research Demokritos, 153 10 Aghia Paraskevi,  
Athens, GREECE <xenul@cyclades.nrcps.ariadne-t.gr>

<sup>2</sup> Rutgers University, Piscataway, NJ 08855-0909, USA

Size selected clusters are considered to be a new building block for the construction of nanostructured materials. This kind of application, however, demands high intensity beams of ionised clusters, which are not easily available. Although cluster sources operating on plasma-discharge sputtering, such as the magnetron or the hollow-cathode source, are extremely efficient providers of ionised cluster, their utilisation for the synthesis of nanostructured materials is limited by the insufficient understanding of coagulation in plasma. In plasma, because of the presence of electrostatic forces, ionisation and coagulation should be inextricably interdependent. These two processes were presently investigated using a hollow-cathode, dc plasma-discharge, and cluster source. Cu clusters were the material studied.

The results of a series of relevant measurements indicate that ionization as well as clustering depends very dramatically on the time interval during which clusters and plasma coexist. Specifically, with respect to the competition between positively and negatively ionized clusters it was found that for short cluster-plasma coexistence intervals almost equal numbers of positive and negative clusters are produced, while for longer coexistence times, longer than about 1 msec, the negative clusters dominate and the number of positive clusters tends to zero.

It is reasonable to expect that the competition between positive and negative clusters in plasma, on which almost nothing was experimentally known before, will affect coagulation very strongly, since clustering of oppositely charged particles is facilitated and that of similarly charged hindered. In fact with respect to clustering it was found that the mean cluster size increases with increasing cluster-plasma coexistence. For instance the mean Cu cluster diameter increases from  $40 \pm 10^{\circ}\text{C}$  to  $110 \pm 8^{\circ}\text{C}$  by increasing the cluster-plasma coexistence time from  $4.0 \times 10^{-4}$  sec to  $7.5 \times 10^{-4}$  sec. Since the cluster-plasma coexistence time can be easily manipulated, e.g. by the introduction of a grounded grid in the discharge chamber to intercept the plasma beam at various distances from the cathode, these findings constitute a novel and practicable means to control the cluster mass of interest in plasma discharge. Implications with respect to the involved mechanisms as well as the construction of nanostructured materials will be discussed.

### DEPOSITED NANO-METRE SIZED IRON CLUSTERS

*T. Åklin<sup>1</sup>, C. Johansson<sup>1</sup>, M. Hansson<sup>1</sup>, M. Andersson<sup>1</sup>, E. Olsson<sup>2</sup>, F. Gustavsson<sup>2</sup>, R. Wäppling<sup>2</sup> and A. Rosén<sup>1</sup>*

<sup>1</sup> Department of Experimental Physics, Chalmers University of Technology and Göteborg University, S-412 96 Göteborg, SWEDEN

<sup>2</sup> The Ångström Laboratory, Uppsala University, S-751 21 Uppsala, SWEDEN

We have produced films of iron clusters in a recently developed high yield laser vaporisation source. The iron clusters were deposited on microslides and the thickness of the obtained films were from 50 to 120 nm. We analysed the films with transmission electron microscopy (TEM), Mössbauer spectroscopy and magnetic measurements. The TEM result shows that the diameters of the deposited iron clusters are in the range from 2 nm to about 10 nm. From preliminary Mössbauer measurements at room temperature we found that the particles undergo fast superparamagnetic relaxation and they contain a-iron, but a small amount of iron oxides could not be ruled out. Mössbauer measurements at lower temperatures will follow these measurements. Hysteresis loops were obtained in the field range of  $\pm 2$  T from 10 K to 295 K. The saturation magnetization of the films was in the range of bulk a-iron. The obtained coercive field,  $B_C$ , and remanence,  $M_r$ , increase with decreasing temperature in the whole temperature range (Fig. 1). This behaviour is typical for a system of mono-domain particles with a wide distribution of sizes. After these first promising results we are planning to reduce the distribution of particle sizes in the films, by varying the parameters of the cluster production.

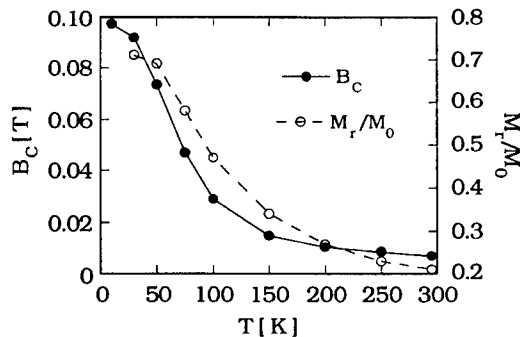


Fig. 1. Coercive field,  $B_C$ , and normalized remanence,  $M_r$ , versus temperature of a film, about 120 nm thick, of iron clusters.  $M_0$  is the magnetization at 0.5 T.

---

**OPTICAL EXTINCTION AND SURFACE MORPHOLOGY OF  
SILICON NANOSTRUCTURES GROWN ON DIELECTRIC SUBSTRATES**

*M. Andersson, A. Iline, F. Stietz and F. Träger*

Fachbereich Physik, Universität Kassel, Heinrich-Plett-Str. 40,  
D-34132 Kassel, GERMANY <iline@physik.uni-kassel.de>

Nanostructures of silicon were grown on dielectric substrates, e.g. CaF<sub>2</sub>, by deposition and surface diffusion of Si atoms with the main objective to correlate the size, shape and density of the generated structures to their optical properties. Along these lines, samples have been prepared under a large variety of experimental conditions. The surface morphology was characterised by scanning force microscopy under ambient conditions and the optical extinction of the silicon structures was measured in the visible and ultraviolet spectral range with wavelengths ranging from 200 to 800 nm.

In order to prepare different Si nanostructures the deposition and growth parameters, in particular the temperature, atom flux and deposition time were varied. Films with nominal thickness of 2 - 20 Si monolayers were made. We find that the substrate temperature T has a particularly pronounced influence on the character of the Si nanostructures. At T = 750 K, the deposited atoms form an amorphous film with sub-nm roughness. At higher temperatures, clusters with lateral dimension of up to 50 nm and heights of up to 10 nm were observed depending on temperature and deposition time.

The optical extinction spectra of the silicon films showed a broad maximum at  $\lambda = 320$  nm and a tail extending throughout the visible spectral range. The cluster samples, on the other hand, exhibited a very weak extinction in the visible followed by an almost monotonous increase to shorter wavelengths. To provide a detailed understanding of the optical properties of the Si nanostructures, theoretical spectra were also calculated using electrodynamics theory and compared to the measured extinction data. Good qualitative agreement between theory and experiment was obtained both for samples consisting of amorphous films and of Si nanoparticles.

The results reported here open up the possibility of preparing semiconductor materials with tailor-made optical properties, particularly in the ultraviolet spectral range.

This work was supported by the Deutsche Forschungsgemeinschaft.

**CLUSTER MODEL OF GAS SENSITIVITY  
NANOSTRUCTURAL SENSORS OF AMMONIA**

*O. I. Bomk<sup>1</sup>, L.G. Il'chenko<sup>2</sup>, V.V. Il'chenko<sup>1</sup>, G.V. Kuznetsov<sup>1</sup>, A.M. Pinchuk<sup>1</sup>,  
V.M. Pinchuk<sup>3</sup> and V.I. Strikha<sup>1</sup>*

<sup>1</sup> Radiophysical Dept., Kiev University, Volodimirska st. 64,  
Kiev 252033, UKRAINE <vai@rpd.univ.kiev.ua>

<sup>2</sup> Institute of Surface Chemistry, Pr. Nauki 31, NAS of Ukraine,  
Kiev 252028, UKRAINE

<sup>3</sup> Polytechnic University, Pr. Peremogi 37, Kiev 252056, UKRAINE

At present there is a large number of works that are devoted to the problems of creation solid-state (semiconductors) gas sensors. In last year's works were shown that using metal superthin films allows essentially increase gas sensitivity of sensors created based on oxides ( $\text{SnO}_2$ ) [1], and Schottky barrier contacts [2]. Many authors' works shown, that superthin film of metals (Pt, Pd, Ag, and other) have island structure and represent on a surface of the semiconductor set clusters by the size 3-10 nanometers. It is clear that without elementary processes understanding, occurring on surfaces, into clusters volume and also on cluster-semiconductor interface, it is impossible to understand a nature of gas sensitivity formation at the gas molecule adsorption. At present work we undertake an attempt of research the processes, occurring on external interface of a superthin metal film at the adsorption of a molecule of ammonia and influence of these processes onto internal functional important metal-silicon interface. Our calculations were carried out in approximation cluster model by NNDO method. The successful application of the cluster model number of authors for energy adsorption and elementary processes catalytic reaction calculation gives us the basis to use it. When simulating the structure of Ti, Ni and silicon clusters (with natural monolayers oxides on interfaces) the technique of univalent pseudo-atoms was used to passivate the extraneous valence bonds at the external interface of clusters. We used an effective technique, which was proposed for fitting the quantum-chemical parameters of boundary pseudoatoms to reproduce certain characteristics of the simulated solid [3]. The most important results of our researches are following: in the result of ammonia molecule adsorption on a surface of metal clusters there are the redistribution charges on metal - silicon interfaces. There was the reduction of electronic density in intermediate space of an elementary cell of surface silicon. This process brings to change of electronic density on silicon atom from 0.85 electron/atom up to 0.7 electron/atom for Si -  $\text{SiO}_2$  - Ni -  $\text{NiO}_2$  cluster. As our calculations show changing of the external ammonia air leads to change in integrated charge on silicon interfacial atom of interface Si -  $\text{SiO}_2$  from 0.4 electron/atom up to 0.7 electron/atom. for cluster Si -  $\text{SiO}_2$  - Ti -  $\text{TiO}_2$ . Such changes charges on interface can result to changes of parameters interfacial dipoles which take a part of formation Schottky barrier and accordingly to changes of I-V characteristics of Schottky barrier diodes.

1. J.Zhang, K.Colbow Sensors and Actuators B 40, 47 (1997).
2. L.M.Lechuga, A.Calle, D.Golmayo, F.Briones. J. Appl. Phys. 70, 3348 (1991).

**POLYMER-IMMOBILIZED NANOSCALE  
AND CLUSTER METAL PARTICLES**

*A.D.Pomogailo*

Institute of Chemical Physics in Chernogolovka, Russian Academy of Sciences,  
142432 Chernogolovka, Moscow, RUSSIA <adpomog@icp.ac.ru>

The possibility of combining the physicochemical properties of metals and polymers in a single material and of regulating these properties through concentration changes has long been under discussion. The progress in this direction is stimulated by the ever-growing interest in this problem shown in many fields of chemistry, physics, and materials science. The essential data on the immobilisation of nanoscale and cluster metal particles in polymeric matrices are considered and systematised for both macroligands and the matrices formed *in situ*. Special attention is paid to the controlled chemical passivation (stabilisation) of extremely active particles of colloidal size using high - molecular - weight compounds. The routes of formation of polymer - immobilised nanoparticles directly in the polymer medium are analysed. This allows the preparation of compositions characterised not only by the most regular distribution of these particles over the bulk of polymer but also by a strong chemical interaction between the components. Studies in the field of polymer-analogous transformations, which offer a promising approach to the binding of mono- and heterometallic clusters as a new direction in the physicochemistry of nanoparticles, are discussed in detail. The peculiarities of the immobilisation of clusters, polynuclear structures, and nanoparticles by synthetic polymers, on the one hand, and by biopolymers, on the other hand, are considered. The basic fields of the application of the products obtained and the prospects of the development of this direction are outlined.

### **CLUSTER-CONTAINING METAL MONOMERS AND THEIR (CO)POLYMERS**

*G.I. Dzhardimlieva, S.I.Pomogailo, and A.D.Pomogailo*

Institute of Chemical Physics in Chernogolovka, Russian Academy of Sciences,  
142432 Chernogolovka, Moscow Region, <dzhardim@icp.ac.ru>

The increasing interest in cluster-containing (co)polymers is nowadays based mainly on two aspects:

- (i) It is reasonable to expect that cluster or cluster complexes incorporated into the polymers would considerably modify polymer materials properties (adhesive, magnetic, thermal, etc.).
- (ii) Cluster-containing polymers are of great interest as catalysts for different reactions, combining the advantages both of homogeneous catalysts (due to solubility or swelling in organic solvents) and heterogeneous ones (due to the increase of cluster stability by their bounding to the polymer which prevents cluster fragmentation or aggregation to large particles).

The reaction of Rh<sub>6</sub>(CO)<sub>16</sub> with 4-vinylpyridine or diphenylphosphorallyl (L) in the presence of N-trimethylammonium oxide proceeds under mild conditions and results in the oxidation of coordinated CO to CO<sub>2</sub>. The main product of this reaction is the monosubstituted derivative Rh<sub>6</sub>(CO)<sub>15</sub>L, the disubstituted Rh<sub>6</sub>(CO)<sub>14</sub>L<sub>2</sub> compound is also produced in a small yield. These products were characterized by IR and <sup>1</sup>H, <sup>13</sup>C, <sup>31</sup>P NMR spectroscopy and by elemental and X-ray analyses. Rh<sub>6</sub>-containing monomers were copolymerized with both styrene and acrylonitrile. Copolymers composition, molecular mass distribution, as well as product's properties were studied.

---

**SIZE DEPENDENT STRUCTURAL TRANSITION CORRELATED  
WITH CATALYTIC ACTIVITY IN NANOSIZED NICKEL PARTICLES**

*O. Tillement, S. Illy and J.M. Dubois*

Laboratoire Science et Génie des Matériaux Métalliques, Ecole des Mines, INPL  
F-54052 Nancy cedex, FRANCE

*Y. Fort*

Laboratoire de Chimie Organique I, Université Henri Poincaré, Nancy I F-54506  
Vandoeuvre-les-Nancy cedex, FRANCE

In recent years, increasing interest has been found in synthesising and processing nanoscale particles and clusters. Physical and chemical properties vary systematically as a function of the size and using ultrafine particles represents a potentially fertile field for materials research. Finely divided powders of metals and alloys have practical implications ranging from microelectronics and materials science to geophysics and catalysts.

In this paper, we develop a new process for preparing ultrafine, equiaxed Ni particles with a nano-size distribution. Stable dispersions of monodispersed Ni clusters were obtained after chemical reduction of Ni (II) salts by activated sodium hydride in organic solvents. The particles were characterised by transmission electron microscopy and X-Ray powder diffraction. Such nanometric metallic powders are easily and reproducibly prepared, not pyrophoric, stable on storage and have an original catalytic behaviour.

We report that according to experimental conditions, size, structure and activity in catalysis can be easily changed. The particles with sizes smaller than 4 nm were found to be hexagonal-closed-packed (hcp), whereas larger ones were face-centred-cubic (fcc). To our knowledge, this is the first observation that unsupported Ni powder may crystallise in the hcp system and that crystalline phase stability is particle size dependent. A strong correlation has been evidenced between size dependent transition and catalytic activity.

**VIBRATIONAL ANALYSIS OF ION IRRADIATED  
SELF-ASSEMBLED MONOLAYERS**

*G. Compagnini, S. Pignataro and O. Puglisi*

Dipartimento di Scienze Chimiche, V.le A.Doria 6 -95125 Catania, ITALY

Nanometric ordered organic ultrathin (1-10 nm) films can be obtained through the use of self assembled techniques. These films are of great interest because of their stability under different conditions due to the formation of a covalent bond with the substrate. For instance, alkanethiole monolayers, self-assembled onto silver or gold substrate, are hydrophobic and resistant to attack by various solvent. Moreover, they are particular interesting because they can be analyzed both by Raman and Infrared techniques using the well known surface enhanced effects.

In this work we would like to present some results on the modification of the vibrational features of self assembled monolayers upon ion irradiation ( $H^+$  100 keV ions) through Surface Enhanced Raman and Infrared Reflection Spectroscopies. In particular low fluences ( $10^{12}$ - $10^{13}$  ions/cm $^2$ ) ion irradiation will be used to induce simple chemical reactions in alkanethiole molecules seen through the loss of CH<sub>3</sub> stretching features and formation of C=C double bonds. Contact angle measurements and Atomic Force Microscopy will also support the results.

**MODELLING OF NANOSTRUCTURAL DESIGN OF ULTRAFINE  
MULLITE POWDER PARTICLES OBTAINED BY ULTRASOUND  
REACTIONAL SPRAYING**

*V. Jokanovic<sup>1</sup>, Dj. Janackovic<sup>2</sup>, P. Spasic<sup>3</sup>, D. Uskokovic<sup>4</sup>*

<sup>1</sup> Institute for Technology of Nuclear and Other Mineral Raw Materials,  
Franchet D`Eperey 86, 11000 Belgrade, YUGOSLAVIA  
<jb39994d@hermes.beotel.yu>

<sup>2</sup> Faculty for Technology and Metallurgy, University of Belgrade,  
Karnegijeva 4, 11000 Belgrade, YUGOSLAVIA

<sup>3</sup> Military Medical Academy, Crnotravska 17, 11000 Belgrade, YUGOSLAVIA

<sup>4</sup> Institute for Technical Sciences, Serbian Academy of Sciences and Arts,  
Knez Mihajlova 35, 11000 Belgrade, YUGOSLAVIA

The theoretical model is discussed enabling determination of size distribution of powder particles on the level of individual particle and the level of its substructure (nanolevel) by knowing the conditions of ultrafine mullite synthesis obtained by reaction spray pyrolysis with ultrawave excitation.

This model gives powder particles distribution spectrum on the whole, the average particle size and populational balances for each discrete value of the spectrum, as well as the average size and distribution of the nanostructural subelements of which the particle is composed.

Experimental data, obtained by a method of scanning and transmission electron microscopy, are in very good agreement with theoretically estimated values.

As it follows, it becomes possible, in so defined periodical physical field, to view the process of the particle genesis from the aspect of its structure and substructure with high level of determinism.

**NANOSCOPIC DYNAMIC FUNDAMENTALS OF RATE PROCESSES  
IN SOLIDS AND APPLICATIONS TO NANOSYSTEMS***Yu.L. Khait*

Solid State Institute, Technion-Israel Institute of Technology, Haifa 32000, ISRAEL

We discuss main ideas and some applications to nanosystems of nano-scopic dynamic electron-related theory at short-lived large energy fluctuations (SLEF's) at atomic particles and SLEF-induced rate processes, phase and structural transformations in solids, interfaces and surfaces summarized in [1,2]. Among the applications are the following: recrystallization and intermixing in damaged [1, 3] and virgin [1,4] Si<sub>n</sub>/Ge<sub>m</sub> strained superlattices of nanometer periods (n= 9, 19; m = 9, 12), formation of Si nanocrystalline nuclei in  $\alpha$ -Si:H(F) - metal interfaces [1,5,6], formation of new germanosilicide phases in Ti/Si<sub>1-x</sub>Ge<sub>x</sub> interfaces [1,7], gradual degradation in semiconductor lasers without [1,8] and under [9] the influence of high pressure (stress) melting without [1,2] and under [1,2,10] the influence of pressure, structural transformation in amorphous materials induced by laser radiation [11], SLEF-induced breaking of the superconducting state in the layered high-T<sub>c</sub> superconductors [12] and other processes. The theory suggests explanations for various observed "anomalies" and puzzling phenomena and gives predictions some of which have been confirmed.

The nanoscopic SLEF-based theory considers the observed phenomena consisting of a great number of SLEF-induced correlated picosecond atomic and electronic processes in nanometer material regions [1-12]. Possible applications of the theory to rate processes and structural and phase transformations in 2-dimensional quantum wells, quantum wires and dots are discussed.

1. Yu. L. Khait, Kinetics and Applications of Atomic Diffusion: Nanoscopic Electron-Affected Stochastic Dynamics (Scitec Pub., Switzerland, 1997).
2. Yu.L. Khait, Phys. Reports 99, 237 (1983).
3. Freiman et. al, Phys.Rev.B 48, 14893 (1993 ).
4. Dettmer et al, Appl.Phys.Lett.66, 2376 (1995).
5. Edelman et al, J.Appl.Phys.75, 7875 (1994).
6. Yu.L. Khait et al, J.Appl.Phys.78, 6504 (1995).
7. W . Freiman et al, Appl.Phys.Lett.69, 3821 (1996).
8. Yu.L. Khait et al, Appl.Phys.Lett.53, 2235 (1988).
9. Yu.L. Khait et al, Appl.Phys.Lett.55, 1170 (1989).
10. Yu. L. Khait , Physica B.139&140, 23'7 (1989) .
11. Abdulhalim et al, Appl.Phys.51, 1170 (1987).
12. Yu.L. Khait., Zs.Phys.B,71, 8 (1988).

**NORMAL MODE ANALYSIS OF OPTICAL POLARISATION RESPONSE  
IN NANOPARTICLE CLUSTERS**

*G.B. Smith and A.J. Reuben*

Applied Physics Department University of Technology, Sydney PO Box 123,  
Broadway NSW, AUSTRALIA <G.Smith@uts.edu.au>

In studying the quasi-static optical response of fine particle clusters and composites techniques which lead efficiently to a normal mode decomposition are shown to be of significant benefit compared to the more conventional approaches which start with the isolated single particle polarisation response. A technique has been developed for establishing the eigen function expansions of the total electrostatic potential based on two distinct coordinate frame systems and appropriate transforms. The development of the structure matrix allows one to determine the value of resonance positions as a function of wavelength for each mode. This will be demonstrated for some important cermet composites in terms of their response at visible and infrared frequencies.

One important observation is that there are many structures for which the fundamental mode is isolated and appears to dominate the response especially when structures have a component with chain like features. Many structures however also have multiple resonances in the range of observation, although overlap of higher order resonances tends to produce a limited number of observable peaks.

**MOLECULAR SIMULATION FOR GAS ADSORPTION ON TiO<sub>2</sub>, RUTILE  
AND ANATASE SURFACES**

*Hsin-Fu Lin<sup>1</sup>, Hong-Ming Lin<sup>1</sup> and Shaw-Ling Hsu<sup>2</sup>*

<sup>1</sup> Dept. of Materials Engineering, Tatung Institute of Technology, Taipei, 104, Taiwan  
*<hmlin@mse.ttit.edu.tw>*

<sup>2</sup> Polymer Science and Engineering, University of Massachusetts, Amherst, MA, USA

To evaluate binding ability of gas adsorbates on TiO<sub>2</sub> (rutile and anatase) particle surface, the molecular simulation is employed to calculate binding energies of gas adsorption on TiO<sub>2</sub> particles. In this study, the simulation for gas adsorption on TiO<sub>2</sub> was performed using the "SORPTION" module in the molecular simulation of Cerius2\_1.6 (Molecular Simulation Inc.). The properties of gas adsorption at the surface of TiO<sub>2</sub> are predicted by Monte-Carlo method. The open force field theory is used to calculate the interaction energies between gas molecules and TiO<sub>2</sub> surface. The results indicate that adsorption property of CO, H<sub>2</sub>S and NO<sub>x</sub> gases on TiO<sub>2</sub> rutile and anatase surfaces can be predicted. Energy analysis shows the energy distribution in the form of number of accepted configurations versus interaction energy. Existence of different energy peaks corresponding to different interaction energies suggests that adsorption of gas adsorbates might occur at various sites at TiO<sub>2</sub> particle surface.

**SYNERGETICS OF NANOSIZABLE STRUCTURES IN METALS  
IN CONDITIONS OF ELECTROSTIMULATED DEFORMATION**

V.A. Petrunin, V.E. Gromov, O.V. Sosnin, V.Ya. Tsellermaer, E.S. Kuchumova, and  
A.V. Gromova.

SibGTU, str. Kirova 42, 654007 Novokuznetsk, RUSSIA

With the growth of the extent degree during the drawing, the channels of deformation localization (CDL) are being formed the evolution of which is followed by the dispersion of fragmented ( subgrained ) structure and by the division of nanostructural particles of iron carbide. The formation of carbide phase as the stabilizing factor for substructures of deformation channels. The physical reason of dispersing the fragmented structure is the decrease of proper stresses ( stabilizing factor ) of fragments dislocations, as the part of stresses is presented by the movable dislocations (the stresses of electron wind).The level of proper stresses in fixed dislocations boundaries of fragments decreases in analogous manner, on which the carbide phase appears. The structure of synergetic theory is close to the scheme of usual phase transitions, therefore, the correlation length for the end sizable system is connected with the correlation length of macroscopic system by ratio  $xL(t)=Lg\{L/x_8(t)\}$  (E. Brezin). The relative correlates in cylindrical configuration have the appearance  $\langle\xi(0)\xi(\tau)\rangle_s \sim m_0 + m \exp(-\tau/\xi_s)$ ,  $\langle\xi(0)\xi(\tau)\rangle_{L \rightarrow \infty} \sim \exp(-\tau/\xi L)$ , where  $\tau$  is axial coordinate, but the correlative length has an appearance as  $\xi L \sim L^2$ ,  $s^{ext} < s_c$ ,  $\xi L \sim L$ ,  $s^{ext} = s_c$ ,  $\xi L \rightarrow \infty \rightarrow \xi_\infty$ ,  $s^{ext} > s_c$  (E.Brezin) ( $s_c$  is the critical stresses of forming the well-regulated states far from equilibrium. Non-equilibrium displacements of the elastic medium for and-sizable structures are the same as for the macrosystem (~ 100 sizes of grain), the correlations length is near the critical point of transformation ( $s^{ext} \geq s_c$ ),  $\xi L \leq L = 10^{-9} m$ ,  $\xi_\infty \leq 10^{-8} m$   $L \rightarrow L_{fr}$  ( $L_{fr}$  is the size of fragment), i.e. due to the end-sizable effects of correlations scale in dislocations structures in the order less (nearly «an atomic level»).

**STRUCTURE TRANSFORMATIONS IN COMPOSITIONS OF COLLOIDAL  
FERROMAGNETIC PARTICLES IN LIQUID CRYSTALS***Andrej Yu. Zubarev and Larisa Yu. Iskakova*

The Ural State University, 51 Lenin Avenue, 620 083 Ekaterinburg, RUSSIA  
<Larisa.Iskakova@usu.ru>

MLC (magnetic liquids on liquid-crystal base) are recently synthesized new type of magnetic systems. They combine peculiarities and properties of liquid crystals with high response to magnetic field as well as with the ability to rearrange cardinally their structure under the action of the field, temperature and other external factors. The known MLC theories are devoted to the systems with low content of colloidal ferroparticles, therefore their magnetic and other interactions were not taken into account. However, in real systems this assumption very often does not hold. Interparticle interactions may induce various transformations in MLS and, therefore, lead to strong modifications of their magnetic, optic, mechanical and other properties. Using statistical analysis, we have constructed thermodynamic model of MLC on a nematic base (ferronematics) with account of magnetic and steric interparticle interaction. The analysis shows that the magnetic interaction of ferroparticles may lead to their condensation and separation of the system on the regions with high and low particle concentrations. This separation is similar to phase transition "gas-liquid". Magnetic field stimulates this phenomenon. We have studied in details phase transitions in thin films of ferronematics when a small film thickness is of principle to us. Under the presence of magnetic field in thin films of liquid crystals the structural phase transition of the 2nd order may occur (it is known as Frederiks transition). The analysis shows that this transition is accompanied by condensation of ferroparticles in the center of a gap. This condensation may be strong and occurs as phase transition "gas-liquid". By this means in thin films of ferronematics Frederiks effect (being the 2nd order phase transition) may stimulate condensation phase transition of the 1st order. We have studied the structure and magnetisation of ferronematics in such a state. Our analysis shows that remagnetisation of thin layers of ferronematics (for example, during Frederiks transition) may be accompanied by the occurrence of non-equilibrium structures. The nematic director in these structures depends periodically on coordinates. If ferronematics director is normal to the gap plane then ferroparticles condensation occurring under the presence of magnetic field may lead to the occurrence of a stable quasi-cylindrical domains stretched along the field (not to separation of the system on two phases). The case of special interest occurs in ferronematics with a frozen non zero magnetisation. Concentration domains in these systems may occur spontaneously. We have estimated critical parameters of domain formation, the dependence of their dimensions, density of their arrangement on the external field, temperature and physical properties of ferronematics.

### **ENERGY AND STRESS FIELDS OF QUASIPERIODIC TILT AND INTERPHASE BOUNDARIES IN NANOSTRUCTURED MATERIALS**

*A.L.Kolesnikova<sup>1</sup>, K.N.Mikaelyan<sup>1</sup>, I.A.Ovid'ko<sup>1</sup> and A.E.Romanov<sup>2</sup>*

<sup>1</sup> Institute of Machine Science Problems, Russian Academy of Sciences, Bolshoj 61,  
Vas.Ostrov, St.Petersburg 199178, RUSSIA <anna@def.ipme.ru>

<sup>2</sup> Ioffe Physico-Technical Institute, Russian Academy of Sciences, Polytechnicheskaya  
26, St.Petersburg 194021, RUSSIA <cromanov@pgpt.ioffe.rssi.ru>

Quasiperiodic tilt and interphase boundaries have been theoretically recognized as structural elements essentially contributing to the properties of nanocrystalline and nanophasse materials, e.g. [1,2]. The stability and the specific role of quasiperiodic boundaries in plastic deformation, relaxation and other processes occurring in nanostructured materials depend on stress-field and energetic characteristics of the boundaries. The main aim of this paper is to calculate the energy and stress field components of quasiperiodic tilt and interphase boundaries in nanostructured materials.

Within the framework of dislocation- and disinclination-structural-unit models [3-6], quasiperiodic tilt boundaries are effectively represented as quasiperiodic sequences of structural units (atomic clusters) associated with grain boundary defects. In this context, the energy and stress field components are calculated here as those of ensembles of grain boundary defects in the boundaries. The dependence of the energetic characteristics of quasiperiodic tilt boundaries on rearrangements of their structural units is revealed.

Quasiperiodic interphase boundaries in nanostructured crystalline film-film and film-substrate systems are studied. The energy and stress field components of such boundaries are calculated here as those of quasiperiodically ordered ensembles of misfit dislocations. The behavioral features of the interphase boundaries, related to quasiperiodicity in translational ordering of their misfit dislocations, are discussed.

- [1] I.A.Ovid'ko, Nanostruct.Mater. 8 (1997) 149.
- [2] I.A.Ovid'ko, In: Nanostructured Materials: Science and Technology, NATO ASI Ser., Edited by G.-M.Chow (Kluwer Acad.Publ., Dordrecht, 1998).
- [3] A.P.Sutton and V.Vitek, Phil.Trans.Roy.Soc.London A 309 (1981) 1.
- [4] A.P.Sutton, Acta Metall. 36 (1988) 1291.
- [5] A.A.Nazarov, A.E.Romanov and R.Z.Valiev, Acta Metall.Mater. 41 (1993) 1033.
- [6] A.A.Nazarov, A.E.Romanov and R.Z.Valiev, Nanostruct.Mater. 4 (1994) 93.

**THERMODYNAMIC BASIS OF FORMATION OF NANOCRYSTALLINE AND AMORPHOUS STRUCTURES BY MECHANICAL ALLOYING***S.D. Kaloshkin, I.A. Tomilin, V.V. Tcherdyntsev*

Department of Physical Chemistry, Moscow Steel and Alloys Institute, Leninsky prosp.,  
4, Moscow, 117936, RUSSIA <iat@phch.misa.ac.ru>

A mechanism of phase formation at mechanical alloying (MA) process based on a thermodynamic model of interaction between components on the interface boundaries is proposed. Binary systems with strongly negative (Ni-Zr, V-Si), close to zero (Fe-Mn, Fe-Co, Fe-Ni) and positive (Fe-Cu, Cu-Co) deviations of mixing enthalpy from the law of ideal solutions were considered. Enthalpy of formation and/or Gibbs energy were calculated for various possible phases of investigated systems. Analysis of driving forces of transformations make it possible to predict a tendency of binary systems to form various structures at MA treatment. The possibility of formation of different phases at MA process, such as amorphous phases, supersaturated solid solutions, and intermetallic compounds was shown. Calculated concentration ranges of phase existence were found to be in a good agreement with experimental results. According to these calculations the final phase composition depends on the temperature (usually from 300 to 700 K) that may be reached in the activation apparatus during MA process. Formation of nanocrystalline structure and, consequently, of very large interface areas between reacting components play a great role in the MA process.

**COMPUTATION OF CAPACITANCES OF Cu<sub>n</sub> NANoclUSTERS**

*P. Senet<sup>1</sup> and M. Hou<sup>2</sup>*

<sup>1</sup> Laboratoire de Physique des Solides, Facultés Notre-Dame de la Paix,  
rue de Namur 61, B-5000 Namur, BELGIUM

<sup>2</sup> Physique des Solides Irradiés CP234, Université Libre de Bruxelles,  
Bd du Triomphe, B-1050 Brussels, BELGIUM

As recently demonstrated for Cu on Au(111) crystal, small metallic clusters can be deposited on a substrate by using a STM in order to form ordered structures [1]. The latter are the precursors of nanodevices with expected unusual electronic transport properties. One of the key factor to understand these properties is the capacitance C of the clusters which is responsible for the well-known Coulomb blockade phenomena. In the present work, this quantity is computed for isolated and assembled Cu<sub>n</sub> clusters (n=2, ..531) by using an atomistic model based on an electron density perturbation theory [2]. The effect of the substrate supporting the nanostructures is described by a dielectric continuum. The equilibrium 0 K configurations of the Cu clusters are evaluated independently by means of heating and cooling cycles modelled classically by molecular dynamics using a tight binding cohesion model [3]. Detail about the method is given. The atomistic calculations of C are compared to much more simple electrostatic approximations the validity of which are thus defined. A good agreement with available experimental data for isolated Cu<sub>n</sub> clusters is obtained.

[1] D. M. Kolb, R. Ullmann and T. Will, Science 275, 1097 (1997).

[2] P. Senet, J. Chem. Phys. 105, 6471 (1996) and in preparation.

[3] G.J. Ackland and V. Vitek; Phys. Rev. B41(1990)10324.

**THE DENSITY OF VALENCE STATES  
OF SMALL DIAMETER CARBON NANOTUBES**

*M. Brjezinskaya<sup>1</sup>, E. Baytinger<sup>1</sup>, V. Kormilets<sup>2</sup>*

<sup>1</sup> Chelyabinsk State Pedagogical University, Lenin av. 69,  
454080 Chelyabinsk, RUSSIA <bmm@cspi.urg.ac.ru>

<sup>2</sup> Physico-technical institute of the Urals branch of Russian Academy of Science,  
Kirov st. 132, Izhevsk 426001, RUSSIA <uufti@fti.udmurtia.su>

The results of electronic structure study for zigzag carbon tubes (3,3) and (4,4) with the diameters relatively 4.16 and 5.46 Å are presented. The number of hexagons along these tube cross-section perimeter is 6 for (3,3) and 8 for (4,4) tubules. Z-coordinate axis coincides with the axis of the tube and x-axis directed along its radius.

Energy bands of nanotubes are calculated by self-consistent full potential linear muffin-tin-orbital method (FP-LMTO) [1]. Band structure of graphene sheet as a testing object was also calculated.

Energy variation of graphite monolayer DOS N(E) well agrees with the known data both for valence and conduction bands. The total valence bandwidth (about 20 eV) also corresponds to the proceeding experimental and theoretical results.

The total valence bandwidth of tubulene (19 eV) is practically the same as that of graphite. This is also true for all carbon structures. The dominant DOS maximum for (3,3) and (4,4) tubules arises due to  $p_x$ -states that can be called  $\pi$ -states analogous to  $\pi$ -electrons of graphite. This feature clearly shifts to the valence band top when the tube diameter diminishes that testifies to the valence electron hybridization mode change.

The conduction states near Fermi level are also sensitive to the folding of graphene sheet in a tube. The energy gap for zigzag (3,3) and (4,4) nanotubes is absent though it is observed in atomic local DOS. The latter is calculated at each of the atoms forming an extended unit cell. The gap of 0.5 eV width exists in local DOS of one of the two adjacent atoms of the cell in  $\bar{A}M$  direction of graphene sheet Brillouin zone. In a case of axial conductivity this effect may cause in a chiral motion of charge carriers.

[1] Weyrich K.H. Phys.Rev. 37, 10269 (1988).

### SURFACE TENSION OF ULTRAFINE PARTICLES

*M.I. Alymov and M.Kh. Shorshorov*

Baikov Institute of Metallurgy of Russian Academy of Sciences,  
Leninsky prospect 49, Moscow 117334, RUSSIA <alymov@lesr.imet.ac.ru>

The consideration of an ensemble of small systems is the main idea of the thermodynamics of small systems worked out by T.L.Hill. The difference between the thermodynamics of disperse systems and macroscopic thermodynamics is in the account of an additional degree of freedom dealt with the size of small system (where a small system is a fine particle). In that case the thermodynamic potential is a function of temperature, pressure and system size. Considering the melting of a fine particle consisting of n atoms, we received

$$s_{sl} = a^{-1} W^{-2/3} N_a^{-1} D H_s n^{1/3} (1 - T_m/T_s) \quad (1)$$

$$s_{sg} = 1.5 a^{-1} W^{-2/3} N_a^{-1} D H_s n^{1/3} (1 - (1 + a n^{-1/3})^{-1} T_m/T_s) \quad (2)$$

where  $T_s$  is the melting temperature of massive material,  $T_m$  is the melting temperature of the ultrafine particle,  $DH_s$  is the melting enthalpy of a mole of the material,  $N_a$  is Avogadro number,  $s_{sl}$  is the solid-liquid surface tension,  $s_{sg}$  is the solid-gas surface tension,  $W$  is an atom volume and  $a$  is the coefficient of particle shape.

The values of  $s_{sl}$  and  $s_{sg}$  for the particles of large size are equal to the same values for massive material. Then, using the experimental data for  $T_m$ , a melting temperature of particles with big radius  $R$ , and  $s_{sl}$  for massive state, we receive  $h$  - the ratio of particle diameter to its height. For example, calculations by equation (1) showed that  $h$  for Sn and Au is equal to 3.5 and 3.0, respectively.

Particles radius  $R$  dependencies of the melting temperature and of the surface tension for ultrafine particles are discussed. The results show that  $s_{sg}$  does not depend on particles size, but  $s_{sl}$  increases, and  $s_{lg}$  decreases as particle size decreases for particles with radius less than 10 nm.

**RECOVERY OF THE EXCESS VOLUME IN ULTRAFINE-GRAINED MATERIALS PRODUCED BY SEVERE PLASTIC DEFORMATION***A.A. Nazarov and R.Sh. Musalimov*

Institute for Metals Superplasticity Problems, Russian Academy of Sciences,  
39 Khalturin str., Ufa 450001, RUSSIA <airat@imspphys.bashkiria.su>

The production of ultrafine-grained (UFG) structure in metals and alloys by severe plastic deformation occurs in extremely non-equilibrium conditions and means the introduction of a high density of point and linear defects in material. Recent experimental studies show that the linear defects mainly accumulate in grain boundaries.

The defects and their elastic fields cause different non-linear effects, which are considered to be the origin of modified properties of UFG materials. One of these effects is the excess volume of UFG materials, which is the object of study in the present paper.

Recent studies of UFG nickel and aluminum alloy by a dilatometric method have shown that during the annealing of as-prepared samples the sample lengths decrease with time at a constant annealing temperature. These experiments are carried out on UFG copper samples prepared by the torsion straining under high pressure. The dependence of the samples' length on annealing time is obtained for a range of temperatures.

The data of early and present experiments are interpreted in terms of the recovery of non-equilibrium dislocation ensembles in GBs taking account for the annealing of non-equilibrium vacancies and grain growth.

Relaxation laws and characteristic relaxation times are calculated for the three types of non-equilibrium dislocation arrays in GBs which are formed during preparation: disordered extrinsic grain boundary dislocation (EGBD) networks, dipoles of triple junction disclinations and ensembles of gliding EGBDs. Formulae are obtained which allow calculating the excess volume of polycrystal due to these defects. The relaxation laws for GB defects complemented with the analysis of vacancy annealing and the grain growth effect allowed to calculate the dependence of UFG sample length on time for the temperatures used in experiments. For the whole range of temperature good agreement is obtained between the theoretical relaxation curves and the data of dilatometric experiments.

This agreement allows to conclude that the structural model of UFG materials produced by severe plastic deformation according to which the properties of these materials are due to the high elastic strains induced by non-equilibrium EGBD arrays can be used for the quantitative study of the properties of UFG materials.

---

**THEORETICAL INVESTIGATION OF THE MICROSCOPICAL  
STRUCTURE SEMICONDUCTOR/THIN METAL FILM  
INTERNAL INTERFACE WITH NANOMETER RESOLUTION**

*L.G. Il'chenko<sup>1</sup> and V.V. Il'chenko<sup>2</sup>*

<sup>1</sup> Institute of Surface Chemistry, Pr. Nauki 31, NAS of Ukraine,  
Kiev 252028, UKRAINE

<sup>2</sup> Radiophysical Dept., Kiev University, Volodimirska st. 64,  
Kiev 252033, UKRAINE <vai@rpd.univ.kiev.ua>

The methods of the experimental investigation "scanning tunnelling microscopy" (STM), "atom force microscopy"(AFM) etc. offered the possibility of direct, real space determination of the surface structure. The result is essentially a contour map of the concrete surface in the external electric field. In the case of the contact between two solids (in the part, between semiconductor and metal) the potential barrier at the interface determines the bulks' properties of the contactive media and very sensitive to the preparation conditions. The last investigations with using the new technique known as ballistic electron emission microscopy (BEEM) shown the nanometer scale lateral variation of the potential relief of the internal interface for the semiconductor/thin metal film structure (in fact the lateral variation of the Schottky barrier (SB) height). In the case of the macroscopically homogeneous interface the nanometer scale lateral variation of the SB height can't be to understand in the framework of the introduction classical point of view.

In this report in the framework of nonlocal electrostatics the theoretical model for a semiconductor/thin metal film junction is proposed. The solution of this problem is found with using the Green function method of nonlocal Poisson equation taking into account the macroscopically (screening) properties of the metal and semiconductor and microscopically structure of the interface simultaneously. It is supposed that the double electric layer in the case of the ideal and macroscopically homogeneous contact is formed by chemical bounding at the interface. The potential barrier (SB) and its lateral change along an interface depending on a nature of chemical bounding and its two-dimensional concentration in limit of one monolayer is designed. It was shown that the electronic structure of the coating thin metal film has a large influence on the SB formation and on the amplitude of the potential relief along the interface. A possibility of potential relief obtaining of intimate contact between two media with taking into account external voltage (image of the internal interface) is discussed.

It is a pleasure to thank F.Cardon, R.van Meirhaeghe and D.Puelman of the Laboratory of Solid State Physics, Gent University (Belgium) for numerous fruitful discussions. One of us (LGI) would like to thank the NATO Scientific Committee for financial support of this work according to NATO Fellowship Grant # P61.1-90/A/02.03/96/551.

**WATER-OXIDE INTERFACIAL TENSION MODELLING & GROWTH  
CONTROL OF SPINEL IRON OXIDE NANOPARTICLES**

*Lionel Vayssières, Jean Pierre Jolivet and Jacques Livage*

University Pierre & Marie Curie, Chimie de la Matière Condensée,  
75252 Paris Cedex 05, FRANCE <[swlva@fki.uu.se](mailto:swlva@fki.uu.se)>

The ability to control the particle size and morphology of nanoparticles is of great importance in view of the rising high-tech applications of nanostructured materials. Achievement of this goal will be reached providing that better fundamental understanding of the thermodynamic and kinetics of nucleation, growth and ageing phenomena involved in the synthesis stage is available.

The major parameter to assess is the interfacial free energy of the system. A model based on Gibbs adsorption equation attempt to quantify the variation of the interfacial tension with the chemical composition of the interface and the dispersion conditions. Proton (or hydroxyl) ions surface adsorption does increase the surface charge density yielding to the lowering of the water-oxide interfacial tension of the system. At maximum surface charge density, i.e. when the surface is electrostatically saturated, the interfacial tension is expected to drop sufficiently allowing the system to attain thermodynamic stability. Assuming a zero interfacial tension at equilibrium, a quantitative treatment is given, yielding to the stability conditions of the system. In the stable area, limited by the PZIT (point of zero interfacial tension), the particles are foreseen to be stabilised and consequently secondary growth phenomenon such as Ostwald ripening is unlikely to occur. Therefore, the size of the particle is expected to be directly related to the precipitation conditions such as pH and ionic strength.

Experimental investigations were carried out on aqueous precipitation of Magnetite ( $\text{Fe}_3\text{O}_4$ ) performed at room temperature. The results showed that thermodynamic stability of nanoparticles may be achieved and that the average particle size may be monitored over an order of magnitude showing narrow size distribution. The excellent agreement between theoretical modelling and experiments yields strong evidence for efficient growth control of metal oxide nanoparticles under low interfacial tension conditions and draws good expectations for future development of nanomaterials and optimisation of their fascinating physical properties.

**BAND GAP CALCULATION OF THIN Si POLYCRYSTALLINE FILMS**

*S.Ménard, A.Saúl, F.Bassani and F.Arnaud d'Avitaya*

Centre de Recherche sur les Mécanismes de la Croissance Cristalline - CNRS,  
Campus de Luminy, case 913, 13288 Marseille Cedex 9, FRANCE

Since the discovery of visible room temperature photoluminescence in porous silicon, many other light-emitting Si-based materials have been fabricated. In 1993 we synthesized a light-emitting Si/CaF<sub>2</sub> multilayers with optical properties similar to oxidized porous silicon. Our Si layers are composed of nanocrystalline grains and present photoluminescence for layer thickness less than 30Å. Absorption measurements performed on these multilayers have shown a large blue-shift of the optical gap with decreasing Si layer thickness, suggesting quantum confinement of the electronic states.

To take into account the polycrystalline character of the Si layers, we have performed tight binding calculations of thin Si films formed of nanocrystalline grains. By varying layer thickness and grain size from 5 to 20Å, we point out that the crystalline quality of the films as well as distance or disorientation between grains, play an important role on the band gap value. The grain structure of the films tends to increase the gap due to increasing carrier confinement. On the opposite, the overlap of the wavefunctions between adjacent grains decreases confinement. We will discuss the importance of the polycrystalline nature of the films in the optical band gap deduced from absorption measurements.

**ATOMIC-SCALE SIMULATIONS OF NANOCRYSTALLINE METALS**

*J. Schiøtz, T. Vegge, F.D. Di Tolla and K.W. Jacobsen*

Center for Atomic-scale Materials Physics (CAMP) and Department of Physics,  
Technical University of Denmark, DK-2800 Lyngby, DENMARK  
[<schiotz@fysik.dtu.dk>](mailto:<schiotz@fysik.dtu.dk>)

Nanocrystalline metals are known to exhibit mechanical properties that are different from (and often superior to) conventional metals, e.g. increased hardness and fracture toughness. We present atomic-scale simulations of the deformation process in nanocrystalline copper using molecular dynamics and realistic many-body potentials. Since we can follow the position and motion of dislocations and grain boundaries, we are able to observe the deformation process directly.

In conventional materials the hardness and yield stress is known to increase with decreasing grain size (the Hall-Petch effect). In our simulations, we observe a *reverse* Hall-Petch effect for grain sizes from 3 to approximately 10 nm, i.e. the metal gets softer when the grain size is reduced. This is in agreement with some experiments, although the experimental situation is not unambiguous, mainly due to the difficulties of preparing samples without microscopic voids. In the simulated materials the reverse Hall-Petch effect is caused by increased deformation in the grain boundaries as the grains get smaller. This grain boundary sliding is the dominating deformation mechanism for grain sizes below 5-10 nm. For materials with larger grains the conventional dislocation-based deformation mechanism is expected to take over.

**TO WHAT EXTENT A CRYSTAL CAN BE SUPERHEATED?**

*Z.H. JIN and K. LU*

State Key Lab of Rapidly Solidified Non-equilibrium Alloys, Institute of Metal  
Research, Chinese Academy of Sciences, Shenyang 110015, CHINA  
[<zhjin@imr.ac.cn>](mailto:zhjin@imr.ac.cn)

Many efforts have been paid recently in understanding the mysteries of superheating behaviours of crystals. However, it seems that a more unified theoretical understanding is still needed. We studied the superheating and melting behaviour of constraint and unconstraint metallic clusters and thin-film crystals using Molecular Dynamics (MD) simulations via many-body type interatomic potentials. For free clusters, the melting points are depressed with decreasing the cluster size. For thin-film crystals with free surfaces, melting occurs anisotropically in analogy with those free surfaces of bulk solids. For constraint cases, heterogeneous nucleation sites of the liquid phase, such as free surfaces or interfaces can be suppressed and melting points of the embedded clusters and confined thin-film crystals can be elevated. The MD data are found to be in reasonable agreement with the relationship between the size and the degree of superheating predicted using the homogeneous nucleation theory. In strengthening the constraint conditions, such as by limiting the nucleation size to be small enough, the melting point can be significantly elevated to and even beyond the upper-limit predicted using other thermodynamic or mechanical models.

**THE SIMULATION OF CHARGE TRANSPORT  
IN THE NANOSTRUCTURE "CAMEL" AND HETEROTRANSISTORS**

*A.S. Bugaev, S.M. Korshunov, S.D. Kuzmichev and V.E. Sorokoumov*

Moscow Institute of Physics and Technology, Dolgoprudny,  
Moscow 141700, RUSSIA <bugaev@quant.fke.mipt.ru>

The progress in modern semiconductor microelectronics stimulates the development of electron device models that take into account many physical processes taking place in such devices. The study of charge transport in semiconductor nanostructures is of fundamental importance, both from the point of view of basic physics and its application to electron devices. The applied aspect of the problem is even more important, since modern electronics depends heavily on sophisticated knowledge of many aspects of charge transport in semiconductors.

The main characteristics of camel- and heterotransistors are determined by peculiarities of transport of non-equilibrium ("hot") electrons in active region of the device. In this area hot electrons are injected from the emitter through the potential barrier at the boundary between the emitter and the base.

Classical kinetic equations for one-particle distribution functions of electrons are used for describing non-equilibrium processes in electron-hole plasma under the influence of self-consistent electric field. Coupled collisions are not taken into account. Character times of nonstationary processes in investigation are chosen much less the times determining generation-recombination processes. The generation-recombination members are omitted in kinetic equation, The scattering of electrons on phonons and impurities are assumed to be three-dimensional and are simulated by Monte-Carlo method. Charge carrier equilibrium equations are solved by the method of stochastic dynamic of macroparticles.

Boundary conditions for equations are determined by the injection and reflection properties of different parts of the boundary and by the electrodes potential and zero normal derivative of potential at the other parts of boundary where the electrodes are absent. Initial conditions are chosen from the condition of quasineutrality in the emitter, base and collector areas.

The investigations of the dynamic operation and optimization of the parameters of nanostructure camel and heterotransistors were carried out. The scientific and applied software package was created for the numerical simulation of nanostructure semiconductor devices by ensemble Monte-Carlo particle method.

**QUANTUM-CHEMICAL TECHNOLOGY OF NANOS**

*E.F.Sheka<sup>1</sup>, V.D.Khavryutchenko<sup>2</sup>, E.A.Nikitina<sup>3</sup>*

<sup>1</sup> Russian Peoples' Friendship University, Moscow, RUSSIA

<sup>2</sup> Institute of Surface Chemistry, National Ac.Sci of the Ukraine, Kiev, UKRAINE

<sup>3</sup> Institute of Applied Mechanics, Russian Ac.Sci., Moscow, RUSSIA

An overlook of what can be done today by a modern quantum chemistry with respect to technologically important nanos is presented. The approach employs semi-empirical SCF LCAO MO methods sophisticatedly developed for supercluster model systems containing up to 999 atoms. A supercluster design is aimed at reproducing a structurally complete fragment of a nanosystem under study and is governed by a "certificate of origin" covering the most distinctive marks of the system. Quantum-chemical (QCh) computations imply both the minimum-energy optimization of the model supercluster structure and the vibrational spectrum determination. The latter is used as the calculation verification on the basis of a comparative study of the calculated and experimental data. A solution of an inverse spectral problem and thus obtaining a corrected force field can be performed if necessary. Particular QCh tools can be used as well to tackle a response of a nanoobject to the application of either an external mechanical stress or an electric field of an arbitrary configuration. The approach lays the foundation for a modern QCh technology of nanos widely differing in chemical composition and structure. It turned out to be extremely fruitful for different kinds of nanoobjects among which there are:

- fine particles of metals, semiconductors, and dielectrics, their bulk and surface properties;
- fine particle modified surfaces, particularly interesting from a viewpoint of an intermolecular interaction occurred on interfaces joining the particle and surrounding;
- surface unit cells of nonreconstructed as well as reconstructed surfaces such as Si(111) and Si(001);
- atomically modified surfaces under an STM tip involving adding and subtraction of atoms from them ;
- nanohills with predetermined properties controllably grown on a substrate by using STM tip, and others.

Technological polymorphism of both bulks and surfaces, chemically stimulated structural phase transition, STM tip induced chemical reactions, ferromagnetism of the Si(111)7x7 surface, a peculiar depth-profile of a chemical activity in homonuclear nanospecies - those are far from being completed list of distinct peculiarities of the nanoobjects studied. Being hardly predicted form a common-sence viewpoint, the findings are direct products of the QCh technology used exhibiting extraordinary possibilities of the latter in the nanos world.

**MAGNETIC ANISOTROPY STUDY IN NANO-SIZED Ni AND Ni/Cu FILMS**

*Y.D. Yao, Y. Liou, S.F. Lee, C. Y. Wu, Y.Y. Chen, G.Z. Huang, H.G. Shiang,  
W.T. Kang, and J.J. Lin*

Institute of Physics, Academia Sinica, Nankang, Taipei 115, Taiwan  
Department of Physics, National Chiao Tung University, Hsinchu 300, Taiwan

Nano-sized Ni and Ni/Cu films with Ni thickness between 1 and 8 Å were prepared by both MBE and evaporation techniques; and Ni and Ni/Cu films with Ni thickness of a few hundred Å were prepared by sputtering technique. Magnetic anisotropy effect was studied with films after annealing below 600 K by SQUID measurement. For thicker Ni films, a shifted magnetic hysteresis loop and a slope change in saturation magnetization were observed below roughly 50 K for properly annealed Ni films. This is analyzed by the effect of exchange anisotropy interaction between the interfaces of the ferromagnetic region and the thin layers of antiferromagnetic oxidized layer formed during annealing. For nano-sized Ni and Ni/Cu films, their magnetoresistance was studied as functions of temperatures between 0.4 and 21 K, and magnetic fields up to 1 T. The thickness of Cu layer for all the samples was kept at 100 Å; and the thickness of the Ni underlayer was varied between 1 and 8 Å. Our experimental data show that the low temperature magnetoresistance of the Cu/Ni films with very thin Ni underlayer behaves more positively than that of Cu films. After analyzing with the weak-localization theory, we have experimentally demonstrated that no magnetic moments are formed in Ni/Cu films with the thickness of Ni underlayer less than 2 Å. We also show that the weak-localization effect is very sensitive to the existence of magnetic moments in the Ni/Cu film system.

**SELF-ASSEMBLY AT THE AIR-WATER INTERFACE:  
IN-SITU PREPARATION OF THIN FILMS  
OF METAL ION GRID ARCHITECTURES**

*Isabelle Weissbuch, Meir Lahav, Leslie Leiserowitz*

Department of Materials and Interface, The Weizmann Institute of Science,  
76100-Rehovot, ISRAEL

The formation, at the air-aqueous solution interface, of thin crystalline films, one to several layers thick (~2-20 nm), of water-insoluble molecules has recently been reported.<sup>1</sup> Thin films of more complex architectures have been generated by the interaction between the insoluble component and various salutes from the subphase. We address whether this approach can be extended to supramolecular multicomponent systems of the form of racks, ladders, grids and cages, in which the coordination array is assembled from either tridentate ligands and octahedral metal ions or from bidentate ligands and tetrahedral metal ions.<sup>2</sup>

We envisaged that spreading the free ligand *L* molecules onto the surface of an aqueous solution containing metal ions could lead to the formation of the grid complex at the air-water interface. Once formed, the complex cations with counterions (that make the salt insoluble in water) would self-assemble into crystalline domains of structure akin to that of the macroscopic crystal. A lateral aggregation process being favored at interfaces, the resulting structure must contain a small number of layers.

Oriented crystalline films, ~11-20 Å thick, of metal ion complexes of the grid type  $[Co_4L_4]^{8+} \cdot 8PF_6^-$  and  $[Ag_9L_6]^{9+} \cdot 9CF_3SO_3^-$ , based on various organic ligands *L*, were prepared *in-situ* at the air-aqueous solution interface. The structure of the complex architectures composed of a 2x2  $Co^{2+}$  and a 2x2  $Ag^+$  grid coordinated to four ligand molecules and a 3x3  $Ag^+$  grid coordinated to six ligand molecules, as well as their molecular organization in thin films were characterized by grazing incidence synchrotron X-ray diffraction and specular X-ray reflectivity measurements performed at the air-aqueous solution interface and by UV, X-ray photoelectron spectroscopy and scanning force microscopy after film transfer onto various solid supports. Such films prepared by self-assembly and transferred to solid surfaces may be of interest for microelectronic technology.

- [1] I. Weissbuch, R. Popovitz-Biro, M. Lahav, L. Leiserowitz, K. Kjaer and J. Als-Nielsen, in: Advances in Chemical Physics, Eds. S. Rice and I. Prigogine, Publ. J. Wiley, New York, **102**, 39-121 (1997).
- [2] J.M. Lehn, Supramolecular Chemistry Concepts and Perspectives, VCH, Weinheim, Germany (1995).

**SUPERCONDUCTIVITY REENTRANCE IN STRONG MAGNETIC FIELDS  
IN Mo/Si MULTILAYERS**

*N.Ya. Fogel, M.Yu. Mikhailov, O.I. Yuzephovich, Yu.V. Bomze and B. Verkin*

Institute for Low Temperature Physics and Engineering, 47 Lenin Avenue,  
310164 Kharkov, UKRAINE <fogel@ilt.kharkov.ua>

Novel reentrance phenomenon is discovered in Mo/Si multilayers which is connected with the nanoscale 1D periodic structure of the system investigated. Reentrance behavior is detected by the resistive method. It occurs in the magnetic fields  $H$  parallel to the layer planes. At some temperature corresponding to the fitting of the vortex cores within semiconducting interlayers a minimum (or a series of minima) appears on resistivity  $R$  vs  $H$  dependence. At lower temperatures the minimum becomes more pronounced and at last transforms into a large zero resistance region (ZRR). After ZRR in the higher magnetic fields the resistance reappears again. In-plane critical current  $J_c$  is the oscillating function of  $H$ , and all the features of  $R$  vs  $H$  and  $J_c$  vs  $H$  dependences are closely correlate.

Reentrance behavior is connected with the influence of the intrinsic pinning and with the specifics of the vortex lattice (VL) structure in layered superconductors. The positions of minima and ZRR depend on the multilayer wavelengths  $s$  and correspond to the stable configurations of commensurate VL's (i.e. VL with the distance between vortices in the orthogonal to the layers direction  $L=N_s$ ;  $N$  is an integer). The experimental data are in quantitative agreement with Ivlev, Kopnin, Pokrovsky theory [1] considering VL structure in the case of a strong intrinsic pinning. Along with ZRR the additional features are often observed on the resistive curves which may be connected with VL metastable states which are dynamically accessible at the  $H$  variation [1, 2]. Hysteretic behavior of ZRR states is also discussed.

1. B.I.Ivlev, N.B.Kopnin, V.L.Pokrovsky, J. Low Temp. Phys. 80, 187 (1990).
2. L.S.Levitov, Phys. Rev. Lett. 66, 224 (1991).

**OPTICAL TRANSMITTANCE OF SEMICONTINUOUS GOLD FILMS**

*N.L. Dmitruk, M.M. Dvoynenko, A.V. Goncharenko, V.R. Romaniuk and E.F. Venger*

Institute of Semiconductor Physics NAS of Ukraine  
Prospect Nauki 45, Kyiv-22, 252650, UKRAINE <avg@isp.kiev.ua>

We deal with ultrathin gold films deposited onto the glass substrates by the thermal evaporation in vacuum. The film thickness at any substrate point depends on the angle of deposition. Thus a sample may be represented as the wedge like strip. The sample preparation conditions were selected so that one end of the strip displayed the metallic behaviour, while another end displayed dielectric behaviour. Between these two ends the percolation threshold was placed whose position was found from the electrical measurements.

We measured film transmittance at fixed light wavelengths in the range of 0.63 - 3.3  $\mu\text{m}$  scanning along the strip. We interpret quantitatively the optical film transmittance by the modified Bruggeman's symmetrical theory that is based on the assumption that our system has a decreased dimension near the percolation threshold. Thus we take into account that this dimension depends on the filling factor (the surface coverage parameter). According to our results an adequate description of the gold film transmittance spectra as a function of the filling factor is possible using our model in a wide range, including the percolation threshold.

## SYNTHESIS OF THIN MOLECULAR SIEVE FILMS

*Jonas Hedlund and Johan Sterte*

Division of Chemical Technology, Luleå University of Technology,  
971 87 Luleå, Sweden <joh@km.luth.se and jost@km.luth.se>

A method which can be used to synthesise thin films of molecular sieves on various supports employing pre-seeding of the substrates has been developed. The method is exemplified by the synthesis of silicalite-1 films on silicon wafers and carbon fibbers, zeolite NA films on alumina wafers, and ZSM-5 films on gold substrates.

The substrates surfaces are first modified to enable adsorption of molecular sieve nano seed crystals from a pre-synthesised and purified sol. Substrates with a negative surface charge at high pH are charge reversed by adsorption of cationic polymer molecules to obtain a positive surface charge. In the case of gold substrates, the gold surface is first silanised by reaction with  $\gamma$ -mercaptopropyl-trimethoxysilane followed by hydrolysis, thus creating a surface with negative charge at high pH. Cationic polymer molecules are then adsorbed on this surface to obtain a positive surface charge in the same manner as with silicon and alumina substrates. Negatively charged nano seed crystals are adsorbed on the modified substrates from a sol with high pH in one or several steps to obtain a monolayer. The adsorbed seed crystals are induced to grow in a synthesis solution at elevated temperature to form a dense and continuous film. The film thickness is controlled by the duration of the treatment with the synthesis solution. Repeated treatment in synthesis solutions can be utilised to further increase the film thickness.

Silicalite-1 seed crystals with an average size of 50 nm were adsorbed on charge reversed silicon wafers. Dense silicalite-1 films with a thickness ranging from 100 to 1000 nm were obtained by treatment of the seeded substrates in a synthesis solution during 10 to 120 h. Hollow fibbers of silicalite-1 were obtained by first synthesising a silicalite-1 film on charge reversed and seeded carbon fibers followed by removal of the carbon fiber support by calcining in air at 600°C

Dense zeolite NA films on alumina supports with film thickness of 320, 520 and 800 nm were synthesised by treatment of seeded supports with a synthesis solution during 7 h in one, two or three synthesis steps, respectively. ZSM-5 films were synthesised by adsorption of 90 nm ZSM-5 seeds on gold substrates modified by silanisation, hydrolysis and charge reversal. Films with a thickness of about 200-250 nm were obtained by treatment of the seeded support in a synthesis solution.

The versatility of the method described, allowing for preparation of thin, and in some cases, ultra thin films of a number of zeolites on various supports, may be of great value in the development of molecular sieve membranes, chemical sensors and other potential application areas. Supported films synthesised by the method have been tested in sensor applications, the adsorption of vapours has been studied both with spectroscopic ellipsometry and with QCM devices.

**SILVERED POLYIMIDE FILMS WITH HIGH REFLECTIVITY**

A. Syzdykova<sup>1</sup>, S. Kudaikulova<sup>1</sup>, G. Boiko<sup>1</sup>, B. Zhubanov<sup>1</sup>, M. Buranbaev<sup>2</sup>, G. Atanbekova<sup>2</sup> and K. Zhumanov<sup>2</sup>

<sup>1</sup> Institute of Chemical Sciences, 106 Valihanov, 480100 Alma-Ata, KAZAKSTAN  
<adm@chem.academ.alma-ata.su>

<sup>2</sup>Physical department of Kazak National State University, Alma-Ata, KAZAKSTAN

The use of metallized reflectors with polymer substrate as solar energy concentrators with high electroconductivity to dissipate charge can significantly reduce the weight and fragility of such mirrors and provide greater flexibility of packaging for subsequent deployment in space application.

In this work we present the results on development of relation between chemical conditions of metallization of polyimide (PI) films by silver, their structure and optical properties. The process of metallization has been conducted by heterogeneous method and consists of three steps: hydrolysis, chelating of modified film by Ag<sup>+</sup> cations, reduction of metal. Hydrolysis step provides thickness of metal incorporation into the film and size of nanoporous. Increase of hydrolysis duration and inclusion of organic solvent into the mixture leads to increase of porous size. Reduction PI/Ag<sup>+</sup> films was carried out by NaBH<sub>4</sub>. Opposite to organic reducing agents sodium borohydride because of high reduction potential (-1,24 V) allows to reduce metal in the bulk of polymer matrix and to obtain strong metal coating. Preliminary complexing of chelated films and NaBH<sub>4</sub> with different ligands allows increasing surface electroconductivity (up to 10<sup>4</sup> S/cm) and reflectivity of thus metallized films.

Films were investigated by X-ray diffraction spectrometry and reflection of the surface was measured at 74° relative incident light of 531 nm (the most intense wavelength of solar radiation). Reflectivity of optical mirror was taken as 100%. Correlation between size of silver nanoparticles and reflectivity coefficient (R%) is as follows:

N <sub>film</sub>	maximum reflectivity, λ nm	R, %	diameter of Ag particle, nm
1	490	38	5,8
2	500	45	8,5
3	505	80	11,3
Optical mirror	508	100	

Films 1 and 2 were obtained at different hydrolysis conditions. Film 3 was prepared by partial reverse diffusion of Ag<sup>+</sup> cations of the film 2 followed by their reduction on the surface of the film. As it seen from these data maximum of reflection shifts to the short-wave region along with decrease of size of incorporated silver nanoparticles. Film 1 is partly transparent and polarizes light. This phenomenon is under investigation at present time.

Thus it can be concluded that at equal conditions of heterogeneous modification of PI films high indexes of surface conductivity and reflectivity are determined by the process of reverse diffusion of metal to the surface.

**INTERLAYER COUPLING IN Mo/Si MULTILAYERS**

*E.I. Buchstab<sup>1</sup>, N.Ya. Fogel<sup>2</sup>, M.Y. Mikhailov<sup>2</sup>, A.S. Sidorenko<sup>3</sup>, O.I. Yuzephovich<sup>3</sup>*

<sup>1</sup> Department of Physics and Solid State Institute, Technion,  
Haifa, ISRAEL <phr32eb@tx.technion.ac.il>

<sup>2</sup> Institute for Low Temperature Physics and Engineering, 47 Lenin Avenue,  
Kharkov, UKRAINE <juzephovich@ilt.kharkov.ua>

<sup>3</sup> Institute of Physics, University of Karlsruhe, Karlsruhe, GERMANY  
<asidoren@fphws01.physik.uni-karlsruhe.de>

Anomalous oscillatory behaviour of superconducting and kinetic parameters has been discovered on Mo/Si multilayers (ML) with a constant Si layer thickness and variable Mo layer thickness  $d$  [1]. The most nontrivial effect among all phenomena mentioned is the oscillating behaviour of the anisotropy parameter  $G$  and of the interlayer coupling strength at the constant thickness of Si layers [2].

Here the interlayer interaction was determined by additional method involving simultaneous measurements of magnetoresistivity above  $T_c$  in magnetic fields parallel and orthogonal to the layers. It allows one to determine the effective thickness of the metal layer  $L$  characterizing interlayer interaction, which is due to the electron tunnelling through barrier [3]. Measurements have been carried out on two series of Mo/Si MLs, one with constant Si layer (25Å) and variable Mo layer thickness and another with constant Mo layer (22Å) and variable Si layer thickness. It appeared that on the first series the  $L$  value oscillates with  $d$  variation too, and oscillations of the both characteristics,  $L$  and  $G$  obtained in the normal and in the superconducting states, correlate closely. The tunnel (Josephson) nature of the interlayer coupling is confirmed by the data obtained on ML series with variable Si thickness. In accordance with the expectations Josephson coupling parameter as well as effective thickness  $L$  depend exponentially on the interlayer distance, tunnel length being about 4Å.

1. E.I.Buchstab, V.Yu.Kashirin, N.Ya.Fogel, V.G.Cherkasova, V.V.Kondratenko, A.I.Fedorenko, and S.A.Yulin, Fiz.Nizk.Temp. **19**, 704 (1993) [Low Temp. Phys. **19**, 506 (1993)].
2. N.Ya.Fogel, O.G.Turutanov, A.S.Sidorenko, E.I.Buchstab, Phys. Rev. B **56**, 2372, 1997.
3. B.L.Altshuler and A.G.Aronov, Modern Problems in Condensed Matter, ed. by M.Pollak and A.L Efros (North-Holland, Amsterdam, 1985), p.1.

---

**ONE PHONON RESONANT RAMAN SCATTERING  
IN QUANTUM WIRES AND FREE STANDING WIRES**

*R. Riera<sup>1</sup>, J.L. Marín<sup>1</sup>, J.M. Bergues<sup>2</sup>, and R.Betancourt-Riera<sup>2</sup>*

<sup>1</sup>Centro de Investigación en Física, Universidad de Sonora, Apdo. 5-088,  
83190 Hermosillo, Sonora, MÉXICO

<sup>2</sup>Departamento de Física de la Universidad de Oriente, 90500, Santiago de Cuba,  
CUBA

The differential cross section (DCS) for an electron Raman scattering (ERS) process in a semiconductor quantum wire (QW) and free standing wire (FSW) of cylindrical geometry is calculated for T = 0K and regarding phonon-assisted transitions. We have given a complete description of the phonon modes of cylindrical structures embedded in another material, which includes a correct treatment of the mechanical and electrostatic matching condition at the surface. We consider the Frohlich interaction and illustrated the theory for GaAs/AlAs system. Electron state are considered assuming complete confinement within the QW. We also assume single parabolic conduction and valence bands. The emission spectra are discussed for different scattering configurations. We study selection rules for the processes. Singularities in the spectra are found and interpreted. The one phonon Raman scattering and ERS studied here can be used to provide direct information about the electron band structured of the system.

**MAGNETIC ORDERING IN TWO-DIMENSIONAL TITANIUM- AND IRON-OXYGEN NANOSTRUCTURES ON DIAMAGNETIC MATRIX**

*N. Bobrysheva, M. Osmolovski and V. Smirnov*

Department of Chemistry, St.Petersburg State University,  
St.Petersburg 198904, RUSSIA <smirnov@moss.pu.ru>

Possibility of magnetic ordering realization in ultra thin layers (3–15 Å) of Ti–O and Fe–O groups on silica, obtained by the method of molecular layering (ML-ALE), is considered in the present work. Magnetic susceptibility of the samples was measured at varied magnetic field strength within the temperature interval 90–290 K.

Studying of magnetic susceptibility of two-dimensional Fe–O and Ti–O nanostructures allowed us to observe unmonotonous dependences of susceptibility on the amount of metal-oxygen groups deposited on the silica. For the samples with various content of Fe–O group in the surface layer (consequently, with various degree of filling of the surface ( $\theta$ ) 0.01, 0.22, 0.4, 0.75, and 1), it was estimated that dependence of magnetic susceptibility on Fe–O groups content in a monolayer has a maximum at  $\theta \approx 0.4$ , and further increase in  $\theta$  leads to the susceptibility decrease. Calculation of specific degree of magnetization, brought to 1g of iron oxide, proved the special state of iron atoms at  $\theta \approx 0.5$ , because spontaneous magnetization was observed only at this value of  $\theta$ . The reason of such a behavior of the samples in magnetic field is discussed and the conclusion is made that there is a two-dimensional magnetic region at the certain amount of Fe–O groups (effect of two-dimensional ferrimagnetism).

Maximum was also observed at the curves under consideration for samples containing Ti–O groups (at  $\theta \approx 0.65$ ). Therewith structurally-induced magnetic effect observed for these samples is associated with the increase in polarization component of diamagnetism, as well as with orienting action of silica core upon Ti–O bonds.

**OPTICAL PROPERTIES OF PHOTOCATALYTICALLY DEPOSITED  
NANOCRYSTALLINE SILVER ON THIN TiO<sub>2</sub> FILMS**

*J. M. Nedeljkovic, M. Dramicanin, T. Rajh\* and M. C. Thurnauer\**

Institute of Nuclear Sciences "Vinca", Laboratory "Gama", P. O. Box 522,  
11001 Belgrade, YUGOSLAVIA <mirjanac@rt270.vin.bg.ac.yu>

\*Chemistry Division, Argonne National Laboratory, Argonne, IL 60439, USA  
<rajh@anlchm.chm.anl.gov>

Thin TiO<sub>2</sub> films were prepared on the glass supports by dip coating technique using colloidal solutions consisting of 45Å particles as a precursor in order to probe the possibility to efficiently deposit silver taking advantage of solid state photocatalytic reactions. Photoirradiation of nanocrystalline TiO<sub>2</sub> films modified with bidentate ligand (alanine) that covalently binds to the surface of TiO<sub>2</sub> and at the same time attach metal ions to the surface of TiO<sub>2</sub> induced reduction of silver ions to their metallic form. Optical properties of metallic island silver films was correlated with microscopy data and possibility to apply this simple procedure in lithography was discussed.

**REACTIVITY OF TWO-DIMENSIONAL OXIDE NANOSTRUCTURES**

*S. V. Menshchikova, L. P. Bogdanova, V. M. Smirnov*

Department of Chemistry, St.Petersburg State University,  
St.Petersburg 198904 RUSSIA <smirnov@moss.pu.ru>

The dependences are studied between chemical composition and structure of two-dimensional synthesized oxide compounds (M-O nanolayers of 3–50 Å on the surface of silica) and its reactivity. Properties of oxide nanostructure have found to depend on spatial atom distribution. Controlling of oxide nanostructures reactivity is considered with the examples of a model catalytic process – hydrolysis of  $\text{CCl}_4$  in the gas phase and reduction of heterogeneous Fe-O groups by hydrogen.

Increased activity of the sample, containing one Ti-O monolayer, observed in the case of catalytic process decreases after deposition of four and more monolayers; therewith the properties of the surface of solid compound become similar to that of the bulk oxide. The possibility is shown to increase the activity of the surface monolayer by changing chemical composition of element-oxygen intermediate monolayer in the samples with the many-component layers.

In the case of heterogeneous reaction of Fe-O reduction the absence of an induction period for two-dimensional nanostructures is established in contrast to the samples obtained by impregnation and precipitation. Characteristics of heterogeneous reaction are discussed.

**CRITICAL MAGNETIC FIELDS AND CROSSOVER IN V/Zr  
QUASIPERIODIC MULTILAYERS**

*V.G. Cherkasova<sup>1</sup>, I.M. Dmitrenko<sup>1</sup>, N.Ya. Fogel<sup>1</sup>, M.Yu. Mikhailov<sup>1</sup>,  
O.I. Yuzephovich<sup>1</sup> and A.N. Stetzenko<sup>2</sup>*

<sup>1</sup> B.Verkin Institute for Low Temperature Physics and Engineering, 47 Lenin Avenue,  
310164 Kharkov, UKRAINE <juzephovich@ilt.kharkov.ua>

<sup>2</sup> Kharkov State Polytechnic University, 27 Frunze St., 310002 Kharkov, UKRAINE

The critical magnetic fields, parallel and perpendicular to the layer planes, have been measured on quasiperiodic Fibonacci multilayers consisting of vanadium and zirconium. Dependence of parallel critical field  $H_c$  on temperature reveals double crossover behavior. This dependence is a square-root-like in the vicinity of transition temperature  $T_c$ , and linear at low temperatures. Between these two ranges of temperature this dependence is power-like:  $H_c \sim (1-T/T_c)^\alpha$ ,  $\alpha=0.78\pm0.01$ . The complicated  $H_c$  vs  $T$  dependence obtained may be explained in terms of Ginzburg-Landau theory for quasiperiodic multilayers [1] as well as in terms of scaling theory for fractal multilayers [2] which takes into account the presence of different structure length scales for the field direction orthogonal to the layers in the case of multilayer systems with complicated sequence of the layers.

1. L.S.Levitov, Pis'ma v JETP 45, 52, 1987.
2. M.G.Karkut, J.-M.Triscone, D.Ariosa, O.Fisher, Phys.Rev.B 34, 4390, 1986.

**STRUCTURAL INVESTIGATION OF SUPERCONDUCTING MULTILAYERS  
CONSISTING OF SEMICONDUCTING MATERIALS**

*A.I. Erenburg<sup>1</sup>, N.Ya. Fogel<sup>1,3</sup>, Yu.V. Bomze<sup>1</sup>, A.Yu. Sipatov<sup>2</sup>, A.I. Fedorenko<sup>2</sup> and  
V. Langer<sup>3</sup>*

<sup>1</sup> B.Verkin Institute for Low Temperature Physics and Engineering, 47 Lenin Avenue,  
310164 Kharkov, UKRAINE <fogel@ilt.kharkov.ua>

<sup>2</sup> Kharkov State Polytechnic University, 27 Frunze Street, 310002 Kharkov, UKRAINE

<sup>3</sup> Department of Inorganic Chemistry, Chalmers University of Technology,  
S-412 96 Göteborg, SWEDEN

There are rather exotic semiconducting superlattices (SL) consisting of monochalkogenides of Pb and Sn which reveal superconductivity at temperatures as high as 6K. Discovery of the new superconducting compositions [1] belonging to the class of semiconducting SL's has made situation even more intriguing, especially because these compositions include wide-gap chalkogenides of rare earth metals (YbS, EuS), one of which (EuS) is ferromagnetic at T<16 K. The origin of superconductivity in these systems did not find yet synonymous explanation. Because superconducting layers in these SL's are confined to the interfaces between two semiconductors [2], the most attractive idea explaining the superconductivity origin is connected with the influence of the misfit dislocation grids existing in the interfacial areas [1]. However, more trivial interpretation is not excluded, namely decomposition of some semiconducting compounds including such superconductors as Pb and Sn.

Here we report the results of the precision X-ray diffractometry and TEM investigations obtained on some of the epitaxially grown superconducting semiconducting SL's. No traces of free Pb are discovered in compositions PbTe/PbS and PbTe/YbS. They do not appear after the aging (during the year or more) too. The free lead is present in composition PbS/EuS. For the former SL's the mismatch of the crystal lattice period's  $a_0$  is large, and the dense grids of dislocations are present in the interfaces. In the latter composition the values of  $a_0$  for two compounds are very close one to another, and misfit dislocations do not appear. This variance in the interface structure is possibly responsible for the difference in the X-ray diffractometry data.

The correlations between superconductivity and the features of the SL structure are discussed. The influence of the aging effect on the structure and superconducting properties of SL's are also under consideration.

1. N.Ya.Fogel, V.G.Cherkasova, A.S.Pokhila, A.Yu.Sipatov, A.I.Fedorenko, Czech J. Phys. 46, Suppl. S2, 727, 1996.
2. I.M.Dmitrenko, N.Ya.Fogel, V.G.Cherkasova, A.I.Fedorenko, A.Yu.Sipatov, Low Temp. Phys. 19, 533, 1992.

**LUMINESCENCE OF DOPED AND UNDOPED ZnO QUANTUM DOTS**

*Kavita Borgohain and Shailaja Mahamuni*

Department of Physics, University of Pune, Pune 411007, INDIA  
<kavita@physics.unipune.ernet.in>

The luminescent properties of undoped ZnO quantum dots encapsulated in various stabilizing agents have been investigated at room temperature. The emission spectra taken at various excitation wavelengths, exhibit two major features. The UV band gap luminescence occurring at about 370 nm and a broad green luminescence band appearing at about 530 nm, which is attributed to defect levels. Interestingly, we have also observed, two features, one at about 420 nm and the other at about 485 nm in the luminescence spectra of ZnO quantum dots. These two features are not observed in the luminescence spectra of bulk ZnO. We attribute the origin of these features to surface defect levels. Substantial difference in the emission spectra have been observed, due to variation in the capping agents. These studies indicate the importance of OH radical on the surface of ZnO quantum dots. In general, it has been observed that surface defects play an active role in the luminescence behaviour of the quantum dots. ZnO quantum dots doped with copper, have also been studied. Doping Cu in ZnO quantum dots having OH radical on its surface, is responsible for quenching green luminescence at 530 nm. On the other hand, OH free, Cu doped, ZnO quantum dots do not exhibit any change in the luminescence behaviour. Variation in size, as well as cappants, which alter surface trap levels, and doping are three different avenues to obtain different emission characteristics.

**ELECTRONIC CONJUGATION BETWEEN SEMICONDUCTOR NANOPARTICLES AND ADSORBED pi-SYSTEMS**

N. A. Kotov<sup>1</sup>, D. Diaz<sup>2</sup> and T. Ni<sup>1</sup>

<sup>1</sup>Department of Chemistry, Oklahoma State University,  
Stillwater, OK 74078, USA <kotov@okway.okstate.edu>

<sup>2</sup>Facultad de Quimica Inorganica, UNAM, Universidad 3000,  
Mexico City 04510, MEXICO

Delocalisation of electrons between semiconductor nanoparticles and adsorbed pi-systems is studied. Thiometalates ( $\text{MoS}_4^{2-}$ ,  $\text{ReS}_4^{2-}$ , and  $\text{WS}_4^{2-}$ ) and copper complexes were shown to bind to the surface of 2.2 nm CdS nanoparticles. By using 2D COSY and NOESY nuclear magnetic resonance spectroscopy (NMR) the conformation of a weakly adsorbed stabiliser on the surface of nanoparticle is established. Problems and perspectives of application of  $^1\text{H-NMR}$  are discussed.

Attachment of thiometalates and a bipyridine copper(II) complex results in the appearance of a strong broad band in UV-VIS absorption corresponding to  $2\text{S}_{3/2}-1\text{S}_e$  transition localised on the surface of nanoparticles and in a substantial transformation of UV-VIS spectra of adsorbing species. New peaks can also be observed in the emission spectra. They are attributed to the transition from a delocalised state to HOMO of nanoparticles. Density functional calculations were employed to determine the position of electronic energy levels in ligands. Comparison with existing experimental and theoretical results reveals that two principal requirements must be met in order to observe effective delocalisation of electrons between a semiconductor core and an organic ligand: (a) energy proximity of LUMO (HOMO) of nanocluster to HOMO (LUMO) of the ligand; (b) strong coupling of the surface states of a quantum dot to its interior states.

**MÖSSBAUER STUDY OF HYPERFINE FIELDS DISTRIBUTION  
IN Fe/Cr SUPERLATTICES**

*I.A. Sergeev, V.N. Gittsovich and V.G. Semenov*

Department of Chemistry, Saint-Petersburg State University,  
Universitetskii pr. 2, St. Petersburg 198904, RUSSIA <ilya@moss.pu.ru>

We have applied  $^{57}\text{Fe}$  Conversion Electron Mössbauer Spectroscopy (CEMS) technique to study the magnetic hyperfine fields (HFF) behavior in  $^{57}\text{Fe}/\text{Cr}$  superlattices. The superlattices have been prepared by means of molecular beam epitaxy on MgO,  $\text{Al}_2\text{O}_3$  and  $\text{SiO}_2$  substrates having different temperature during operating. The sample consists of 30 (Fe/Cr) bilayers with the Cr layer thickness chosen so as to exhibit antiferromagnetic coupling of  $^{57}\text{Fe}$  layers.

A technique enabling to extract information on HFF and Fe atoms environment in interface area as well as on spin texture for separate HFF components from the set of experimental spectra is proposed. A necessary spectra set is being obtained when measuring CEMS spectra at three mutually orthogonal directions. This number of experimental data enabled us to get totally texture free spectra as well as spectra with 2nd and 5th Zeeman sextet lines suppressed or with intensity change being controlled. Two main parts in HFF distribution function have been obtained as result of such spectra computation. The first part is referred to atoms located within Fe layers, the second part results from Fe atoms located in interface area where considerable mixture of Fe and Cr takes place. The above mentioned is justified by the strict dependence of these parts portion change on Fe layers width in superlattice. A correlation between HFF value and chemical shift is established. As a result of computation the problem of possible noncollinearity of magnetic moments of antiferromagnetically ordered Fe layers in given samples is discussed.

The work has been funded by RFBR grant No. 96-03-33342a.

**NANOCRYSTALLINE OXIDE AND NITRIDE FILMS FABRICATION  
USING LASER AND PLASMA PROCESS**

*Tomoaki Ikegami, Masaaki Yamazato, Yukihiko Yamagata, Kenji Ebihara and  
Grishin Alexander\**

Kumamoto University, Dept. of Electrical and Computer Engineering,  
2-39-1 Kurokami, Kumamoto, Kumamoto 860-8555, JAPAN  
<ikegami@eecs.kumamoto-u.ac.jp>

\*Department of Condensed Matter Physics, Royal Institute of Technology,  
Teknikringen 14, S-100 44 Stockholm, SWEDEN

Oxide thin films such as YBCO superconducting and ferroelectric PZT and PLZT, nitride films like Carbon Nitride and Titanium Nitride and Diamond Like Carbon were prepared by using the pulsed excimer laser deposition method, and plasma and ion processing techniques such as RF sputtering and ion implantation. During the processing optical emission and mass spectroscopy, and probe measurement of the process plasma were conducted to characterise the plasma. Comprehensive characterisation of fabricated films and correlation between nanocrystalline structure and functional properties were investigated. Application of these films were also investigated; heterostructures consisted of YBCO and PZT films for a fatigue-free FeRAM and an electron emitting device, TiN films for buffer layer and tribological, low-wear, protective coating, and PLZT film for a pyroelectric sensor.

**NANOLAYERED CHALCOGENIDE GLASS STRUCTURES  
FOR OPTICAL RECORDING***A. Kikineshi, A. Mishak, V. Palyok and M. Shiplyak*

Department of Solid State Electronics, Uzhgorod State University,  
Pidhirna str. 46, Uzhgorod, 294000, UKRAINE <kiki@sse.univ.uzhgorod.ua>

A number of As(Sb,Ge)-S(Se,Te)-based binary or more complex glasses and amorphous selenium (a-Se) are light-sensitive semiconductors, which possess photo- and thermoinduced structural transformations between amorphous-amorphous or amorphous-crystalline states. These transformations determine different optical memory effects, connected with optical absorption, reflection or refractive index changes [1]. The parameters of corresponding reversible or irreversible information recording processes may be varied by changing the composition, technology of metastable amorphous layers, which are usually few micrometers thick. New method for tailoring these processes and recording materials was realised in nanolayered, superlattice-like structures [2].

Sensitive layers are sandwiched between non-sensitive, or both in a periodical structure are sensitive to the light, so stimulated structural transformations inside the 3-15 nm thick sub-layers and/or interdiffusion processes occur under the influence of light (usually laser beams with necessary wavelengths and energy density). So far as some thermodynamical, mechanical, electrophysical and optical parameters of nanoparticles, nanolayers differ from the bulk (thick layer) of the same material, the structural transformations and optical recording parameters may be changed, improved. The mechanisms of structural transformation processes (ordering- disordering in glassy matrix or crystallisation), as well as interdiffusion were investigated both by the analysis of optical recording parameters and by optical transmission, Raman scattering, TEM and AFM microscopy measurements.

Two main types of nanolayered structures (NS) were investigated: Se-Te/As-Se based NS with strong interdiffusion effects and more stable As-S/a-Se, As-S/As-Se based NS. Samples were prepared by cyclic vacuum thermal evaporation on amorphous or crystalline substrata. It was shown that quantum confinement effects cause the optical absorption shift towards higher energies. The change of the volume and surface energy ratio in the cases of different neighbouring materials causes the shift of the glass softening temperature and main stress relaxation times. So the spectral sensitivity, thermal stability of the optically recorded amplitude-phase relief, for example hologram, its efficiency may be changed. Operated sensitivity for digital recording was also realised due to the interdiffusion in Se-Te based nanolayered structures.

1. F.Kikineshi, A. Mishak in: Physics and Applications of Non-Crystalline Semiconductors in Optoelectronics (1997) Ed. by A. Andriesh and M. Bertolotti, NATO ASI Series, 3. High Technology- Vol.36.pp.249-257.
2. Kikineshi (1995), Optical Engineering, Vol.34, pp.1040-1043.

**PROPERTIES OF RECOMBINATION PROCESSES  
IN QUANTUM DOT LASER EMITTING AT 1.9  $\mu\text{m}$** 

*N.Yu. Gordeev, V.I. Kopchatov, V.M. Ustinov, A.E. Zhukov, A.Yu. Egorov, A.R. Kovsh,  
P.S. Kop'ev, and S.V. Zaitsev*

A.F.Ioffe Physical-Technical Institute of the Russian Academy of Sciences,  
Politekhnicheskaya 26, St.Petersburg 194021, RUSSIA <Gordeev@switch.ioffe.rssi.ru>

Ultralow threshold current density of  $62 \text{ A/cm}^2$  at RT has been achieved in lasers based on InGaAs/AlGaAs/GaAs quantum dots (QD) [1]. However in such structures the range of emitting wavelength is limited by the value of  $1.3 \mu\text{m}$ . Recently we reported about the InAs/InGaAs/InP QD laser with threshold current density as low as  $11 \text{ A/cm}^2$  at 77 K emitting at  $1.9 \mu\text{m}$  [2].

In the present work we study properties of emitting recombination in these heterostructures and processes interrupting lasing at RT. Lasing was observed at the temperature range from 77 to 200 K and characterized by the parameter of  $T_0=25 \text{ K}$ . Investigation of threshold current density vs. cavity losses dependence showed pronounced increasing of the threshold current density for laser with cavity losses above  $50 \text{ cm}^{-1}$  and the shift of the lasing wavelength to  $1.7 \mu\text{m}$ . Differential quantum efficiency decreases by a factor of 4.5 at increasing temperature from 77 K to 200 K. We explain such behavior as a saturation of the gain through the QD states and pronounced carrier delocalisation from the quantum dots. Using stripe geometry lasers with various cavity length we have estimated the internal quantum efficiency of stimulated emission to be as low as 40 % at 77 K. The remaining 60 % of carriers recombine in spontaneous mode via the excited states of QD and the states of wetting layer affirming the existence of the strong carrier delocalisation.

We assume that using the InGaAlAs alloy having higher value of the bandgap as a QD matrix will lead to a suppress of the thermal evaporation of carriers from the QD states. This increases internal quantum efficiency of stimulated emission and finally must provide lasing through the QD states at  $1.9 \mu\text{m}$  at room temperature.

1. V.M.Ustinov, A.Yu.Egorov, A.E.Zhukov, M.V.Maksimov, A.F.Tsatsulnikov, N.Yu.Gordeev, S.V.Zaitsev, Yu.M.Shernyakov, N.A.Bert, P.S.Kop'ev, Zh.I.Alferov, N.N.Ledentsov, J.Bohrer, D.Bimberg, A.O.Kosogov, P.Werner, U.Gosele "Low-threshold injection lasers based on vertically coupled quantum dots", Journal of Crystal Growth 175/176, 689-695 (1997 ).
2. A.E.Zhukov, A.Yu.Egorov, A.R.Kovsh, V.M.Ustinov, S.V.Zaitsev, N.Yu.Gordeev, V.I.Kopchatov, A.V.Luney, A.F.Tsatsulnikov, B.V.Volovik, N.N.Ledentsov, P.S.Kop'ev, "Low threshold quantum dot laser emitting at  $1.9 \mu\text{m}$ ", to be published in Semiconductors (1998).

### **SELF-ASSEMBLY OF SURFACE COMPOSITE INORGANIC/ORGANIC THIN FILMS**

*N. Kovtyukhova\*, P.J. Ollivier, and T.E. Mallouk*

Department of Chemistry, 152 Davey Laboratory, The Pennsylvania State University  
University Park, PA 16802, USA <tom@chem.psu.edu>

\*Institute of Surface Chemistry, NAN of Ukraine, 31, Pr.Nauky,  
252022 Kyiv, UKRAINE <nik@surfchem.freenet.kiev.ua>

The self-assembly of unilamellar inorganic sheets and organic macromolecules, which are held together by non-specific bonding forces at the solid/solution interface, represents a new approach to making functional surface heterostructures.

The approach described in this work is based the exfoliation of lamellar solids, such as MoS<sub>2</sub> and graphite oxide (GO) to produce colloids of pseudo two-dimensional nanoparticles. The self-assembly procedure consists of layer-by-layer deposition of these two-dimensional anion sheets prepared and cationic "spacers" (e.g. polymers), which alternate along the stacking axis. Using Atomic Force Microscopy (AFM) as a direct observation technique, questions of fundamental and practical importance have been addressed:

- what does the first layer of the sheets adsorbed on a substrate look like on the nanoscale?
- can we affect the quality of inorganic mono- and multilayers by varying the conditions of their deposition, and the chemical composition of the substrate surface?

We report here a detailed study of the preparation and characterisation of ultrathin MoS<sub>2</sub> and GO films on silicon. These films are grown from sols of the exfoliated layered compounds and polyallylamine hydrochloride. The lateral dimensions of the exfoliated particles have been determined by Transmission Electron Microscopy (TEM), and are in the range of several tens to several thousands nanometers. AFM images show that the thickness of the first layer of MoS<sub>2</sub> and GO particles is 9-20 Å, which equals thickness of single- and/or double-layer sheets of the lamellar compounds under investigation. The lateral dimensions of the sheets and their packing in the first adsorbed layer depend on the chemical composition of the Si surface and pH of the starting sol. AFM images of the MoS<sub>2</sub> and GO multilayer films deposited in four adsorption cycles show neither well-resolved sheets nor voids between them. Hence these multilayer films completely cover the substrate surface. Depending on the chemical composition of the Si surface and pH of the starting GO sol, the thickness (estimated by ellipsometry) of the four layer films ranged from 7.5 to 12.5 nm for MoS<sub>2</sub> and from 105 to 150 nm for GO. The roughness varied from 1.3-2.2 nm for MoS<sub>2</sub> films and from 1.2 - 2.7 nm for GO.

**CAPTURE OF EXCITON MOLECULES BY QUANTUM DOTS AND  
ISOELECTRONIC IMPURITIES IN MULTIVALLEY SEMICONDUCTORS***A.A. Rogachev*

A.F.Ioffe Physical-Technical Institute of RAS,  
St.Petersburg 194021, RUSSIA <trirog@mail.wplus.net>

Electrons and holes can be captured by small size quantum wells, i.e. by quantum dots, and by isoelectronic impurities. Dots are also capable to capture excitons and biexcitons. In the present work for the first time, theoretical and experimental consideration is given to the formation of exciton molecules containing three or four excitons in one dot. Existence of such exciton molecules is possible only in multivalley semiconductors [1,2]. The conduction and valence bands of such semiconductors as GaP, AlAs, AlSb, Ge and Si have several energy minima. The Coulomb interaction of electrons and holes in multivalley semiconductors results in formation of exciton molecules, i.e. not only of biexcitons, but also of essentially stronger bound triexcitons and tetraexcitons. Both free and bound on dots excitons can be strongly binded because in multivalley semiconductors up to four holes can be located in ground state (s-state). The number of electrons in ground state can be significantly larger, for example, in GaP there can be 6 electrons, in Ge - 8 and in Si - 12 electrons. We recently showed experimentally and theoretically that while the dot depth increases, first, the captured exciton molecule radius essentially decreases and only after, with the dot depth still increasing, the electron energy level rises. At further increase of the dot depth electrons and holes are captured independently and the Coulomb interaction of electrons and holes may be considered as a small correction. Kinetics of the formation of free and bound on quantum dots exciton molecules was studied. The capture by dots of electrons, holes, excitons and free exciton molecules was considered. An important feature of formation of exciton molecules captured by dots is the presence of tunnel transitions of electrons and holes between dots. It is shown that for GaP-Bi the tunnel transitions between isoelectronic impurities of *Bi* of the concentration higher than  $10^{17} \text{ cm}^{-3}$  determine distribution of dots with respect to the number of captured excitons, which does not depend on the excitation level in a wide range of excitation. In principle, two energy levels of excitons in dots are possible, namely, a level of 1s-state holes and a level with a lower binding energy, in which several holes occupy the 2p-state. Electrons on both levels occupy the 1s-state.

**MODIFIED SOL-GEL PROCESSING OF NANOSTRUCTURED  
THERMAL BARRIER COATINGS**

*L.K. Kurihara<sup>1</sup> and G.M. Chow*

Naval Research Laboratory, Materials Science and Technology Division,  
Washington DC 20375, USA <kurihara@anvil.nrl.navy.mil>

<sup>1</sup> also at Potomac Research International, Fairfax, VA 22030, USA

Nanostructured thermal barrier coatings (TBC) with a large number of grain boundaries and controlled porosity are of interest because of increased phonon scattering leading to a decrease in the thermal conductivity. Solution chemistry, in particular, sol-gel techniques offer the advantages of the molecular or atomic scale tailoring of the precursors, and the ability to coat planar and hidden surfaces with complex shapes. However, traditional sol-gel techniques are often limited to the preparation of thin films. When thick coatings are deposited, the drying and densification steps must be carefully controlled to minimize associated large capillary stresses, which cause cracking. In this work, a modified sol-gel approach, i.e. doping the gel with nanoparticles, is investigated for the preparation of thick, crack-free nanostructured TBCs. Coatings of alumina stabilized zirconia (ASZ), and yttria stabilized zirconia (YSZ) with different nanoparticle loadings are synthesized. The effects of processing parameters such pH, particle loading, and post-deposition heat treatment on the structure, microstructure and properties of the coatings are studied.

**THE COATING OF AMORPHOUS IRON NANOPARTICLES  
BY LONG-CHAIN ALCOHOLS**

*Gina Kataby<sup>1</sup>, Avi Ulman<sup>2</sup>, Ruslan Prozorov<sup>3</sup> and Aharon Gedanken<sup>1</sup>*

<sup>1</sup> Department of Chemistry, Bar-Ilan University,

Ramat-Gan 52900, ISRAEL <kataby@ashur.cc.biu.ac.il>

<sup>2</sup> Department of Chemistry, Polytechnic University, Brooklyn, NY 11201, USA

<sup>3</sup> Institute for Superconductivity, Department of Physics, Bar-Ilan University,  
Ramat-Gan 52900, ISRAEL

Coatings of long alkyl-chain alcohol and acids on nanophased amorphous iron nanoparticles have been carried out using the self-assembled technique. The formation of chemical bonds between the substrate and the surfactants was demonstrated by FTIR and XPS measurements. The superparamagnetic nature of fine-coated nanoparticles was detected in the magnetization measurements. Thermal stability (TGA and DSC) and floatability properties were also measured. The amorphous iron nanoparticles were prepared according to the process outlined by Suslick, using sonochemical technique.

**SOL-GEL DERIVED SILICA FILMS DOPED  
BY CuS AND CuInS<sub>2</sub> SMALL PARTICLES**

*V. S. Gurin<sup>1</sup>, V.B. Prokopenko<sup>2</sup>, A.A. Alexeenko<sup>2</sup> and I.M. Melnichenko<sup>2</sup>*

<sup>1</sup> Physico-Chemical Research Institute, Belarusian State University, Leningradskaja str.  
14, Minsk, 220080, BELARUS <postmaster@phchinst.belpak.minsk.by>

<sup>2</sup> Advanced Materials Research Laboratory, Gomel State University,  
Gomel 246699, BELARUS <vit@prl.gsu.gomel.by>

Ultrafine semiconductor particles in different media have attracted significant attention in connection with their unique optical, electrical, magnetic, and other properties. Thin films are one of many possible realizations of solid materials which can be useful for different studies and are perspective for application. Semiconductor-doped films are good instance of nanocomposites when both a film-forming medium and dopants can have size-dependent peculiarities. In the report we consider the preparation features of silica films with small particles of binary semiconductors with complicated band structure (Cu<sub>x</sub>S, Cu<sub>x</sub>Se) and ternary compounds - copper-indium sulfide (CuInS<sub>2</sub>) by the method of chemical transformation of metal oxides. Silica matrix in such system is appear as both useful inert medium to explore gas-solid and solid-solid chemical processes and high-quality base for optical and electrophysical applications.

Silica films were produced by conventional sol-gel technique with inclusion of solvable copper and indium salts at the sol step of process. Uniform sol-gel coatings with metal oxide particles can be formed on different substrates after heat treatment and transformed into sulfides by exposure in the hydrogen sulfide atmosphere. Copper selenide was formed after the reduction of copper in hydrogen atmosphere with subsequent selenization in selenium vapour. In the course of sulfidization a few non-stoichiometric phases Cu<sub>x</sub>S were identified and their optical properties were studied. CuInS<sub>2</sub> nanoparticles with chalcopyrite lattice were formed by this method for the first time. Chemical composition of films and particle characterization was performed by optical spectroscopy, XRD, XPS, TEM, RBS at different steps of the transformations.

In the set of film materials presented the quantum-size effect is combined with chemical factors and indirect-direct band transformations. They possess specific optical absorption with additional near-IR bands that is absent for conventional II-VI and I-VII semiconductors.

**PHOTOEMISSION STUDY OF CdS QUANTUM DOTS**

*Jagjit Nanda, Beena Annie Kuruvilla and D.D. Sarma*

Solid State and Structural Chemistry Unit, Indian Institute of Science,  
Bangalore 560 012, INDIA <nanda@sscu.iisc.ernet.in>

Semiconductor quantum dots exhibit size dependent electrical and optical properties. Confinement of the charge carriers (electrons and holes) in all the three dimension leads to an increase of the band gap with decreasing size of the crystallites resulting into size dependent properties. Such effect is known in the literature as quantum confinement effect. CdS is a typical II-VI semiconductor having a band gap of 2.40 eV and shows strong quantum confinement effect. We have synthesized two sizes of CdS quantum dots having an average diameter of 22 Å and 44 Å both in the strong confinement limit i.e less than the bulk CdS Bohr exciton diameter which is around 60 Å. These quantum dots were prepared by the capping the surface of CdS nanocrystallites (during growth) with organic ligands to prevents agglomeration. In our case we have used Thioglycerol as the capping material. The UV absorption spectra of the CdS quantum dots show sharp excitonic features with the edge shifted towards higher energy compared to the bulk CdS. Such sharp features indicate a narrow size distribution. The X-ray diffraction shows broad peaks corresponding to bulk CdS which has a cubic phase. We report the photoemission results on these CdS quantum dots. The Sulphur 2p core-level spectrum shows three distinct features. We identify this to three types of sulphur present in the dots. Sulphur belonging to the CdS core, surface sulphur and sulphur of the capping layer. The experimental S 2p spectrum was fitted for both sizes. An estimate regarding the size of the dots was obtained by calculating the photoelectron intensity using the mean escape depth formula and comparing it with the fitted experimental intensities. The sizes agrees well with the size obtained from optical and structural techniques. Apart from this detail valence band studies explaining the shift in the valence band with respect to the size will be discussed.

**SURFACE MORPHOLOGY AND COMPOSITIONAL VARIATIONS  
IN MOLECULAR BEAM EPITAXY GROWN  $\text{GaN}_x\text{As}_{1-x}$  ALLOYS**

*O. Zsebök, J.V. Thordson, L. Ilver and T.G. Andersson*

Applied Semiconductor Physics, Division of Microelectronics and Nanoscience,  
Department of Physics and Engineering Physics, Chalmers University of Technology  
and Göteborg University, S-412 96 Göteborg, SWEDEN <zseboeck@fy.chalmers.se>

The zinc blende  $\text{GaN}_x\text{As}_{1-x}$  alloy has a large span in lattice constant, 4.50 - 5.65 Å, and gap 1.42 - 3.45 eV. The large band gap is of great potential for optical devices operating with visible light. Since there is no substrate that fits the lattice constant of the alloy, structural defects with sizes from the nm-scale will develop in the film such as nanopipes, etc. We have studied the  $\text{GaN}_x\text{As}_{1-x}$  alloy with compositions from isoelectronic doping concentrations up to GaN. The layers were grown on GaAs (001) substrates in a molecular beam epitaxy (MBE) system using an RF activated plasma source. The structures were grown with thickness between 2 and 6 µm on GaAs (100) substrates at 580 °C. The main growth parameters were the N<sub>2</sub>-flux, which was varied between 0.05 and 1.00 sccm, and the RF power. The average nitrogen content in the film was determined by secondary ion mass spectrometry (SIMS). High resolution X-ray diffraction (HRXRD) showed one peak corresponding to  $\text{GaN}_x\text{As}_{1-x}$ , with ~2% nitrogen, but also a weaker peak for the zinc blend GaN. Studies by high-resolution scanning electron microscopy (SEM) revealed that the isoelectronically doped samples (~10<sup>18</sup> cm<sup>-3</sup> of N in GaAs) had a surface quality similar to pure GaAs. On the alloy samples morphological defects were detected. Elliptically shaped holes of 3 - 4 µm were present having a conical shape in cross-section with a depth of approximately 2 µm, possibly arising at a surface lattice defect. Auger electron spectroscopy (AES) point analysis, with a spot diameter of less than 500 nm, and energy dispersive X-ray spectroscopy (EDX) revealed strong lateral variations in composition. There was a significantly higher nitrogen content accumulated in the side walls of the holes (possibly pure GaN single crystals of nm-size) compared to the flat surface. At high nitrogen compositions, GaN(As), crystalline surface features with sizes of 1-2 µm were seen. According to high-resolution AES and EDX characterisations the composition of the rounded features was close to GaN, while the As had been incorporated into prolonged particles. The general surface roughness was best for samples with the smallest amount of As. Larger mixing gave worse crystal quality as alloy compositions in the intermediate range had the worst surface roughness, more than 100 nm.

**INFLUENCE OF THE STRONG ELECTROMAGNETIC WAVE  
ON THE OPTIC PROPERTIES OF THE QUANTUM WELLS  
IN THE QUANTUM CONFINEMENT STARK EFFECT CONDITION**

*V.A. Petrov and V. B. Sandomirsky \**

Institute of Radio Engineering & Electronics, Russian Academy of Sciences,  
Mokhovaya 11, Moscow 103907, RUSSIA <vpetrov@mail.cplire.ru>

\* Dept. of Phys., Bar-Ilan Univ., 100 Raman-Gan, ISRAEL

Recently, interest has increased sharply in the investigation of the possibility of noncontact modulation of optical properties of quantum wells (QWs) by a strong electromagnetic wave (SEMW). First of all, the manifestation of the effect of a SEMW on the exitonic absorption in the GaAs QW due to the *optical* Stark effect should be noted here<sup>1</sup>.

Previously, we pointed to another possibility of using a SEMW for the modulation of the optical absorption edge in QWs. We calculated the interband absorption coefficient of a weak wave of  $\omega$  frequency ( $\hbar\omega = E_g$ ) in the presence of another, strong  $\Omega$  frequency ( $\hbar\Omega \ll E_g$ ) and  $E$  optical field SEMW in the CaAs-type QW ( $E_g$  is the optical width of the forbidden band in the QW) and showed that quasienergetic additions to the energies of electrons and holes appearing in the field of the SEMW  $\Delta_{d,h}(E) = e^2 E^2 / 2m_{d,h}^* \Omega^2$  in the case of circular polarization ( $e$  is an electron charge,  $m_{d,h}^*$  are effective masses of electrons and holes) can be considered as a shift of the optical absorption edge of the weak wave in the QW *toward the short-wave spectrum part*<sup>2</sup>. Recently, this effect was detected experimentally in the InGaAs-type quantum wells<sup>3</sup>.

In this work we investigated theoretically similar effects of the SEMW in the QWs and quantum wires in the presence of a *strong constant electric F field*, which was directed along the normal to the plane of the QW or to the axis of the quantum wire (quantum confinement Stark effect). We examined the situation when the  $E$  optical field of a SEMW lies in the plane of the QW or directed along the quantum wire axis. In the approximation of the isolated bands quasienergetic spectrums of electrons and holes as well as *exact* nonstationary wave functions of particles in a QW and a quantum wire in the presence of the constant electric field and the SEMW were found. Linear and circular polarization of a strong wave was investigated. We calculated the interband absorption coefficient of a weak wave and showed that the magnitude of the total shift  $\Delta$  of the optical absorption edge is equal:  $\Delta = \Delta_{d,h}(E) - \Delta_{d,h}(F)$  since the strong wave and the constant electric field shifted the edge to the opposite sides. The calculations showed that for the GaAs-type QW and  $\hbar\Omega = 13.7$  meV,  $E \approx 1.3 * 10^4$  V/cm ( $I \approx 1$  MW/cm<sup>2</sup> is the intensity a of strong wave)  $\Delta_{d,h}(E) \approx 5$  meV for the wave with circular polarization. In the QWs  $\Delta_{d,h}(F)$  may be easily made both more and less than  $\Delta_{d,h}(E)$ .

1. A. Von Lehmen et al., Optics Lett. 11, 609 (1986).

**NANOSTRUCTURED MODEL BIOMATERIAL SURFACES PREPARED BY  
ADSORPTION OF CHARGED POLYSTYRENE PARTICLES ON TITANIUM**

*P. Hanarp, D. Sutherland and J. Gold*

*Q.*

Dept. of Applied Physics, Chalmers University of Technology,  
S-412 96 Göteborg, SWEDEN <f93peha@dd.chalmers.se>

The chemistry and structure of biomaterial surfaces influences the biological response to an implant. Recent studies have shown that even nanometer structural features may enhance cell spreading, adhesion and activation on model implant surfaces.<sup>1</sup> To provide nanostructured surfaces for cell culture studies, we have used a method based on adsorption of charged polystyrene particles on titanium. This is an easy yet powerful method to produce large surface areas with a controlled nanostructure.

Surfaces of silicon wafers, pre-coated with 20 nm of thermally evaporated Ti, were treated with aluminium chloride hydroxide giving a net positive charge at neutral pH. The surfaces were exposed to dilute aqueous solutions of colloidal polystyrene particles (diameter 110±5 nm, White-sulphate Latex, IDC Portland, OR), and the negatively charged particles adsorbed onto the surfaces randomly by electrostatic interactions. A sub-monolayer of particles was obtained with coverage controlled either by salt concentration (NaCl) in the colloidal solution for equilibrium adsorptions or particle concentration and adsorption time in interrupted (non-equilibrium) adsorptions. A thin film of Ti (60 nm) was evaporated on top of the particles to provide a chemically homogenous surface. Scanning electron microscopy (SEM) and image analysis software were used to characterise the particle packing density and spacings.

Surfaces with controlled nanotopography (i.e. 2D nanoporous surfaces) were produced by adsorbing sub-monolayers of 110 nm, negatively charged polystyrene particles onto positively charged Ti surfaces. The average distance between the particles (or area coverage) was controlled by the salt concentration in the colloidal solution. A high salt concentration screens the interparticle electrostatic repulsion (Debye screening) resulting in a reduced interparticle spacing and increased coverage. By varying the salt concentration, we have produced surfaces with 8-26 % area coverage of evenly spaced particles. At higher coverages, 2D (and some 3D) aggregation of particles was observed, probably caused by attractive capillary forces between close particles when drying the samples. Radial distribution functions (rdfs) for the particles were in good qualitative agreement with the soft disk random sequential adsorption (RSA) model.<sup>2,3</sup>

Adsorption of polystyrene particles onto Ti surfaces is a quick and easy method to produce uniform nanostructures over large surface areas. Particle size and coverage may be varied to produce the required surface structure. Fabrication of controlled 3D nanoporous particle films is also possible using this method, where repeated adsorption of particles and repeated charging of the substrate results in multilayer formation. The samples that we are making are intended for cell culture studies, which are in progress.

**ELABORATION OF SI NANOWIRES OR DOTS  
ON CaF<sub>2</sub> V-GROOVED SURFACES**

*F. Bassani, S. Ménard, A. Ronda and F. Arnaud d'Avitaya*

Centre de Recherche sur les Mécanismes de la Croissance Cristalline - CNRS, Campus de Luminy, case 913, 13288 Marseille Cedex 9, FRANCE <bassani@crmc2.univ-mrs.fr>

Since the discovery of efficient photoluminescence in porous silicon, much effort has been devoted to the fabrication of other visible-light emitting Si-based materials. Recently, we demonstrated room-temperature luminescence in nanocrystalline Si/CaF<sub>2</sub> multilayers grown by molecular beam epitaxy (MBE). At the present time, there is still a debate on the shape and size of Si nanostructures optically active in the visible range. Since the dimensionality of such Si nanostructures seems to be a key factor, self-organized Si nanostructures such as nanowires or dots might be realized by using surfaces which naturally present a regular array of steps. In that purpose, we have studied the first nucleation steps of Si on CaF<sub>2</sub> V-grooved surfaces previously deposited on Si(110) substrates.

In the first part, we investigate the initial stages of growth of CaF<sub>2</sub> on Si(110) substrates by using reflection high energy electron diffraction, atomic force microscopy and scanning electron microscopy. With this particular orientation, a regular array of CaF<sub>2</sub> ridges and grooves extending along the [-110] direction is obtained.

In the second part, we report on the growth of Si on these CaF<sub>2</sub> V-grooved surfaces. Due to the difference in surface free energy, Si grows in a three dimensional way on CaF<sub>2</sub> and forms islands whatever the deposition temperature. We point out that by using low-energy electron-beam exposure of the CaF<sub>2</sub> surface or by choosing appropriated MBE growth conditions, the growth mode of Si on CaF<sub>2</sub> can be significantly changed. That allows the Si to wet the CaF<sub>2</sub> surface more readily and consequently to get Si nanowires more elongated along the direction of the grooves.

### **MICROSTRUCTURE OF PLASMA SPRAYED NANOSCALE TUNGSTEN CARBIDE-COBALT COATINGS**

*M. Scholl, M. Becker and D. Atteridge*

Oregon Graduate Institute of Science and Technology Department of Materials Science  
and Engineering P.O. Box 91000 Portland, OR 97291-1000, USA

A  $\sim 120 \pm 10$  micron WC-15Co powder consisting of nanoscale WC in a cobalt matrix was sprayed using a high energy plasma system. For comparison a conventional  $\sim 45 \pm 11$  micron WC-12Co powder was sprayed under similar conditions. This high energy plasma system differs from conventional plasma systems by working at lower currents (up to 500 amps) and high voltages (exceeding 500 volts). The plasma system was operated at a nominal 150 kilowatts and over a wide range of gas flows which yielded plasma velocities from sub-sonic to OVER MACH 2. Nitrogen primary plasma gas flows ranged from 200 to 300 slpm and hydrogen secondary gas flow ranged from 0 to 100 slpm. For selected cases, a carburizing atmosphere was introduced to minimize decarburization. The working distance was also varied. An experimental design was used to maximize information content and expedite analysis over the wide range of operating conditions. The resulting coatings were sectioned and examined metallographically and microhardness tests performed.

The microstructure of the nanoscale coating was resolvable only at high magnifications in a scanning electron microscope (SEM) and by transmission electron microscopy (TEM), showing carbides about 100 nm in size. In contrast the carbides in the conventional WC-12Co material were 5 to 10 microns. At low resolution in the optical microscope, the nano-scale carbides were only identifiable by morphology changes in the surface of the sample due to variations in polishing characteristics. With both conventional and nano-scale starting powders, the coating porosity was very low, especially in the nanoscale WC-15Co coatings where microscopic porosity was not observable in the optical microscope. Amorphous and microcrystalline regions in the cobalt matrix were identified by transmission electron microscopy (TEM). Hardnesses ranged from 850 to 1100 HK500 depending on the operating parameters for the nanoscale WC-Co. The hardness of the conventional WC-Co was about 920 HK500. Despite the wide variation in deposition parameters the nanoscale coatings obtained from the type of feedstock used showed little variation in microstructure and hardness.

Continuing research is defining the nanoscale microstructure using high resolution transmission electron microscopy to adequately resolve the microstructure. The microchemistry of the carbides and the cobalt matrix is also being examined AND other tribological performance tests are being conducted.

**PROPERTIES OF PLASMA SPRAYED NANOSCALE  
TUNGSTEN CARBIDE-COBALT COATINGS***M. Scholl, M. Becker and D. Atteridge*

Oregon Graduate Institute of Science and Technology Department of Materials Science  
and Engineering P.O. Box 91000 Portland, OR 97291-1000, USA

A  $\sim 120 \pm 10$  micron WC-15Co powder consisting of nanoscale WC in a cobalt matrix was sprayed using a high energy plasma system. For comparison a conventional  $\sim 45 \pm 11$  micron WC-12Co powder was sprayed under similar conditions. The plasma system differs from conventional systems by working at lower currents (up to 500 amps) and high voltages (up to 500 volts). The plasma system was operated at a nominal 150 kilowatts and over a wide range of gas flows which yielded plasma velocities from subsonic to supersonic. Nitrogen primary plasma gas flows ranged from 175 to 300 slpm and hydrogen secondary gas flow ranged from 0 to 100 slpm. The working distance was also varied. An experimental design was followed to maximize the information content over the wide range of parameters. The resulting coatings were sectioned and examined metallographically and microhardness tests performed. For performance tests, coatings were tested under three-body abrasion in a ASTM G-65 Dry-Sand-Rubber-Wheel test with silica sand. The results of the abrasion tests were compared to other coating materials and to common cast abrasion resistant materials. The coatings are also being evaluated in pure sliding in an Amsler twin-roller machine which also allowed the coefficient of friction to be measured.

The microstructure of the nanoscale coating was resolvable only at high magnifications in a scanning electron microscope showing carbides about 100 nm in size. In contrast the carbides in the conventional WC-12Co material were 5 to 10 microns. With both types of starting powders, the coating porosity was very low, especially in the nanoscale WC-15Co coatings where microscopic porosity was not observable in the optical microscope. Amorphous and microcrystalline regions in the cobalt matrix were identified by transmission electron microscopy (TEM). Hardnesses were ranged from 850 to 1100 HK500 depending on the operating parameters for the nanoscale WC-Co. The hardness of the conventional WC-Co was about 920 HK500. Despite the wide variation in deposition parameters the nanoscale coatings showed little variation in microstructure and hardness. The abrasive wear resistance of the nanoscale WC-15Co coatings was equivalent to other best of the conventional WC-12Co coatings tested, as well as to Cr<sub>3</sub>C<sub>2</sub>-25NiCr coatings. There was much greater scatter in the wear tests of the conventional WC-Co but little in tests of the nanoscale WC-Co. In comparison to cast high chromium irons, a 25Cr white iron and a 20Cr-2Mo-1.5Ni-1.5Cu white iron, the nanoscale WC-Co coatings had similar wear resistance. Additionally despite being deposited over extremes of deposition parameters, the wear resistance of the nanoscale WC-Co coatings varied only slightly.

**OPTICAL PROPERTIES OF PbS-CdS COATED SEMICONDUCTOR NANOPARTICLES**

*Beena Annie Kuruvilla, Jagjit Nanda and D.D. Sarma*

Solid State and Structural Chemistry Unit, Indian Institute of Science,  
Bangalore 560 012, INDIA <beena@sscu.iisc.ernet.in>

Study of semiconductor nanocrystallites, particularly belonging to II-VI, III-V and IV-VI groups has been a topic of intense research over last two decades due to their novel electrical and optical properties which are different from the bulk. Quantum confinement of electron and holes in all three dimension leads to an increase in the effective band gap with decreasing crystallite size. Consequently the optical absorption and emission of nanocrystallites shifts to higher energies. Recently there has been some attempts to synthesize coated semiconductor nanoparticles in which on the top of one semiconductor nanoparticles another semiconductor of different material is grown. The electrical and optical properties such core - shell structures are more interesting compared to single nanoparticles. We have synthesized two series of PbS-CdS coated semiconductor nanoparticles in which PbS is coated on the CdS nanoparticles. First CdS nanoparticles having average diameter of 22 Å and 44 Å were synthesized using a method given by Vossmeyer et. al. The nanoparticles solution was then refluxed for few hours with Lead salt (in this case  $\text{Pb}(\text{NO}_3)_2$ ). The thickness of the PbS layer was varied by changing the Pb/Cd ratio. These particles were structurally characterized by X-ray diffraction and X-ray Photoelectron Spectroscopy. The uv absorption spectra of the coated nanoparticles are broadened and shows a systematic shift towards lower energy with increasing Pb/Cd ratio with respect to bare CdS nanoparticles. This can be due to the distribution of the shell thickness. The photoluminescence (PL) spectra of the coated nanoparticles shows interesting features. Bare CdS nanoparticles shows broad trapped luminescence due to the defect states on the surface of the nanoparticles with band edge luminescence completely suppressed. With increasing PbS coating the band edge luminescence is considerably enhanced indicating the quenching of the defect states.

**THE SCANNING ELECTRON MICROSCOPY OF  $(\text{Bi}_2\text{S}_3)_{0.40}(\text{CdS})_{0.60}$  THIN FILM ON GLASS AND Si <111> SUBSTRATES***Susama Misra*

Department of Physics, Ravenshaw College, Cuttack-753003, INDIA

The  $(\text{Bi}_2\text{S}_3)_{1-x}(\text{CdS})_x$  thin film prepared by electroless deposition [1] for the first time was studied by scanning electron microscopy and Rutherford backscattering. The  $(\text{Bi}_2\text{S}_3)_{0.40}(\text{CdS})_{0.60}$  film was deposited on glass and Si<111> substrates to study the effect of substrate on the microstructure. The as-grown  $(\text{Bi}_2\text{S}_3)_{0.40}(\text{CdS})_{0.60}$  film of Si<111> was found comparable to the annealed film showing more homogenous nature than that for the as-grown film on glass. The as-grown film on glass showed smaller grain size in comparison to Si<111>. The grain size on Si<111> varied between 0.1 to 0.25  $\mu\text{m}$  whereas the combined grain showed maximum size of  $\sim 1.2 \mu\text{m}$  at 54 K magnification. The as-grown film on Si<111> showed larger combined grain growths showing columnar nature in comparison to the film on glass. This type of preferential growth of film on Si<111> was found possible for the annealed film on glass substrate.

The roughness of the  $(\text{Bi}_2\text{S}_3)_{0.40}(\text{CdS})_{0.60}$  thin film was studied by stylus (32 nm) and Rutherford backscattering (30 nm) methods showing excellent agreement in the results. The composition was found out by using the 3.07 MeV  $\text{He}^{++}$  ion projectile from the 3 MV tandem pelletron accelerator of the Institute of Physics, Bhubaneswar. The results confirmed that the composition was independent of the nature of the substrate. Nonuniformity in the backscattering spectrum for the sulphur peak may account for the roughness of the sample. The presence of oxygen in the spectrum indicates presence of oxide in the film. However depth profiling of the RBS spectra in addition to other chemical studies will explain the presence of oxides if any. It is further concluded that  $(\text{Bi}_2\text{S}_3)_{0.40}(\text{CdS})_{0.60}$  film on Si<111> substrate yields better microstructural properties in comparison to glass substrate.

[1] S.Misra and H.C.Padhi, Jl. of Appl. Phy. 75 (1994) 4576.

**NANOCRYSTALLINE SILICON CARBIDE FILMS  
BY CHEMICAL VAPOR SYNTHESIS**

*S. Seifried, M. Winterer and H. Hahn*

Darmstadt University of Technology, Department of Materials Science,  
Thin Films Division, Petersenstr. 23, 64287 Darmstadt, GERMANY  
[<hhahn@hrzpub.tu-darmstadt.de>](mailto:hhahn@hrzpub.tu-darmstadt.de)

Nanocrystalline films in the system Si-C with grain sizes below 50 nm and thickness up to 150 microns have been prepared by a modified Chemical Vapour Deposition method, the Chemical Vapour Synthesis.

Hot-wall reaction of tetramethylsilane under inert conditions is carried out on different substrate materials at temperatures between 800°C and 1100°C by using direct precursor mass flow. The dependence of reactor position on film-thickness and growth-mode is examined. Furthermore, the influence of other processing parameters, specifically, precursor partial pressure, total pressure and temperature on microstructure and properties is investigated.

### MODIFIED POLYIMIDE STRUCTURES

*Saule K. Berzhanova, Natalya B. Stepanenko and academician Bulat A. Zhubanov*

Institute of Chemical Sciences, 106 Valihanov, 480100 Alma-Ata, KAZAKHSTAN  
<adm@chem.academ.alma-ata.su>

The creation of uniform composite polyimide (PI) on metal is actual because of low adhesive properties of PI-lacquers. In this work we present the results on modification of PI structure has been carried out by using of Si-organic structures with various length of Si-organic chain that introduced into the amine components of PI composites. The optimum of Si-organic length at n=9 of oligodimethylsiloxane units has shown the best effect of adhesive properties to the steel plate and copper wires as a isolation enameled coating with a good elasticity, hydrolytic stability and ability to heat hardening at lower temperatures. The obtained improved characteristics have been testified in the semiindustrial conditions of wire production.

There are some advantages from the modification of polyurethane (PU) materials by the use of imide cycles into the polyolic compound. It was established an optimum of isocyanate indexes for the synthesis of stable elastic foams on a basis of oligoesters vary in structures. The modified additives have shown properties of final PU composites with a further application in the reaction injection molding (RIM).

The modification of fluorinated bis  $\beta$ -diketonates contained the rare earth metals (Er, Yb) by polycondensation and polyrecombination methods leads to formation of soluble modeling compounds of Er-, Yb-polychelates on the basis of hexafluoroacetylacetone. The fluorinated derivative of tetracetylene may be applied as an efficient tetra-ligand for the rare earth metals in order to obtain soluble polychelates with the specific optical property such as a resistance to the IR-impulse (Nd) radiation generated at the frequency of  $9430\text{cm}^{-1}$  ( $\lambda=1,06\ \mu$ ) with a further luminescence in a visible range.

The peculiarities of imidization of polyamic acid (PAA) of alycyclic structure have been investigated under the  $\text{CO}_2$  -continuous laser radiation ( $\lambda=10,6\ \mu$ ). There are obtained the optimum conditions of laser imidization on the thin PAA-films ( $5-10\mu$ ) and investigated some dependencies on imidization degree (i, %) under the operated radiation.

**SINTERING BEHAVIOUR OF NANOCRYSTALLINE Y<sub>2</sub>O<sub>3</sub>**

*P. Merkert, P. Schneider, H. Hahn and J. Rödel*

TU Darmstadt, Fachbereich Materialwissenschaft, Petersenstr. 23, Geb. 73a  
64287 Darmstadt, GERMANY <merkert@hrzpub.tu-darmstadt.de>

Nanocrystalline yttria with a grain size of 27 nm was produced by inert gas condensation. Pellets of 10 mm diameter were subsequently pressed uniaxially at 5-10 kN and cold isostatically at 400 kN. Sintering studies were performed at temperatures between 1200°-1300°C for 10-960 min to obtain densities from 60-100% theoretical density. The grain size was measured by the linear intercept method as a function of density. Sintering paths of yttria were obtained and discussed in comparison to microcrystalline yttria. To observe changes in pore size distributions during sintering BET-measurements were carried out for all densities. Fracture strength was either measured by biaxial (ball-on-three-ball-configuration) flexure or four-point bending test.

**MICROSTRUCTURE, STRENGTH AND PLASTICITY  
OF NANOPHASE MATERIALS***N.I. Noskova*

Institute of Metal Physics Ural Division of Russian Academy of Sciences,  
S.Kovalevskaya str. 18, GSP-170 Ekaterinburg 620219, RUSSIA

The nanophase Fe-, Co-, and Pd-based alloys was shown to form through crystallization from an initially amorphous state at various temperatures (723-943 K) after holdings for various times. The nanophase Fe- and Co- based alloys were obtained by rapid crystallization (within several seconds) at elevated temperature (853-943 K). The nanophase alloy  $Pd_{81}Cu_7Si_{12}$  was produced by rapid quenching of a melt and crystallized during creep tests in the temperature range between 673 and 773 K.

The microstructure of the nanocrystalline alloys was studied *in situ* at different stages of crystallization of the amorphous ribbons in the column of an electron microscope. Specific features of the structure of nanometer-sized grains and of phase composition of the alloys were established depending on the schedule of the crystallization annealing. High-resolution transmission electron microscopy (HREM) was used to study the structure of nanophase crystals and their interfaces in multiphase nanocrystalline alloys. It was shown that the interfaces between chemically similar nanophases may have different structures; they may represent crystalline junction (with a transition region of no more than 0.2 nm in width) between nanocrystals whose lattices are misoriented by 2-70°; be twin boundaries; or have a more complex structure with dislocations; or even have an amorphous structure. Interphase interfaces between nanophases with different chemical compositions may represent a transition crystalline layer, or a strongly elastically distorted quasi-amorphous layer of up to 2 nm in thickness or even may have a different chemical composition. When grains of chemically different nanophases are joined, their lattices undergo internal elastic distortions and dislocation dipoles are formed inside nanocrystals.

The nanophase state of the alloys was found to be have lower strength and plasticity (as compared to those of the alloy in the amorphous state) irrespective of the crystallization temperature (623-923 K). Rapid crystallization of metallic glass at an elevated temperature under rapid heating and cooling was shown to result in a significant gain in the strength for the alloy  $Fe_5Co_{70}Si_{15}B_{10}$  at 300 K, for the alloy  $Pd_{77.5}Cu_6Si_{16.5}$  at 573 K and for the alloy  $Fe_{73.5}Cu_1Nb_3Si_{13.5}B_9$  at 673 K. The crystallized  $Pd_{81}Cu_7Si_{12}$  may exhibit a sufficiently high plasticity (from 15 to 80%) under the creep condition if it has an amorphous-crystalline structure or if the grain size does not exceed 10 nm. Defects caused by deformation of the nanophase alloy were studied. The defects in the deformation structure of the alloy indicate the appearance of specific deformation channels in the nanophase alloy.

**MECHANICAL BEHAVIOUR OF NANOCOMPOSITE  
Al-X-Zr (X = Cu, Si, Ni) ALLOYS**

*Dheepa Srinivasan and K. Chatopadhyay*

Department of Metallurgy, Indian Institute of Science, Bangalore 560 012, INDIA

Hypo eutectic Al-X (X=Cu, Si, Ni) alloys with Zr additions (1-3 at%) were synthesised using the melt spinning technique. The effect of rapid solidification as well as the ternary Zr addition results in a fine grained microstructure with large volume fractions of stable/metastable intermetallic phases, in all the cases. The nanocomposites display high hardness values (~3-4 GPa), from microhardness measurements. Mechanical properties of these multiphase high strength Al alloys are being studied. Tensile testing of the melt spun foils is carried out both at room and elevated temperatures to look into the possibility of producing alloys that are potentially superplastic. In this investigation the experimental results of the deformation behaviour are correlated with the observed microstructure.

**STRUCTURE AND MAGNETIC PROPERTIES  
OF NANOSTRUCTURED  $\text{Fe}_{40}\text{Ni}_{38}\text{Mo}_4\text{B}_{18}$**

*J. Li<sup>1</sup>, Z. Su<sup>1</sup>, H. Hahn<sup>2</sup>, F.L. Wei<sup>3</sup>, Z. Yang<sup>3</sup>, T.M. Wang<sup>1</sup>, S.H. Ge<sup>4</sup>*

<sup>1</sup>Department of Materials Science, Lanzhou University, Lanzhou 730000, CHINA

<sup>2</sup>Department of Materials Science, Technical University of Darmstadt,  
64287 Darmstadt, GERMANY

<sup>3</sup>Applied Magnetism Laboratory of SEC, Lanzhou University, Lanzhou 730000, CHINA

<sup>4</sup>Department of Physics, Lanzhou University, Lanzhou 730000, CHINA

With the purpose to search new soft magnetic nanostructured alloys, the amorphous  $\text{Fe}_{40}\text{Ni}_{38}\text{Mo}_4\text{B}_{18}$  alloy has been heat-treated to obtain the nanostructure. Nanostructured  $\text{Fe}_{40}\text{Ni}_{38}\text{Mo}_4\text{B}_{18}$  specimens with a wide range of different nanostructures can be produced by annealing the amorphous alloy in the temperature range from 700 K to 1060 K. The nanostructured  $\text{Fe}_{40}\text{Ni}_{38}\text{Mo}_4\text{B}_{18}$  specimens prepared between 700 K and 760 K have a microstructure of the 4-9 nm fcc (Fe,Ni) solid solution crystallites embedded in the amorphous matrix. The nanostructured  $\text{Fe}_{40}\text{Ni}_{38}\text{Mo}_4\text{B}_{18}$  specimens obtained between 780 K and 910 K show a polycrystalline microstructure of the major cubic  $(\text{Fe},\text{Ni},\text{Mo})_{23}\text{B}_6$  phase with grain sizes from 20 nm to 40 nm and the minor fcc (Fe,Ni) solid solution crystallites of about 10 nm. The nanostructured  $\text{Fe}_{40}\text{Ni}_{38}\text{Mo}_4\text{B}_{18}$  specimens produced between 930 K and 1060 K represent a polycrystalline microstructure of the 12-25 nm fcc (Fe,Ni) solid solution crystallites and the 45-240 nm cubic  $(\text{Fe},\text{Ni},\text{Mo})_{23}\text{B}_6$  crystallites.

Magnetic measurements revealed that the nanostructured  $\text{Fe}_{40}\text{Ni}_{38}\text{Mo}_4\text{B}_{18}$  obtained by annealing the amorphous  $\text{Fe}_{40}\text{Ni}_{38}\text{Mo}_4\text{B}_{18}$  alloy at 740 K has the highest initial permeability, the highest maximal permeability, the lowest coercivity, the maximal saturation induction, and the lowest saturation magnetostriction. The optimal magnetic properties of this nanostructured specimen can be understood by considering the combination of the zero anisotropy and the lowest saturation magnetostriction.

**BEHAVIOR AND BONDING MECHANISMS OF ALUMINUM  
NANOPARTICLES BY ELECTRON BEAM IRRADIATION***BingShe XU and Shun-Ichiro TANAKA*

Tanaka Solid Junction Project, ERATO, Japan Science and Technology Corporation,  
1-1-1 Fukuura, Kanazawa-ku, Yokohama 236, JAPAN

Activities such as migration, rotation and revolution, and bonding behavior of aluminum nanoparticles under electron beam irradiation have been investigated using a high-resolution transmission electron microscope (HRTEM) on a stage at room temperature. It was determined that the driving force of the migration, rotation and revolution of the Al nanoparticles was a momentum transfer from spirally trajected electrons and ions inside the pole piece of the HRTEM. It is estimated that before Al nanoparticles bonded, the migration distance  $x$  changed with time  $t$  as  $x = k_0 \cdot \log t$ . Furthermore, adjacent Al nanoparticles came into contact and bonded via necking. The Al/Al grain boundaries and the twin boundaries migrated to the nanoparticle surface. Finally, these boundaries disappeared, which produced a single particle or a single crystal. The bonding mechanisms are different from these of surface diffusion, volume diffusion, grain boundary or viscous flow. The bonding driving forces were the surface energy of the nanoparticle and momentum transfer from high energy electrons or ions (knock-on effect). The bonding-growth kinetic model of  $\log(r/R) = 0.3 \cdot \log t$  has been suggested. It is also clear that heating by electron irradiation is not a major controlling factor for the Al nanoparticle activities and the bonding processes.

**THE CRYSTALLIZATION OF AMORPHOUS AND FORMATION  
OF BULK NANOCRYSTALLINE IN ZR-BASED ALLOYS**

*Min Qi, A. Sagel and H.J. Fecht*

Department of Electronic and Magnetic Materials  
University of Ulm, Albert-Einstein-Allee 41, 89081 Ulm, GERMANY

More and more attention has drawn to nanocrystalline materials because their potential application prospect. However, most nanocrystallines obtained up to now were in either powder or thin film because the limit of producing process. The successful synthesis of bulk amorphous alloys by Greer, Inoue and Johnson provides the possibility of preparing bulk nanocrystalline alloy through crystallizing bulk amorphous phase. We prepared a  $Zr_{60}Al_{10}Ni_9Cu_{18}B_3$  amorphous alloy bar with 3 mm in diameter by arc-melting plus sucking its melt into a copper tube with 3 mm diameter. The present paper investigated the stability of  $Zr_{60}Al_{10}Ni_9Cu_{18}B_3$  amorphous alloy bar produced by the above method, the kinetics of crystallization, microstructure by transition electronic microscopy, differential scanning calorimeter. The results show that homogeneous amorphous has been got by arc-melting plus sucking the above alloy melt into copper tube with 3 mm diameter. The characteristic temperature parameters for this alloy are:  $T_g = 655$  K,  $T_x = 753$  K and  $\Delta T_x (=T_x - T_g) = 98$  K. The thermodynamic analysis show that the activation energy of crystallization for this alloy is about 221 KJ/mol. Kinetic analysis indicates that with different isothermal annealing, the Johnson-Mehr-Avrami kinetic curves ( $1n[-\ln(1-X_v)] - 1nt$ ) have different type, The curves at both 693 K and 703 K are nearly straight lines. The Avrami exponent  $n$  of the present alloy is about 3.2 when isothermal treating at 693 K as well as 703 K. when annealing above 720 K, the logarithmic plots according to JMA equation are consisted of two parts of straight lines which have different slope, indicating there are different crystallization mechanisms during different stage of annealing. Homogeneous nanocrystalline can be steadily got through annealing amorphous.

**STRUCTURE AND MAGNETIC PROPERTIES  
OF Ag<sub>x</sub>-Co<sub>1-x</sub> NANOPARTICLES**

*Hong-Ming Lin<sup>1</sup>, Chiun-Yen Tung<sup>1</sup>, S.J. Tzeng<sup>1</sup>, W.L. Tsai<sup>1</sup>, Y. Hwu<sup>2</sup>, Y.D. Yao<sup>2</sup> and  
Pee-Yew Lee<sup>3</sup>*

<sup>1</sup> Dept. of Materials Engineering, Tatung Institute of Technology,  
Taipei, 104, Taiwan <hmlin@mse.ttit.edu.tw>

<sup>2</sup>Institute of Physics, Academia Sinica, Nankang, Taipei, 115, Taiwan

<sup>3</sup>Institute of Materials Eng., National Taiwan Ocean University, Keelung, Taiwan

The nanocrystalline Ag<sub>x</sub>-Co<sub>1-x</sub> solid solutions are prepared by the gas condensation method. Ag and Co are immiscible both in solid and liquid states, so the liquid quenching technique is not suitable to form solid solution in this system. In this study, Ag and Co elements are co-evaporated and condensed on liquid nitrogen cold-trap to form the solid solution of nanocrystalline (NC) Ag<sub>x</sub>-Co<sub>1-x</sub>.

DSC results show there is an endothermic reaction occurs at about 350°C that indicates the dissolution of NC Ag<sub>x</sub>-Co<sub>1-x</sub> solid solution. The XRD patterns of as-received NC Ag<sub>x</sub>-Co<sub>1-x</sub> system reveal only broadening peaks of Ag, but after heat treatment up to 380°C, the Co-hcp lines are observed, indicating Co-hcp phase formed by segregation of Co atoms from Ag lattice. The similar phenomena also observed by TEM electron bombardment. The results of VSM analysis show that both saturation magnetization (Ms) and remanence (Mr) increase after heat treatment, these may suggest that the quantity and the cluster size of ferromagnetic phase precipitates may alter their origin magnetic properties.

**MAGNETIC CHARACTERIZATION OF PURE NANO-IRON**

Boxiong Qin<sup>1</sup>, Xixiang Zhang<sup>2</sup>, Gang Liu<sup>1</sup> and J. Tejada<sup>3</sup>

<sup>1</sup> Dept. of Welding , College of Mechanical Engineering, Tianjin University,  
Tianjin 300072, CHINA

<sup>2</sup> Dept. of Physics, Hong Kong University of Science & Technology,  
Clear Water Bay, Kowloon, Hong Kong, CHINA

<sup>3</sup> Fac. Fisica, Univ. Barcelona, Diagonal 647, 08028 Barcelona, SPAIN

The purity (99.9wt%) of the nano-Iron produced by the coercive evaporation process has been verified by plasma emission-spectrometry, Mössbauer analyser and XRD. Meanwhile, it is confirmed that the micro-structure of Fe nanoparticle consists in -lattice. The magnetic characterization of the nano-Iron are evaluated by SQUID. It is shown that the magnetization of the Fe nanopowder is dependent upon the temperature and particle size. At room temperature the saturation magnetization is 170emu/g in the particle size in the order of 35 nm. In the temperature range of 10 to 290K, with temperature rising the coercivity goes down. Within the mean particle size range of 15-75 nm the coercivity comes to the climax in the particle diameter in the order of 35 nm.

**DETERMINATION OF ELASTIC PROPERTIES  
OF FUNCTIONAL GRADED NANOSTRUCTURED COATINGS**

*Sergey M. Aizikovich, Leonid I. Krenev and Nadejda A. Serova*

Rostov State University, Institute for Mechanics and Applied Mathematics,  
P.O.Box 4845, Rostov-on-Don,344090, RUSSIA <aizsm@gis.rnd.runnet.ru>

Coating of substrates by specially engineered multilayers (functional graded coatings) or the base of nanomaterials is one of the most promising approaches to the extension of useful life time of articles. However, the present day techniques of evaluation of the mechanical properties of such structures are very inadequate.

Nanoindentation is a technique developed to measure the hardness of 'surfaces' and thin films which utilises very low loads and senses the indentation depth. Once a measurement technique is developed to determine the mechanical properties of the functionally graded coatings, it could be used to improve their mechanical properties.

The determination of mechanical properties of these coatings is critical for the product quality control. In literature several methods for determining different mechanical properties of a non-homogeneous material have been suggested. While some highly precise instruments make it possible to perform non-destructive indentation tests for non-homogeneous material, there has not yet been a reliable method for interpreting the testing results. A method of both mathematical simulation of standard nano-indentation tests and for test results interpretation is discussed in this paper and is applied to estimate the non-homogeneity characteristics of coatings non-homogeneous in the direction of thickness. A technique for non-destructive control of mechanical characteristics of non-homogeneous materials using a spherical indenter penetration also is described. Limits of the elastic deformation, the size of the indenter and elastic loading limits for non-homogeneous materials are discussed. Recommendation for performing experiments is also given.

**SYNTHESIS AND MAGNETIC CHARACTERISTICS  
OF SOLID-HDDR  $\text{PrFe}_{10}\text{VMoNy}$  NANOCRYSTALLINE ALLOYS**

*Z.Q. Jin, W. Tang, J.R. Zhang, S.L. Tang, L.Y. Lu and Y.W. Du*

National Laboratory of Solid State Microstructures and Institute of Solid State Physics,  
Department of Physics, Nanjing University, Nanjing 210093, CHINA <ufp@nju.edu.cn>

Isotropic  $\text{Pr}(\text{Fe},\text{V},\text{Mo})_{12}\text{Ny}$  nanocrystalline compounds have been fabricated by solid-HDDR (hydrogenation-disproportionation-desorption-recombination) and subsequent nitrogenation processes. The phase component, microstructure and magnetic properties of the samples have been investigated systematically using x-ray diffraction, thermomagnetic analysis and magnetic measurements. The disproportionation of the  $\text{Pr}(\text{Fe},\text{V},\text{Mo})_{12}$  matrix phase with hydrogen results in the formation of a nanocrystalline mixture consisting of  $\text{PrH}_{2+\delta}$ ,  $\text{Fe}_2(\text{Mo},\text{V})$  and  $\alpha$ -Fe. As the hydrogenated samples are degassed at 923 K in a vacuum for 15 min, a metastable  $\text{TbCu}_7$ -type crystal structure is presented. With increasing dehydrogenation time to 2 h or temperature to 973 K, the  $\text{TbCu}_7$ -type phase transforms into  $\text{Pr}(\text{Fe},\text{V},\text{Mo})_{12}$  compounds by accompanied with the decrease of the Curie temperature. Above 1173 K,  $\text{Pr}(\text{Fe},\text{V},\text{Mo})_{12}$  partially decomposes and the amount of  $\alpha$ -Fe increases with the growth of grains, resulting in the apparently degrades of magnetic properties. The optimum temperature for the HDDR process is 1073 K for preparing the isotropic  $\text{Pr}(\text{Fe},\text{V},\text{Mo})_{12}\text{Ny}$  magnets. Upon nitrogenation at 773 K, the Curie temperature is found to be 616 K for 1:12 type nitrides, however, it is undefined for  $\text{TbCu}_7$  type nitrides due to the broaden of magnetic-order transition. The optimum coercivity of 3.5 kOe with a magnetization up to 131 emu/g at a field of 2 T is obtained for 1:12 compounds without fine milling. The solid-HDDR process proved to be very rapid and effective for homogenizing the as-cast alloys.

**THERMAL CONDUCTING BEHAVIOR  
OF NANOSTRUCTURED Y-TZP COMPACTS**

*Z.Qian and J.L.Shi*

State key Lab. of High Performance Ceramics and Superfine Microstructure, Shanghai  
Institute of Ceramics, 1295 Ding-xi Road, Shanghai, CHINA

The compacts of Y-TZP (yttria stabilized tetragonal zirconia polycrystalline) with different crystallite size from about 8 nm to about 80nm were fabricated, and the thermal conductivity of the compact materials were measured. It was found that the thermal conducting behavior of the materials was strongly dependent on the crystallite size, density and temperature. The most distinguished feature of the materials is that the thermal conductivity of compacts with crystallite size smaller than about 50 nm increases with the increase of measuring temperature, while materials of the crystallite size larger than about 50 nm show the decreased thermal conductivity with the increase of temperature, which is similar to micrometer-sized Y-TZP material. The unusual thermal conducting behavior of the nanostructured materials was discussed.

**FORMATION OF NANOSTRUCTURES AND OF POWDER  
CONSOLIDATION OF Nd(Pr)FeB ALLOYS BY SPD-METHOD.**

V.V. Stolyarov and D.V. Gunderov,

Institute of Physics of Advanced Materials, Ufa State Aviation Technical University,  
K. Marx 12, Ufa, 450000, RUSSIA <vlst@ippm.rb.ru>

Traditional methods of processing ultrafine-grained state in NdFeB alloys are rapid quenching and ball-milling. On the basis of these methods technological processes of fabrication of magnetic hard materials with records properties were developed.

Present investigations show that a non-traditional method of severe plastic deformation (SPD) at room temperature results in formation of a metastable ultrafine-grained structure and at maximum strain values in a quasiamorphous structure of Nd(Pr)FeB alloys. The SPD method involves conducting torsion straining under high pressure ( $P = 5 - 12$  GPa) on Bridgman anvils. It was established that Nd(Pr)FeB alloys of various composition display almost similar dependencies of their structure and magnetic properties on strain values. At the same time starting composition of an alloy exerts considerable influence on sequence of structural transformations during deformation. Heat treatment of the severe plastic deformed Nd(Pr)FeB alloys leads to formation of an ultra fine-grained high coercive state (to 2240 kA/m in the  $\text{Pr}_{20}\text{Fe}_{73.5}\text{B}_5\text{Cu}_{1.5}$  alloy after SPD and annealing).

SPD methods (conducted at room temperature) also allow us to fabricate compacts out of nanocrystalline rapidly quenched, gas-atomised and ball-milled NdFeB powders with density almost equal to 100%. It is very important that in compacts processed by SPD methods the metastable amorphous and nanocrystalline state is still preserved.

**STRUCTURE AND OPTICAL PROPERTIES  
OF NANOCRYSTALLINE GERMANIUM AND SILICON**

*R.K. Islamgaliev<sup>1</sup>, R. Kuzel<sup>2</sup>, S. Mikov<sup>3</sup>, E. Obraztsova<sup>4</sup>, F. Chmelik<sup>2</sup> and R.Z. Valiev<sup>1</sup>*

<sup>1</sup>Institute of Physics of Advanced Material, Ufa State Aviation Technical University,  
K.Marx 12, Ufa 450000, RUSSIA

<sup>2</sup>Department of Metal Physics, Charles University, Ke Karlovu 5,  
12116 Prague 2, CZECH REPUBLIC

<sup>3</sup>Ulyanovsk State University, Ulyanovsk 432000, RUSSIA

<sup>4</sup>General Physics Institute, Moscow 117942, RUSSIA

TEM, XRD, Raman scattering and measurements of photoluminescence spectra were used in this work in order to study the structure and optical properties of nanocrystalline germanium and silicon processed by severe plastic deformation.

TEM images have shown that the structure of samples is characterised by lognormal grain size distribution with a mean grain size of about 20 nm and by significant fraction of high angle grain boundaries. High level of internal elastic strains was revealed by X-ray analysis. Spectra of Raman scattering showed widening of peaks, their shift to lower frequencies and appearance of an additional peak. Exhibition of photoluminescence was revealed in a visible area of the spectrum in the as-prepared samples of nanocrystalline silicon. A significant difference of a mean grain size estimated by TEM, XRD and Raman scattering is noticed.

The obtained results are discussed on the basis of a structural model of a nanostructured state. According to this model, severe plastic deformation results not only in very small grain size but also in the formation of a specific grain boundary defect structure associated with high level of internal elastic strains and distortions of crystal lattice in the near boundary area. Such an unusual structure of semiconductors subjected to severe plastic deformation is responsible for their unique optical properties.

**AGEING EFFECTS IN METASTABLE NANOSTRUCTURED ALLOYS.**

*V.V. Stolyarov and R.Z. Valiev.*

Institute of Physics of Advanced Materials, Ufa State Aviation Technical University,  
Ufa 450025, RUSSIA <vlst@ippm.rb.ru>

Bulk nanostructured ultrafine-grained materials can be successfully processed by severe plastic deformation [1]. Moreover, severe plastic deformation can also result in formation of metastable states associated with supersaturated solid solutions. In the present work nanostructured metastable alloys are processed by two methods: (1) severe torsion straining under high pressure of the alloys 01959 (Al-6.1%Zn-2.8%Mg-1%Cu-0.37%Zr) and VT6 (Ti-6%Al-4.5%V) in the quenched state; (2) severe torsion straining of the alloy Al-11%Fe; this alloy is immiscible in the cast state but can form supersaturated solution iron in aluminium after deformation [2,3]. Processes of ageing are studied in the fabricated alloys by methods of transmission electron microscopy and X-ray structural analysis as well as by changes in mechanical properties.

It was established that severe plastic deformation results in refinement of structure to the mean grain size of matrix phase 70 nm in the alloy 01959 and 100 nm in the Al-11%Fe and VT6 alloys. The formed structure has high angle grain boundaries.

In the deformed state all alloys display higher values of microhardness as compared to the as-received state by a factor of 2-3. Additional significant hardening of the alloys occurs during following natural or artificial ageing. The achieved level of microhardness (3000 MPa) and strength (750 MPa) is a record for this type of aluminium alloys.

The observed structural features and the possible operating mechanisms of hardening in the nanostructural alloys during ageing, in particular, solid solution hardening, structural strengthening directly connected with grain refinement and precipitation hardening, are discussed.

1. R.Z. Valiev, ed., Ultrafine-Grained Materials Produced by Severe Plastic Deformation, Special Issue, Ann. Chim. Mat. Sci., Fr., 21, 6-7 (1996).
2. V.V. Stolyarov, V.V. Latysh, V.A. Shundalov, D.A. Salimonenko, R.K. Islamgaliev, R.Z. Valiev, Mater. Sci. Eng. A 234-236 (1997) 339-342
3. O.N. Senkov, F.H. Froes, V.V. Stolyarov, R.Z. Valiev and J. Liu, Proc. of 5th Int. Conf. Advanced Particulate Materials and Processes, Eds F.H. Froes and J. Hebeisen, April 1997, West Palm Beach, USA

**MAGNETIC PROPERTIES AND STRUCTURE  
OF NANOCRYSTALLINE Fe-Al AND Fe-Ni ALLOYS**

*Elzbieta Jartych<sup>1</sup>, Jan K. Zurawicz<sup>1</sup>, Dariusz Oleszak<sup>2</sup> and Marek Pekala<sup>3</sup>*

<sup>1</sup> Technical Univ. of Lublin, Dept. of Experimental Physics, ul. Nadbystrzycka 38,  
20-618 Lublin, POLAND <jartych@antenor.pol.lublin.pl>

<sup>2</sup> Warsaw Univ. of Technology, Dept. of Materials Science and Engineering,  
ul. Narbutta 85, 02-524 Warsaw, POLAND

<sup>3</sup> Univ. of Warsaw, Dept. of Chemistry, Al. Zwirki i Wigury 101,  
02-089 Warsaw, POLAND

In this work the magnetic and structural properties of nanocrystalline Fe-Al and Fe-Ni alloys were determined. Alloys were prepared by the mechanical alloying process in a conventional horizontal low energy ball mill in case of Fe-Al and in a high-energy ball mill in case of Fe-Ni. The standard X-ray diffraction, Mössbauer and magnetic studies were carried out on the powder samples.

The structural investigations proved that in the low energy mechanical alloying process of Fe and Al the disordered bcc solid solution was formed up to 50 at.% Al. The final products of milling were nanocrystalline and exhibited interesting magnetic properties somewhat different as compared with microcrystalline alloys. The following effects were observed:

- (i) the mean hyperfine magnetic fields and the magnetic ordering temperatures were higher in the nanocrystalline Fe-Al alloys than in the microcrystalline alloys;
- (ii) the average magnetic moments per Fe atom  $\langle\mu_{Fe}\rangle$  in nanocrystalline Fe-30 at.% Al and Fe-40 at.% Al were about 10 % smaller as compared with the corresponding microcrystalline alloys while in equitoxic FeAl alloy  $\langle\mu_{Fe}\rangle$  was significantly larger than that obtained for microcrystals due to the ferromagnetic interactions.

In case of Fe-Ni alloys the bcc solid solution is formed during milling for the composition with 20 at.% Ni, while for the 35 at.% Ni the fcc solid solution was obtained. Both mechanically synthesised alloys were ferromagnetic and no Invar effect was observed for 35 at.% Ni.

**INVESTIGATION OF THE SOFT MAGNETIC PROPERTIES  
OF FeCuNbB ALLOYS**

*T. Girhardt<sup>1</sup>, J. Hess<sup>1</sup>, A. Grabias<sup>2</sup>, M. Kopcewicz<sup>2</sup>, D. Ramin<sup>3</sup>, W. Riehemann<sup>3</sup>*

<sup>1</sup> Institut für Metallphysik und Nukleare Festkörperphysik, TU Braunschweig,  
Mendelssohnstr. 3, 38106 Braunschweig, GERMANY <J.Hesse@TU-BS.DE>

<sup>2</sup> Institute of Electronic Materials Technology, Wolczynska Str. 133,  
PL-01-919 Warsaw, POLAND

<sup>3</sup> Institut für Werkstoffkunde und Werkstofftechnik, TU Clausthal,  
Agricolastr. 6, D-38678 Clausthal-Zellerfeld, GERMANY

The alloy system of  $\text{Fe}_{86-x}\text{Cu}_1\text{Nb}_x\text{B}_{13}$  ( $x=4,5,7$ ) was subject to an investigation of its soft magnetic properties. The amorphous ribbons were annealed for 1 hour at different temperatures, in order to obtain samples in different crystallisation states, including nanocrystalline state. After that, a phase analysis was done using room temperature Mössbauer spectrometry. The soft magnetic properties were studied using the Mössbauer effect in radio frequency (rf) magnetic fields. We could show that classical measurements, like those of the coercive force  $H_C$ , correspond well to the results obtained by our rf Mössbauer measurements. The results show that the appearance of FeB-phases impairs the good soft magnetic properties of this alloy system.

**SOFT MAGNETIC PROPERTIES OF Fe(Cu,Nb)SiB ALLOYS EVIDENCED BY  
MÖSSBAUER EXPERIMENTS IN RADIO FREQUENCY MAGNETIC FIELDS**

*T. Graf<sup>1</sup>, J. Hesse<sup>1</sup> and M. Kopcewicz<sup>2</sup>*

<sup>1</sup> Institut für Metallphysik und Nukleare Festkörperphysik, TU Braunschweig,  
Mendelssohnstr. 3, 38106 Braunschweig, GERMANY <J.Hesse@TU-BS.DE>

<sup>2</sup> Institute of Electronic Materials Technology, Wolczynska Str. 133,  
PL-01-919 Warsaw, POLAND

Conventional (transmission) Mössbauer effect investigations on alloys exhibiting a nano structure deliver valuable information about the alloys microstructure. The application of a radio frequency magnetic field parallel to the absorber plain causes the Mössbauer effect to become a very sensitive tool for detecting soft magnetic properties. These features are due to two effects, the appearing of side bands in the spectra and the collapse of the spectrum. Recently it was discovered that in multiple phase alloys like nanostructured Fe(Cu,Nb)SiB a partial collapse of the components in the spectrum appears if the amplitude of the radio frequency magnetic field is chosen properly.

In this contribution we demonstrate the abilities of this measurement method comparing well-known results about magnetostriction and coercivity with the information content of the Mössbauer spectra collected at different compositions of the Fe(Cu,Nb)SiB alloys.

**HETEROVALENT CLUSTERS OF COPPER ATOMS IN LAYERED SUPERCONDUCTING OXIDES AND THEIR SOLID SOLUTIONS**

*N. Bobrysheva, M. Mikhailova, N. Chezhina and M. Osmolovski*

Sankt-Petersburg State University, Universitetskii pr.2, St.Petersburg,  
Petrodvorets 198904, RUSSIA <chezhina@nc2490.spb.edu>

Complex investigation of magnetic properties (magnetic susceptibility, malefic dilution, magnetic dependent microwave absorption) of superconducting (SC) complex oxides  $\text{La}_{1.85}\text{Sr}_{0.15}\text{CuO}_4$ ;  $\text{La}_{1.85}\text{Sr}_{0.15}\text{Cu}_{0.9}\text{Li}_{0.1}\text{O}_4$ ;  $\text{La}_{1.85}\text{Ba}_{0.15}\text{CuO}_4$ , and their solid solutions in diamagnetic solvents results in a conclusion about their submicroheterogeneous structure the presence of stable nanofragments in them, responsible for superconductivity.

The study of the  $y(\text{La}_{1.85}\text{Sr}_{0.15}\text{CuO}_4)(1-y)(\text{LaSrAlO}_4)$  system ( $0.01 < y < 1$ ) have shown that SC properties are preserved even at a very lame dilution (up to 90 mol % of the diamagnetic solvent), the temperature of the transition to SC state ( $T_c$ ) being 37 K and invariable on dilution. An adequate description of magnetic and electric properties is possible if we suggest that an elementary structural unit, responsible for these properties, is a cluster of copper and oxygen atoms of the Cu(II)-O-Cu(III)-O-Cu(II) type. Then, on the basis of structural parameters of the oxide, the minimal size of the cluster (i.e. the size of the nanofragment, stable toward dilution) is 0.78 nm. The inevitable integration of the nanofragments, as the concentration of the solid solution increases, does not result in the changes in  $T_c$ , i.e the structural nanofragment is an elementary superconducting fragment.

A similar situation is realized also in the solid oxide  $\text{La}_{1.85}\text{Sr}_{0.15}\text{Cu}_{0.9}\text{Li}_{0.1}\text{O}_4$ , where the replacement of a part of copper atoms by lithium does not result in a decrease in  $T_c$  (~36 K).

A decisive proof of the submicroheterogeneous structure of perovskite-like oxides seems to us to be the properties of the  $y(\text{La}_{1.85}\text{Sr}_{0.15}\text{CuO}_4)(1-y)(\text{LaSrAlO}_4)$  system ( $0.01 < y < 1$ ). Concentrated solutions have the layered structure ( $y > 0.5$ ); diluted solutions have the  $\beta\text{-K}_2\text{SO}_4$  type structure, where Cu and Al atoms are situated in isolated tetrahedron of oxygen atoms. Nevertheless  $T_c$  is 35 K. for the pure oxide, decreases to 14 K upon introduction of 15 mol% of the solvent and does not change further up to its content of 85 mol%. These data convincingly show that the character of the term splitting of copper atoms ( $\text{O}_h$  or  $\text{T}_d$ ) within the clusters - nanofragments does influence  $T_c$  but does not affect the very fact of the SC evoking. The stability of the clusters is suggested to be determined by an additional Coulomb interaction in the resulting quasi-particles of exciton type (Cu(III) - positive charge, hole, Cu(II) - negative charge, electron).

**MAGHEMITE NANOPARTICLES :  
FORMATION UNDER HYDROTHERMAL CONDITIONS**

*M.G. Osmolovski, V.N. Gittsovich and V.G. Semenov*

St. Petersburg State University, Universitetskii pr.2, Sankt-Petersburg,  
Petrodvorets 198904, RUSSIA <chezhina@nc2490.spb.edu>

It is known that the hydrothermal decomposition of iron(III) hydroxide in an alkali medium (pH =11 - 12) in the presence of organic complexing agents - polycarboxylic acids or phosphonic acids allows ultrafine particles of  $\alpha$ -Fe<sub>2</sub>O<sub>3</sub> to be obtained. These particles always have a narrow distribution by the sizes. The shape of the particle (from sphere to spindle) also can be regulated.

During the study we have found that the chemical processes can be represented as crystallization of the oxide within one colloid aggregate of the hydroxide nanoparticles. The diameter of the aggregate depends on the concentration and type of complexing agent.

At the ratio of complexing agent/iron  $5 \times 10^3$ -  $2 \times 10^2$  mol/mol nanodispersed  $\gamma$ -Fe<sub>2</sub>O<sub>3</sub> results from the reaction. The particle sizes were determined by the SSA and TEM methods. In the case of the powder with the linear size of the particles about 80 nm the magnetic properties were studied (by the Faraday method in the range 80 - 293 K) and Mossbauer spectra. The extrapolation of the specific magnetization of saturation to  $1/H = 0$  results in  $\sigma = 2.5 \text{ A} \times \text{m}^2/\text{kg}$  at 293 K. At room temperature and zero applied field the Mossbauer spectrum consists of superparamagnetic center peaks (doublet).

**EXPERIMENTS ON THE POSSIBLE USE  
OF NANOSCALE PARTICLES AS NANOCOMPASS**

*E. del Barco, J.M. Hernandez, A. Julia, R. Ziolo and J. Tejada.*

Dpto. Fisica Fundamental. Universidad de Barcelona,  
Diagonal, 647. 08028 Barcelona. SPAIN <edb@ffn.ub.es>

In this paper we describe experiments we have carried out using small magnetic particles embedded in different polimeric matrixes. Our main conclusion, which is based on both low and high field measurements, is that the low temperature viscous behaviour of the nanoparticles dispersed in the polimeric matrix is due to the existence of cavities inside which the particles are free.

**SIZE AND SHAPE EFFECT ON THE CANTED ANTFERROMAGNETISM  
IN  $\alpha\text{-Fe}_2\text{O}_3$  PARTICLES**

*D. Fiorani, L. Suber, A. Garcia, A.M. Testa, P. Imperatori, J.L. Dormann<sup>1</sup>, M. Angiolini<sup>2</sup> and A. Montone<sup>2</sup>*

ICMAT, CNR, C.P. 10, 00016 Monterotondo Stazione (Roma), ITALY

<sup>1</sup> Lab. de Magnetisme et d'Optique, CNRS, 78035 Versailles, FRANCE

<sup>2</sup> ENEA, CR Casaccia, INN-NUMA, C.P. 2400, 00100 Roma, ITALY

<Fiorani@nserv.icmat.mlib.cnr.it>

The magnetic properties of  $\alpha\text{-Fe}_2\text{O}_3$  particles of different shape (spherical, rhombohedral and acicular) and size have been investigated by magnetization and Mössbauer spectroscopy measurements. For spherical (average diameter between 10 and 50 nm) and rhombohedral (average edges between 30 and 50 nm) particles samples, the spin reorientation Morin transition  $T_M$  (263 K in the bulk) was found to decrease with decreasing particle size. On the other hand, for acicular particles samples (average major axis between 400 and 500 nm, minor axis between 90 and 100 nm), the Morin temperature was observed only after annealing. In some spherical and rhombohedral samples, a small fraction of superparamagnetic nanoparticles is also present, as shown by a broad maximum in the low field ( $H = 20$  Oe) magnetization centered between 30 and 60 K, depending on the sample, and by the superposition of a magnetic sextuplet and a superparamagnetic doublet in Mossbauer spectra at room temperature. Field dependent magnetization measurements show that the magnetization consists of the sum of two contributions:  $M = M_0 + c_{AF}H$ , where  $c_{AF}$  is the antiferromagnetic susceptibility and  $M_0$  is due both to the weak ferromagnetism, induced by the canting of the two sublattices, and the uncompensated spins due to the reduced particle size. Both  $c_{AF}$  and  $M_0$ , whose temperature dependences were investigated in detail, show a clear change of behaviour at  $T_M$ . A spin flop transition, revealing the reorientation of the sublattices magnetization in a direction perpendicular to the applied field, is observed at a few tesla (e.g.  $H_{sf} \sim 3$  T for acicular particles).

**ANOMALIES IN MAGNETIC PROPERTIES OF Fe-O TWO-DIMENSIONAL  
NANOSTRUCTURES ON THE SURFACE OF DIAMAGNETIC MATRIX**

*E. V. Charnaya<sup>1,2</sup>, K. J. Lin<sup>1</sup>, V. M. Sarnatskii<sup>1,2</sup>, C. Tien<sup>1</sup>, and V. M. Smirnov<sup>2</sup>*

<sup>1</sup> National Cheng Kung University, Tainan, Taiwan

<sup>2</sup> St.Petersburg State University, St.Petersburg 198904, RUSSIA  
<sarnazki@onti.niif.spb.ru>

The problem of magnetic ordering realization in the ultra-thin layers obtained by the method of molecular layering (ML-ALE) is considered. Magnetization of Fe-O ionic layers (3–15 Å) on the silica surface is studied within temperature interval 50–300 K using an SQUID magnetometer. Samples containing various amount of Fe-O groups in the surface layer with terminal organic ligands (sample (mmole/g): 1 - 0.38, 2 - 0.26) have shown unusual magnetic properties. Zero field cooled (ZFC) and field cooled (FC) magnetization versus temperature were measured at H 200 Oe. ZFC and FC are almost similar for sample no. 1, whereas ZFC magnetization for sample 2 is twice higher than the FC one. Magnetization versus magnetic field curves measured at low temperature for sample 2 revealed a weak ferromagnetism, the hysteresis loop are merged near 2000 Oe. When cooled in high magnetic field the hysteresis loops are shifted. The overall behavior of sample 2 showed a weak ferromagnetism at low temperature and very smeared phase transition into a magnetic ordered state.

**MAGNETIC DIPOLE EFFECTS  
IN THE OPTICAL PROPERTIES OF NANOCOMPOSITES**

*G.A. Niklasson and E. Wäckelgård*

Department of Materials Science, Uppsala University,  
P.O. Box 534, S-75121 Uppsala, SWEDEN

We analyse the optical properties of nanocomposites consisting of small metallic particles dispersed in a dielectric matrix. The optical response of nanoparticles is usually dominated by the electric dipole term, but in special cases the magnetic dipole contribution may also be important. We show that the magnetic dipole response is actually dominant when the real part of dielectric function of the matrix material goes through zero and the imaginary part is small. For dielectric materials this happens in the infrared wavelength range. The interactions of photons with phonons give rise to the polariton absorption. The dielectric function of the dielectric can to a very good approximation be described with the Lorentz model. The real part is zero and the imaginary part is small at the longitudinal phonon frequency,  $\omega_{\text{LO}}$ . Around this frequency we anticipate that the optical properties of metal-dielectric composites will be largely due to magnetic dipole effects. This observation may explain certain anomalies observed earlier for nickel-alumina and cobalt-alumina composites. Around  $\omega_{\text{LO}}$ , the dielectric function was observed to fall outside the rigorous Bergman-Milton bounds, which are valid for the electric dipole response.

**POSITIVE MUONS IN NANOCRYSTALLINE TRANSITION METALS:  
DIFFUSION AND MAGNETIC NANOSTRUCTURE**

*O. Hartmann, R. Wäppling and M. Ekström*

Dept. of Physics, Uppsala University S-75121 Uppsala, Sweden

B.Heisel, M.Schmelzer, H.Natter and R.Hempelmann,

Physical Chemistry, University Saarbrücken, D-66123 Saarbrücken, Germany

Positive muons in condensed matter can be considered as hydrogen isotopes with a rich variety of diffusion effects due to their light mass. Furthermore, due to their magnetic moment, positive muons are powerful atomistic probes for local magnetic fields.

A systematic mSR study on nano-Cu (as a non-magnetic transition metal) demonstrates that the diffusion of m+ in nanocrystalline metals is influenced by both features of the nanostructure, i.e. by the very small grain size and by the comparatively large fraction of grain boundaries. The former effect yields a size effect of the phonon-assisted muon tunnelling, but only at particle diameters below 20 nm. The latter feature, in samples with crystallite sizes above 20 nm, establishes a connection between m+ diffusion and volume fraction of grain boundary regions [1].

Systematic mSR studies on nano-Ni and nano-Co (as ferromagnetic transition metals), again as a function of grain size, give insight into the magnetic nanostructure. The muon allows to distinguish between a (narrow) geometrical grain boundary (with topological disorder) and a broad one, in accordance with the model of Kronmüller [2]. In the framework of a special two-state model for the muon diffusion in nano-Ni, we are able to estimate the thickness of the magnetically disordered region which increases approximately linearly with temperature.

[1] M.Soetratmo, H.Natter, R.Hempelmann, O.Hartmann, R.Wäppling and M.Ekström,  
Hyperfine Interactions **105**, 245-252 (1997).

[2] H. Kronmüller, Basic magnetic properties of nanocrystalline particles and particle  
ensembles, in A.Hernando, Nanomagnetism, Kluwer Academic Publ., Amsterdam  
1993.

---

**DIFFUSION-INDUCED CREEP OF POLYCRYSTALLINE  
AND NANOSTRUCTURED METALS.***Yu.R. Kolobov*

Institute of Strength Physics and Material Science, RAS  
Pr. Academicesky 2/1, 634021 Tomsk, RUSSIA <ispms@ispms.tomsk.su>

Kinetic mechanisms of phenomena to be induced by the diffusion on the grain boundaries in polycrystalline and nanostructured (NS) materials have been analyzed. It is found that the diffusion-induced activation of grain-boundary sliding, creep and superplasticity occur under the conditions where a certain kinetic diffusion regime is realized. For the known values of the grain boundary and volume diffusion coefficients the conditions of occurrence of these processes (temperature and time intervals) can be determined by the computational procedures. This approach makes the basis for predicting the effect of diffusion-induced loss of strength in polycrystalline and nanostructured materials.

By way of example of Ni and Cu nanostructured (grain size 100 - 200 nm) it was shown that the effect of diffusion induced loss of strength by creep was much observed at temperatures low than 400 K in comparison with polycrystalline condition with grain size 50  $\mu\text{m}$ .

It was supposed that the physical reason for the decrease in the temperature for the effect to manifest itself is much higher value of diffusion coefficients of impurities in nanostructures.

For instance, the diffusion investigation conducted on a Ni(Cu) system (the impurity is in round brackets) using the method of the secondary ion mass-spectroscopy (SIMS) has shown that values of grain boundary diffusion coefficient of Cu in nanostructured Ni at temperatures from 398 to 573 K exceeded the coarse-grained ones by 5-6 orders of magnitude.

**INFLUENCE OF GRAIN BOUNDARY DIFFUSION FLUXES OF IMPURITY  
ON THE VALUE OF CREEP ACTIVATION ENERGY  
OF NANOSTRUCTURED AND COARSE-GRAINED NICKEL**

*Ratochka I.V., Grabovetskaya G.P., Kolobov Yu.R. and Ivanov K.V.*

Institute of Strength Physics and Material Science, RAS.  
Pr. Academichesky 2/1, 634021 Tomsk, RUSSIA <ispms@ispms.tomsk.su>

The transitions of apparent activation energy value ( $Q_c$ ) of nanosrtuctured (NS) nickel produced by equal-channel angular pressing (grain size 0.1-0.3  $\mu\text{m}$ ) and coarse-grained nickel (grain size-5  $\mu\text{m}$ ) have been investigated during plastic deformation in vacuum and under the influence of copper grain boundary diffusion fluxes from the external source (coating) at temperature range 423-473K. The effect of considerable decrease of creep resistance under grain boundary diffusion fluxes of impurity has been found. Herewith maximum of the effect takes place at 873K for coarse-grained nickel and at more low temperature for NS one (423K). Noted singularity is shown to be connected with more higher value of grain boundary diffusion coefficient in NS state (increase on 5-6 order of magnitude). It has been established that for NS nickel creep in vacuum  $Q_c = 115 \pm 15$  kJ/mol. For coarse-grained nickel creep under the same conditions  $Q_c = 270 \pm 15$  kJ/mol which corresponds to apparent activation energy value of volume self-diffusion. Decrease of creep apparent activation energy is assumed to be caused by specialty of plastic deformation development in NS state. For NS nickel creep under influence of copper grain boundary diffusion fluxes from the coating at 423K (it corresponds to maximum value of creep acceleration effect)  $Q_c = 70 \pm 15$  kJ/mol which nearly check with activation energy of copper grain boundary diffusion into NS nickel ( $Q=60.2$  kJ/mol). Simultaneously at 473K  $Q_c$  value for NS nickel coated by copper is the same with  $Q_c$  value of samples without coating (no acceleration effect). One supposes that  $Q_c$  value transition for NS nickel under creep acceleration effect is connected with change of main deformation mechanism from intracrystalline dislocation sliding to grain boundary sliding. Hence creep acceleration effect for NS nickel as well as for coarse-grained one is caused by increase of grain boundary sliding contribution to total deformation.

**INVESTIGATION OF POSSIBILITY TO GET SUPERPLASTIC STATE  
OF NANOSTRUCTURED COPPER**

*K.V. Ivanov, L V. Ratochka and Yu.R. Kolobov.*

Institute of Strength Physics and Material Science, RAS.  
Pr. Academicesky 2/1, 634021 Tomsk, RUSSIA <ispms@ispms.tomsk.su>

The possibility of realisation of superplastic state of nanostructured (NS) copper (grain size 0.1-0.3  $\mu\text{m}$ ) produced by equal-channel angular pressing has been studied during creep and tensile tests in vacuum and under the influence of aluminium grain boundary diffusion fluxes from external source (coating). It has been established that the creep curves of NS copper at 373-473K have conventional three-stage form except the curves at 473K and loads less than 140 MPa which have five stages. Herewith plasticity of the copper rises strongly (from 10% to 50%). Such character of the creep is supposed to be caused by process of dynamic recrystallisation during deformation. The creep acceleration effect for NS copper under the influence of diffusion fluxes through aluminium grain boundary is found. The effect takes place at lower temperatures as compared with coarse-grained state. The decrease of the effect display temperature is supposed to be caused by the essential increase of diffusion coefficients of aluminium in NS copper beside coarse-grained one. It has been established that at 473K strong increase of strain rate sensitivity takes place during deformation of copper under influence of aluminium diffusion fluxes ( $m=0.5$ ) in comparison with pure copper ( $m=0.19$ ). One supposes it may be caused by increase of grain boundary sliding contribution to total deformation. However superplasticity does not realise under indicated conditions. Superplasticity does not realise during NS copper tensile tests at 293-973K and  $\dot{\epsilon}^* = 3.3 \cdot 10^3 \text{ s}^{-1}$  also. So nanostructure existence is not enough for metal polycrystal transition to superplastic state.

**MAGNETIC SUSCEPTIBILITY OF NANOCRYSTALLINE  
PARTICLES OF DISELENIDES OF V (Nb) AND VI (Mo, W)  
METALS OF PERIODIC SYSTEM**

*G.V. Lashkarev, A.I. Dmitriev, L.M. Kulikov, and A.A. Semjonov-Kobzar.*

Institute for Problems of Materials Science, 3 Krzhizhanovsky st.,  
252142 Kiev, UKRAINE <lashk@ipms.kiev.ua>

The temperature dependence of magnetic susceptibility (MS) of d-transition metals diselenides of V (Nb) and VI (Mo, W) group of the Periodic System is investigated. NbSe<sub>2</sub> in the bulk state has a metallic conductivity (free and valence zone are overlapped). MoSe<sub>2</sub> and WSe<sub>2</sub> are semiconductors with energy gap 1.6 and 1.35 - 1.6 eV accordingly. The dimensions of initial particles before dispersion are 10 - 40 μm. Dispersion of diselenides up to nanocrystalline dimensions was fulfilled by special intercalation upon ultrasonic and electrochemical influence.

MS of diselenides powders with metallic and semiconducting conductivity changes in opposite ways by their dispersion. NbSe<sub>2</sub> with metallic conductivity is a Pauli paramagnet in initial state. It becomes diamagnet after dispersion up to particles dimensions about 25 - 140 nm. The transition paramagnet - diamagnet is not connected with powders oxidation. The density of state decrease is a reason for downsizing of Pauli paramagnetism in a comparison with MS of crystal lattice ( $|\chi_{\text{lattice}}| > \chi_{\text{Pauli}}$ ).

An intercalation of NbSe<sub>2</sub> by Cu at powder dispersity up to 5 nm does not lead to a change of MS sign. Apparently the change of density of states on Fermi surface at intercalation by Cu and at dispersion compensates one another and does not change MS magnitude essentially.

Semiconducting MoSe<sub>2</sub> and WSe<sub>2</sub> powders are diamagnets in initial state. Their MS is defined by susceptibility of crystal lattice. But they become Pauli paramagnets after dispersion up to dimensions of 15 - 95 nm. By dispersion the cutting of atom chemical bonds on particles surface occurs. One can suppose that a great concentration of free electrons appears. Along with high density of states on Fermi surface it leads to a correlation ( $|\chi_{\text{lattice}}| < \chi_{\text{Pauli}}$ ). The last determines the positive sign of MS in nanocrystalline MoSe<sub>2</sub> and WSe<sub>2</sub>.

**MAGNETIC PROPERTIES OF MECHANICALLY ALLOYED  
NANOCRYSTALLINE Ni<sub>3</sub>Fe**

*C.N. Chinnasamy, A. Narayanasamy, K. Chattopadhyay\* and N. Ponpandian*

Department of Nuclear Physics and Materials Science, Centre University of Madras,  
Guindy Campus, Chennai 600 025, INDIA <madphy@iitm.ernet.in>

\*Centre for Advanced Study, Department of Metallurgy, Indian Institute of Science,  
Bangalore 560 012, INDIA.

Disordered Ni<sub>3</sub>Fe alloy was prepared by mechanical alloying of elemental powders in a planetary ball mill (Fritsch Pulverisette ‘P5’) in toluene atmosphere. X-ray diffraction analysis reveals that the initially sharp diffraction peaks significantly broaden after 30 hours of milling. The broadening of Bragg peaks is caused by both the small size of the diffracting grains and by atomic level strain. In the early stages of milling the crystal size decreases rapidly to less than 20 nm. Further refinement proceeds slowly and reaches a saturation value of 10 nm. About 5% iron is found to be present even after 144 hours of milling. This may be a consequence of the lower milling intensity (200 rpm). When the milling intensity was increased (300 rpm), Ni<sub>3</sub>Fe phase was fully formed even at 50 hours of milling and no unreacted Fe was detected. The chemical composition and morphology of the powder have been studied by using EDAX and SEM analysis respectively.

The saturation magnetisation and coercivity were measured as a function of milling time by using Vibrating sample Magnetometer. The hyperfine field distributions obtained from the Mössbauer studies for different milling hours of the sample reveal that the alloy is highly disordered. The average hyperfine field value of 27.5 Tesla is attributed to the disordered Ni<sub>3</sub>Fe phase. The results of the atomic ordering studies will also be discussed.

**LOCAL MAGNETIC PROPERTIES OF NANOCRYSTALLINE Ni AND Pd-Fe**

*St. Lauer<sup>1</sup>, Z. Guan<sup>1</sup>, H. Wolf<sup>1</sup>, H. Natter<sup>2</sup>, M. Schmelzer<sup>2</sup>, R. Hempelmann<sup>2</sup> and  
Th. Wichert<sup>1</sup>*

<sup>1</sup> Technische Physik, <sup>2</sup> Physikalische Chemie, Universität des Saarlandes,  
D-66041 Saarbrücken, GERMANY <thw@tech-phys.uni-sb.de>

Nanocrystalline Ni and Pd-Fe samples are characterised on a local scale using perturbed gg angular correlation spectroscopy (PAC). The magnetic hyperfine field and electric field gradient (EFG) are measured at the site of radioactive  $^{111}\text{In}$  probe atoms.

Nanocrystalline Ni is prepared by pulsed electrodeposition and is doped *in-situ* with  $^{111}\text{In}$  by adding radioactive  $^{111}\text{InCl}_3$  to the electrolyte. The resulting grain size is determined by X-ray diffraction to about 40 nm. The  $^{111}\text{In}$  atoms are incorporated at substitutional lattice sites, which is indicated by the PAC spectrum showing two sites with slightly different magnetic fields of 6.7 T and 6.5 T. The hyperfine field of 6.7 T, known from polycrystalline Ni, is detected by about  $f_1 = 40\%$  of the  $^{111}\text{In}$  atoms, whereas  $f_2 = 60\%$  of the probe atoms are exposed to the slightly reduced magnetic field of 6.5 T. The second component  $f_2$  is converted to that of polycrystalline Ni  $f_1$ , if the sample is annealed at temperatures between 400 K and 600 K. This process is accompanied by growth of the crystallites. Therefore, the component  $f_2$  seems to be characteristic for nanocrystalline Ni. For this component ( $f_2$ ) it is also observed that the alignment of the magnetic domains by an external magnetic field happens at a lower value than for polycrystalline Ni ( $f_{r1}$ ).

Nanocrystalline Pd-Fe alloys with a grain size down to 15 nm are obtained by ball-milling of Pd powder, which is accompanied by the incorporation of Fe impurity atoms. It is known that Pd-Fe alloys become ferromagnetic if the iron content exceeds 0.1 at%. The PAC investigations yield information on the formation of defects during ball-milling by the detection of characteristic EFG. Additionally, a distribution of magnetic hyperfine fields is observed, indicating ferromagnetic order of the Pd-Fe samples. The distribution of magnetic fields is centred at 7.5 T with a width of 4 T. After heating the sample at 880 K, the centre of the distribution is shifted to 12 T and the width is reduced to 1.5 T. The reduced width of the field distribution is assigned to the transformation from the disordered solid solution obtained by ball-milling to an ordered  $\text{Pd}_3\text{Fe}$  compound. The local magnetic field vanishes at a Curie temperature of about 470 K.

The financial support by the DFG within the SFB 277 is acknowledged.

**PINNING OF MAGNETIC DOMAIN WALLS AT LINE CROSSINGS  
IN MESOSCOPIC Co STRUCTURES**

*F.G. Aliev, E. Seynaeve, A. Volodin, K. Temst, C. Van Haesendonck, and Y.  
Bruynseraede*

Laboratorium voor Vaste-Stoffysica en Magnetisme, Katholieke Universiteit Leuven,  
Celestijnlaan 200D, B-3001 Leuven, BELGIUM <Aliev.Farkhad@fys.kuleuven.ac.be>

Artificial engineering and imaging of the magnetic properties of nanostructured magnetic films are important from a fundamental as well as a technological point of view. We report on the magnetic properties of magnetic Co line structures with a submicrometer cross section ( $0.17 \times 0.017 \mu\text{m}^2$ ) and a length  $L$  up to  $5 \mu\text{m}$ . The desired Co line pattern is obtained by deposition of 17 nm thick Co films in lift-off profiles. The lift-off profiles are defined by electron beam lithography on oxidised Si wafers which are kept at room temperature during the evaporation of the Co films from a Knudsen cell in a molecular beam epitaxy system. We have shown that the Hall effect can be a very useful tool for an analysis of the magnetic order at submicrometer scale. The measurements of the Hall effect show that the magnetisation of the Co structures is reversible for  $L \leq 1 \mu\text{m}$  and becomes irreversible for  $L \geq 5 \mu\text{m}$ . Magnetic force microscopy and magnetoresistance measurements reveal that the reversibility is linked to the pinning of the magnetic domain walls at the crossing of the lines and the voltage probes. For  $L \geq 5 \mu\text{m}$  additional domain walls appear inbetween the voltage probes, resulting in hysteresis effects for the electrical transport properties. We conclude that the voltage probes, which are unavoidably present in electrical transport measurements, are able to pin the domain walls. This provides the possibility to independently investigate the magnetoresistance of single magnetic domains as well as to estimate the additional resistance related to the area in the vicinity of a domain wall.

This work has been supported by the Fund for Scientific Research - Flanders (FWO) as well as by the Flemish Concerted Action (GOA) and the Belgian Inter-University Attraction Poles (IUAP) research programs.

**ON ELECTRON-ELECTRON SCATTERING MECHANISMS  
IN 2D DEGENERATED SYSTEMS**

*R.N.Gurzhi, A.N. Kalinenko, A.I. Kopeliovich and A.V. Yanovsky*

B.I. Verkin Institute for Low Temperature Physics & Engineering, Academy of Sciences of Ukraine, Lenin  
Ave. 47, Kharkov 310164, UKRAINE <kopeliovich@ilt.kharkov.ua>

The detailed quantitative theory of electron-electron scattering processes in 2D degenerated systems in GaAs(AlGaAs) heterostructures has been developed on the basis of analytical treatment and numerical calculations. We have found the conditions and intervals of values of characteristic parameters in which specific properties of 2D relaxation predicted previously on the theoretical level manifest themselves, such as

- (i) slow evolution of nonequilibrium electron distributions which are antisymmetrical in momentum;
- (ii) the flow of holes moving almost antiparallel to electrons emitting them.

New effects, i.e. a secondary beam of electrons scattered back and a narrow beam of holes moving in the direction of injection, have been found. It has been shown that these effects occur only at scattering of high-energy electrons and they disappear at the temperature of system, which is approximately equal to 1/3 of this energy. Spatially inhomogeneous distributions arising in the conditions of real experiment in the first stages of evolution of electron beams have been studied as well.

**RESPONSE OF 2D ELECTRON GAS  
TO A NONSTATIONARY INJECTED ELECTRON BEAM**

*A.I. Kopeliovich, A.N. Kalinenko and A.V. Yanovsky*

B.I. Verkin Institute for Low Temperature Physics & Engineering, Academy of Sciences of Ukraine,  
Lenin Ave. 47, Kharkov 310164, UKRAINE <kopeliovich@ilt.kharkov.ua>

Electron beams injected into two-dimensional electron gas (2DEG) are used to study collimation effects<sup>1</sup> and electron-electron scattering.<sup>2</sup> The present report shows a possibility to use injected beams for studying the dynamic screening processes in 2DEG. As one can show, the potential and current long-range effects are characteristic of nonstationary injected electron beam. Thus, the potential, created by a bunch of electron that was injected due to impulse potential difference, applied to a point contact, is following:  $\varphi \approx qr_0r^{-2}f(\theta)$ , where  $r$  is the distance from an electron bunch moving with a Fermi velocity  $u$ ,  $\theta$  is the angle between  $u$  and  $r$ ,  $r_0$  is the screening radius,  $q$  is the total beam charge. (Here we remember that a resting screening charge creates a potential  $\varphi \propto r^{-3}$  at  $r \gg r_0$ ). The charges screening a moving bunch create the current which density decreases as  $r^{-2}$ . The indicated potential and current long-range effects of bunch can appear to be an experimentally observed effect.

The following experimental realization of long-range effect is more promising for the observation. Let us apply the ac voltage to a point contact and create a beam-wave in this way. We will receive the following expression for the addition to electron charge density without taking into account the screening charges

$$\delta\rho_0 = A\delta(y)\exp\{i(x-ut)\xi\}, \xi = \omega_0/u,$$

where  $\omega$  is the frequency of applied voltage,  $A$  is the constant. The potential created by a screened beam-wave is following

$$\varphi \approx Ar_0\xi\eta(\xi y)\exp\{i(x-ut)\xi\}.$$

Here function  $\eta(z) \approx 1$  at  $z \leq 1$  and  $\eta(z) \approx z^{-2}$  at  $z \gg 1$ . This potential is created mainly by electrons of gas accelerated by a beam field and moving with a velocity close to  $u$ . A wave length  $\xi^{-1}$  is smaller than a ballistic path of beam (which is approximately equal to  $10 \text{ fm}$ ) at  $\omega > 10^{10}$ .

1. Molenkamp, A.A. M.Starring, C.W.J. Beenakker, R. Eppenga, C.E. immering, J.G. Williamson, C.J.P.M. Harmans and C.T. Foxon, Phys.Rev. B 41, 1274 (1990).
2. L.W. Molenkamp, M.J.P. Brugmans, H.Van Houten and C.T. Foxon, Semicond. Sci. Technol. 7, B228 (1992).

**STRUCTURE AND MECHANICAL BEHAVIOUR OF A COMMERCIAL  
Al-Mg ALLOY AFTER EQUI-CHANNEL-ANGULAR EXTRUSION**

*M.V. Markushev<sup>1</sup>, M.Yu. Murashkin<sup>1</sup>, P.B. Prangnell<sup>2</sup> and O.A. Maiorova<sup>1</sup>*

<sup>1</sup> Institute for Metals Superplasticity Problems Russian Academy of Sciences,  
Khalturn 39, Ufa 450001, RUSSIA <mvmark@metall.ugatu.ac.ru>

<sup>2</sup> Manchester Materials Science Centre, Grosvenor Street,  
Manchester, M1 7HS, UK <philip.prangnell@umist.ac.uk>

The production of nano-scale structures in bulk samples of the commercial non-heat treatable aluminium alloy 1560 (Al-6Mg-0.6Mn) has been investigated, using a thermomechanical treatment, involving the process of equi-channel-angular extrusion (ECAE). The ECAE tooling used, allows the possibility of grain refinement to the nano-scale in rod samples of 20mm in diameter. The process deforms materials in shear to extremely high strains with a minimum change in the sample geometry. The billet size is only limited by the die set used and can easily be scaled up in a commercial production process.

With the optimum thermomechanical treatment, an ultra-fine grain structure with grains of 200-400nm in size was produced. The features of the as-received structure, and its evolution during post-deformation annealing, have been studied. It was established that heating above 200°C leads to rapid grain coarsening through secondary recrystallisation, by the formation and growth of discrete grains several microns in size.

The mechanical behaviour of the alloy was studied at room temperature static tension and bending, in the as-ECA extruded condition, after further cold rolling, as well as after annealing at 200°C (grain size  $d \approx 400$  nm) and at 350°C ( $d = 5$  mm). The alloy's strength, ductility, and fracture toughness characteristics were analyzed as a function of the microstructural state. It was found that grain refinement to the nano-scale led to a prominent increase in the alloy strength and decrease in ductility and toughness. It was shown that there was a significant drop in the resistance to both static crack formation and growth with transition from fine grained to nanostructures. The latter was mainly caused by a greater macrolocalization of plastic flow during deformation of the nanostructured material.

The influence of the alloy structural state on the phenomenon of flow stress instabilities is discussed.

**PECULIARITIES OF MECHANICAL BEHAVIOUR AND STRUCTURAL  
CHANGES IN COMMERCIAL AL ALLOYS WITH NANOCRYSTALLINE  
STRUCTURE DURING HIGH RATE SUPERPLASTICITY**

*N.K. Tsenev<sup>1</sup>, A.M. Shammazov<sup>1</sup> and P. Berbon<sup>2</sup>*

<sup>1</sup>Ufa State Petroleum Technical University, 1 Kosmonavtov str.,  
Ufa 450062, RUSSIA <tsenev@ippm.rb.ru>

<sup>2</sup>Department of Materials Science and Mechanical Engineering,  
University of Southern California, Los Angeles, CA 90089-1453, USA

In the present work there was studied behaviour of "stress - strain" curve ( $\sigma$  -  $\epsilon$ ) at low temperature high rate superplasticity in commercial Al alloys of Al-5.5%Mg-2.2%Li-0.12%Zr-0.12Sc(1421) and Al-2.65%Cu-2.2%Li-0.12Zr (1460) systems with nanocrystalline structure ( $d=0.5\text{--}0.8 \mu\text{m}$ ). Three areas are distinctly distinguished in curve  $\sigma$  -  $\epsilon$  during high strain rates ( $\dot{\epsilon} > 10^2 \text{ s}^{-1}$ ): 1) area of low flow stress values ( $\epsilon \approx 10\text{--}20\%$ ), 2) area of sharp increase of acting stresses ( $\epsilon \approx 20\text{--}35\%$ ) and 3) flow plastic area ( $\epsilon > 35\%$ ). At low strain rates  $\dot{\epsilon} \leq 10^3 \text{ s}^{-1}$  there observed only two areas (in the initial stage the area of low flow stress values is absent).

It is revealed that maximum elongation, more than 1000%, and high coefficient values of flow stress rate sensitivity for alloys with nanocrystalline structure are achieved at strain rates  $10^2 \text{ s}^{-1}$  and deformation temperature of 623 K. With all that an uniform elongation of samples was observed. Failure of samples was conducted at angle of 90° to the deformation axle, practically without formation of a neck.

An increase ( $\dot{\epsilon}=10^1 \text{ s}^{-1}$ ) or decrease ( $\dot{\epsilon}=10^3 \text{ s}^{-1}$ ) of strain rate leads to a sharp localisation of deformation, i.e. formation of a neck and considerable decrease of a maximum relative elongation.

Questions of calculations of true values of stress - strain curve, taking in to account deformation localisation was discussed and criticised.

Structure of nanocrystalline 1421 and 1460 alloys in initial states (before superplastic deformation) and after different stages of low temperature high rate superplasticity was studied by transmission electron microscopy.

Physical nature of the effect appearance and vista for commercial application of nanocrystalline materials is being discussed in the given work.

**ELECTRIC RELAXATION IN CONDUCTING  
METAL-INSULATOR NANOCOMPOSITES**

*A.B. Pakhomov<sup>1</sup>, S.K. Wang, and X. Yan*

Department of Physics, The Hong Kong University of Science and Technology  
Clear Water Bay, Kowloon, Hong Kong <PHALEC@usthk.ust.hk>

<sup>1</sup>On leave from A.F. Ioffe Physical Technical Institute,  
Saint-Petersburg 194021, RUSSIA

We report impedance measurements in (NiFe)-(SiO<sub>2</sub>), Pt-SiO<sub>2</sub> and Au-SiO<sub>2</sub> co-sputtered nanocomposite films at the metal-insulator transition and in the metallic state. At least three relaxation processes were identified in the impedance behaviour. This behaviour may be related to polarisation and tunnelling between clusters of metal granules, between isolated metal granules, or between isolated metal atoms.

The 0.5-1.0 mm thick nanocomposite samples were prepared by co-sputtering on glass substrates. The metal volume fraction measured by EDAX was between 0.52 and 0.72. The composites consist of very small crystalline metal granules (the minimum diameters down to less than 1 nm) immersed in the amorphous insulating matrix. The granule sizes follow an exponential distribution. A considerable fraction of metal is present in a form of dissolved impurity atoms. In the lower concentration samples the dc conduction is thermally activated. The higher concentration samples are metallic at room temperature, but have logarithmic temperature dependence at lower temperatures.

The impedance  $Z = R + iX$  was measured along the sample plane in the frequency range between 20Hz<f<1MHz, with a four - terminal method. The absolute value of the negative reactance -X shows a peculiar low frequency behaviour. For a conducting system with an internal capacitance C, where R and C are in parallel, one could expect  $-X \sim f$  at low frequency. Instead, the value of -X has a minimum at a frequency  $f_m$ , which increases with increasing metal volume fraction. As the frequency decreases below  $f_m$ , the -X value is increasing, with at least one small maximum imposed on this general behaviour.

At intermediate or high frequency we observe a behaviour which can be described by percolation scaling theories. Presence of tunnelling between percolation clusters is reflected in the dependence of effective capacitance on frequency. We relate the low frequency features to relaxation associated with activated charge transfer between neighbouring isolated metal grains, or between metal atoms in the insulating matrix.

**LOW-TEMPERATURE MÖSSBAUER STUDIES  
OF NANOGLASS Fe<sub>79</sub>B<sub>21</sub> POWDER PREPARED BY CHEMICAL REDUCTION**

*G.Y. Wu<sup>1</sup>, J.Z. Jiang<sup>2</sup>, and X.P. Lin<sup>1</sup>*

<sup>1</sup> Jiangsu Institute of Chemical Engineering, Changzhou, Jiangsu, CHINA.

<sup>2</sup> Department of Physics, Building 307, Technical University of Denmark,  
DK-2800 Lyngby, DENMARK

After the discovery of the preparation of nanoglass TM-B (TM=Fe, Co, Ni) powders [1], there has been considerable interest in this field [2]. Here we report an on-going project on the low-temperature magnetic behavior of nanoglass Fe<sub>79</sub>B<sub>21</sub> powder prepared by the chemical reduction. We have performed Mössbauer measurements in a temperature range from 5 to 295 K for the powder and one amorphous Fe<sub>80</sub>B<sub>20</sub> ribbon prepared by melt-spinning method for comparison. These results showed that the average magnetic hyperfine field of the nanoglass Fe<sub>79</sub>B<sub>21</sub> powder followed the Block's law, H(T)/H(0)=1-BT<sup>3/2</sup>, in the temperature range studied, indicating excitations of long-wavelength spin waves. The value of B parameter for the powder is found to be about 2.8 x 10<sup>-5</sup> K<sup>-3/2</sup>, larger than 2.2 x 10<sup>-5</sup> K<sup>-3/2</sup> found for the ribbon sample. This suggests that the local structural environments in the powder sample contain a high degree of disorder than in the ribbon sample.

- [1] J. van Wijngaarden, S. Mørup, C.J.W. Koch, S.W. Charles and S. Wells, *Nature* **322**, 622 (1986).
- [2] See for example, D. Buchkov et al., *J. Magn. Magn. Mater.* **62**, 87 (1986); A. Inoue et al., *Metall. Trans.* **19A**, 2315 (1988); S. Wells et al., *J. Phys.: Condens. Matter* **1**, 8199 (1989); J. Jiang et al., *J. Non-Cryst. Solids* **116**, 247 (1990); **124**, 139 (1990); S. Linderoth and S. Mørup, *Physica Scripta* **45**, 408 (1992).

**ON THE BEHAVIOUR OF MECHANICALLY MILLED Fe-Cu MATERIALS  
UNDER HIGH PRESSURE AND TEMPERATURE***J.Z. Jiang<sup>1</sup>, J.S. Olsen<sup>2</sup>, L. Gerward<sup>1</sup>, and S. Mørup<sup>1</sup>*<sup>1</sup> Department of Physics, Building 307, Technical University of Denmark,  
DK-2800 Lyngby, DENMARK<sup>2</sup> Niels Bohr Institute, Oersted Laboratory, DK-2100 Copenhagen, DENMARK

High-energy ball milling is widely used for the preparation of nanostructured metals, ceramic and cermets. In our previous works, we have succeeded in alloying immiscible metal systems, e.g. Fe-Cu [1], and immiscible ceramic systems, e.g. Fe<sub>2</sub>O<sub>3</sub>-Al<sub>2</sub>O<sub>3</sub> and Fe<sub>2</sub>O<sub>3</sub>-SnO<sub>2</sub> [2]. The alloying processes the microstructures of the metastable alloys and their electrical and magnetic properties have been investigated. Here we present an ongoing project on mechanically milled Fe-Cu samples with respect to the compressibility and phase transformations under high pressure and temperature. In this work, high-pressure and high-temperature x-ray powder diffraction measurements were performed using synchrotron radiation in the multi-anvil device MAX80 at HASYLAB in Hamburg, Germany. Similarities and differences on the compressibility and phase transformations in nanostructured Fe, Cu, and FeCu alloys, and the corresponding bulk materials will be presented and discussed.

- [1] J.Z. Jiang et al. *Appl. Phys. Lett.* **63**, 1056 (1993); **63**, 2768 (1993); and J.Z. Jiang et al., *J. Phys. Condens. Matter* **6**, L227 (1994); **6**, L343 (1994).
- [2] J.Z. Jiang et al., *Mater. Sci. Forum* **225-227**, 489 (1996); J.Z. Jiang et al., *Phys. Rev. B* **55**, 11 (1997); **55**, 14830 (1997); and J.Z. Jiang et al., *J. Phys. D: Appl. Phys.* **30**, 1459 (1997).

**IMPROVING THE MAGNETIC PROPERTIES OF NANOCRYSTALLINE  
 $\text{Fe}_{73.5}\text{Cu}_1\text{Nb}_3\text{Si}_{13.5}\text{B}_9$  BY HEAT TREATMENT OF THE MELT***H.Chiriac, Marilena Tomut and Maria Neagu*

National R&D Institute for Technical Physics, Blv. Mangeron 47,  
6600 Iasi 3, ROMANIA <[marilena@phys-iasi.ro](mailto:marilena@phys-iasi.ro)>

Viscosity measurements on liquid  $\text{Fe}_{73.5}\text{Cu}_1\text{Nb}_3\text{Si}_{13.5}\text{B}_9$  alloy reveal irreversible changes that take place in the melt during heating. This behaviour was assigned to temperature dependence of the short range ordering present in the melt. The aim of this paper is to study the effect of the heat treatment of the melt on the magnetic properties of the nanocrystalline  $\text{Fe}_{73.5}\text{Cu}_1\text{Nb}_3\text{Si}_{13.5}\text{B}_9$  alloys, obtained by controlled crystallisation of rapidly solidified ribbons, by taking into account the inheritance of the short range ordering present in the melt.

Nanocrystalline ribbons were obtained with different heat treatment of the melt above and below a critical temperature inferred from viscosity measurements. The crystallisation of the amorphous alloy was followed by DTA and X-ray diffraction. The influence of the melt heat treatment on the britleness, coercivity and saturation magnetostriction was studied.

Correlation of the results on the crystallisation kinetics, magnetic properties in nanocrystalline state and viscosity of the melt allowed us to draw conclusions concerning the influence of the structural units existing in the melt on the crystallisation of  $\text{Fe}_{73.5}\text{Cu}_1\text{Nb}_3\text{Si}_{13.5}\text{B}_9$  amorphous alloys and on the possibility of improving the application oriented magnetic properties by suitable heat treatment of the molten master alloy.

---

**IN-SITU CHARACTERIZATION OF CAPPED NANO PARTICLES  
USING SPECTROSCOPIC ELLIPSOMETRY TECHNIQUE**

*D.P. Acharya and B.R. Mehta,*

Thin Film Laboratory, Physics Department, Indian Institute of Technology,  
N. Delhi 110016, INDIA <brmehta @physics.iitd.ernet.in>

Spectroscopic ellipsometry technique is an extremely sensitive non destructive technique for the characterization of surfaces, interfaces and thin films. Small microstructural and stoichiometric changes can be quantitatively and accurately determined by measuring the changes in the polarization state of the incident light . In the present study, spectroscopic ellipsometry technique has been used for the in-situ analysis of the optical properties of CdS nano particles. These nano particles have been grown by chemical capping method using thiophenol as the capping agent. Thiophenol controls the size of the nano particles by forming capping bonds at the surface of the growing particle. These capped nano particles can also be easily dispersed in organic solvents. A special sample enclosure having quartz windows has been designed and fabricated to characterize the semiconductor nano particles dispersed in the liquid media using rotating polarizer spectroscopic ellipsometer in the reflection mode. The incident light passes through the solution containing the nano particles and is reflected into the detector through the analyzer. The changes in the observed  $\epsilon_1$  and  $\epsilon_2$  spectra has been related with the size and composition of the semiconductor nano particles. Using the present technique,  $\epsilon_1$  and  $\epsilon_2$  spectra of the CdS nano particles have been obtained at different stages of growth.

**AG/SIO<sub>2</sub> CERMETS MADE BY RADIO-FREQUENCY SPUTTERING;  
MICROSTRUCTURE AND OPTICAL PROPERTIES**

*S. Fagnent<sup>1</sup>, L. Sauques<sup>1</sup>, M.C.Sainte Catherine<sup>1</sup>, C. Sella<sup>2</sup> and S. Berthier<sup>3</sup>*

<sup>1</sup> DGA/DCE/CREA 16 bis Av Prieur de la Cote d'Or  
94114 Arcueil, FRANCE <fagnent@etca.fr>

<sup>2</sup> Laboratoire d'Optique des Solides CNRS Meudon Bellevue,  
1 Pl. Aristide Briand, 92195 Meudon Bellevue, FRANCE

<sup>3</sup> Laboratoire d'Optique des Solides, Universite Pierre et Marie Curie,  
4 Place Jussieu, 75005 Paris, FRANCE

Ag/SiO<sub>2</sub> cermet films have been deposited by radio frequency cosputtering. Two ways of achievement were chosen: Ag discs or sectors with several configurations on SiO<sub>2</sub> target were investigated. Large Ag volume fraction range has been covered. Ultra Violet, visible and infrared optical properties (wavelength: 0.3-20 micrometers) were achieved. With help of effective medium theories (among others) interpretation of optical properties is proposed in accordance with the microstructural studies (TEM, MEB) and techniques of deposition. Particularly emphasis has been placed on the study of the deduced absorption (Absorption=1-Reflexion-Transmission) properties. X grazing diffraction, SIMS, thickness and percolation threshold by four points probe conductivity measurements were also achieved. Further investigations are in progress on Ag/Al<sub>2</sub>O<sub>3</sub> cermets.

Acknowledgment: This research was supported by the « Delegation Generale pour l'Armement (DGA) » (France).

**Bibliography:**

1. Cohen, G.D. Cody, M.D. Coutts and Abeles, Phys Rev B 8, 3689 (1973).
2. Gajdardziska-Josifovska, R.C. McPhedran, D.R. McKenzie and R.E. Collins, Appl. Optics 28, 2744 (1989).
3. Abeles and J.I Gittleman, Appl. Optics 15, 2328 (1976).
4. Gajdardziska-Josifovska, R.C. McPhedran, D.J.H. Cockayne, D.R. McKenzie and R.E. Collins, Appl. Optics 28, 2736 (1989).
5. Emeric, A. Emeric, Thin Solid Films, 1, 13-30 (1967).
6. T.Kume, T. Amano, S. Hayashi, K. Yamamoto, Thin Solid Films 264, 115-119 (1995).
7. Kreibig, M. Vollmer, Optical Properties of Metal Cluster, (1995).
8. P.Gadenne, M.Gadenne, Y.Yagil, G.Deutscher, Phys. A 207, 228-233 (1994).
9. M.H.Lee, I.T.H. Chang, B. Cantor, Materials Science and Engineering, A179-A180, 545-551 (1994).
10. Priestley, B. Abeles and R.W. Cohen, Phys. Rev. B 12, 2121 (1975).

**GRAIN-SIZE DEPENDENCE OF MAGNETIZATION  
IN NANOCRYSTALLINE Ni AND Co**

M. Schmelzer<sup>1,3</sup>, H. Natter<sup>1,3</sup>, R. Hempelmann<sup>1,3</sup>, C. E. Krill<sup>2,3</sup> and  
R. Birringer<sup>2,3</sup>

<sup>1</sup> Physikalische Chemie, <sup>2</sup> Technische Physik, <sup>3</sup> Sonderforschungsbereich 277  
Universität Saarbrücken, D-66123 Saarbrücken, GERMANY

According to the random anisotropy model as applied by Herzer to fine-grained magnetic materials [1], certain macroscopic magnetic properties of nanocrystalline ferromagnets are expected to exhibit a pronounced grain-size dependence for average grain sizes near the exchange length  $L_{ex} = \sqrt{A/K_1}$  (determined by the exchange constant A and the anisotropy constant K<sub>1</sub>).

Using the technique of pulsed electrodeposition, it is possible to prepare porosity-free nanocrystalline materials with a high degree of control over the shape of the resulting grain-size distribution [2]. By this method we have synthesized a series of nanocrystalline Ni an Co samples with average grain sizes between 8 and 77 nm and a narrow size distribution, as determined by X-ray diffraction peak-profile analysis [3]. Such samples represent attractive systems for testing the predictions of the random anisotropy model for single-phase nanocrystalline ferromagnets.

Measurements of the magnetic properties of the nano-Ni and nano-Co samples, performed by vibrating sample magnetometry, find that the saturation magnetisation exhibits hardly any dependence on grain size. The maximum permeability, on the other hand, increases monotonically with decreasing grain size, while the coercivity passes through a pronounced maximum. The grain size at which this maximum occurs coincides roughly with the literature values for L<sub>ex</sub> in Ni and Co.

- [1] G. Herzer, *Grain Size Dependence of Coercivity and Permeability in Nanocrystalline Ferromagnets*, IEEE Trans. Magn. **26** (1990) 1397.
- [2] H. Natter, M. Schmelzer und R. Hempelmann, *Nanocrystalline Nickel and Nickel-Copper-Alloys: Synthesis, Characterization and Thermal Stability*, J. Mater. Research (1998), in print
- [3] C. E. Krill and R. Birringer, *Estimating Grain-Size Distributions in Nanocrystalline Materials from X-ray Diffraction Profile Analysis*, Phil. Mag. A (1998), in print

**NANOCRYSTALLINE NH<sub>4</sub>MnF<sub>3</sub> WITH CONTROLLED GRAIN SIZE:  
SYNTHESIS AND ANTIFERROMAGNETISM**

*M. Roth<sup>1</sup>, R. Hempelmann<sup>1</sup>, O. Borgmeier<sup>2</sup>, T. Eifert<sup>2</sup> and H. Lueken<sup>2</sup>*

<sup>1</sup> Physikalische Chemie und Sonderforschungsbereich 277,

Universität Saarbrücken, D-66123 Saarbrücken, GERMANY

<sup>2</sup> Anorganische Chemie, RWTH Aachen, D-52074 Aachen, GERMANY

Nanocrystalline NH<sub>4</sub>MnF<sub>3</sub> was prepared by precipitation in the inverse micelles of w/o-microemulsions using mixtures of ammonium substituted AOT and n-heptane which are able to stabilize large contents of concentrated NH<sub>4</sub>F and Mn(OAc)<sub>2</sub> aqueous solutions. In the subsequent coagulation with acetone, NH<sub>4</sub>(OAc) is formed which can quantitatively be removed by transformation into acetamid. By appropriate variation of the synthesis parameters the volume averaged crystallite diameter, as measured by X-ray diffraction line shape analysis, can be tuned to values of 10 nm  $\leq \langle D \rangle_{vol} \leq$  60 nm [1]. The magnetic measurements have been performed using a SQUID magnetometer in the temperature range between 1.7K and 300K at magnetic fields between 0.01 and 5T.

For a bulk NH<sub>4</sub>MnF<sub>3</sub> reference sample (cubic perovskite for T > 182K, tetragonally distorted below) we observe a Curie-Weiss paramagnetism above T ≈ 150K. The molar magnetic susceptibility,  $\chi_{mol} = C / (T - \Theta_p)$  with  $\Theta_p = -140$ K, correlates with the expected magnetic spin moment,  $\mu = 5.9\mu_B$ ; the structural phase transition can be recognised by a slight anomaly of  $\chi_{mol}(T)$ . Below T<sub>N</sub> = 75K antiferromagnetic ordering occurs, but with weak ferromagnetic contributions due to spin canting, in agreement with literature results [2].

For nanocrystalline NH<sub>4</sub>MnF<sub>3</sub> we observe the following changes of the magnetic properties with decreasing particle size (which are pronounced for  $\langle D \rangle_{vol} < 30$  nm):

- The strength of the antiferromagnetic exchange interaction decreases which is evident from the decrease of  $|\Theta_p|$  and T<sub>N</sub> and the increase of  $\chi_{mol}$ .
- The ferromagnetic contribution decreases as can be concluded from the magnetic field dependence of the  $\chi_{mol}$  vs. T plots for T < T<sub>N</sub>.

Theoretically, the observed magnetic properties in the paramagnetic state can be understood in terms of the high-temperature susceptibility series for the simple cubic Heisenberg S = 5/2 antiferromagnetic (applied to the cubic phase) and the corresponding tetragonal model (applied to the tetragonal phase).

- [1] M. Roth and R. Hempelmann, *The Synthesis of Nanocrystalline NH<sub>4</sub>MnF<sub>3</sub> - A Preparation Route to Produce Size-Controlled Precipitates via Microemulsion Systems*, Chemistry of Materials **10**, 78 (1998)
- [2] J. Bartolomé, R. Burriel, F. Palacio, D. Gonzales, R. Navarro, J. A. Rojo and L. J. de Jongh, *Magnetic Properties of Weak Ferromagnet NH<sub>4</sub>MnF<sub>3</sub>*, Physica **115**, 190 (1983)

**SPIN-GLASSLIKE BEHAVIOR OF  
IRON-NITRIDE NANOPARTICLES SYSTEMS***H. Mamiya and I. Nakatani*

National Research Institute for Metals, Tsukuba 305, JAPAN  
<mamiya@nrim.go.jp and nakatani@nrim.go.jp>

Glassy behaviour has been intensively investigated in ferromagnetic fine particle systems with the random anisotropy and the dipolar interactions. However, the similar behaviour is also observed for the blocking phenomena of isolated particles. To clarify the difference between them, the magnetisation in equilibrium  $M_{eq}$ , in addition to the field cooled and zero field cooled magnetisation ( $M_{FC}$  and  $M_{ZFC}$ ), is discussed. We also discuss the critical phenomena and the slow dynamics.

Samples are two frozen iron-nitride magnetic fluids with uniform particles whose diameters are about 6 nm. One is a dense magnetic fluid as interacting particles, and another is its dilution as isolated particles. Because their carrier liquids (kerosene) are solidified in a zero field, the particles can be considered to have randomly oriented easy axes. We estimate  $M_{eq}$  as the convergent value of the relaxation curves for various initial states.

For both samples, the same behaviour, a plateau of  $M_{FC}(T)$  and a difference between  $M_{FC}(T)$  and  $M_{ZFC}(T)$ , is observed at weak fields at low temperatures. However,  $M_{eq}(T)$  completely differs in the diluted sample and the dense sample.  $M_{eq}(T)$  of the diluted sample seems to be inversely proportional to the temperature even in the temperature range in which  $M_{FC}(T)$  is constant, while  $M_{eq}(T)$  of the dense sample is nearly the same with  $M_{FC}(T)$  in the temperature range. These indicate that the plateau of  $M_{FC}(T)$  for the isolated particles is caused by a finite measurement time and that the equilibrium state is superparamagnetic in the entire temperature range. On the other hand, the plateau of  $M_{eq}(T)$  for the interacting particles shows that the magnetic moments freeze cooperatively below a temperature  $T_g$ .

The nonlinear susceptibility for the dense sample sharply increases with decreasing temperature above  $T_g$ . Below about  $T_g$ , we observe a broadened relaxation time distribution that depends on the history of the system. Such behaviour is not observed for the diluted sample. These results indicate that the freezing of the magnetic moments for the interacting particles is different from the blocking for isolated particles and quite similar to the freezing of spin glass.

**NANOSCALE CHARACTERIZATION AND MODELING OF  
THE MAGNETIZATION BEHAVIOR IN NANOSTRUCTURED METALS**

*J.F. Löffler, H.-B. Braun and W. Wagner*

Paul Scherrer Institut, CH-5232 Villigen PSI, SWITZERLAND <joerg.loeffler@psi.ch>

Magnetic small-angle neutron scattering (SANS) was performed on nanostructured Fe, Co and Ni in order to investigate the field dependence of the intergranular magnetic correlations on the nanometer scale. The magnetic scattering is anisotropic, i.e. it varies with the angle between the scattering and the magnetization vector. Thus, the anisotropic distortion of the lines of equal intensity on a two-dimensional SANS detector is a direct measure for the magnetic correlations regarding spatial extension, magnitude and magnetization direction of correlated regions relative to the external field. In intermediate fields between 0.8 and 1.5 kOe the SANS measurements on nanostructured Fe and Co with small grain sizes show a net magnetic component perpendicular to the external field, correlating many grains over distances larger than 40 nm. We further observe that this net magnetic component is more pronounced for a decreasing bulk anisotropy. For larger external fields the usual ferromagnetic alignment was obtained.

To analyze the SANS data, we assumed a model of spherical ferromagnetic domains embedded in a homogeneous magnetic matrix with the domains having the magnetization tilted relative to that of the matrix. Based on this model we calculated the magnetic scattering as a projection onto the two-dimensional detector. Comparing the experimental data with the calculated SANS intensities, we found agreement when the domains and the matrix have the same modulus of magnetization. This agreement in general supports the interpretation that domains, confining several grains, in intermediate fields are still tilted out of the external field direction. Furthermore, with increasing magnetic field, the clusters become unstable at a critical field and flip into the stable state directed towards the external field direction. This critical field depends on the angle between the local anisotropy axis and the external field, as described by the original Stoner-Wohlfarth model. By modifying this model to consider the magnetic exchange between the grains, we can quantitatively explain the magnetization behavior as a function of the external field. In intermediate fields for example, the tilting angle of the clusters is up to 70° with the consequence that such clusters induce a perpendicular net magnetic component as observed by the experiment.

**EXCHANGE ANISOTROPY IN FINE COBALT PARTICLES**

*A. Petrov, S. Belogurov and I. Kudrenitskis*

Nuclear Research Centre Latvian Academy of Sciences, Salaspils, LATVIA

Exchange anisotropy in fine cobalt particles with different diameters in the range 14-110 nm covered by oxidized layer was investigated. It is known, that after cooling of such particles in external magnetic field the shift of magnetic hysteresis loop is observed due to exchange interaction at the interface Co-CoO.

Assuming that for separate particle exchange anisotropy easy direction coincides with the direction of external magnetic field, and using expression for an energy of particle in external magnetic field, the relation between the value of hysteresis loop shift and exchange interaction energy at the Co-CoO interface was found. For the particles of all sizes, but the smallest one, this value was equal to  $0.29 \pm 0.02$  erg/cm<sup>2</sup>. For the particles of the smallest size with cobalt core radius  $r = 4$  nm this value was equal to  $0.21 \pm 0.02$  erg/cm<sup>2</sup>, that may be due to different kinds of size effects.

Using X-ray structural analysis the structure of particles was also investigated. These investigations have shown that cobalt core is surrounded by thin layer of CoO, that provides existence of exchange anisotropy, and which, in turn, is covered by Co<sub>3</sub>O<sub>4</sub> layer.

**CRYOCHEMICAL SYNTHESIS AND PHYSICAL-CHEMICAL PROPERTIES  
OF NANO-DISPERSED METALLOPOLYMERS**

*V.V. Zagorskii, S.V. Ivashko, V.E. Bochenkov and G.B. Sergeev*

Department of Chemistry, Moscow State University, 119899 Moscow, RUSSIA  
*<gbs@cryo.chem.msu.su>*

New nanodispersed metallopolymer (Ag, Na, Mg, Pb, Mn, Ca, Sm) films have been obtained via low temperature codeposition of metal and reactive para-xylylene monomer vapours at 100 K. It was shown by TEM results that metals formed globe-like particles of 5-8 nm size and uniformly distributed in polymer matrix. Electric conductivity of the films obtained were studied as during the components codeposition, by the samples annealing at 80-300 K and also at constant temperature.

The results for Ag- and Ca-containing samples on monomer and polymer supports are in accordance with the metal chemical activity. In the case of chemically inert silver the annealing of the prior insular film sample at 100 K led to sharp increase in conductivity values due to rising of silver atoms and clusters mobility. In the case of chemically active Ca annealing of the sample led to sharp decrease in conductivity values . It could be resulted from the reaction of Ca-nanoclusters with monomer and guttering effects. Adsorption of residual gases and monomer at the surface of Ca-nanoparticles could cause the decrease of electrical conductivity value. The same results have been obtained for Sm-systems. Pb-poly-para-xylylene systems possess the intermediate electrical conductivity values between Ag- and Ca(Sm) -containing systems. More complicated electrical behaviour of Mn-para-xylylene samples is connected with the formation of stable  $\pi$ -complexes of metallic Mn with monomer molecules. The existence of stable Mn-para-xylylene  $\pi$ -complexes were shown by reflection IR-spectroscopy.

Electrical-conductivity measurements were made for bimetallic Pb/Sm, Na/Ag and Na/Pb-systems. The results are very similar to the superposition of the electric conductivity curves for the neat metals. Thus the results obtained show the perspectives of the use of electric conductivity measurements in-situ during metal-polymer samples formation for their complex characterisation.

**Acknowledgements.** The work was partially supported by RFBR grant N 96-03-33970a and International OMMEL programme.

**A COMPARATIVE STUDY ON THE ELECTRICAL AND  
MAGNETIC BEHAVIOUR OF CO-SPUTTERED AND  
MULTILAYER NANOCOMPOSITE  $\text{Ni}_x(\text{SiO}_2)_{1-x}$  THIN FILMS**

*Horia Chiriac, Florin Rusu, Maria Ursean and Mihai Lozovan*

National Institute of R&D for Technical Physics,  
47 Mangeron Blvd., 6600 Iasi 3, Romania <lozovan@uaic.ro>

Granular metal films with nanocrystalline to amorphous structure are of great interest for applications in the field of miniature sensors [1-3,5]. These materials exhibit important changes in their physical properties when the volume fraction of metal decreases under a critical value, known as the percolation threshold. The physical properties of granular metal films are strongly dependent on the deposition conditions and subsequent thermal treatments, so one can obtain artificially structured materials with tailored properties, by properly choosing the process parameters [2-4].

In this paper we present some results on the conductivity and magnetic properties of  $\text{Ni}_x(\text{SiO}_2)_{1-x}$  thin films, with metal contents between 40% and 60% (near the percolation threshold), in view of using these films for technological applications. The co-sputtered films have been deposited by composite target and the multilayer films have been obtained by sequential sputtering of two targets. The conductivity, TCR and magnetisation measurements revealed the presence of the percolation threshold at Ni contents in the films of about 50%, as predicted in theory, for both film categories in discussion. We also made Hall measurements, which confirm the percolation threshold at about 50 % of metal content in films. These phase transitions, concerning the conductivity and magnetic behaviour of  $\text{Ni}_x(\text{SiO}_2)_{1-x}$  granular metals make them interesting for the field of thin film sensors (for temperature, displacement, force etc), or magnetic recording media.

1. T.E.Schlesinger &all. - J.Appl.Phys. 70 (6), 15 Sept. 1991
2. C.L.Chien - J.Appl.Phys. 69 (8), 15 April 1991
3. B.Abeles &all. - Adv.Phys.24, 407 (1975)
4. A.Gavrin, C.L.Chien - J.Appl.Phys.67, 938 (1990)
5. A.Heinrich &all. - Thin Solid Films, 223 (1993), 311-319

---

**MAGNETIC PROPERTIES OF FINEMET IN DEPENDENCE OF  
NANOCRYSTALLISATION CONDITIONS AND SURFACE TREATMENT**

*D. Ramin and W. Riehemann*

Institute of Materials Engineering and Technology, Technical University Clausthal,  
Agricolastraße 6, D-38678 Clausthal-Zellerfeld, GERMANY  
<detlef.ramin@tu-clausthal.de>

Amorphous  $\text{Fe}_{73.5}\text{Si}_{13.5}\text{Cu}_1\text{Nb}_3\text{B}_9$  crystallises at temperatures of about 580°C to a soft magnetic material called FINEMET with superior properties like very low coercitivity of less than 1 A/m, low AC losses, and high saturation magnetisation. Although the nanostructure of FINEMET is very insensible to small variations of annealing parameters some magnetic properties like coercitivity and dynamic power losses vary substantially.

Strips of  $\text{Fe}_{73.5}\text{Si}_{13.5}\text{Cu}_1\text{Nb}_3\text{B}_9$  were nanocrystallised under different heat treatment conditions. The annealing temperature, heating and cooling rate were varied and ambient magnetic fields were applied during nanocrystallisation. After heat treatment the dynamic hysteresis loops of each specimen was measured with a computer controlled device in the frequency range between 3.2 Hz and 20 kHz at polarisations from 0.6 T to 1.0 T. Several types of specimens were used for measurement including samples surface treated prior to heat treatment. It was found that the coercitivity as well as the dynamic power losses vary considerably with different nanocrystallisation conditions.

**A MULTIPLE SCATTERING APPROACH  
TO SOLVE THE RADIATIVE TRANSFER EQUATION**

*William E. Vargas<sup>1</sup> and Gunnar A. Niklasson<sup>2</sup>*

<sup>1</sup> Centro de Investigación en Ciencia e Ingeniería de Materiales and Escuela de Física,  
Universidad de Costa Rica, San José, COSTA RICA

<sup>2</sup> Department of Materials Science, Uppsala University,  
Box 534, S-751 21 Uppsala, SWEDEN

The optical properties of a particulate slab perpendicularly illuminated with unpolarized collimated radiation are considered. The slab consists of homogeneous spherical particles randomly distributed in a non absorbing matrix. The radioactive transfer equation is written in terms of amounts of radiation emerging from multiple scattering events, and taking into account the reflections of the diffuse radiation at the boundaries of the slab. The angular and optical depth dependence of each scattering order, as well as the total diffuse radiation, can be easily computed in terms of particle size and concentration, relative refractive index of the particles, and wavelength of the impinging radiation. Effective values of the scattering and absorption coefficients of the slab have been obtained in terms of the corresponding scattering and absorption cross sections of the particles, and mean values of the average path-length parameter and forward scattering ratio.

**ELECTRONIC STRUCTURE OF A CLUSTER-ASSEMBLED  
NANOCRYSTALLINE SILVER FILM INVESTIGATED WITH HREELS**

*M. Andersson, C.-M. Grimaud, L. Siller and R.E. Palmer*

Nanoscale Physics Research Laboratory, School of Physics and Astronomy,  
The University of Birmingham, Edgbaston, Birmingham, B15 2TT, UK  
<M.T.Andersson@bham.ac.uk>

High-resolution electron energy loss spectroscopy (HREELS) provides a powerful in-situ method to explore the electronic and optical properties of nanostructures and thin films. We have produced a nanocrystalline film of silver by deposition [1] of size-selected Ag<sup>3-</sup> clusters on highly oriented pyrolytic graphite. The substrate was at room temperature during deposition and therefore the silver clusters were mobile and aggregated into islands with a size of a few nanometers, as imaged with scanning tunnelling microscopy. The electronic structure of the clusters was investigated with angle-resolved HREELS. The spectrum is similar to that of a bulk silver surface and exhibits the following features: a strong plasmon peak around 3.8 eV, electron-hole pair excitations above that energy and a weak peak around 8 eV.

The investigation was focused on the plasmon peak at 3.8 eV. The dispersion of the position and the width of the peak was measured by varying the detection angle of the scattered electrons. There is a weak positive dispersion of both the peak position and width, i.e. both the plasmon energy and width increase as a function of momentum parallel to the surface. The data is compared with corresponding investigations of single-crystalline silver surfaces [2], where the energy dispersion especially is much stronger. We discuss possible causes for the observed behaviour which could be the finite thickness of the film and the substrate interaction, the relaxation of momentum conservation for small particles and the fact that the island surfaces are curved/faceted rather than parallel to the substrate.

[1] S.G. Hall et al., Rev. Sci. Instrum. 68 (1997) 3335.

[2] M. Rocca, Surf. Sci. Rep. 22 (1995) 1.

## OXYGEN DIFFUSION IN NANOCRYSTALLINE MONOCLINIC $\text{ZrO}_2$

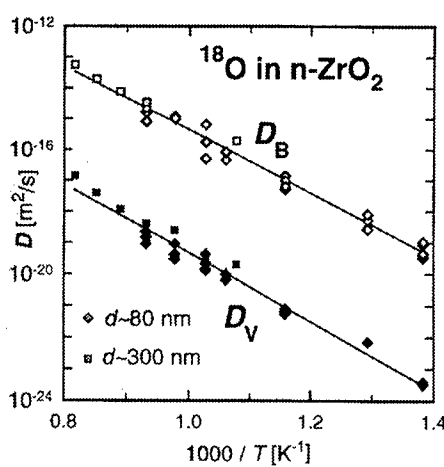
*U. Brossmann<sup>1</sup>, U. Sodervall<sup>2</sup>, R. Würschum<sup>1</sup> and H.-E. Schaefer<sup>1</sup>*

<sup>1</sup> Universität Stuttgart, Institut für Theoretische und Angewandte Physik,  
D-7550 Stuttgart, GERMANY

<sup>2</sup> Chalmers University of Technology, Department of Microelectronics,  
S-41296 Göteborg, SWEDEN

Diffusion plays a key role in determining important properties of oxide ceramic materials, such as sintering behavior, ductility and creep resistance. The investigation of the oxygen diffusion in undoped  $\text{ZrO}_2$  has so far been limited to gas exchange experiments. In the present study, depth profiles of the oxygen diffusion in nanocrystalline, undoped  $\text{ZrO}_2$  with a monoclinic structure were obtained using  $^{18}\text{O}$  as tracer and SIMS profiling. Samples of mainly tetragonal  $\text{ZrO}_2$  with a crystallite size of 5-10 nm were prepared from 99.8 % pure Zr metal by DC sputtering and crystallite condensation in an inert gas atmosphere, oxidation and in-situ consolidation of the n-  $\text{ZrO}_2$  powder. Pressureless sintering at temperatures of 950 to 1050°C lead to 97-99% density and a crystallite size of 80 to 300 nm.

X-ray diffraction measurements<sup>1</sup> on samples annealed at different temperatures up to 800°C showed a gradual transformation to the monoclinic phase and the stability of the tetragonal phase at ambient temperature for crystallites up to 15 nm of size.



Diffusion anneals were carried out in an atmosphere of about 100 hPa of 97% enriched  $^{18}\text{O}$  in the temperature range of 450 to 950 °C. The penetration depths ranged between about 0.1 and 2 microns after annealing times of 5 min to 95 h. The shape of diffusion profiles could be quantitatively understood with a model based on diffusion from a constant source under type B kinetics and a small contribution from residual porosity. The interface diffusion of oxygen in mono-clinic n-  $\text{ZrO}_2$  was found to be 3 to 4 orders of magnitude faster than volume diffusion over the entire temperature range studied. No influence of the crystallite size was observed.

The activation energies for both volume and interface diffusion,  $Q_V = 2.2 \text{ eV}$  and  $Q_B = 1.95 \text{ eV}$ , are considerably higher than values found in CaO- or  $\text{Y}_2\text{O}_3$ -stabilized  $\text{ZrO}_2$  but much lower than in the highly stoichiometric MgO or  $\text{Al}_2\text{O}_3$ .<sup>2</sup> These data suggest, that the oxygen diffusion in pure  $\text{ZrO}_2$  is dominated by a thermally activated formation and migration of vacancies on the oxygen sublattice.

**INTERNAL FRICTION AND THE YOUNG'S MODULUS CHANGE  
ASSOCIATED WITH AMORPHOUS TO NANOCRYSTALLINE  
PHASE TRANSITION IN Mg-Ni-Y ALLOY.**

*Y.M. Soifer, N.P. Kobelev<sup>1</sup>, I.G. Brodova, A.N. Manukhin<sup>2</sup> and E.Korin, L.Soifer<sup>3</sup>*

<sup>1</sup> Institute of Solid State Physics, RAC, Chernogolovka 142432, Moscow, RUSSIA

<sup>2</sup> Institute of Metal Physics, RAC, Kovalevskaya Str., Ekaterinburg 620219, RUSSIA

<sup>3</sup> Department of Chemical Engineering, Ben-Gurion University of the Negev,  
P.O. Box 653 84105, ISRAEL

The internal friction and Young's modulus of amorphous Mg<sub>84</sub>Ni<sub>12.5</sub>Y<sub>3.5</sub> alloy obtained by the melt spinning technique have been measured by a vibrating reed method at frequency of 250 Hz at heating and cooling runs in the temperature range from 300K to 650K. The structure of the samples after annealing was determined by the x-ray diffraction technique. The crystallisation kinetics of the alloy was studied by the differential scanning calorimetry (DSC). The Young's modulus measurements reveal the irreversible multi-step increase (up to 35%) during the specimen annealing in the temperature range investigated. The Young's modulus changes are accompanied by the irreversible internal friction peaks and they are observed in the same temperature intervals where the anomalies of DSC spectrum are displayed. The results obtained are explained by the structural rearrangement (mainly, a topological ordering and a crystallisation process) from amorphous to nanocrystalline state during the annealing. Mechanisms responsible for both the Young's modulus changes and internal friction spectrum in Mg-Ni-Y alloy are discussed.

**INTERNAL FRICTION IN MICROCRYSTALLINE METALS**

V.N. Chuvil'deev<sup>1</sup>, M.Yu. Gryaznov<sup>1</sup>, V.I. Kopylov<sup>2</sup> and A.N. Sysoev<sup>1</sup>

<sup>1</sup> Nizhny Novgorod Research Physical-Technical Institute,  
Gagarina Av. 23/3, 603600 Nizhny Novgorod, RUSSIA

<sup>2</sup> Physical-Technical Institute of Belorussian Academy of Sciences,  
Zhodinskaya st. 4, Minsk 220730, BELORUSSIA

There were carried out experimental investigations of elastic and non-elastic characteristics of microcrystalline copper (99.98%) and nickel (99.98%). The materials studied had special microstructure with characteristic size of the structural elements ~100 nm. This structure was obtained by special methods of intensive plastic strain (ECAP - technology). For measuring of the elastic and non-elastic the forced bending mode method characteristics was used for the samples with free ends at the frequency 1-2 kHz. The form of the samples was a plate having the characteristic sizes 2×14×80 mm. In the course of experiments there were defined the elasticity modules E and the internal friction values  $Q^{-1}$  in conditions of continuous heating from 20°C to 350°C for Cu and from 20°C to 400°C for Ni and isothermal annealing at the temperature 120 - 215°C for Cu and 230 - 300°C for Ni.

The investigations showed that the internal friction  $Q^{-1}$  of the microcrystalline materials differs essentially from the corresponding values for the large crystal materials. In the process of isothermal annealing of the microcrystalline samples, the values E and  $Q^{-1}$  are changed essentially, approaching gradually the characteristic values of the annealed material. At the same time the rate and the character of these changes depend on the annealing temperature T. As a rule when T is increasing, the recovery process intensity is increasing. The activation energy of these processes (recovery) in copper is close to the activation energy of the grain-boundary self-diffusion. In nickel the activation energy of the recovery processes is changing non-monotonously during annealing. During the isothermal exposure of copper and nickel, we have found new internal friction peaks that were not observed before. In copper at the level of  $5 \cdot 10^{-4}$  when the background values are  $\sim 10^{-4}$  (at T=200°C the peak is observed when the exposure is 240 min, at T=215°C the peak is when the exposure is 210 min). For nickel the peak is at the level  $1.5 \cdot 10^{-3}$  when the background level is  $8 \cdot 10^{-4}$  (at T=240 °C the peak is observed after the 90 min exposure; at T=250°C it is observed after the 180 min annealing). In this work there was proposed the internal friction model allowing to explain the observed laws.

---

**MODEL OF NONEQUILIBRIUM GRAIN-BOUNDARY DIFFUSION  
IN MICROCRYSTALLINE MATERIALS***V.N. Chuvil'deev*

Nizhny Novgorod Research Physical-Technical Institute, Gagarina 23/3,  
Nizhny Novgorod 603600, RUSSIA <fmv@phys.unn.runnet.ru>

There was carried out theoretical investigation of the structure, thermodynamical parameters and diffusive characteristics of equilibrium and non-equilibrium high angular grain boundaries. It is explained that the boundary structures may be described using the "islands model". At the same time the free volume is the main parameter characterising distribution of the islands and, correspondingly, the boundary structural state. There is proposed a model allowing explaining the dependence of the free energy and the boundary entropy value on the value of the material free volume and thermodynamical constants. There is proposed a new model of diffusion in the boundary having an islands structure. The model is based on the ideas of heterophase fluctuations when there are changed the sizes of the islands having high diffusivity. There were carried out the calculations of the enthalpy, entropy and diffusion activation energy for some pure metals.

There is described the structure and the properties of non-equilibrium grain boundaries. There is explained that anomalies in diffusive parameters and thermodynamical characteristics of non-equilibrium boundaries are the result of their free volume increase at the expense of the free volume introduced by lattice dislocations hit into the boundaries and implementing the intragranular deformation. There were obtained equations describing the boundary energy and their diffusive parameter changes during their interaction with separate dislocations and with lattice dislocation flow. There was defined the grain-boundary diffusion coefficient dependence on the deformation rate and on the material structure parameters.

In the work there is analysed the role of the deformation-stimulated diffusion in the nano- and microcrystalline materials. There are also discussed the processes of the grain boundary sliding deformation-stimulated migration and the grain growth.

**PRESSURE SINTERING OF ULTRAFINE IRON AND NICKEL POWDER***M.I. Alymov*

Baikov Institute of Metallurgy of Russian Academy of Sciences,  
Leninsky prospect 49, Moscow 117334, RUSSIA <alymov@lesr.imet.ac.ru>

Pressure sintering of iron and nickel ultrafine powder (UFP) was conducted using three methods: uniaxial pressure of upsetting forging without molds, hot isostatic pressing (HIP) method and high-temperature pressing (HTGE). UFP were prepared by chemical method. Observation of the microstructure and measurements of the mass density, average grain size and mechanical properties of the sintered compacts were carried out. The uniaxial pressure sintering was performed at temperatures 670-1370K and pressures 90-380 MPa in vacuum and in hydrogen atmosphere. Green compacts, which were  $\phi 5 \times 15$  mm in size and 40-55% in relative density, were made by die-pressing. No lubricant was used in the pressing operation. The critical sintering temperature for complete densification decreased under 380 MPa to 740 K. The minimum average grain size and the highest hardness of fully dense compacts was 100 nm and 5GPa, respectively.

The HIP and HTGE methods have been applied to obtained bulk high-density compacts. Short duration action of the pressure and temperature by HTGE method permits to obtain high density bulk compacts with low grain size and high strength.

The kinetic approach to the analysis of UFP sintering mechanisms is developed allowing for size particle factor. The sintering maps were calculated.

**MECHANICAL BEHAVIOR OF Fe-6Mn-2Ni-Mo-V  
WITH ULTRA FINE-GRAINED STRUCTURE**

*I.Yu. Pyshmintcev<sup>1</sup>, V.A. Khotinov<sup>1</sup>, S.B. Mikhailov<sup>1</sup>, V.A. Korznikov<sup>2</sup> and  
R.R. Mulyukov<sup>2</sup>*

<sup>1</sup> Ural State Technical University, Mira str.19, Ekaterinburg 620002, RUSSIA  
[<tom@dialup.ustu.ru>](mailto:tom@dialup.ustu.ru)

<sup>2</sup> Institute for Metals Superplasticity Problems, Russian Academy of Sciences,  
Khalturina, 39, Ufa 450001, RUSSIA <[radik@imspphy.bashkiria.su](mailto:radik@imspphy.bashkiria.su)>

The samples out of a high-strength martensite alloy were subjected to heavily “warm” deformation rolling with a consequent annealing alloy with the purpose to improve a combination of strength and plasticity via creation of an ultra fine-grained structure. It was established that varying parameters of treatment could result in significant changes of regularities of phase transformations and mechanical behaviour of a material. As compared to the state after traditional heat treatment a concurrent increase in viscosity and strength by a factor of 1.5 was achieved. The investigations of amplitude and temperature dependencies of internal friction were conducted to reveal the influence of parameters of treatment on structure and properties of the material.

**APPLICATION OF NANOPOWDERS TO HIGH TEMPERATURE  
SINGLE CRYSTAL FIBER SENSOR**

*Yan-qi WANG and Xi-jun WU*

Department of Materials Science and Engineering, Zhejiang University,  
Hangzhou 310027, CHINA <mse\_xjwu@ema.zju.edu.cn>

ZrO<sub>2</sub>, CuO, Al<sub>2</sub>O<sub>3</sub> and SiO<sub>2</sub> mixed powders, with different powder sizes ranged from 7 to 72 nm (nanopowders) and 1.2 to 2.4  $\mu$ m (micropowders) respectively, were used to coat the head of the sapphire single crystal fiber. The effect of the powder size upon the sensor's properties was studied. The results indicated that the coating with nanopowders greatly improves the optical stability, the adhesive strength and the thermal shock resistance of the sensor. The response time of the sensor coated with nanopowders is 0.005 s, which is obviously shorter than that of the sensor coated by micropowders, 0.48 s. Above results have been used to improve the performance of this kind of temperature sensor. The microstructures of the mixed powders on the sensor's properties were also studied.

**MICROHARDNESS AND SUBMICROCRYSTALLINE STRUCTURE OF STAINLESS STEELS OBTAINED BY SEVERE PLASTIC DEFORMATION**

*S.V. Dobatkin, R.Z. Valiev\*, L.M. Kaputkina, N.A. Krasilnikov\*, M.A. Kazakov, and O.V. Sukhostavskaya*

Moscow State Steel and Alloys Institute, Leninsky prospekt 4,  
117936 Moscow, RUSSIA <ctmo@ns.misa.ac.ru>

\*Ufa State Aviation Technical University, K. Marx 12, 450000 Ufa, RUSSIA

Structure and properties of stainless steels (austenitic 0.08% C - 18% Cr - 10% Ni - 0.5% Ti and ferritic 0.08% C - 18% Cr - 0.5% Ti) after severe plastic deformation at room temperature were investigated. Deformation was performed by torsion (after preliminary compression on 50%) under 6 GPa pressure up to 9 revolutions that corresponds to a strain degree  $e = 6.3$  of the samples having initial size  $\varnothing 10 \times 1$  mm.

Severe plastic deformation significantly increases the microhardness of both steels. If austenitic and ferritic steels in initial hot-rolled state had microhardness  $H_m = 1.9$  and 1.6 GPa, after preliminary compression - 3.6 and 2.6 GPa, than after intense deformation by torsion  $e = 6.3$  the values of microhardness increase up to ~ 6 GPa and ~ 7 GPa, accordingly. One can see that ferritic steel having lower initial value of microhardness strengthens more strongly. The  $H_m = f(e)$  dependence confirms it. Monotonous increasing in microhardness values of ferritic steel finishes at  $e = 5.7$  (5 revolutions) and  $H_m$  values remain approximately constant up to  $e = 6.3$  (9 revolutions). While in austenitic steel monotonous increasing in microhardness takes place right up to  $e = 6.3$ .

The microhardness measurements found out non-uniformity of strain and structure along diameter and thickness of the samples. The measurements were carried out in the centre ( $H_m^0$ ), in the middle of a radius ( $H_m^{1/2R}$ ) and at the ends ( $H_m^R$ ) of the samples on the surface and central planes (central plane is perpendicular to the axis of torsion and crosses the middle of the sample's height). The values of microhardness increase from  $H_m^0$  to  $H_m^R$  in both steels, both planes and for all strain degrees. The difference between  $H_m^{1/2R}$  and  $H_m^0$  is more significant, than between  $H_m^{1/2R}$  and  $H_m^R$ . In ferritic steel the difference between microhardness in the center and at the ends of the samples are two times higher than in the austenitic steel. The values  $H_m$  at the central plane are lower, than at the surface. It should be noted that microhardness even in the centre of samples in both steels where strain degree is minimum has sufficiently high values  $H_m^0 \geq 5$  GPa.

Electronmicroscopic investigation showed the submicrostructure formation during severe plastic deformation. Structure elements in ferritic steel have sizes of 40-150 nanometers after  $e = 6.3$ . A character of the electron diffraction pattern allows to approve about presence both low- and high-angle boundaries between structure elements. Submicrocrystalline structure was formed during intense deformation by torsion since after preliminary compression the cellular structure with low-angle misorientation of boundaries one can observed.

**CHARACTERISTIC FUNCTIONS OF NANOSTRUCTURED MATERIALS***V. Garrido and D. Crespo*

Dept. Física Aplicada, Univ. Politècnica de Catalunya, Campus Nord,  
Modul B4, 08034 Barcelona, SPAIN <crespo@benard.upc.es>

Nanostructured materials are often obtained by first order phase transformations, driven by nucleation and subsequent growth of particles in a volume or at an interface. A recently developed mean field model (PKJMA), grounded on the Avrami hypotheses plus a populational description [1] allows to increase the knowledge on the microstructures obtained by such kinetics [2]. However, most of the macroscopical properties of the materials are related to their spatial correlation functions. To calculate them, a general relationship between the autocorrelation function  $C_1(r,t)$  and the droplet size-shape distribution was obtained by using self-similarity arguments [2]. Furthermore, we derived some relationships which allow us to obtain the remaining correlation functions from  $C_1(r,t)$ , the untransformed volume fraction,  $M_0(t)$ , and the degeneracy parameter  $p$ . An exact expression for the autocorrelation function was obtained for isotropic growth using a system scaling length.

Since the PKJMA model is less restrictive than previously existing theories, the correlation functions can be obtained for any dependence of the kinetic parameters. The procedure is illustrated by calculating the correlation functions corresponding to the nanostructures developed in partitioning transformations, considering diffusion controlled growth with soft impingement and decreasing nucleation rate.

- [1] D. Crespo and T. Pradell, *Phys. Rev. B* **54**, 3101 (1996).
- [2] D. Crespo, T. Pradell, M.T. Clavaguera-Mora and N. Clavaguera, *Phys. Rev. B* **55** 3435 (1997).
- [3] V. Garrido and D. Crespo, *Phys. Rev. E* **56**, 2781 (1997).

---

**NMR RELAXATION AND LINESHAPE STUDY ON Li<sup>+</sup> DIFFUSION  
IN NANOCRYSTALLINE LAYER-STRUCTURED Li<sub>x</sub>TiS<sub>2</sub>**

*Rudolf Winter and Paul Heitjans*

Institut für Physikalische Chemie und Elektrochemie, Universität Hannover,  
Callinstr. 3a, 30167 Hannover, GERMANY <rudi@curie pci.uni-hannover.de>

Hexagonal TiS<sub>2</sub> is known as a layer-structured material which can be used as a host for intercalation compounds. Two-dimensional diffusion of Li ions takes place along the layers. The influence of the structural heterogeneity, introduced into the layered material by decreasing the grain size, on the Li diffusion is the objective of this study.

Nanocrystalline (n-)Li<sub>x</sub>TiS<sub>2</sub> was prepared by chemical Li intercalation into polycrystalline TiS<sub>2</sub> and subsequent high-energy ball milling. The average grain size, as measured by X-ray diffraction line broadening, is in the 10 nm range. As reference, also polycrystalline and amorphous Li<sub>x</sub>TiS<sub>2</sub> samples were studied.

Temperature and frequency dependent <sup>7</sup>Li spin-lattice relaxation rate measurements were carried out in the laboratory ( $T_1^{-1}$ ) and in the rotating ( $T_{1p}^{-1}$ ) reference frames. The activation energy  $E_a$  obtained from the low-temperature flank of the diffusion-induced relaxation rate peak in an Arrhenius-type, *i.e.*  $\log T_1^{-1}(T^{-1})$ , representation, is about 160 meV (as compared to 190 meV for the polycrystalline and 66 meV for the amorphous material). The frequency exponent in  $T_1^{-1} \sim v_0^{-\beta}$  is  $\beta \approx 0.6$ .

The shape of the central line of the <sup>7</sup>Li NMR spectra was measured as a function of temperature. In the rigid lattice limit, *i.e.* below 250 K, a single-Lorentzian function is appropriate to fit the line shape. In the range 250 K  $\leq T \leq$  400 K, a double-Lorentzian form is obtained with a constant broad component (bulk material) and a motionally narrowed component (interface material) the intensity of which is increasing up to about 50%. Above 400 K, the broad component becomes motionally narrowed as well.

The increasing intensity of the narrow spectral component with temperature indicates an inhomogeneous structure within the interface regions: motional narrowing does not start at the same temperature for all interface Li sites due to their different local environment. The small difference in  $E_a$  of the nano- and polycrystalline Li<sub>x</sub>TiS<sub>2</sub> is a consequence of the two-dimensional diffusion mechanism: Li ions diffusing within a layer and on the surface of a nanocrystallite experience similar potential barriers. An amorphous-like structure of the interface material can be excluded for the layer-structured material, as this would imply significantly lower  $E_a$  like in the amorphous sample.

**THERMAL STABILITY OF NANOCRYSTALLINE GOLD FILM  
PREPARED BY GAS DEPOSITION METHOD STUDIED BY BENDING TEST**

*M. Kobiyama, T. Inami and S. Okuda*

Faculty of Engineering, Ibaraki University, 4-12-1, Nakanarusawa,  
Hitachi, Ibaraki 316, JAPAN <kobiyama@hit.ipc.ibaraki.ac.jp>

Thermal stability of nanocrystalline gold film prepared by gas deposition method was studied by means of mechanical behavior. Gold (99.999%) was evaporated in He gas to obtain nano-sized gold particles. Then, by a pressure difference, the particles were transferred through a fine tube from evaporation chamber into deposition chamber and deposited onto a glass substrate which were fixed on the stage movable in X and Y directions. Specimen size was about 1x4 mm with thickness 10-20  $\mu\text{m}$  with various grain sizes (7 nm-30 nm). The specimens were annealed for 1h at each temperature in vacuum, with heating rate of 1 K/min. Grain size was estimated from scanning tunnelling microscope (STM) observations.

Mechanical behaviour of specimens were studied by bending test under an optical microscope equipped with video-camera. After each step-wise increase in bending strain, a bending load was released and residual strain of the specimen was measured.

For the bending test at room temperature, specimens as deposited revealed a complete elastic deformation up to  $\epsilon \sim 1-0.5\%$ , i.e. showed a very large elasticity, and the residual strain was found to decrease with increasing grain size in agreement with the grain boundary sliding effect. Comparing specimens as deposited and after annealing treatments, thermal stability was found to increase with decreasing grain size. For example, the specimens with grain size 25 nm showed almost no recovery even after the annealing below 673 K and below 773 K for the bending tests at room temperature and at 77K, respectively.

Further, detailed results on the grain size on the above deformation behaviour will be presented.

**MECHANICAL CRYSTALLIZATION OF  
AMORPHOUS FeZrBCu SOFT MAGNETIC MATERIAL**

*J.Friedrich, U. Herr and K. Samwer*

Institute of Physics, University of Augsburg, Memminger Str. 6,  
86135 Augsburg, GERMANY

Nanocrystalline Fe-base soft magnetic materials with high saturation magnetization can be obtained by crystallization of FeZrBCu amorphous precursors. In contrast to the conventional thermal crystallization, mechanical crystallization provides an alternative route for the generation of nanocrystalline materials. We report about an experimental study of mechanical crystallization of FeZrBCu melt spun ribbons in a high energy ball mill. Special emphasis is put on the early stages of the transformation. X-ray diffraction, Moessbauer spectroscopy and magnetization measurements have been used to characterize the material. We find a continuous increase of the saturation magnetization with milling time accompanied by an increase of the crystalline fraction. The coercivity shows a different behavior with a large increase after short milling. The possible influence of the deformation process on the magnetic anisotropy and the coercivity is discussed. The results are compared with the phase formation and magnetic properties during mechanical alloying of FeZrBCu powder mixtures which also yields nanocrystalline material.

The project has been funded by the Deutsche Forschungsgemeinschaft.

**INFLUENCE OF MICROSTRUCTURE ON MAGNETIC BEHAVIOUR  
IN NANOCRYSTALLINE Fe-Nb-B-(Cu) ALLOYS**

*I. Škorvánek<sup>1</sup>, J. Marcin<sup>1</sup>, B. Idzikowski<sup>2</sup>, P. Duhaj<sup>3</sup>, J. Kováč<sup>1</sup> and V. Kavečansky<sup>1</sup>*

<sup>1</sup> Institute of Experimental Physics, Slov. Acad. Sci., 043 53 Košice, SLOVAKIA

<sup>2</sup> Institute of Molecular Physics, Polish Acad. Sci., 60-179 Poznan, POLAND

<sup>3</sup> Institute of Physics, Slovak Acad. Sci., 842 28 Bratislava, SLOVAKIA

The formation of a nanocrystalline microstructure and its influence on magnetic behaviour in  $\text{Fe}_{80}\text{Nb}_7\text{B}_{12}\text{Cu}_1$  and Cu-free  $\text{Fe}_{81.5}\text{Nb}_{6.5}\text{B}_{12}$  alloys is investigated in series of specimens prepared by primary crystallisation of melt-spun amorphous ribbons. The crystallisation behaviour of investigated alloys is studied by differential scanning calorimetry and by thermomagnetic measurements. The bimodal shape of the first broad exothermic peak in the DSC thermogram of the Cu-free  $\text{Fe}_{81.5}\text{Nb}_{6.5}\text{B}_{12}$  alloy clearly indicates the two-stage nature of bcc-Fe phase formation process, which was recently reported for the alloys of similar composition. It is shown that addition of Cu to the FeNbB system results in a decrease of crystallisation temperature and only single exothermic peak that corresponds to the formation of bcc-Fe phase is evident on the DSC curve. The transmission electron microscopy is used in order to obtain direct microstructural evidence of the various stages of crystallization in selected samples. The changes in microstructure upon annealing of parent amorphous ribbon in the temperature range 400°C - 650°C were examined by X-ray diffraction. The relative amount of crystalline phase and the average grain size of nanocrystalline particles were estimated from the corresponding X-ray diffractograms as a function of annealing temperature.

The magnetic behaviour is investigated by the VSM-magnetometry and by quasi-static hysteresis loop measurements. The saturation magnetisation was experimentally studied as a function of measuring temperature over the temperature range from 4.2 K to 800 K. It is shown that the remarkable increase of Curie temperature of amorphous rest matrix (up to 70 K for the  $\text{Fe}_{81.5}\text{Nb}_{6.5}\text{B}_{12}$  samples) takes place with increase of volume fraction of bcc-Fe nanocrystals. The results of hysteresis loop measurements performed at room and liquid nitrogen temperature have revealed marked deterioration of soft magnetic properties during the first stages of nanocrystallization. This deterioration is significant namely for Cu-free  $\text{Fe}_{81.5}\text{Nb}_{6.5}\text{B}_{12}$  alloys at room temperature, where the weak magnetic matrix shows reduced capability to transmit the exchange coupling between nanocrystalline grains. For the samples with larger volume fraction of nanocrystalline phase the increase of annealing temperature results in the decrease of coercivity. The observed magnetic softening with increasing volume fraction of nanocrystalline phase can be explained by the decrease of intergranular distances as well as by the changes in magnetic properties of retained amorphous matrix, which allow stronger exchange coupling between bcc-Fe nanocrystals.

**DISORDER-ENHANCED COERCIVITY  
IN MECHANICALLY MILLED Sm-Co ALLOYS**

*Diandra L. Leslie-Pelecky<sup>1</sup> and Richard Schalek<sup>2</sup>*

<sup>1</sup> Department of Physics & Astronomy and Center for Materials Research,  
University of Nebraska, Lincoln, NE 68588-0111, USA <[diandra@unlinfo.unl.edu](mailto:diandra@unlinfo.unl.edu)>

<sup>2</sup> Composite Materials and Structures Center, Michigan State University,  
East Lansing, MI 48824, USA

Mechanical milling can create or modify nanostructure by refining grain size and by introducing atomic-level disorder. Recent studies of mechanically milled ferrimagnets and antiferromagnets show that a combination of atomic-level disorder and missing bonds can form a spin-glass-like layer on the surface of the particle (or in the interphase) that results in increased coercivity, long-time decay of the magnetization and shifted hysteresis loops.<sup>1,2</sup> We have observed similar features (shifted hysteresis loops and large increases in coercivity) in mechanically milled SmCo<sub>5</sub>. Pre-alloyed powder is milled in a SPEX 8000 mixer/mill for times from 15 minutes to 28 hours. The room-temperature coercivity dramatically increases from 2.5 kOe in the as-received state to a maximum of 16 kOe after two hours of milling. Remanence ratios are on the order of 0.8 regardless of whether or not the powders have been aligned prior to measurement. Low-temperature hysteresis loops for samples with higher coercivities show two-phase behavior not evident at room temperature, with the degree of two-phase character of the loops directly correlated to the dependence of the coercivity on milling time. The hysteresis loops at temperatures below 250 K also exhibit large shifts toward negative field (up to 10 kOe at 5 K), with the magnitude of the shift also correlated to the coercivity. Shifts are observed in both field-cooled and zero-field-cooled states. Small room-temperature shifts are observed for some milling times. While increases in the coercivity and remanence ratio are expected for samples with coupling between hard and soft ferromagnetic materials, shifts in the hysteresis loop generally are not characteristic of exchange-spring magnets. We propose that spin disordering induced by milling is responsible for the enhanced coercivity and remanence ratio and shift observed in these materials and compare our results to those of measurements in ferrimagnets and antiferromagnets.

1. R.H. Kodama, A.E. Berkowitz, E.J. McNiff, Jr. *et al.*, "Surface Spin Disorder in NiFe<sub>2</sub>O<sub>4</sub> Nanoparticles," Phys. Rev. Lett. **77**, 394 (1996).
2. R.H. Kodama, Salah A. Makhoul and A.E. Berkowitz, "Finite Size Effects in Antiferromagnetic NiO Nanoparticles." Phys. Rev. Lett. **79**, 1393 (1997)

### THE SONOCHEMICAL SYNTHESIS OF ACICULAR AMORPHOUS NANOPARTICLES IN MAGNETIC FIELD

*Tanya Prozorov<sup>1</sup>, Ruslan Prozorov<sup>2</sup>, Yuri Koltypin<sup>1</sup> and Aharon Gedanken<sup>1</sup>*

<sup>1</sup> Department of Chemistry, Bar-Ilan University,  
Ramat-Gan 52900, ISRAEL <prozorr@ashur.cc.biu.ac.il>

<sup>2</sup> Institute for Superconductivity, Department of Physics, Bar-Ilan University,  
Ramat-Gan 52900, ISRAEL

The sonochemical irradiation of Fe (CO)<sub>5</sub> solution in decaline has been carried out with and without external magnetic field. Direct TEM measurements reveal that sample obtained without magnetic field consists of sponge-like particles of mean size of about 25 nm, whereas the sample, synthesized in 7 kGauss applied magnetic field consists of highly acicular particles of 50 nm in length and 5 nm in diameter. Our finding sheds light on the process of particle nucleation during sonication. It cannot be a diffusion-assisted growth, because of very small time scale, therefore we conclude that particles are forced to form an acicular entity by direct magnetic interactions. The amorphous nature of obtained substance was verified by XRD measurements, SAED and thermal analysis.

The M vs. T measurements indicate the giant shift of the blocking temperature of about 50 K toward higher values for the sample, obtained in magnetic field (see Fig.1).

We attribute the observed shift to the significant enhancement of the particle shape magnetic anisotropy. This is also confirmed by measurements of the magnetic relaxation.

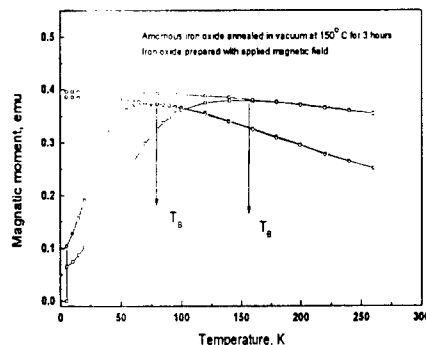


Figure 1. ZFC and FC for iron oxide prepared with applied magnetic field 7 kG.

**STRUCTURAL AND MAGNETIC STUDIES OF Co-CONTAINING  
NANOCRYSTALLINE SOFT MAGNETS**

*R.S. Taylor, W.R. Wilson, R.H. Yu, J.Q. Xiao, and K.M. Unruh*

Department of Physics and Astronomy University of Delaware Newark,  
DE 19716, USA <kmu@udel.edu>

Nanocrystalline materials with soft magnetic properties have been prepared by appropriate heat treatments of rapidly quenched amorphous Fe-Co-Si-B-Nb-Cu and Fe-Co-Zr-B-Cu alloys over a wide range of Fe/Co ratios. The structure and thermal stability of the nanocrystalline phase has been characterized by x-ray diffraction (XRD), transmission electron microscopy (TEM), differential scanning calorimetry (DSC), and differential thermal analysis (DTA) measurements. In addition to the characterization measurements, a systematic series of magnetic measurements have been carried out in order to determine the magnetization, coercivity, and magnetostriction of these materials as a function of the Fe/Co ratio from room temperature to above 600°C. The results of these measurements have shown that Co can successfully be substituted for Fe in both classes of alloys without a significant degradation in the soft magnetic properties, and that as a result increased saturation magnetizations and Curie temperatures can be achieved. The combination of enhanced saturation magnetization, Curie temperature, and small coercivity offers the potential for new technological applications, particularly at elevated temperatures.

This work has been supported by the Air Force Office of Scientific Research under contract no. 49620-96-1-0434.

**STRUCTURAL CONFIGURATION AND MAGNETIC PROPERTIES  
OF THE RAPIDLY SOLIDIFIED CuCo ALLOY**

*E. Bonetti<sup>1</sup>, L. Del Bianco<sup>1</sup>, L. Savini<sup>1</sup>, P. Tiberto<sup>2</sup>, F. Vinai<sup>2</sup>*

<sup>1</sup>Dipartimento di Fisica, Università di Bologna and Istituto Nazionale per la Fisica della Materia, Viale Berti Pichat 6/2, I-40127 Bologna, ITALY

<sup>2</sup>Istituto Elettrotecnico Nazionale Galileo Ferraris and Istituto Nazionale per la Fisica della Materia, I-10125 Torino, ITALY

The interest grown during the last years in granular systems has been mainly determined by the possibility to observe a giant magnetoresistance (GMR) effect when particular microstructural conditions are achieved. In particular, the CuCo solid solution obtained by ultra rapid quenching is reported to show enhanced GMR after suitable thermal treatments that induce the development of Co nanometric precipitates, with superparamagnetic behaviour, in the Cu matrix.

$\text{Cu}_{1-x}\text{Co}_x$  ( $x = 0.03, 0.06, 0.1, 0.12, 0.15$ ) ribbons have been synthesised by planar flow casting in He atmosphere. Measurements of elastic energy dissipation coefficient and dynamic Young's modulus have been performed as a function of temperature, in the 300-900 K range, and as a function of time at selected temperatures.

The results provide useful information on the structural features of the as-cast ribbons and on their microstructural evolution with temperature. In particular, annihilation of excess vacancies, relaxation of internal stresses, precipitation and coarsening of Co at the dislocations and at the Cu grain boundaries are the processes invoked to account for the different anelastic behaviours observed in the samples. Complementary magnetic measurements (hysteresis loops, GMR) have been performed on the same ribbons in order to establish a relationship between magnetic properties and structural configuration. The influence of the synthesis parameters, such as the quenching rate, on the state of dispersion of cobalt in the Cu matrix has been also studied by carrying out a similar analysis on ribbons with the same Co content but obtained with different wheel velocities.

**MECHANICAL BEHAVIOUR OF Ni<sub>3</sub>Al-L1<sub>2</sub> ORDERED COMPOUND  
ENTERING THE NANO-GRAIN SIZE REGIME**

*E.Bonetti, E.G.Campari, L.Pasquini, E.Sampaolesi and G.Scipione*

Dipartimento di Fisica dell'Università di Bologna and Istituto Nazionale per la Fisica della Materia, viale Berti-Pichat 6/2, I-40127 Bologna, ITALY <bonetti@df.unibo.it>

The Nickel Aluminide Ni<sub>3</sub>Al with the L1<sub>2</sub> ordered structure exhibits a variety of temperature dependence of the flow stress (TDFS) and particularly an 'anomalous' increase of the flow stress with temperature up to 800 K. The models which try to account for this behavior involve locking processes resulting from intrinsic dislocation core transformations. The positive temperature dependence of the flow stress was attributed to splitting of superpartial dislocation pairs into segments lying in the (111) and (010) planes, with the dislocation segments lying in the (010) plane acting as pinning centre for the dislocation.

An effect of thermally activated dislocation pinning in these intermetallics was also detected by means of dynamic elasticity modulus measurements by mechanical spectroscopy. In single crystals with the L1<sub>2</sub> composition the modulus increases reversibly from room temperature up to about 800-900 K. At temperatures in this range the crystal slip systems change and the yield stress increase with temperature stops.

In the nanocrystalline intermetallic produced by ball milling the anelastic behaviour is quite complex, depending on the long-range order degree and grain size. The structural conditions under which the anomalous temperature increase of the modulus is absent have been checked and moreover the role of the interfaces in the high-temperature anelastic regime behaviour was established. A comparison of the experimental results on monocrystalline, polycrystalline and nanocrystalline samples was performed and a phenomenological description of the different behaviour is presented.

**ANNEALING EFFECTS OF MAGNETIC PROPERTIES IN Fe<sub>83</sub>Zr<sub>7</sub>B<sub>8</sub>Cu<sub>2</sub>**

*Cheol Gi Kim<sup>1</sup>, Gil-Ho Ryu<sup>2</sup>, Seong-Cho Yu<sup>2,3</sup>, and K.V. Rao<sup>3</sup>*

<sup>1</sup>Dept. of Physics, Sun Moon Univ., Chung-nam, 336-840, KOREA

<sup>2</sup>Dept. of Physics, Chungbuk National University, Cheongju, 361-763, KOREA

<sup>3</sup>Dept. of Cond. Mat. Phys., Royal Inst. of Tech., S-10044 Stockholm, SWEDEN

The magnetic properties of giant magneto-impedance(GMI), permeability, and low temperature magnetization were measured in Fe<sub>83</sub>Zr<sub>7</sub>B<sub>8</sub>Cu<sub>2</sub> alloys before and after the annealing at 500 and 550 , respectively. Amorphous Fe<sub>83</sub>Zr<sub>7</sub>B<sub>8</sub>Cu<sub>2</sub> ribbons were prepared by rapid quenching technique in Ar atmosphere. GMI profile during a half cycle of magnetization under a slowly varying magnetizing field of 0.01 Hz showed a sharp maximum around zero field. GMI is associated with the domain dynamics of the wall motion and rotational magnetization[1]. The contribution from wall motion is dominant over the rotational magnetization in the frequency range in the usual amorphous samples. As the frequency increases over a few hundreds kHz, the dip in the GMI profile appeared, showing that the wall motion begins to be damped, in turns, the effect of rotational magnetization on GMI is comparable to that of wall motion. In contrast to the GMI characteristics for the high frequency in the usual amorphous materials, the dip in the GMI profiles doesn't appear in as-quenched, 500 and 550 annealed Fe<sub>83</sub>Zr<sub>7</sub>B<sub>8</sub>Cu<sub>2</sub> samples up to 1 MHz. It means that the damping of wall motion is not significant up to this frequency. The magnitude of GMI, Z<sub>H=sat</sub> - Z<sub>H=0</sub>, decreased in the 500 annealed sample compared to that of as-quenched one, may be due to the crystalline sites hindering the magnetization. But this value increased again in the 550 annealed sample, which can be explained by the change of average grain size of the sample because of its different annealing temperature.

[1] L. V. Panina et al., IEEE Trans. Mag. **31**, 1249 (1995).

**SUPERFLUIDITY AND QUANTUM VORTICES IN SYSTEMS WITH  
PAIRING OF SPATIALLY SEPARATED ELECTRONS AND HOLES.***S.I. Shevchenko and S.V. Terent'ev*

B.I. Verkin Institute for Low Temperature Physics&Engineering Academy of Sciences  
of Ukraine, Lenin Ave., Kharkov 310164, UKRAINE <[shevchenko@ilt.kharkov.ua](mailto:shevchenko@ilt.kharkov.ua)>

A possibility for the existence of rather unusual superconductivity mechanism due to pairing of spatially separated electrons and holes (PSSEH) has been predicted by Shevchenko and independently by Lozovik and Yudson (SLY) about 20 years ago. The main feature of this superconductivity mechanism consists in that an electron supercurrent is accompanied by a hole supercurrent that is equal in value to the former one. For a long time the predictions of SLY escaped experimentalists attention, until progress in microelectronics resulted in the creation of the required structures. There are experimental papers which report the observation of phenomena associated with the discovery of the superconductivity mechanism predicted by SLY.

In this report a possibility of appearance of planar vortices in PSSEH systems is demonstrated. The term "planar" implies the vortices in which electron-hole pairs rotate as a whole in the structure plane. Like in the Onsager-Feynman case, the velocity field of the planar vortices decreases with the distance from the vortex centre by the  $1/r$  law (not exponentially as in ordinary superconductors). This leads pairing of vortices with opposite circulations and the superconducting transition in the PSSEH systems by Berezinskii-Kosterlitz-Thouless mechanism. On the other hand the planar vortices can interact with the external magnetic field, just like the Abrikosov vortices do. It is shown that the magnetic field which two-dimensional divergence differs from zero can lead to the appearance of a macroscopic number of quantized vortices with equal circulation. The vortex structure formed in the magnetic field of two-dimensional ring current is thoroughly investigated and it is shown that the vortex structure is ordered but it is non-invariant under translations.

The temperature of superconducting transition of PSSEH systems in a strong magnetic field perpendicular to a structure plane has been found and the behavior of these systems in crossed electric and magnetic fields has been studied. It is shown that the crossed fields can lead to an effect similar to flux quantization in ordinary superconductors. If the two-dimensional divergence of the electric field is not equal to zero, the crossed fields create a macroscopic number of planar vortices with the same circulations. The vortex structure is determined by behavior of electric field in space. In the electric field of two-dimensional charged disk the vortices are to form a regular lattice.

**MÖSSBAUER STUDY OF THE NANOCRYSTALLINE  $\text{Fe}_{80}\text{Ti}_7\text{B}_{12}\text{Cu}_1$  ALLOY**

*A. Grabias, M. Kopcewicz and B. Idzikowski\**

Institute of Electronic Materials Technology, Wólczyńska 133,  
01-919 Warszawa, POLAND

\*Institute of Molecular Physics, Polish Academy of Sciences, M. Smoluchowskiego 17,  
60-179 Poznań, POLAND

Amorphous  $\text{Fe}_{80}\text{Ti}_7\text{B}_{12}\text{Cu}_1$  alloy exhibits two stages of crystallisation. Annealing at temperatures between the first and second exothermic peaks at the differential scanning calorimetry curve enabled us to obtain a microstructure consisting of nanocrystalline bcc-Fe grains embedded in the retained amorphous matrix. Such a nanocrystalline structure exhibits a combination of very good soft magnetic properties (low coercivity, high saturation magnetisation and permeability) as it has been revealed for Fe-Me-B alloys (Me = Zr, Nb, Ti or Ta). These alloys have superior magnetic properties (higher saturation magnetisation and permeability) as compared to more conventional FeCuNbSiB alloys. Good soft magnetic properties result from the significant reduction of effective magnetic anisotropy due to (i) exchange interaction between bcc-Fe nanocrystalline grains and (ii) the reduction of the magnetostriction.

In this study we present investigation of the structure and magnetic properties of the nanocrystalline  $\text{Fe}_{80}\text{Ti}_7\text{B}_{12}\text{Cu}_1$  alloy by Mössbauer effect. The experiments were performed for FeTiBCu alloy in the as-quenched amorphous state and after annealing for 1 h at temperatures of 440, 470, 520, 570 and 620°C. Conventional transmission Mössbauer spectroscopy was used for phase identification and determination of their relative contents. Unique rf-Mössbauer technique, in which Mössbauer spectra are measured during exposure of samples to a magnetic radio-frequency (rf) field, was applied to study magnetic properties of the  $\text{Fe}_{80}\text{Ti}_7\text{B}_{12}\text{Cu}_1$  alloy. The intensity of the 61 MHz field ranged from 0 to 20 Oe.

The rf field induces in ferromagnetic materials two effects – rf collapse and rf sidebands. The rf collapse, which is very sensitive to local anisotropy fields, depends strongly on thermal treatment of FeTiBCu alloy. The complete rf collapse of the magnetic hyperfine structure (hfs) occurs only in the amorphous phase. The nanocrystalline phase yields partly collapsed magnetic hfs spectral components revealing that the magnetic anisotropy of the bcc-Fe nanocrystals is larger than that of the amorphous phase. The rf sidebands, directly related to magnetostriction, markedly decrease when the nanocrystalline bcc-Fe phase is formed, indicating decrease of magnetostriction. The rf-Mössbauer experiments performed as a function of the rf field intensity provided detailed information on anisotropy fields related to the size distribution of bcc-Fe grains.

**NANOCRYSTALLIZATION PROCESS IN ALLOYS AL-Y-Ni-Fe**

*K. Pêkaa<sup>1</sup>, P. Jaskiewicz<sup>1</sup> and J. Latuch<sup>2</sup>*

<sup>1</sup> Institute of Physics, Warsaw University of Technology, ul. Chodkiewicza 8,  
02-524 Warsaw, POLAND <pekalam@adam.mp.pw.edu.pl>

<sup>2</sup> Department of Materials Science and Engineering, Warsaw University of Technology,  
ul. Narbutta 85, 02-524 Warsaw, POLAND

Nanocrystallization process in AlYNiFe alloys was investigated by structural, electrical resistivity and DSC measurements. Nanocrystalline alloys were prepared by two methods. First series of alloys was made by a melt spinning at relatively slow velocity of the copper roller. The second series was obtained from the amorphous alloys produced at higher roller velocity, which were then subjected to the annealing above the nanocrystallization temperature. The initial content of the fcc Al nanocrystals in the amorphous matrix was increased during nanocrystallization. The electron transport properties of two series of alloys were compared and substantial differences were discussed. The temperature coefficient of resistivity of the first series was negative and diminished with the increasing nanocrystalline fraction. Nanocrystallization of the first series proceeds with higher rate than for the amorphous alloy. Such a behavior is in contrast to the second series of alloys exhibiting a positive temperatures coefficient of resistivity. Nanocrystallization rate of these alloys is comparable with rates of amorphous alloys. It was observed that alloys of both the series containing any initial fraction of the nanocrystalline phase complete their crystallization process at relatively higher temperature. Discussion of these properties will be presented.

**ANOMALY OF THE HALL-PETCH RELATION  
FOR NANOCRYSTALLINE MATERIALS**

*Zaichenko S.G. and Glezer A.M.*

Institute of Physical Metallurgy I.P.Bardin State Scientific Center of Ferrous  
Metallurgy 2 Baumanskaya, 9/23, Moscow 107005, RUSSIA

One of the important peculiarities of the mechanical behavior of nanocrystalline materials (NCs) obtained by various methods including crystallization from amorphous precursor is a deviation of yield stress  $\tau_y$ , from the Hall-Petch relation since some critical average grain size  $D_{cr}$ . The dependence of  $\tau_y$  on the average grain size as a rule has a point of inflection at  $d = D_{cr}$ . To clarify this event we have solved a double-periodical task in the framework of micropolar elastic theory and have obtained the dependence of stress concentration coefficient  $S$ , on  $d$  and internal geometrical characteristics of intergranular (amorphous) and crystalline phases. In this case a structure of NCs is considered as analogous with that of polycomposition material having different shear modulus for grain and amorphous (intergranular) phase. It was obtained that when  $d < D_{cr}$ ,  $\tau_y$  increases in proportion to  $d^{1/2}$  and when  $d > D_{cr}$ ,  $\tau_y$  obey to the Hall-Petch relation.  $D_{cr}$  was established as 20-30 nm. Mechanism of NCs plastic deformation is proposed that its main peculiarity is a formation of disclination network at the junctions of intergranular boundaries. Theoretical and experimental results found to be in good agreement for a number of NCs.

**MAGNETIC SUSCEPTIBILITY OF NA<sub>1</sub>YI OCRYSTALLINE PARTICLES OF DISKLENIDES OF V (Nb) AND VI (Mo, W) METALS OF PERIODIC SYSTEM**

*G.V. Lashkarev, A.I. Dmitriev, L.M. Kulikov and A.A. Semyonov-Kobzar*

Institute for Problems of Materials Science, 3 Krzhizhanovsky st.,  
252142 Kiev, UKRAINE <lashk@ipms.kiev.ua>

The temperature dependence of magnetic susceptibility (MS) of d-transition metals diselenides of V (Nb) and VI (Mo, W) group of the Periodic System is investigated. NbSe<sub>2</sub> in the bulk state has a metallic conductivity (free and valence zone are overlapped). MoSe<sub>2</sub> and WSe<sub>2</sub> are semiconductors with energy gap 1.6 and 1.35 - 1.6 eV accordingly. The dimensions of initial particles before dispersion are 10 - 40 μm. Dispersion of diselenides up to nanocrystalline dimensions was fulfilled by special intercalation upon ultrasonic and electrochemical influence.

MS of diselenides powders with metallic and semiconducting conductivity changes in opposite ways by their dispersion NbSe<sub>2</sub> with metallic conductivity is a Pauli paramagnet in the initial state. It becomes diamagnet after dispersion up to particle dimensions about 25 - 140 nm. The transition paramagnet - diamagnet is not connected with powders oxidation. The density of state decrease is a reason for downsizing of Pauli paramagnetism in a comparison with MS of crystal lattice ( $|\chi_{\text{lattice}}| > |\chi_{\text{Pauli}}|$ ).

An intercalation of NbSe<sub>2</sub> by Cu at powder dispersity up to 5 nm does not lead to a change of MS sign. Apparently the change of density of states on Fermi surface at intercalation by Cu and at dispersion compensates one another and does not change MS magnitude essentially.

Semiconducting MoSe<sub>2</sub> and WSe<sub>2</sub> powders are diamagnets in the initial state. Their MS is defined by susceptibility of crystal lattice. But they become Pauli paramagnets after dispersion up to dimensions of 15 - 95 nm. By dispersion the cutting of atom chemical bonds on particles surface occurs. One can suppose that a great concentration of free electrons appears. Along with high density of states on Fermi surface it leads to a correlation ( $|\chi_{\text{lattice}}| > |\chi_{\text{Pauli}}|$ ). The last determines the positive sign of MS in nanocrystalline MoSe<sub>2</sub> and WSe<sub>2</sub>.

**NMR INVESTIGATION ON ION DYNAMICS AND STRUCTURE  
IN NANOCRYSTALLINE AND POLYCRYSTALLINE LiNbO<sub>3</sub>***D. Bork and P. Heitjans*Institut für Physikalische Chemie und Elektrochemie  
Universität Hannover, Callinstr. 3-3a, 30167 Hannover, GERMANY

Nanocrystalline (n-) LiNbO<sub>3</sub> was prepared from commercially available polycrystalline (p-) material through high-energy ball milling using a SPEX 8000 mill. The resulting grain size was determined from XRD measurements and TEM images. Thermal stability ranges of the samples were examined by DTA indicating that, in order to exclude grain boundary relaxation and grain growth, NMR measurements on n-LiNbO<sub>3</sub> had to be restricted to temperatures below 460 K. Here we report results obtained from NMR experiments performed on a n-LiNbO<sub>3</sub> sample with an average grain size of 23 nm. Corresponding measurements on p-LiNbO<sub>3</sub> were done for reference purpose since, concerning spin-lattice relaxation in LiNbO<sub>3</sub>, there are no data available in literature yet. On n-LiNbO<sub>3</sub> we carried out NMR measurements of the <sup>7</sup>Li spin-lattice relaxation rate  $T_1^{-1}$  at frequencies between 24 MHz and 78 MHz in the temperature range from 140 K to 460 K in comparison with corresponding experiments on p-LiNbO<sub>3</sub> in the range from 300 K to 1400 K which in each case covered the low-temperature side of the diffusion induced  $T_1^{-1}$  peak. Plotting the results in the usual  $\log T_1^{-1}$  vs.  $T^{-1}$  Arrhenius diagram revealed a reduced activation energy in n-LiNbO<sub>3</sub> as compared to the p-material. Investigations of the spin-lattice relaxation rate in the pulsed rotating reference frame  $T_{1c}^{-1}$  at frequencies from 15 kHz to 43 kHz and temperatures between 300 K and 990 K yielded an asymmetric peak in the Arrhenius plot for p-LiNbO<sub>3</sub>. In analogous experiments on n-LiNbO<sub>3</sub> carried out from 140 K to 450 K only a weakly temperature dependent background of the relaxation rate was observed. The frequency dependencies of the spin-lattice relaxation rate according to the power law  $T_1^{-1} \propto \nu^{-\beta}$  in both n-LiNbO<sub>3</sub> and p-LiNbO<sub>3</sub> are characterized by values between  $\beta = 1.1$  and  $1.5$ . This as well as the asymmetric peak in the Arrhenius plot for p-LiNbO<sub>3</sub> represent deviations from standard BPP behavior in both samples.

In n-LiNbO<sub>3</sub> the motional narrowing of the central line in the <sup>7</sup>Li NMR spectrum starts at 250 K and is almost completed at 450 K whereas in p-LiNbO<sub>3</sub> the motional narrowing is detected between 650 K and 990 K.

The fast diffusion of Li ions in n-LiNbO<sub>3</sub> indicated by the reduced activation energy and the shift of the motional narrowing to lower temperatures is a consequence of the underlying heterogeneous structure, which can be identified by the characteristic <sup>7</sup>Li NMR lineshape. At 450 K the central NMR line is a superposition of two contributions: first a narrow component from diffusing Li ions in the grain boundaries and second a broad part from immobile Li ions in the grains. In contrast, for p-LiNbO<sub>3</sub> a structuring of the central line cannot be detected at any temperature.

**DAMPING FACTORS OF DE HAAS-VAN ALPHEN OSCILLATIONS  
IN THE VORTEX STATE OF SUPERCONDUCTING MULTILAYERS**

*V.M.Gvozdikov and M.V. Gvozdikova*

Department of Physics, Kharkov State University, 310077 Kharkov, UKRAINE  
<Vladimir.M.Gvozdikov@univer.kharkov.ua>

Experiments show that below the upper critical field, i.e. in the vortex state, both de Haas-van Alphen oscillation frequencies and effective masses are unchanged from their values in the normal state, whereas the amplitude of these oscillations experience additional damping in the vortex state. In spite of a progress in theoretical understanding of physics beyond dHvA effect in a two-dimensional superconductors some points remain unclear yet. In this connection we have considered microscopically dHvA oscillations in a vortex-lattice state of layered superconductors and shown that factors of damping of these oscillations are: a) additional electron scattering on vortex-lattice imperfections, resulting in a Dingle-like exponential factor depending on the order parameter and magnetic field,  $H$ , b) Landau level broadening into dispersive bands caused by periodic vortex-lattice, c) the energy gap at the Fermi level, d) the layer-factor, depending on the stacking of the layers. Factors b)-d) damp dHvA amplitudes in a nonexponential fashion. In particular, the factor d) modulating dHvA oscillation due to the layered structure of superconductors is determined by the one-dimensional density of states,  $g(E)$ , related with the electronic transport across the layers. It is periodic function in  $1/H$  with frequencies depending on location of singularities in  $g(E)$  (van Hove singularities and the ones due to the stacking faults). This result provides a basis for determination, of the layer structure of multilayers by experimental detection of these modulating oscillations.

**3D TRANSITION FERROMAGNETIC METAL NANO-CRYSTALS  
PREPARED WITH GAS DEPOSITION METHOD (GDM)**

*Yuji Sasaki, Manabu Hyakkai, Eiji KITA, Hisanori Tanimoto<sup>1</sup> and Akira Tasaki*

Center for TARA and Institute of Applied Physics, <sup>1</sup>Institute of Materials Science,  
University of Tsukuba, Tsukuba, Ibaraki 305-8573, JAPAN <kita@bk.tsukuba.ac.jp>

Gas deposition method has been developed for a new handling way of ultra-fine particle (UFP) and is considered to be one of suitable method to produce nano-crystalline materials. The method is based on the UFP formation with an inert gas evaporation. After the formation in an evaporation chamber, UFP are transferred into a deposition chamber by an inert gas flow and are piled up on to the substrate. In this paper, we report the application of this technique to the formation of 3d transition metal nanocrystals and their structure. Compared with noble metals, transition metals are easy to be oxidized. Special attention must be paid to impurities in the inert gas used during the preparation. The purity was kept at remarkably high by using a He circulating system. The metals of Fe, Co, and Ni were evaporated by RF heating using a ZrO<sub>2</sub> linear set in a tungsten crucible. X-ray diffraction study reveals the same crystal structure as those of bulk states for Fe and Ni (bcc and fcc), while the Co nanocrystal has modified structure from the fcc structure. From the simple analysis of the line profile, the averaged grain sizes are ranged between 10 and 20 nm. In STM photographs, the fine grains with same size as that estimated by X-ray patterns are shown and the secondary structure composed of fine particles with the size of 100nm are found in almost all samples irrespective to the sort of metals. The magnetization is also a good probe for oxidization because the magnitude of magnetization for the unit weight of ferromagnetic elements must decrease by the formation of their oxides. The values are more than 95 % of bulk except for samples with loose packing, which were prepared with lower pressure difference between the evaporation and deposition chambers. GDM is also found to be a good technique to deal with ultra fine particles of 3D metals because oxidization is well suppressed during the fabrication process.

**ANOMALIES IN MAGNETIC PROPERTIES OF Fe-O TWO-DIMENSIONAL  
NANOSTRUCTURES ON THE SURFACE OF DIAMAGNETIC MATRIX**

E.V. Charnaya<sup>1</sup>, K.J. Lin<sup>1</sup>, V.M. Sarnatskii<sup>2</sup>, C. Tien<sup>1</sup>, and V.M. Smirnov<sup>2</sup>

<sup>1</sup> National Cheng Kung University, Tainan, Taiwan

<sup>2</sup> St.Petersburg State University, St.Petersburg 198904, RUSSIA

The problem of magnetic ordering realisation in the ultra-thin layers obtained by the method of molecular layering (ML-ALE) is considered. Magnetisation of Fe-O ionic layers on the silica-gel surface was studied within the temperature range 5 to 300 K using a SQUID magnetometer. Samples containing various numbers of the Fe-O groups in surface layers with terminal organic ligands (samples (mmol/g): 1 - 0.38, 2 - 0.26) have shown unusual magnetic properties. The zero field cooled (ZFC) and field cooled (FC) magnetisation versus temperature were measured at H=200 Oe. The ZFC and FC curves were almost similar for the sample 1, whereas the ZFC magnetisation for the sample 2 at low temperatures was twice the FC one. The magnetisation versus magnetic field curves measured at low temperature for the sample 2 revealed a weak ferromagnetism, the hysteresis loops were merged near 2000 Oe. When cooled in high magnetic field, the hysteresis loops were shifted. The overall behaviour of the sample 2 showed a weak ferromagnetism at low temperature and a very smeared phase transition into a magnetic ordered state.

This work has been funded by RFBR, grant N 96-03-33990, and by NSC of Taiwan, grant 87-2811-M-006-0009.

**PARAMAGNETIC SUSCEPTIBILITY  
OF THE THERMICALLY TREATED Co-BASED AMORPHOUS ALLOYS**

*M. Zakharenko, M. Babich, T. Tsvetkova and I. Yurgelevych*

Taras Shevchenko University, 64 Volodymyrska st., 252033 Kyiv, UKRAINE  
*<nikolay@physmet.ups.kiev.ua>*

Amorphous metallic alloys are the subjects of great scientific interest because of their unique combination of physical properties. However, the physical properties of amorphous alloys are known to be modified under action of a numerous destabilizing factors such as temperature, mechanical treatment, and irradiation by different particles, etc due to processes of structural relaxation.

In this work the temperature dependence of paramagnetic susceptibility  $\chi(T)$  of as-quenched and annealed amorphous  $\text{Co}_{72}\text{Fe}_{5.7}\text{Ni}_{12.2}\text{Si}_{6.5}\text{B}_{3.6}$  alloy (composition is in wt %) were investigated using Faraday technique. The samples prepared by melt spinning were annealed for 10 min at the temperatures  $T_a=350, 375, 400, 450$  and  $500^\circ\text{C}$ . At the room temperature they are ferromagnetic with Curie temperature  $T_c$  near 520 K. So, the  $\chi(T)$  dependence were investigated in the temperature range  $T_c < T < T_x$  ( $T_x$  is a crystallization temperature) both for as-quenched and annealed samples. These curves were found to obey Curie-Weiss law:

$$\chi = \chi_0 + \frac{N\mu^2}{3k(T - \theta)}.$$

The values of effective magnetic moment per metallic atom  $\mu$  and paramagnetic Curie temperature  $\theta$  were calculated from  $\chi(T)$  curves. It should be noted that  $\mu$  is rising with  $T_a$  (from  $2.29\mu_B$  for as-quenched alloy to  $2.77\mu_B$  for  $T_a=500^\circ\text{C}$ ), while no essential changes in  $\theta$  were observed. The regularities of  $\mu$  changes under isochronal annealing considered being a result of constituent atoms' spatial redistribution in comparison with as-quenched alloy and clusterisation processes (formation of microinhomogeneities enriched by transition metals atoms). Such microinhomogeneities are seemed to behave as superparamagnetic particles.

---

**DUCTILITY OF NANOCRYSTALLINE ZIRCONIA BASED  
CERAMICS AT LOW TEMPERATURES**

*U. Betz, H. Hahn*

Darmstadt University of Technology, Department of Materials Science,  
Thin Films Division, Petersenstr. 23, 64287 Darmstadt, GERMANY  
<hhahn@hrzpub.tu-darmstadt.de>

The ductile behaviour of nanophase yttria doped zirconia ceramics was investigated during low-temperature deformation experiments. Ceramics were produced by following a standard processing route of mechanical compaction of the dispersion mixed nanoparticles synthesized by the inert gas condensation or chemical vapour condensation technique and pressureless sintering. Uniaxial forming in tension has been performed in air at temperatures below 0.5 T<sub>m</sub>. The influence of initial grain size and porosity on strain and strain-rate has been a topic of interest as well as the microstructural evolution during deformation. Constant load tests and tests with stress- and temperature-jumps have been carried out to estimate the thermomechanical parameters, strain-rate-sensitivity exponent, activation energy and grain-size exponent of 5 mol% yttria partially stabilized zirconia. A maximum elongation of about 60 % has been achieved with a 5 mol% Y<sub>2</sub>O<sub>3</sub> + ZrO<sub>2</sub> + 12 wt.% Al<sub>2</sub>O<sub>3</sub> composite ceramic at 1250°C. The results were related to a deformation model based on mesoscopic grain boundary sliding.

**EFFECT OF HIGH HYDROSTATIC PRESSURE ON THE FERROELECTRIC PROPERTIES OF EPITAXIAL  $\text{PbTiO}_3/\text{YBa}_2\text{Cu}_3\text{O}_{7-x}$  NANOSTRUCTURES**

A.M. Grishin, S.I. Khartsev, P. Johnsson and K.V. Rao

Department of Condensed Matter Physics, Royal Institute of Technology  
S-100 44 Stockholm, SWEDEN

At first time dielectric permittivity, loss  $\tan \delta$ , and polarization  $P-E$  loop in epitaxial pulsed laser deposited  $\text{PbTiO}_3(200 \text{ nm})/\text{YBa}_2\text{Cu}_3\text{O}_{7-x}(600 \text{ nm})/\text{LaAlO}_3$  heterostructures have been measured in the high-pressure vessel. Ferroelectric properties have been found to be suppressed monotonously: remnant polarization decreases from  $42 \text{ mC/cm}^2$  to  $15 \text{ mC/cm}^2$ , coercive force decreases from  $150 \text{ kV/cm}$  to  $65 \text{ kV/cm}$  while dielectric permittivity increases almost three times with the hydrostatic pressure increase up to 8 kbar. The effects are described in the model of anisotropic compression of the epitaxial substrate/film structure.

**MAGNETISATION REVERSAL OBSERVATION AND MANIPULATION  
OF CHAINS OF NANOSCALE MAGNETIC PARTICLES  
USING THE MAGNETIC FORCE MICROSCOPE**

*J. Wittborn , K.V. Rao , R .Proksch<sup>1</sup>\*, I. Revenko<sup>2</sup>\*, E .Dan. Dahlberg<sup>3</sup> and  
D. A. Bazylinski<sup>4</sup>*

Department of Condensed matter physics , KTH , Teknikringen 14,  
SE-10044 Stockholm, Sweden.

<sup>1</sup> Dept. of Physics, St Olaf College and Magnetic Microscopy Center,  
University of Minnesota, Minneapolis, MN55455, USA

<sup>2</sup> Dept. of Physics, St Olaf College, Northfield, MN 55057, USA

<sup>3</sup> Magnetic Microscopy Center, School of Physics and Astronomy,  
University of Minnesota, Minneapolis, MN 55455, USA

<sup>4</sup> Dept. of Microbiology, Immunology and Preventive Medicine,  
Iowa State University, Ames, Iowa, USA

\*Present address: Digital Instruments, SantaBarbara, CA 93117, USA

The magnetization reversal of chains of fifty nanometer, magnetic particles has been studied using Magnetic Force Microscopy (MFM) in an applied field. The magnetic particles, magnetosomes biomimicized by magnetotactic bacteria, are single crystal  $\text{Fe}_3\text{O}_4$  with a narrow size distribution. The samples studied consisted of three long chains composed of 35 to 80 magnetosomes. A method for extracting Switching Field Distributions (SFD's) from sets of MFM images of such chains was developed. The method consists of making MFM images in consecutively incremented applied fields (increasing and decreasing), effectively taking the chain through a hysteresis loop. The series of consecutive images were then subtracted, resulting in a series of images showing the change in sample magnetization between the incremented fields. The switching field,  $H_s$  for a segment was defined as the average of the two field values in between which the largest change in magnetization occurred. The magnetization change was quantified by the integrated change in MFM signal over the chain segments in order to get the SFD. For most of the chain segments the SFD had only two sharp peaks, thus corresponding to a square hysteresis loop. We defined the coercivity,  $H_c$  as the average of the absolute value of the two switching fields. The hysteresis loops were done at different angles between the applied field and the long axis of the chains. Additionally, multiple hysteresis loops were made for the same chain, showing that the field from the tip affects the sample magnetization. The coercivity was found to increase with the number of particles in a chain up to 7 or 8 particles and then slowly decrease with increasing number of magnetosomes. After the initial reversal observations, one of the chains was cut into smaller pieces using the MFM-tip, thus producing separated chain segments, presumably with altered inter-particle interactions. The separated chain segments were found to have lower coercivities than unseparated chain segments. We attribute the lower coercivity to reduced magnetostatic interactions between the chain segments.

**X-RAY ABSORPTION STUDY IN NANOCRYSTALLINE Fe, Co, Ni AND Cu METALLIC POWDERS**

*L. Y. Jang<sup>1</sup>, Y. D. Yao<sup>2</sup>, and Y. Y. Chen<sup>2</sup>*

<sup>1</sup> Synchrotron Radiation Research Center, Hsinchu 300, Taiwan

<sup>2</sup> Institute of Physics, Academia Sinica, Taipei 115, Taiwan

X-ray absorption fine structure (XAFS) measurements can provide useful information about the chemical bonding, the ordering factor, and the electronic configuration etc. around a local element. Thus it is well suited for investigating the local environment around the constituent atoms in nanocrystalline materials. In nanocrystalline materials, their fundamental properties are very different from that of the bulk samples. In this investigation the XAFS technique was used to study the local environment of nanocrystalline Fe, Co, Ni, and Cu powders. From the k edge spectrum measurements, we find that the coordination number in nanocrystalline samples for Fe and Co is 8.6 and 7.4, respectively, which is a little bit larger than that of bulk samples; however, it is reversed for Ni and Cu. In general, the bond lengths in both nanocrystalline and bulk metallic powders we studied are roughly the same. The order factor etc. is variant, which is dependent on the historical conditions of the samples. For electronic configuration, for example, considering the nanocrystalline Ni samples after annealing between 300 and 900 C, their ordering factor and coordination number slowly approach to the bulk value, however, according to their absorption curves, the electronic configuration remains the same. The mean-square disorder factor of nanocrystalline samples is always larger than that of the bulk samples, this means that the ordering factor is significantly reduced in nanocrystalline materials. For example, the mean square disorder factor for nanocrystalline Fe, Co, and Cu samples is  $0.0064 \pm 0.0008$ ,  $0.0117 \pm 0.0025$ , and  $0.0083 \pm 0.0005$ , respectively; they are slightly larger than the values of  $0.0004 \pm 0.0003$ ,  $0.0068 \pm 0.0005$ , and  $0.0078 \pm 0.004$  for bulk Fe, Co, and Cu, respectively. According to the analysis of our experimental data, we conclude that both ordered disordered crystalline phases can exist in nanocrystalline metallic powders, but the gas-like feature was not observed. Details will be discussed.

**SINTERING OF BIMODAL ALUMINA POWDER MIXTURES  
WITH THE NANOCRYSTALLINE COMPONENT***B.G. Ravi and R. Chaim*

Department of Materials Engineering,  
Technion - Israel Institute of Technology Haifa 32000, ISRAEL

Packing characteristics and sintering behavior of the bimodal mixtures of nano (130 nm) and conventional alumina ( $\sim 1 \mu\text{m}$ ) powders were investigated. Green density of the nanocrystalline particle compact was lower than that of the coarse particles. Increase in the packing density was observed at 70% coarse particle composition. The powder shrinkage characteristics were determined by dilatometry. The cold pressed compacts were sintered within the temperature range of 1200°C to 1400°C. The pattern of the green density versus composition was maintained in all sintering temperatures. Grain size and its distribution as a function of temperature were analyzed for isothermally sintered specimens. The activation energies for initial stage of sintering at constant heating rate were determined. Activation energies obtained from the shrinkage data were compared to those from the isothermal sintering experiments and the exact mechanisms associated with different stages of sintering were analyzed.

**NANOSTRUCTURE AND MICROHARDNESS  
OF Al<sub>86</sub>Ni<sub>11</sub>Yb<sub>3</sub> NANOCRYSTALLINE ALLOY***G.E. Abrosimova, A.S. Aronin and Yu.V.Kir'janov*

Institute of Solid State Physics RAS, Chernogolovka, RUSSIA &lt;yukir@issp.ac.ru&gt;

*T.Gloriant and A.L.Greer*

Dept. of Mat. Sci. And Metallurgy, University of Cambrige, Cambrige, UK

The formation, structure and thermal stability of a nanocrystalline Al<sub>86</sub>Ni<sub>11</sub>Yb<sub>3</sub> alloy were studied by differential scanning calorimetry, X-ray diffraction, transmission electron microscopy and high resolution electron microscopy. Nanocrystalline material was obtained by controlled crystallization of melt-spun amorphous alloy. The crystallization of the alloy begins at 149°C (heating rate is 20 K/min) with  $\alpha$ -Al nanocrystal formation. After this primary crystallization the grain size of Al nanocrystals is about 10 nm. The  $\alpha$ -Al particles are dispersed uniformly in the residual amorphous matrix. The diameter of  $\alpha$ -Al particles, phase composition and microhardness of samples are examined for annealed alloys as function of fraction crystallized. The microhardness increased up to 4 GPa. The solute enrichment of remaining amorphous phase during the crystallization was supposed to play an important role in the increasing of the microhardness.

**Ni-Mo-B ALLOYS: NANOSTRUCTURE FORMATION AND PROPERTIES**

*A.S. Aronin, G.E. Abrosimova, Yu.V. Kir'yanov and I.I. Zver'kova*

Institute of Solid State Physics RAS, Chernogolovka, RUSSIA <aronin@issp.ac.ru>

The formation, thermal stability and properties of nanocrystalline  $\text{Ni}_{100-x-y}\text{Mo}_x\text{B}_y$  ( $27 < x < 31.5$ ,  $y = 5, 10$ ) were studied by X-ray diffraction, differential scanning calorimetry, transmission and high resolution electron microscopy and microhardness measurements. Crystallization of melt-quenched amorphous alloys at  $600^\circ\text{C}$  leads to the formation of nanocrystalline structure; the nanocrystal size is 15-25 nm and increases slightly with the annealing time. The grain size in the near surface layer was found to be larger than the grain size in the bulk. The lattice parameters of nanocrystals were found to depend on the alloy composition and the annealing duration. These changes are attributed to the different initial composition of the nanocrystals and to the simultaneous diffusion of Mo and B from the nanocrystals to the amorphous matrix. The stability of the nanocrystalline structure results from the thermal stability of the amorphous matrix, which insulates the nanocrystalline grains from each other; the crystallization temperature of amorphous matrix increases during the annealing owing to the enriching with B and Mo. The microhardness has been observed to increase when the nanocrystalline structure is formed and increases further with the growth of the nanocrystals. This behavior is inverse to Petch-Hall law and it may be explained by the increase of the B and Mo content in the amorphous matrix. The nanocrystalline structure (nanocrystals and amorphous layers between them) decomposes during further annealing into the equilibrium phases:  $\text{Ni}_3\text{Mo}$ ,  $\text{Mo}_2\text{B}$  and Ni. The  $\text{Ni}_3\text{Mo}$  phase may be formed from the nanocrystalline solid solution.

Financial support of RFBR (grant N 96-02-19582) is gratefully acknowledged.

**MICROSTRUCTURE STUDY ON NANOPHASE POWDER  
OF INDIUM TIN OXIDE***Yuzun Gao, Yonghong Li and Taosong Zhang*

General Research Institute for Non-Ferrous Metals, Beijing, 100088, CHINA  
[<Grimhvem@public3.bta.net.cn>](mailto:<Grimhvem@public3.bta.net.cn>)

Nanophase indium tin oxide (ITO) powder has extensive application in electron industry. Especially high density fine grain ITO target can minimize ion bombardment damage because of the fine grain crystal of nanophase. The sputtering ITO films from this kind of target have good homogeneity. In this paper, X-ray diffractometry and transmission electron microscopy (TEM) were used to study the structure change of ITO powder during different stage of annealing process. ITO powder is prepared from indium-tin hydroxide. Co-precipitation method was used to prepare indium tin hydroxide. Indium tin hydroxide has the structure of cubic crystal. The hydroxide with cubic structure transformed to amorphous after heat treatment at 250°C for 1hr. When the heat treatment temperature is higher than 280°C, the amorphous transformed to indium tin oxide with cubic crystal structure. After heat treatment at 600°C for 1hr, the particle size of indium tin oxide is 8-20 nm. The weight rate of In:Sn is near 9:1. Its granule has spherical shape. The dispersity is good.

**NANOMETER SIZED ZnO WITH NOVEL MORPHOLOGY  
AND ITS METASTABLE STATE CHARACTERISTICS**

*Zhizhong Yang, Zequn Li, Kangtai Tang, Hui Ou, and Yingyi Fu*

Guangzhou Institute of Chemistry, Academia Sinica.  
P. O. Box 1122, Guangzhou 510650, CHINA.

According to the dynamic laser light scattering (DLLS), TEM and computer simulation on the formation and agglomeration mechanism of nanoparticles in micelle or microemulsion different type of 'microreactor' formation conditions and special non-ionic surfactants have been selected. Size and shape-controlled nanometer sized ZnO with variable shapes including spherical, rod-like, laminar, vehicle and sponge were prepared by means of controlled catalytic hydrolyzation and ultrasonic chemical reaction in the designed 'microreactor'. The structure, morphology, particle size and size distribution of the above-mentioned nanoparticles have been characterized by TEM, IR, X-ray diffraction, LLS, DLLS, UV-visible spectroscopy analysis. Nanometer sized ZnO with different size, concentration and degree of aggregation suspended in cyclohexane have shown different light transmission and absorption properties, and after post treatment to overcome energy barrier, such as heating at assigned temperature for certain time the colour and transparency were changed gradually. It predicted that the occurring of different equilibrium stable state conforming the different metastable state of ZnO nanoparticles. The nanocomposite consisting of ZnO nanoparticles and various modified methacrylates with different polarity and polymerization shrinkage were prepared by UV radiation induced fast polymerization. Their novel optical properties due to the different particle size, ZnO concentration, the interaction between ZnO nanoparticles and matrix resins, degree of aggregation and the morphology of clusters were characterized by TEM, LLS, UV-visible spectroscopy and non-linear optical property measurements. The similar metastable state characteristics also have been observed in these nanocomposites.

**Cu CLUSTERING AND Si PARTITIONING  
IN THE EARLY CRYSTALLIZATION STAGE  
OF AN  $\text{Fe}_{73.5}\text{Si}_{13.5}\text{B}_9\text{Nb}_3\text{Cu}_1$  AMORPHOUS ALLOY**

*K. Hono, M. Ohnuma, D.H. Ping and H. Onodera*

National Research Institute for Metals , 1-2-1 Sengen , Tsukuba 305, JAPAN

A nanocrystalline Fe-Si-B-Nb-Cu alloy, known as FINEMET, is a very attractive soft magnetic material exhibiting excellent permeability while maintaining a high saturation magnetization [1]. This material is prepared by annealing a melt-spun  $\text{Fe}_{73.5}\text{Si}_{13.5}\text{B}_9\text{Nb}_3\text{Cu}_1$  amorphous ribbon at temperatures in the range of 520-580°C. The microstructure produced by the primary crystallization reaction consists of nanoscale a-Fe grains embedded in the remaining amorphous matrix.

The mechanism of such a nanocomposite microstructure has been a subject of numerous studies. Although earlier APFIM and EXAFS works convincingly showed presence of Cu clusters prior to the onset of crystallization reaction, how Cu clusters stimulate nucleation of the  $\alpha$ -Fe(Si) has been speculative, because no spatial information have been obtained by these techniques. The aim of this paper is to report definite new experimental results by three dimensional atom probe (3DAP) and high resolution electron microscopy (HREM) concerning the role of Cu clustering to nanocrystallization of a Fe-Si-B-Nb-Cu amorphous alloy.

Cu atom clusters have been confirmed by 3DAP elemental mapping in the amorphous state after annealing below the crystallization temperature (Fig. 1). The density of these clusters are in the order of  $10^{24} \text{ m}^{-3}$ , which is comparable to that of the  $\alpha$ -Fe(Si) grains in the optimum nano-crystalline microstructure. In the early stage of primary crystallization, Cu clusters are in intimate contact with the  $\alpha$ -Fe(Si) nanocrystals, suggesting that each  $\alpha$ -Fe(Si) primary particles are heterogeneously nucleated at the site of Cu clusters. In the early stage of crystallization, the concentration of Si is lower in the primary crystal than in the amorphous matrix phase, unlike in the late stage of the primary crystallization, where Si partitions into the a-Fe phase with a composition of approximately 20 at.%.

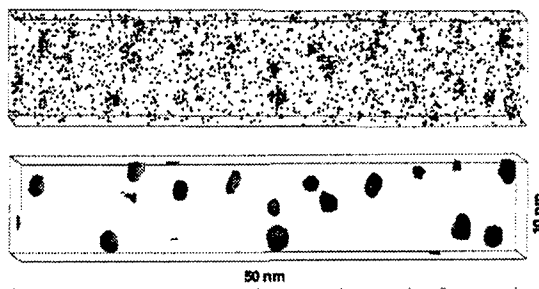


Fig. 1. 3DAP elemental mapping of Cu and iso-concentration surface of 6 at.% Cu in  $\text{Fe}_{13.5}\text{Si}_9\text{B}_3\text{Nb}_1\text{Cu}$  melt-spun alloy annealed at 400°C for 60 min.

- Y. Yoshizawa, S. Oguma and K. Yamauchi, *J. Appl. Phys.* **64**, 6044 (1988).

**NONEQUILIBRIUM PHASE TRANSITION OF Nd<sub>3</sub>(Fe,Ti)<sub>29</sub> COMPOUND  
DURING MECHANICAL MILLING**

*S.L. Tang, X.M. Jin\*, B.W. Wang\*, Z.Q. Jin, S.Y. Zhang and Y.W. Du*

National Laboratory of Solid State Microstructures and Department of Physics,  
Nanjing University, Nanjing 210093, CHINA <ufp@nju.edu.cn>

\* Institute of Metal Research, Chinese Academy of Sciences, Shenyang 110015,  
CHINA

A nonequilibrium phase transition has been found during mechanical milling of monoclinic Nd<sub>3</sub>(Fe,Ti)<sub>29</sub> compound. The transition process and the mechanically milled products have been investigated by x-ray diffraction, transmission electron microscopy, and ac initial susceptibility. The results show that mechanical milling results in the transformation of Nd<sub>3</sub>(Fe,Ti)<sub>29</sub> compound into a nanostructure during the early stage of milling, and then generates it to decompose to the hexagonal TbCu<sub>7</sub>-type Nd(Fe,Ti)<sub>7</sub> disorder phase and  $\alpha$ -Fe(Ti), and finally transforms the material to the mixture of an amorphous phase and  $\alpha$ -Fe(Ti). The structure of mechanically milled Nd(Fe,Ti)<sub>7</sub> phase is similar to but not exactly identical with that of annealed Nd(Fe,Ti)<sub>7</sub> phase. The magnetic-ordering transition of the former is broader than that of the later. The broadening of the magnetic-ordering transition can be attributed to the effect of the nanostructure, and the unhomogeneity of the concentration of Nd(Fe,Ti)<sub>7</sub> phase.

**NANOSTRUCTURES FROM SEVERE PLASTIC DEFORMATION AND  
MECHANISMS OF LARGE-STRAIN WORK HARDENING***I.V. Alexandrova and R.Z. Valiev*

Institute of Physics of Advanced Materials, Ufa State Aviation Technical University,  
K.Marksa 12, 450000 Ufa, RUSSIA <igor@ippm.rb.ru>

Recent investigations revealed that intense plastic deformation, namely, large deformations at high applied pressure, give a possibility to process the bulk nanostructured materials. The grains in these materials have a size as much as a few dozens of nanometers and high angular random boundaries [1,2]. These materials are of a great interest due to their both unusual physical and mechanical properties and deformation behaviour.

At the same time the question related to the nature of formation of nanostructures at severe plastic deformation is still a subject of many discussions.

To clear up this problem in the present investigation results of the evolution of the nanostructure at the process of severe plastic deformation are represented and discussed in the frameworks of recent approach to large-strain work hardening mechanisms [3,4]. A special attention is paid to TEM and X-ray evidences of the formation of high angle grain boundaries. It is shown that the increase in the deformation degree results in qualitative transformations in the structure of materials at the achievement of large strains characteristic of severe plastic deformation techniques.

1. R.Z. Valiev, A.V. Korznikov, R.R. Mulyukov, Mater. Sci. Eng. A168, 141 (1993).
2. Ultrafine-grained materials, prepared by severe plastic deformation, R.Z. Valiev, edit., 1996, Annales de Chimie. Science des Materiaux 21, 396 (1996).
3. T. Ungár, M. Zehetbauer, Scr. Mater. 35, 1467 (1996).
4. M. Zehetbauer, Acta metall. mater. 41, 589 (1993).

**ELASTIC STRAIN DISTRIBUTION FROM GRAIN BOUNDARIES IN  
ULTRAFINE-GRAINED COPPER***R.K.Islamgaliev*

Institute of Physics of Advanced Materials, Ufa State Aviation Technical University,  
K.Marx 12, Ufa 450000, RUSSIA

It is known that ultrafine-grained materials processed by severe plastic deformation are characterised by small grain size and high level of elastic strain [1]. In order to study elastic strain distribution from grain boundaries the method based on the TEM observation of the thickness fringes behaviour [2] is developed in this work.

Pure copper processed by equal channel angular pressing was used for investigations. TEM studies were performed using transmission electron microscope JEM-2000FX. The structure of as-prepared samples was characterised by a mean grain size of 0.3 nm, high angle grain boundaries and high dislocation density.

The dependence of the thickness fringes width on the tilt angle was studied for both usual and spread diffraction contrasts at grain boundaries. Experimental results are discussed in the framework of dynamic theory of contrast.

The dependence of elastic strains on the distance from grain boundaries having usual diffraction contrast is revealed. It is shown that the value of elastic strains reaches maximum level of  $2.6 \times 10^{-3}$  at the distances equal to 7-8 lattice parameters from grain boundary, that is 2-3 times higher than the average value of elastic strains in ultrafine-grained copper determined by X-ray analysis of diffraction peak profile. The grain with spread diffraction contrast has demonstrated even a higher level of elastic strains of  $4.5 \times 10^{-3}$ .

Although X-ray analysis shows lower average value of elastic strains in the sample, the direct observation by HREM confirms a high level of local elastic distortions of crystal lattice near grain boundaries caused by high density of the grain boundary dislocations [1].

Thus, the obtained results have demonstrated that the important feature of ultrafine-grained materials processed by severe plastic deformation is a specific defect structure of grain boundaries associated with high level of elastic strains and distortions of crystal lattice. Moreover, there is inhomogeneous elastic strain distribution inside grains with maximum level at the distance equal to 7-8 lattice parameters from grain boundaries.

1. Ultrafine-grained materials produced by severe plastic deformation, Special issue.  
Ed. by R.Z.Valiev. Annales de Chimie - Science des Materiaux (1996).
2. R.K.Islamgaliev, R.Z.Valiev. Solid State Physics. 37 (12) (1995) 3597.

**PHASE TRANSFORMATION IN RAPIDLY QUENCHED AND  
ANNEALED Mg<sub>80</sub>Ni<sub>15</sub>Y<sub>5</sub> ALLOY***I. Brodov and A. Manukhin*

Institute of Metal Physics, Ural division of Russian Academy of Science,  
S. Kovalevskaya st. 18, GSP-170, 620219 Ekaterinburg, RUSSIA  
<crystal@ifm.e-burg.su>

The purpose of this work is to investigate features of the structure formation in Mg<sub>80</sub>Ni<sub>15</sub>Y<sub>5</sub> alloy prepared by rapid quenching from the melt and the thermal stability of amorphous state in the following annealing.

Mg<sub>80</sub>Ni<sub>15</sub>Y<sub>5</sub> alloy were prepared by the pure element mixture melt in an aluminum crucible under KCl-NaCl slag-cover at the temperature of 1000 K. Rapidly quenched specimens in form of ribbons were prepared by melt spinning on the copper drum surface under vacuum. The range of cooling rates V was 2.5×10<sup>5</sup>...3×10<sup>6</sup> K/s. The melt heating temperature was 880 K.

Differential thermal analysis (DTA) was performed under Ar atmosphere at the heating rate of 4 K/min in the temperature range of 350 to 770 K. DTA method was used to study amorphous alloy crystallisation specialities and to determine annealing regimes. The phase analysis of amorphous and annealed ribbons was carrying out by X-ray diffraction technique with Cu K<sub>α</sub> monochromatic radiation.

It was established that ribbons were prepared at V=2.5×10<sup>5</sup> K/s have the crystalline structure of triple metastable quasieutectic. X-ray amorphous specimens were produced at V≥10<sup>6</sup> K/s.

According DTA method their crystallisation begins at 426 K temperature and realises through several stages. Amorphous ribbons were heated to 438 and to 478 K temperature during 5 min. This heat treatment causes the formation of Mg<sub>13</sub>Ni<sub>12</sub>Y<sub>4</sub> nanocrystalline phase. At the annealing temperature of 438 K nanocrystals of 6 nm in size are formed. The increase in the heating temperature up to 478 K increases one up to 14 nm and causes the formation on the second nanocrystalline phase enriched magnesium.

---

**INFLUENCE OF ION THINNING ON THE MICROSTRUCTURE  
OF NANOPHASE METAL**

*Yonghong Li, Yuzun Gao and Taisong Zhang*

General Research Institute for Non-Ferrous Metals, Beijing 100088, CHINA  
<Grimhvem@public3.bta.net.cn>

There are more grain boundaries in nanophase materials. A large amount of free energy is stored on the grain boundaries. Nanophase material is instability thermodynamically and easy to occur recrystalline, especially for metals with low melt point. In the present paper, transmission electron microscopy was used to investigate the microstructure of nanophase metal copper. The powder with particle size of 15 nm prepared by chemical method was pressed into sheet. Then two types of samples for TEM observation were prepared by ion milling with 5kV argon ion at 12° incident angle under conditions of room temperature and liquid nitrogen temperature. TEM examination showed that the microstructure in the sample prepared under liquid nitrogen cooling condition maintained the characteristic of nanophase materials, while that thinned at room temperature had some of abnormal growth grains already. In situ observation in HVEM under heating provided the evidence of abnormal growth grains. The cause of formation of abnormal growth grains in TEM sample prepared at room temperature is discussed.

**STRUCTURAL AND MAGNETIC INFORMATION ABOUT A  
NANOSTRUCTURED FERROMAGNETIC Fe-Cu-Nb-B ALLOY BY NOVEL  
MODEL INDEPENDENT EVALUATION OF MÖSSBAUER SPECTRA**

*O. Hupe<sup>1</sup>, H. Bremers<sup>1</sup>, J. Hesse<sup>1</sup>, A. Afanas'ev<sup>2</sup> and M. Chuev<sup>2</sup>*

<sup>1</sup> Institut für Metallphysik und Nukleare Festkörperphysik, TU Braunschweig,  
Mendelssohnstr. 3, 38106 Braunschweig, GERMANY <J.Hesse@TU-BS.DE>

<sup>2</sup> Institute of Physics and Technology, Academy of Sciences of Russia,  
Krasikov Street 25a, 117218 Moscow, RUSSIA

Mössbauer spectrometry is an excellent tool for investigating nanostructured materials. We demonstrate on complex spectra of a nanostructured Fe-Cu-Nb-B alloy vs. temperature a novel evaluation technique. The spectra consist of several parts due to nanocrystalline iron, amorphous and interfacial phases. Such complex spectra recently were successfully described by a two hyperfine field distribution model (M. Miglierini and J.M. Greneche, J.Phys.:Condens. Matter 9(1997) 2303-2347). In our case the spectral model is not prescribed ahead of time, but is derived directly in the course of fitting the spectrum applying a new idea and the DISCOVER program (A.M. Afanas'ev and M.A. Chuev JETP 80(1995) 560-567). First the measured spectra are described with a rather big number of single Lorentzian lines, which gives the best fit. This number of lines is restricted by the fluctuation of the counting rates in the spectrum. While reducing the number of lines step by step by introduction of 'bounds' like hyperfine field or quadrupole splitting, a physical model is arising. It is not necessary to presuppose any restrictions, e.g. that the spectrum has to be described with two different distributions of hyperfine fields. We present measurements on  $\text{Fe}_{79}\text{Cu}_1\text{Nb}_7\text{B}_{13}$ , their evaluation i.e. hyperfine fields and their distribution and give the temperature dependence of all other parameters describing the spectra.

**NANOCRYSTALLISATION OF FeCuNbB ALLOYS**

*T. Girchardt<sup>1</sup>, B. Friedrichs<sup>2</sup>, E. Woldt<sup>2</sup>, J. Hesse<sup>1</sup>*

<sup>1</sup> Institut für Metallphysik und Nukleare Festkörperphysik, TU Braunschweig,  
Mendelssohnstr. 3, 38106 Braunschweig, GERMANY <J.Hesse@TU-BS.DE>

<sup>2</sup> Institut für Werkstoffkunde, TU Braunschweig, Langer Kamp 8,  
D-38106 Braunschweig, GERMANY

We investigated the alloy system of  $\text{Fe}_{86-x}\text{Cu}_1\text{Nb}_x\text{B}_{13}$  ( $x=4,5,7$ ) in order to obtain information on the crystallisation behaviour of the amorphous precursor alloy and the resulting structural composition. Onset temperatures of different crystallisation steps were studied with DSC measurements. Dilatometric and thermomagnetic measurements as well as those of the electrical resistivity were applied in order to detect changes not being correlated with a change of the heat capacity. For a structural investigation, Mössbauer effect and electron diffraction experiments were done. Our results show that - up to a certain annealing temperature depending on the Nb content - there is only a nanocrystalline -Fe phase, embedded in an amorphous matrix. At higher annealing temperatures crystalline FeB-phases appear.

**CHARACTERISTICS OF NANOMETER-SIZED YSZ POWDERS PRODUCED  
BY EVAPORATING THE TARGET BY A PULSED CO<sub>2</sub>-LASER**

*Y.A. Kotov, V.V. Osipov, O.M. Samatov and M.G. Ivanov*

Institute of Electrophysics, Ural Division of the Russian Academy of Sciences  
Komsomolskaya Str. 34, 620049 Ekaterinburg, RUSSIA <razrad@ief.intec.ru>

Targets made from coarse YSZ powder with a Y<sub>2</sub>O<sub>3</sub> content of 10.25 mol. % were evaporated by a pulsed CO<sub>2</sub>-laser operating with a frequency of 400 Hz. With the radiation pulse duration of 180 µs, with the average power of 600 W, and with the condensation of vapor in a stream of cleaned air, cubic-structure YSZ particles were obtained which had a shape close to spherical. Particle size distribution was close to a lognormal distribution with  $d_g = 10$  nm and  $\sigma = 1.75$ . The measured specific surface of the powder was 65 m<sup>2</sup>/g, while the Y<sub>2</sub>O<sub>3</sub> content reduced to 10 mol.%.

As the productivity was 20g/h and the raw material used is cheap enough, this method holds much promise for the production of nanometer-sized powders of complicated chemical compounds, especially when the average radiation power is raised.

**SYNTHESIS AND CHARACTERIZATION  
OF POLYMER-METALLIC NANOCOMPOSITES  
VIA MICROEMULSION REACTION / POLYMERIZATION**

*L.M. Gan<sup>1,2</sup>, C.H. Chew<sup>2</sup>, P.Y. Chow<sup>2</sup>, C.H. Quek<sup>2</sup> and P.F. Chong<sup>3</sup>*

<sup>1</sup>Institute of Materials Research and Engineering, 119260, SINGAPORE

<sup>2</sup>Dept. of Chemistry, National University of Singapore, 119260, SINGAPORE

<sup>3</sup>Dept. of Materials Science, National University of Singapore, 119260, SINGAPORE  
<scip7016@nus.edu.sg>

The development of novel bulk materials with inorganic/organic compounds that have modulated compositions on the nanometer scale is at the forefront of research. Recently, much interest has been shown in ultrafine metal particles. Metal-containing composites are of particular interest for producing materials with tailored electrical and optical properties. In this paper, we report the synthesis of gold or silver nanoparticles in the bicontinuous microemulsions using a nonionic polymerizable surfactant  $\omega$ -methoxy poly(ethylene oxide)<sub>40</sub> undecyl  $\alpha$ -methacrylate (PEO-R-MA-40), 2-hydroxyethyl methacrylate (HEMA), methyl methacrylate (MMA) and aqueous gold or silver solution which are first formulated. The reduction of gold or silver nanoparticles occurred *in situ* in the presence of a photoinitiator, which also caused the system to polymerize simultaneously. These coloured polymeric composites can be fabricated in the form of film, sheet and block. The size of the metallic particles in the polymerized materials was found to be within 10-20 nm in diameter by transmission electron microscopy.

**LOCAL ATOMIC STRUCTURE OF NANOCRYSTALLINE Pd  
AND SUBMICROCRYSTALLINE Cu BY EXAFS***Yu.A. Babanov, L.A.Blaginina and R.R. Mulyukov<sup>1</sup>*

Institute of Metal Physics, Russian Academy of Sciences,  
GSP-170, 620219 Ekaterinburg, RUSSIA <domen@ifm.e-burg.su>

<sup>1</sup> Institute of Metals Superplasticity Problems,  
Khalturina 39, 450001 Ufa, RUSSIA

EXAFS spectra of nanocrystalline (nc) Pd and submicrocrystalline (smc) Cu are presented. The sizes of crystallites are 15 nm for 'as prepared' compacted sample of nc Pd produced by gas condensation technique and 14 nm after additional compaction at 100°C (Haubold T. et al, Phys. Lett.A, 1989, v.135, 8,9, p.461). Submicrocrystalline Cu samples with grain size of 100-200 nm were prepared by severe plastic deformation.

EXAFS measurements of Pd samples with optimal thickness were performed using synchrotron radiation at 77 K. Measurements for Cu samples were carried out using laboratory EXAFS spectrometer at 300 K. Spectra have been analyzed by the regularization method of solving the EXAFS integral equation. Atomic density distribution functions were determined.

The results obtained show that the short-range order of nc Pd and msc Cu is similar the short range order of coarse-grained crystalline samples but the first neighbour coordination numbers N are smaller. The decrease of N in comparison with theoretical value for fcc structure are 6% for nc Pd and 3% for msc Cu.

**HYDROXIDES AS PRECURSORS OF NANOCRYSTALLINE OXIDES**

*X. Bokhimi<sup>1</sup>, A. Morales<sup>1</sup>, M. Portilla<sup>2</sup> and A. García-Ruiz<sup>3</sup>*

<sup>1</sup> Institute of Physics, The National University of Mexico (UNAM), A. P. 20-364,  
01000 México D. F., MEXICO <bokhimi@fenix.ifisicacu.unam.mx>

<sup>2</sup> Faculty of Chemistry, UNAM, A. P. 70-197, 01000 México D. F., MEXICO

<sup>3</sup> UPIICSA, The National Polytechnic Institute (IPN), Té No. 950 Esq. Resina,  
08400 México D. F., MEXICO

Nanocrystals of zirconia, titania, alumina and iron oxide were prepared by chemical methods with hydroxides as precursors. Crystallite size of the phases was controlled through dehydroxilation and oxidation of the samples. Hydroxides were obtained by hydroxilation of salts or alkoxides of the metal. The systems were characterized by X-ray powder diffraction, DTA, TGA and DSC. We analyzed the evolution of these hydroxides as a function of temperature, emphasizing the transformations of the atomic distributions, which were amorphous or crystalline. The analysis of the atomic distribution was done by refining the crystalline structures with the Rietveld method, and by Fourier filtering the diffraction pattern of the amorphous phases. With these techniques we obtained information about the crystallography of the system, even in the initial stage of crystallization, where the crystallites were extremely small. Zirconium, titanium, and aluminum hydroxides were amorphous. The amorphous structure of zirconium hydroxide, which had the same local order as tetragonal zirconia, was produced by the random condensation of the monomeric zirconyl group  $[Zr_4(OH)_8(OH_2)_{16}]^{8+}$ . Partial dehydroxilation of zirconia samples gave rise to nanocrystalline tetragonal zirconia stabilized by the remaining hydroxyl ions in its lattice. The structure of the titanyl group associated to the amorphous titanium hydroxide was not clear; its best approximation was given by  $Ti(OH)_3^+$ . Partial dehydroxilation of titania samples produced a mixture of nanocrystalline anatase and nanocrystalline brookite. Aluminum hydroxide was produced by the random condensation of the monomeric group  $[Al(OH_2)_6]^{3+}$ . Iron hydroxide,  $Fe(OH)_2$ , was crystalline with iron atoms at the center of OH octahedra. Oxidation of aluminum and iron hydroxides produced the oxyhydroxides  $AlOOH$  and  $FeOOH$ , which were the precursors to obtain nanocrystalline alumina and nanocrystalline iron oxide.

**NANOCRYSTALLINE TETRAGONAL ZIRCONIA STABILIZED  
WITH YTTRIUM AND HYDROXYL IONS**

X. Bokhimi<sup>1</sup>, A. Morales<sup>1</sup>, O. Novaro<sup>1</sup>, T. López<sup>2</sup>, R. Gómez<sup>2</sup>, T. D. Xiao<sup>3</sup> and  
P. R. Strut<sup>3</sup>

<sup>1</sup> Institute of Physics, The National University of Mexico (UNAM), A. P. 20-364,  
01000 México D. F., MÉXICO <bokhimi@fenix.ifisicacu.unam.mx>

<sup>2</sup> Department of Chemistry, Universidad Autónoma Metropolitana Iztapalapa,  
A. P. 54-534, 09340 México D. F., MÉXICO

<sup>3</sup> Inframat Corporation, 20 Washington Av., Suite 106, North Haven,  
CT 06473-2342, USA.

Nanocrystalline tetragonal zirconia was stabilized with yttrium and with hydroxyl ions. Yttrium-stabilized tetragonal zirconia was prepared via the hydrolysis of an aqueous solution of zirconyl chloride and yttrium chloride. Hydroxyl-stabilized tetragonal zirconia was prepared by using the sol-gel technique with zirconium n-butoxide as precursor and HCl, H<sub>2</sub>SO<sub>4</sub>, C<sub>2</sub>H<sub>4</sub>O<sub>2</sub>, and NH<sub>4</sub>OH as hydrolysis catalysts. Samples were characterized with X-ray powder diffraction, DTA, TGA, and infrared spectroscopy. The structure of the crystalline phases was refined with the Rietveld method. For both systems, samples were amorphous when they were annealed below 300°C in air. The local order in the amorphous phases was the same as in tetragonal zirconia, and was determined by the disordered condensation of the monomeric zirconyl group [Zr<sub>4</sub>(OH)<sub>8</sub>(OH<sub>2</sub>)<sub>16</sub>]<sup>8+</sup>. Since in the samples doped with yttrium, we observed only one amorphous phase, we propose that in the zirconyl group yttrium already substituted zirconium atoms when zirconium and yttrium salts were mixed in the aqueous solution; zirconyl group was transformed into the [Zr<sub>4-x</sub>Y<sub>x</sub>(OH)<sub>8</sub>(OH<sub>2</sub>)<sub>16</sub>]<sup>(8-4x)+</sup> ion. Dehydroxilation of the samples above 300°C initiated the formation of the nanocrystalline tetragonal phase. At high yttrium concentrations the stabilized phase was not tetragonal but cubic zirconia. When the samples were annealed in air at temperatures above 400°C, yttrium-stabilized nanocrystalline tetragonal zirconia remained stable, but the hydroxyl-stabilized nanocrystalline tetragonal zirconia was irreversibly transformed into nanocrystalline monoclinic zirconia, because the hydroxyl ions that stabilized the structure left its lattice. When dehydroxilation was complete, at high temperatures, the only phase present in the sample was monoclinic zirconia.

### **MORPHOLOGICAL CHARACTERISATION OF NANOCRYSTALS WITH LAYERED STRUCTURES**

*D. V. Szabó and D. Vollath*

Forschungszentrum Karlsruhe, Institut für Materialforschung III  
P.O. Box 3640, D- 76021 Karlsruhe, GERMANY <dorothee.szabo@imf.fzk.de>

Nanocrystalline compounds with layered structures, such as MoS<sub>2</sub>, WS<sub>2</sub>, SnS<sub>2</sub>, WSe<sub>2</sub>, or ZrSe<sub>2</sub> show interesting structural features. Tenne et al. [1] found nested fullerene like onion crystals in WS<sub>2</sub> or MoS<sub>2</sub> in thin films on quartz substrates.

Within this study nanoscaled sulphide or selenide particles were synthesised using the microwave plasma process [2,3]. The plasma is powered either from a magnetron with a frequency of 2.45 or 0.915 GHz. The reactions are performed in quartz tubes passing the microwave cavities. The vaporised precursors, chlorides or carbonyls of the metals, and H<sub>2</sub>S or SeCl<sub>4</sub> for the chalcogenides are introduced into argon carrier gas. The nanoparticles are formed in the plasma zone at the intersection between the reaction tube and the microwave wave guide. The reaction time in the plasma zone is in the range of a few milliseconds. In general, performing the synthesis at 2.45 GHz means lower reaction temperature and shorter residence time in the plasma, compared to a synthesis performed at 0.915 GHz. The morphology of the nanoparticles is characterised by high resolution electron microscopy (Philips CM 30ST). The lattice fringes were evaluated quantitatively in the Fourier space.

Depending of the synthesis parameters, different morphologies are observed. Besides more or less spherical particles, many non-equilibrium particles exhibiting odd shapes, bent lattice planes, varying distances between the planes or step dislocations are found.

In the case of MoS<sub>2</sub> (2.45 GHz) irregularly shaped non-equilibrium particles with sizes from 5 to 8 nm are formed. Additionally, at longer residence times bent lattice planes, varying distances between the planes and nested structures are present. In the case of WS<sub>2</sub> (2.45 GHz) layered, small and uniform particles are formed. With increasing residence time and temperature the particles consist of more layers. Additionally, fullerene like onion crystals are found. Rope-like layered structures of a length up to about 50 nm, containing dislocations are present in SnS<sub>2</sub> synthesised at 2.45 GHz. The SnS<sub>2</sub> ropes consist of about 8 to 10 layers.

In contrast to WS<sub>2</sub>, glassy particles are found in WSe<sub>2</sub> produced at low temperature. At higher temperatures the particles exhibit sizes around 5 nm. These particles are crystallised in a different but not layered structure. During observation in the electron microscope these particles change their structure into an expected layered one. In ZrSe<sub>2</sub> layered, rope like structures and fullerene like onions are found. These particles contain highly distorted lattice planes and varying distances between the layers.

- [1] R. Tenne, L. Margulis, M. Genut, G. Hodes: Nature 360(1992) 444-446
- [2] D. Vollath, D. V. Szabó, B. Seith, German patent application 19628357.4 (1996)

**DEPENDENCE OF MICROSTRUCTURE ON DEPOSITION CONDITIONS IN  
R.F. SPUTTERED TIN OXIDE FILMS FOR GAS SENSING APPLICATIONS**

*A.M. Serventi<sup>1</sup>, M.C. Horrillo<sup>2</sup>, D.G. Rickerby<sup>1</sup> and R.G. Saint-Jacques<sup>3</sup>*

<sup>1</sup> Institute for Advanced Materials, European Commission Joint Research Centre,  
21020 Ispra VA, ITALY

<sup>2</sup> Laboratorio de Sensores, Centro de Tecnologias Fisicas, C.S.I.C.,  
Calle Serrano 144, 28006 Madrid, SPAIN

<sup>3</sup> INRS-Énergie et Matériaux, 1650 montée Sainte-Julie,  
Varennes, Québec, J3X 1S2, CANADA

The structure of nanograin tin oxide thin films deposited on polycrystalline alumina substrates by r.f. magnetron sputtering has been examined by cross-section transmission electron microscopy. Two principal types of growth microstructure were observed: a compact columnar structure and a porous equiaxes structure, together with an intermediate structure that was equiaxed near the substrate but columnar near the film surface. The type of structure is dependent on the substrate temperature, deposition rate and the percentage of oxygen present in the residual gas in the vacuum chamber. The film texture is isotropic, even in the case of the columnar structure, irrespective of the local morphology or crystallographic orientation of the substrate. However, these factors do affect the degree of porosity and columnarity. These results are discussed in relation to the sensitivity of the films to carbon monoxide and propanal in the operating temperature range 200-350°C.

**CRYSTALLINE AND MAGNETIC NANOSTRUCTURES IN A GLASS  
CERAMIC CHARACTERIZED BY SMALL ANGLE NEUTRON SCATTERING**

*A. Wiedenmann<sup>1</sup>, U. Lembke<sup>2</sup> and A. Hoell<sup>2</sup>*

<sup>1</sup>Hahn-Meitner Institut Berlin, GERMANY

<sup>2</sup> Universität Rostock, GERMANY

New nanosized spinel ferrites with potential applications to storage devices have been produced via the glass crystallisation method. By suitable heat treatment of the Ca-Si-B-Fe-oxide glass nanocrystalline magnetite  $\text{Fe}_3\text{O}_4$  with spinel structure embedded in a non-magnetic matrix can be developed.<sup>1</sup>

Small Angle Neutron Scattering (SANS) was applied to investigate simultaneously compositional and magnetic correlations in the glass ceramic obtained. A bimodal volume size distribution was found for the nanocrystalline phase with maxima centered at radii of 2.5 nm and 10 nm, respectively. The magnetic scattering behaviour is characteristic for superparamagnetism of single-domain particles following the Langevin statistics. However, the magnetic microstructure is not congruently shaped with the crystalline one. Both fractions of nanocrystals must be attributed to the magnetite phase but they are composed by a small ferrimagnetic core surrounded by a non-magnetic surface layer.

1. A. Hoell, R. Kranold, U. Lembke, R. Brückner, R. Müller, P. Görnert, A. Schüppel, Ber. Bunsenges. Phys. Chem. **100**(1996) 146-160

**NEUTRON SCATTERING INVESTIGATIONS OF NANOSCALED  
MICROSTRUCTURES IN BULK AMORPHOUS ALLOYS***A. Wiedenmann, U. Keiderling, U. Gerold and M.-P. Macht*Hahn-Meitner Institut Berlin, Glienickerstrasse 100,  
D 14109 Berlin, GERMANY <Wiedenmann@hmi.de>

New metallic Zr-Ti-Cu-Ni-Be glasses have been recently developed which permits the formation of large bulky ingots at low cooling rates.[1]. These materials reveal strong resistance against crystallisation in the supercooled liquid (SCL) state in a wide range of about 50 K above the glass temperature  $T_g = 320^\circ\text{C}$ . In this paper we review the results of a comprehensive study of the evolution of the microstructure and of the local atomic order upon heat treatments combining Small Angle-(SANS), Wide Angle Neutron Scattering (WANS) and X ray diffraction (XRD).

Annealing of the amorphous alloy in the SCL state above  $T_g$  gives rise to a SANS profile with a characteristic time and temperature dependent intensity maximum [2]. This profile which exhibits dynamically scaling [3] is attributed to decomposition into a pseudo-periodic microstructure consisting of nanosized droplets embedded in the amorphous matrix [2-5]. WANS and XRD revealed clearly the amorphous state by the absence of any enlarged Bragg reflection and the modulation of the diffuse scattering. The total pair correlation function  $G(r)$  exhibits three distinct peaks corresponding to first nearest neighbour pairs. Only minor differences in  $G(r)$  occur above and below  $T_g$ .

The kinetics of the decomposition as measured by *in-situ* SANS was modelled by nucleation and diffusion limited growth of amorphous precipitates and by ordering effects due to hard-core-like interactions of depletion zones around the droplets [5].

Above  $T_{x1} = 673\text{K}$  partly crystallisation and growth of a nanocrystalline phase is observed by SANS, WANS and XRD. The size and structure has been determined and confirmed by TEM [6].

The crystallisation kinetics at  $T_{x1}$  is tremendously slowed down when the alloy is previously decomposed by annealing in the SCL state which implies that phase separation is at the origin of the enhanced thermal stability of this glass [4].

- [1] Johnson, W.L., Peker, A: *Appl. Phys. Lett.* **63** (1993) 23425
- [2] Wiedenmann, A., Keiderling, U., Macht, M.-P., Wollenberger, H.: *Mat. Science Forum* **225-227** (1996). 71-76
- [3] Wiedenmann, A., Liu J.M.: *Solid st. comm.* **100** (1996) 331-334
- [4] Liu, J.-M., Wiedenmann, A., Gerold, U., Wollenberger, H.: *phys. stat. sol. (b)* **199** (1997) 379-392
- [5] Hermann, H., Wiedenmann, A., Uebel, P. *J.Phys C* **9** (1997) L501-L516
- [6] Macht, M.-P., Wanderka, N., Wiedenmann, A., Wollenberger, H., Wei, Q., Fecht, H.J., Klose, S.: *Mat. Science Forum* **225-227** (1996). 65-7

**NEW Gd-Al NANOPHASE OBTAINED BY CRYSTALLIZATION  
OF  $Gd_4Al_3$  METALLIC GLASS**

*V. Petkov<sup>1</sup>, T. Spassov<sup>2</sup>, S. Suriñach<sup>3</sup> and M.D. Baro<sup>3</sup>*

<sup>1</sup> Faculty of Physics, Sofia University, Sofia-1126, BULGARIA  
*<petkov@phys.uni-sofia.bg>*

<sup>2</sup>Faculty of Chemistry, Sofia University, Sofia-1126, BULGARIA

<sup>3</sup>Dept. Física, Universitat Autònoma de Barcelona,  
 Bellaterra, E08193 Barcelona, SPAIN *<baro@cc.uba.es>*

Crystallization behaviour of  $Gd_4Al_3$  metallic glass, obtained by the melt-spinning method, has been studied by X-ray diffraction (XRD) and differential scanning calorimetry (DSC). It has been found that the crystallization of  $Gd_4Al_3$  glass is a two-stage process with the first stage occurring at approximately 710 K - 715 K and the second - at approximately 770 K. This behaviour is clearly illustrated in Fig. 1. As the analyses of XRD data showed, the product of the first stage of the crystallization of  $Gd_4Al_3$  glass is a new crystalline phase with a nominal composition  $Gd_4Al_3$  that has not been reported so far. The new phase has a primitive tetragonal (t) lattice with parameters  $a = b = 15.4893(8)$ ,  $c = 5.3020(5)$ . The emerging and growth of t- $Gd_4Al_3$  is illustrated in fig 2. By profile analyses of XRD patterns, it has been found that the size of the crystallites of t- $Gd_4Al_3$  varies between 70 Å to 90 Å when the crystallization is carried out at 710 K - 715 K, respectively, i.e. the newly observed t- $Gd_4Al_3$  is a typical nanophase. No further growth of the crystallites of t- $Gd_4Al_3$  has been found to take place with the increase of the temperature of crystallization. Instead, a decomposition of t- $Gd_4Al_3$  into well-known tetragonal  $Gd_3Al_2$  and cubic  $GdAl$ , which turns out to be the second stage in the crystallization of  $Gd_4Al_3$  glass has been observed.

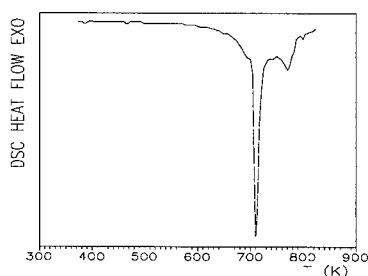


Figure 1. DSC scan for  $Gd_4Al_3$  metallic glass (heating rate 20 K/min)

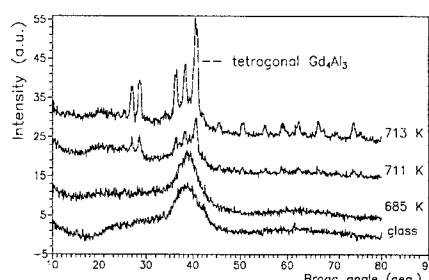


Figure 2. XRD patterns of the product of the first stage of the crystallization of  $Gd_4Al_3$  metallic glass

**ANOMALOUS ACCOMMODATION PHENOMENA TAKING PLACE  
DURING THE STRAIN-INDUCED FORMATION  
OF A SUPERFINE HCP STRUCTURE IN Fe-Ni ALLOYS**

*V.A. Shabashov and A.G. Mukoseev*

Institute of Metal Physics, Ural Branch of Russian Academy of Sciences,  
Yekaterinburg 620219, RUSSIA

The Mössbauer spectroscopy method was used to analyze the superfine  $\epsilon$  phase having an HCP lattice in a two-phase ( $\gamma+\epsilon$ ) structure produced by pressure strain in FCC iron-manganese alloys, which are stable under standard conditions.

Mössbauer data were obtained for the two-phase  $\gamma+\epsilon$  structure at different pressures and volumes of the  $\gamma \rightarrow \epsilon$  transformation.

Large anomalous changes were found to occur in the isomer shift of the  $\epsilon$  phase being formed. These changes are due to the fact that the electronic structure of the HCP lattice is highly sensitive to the alteration of the interatomic distance during the martensite-type phase recrystallization.

The anomalous changes in the fundamental physical characteristics of the superfine structure of the Fe-Mn alloy were treated in terms of the accommodation model of a nanodimensional duplex structure having developed phase boundaries.

**BORON-CONTAINING NANOPARTICLES AND THEIR CONTRIBUTION TO  
THE THEORY AND PRODUCTION OF NEW MATERIALS***Iovka Dragieva and Zdravko Stoynov*

Bulgarian Academy of Sciences, CLEPS, 1113 Sofia, BULGARIA  
<banchem@bgearn.acad.bg> or <iovka@cleps.acad.bg>

It is now known that through the chemical reduction of water salt solutions of transition metals with sodium or potassium borohydride it is possible to produce nanoscale amorphous particles, containing boron to 20 atomic %[1]. Most studies on application of borohydride reduction products in practice have been directed towards procedures for the preparation of various compositions and properties particles [2].

Recently we succeeded in the preparation of nanoparticles by the same method, but in a typical nanocrystalline state [3]. By means of photoelectron spectroscopy study it was established the difference between amorphous and crystalline nanoparticles containing similar percent boron. The binding energy (BE) of B1s electrons to the nuclei of boron atoms has only one value in nanocrystalline particles, while in amorphous particles B1s electrons have two kinds of binding energy(BE). Both states ( B<sup>I</sup>, 188.5 eV) and ( B<sup>II</sup> 191.7) eV can be quantitatively equal, especially in the magnetically disordered amorphous state[4].

The comparative investigations by impedance and photoelectron spectroscopy of the state of boron atoms in amorphous magnetic ribbons for toroidal transformer production show the presence of two binding energies of B1s electrons to boron nuclei irrespective of the shape, size, composition , and methods of production of the amorphous materials [5].

We suppose that the presence of two state of binding energies of *B 1s* , *N 1s*, *C 1s* (and *O 1s* ) electrons to the nuclei of these atoms in all materials pre-determines the appearance of the amorphous state.

- [1] I. Dragieva *et al.* , *J. Less Common Met.* **67**, 375(1979).
- [2] I. Dragieva, *AIP Conference Proceedings* **231**, *BORON-RICH SOLIDS*, Albuquerque, NM 1990, Eds: D. Emin et al., AIP, New York , 516(1991).
- [3] I. Dragieva *et al.*, *IEEE Trans. MAG-28*, 3183(1992).
- [4] V. Krastev, M. Stoycheva, E. Lefterova, I. Dragieva, Z. Stoynov, *J. Alloys and Compounds*, **240**, 186 (1996).
- [5] I. Dragieva, Z. Stoynov, I. Nikolaeva, V. Krastev, *J. Solid State Chem.* **133**, 273 (1997).

## ELECTROCHEMICAL PREPARATION OF WATER-SOLUBLE METALLIC NANOPARTICLES STABILIZED BY SURFACTANTS

*Michael G. Koch and Manfred T. Reetz*

Max-Planck-Institut für Kohlenforschung, Kaiser-Wilhelm-Platz 1, D-45470 Mülheim,  
a.d. Ruhr, GERMANY <kochm@mpi-muelheim.mpg.de>

The electrochemical synthesis of tetraalkylammonium salt stabilized transition metal colloids in organic solvents has been reported previously by our group.<sup>1-5</sup> The solubility of these nanoparticles can be tuned by the choice of the alkyl chain length of the tetraalkylammonium salt.<sup>3,4</sup>

Now we demonstrate that our electrochemical method can also be applied to the clean preparation of transition metal nanoparticles that dissolve in aqueous media. Therefore two different synthetic procedures have been developed. In the first one a sacrificial anode, e.g. Pd or Ni, is used as metal source in a THF/MeCN solution of the surfactant. The cathodic reduction of the resulting metal ions is followed by particle growth and finally precipitation of the stabilized colloid from solution. In the second method a metal salt, e.g. Pd(OAc)<sub>2</sub>, is electrochemically reduced in an aqueous surfactant solution resulting in stable metal hydrosols. The surfactants that we use in order to protect these particles from agglomeration are of the zwitterionic type such as sulfobetaines, C<sub>n</sub>H<sub>2n+1</sub>Me<sub>2</sub>N<sup>+</sup>C<sub>3</sub>H<sub>6</sub>SO<sub>3</sub><sup>-</sup>, and carboxybetaines, C<sub>n</sub>H<sub>2n+1</sub>Me<sub>2</sub>N<sup>+</sup>C<sub>3</sub>H<sub>6</sub>CO<sub>2</sub><sup>-</sup>.

Various mono- and bimetallic colloids (particle size 2-6 nm) have been prepared which exhibit high catalytic activity in solution and on solid support. We found that the stability and aggregation behaviour of these hydrosols strongly depends on the chain length of the surfactants and therefore on their critical micelle concentration (cmc). The minimum chain length necessary to stabilize the colloids is C9, while the upper limit for sufficient stabilization is given by C16. The hydrosols remain stable if the total amount of stabilizer is above the cmc value.

These results lead us to the assumption that the micelles itself rather than the monomeric surfactants are responsible for the stabilization of the colloidal assemblies. This could be confirmed by small angle X-ray scattering (SAXS) experiments which also revealed that the 4 nm palladium colloids form aggregates of about 50 nm size in aqueous solution. The SAXS particle sizes are in good agreement with those derived from TEM measurements.

<sup>1</sup> M.T. Reetz, W. Helbig, *J. Am. Chem. Soc.* **1994**, *116*, 7401

<sup>2</sup> M.T. Reetz, S.A. Quaiser, *Angew. Chem. Int. Ed. Engl.* **1995**, *34*, 2240

<sup>3</sup> M.T. Reetz, W. Helbig, S.A. Quaiser, *Chem. Mater.* **1995**, *7*, 2227

<sup>4</sup> M.T. Reetz, W. Helbig, S.A. Quaiser, U. Stimming, N. Breuer, R. Vogel, *Science* **1995**, *267*, 367

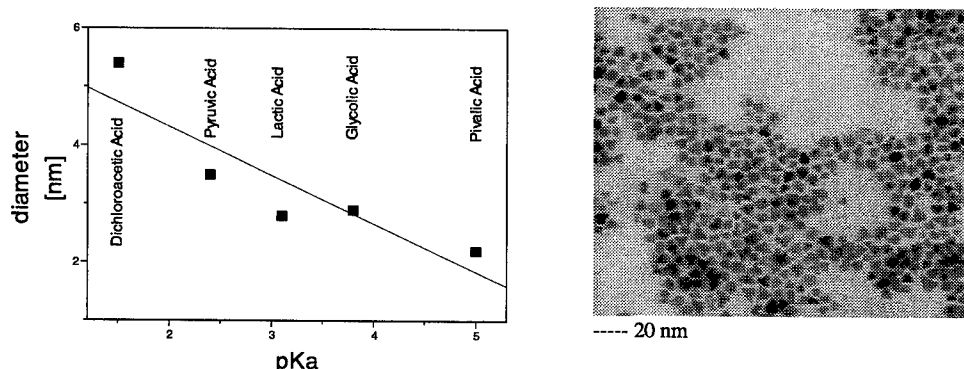
<sup>5</sup> M.T. Reetz, S.A. Quaiser, R. Breinbauer, B. Tesche, *Angew. Chem. Int. Ed. Engl.* **1995**, *34*, 2728

### SIZE AND SHAPE SELECTIVITY IN THE SYNTHESIS OF NANOSTRUCTURED METAL COLLOIDS

*Matthias Maase, Bernd Tesche and Manfred T. Reetz\**

Max-Planck-Institut für Kohlenforschung, Kaiser-Wilhelm-Platz 1, 45470 Mülheim  
a.d. Ruhr, GERMANY <mmaase@mpi-muelheim.mpg.de>

Recently, we have reported the size selective synthesis of a variety of transition metal colloids by means of electrochemical reduction.<sup>1</sup> Using chemical reduction, particle size is supposed to be mainly governed by the kinetics of nucleation and particle growth.<sup>2</sup> In the present study we show that the redox potential of the reducing agent affects the kinetics hence the particle size. Several novel THF soluble tetraoctylammonium carboxylates were used as reducing agents and colloid stabilizer simultaneously. The reducing strength of the carboxylates has been estimated by the pK<sub>a</sub> value of the corresponding acid hence the appropriate reducing agents have been picked just by comparing well-known thermodynamic properties. The oxidation potentials of the compounds under experimental conditions were determined later by Cyclic Voltammetry. All experiments were run under exactly the same conditions. The reducing agents were quite similar in structure only differing in the  $\alpha$ -substituent of the carboxylate. Using these different reducing agents we were able to synthesise palladium nanoparticles in the range of 2 to 6 nm. Tetraoctylammonium glycolate turned out to give triangular shaped particles with an abundance of up to 60%. This is the first example of a reducing agent that controls both size and shape of the nanoparticles while additionally acting as a stabilizer. Considering the results of EL-SAYED,<sup>3</sup> the carboxylate group seems to be responsible for affecting the nanocrystal growth thus determining its shape. For palladium nanocolloids, this is the first time that shape selectivity has been observed.



<sup>1</sup> M.T. Reetz, W. Helbig, *J. Am. Chem. Soc.* **1994**, *116*, 7401

<sup>2</sup> J. Turkevich, J. Hillier, P.C. Stevenson, *Discuss. Faraday Soc.* **1951**, *55*

<sup>3</sup> T. S. Ahmad, Z.L. Wang, T.C. Green, A. Henglein, M. A. El-Sayed, *Science* **1996**, *272*, 1924

**Fe<sub>2</sub>O<sub>3</sub> NANOPARTICLES SUPPORTED ON SILICON CARBIDE***C. Estournès*

I.P.C.M.S. Groupe des Matériaux Inorganiques UMR 46 CNRS, ULP, ECPM.  
23, rue du Loess B.P. 20/CR 67037 Strasbourg Cedex, FRANCE

*N. Keller, C. Pham-Huu and M.J. Ledoux*

Laboratoire de Chimie des Matériaux Catalytiques, IPCMS GMI, ECPM,  
1, rue Blaise Pascal 67008 Strasbourg Cedex, FRANCE

Nanosized particles of iron oxide (Fe<sub>2</sub>O<sub>3</sub>) supported on high surface area (25 m<sup>2</sup>/g) silicon carbide are prepared by wetness impregnation of the support (SiC) with an aqueous solution of iron nitrate in two successive operations with an intermediate drying at 110°C. The sample is then calcined at 400°C for 2h and subsequently thermally treated at different temperatures between 400 to 600°C. The changes occurring during these treatments are followed by X-ray diffraction, Mössbauer spectroscopy, Transmission Electron Microscopy (TEM) and static magnetic measurements. Depending on the temperature several forms of iron oxide can be obtained, amorphous phase, γ-Fe<sub>2</sub>O<sub>3</sub> and α-Fe<sub>2</sub>O<sub>3</sub>, and these phases are homogeneously dispersed on the SiC surface. XRD patterns of this material after calcination at 400°C up to 550°C contained only diffraction lines of β-SiC and almost no traces of iron oxides. Static magnetic and Mössbauer measurements show the presence of γ-Fe<sub>2</sub>O<sub>3</sub> and amorphous phases which progressively transform into α-Fe<sub>2</sub>O<sub>3</sub> when increasing calcination temperatures up to 600°C.

However, when the intermediate calcination is performed at 400°C instead of 110°C between the two successive impregnations, XRD patterns show the presence of hematite. Magnetic measurements of this composite material exhibit hysteresis loops with high coercive fields, increasing from 5800 to 7500 Oe, while the maximum of magnetization (at 16000 Gauss) decreases when the treatment temperature increases up to 600°C. This phenomenon can be attributed to the presence of elongated particles, induced by the intermediate calcination at 400°C, as shown by TEM.

**STRUCTURAL EVOLUTION OF THE AMORPHOUS MATRIX IN SOFT  
MAGNETIC NANOCRYSTALLINE ALLOYS**

*A. Cziráki<sup>1</sup>, I. Gergs<sup>1</sup>, L.K. Varga<sup>2</sup>, A Lovas<sup>2</sup> and I. Bakonyi<sup>2</sup>*

<sup>1</sup>Eötvös University, Department of Solid State Physics, Múzeum krt. 6-8,  
H-1088 Budapest, HUNGARY

<sup>2</sup>Research Institute for Solid State Physics and Optics, Hungarian Academy of  
Sciences. H-1525 Budapest, P.O.B. 49, HUNGARY

Detailed transmission electron microscopy (TEM) investigations have revealed that each of the bcc nanograins are surrounded by an amorphous shell in optimally heat-treated nanocomposites obtained by partial crystallisation of Fe<sub>73.5</sub>Si<sub>13.5</sub>B<sub>9</sub>Nb<sub>3</sub>Cu<sub>1</sub> (Finemet) and Fe<sub>86</sub>B<sub>6</sub>Zr<sub>7</sub>Cu<sub>1</sub> type amorphous alloys. No clustering of the bcc nanograins has been observed. In samples heat-treated above the optimum temperatures, relatively large (~50 nm) grains of Fe<sub>3</sub>B(Nb) and Fe<sub>3</sub>Zr(B) based compounds have been identified by both X-ray diffraction and selected area electron diffraction (SAED). In the Fe<sub>86</sub>B<sub>6</sub>Zr<sub>7</sub>Cu<sub>1</sub> type amorphous alloys an inner SAED ring appears already in the optimally annealed samples, which precedes the occurrence of the SAED spots of the crystalline compounds formed at higher annealing temperatures only, indicating a compound-like chemical composition of the remaining amorphous matrix in which the grain-growth inhibitor elements are supersaturated. Density and magnetic measurements as a function of annealing temperature have been used to monitor the amorphous-nanocrystalline transformation and to assert the optimal state.

**PHASE TRANSFORMATIONS IN NANOCRYSTALLINE MECHANICALLY  
ALLOYED Ni-Mo POWDERS**

D.Oleszak, V.K.Portnoy<sup>1</sup> and H.Matyja

Department of Materials Science and Engineering, Warsaw University of Technology,  
Narbutta 85, 02-524 Warsaw, POLAND <daol@inmat.pw.edu.pl>

<sup>1</sup>Department of Chemistry, Moscow State University, Moscow, RUSSIA

Ni-Mo based alloys are widely used in the industry due to their good electrocatalytic properties. However, many investigations are aimed towards improving the properties of the Ni-Mo alloys. It can be achieved by changing the microstructure of the alloys from microcrystalline into nanocrystalline one. Among the possibilities of producing nanostructured materials is mechanical alloying (MA) technique.

The aim of this work was to investigate the phase and structural transformations in the Ni-Mo alloys produced by high and low-energy MA. The formation processes of various nanocrystalline equilibrium and non-equilibrium phases in the alloys were studied and their thermal stability was determined. The influence of milling parameters on the mechanical alloying processes was studied as well. X-ray diffraction and differential scanning calorimetry (DSC) were employed as the experimental techniques

For Ni - 20 at.% Mo powder mixture MA resulted in the formation of nanocrystalline supersaturated Ni(Mo) solid solution with lattice parameter 3.612 Å. The crystallite size and strain level of the fcc Ni(Mo) solid solution were about 30 nm and 0.8%, respectively.

MA of the Ni - 43 at.% Mo powder mixture led to the formation of an amorphous phase, with small amount of unreacted nanocrystalline Mo. Additionally, a new phase described as bcc one with lattice parameter 3.43 Å, was formed after milling in a low energy device. Heating the samples synthesized in both mills resulted in the formation of another new phase defined as fcc with lattice parameter 10.954-11.098 Å, depending on the mill employed.

**NANOCRYSTALLINE BCC SOLID SOLUTIONS OF Al-Fe-V SYSTEM  
PREPARED BY MECHANICAL ALLOYING**

*V.I. Fadeeva, V.K. Portnoy, YU.V. Baldohin, G.A. Kotchetov and H. Matyja<sup>1</sup>*

Department of Chemistry, Moscow State University, Moscow, RUSSIA

<sup>1</sup>Department of Materials Science and Engineering, Warsaw University  
of Technology, Narbutta 85, 02-524 Warsaw, POLAND

Elemental powder mixture of the composition  $\text{Al}_{50}\text{Fe}_{50-x}\text{V}_x$  ( $x = 5, 15, 25$  at. %) were mechanically alloyed in a water cooled high energy planetary ball mill in an argon atmosphere. Stainless steel vials and balls were used. The powders obtained after MA and subsequent heating were examined by X-ray diffraction (XRD) and Mössbauer spectroscopy.

The changes in the lattice parameter, crystallite size and microstrains of the  $\text{Fe}(\text{Al},\text{V})$  solid solution were studied.

It was found that after milling of the  $\text{Al}_{50}\text{Fe}_{50-x}\text{V}_x$  powders mixture the  $\text{Fe}(\text{Al},\text{V})$  solid solution with crystallite sizes 10 nm was formed. Mössbauer spectra show that the  $\text{Fe}(\text{Al},\text{V})$  solid solutions were partially ordered though the superstructural lines on XRD patterns were absent.

Annealing of the  $\text{Al}_{50}\text{Fe}_{50-x}\text{V}_x$  powder mixture leads to the following structural transformations depending on the vanadium content: for  $x=5$  at.% the  $\text{Fe}(\text{Al},\text{V})$  solid solution becomes ordered (B2 type structure and the long range order parameter achieves 0.72), for  $x=15$  at.% and  $x=25$  at.% the solid solution transforms into a two phase state. One of these phases was identified as the B2 type phase with the LRO parameter of 0.55, the second one as a cubic (D8a) with the lattice parameter  $a=1.1769$  nm.

**COMPARISON OF SIGMA PHASE FORMATION  
IN COARSE GRAINED AND NANOCRISTALINE Fe-Cr-Sn ALLOYS**

*B.F.O. Costa, G. Le Caer\*, N. Ayres de Campos*

Departamento de Física da Universidade,  
P-3000 Coimbra, PORTUGAL <benilde@gemini.ci.uc.pt>

\*LSG2M, CNRS UMR 7584, Ecole des Mines,  
F-54042 Nancy Cedex, FRANCE <lecaer@mines-u.nancy.fr>

Fe-Cr-Sn alloys with Sn compositions ranging from 0 to 6 at% were prepared by melt and by mechanical alloying. Coarse grained and nanocrystalline alloys were obtained in each case, with size of grains of about 50 µm and 10 nm, respectively. The influence of the size of grains and the Sn content on the sigma-phase transformation was studied by means of <sup>57</sup>Fe and <sup>119</sup>Sn Mössbauer spectroscopy and electron transmission microscopy. X-ray diffraction measurements were also performed in order to characterise the transformation.

It is observed that the rate of formation of the sigma-phase is higher for as-milled alloys, and decreases with the increase of Sn concentration for both kinds of samples. In coarse-grained alloys, Sn precipitates at grain boundaries, blocking the nucleation sites of the sigma-phase. This seems to be the main reason for the retardation process. In mechanically alloyed Sn extended solid solutions, a large density of nucleation sites exists for the sigma-phase, but its growth is controlled by the removal of the excess of tin from the mother solid solution.

**CHARACTERISATION OF THE MICROSTRUCTURE OF  
NANOPHASE Ni AND ITS INFLUENCE ON MECHANICAL PROPERTIES:  
A MOLECULAR DYNAMICS COMPUTER SIMULATION**

*H. Van Swygenhoven<sup>1</sup>, M. Spaczer<sup>1</sup>, D. Farkas<sup>2</sup> and A. Caro<sup>3</sup>*

<sup>1</sup> Paul Scherrer Institute, CH-5232 Villigen PSI, SWITZERLAND <helena.vs@psi.ch>

<sup>2</sup> Virginia Polytechnic Institute, 213 Holden Hall, Blacksburgh, VA, USA

<sup>3</sup> Centro Atomico Bariloche, 8400 Bariloche, ARGENTINA

The microstructure of computer generated Ni nanophase samples with mean grain sizes ranging from 3 to 12 nm is studied by means of pair distribution functions, coordination number, atom energetics, visual inspection of slices and local crystalline order in terms of a bond analysis technique. In the bond analysis technique six categories of atoms are defined: *perfect fcc*, atoms having a local fcc order till fourth neighbors, *good fcc*, atoms having a local fcc order till first neighbors, *perfect hcp*, atoms having a local hcp order till fourth neighbors, *good hcp* atoms having a local hcp order till first neighbors, atoms having other 12 coordinated combinations, and finally the non-12 coordinated atoms. Making a difference between atoms with a local fcc or hcp order up to both fourth and first neighbors helps identifying the hcp atoms which might be outside the boundaries and those which are in the boundaries.

Two types of samples are considered: those with random crystallographic orientation, representing samples with mainly high angle grain boundaries, and those originated from the same seeds as before, but with a limited misorientation, representing samples with mainly low angle grain boundaries. The mean grain size of the samples vary between 3 and 12 nm, each containing at least 15 grains.

The nature of the grain boundary structure in the different type of samples is studied and the influence on the sample density, grain boundary density and the excess grain boundary enthalpy is discussed and compared with experimental values found in literature.

The influence of the grain size on the plastic deformation is discussed in terms of a model based on grain-boundary viscosity controlled by a self diffusion mechanism at the disordered interface, which is activated by thermal energy and stress. The model is fitted to the results of both low angle samples and high angle samples.

**STRUCTURAL PROPERTIES OF NANOSIZE Ni<sub>3</sub>Al**

V. Bonny<sup>1,2</sup>, H. Van Swygenhoven<sup>2</sup>, W. Wagner<sup>2</sup>, D. Segers<sup>3</sup>, and J. van der Klink<sup>1</sup>

<sup>1</sup> Ecole Polytechnique Fédérale de Lausanne, CH-1015 Ecublens, SWITZERLAND  
<Vincent.Bonny@psi.ch>

<sup>2</sup> Paul Scherrer Institut, CH-5232 Villigen PSI, SWITZERLAND

<sup>3</sup> RUG, Department of Subatomic and Radiation Physics, NUMAT,  
Proeftuinstraat 86, B-9000 Gent, BELGIUM

Ni<sub>3</sub>Al is produced by the inert-gas condensation technique as nanosized powder and also as consolidated nanophase material. We investigate the structural parameters, i.e. grain size, crystalline structure, chemical order and free volume as a function of the condensation and consolidation parameters. Grain size and crystalline structure are investigated by X-ray diffraction and electron microscopy, the chemical order by means of Nuclear Magnetic Resonance, and the free volume distribution by means of positron annihilation. The smallest clusters obtained are in the size range of 5 to 6 nm, and in the compacted material a grain size of the same order is obtained. In both, the powder and the compacted material, well established chemical order can be verified from the line width in the NMR spectra. The influence of compaction parameters on the chemical order and the crystalline structure are discussed.

---

**CRYOCHEMICAL SYNTHESIS OF BIMETALLIC NANOPARTICLES IN SILVER - LEAD - METHYLACRYLATE SYSTEM**

*Boris M. Sergeev, Gleb B. Sergeev and Andrei N. Prusov*

Chemistry Department, Moscow State University, 119899, Moscow, RUSSIA  
<gbs@cryo.chem.msu.su>

Bimetallic nanoparticles with a homogeneous or layer-by-layer distribution of composing metal atoms are important in catalysis, molecular electronics, and serve as models for the study of alloys formation.

Organosols of mono- and bimetallic nanoparticles were synthesised *via* vacuum ( $10^{-3}$ - $10^{-4}$  Torr) low-temperature co-deposition of metal(s) and organic monomer - methylacrylate (MA) vapours onto the liquid-N<sub>2</sub> cooled wall of the glass reactor chamber with subsequent heating of the solid co-condensate up to room temperature.

It was found that under conditions of joint condensation of Ag with MA silver-initiated polymerisation took place of the monomer. According to the estimates, the degree of conversion of MA was 1-2%. Apparently, the macromolecules arising in polymerisation are bound fairly strongly to silver thus forming a shell preventing aggregation of  $\leq 15$  nm-sized particles.

Polymerisation yields in Pb/MA and Ag/Pb/MA systems were found to be negligible. In our opinion, the observed difference between the Ag/MA and Ag/Pb/MA systems may be due to non-additivity in chemical properties of bimetallic particles, or to effective inhibition of the silver- initiated polymerisation of MA by Pb atoms. It is obvious that low-molecular MA is less effective in stabilising ligand than corresponding polymer. This is the cause of aggregation of both Pb and Ag/Pb nanoparticles ( $\leq 5$  nm in size) in cryochemically prepared organosols.

Surface plasmon absorption band in Ag/MA organosol is centred at 416-420 nm. In Ag/Pb/MA sol in argon gas this band is red-shifted to 438 nm. After exposure Ag/Pb/MA sols to air we observed further progressive red shift of the band to 466 nm. Though detailed interpretation of the absorption spectra of metal colloids is rather complicated, TEM data obtained in the work make it possible to connect observed red shift 416 nm-420 nm  $\rightarrow$  438 nm mainly to the aggregation of Ag/Pb nanoparticles. Oxidation of lead in air may decrease the stability of the bimetallic nanoparticles and cause their further aggregation. In this case, red shift of the silver plasmon absorption band from 438 nm to 466 nm may indicate the progressive aggregation of Ag/Pb particles and changes in their electronic state upon oxidation.

Further investigations will be directed towards the elucidation of the dependence of both optical properties and chemical reactivity of bimetallic nanoparticles on their composition, surface ligand layer nature and structure.

**CHARACTERIZATION OF Al-RICH Al-Fe ALLOYS PREPARED BY BALL MILLING**

*F. Zhou<sup>1,2</sup>, R. Liick<sup>2</sup> and K. Lu<sup>1</sup>*

<sup>1</sup> State Key Laboratory for RSA, Institute of Metal Research,  
Chinese Academy of Sciences, Shenyang 110015, CHINA

<sup>2</sup> Max-Planck-Institut für Metallforschung, Seestr. 92. D-70174 Stuttgart, GERMANY

Metastable  $\text{Al}_x\text{Fe}_{100-x}$  ( $x = 70$  to  $90$  at.%) alloys have been prepared by ball milling of elemental powders. Results after long milling times were as follows:

- (i)  $x \leq 70$  supersaturated nanostructured bcc solid solution,
- (ii)  $75 \leq x \leq 85$  amorphous and
- (iii)  $x = 90$  two-phase mixture of amorphous and supersaturated nanostructured fcc solid solution.

By use of DSC (differential scanning calorimetry) and MTA (magnetothermal analysis) stability and transformation behavior were analysed. We report on formation of these metastable alloys, characterization by X-ray investigation and transformation. In the present paper we focus on magnetic measurements on  $\text{Al}_{70}\text{Fe}_{30}$ , where indication of several stages of transformation has been found.

**FUNCTIONAL SELF-ASSEMBLED MONOLAYERS ON GOLD  
FOR THE SELECTIVE RECOGNITION OF NEUTRAL MOLECULES  
AND CATIONS FROM AQUEOUS SOLUTIONS**

*Stefano Levi, Frank C. J. M. van Veggel, Bart-Hendrik Huisman, Simon Flink,  
Arianna Friggeri, Marcel Beulen, and David N. Reinhoudt*

Laboratories of Supramolecular Chemistry and Technology,  
Faculty of Chemical Technology, University of Twente, P.O. Box 217,  
7500 AE Enschede, THE NETHERLANDS <S.Levi@ct.utwente.nl>

Organic molecules with functional groups for the selective recognition of neutral molecules and cations from aqueous solutions have been self-assembled on gold surfaces. Characterisation of these highly ordered monolayers has been done by XPS, SIMS, grazing-angle FT-IR, contact angle measurements, cyclic voltammetry (CV), and electrochemical impedance spectroscopy (EIS). Some layers have also been studied by AFM showing two different hexagonal lattices depending on the experimental conditions. These two lattices are commensurate and could be identified with the molecular structure of the adsorbate.

The recognition of neutral molecules, like p-nitrobenzoic acid and p-nitrophenol, has been studied by surface plasmon resonance (SPR). These measurements showed that some of the layers have a stronger interaction with the guest than the reference layer. The "best" reference layer proofed a hydroxy-terminated alkanethiol.

Crown ethers like 12-crown-4 and 15-crown-5 having a substituent with a thiol moiety form self-assembled monolayers on gold that bind cations from the aqueous phase. The binding event could be registered by CV and EIS using a  $\text{Ru}(\text{NH}_3)_6^{3+}$  as "marker" ion. The 12-crown-4 derivative shows a large selectivity of  $\text{Na}^+ > \text{K}^+ >> \text{Li}^+, \text{Cs}^+, \text{Mg}^{2+}$ , and  $\text{Ca}^{2+}$ . The 15-crown-5 derivative has a large selectivity of  $\text{K}^+$  over  $\text{Na}^+$ . The selectivity is due to sandwich formation, i.e. the binding a cation by two crown ethers, which could be shown by "diluting" the crown ether in the monolayer by alkanethiols.

Sams of sulfides with a ferrocene on one end of the molecule and a carboxylic acid on the other show a redox behaviour that is dependent on the pH of the solution. The oxidation of the ferrocene is more anoxic when the carboxylic acids are deprotonated because of stabilisation of the ferrocinium. This change of the redox potential is being used as sensing principle.

**ORDERING OF NANOCRYSTALLINE FeAl PRODUCED  
BY CLUSTER CONDENSATION**

*K. Reimann and H.-E. Schaefer*

Institut für Theoretische und Angewandte Physik, Universität Stuttgart  
Pfaffenwaldring 57, 70550 Stuttgart, GERMANY  
[<Klaus.Reimann@itap.physik.uni-stuttgart.de>](mailto:<Klaus.Reimann@itap.physik.uni-stuttgart.de>)

In order to study the interplay of ordering phenomena, strain relaxation, and crystallite-size stability, nanocrystalline  $\text{Fe}_{50}\text{Al}_{50}$  and  $\text{Fe}_{60}\text{Al}_{40}$  alloys were prepared by sputtering, crystallite condensation in an Ar atmosphere and subsequent compaction (2–4 GPa) at room temperature. The lattice structure is B2 as in coarse-grained FeAl but with a significantly lower degree ( $\leq 50\%$ ) of order. The crystallite size is below 30 nm and internal strains exceed 1.5 % in the {110} directions. The ordering process takes place mainly in the temperature range from 420 to 470 K. This is measured by the x-ray intensities of the superlattice reflections. The crystallite size remains smaller than 50 nm even after annealing at 0.8  $T_m$  (melting temperature  $T_m=1488$  K) as evidenced by transmission electron microscopy. The annealing behavior of cluster condensed nanocrystalline FeAl is compared to ball-milled FeAl. Furthermore, the decreases of the internal strains and of the lattice parameter during annealing are discussed. First results of magnetothermal analysis studies will be presented.

**CHARACTERISTICS OF NANOSTRUCTURED TiO<sub>2</sub> POWDERS  
SYNTHESIZED BY COMBUSTION FLAME-CHEMICAL  
VAPOR CONDENSATION PROCESS**

*B.K.Kim, G.G.Lee, G.H.Ha and D.W.Lee*

Korea Institute of Machinery & Materials, KOREA

Combustion Flame-Chemical Vapor Condensation (CF-CVC) process that can produce a nanostructured powder continuously has been used to produce non-agglomerated TiO<sub>2</sub> powder. This process involves precursor pyrolysis and condensation in a reduced pressure environment. The process parameters such as flame temperature, precursor concentration in the carrier gas are varied and the synthesised powders are characterised for crystal structure, chemical composition, and particle size by using TEM, X-ray, BET and TGA. The effects of processing parameters on TiO<sub>2</sub> powder characteristics are briefly considered.

**CHARACTERIZATION OF FERRITES SYNTHESIZED BY MECHANICAL ALLOYING AND SOFT CHEMISTRY**

*N. Millot<sup>1</sup>, S. Begin Colin<sup>2</sup>, P. Perriat<sup>1</sup>, G. Le Caër<sup>2</sup>*

<sup>1</sup> Laboratoire de Recherches sur la Réactivité des Solides, U.M.R. 5613,  
BP 400, 21011 Dijon Cedex, FRANCE

<sup>2</sup> Laboratoire de Science et Génie des Matériaux Métalliques, U.M.R. 7584,  
Ecole des Mines, 54042 Nancy Cedex, FRANCE <begin@mines.u-nancy.fr>

Numerous studies have been devoted for many years to the particular properties of nanocrystalline materials, which are characterised by the existence of a significant fraction of atoms residing in defect environments. In this nanoscale regime, particles exhibit volume and surface effects which are not observed in the associated coarse-grained materials. A characterisation of grains and of grain boundaries is important for a deep understanding of their behaviour. For the purpose of comparing nanostructured materials prepared by different synthesis methods, nanocrystalline Fe-based spinels were synthesised using two different routes: soft chemistry and high-energy ball milling. In the former synthesis method, precipitation in an aqueous solution is followed by thermal annealing under a reducing mixture of N<sub>2</sub>/H<sub>2</sub>/H<sub>2</sub>O gases. In the latter method, the spinel phase is directly formed in the mill at room temperature and under argon atmosphere from an initial powder mixture of Fe, Fe<sub>2</sub>O<sub>3</sub> and TiO<sub>2</sub> in stoichiometric proportions. The as-prepared powders are characterised by X-ray diffraction, scanning and transmission electron microscopy, surface area measurements and Mössbauer spectrometry. In both cases, the average crystallite size is about 15 nm, but whereas in the case of mechanosynthesis, the ball-milled powders consist of aggregates, those obtained by soft chemistry are very well dispersed. Comparison of both types of ferrites show that oxidation phenomena occur thus at the surface of grains in the soft chemistry powders and lead to materials with a higher deviation d from stoichiometry Fe<sub>3-x</sub>M<sub>x</sub>O<sub>4+d</sub> than those formed from mechanical alloying. Mössbauer spectra agree with the previous conclusions on the differences in oxidation behaviour and in crystallite size distribution. They demonstrate that heterogeneities of titanium content exist in soft chemistry powders while a superparamagnetic behaviour is evidenced in the mechanosynthesised ferrites at room temperature.

**STRUCTURAL CHARACTERIZATION OF ULTRA DISPERSED (NANO-) MATERIALS AS MIDDLE BETWEEN AMORPHIC AND CRYSTALLINE***V.F. Petrunin*

Moscow Engineering Physics Institute, Kashirskoe sh., 31, Moscow 115409, RUSSIA  
*<petrunin@onil724a.mephi.ru>*

When the size of small particles becomes comparable with a characteristic distance of some other physical phenomenon (size of domain, length of phonon or electron free path, the dimension of defects, etc.), then various dimensional effects can occur [1,2]. Model computations concerning the atomic arrangement in small particles have been undertaken using the methods of molecular dynamics. Calculations were made for two small particles: one of 736 nickel and other of 1047 gold atoms. In both cases the calculated values of interatomic distances along various crystallographic directions are essentially decreased in the centre of the particle and also much decreased as the surface is approached in all directions. Such changes of interatomic separation correspond to an inhomogeneous distortion. Theoretical treatment of the impurity atoms distribution inside the small particle showed also its nonergodic character along the radius. Electron, X-Ray and mainly neutron diffraction experiments carried out to estimate the validity of the model above.

The high resolution electron images of small gold particles are in qualitative agree with the monotonical decreasing of interplanar distances near the surface. By the neutron and X-Ray analysis of ultrafine TiN and ZrN powders were established that their particles size diminution leads to a regular decrease of the lattice constant (up to 0,3%) and the increase of the root-mean square atom displacements (up to 20%). Considerable microdistortion of ultradispersed ZnN crystal lattice was discovered by means of harmonic analysis of asymmetrical peaks profiles. It was found that a part of oxygen impurity atoms could penetrate into the nitride lattice replacing mainly nitrogen atoms. It was shown by the neutron diffraction technique that solid solution of oxygen in a small nickel particle is characterised by a spatially inhomogeneous concentration distribution manifested in an inhomogeneous extension of the lattice and in an increasing of the mean square atomic displacements.

The generalising of all theoretical and experimental results allows suggesting model of UDM's atomic arrangement, which illustrates the possibility of transition from crystalline to amorphous state through ultradispersed one. So UDM atomic structure is peculiar, midway between the crystalline and amorphous states. The reasons of this peculiarity are significant surface energy, small size of crystallite and extreme conditions of preparing.

[1] Morokhov I.D., et al - Sov. Phys. Usp., No.4 (1981), 295-316.

[2] Pertunin V.F., - J. Mendeleev Chem. Soc. (in Russian), v.7, No.2 (1991), 146-150.

**NANO-STRUCTURAL POLYACETYLENE-LAYERED  
PHOSPHATE COMPOSITE**

*Shunro Yamaguchi and Koichi Niihara*

Osaka University, The Institute of Scientific and Industrial Research,  
8-1 Mihogaoka, Ibaraki, Osaka 567, JAPAN <shunro@sanken.osaka-u.ac.jp>

There has been interested in development of functional organic-inorganic nano-composite in recent years. Recently, we found that long chain diacetylene compound was intercalated into layered phosphate to afford the nano-structural diacetylene-layered phosphate intercalation compound. The organic - inorganic hybrid material was irradiated with gamma ray to polymerise diacetylene. The polymerized hybrid material with nanostructure possesses conducting property and is a potent material for molecular rectifier. Structure and electric properties of the nano-structural polyacetylene-layered phosphate intercalation compound are presented.

**MAGNETIC PROPERTIES OF THE RESIDUAL AMORPHOUS PHASE IN  
NANOCRYSTALLINE Fe-Zr-B-Cu ALLOYS.**

*T. Kemény, D. Kaptás, J. Balogh, L.F. Kiss, L.K. Varga and I. Vincze*

Research Institute for Solid State Physics and Optics, P.O.Box 49,  
H-1525 Budapest, HUNGARY <kemeny@power.szfki.kfki.hu>

Melt spun amorphous  $\text{Fe}_{92-x}\text{B}_x\text{Zr}_7\text{Cu}_1$  ( $2 \leq x \leq 12$ ) alloys have been heat treated to the end of the first crystallisation stage indicated by Differential Scanning Calorimetry. It has been verified by transmission electron microscopy and X-ray diffraction that Fe-rich nanocrystalline bcc phase is formed in this process. The low and high temperature Mössbauer results including also external magnetic field studies make it evident that the bcc phase contains a non-negligible amount of dissolved Zr and B. These results also indicate that the chemical composition of the residual amorphous phase is significantly shifted, approaching the  $\text{Fe}_{67}(\text{Zr},\text{B})_{33}$  ratio.

Melt quenched  $\text{Fe}_{67}(\text{Zr},\text{B})_{33}$  alloys have been prepared for a direct comparison with the residual amorphous phase. It is established that amorphous alloys are only produced for the compositions where the B:Zr ratio exceeds unity. Different properties (Curie temperature and Fe hyperfine field) related to the magnetic behaviour are compared for the bulk amorphous alloys and for the residual amorphous phase of the nanocrystallised samples. The comparison indicates that the magnetic and hyperfine properties of the nanosized amorphous phase are not significantly different from its bulk counterpart.

### **NEW HIGH PIEZOELECTRIC COUPLING PLuNT BINARY SYSTEM CERAMICS**

*A. Sternberg, L. Shebanovs, M. Antonova, M. Livinsh, J.Y. Yamashita\*,  
I. Shorubalko and A. Spule,*

Institute of Solid State Physics, University of Latvia, LATVIA <stern@latnet.lv>

\* Toshiba Corporation, Kawasaki, JAPAN

Solid solutions of the  $(1-x)\text{Pb}(\text{Lu}_{1/2}\text{Nb}_{1/2})\text{O}_{3-x}\text{PbTiO}_3$  (PLuNT) binary system have been synthesised for the first time. Hot-pressed (temperature  $930^\circ\text{C}$  to  $1130^\circ\text{C}$ , pressure 25 MPa) ceramics series have been obtained in the interval  $0 < x < 0.80$  to study the structural, dielectric and piezoelectric properties.

At room temperature the phases change from monoclinic (M)  $x < 0.38$  (pseudo-cubic at  $x \approx 0.2$ ) to tetragonal (T) at  $x > 0.48$ . Pure lutetium niobate (PLuN) has a pronounced long-range order in the B sublattice (the X-ray diffraction contains superstructure maxima of a pseudo-monoclinic symmetry) and a sharp antiferroelectric phase transition at  $\sim 258^\circ\text{C}$ . The morphotropic region extends over the interval  $x = 0.38-0.49$ , the concentration ratio  $M:T \equiv 1$  (morphotropic phase boundary – MPB) corresponds to  $x = 0.41$ . Within this interval, compared to the classical piezoelectric ceramics PZT, a rather strong distortion of the unit cell is maintained -  $(c/a-1) \geq 0.02, \geq 90.37^\circ$ . For this reason the pure PLuNT is a "hard" piezoelectric. The maximum values of the electromechanical coupling coefficients  $k_p = 0.663$ ,  $k_t = 0.481$ ,  $k_{31} = 0.355$  of PLuNT  $(1-x)/x$  ceramics are attained for compositions near the monoclinic / tetragonal MPB - PLuNT 59/41.

The PLuNT system, having the highest  $T_m$  ( $> 350^\circ\text{C}$ ) among binary  $\text{Pb}(B',B'')\text{O}_3$ -PT perovskites is favourable for high temperature piezoelectric sensors and actuators, and may be of interest as promising basis for thin film and single crystal performance.

**THE CRYSTALLINE-TO-AMORPHOUS TRANSFORMATIONS  
IN THE TiH<sub>2</sub>-Fe SYSTEM DURING BALL MILLING**

*A.A. Novakova<sup>1</sup>, O.V. Agladze<sup>1</sup>, R.S. Gvozdover<sup>1</sup> and B.P. Tarasov<sup>2</sup>*

<sup>1</sup> Department of Physics, Moscow State University,  
117234 Moscow, RUSSIA <ova@runar.phys.msu.su>

<sup>2</sup> Institute for New Chemical Problem RAS, 142432 Chernogolovka, RUSSIA

Elemental equiatomic TiH<sub>2</sub>-Fe powder mixtures were mechanically alloyed in high energy ball mill under Ar through different time. The phase analysis was performed by X-ray diffraction. The transformations up to amorphous state during milling process were checked by low temperature Mössbauer spectroscopy and SEM. An amorphous phase coexisting with crystalline hydride was obtained. We have analyzed the influence of hydrogen inclusive in TiH<sub>2</sub> structure on the amorphization process. The thermal stability of the MA sample was studied by means of DTA method.

## NANOSTRUCTURED PRECIPITATES: EXPERIMENTAL VERSUS EXACT THEORETICAL PROFILES

V. Garrido<sup>1</sup>, D. Crespo<sup>1</sup>, E. Pineda<sup>2</sup>, T. Pradell<sup>2</sup> and M. Capitán<sup>3</sup>

<sup>1</sup> Dept. Física Aplicada, Univ. Politècnica de Catalunya, Campus Nord,  
Modul B4, 08034-Barcelona, SPAIN <crespo@benard.upc.es>

<sup>2</sup> ESAB, Univ. Politècnica de Catalunya. Urgell 187, 08036 Barcelona, SPAIN.

<sup>3</sup> European Synchrotron Research Facility, BP 220-F-38043 Grenoble Cedex, FRANCE

Small Angle X-Ray Scattering (SAXS) is one of the few techniques suitable for the determination of the grain size distribution of nanostructured materials. Although a general theory is well established since the fifties assuming a-priori knowledge of the precipitates shape, no exact theory was available for materials obtained by nucleation and growth kinetics, where the impingement between grains provokes the sphericity loss of the grains.

A recently developed kinetic model grounded on the thermodynamic factors which drive the transformation of the amorphous matrix into crystalline precipitates [1] allows to theoretically determine the grain size distribution of materials undergoing such first order phase transitions. It has been tested in the primary crystallization of the amorphous Fe<sub>73.5</sub>Cu<sub>1</sub>Nb<sub>3</sub>Si<sub>17.5</sub>B<sub>5</sub> giving excellent agreement with the experimental data (macroscopical and TEM, [2]). Further theoretical development has allowed us to determine the spatial autocorrelation function of such systems without any approximation [3] and, consequently, the scattering profile associated to the grain size distribution in the SAXS spectra without supposing any specific shape in the precipitates. On the contrary, the effect of the impingement between neighbour grains during the transformation, which results in a loss of sphericity, is fully taken into account.

We present the comparison of these theoretical results with SAXS experimental spectra obtained at the European Synchrotron Research Facility.

- [1] D. Crespo, T. Pradell, M.T. Clavaguera-Mora & N. Clavaguera, *Phys. Rev. B* **55**, 3435 (1997).
- [2] T. Pradell, D. Crespo, N. Clavaguera, J. Zhu & M.T. Clavaguera-Mora, *Nanos. Mater.* **8**, 345 (1997).
- [3] V. Garrido & D. Crespo, *Phys. Rev. E* **56**, 2781 (1997).

**ANOMALOUS DECREASING OF THE HYPERFINE MAGNETIC FIELD I  
N THE TOP LAYER OF Fe/Cr MULTILAYER COVERED BY Zr OBSERVED  
BY MÖSSBAUER REFLECTOMETRY**

*M.A. Andreeva<sup>1</sup>, A.I. Chumakov<sup>2</sup>, S.M. Irkaev<sup>3</sup>, K.A. Prochorov<sup>4</sup>, R. Ruffer<sup>2</sup>,  
N.N. Salaschenko<sup>4</sup> and V.G. Semenov<sup>5</sup>*

<sup>1</sup> Dept. of Physics, Moscow State University, 117234, Moscow, RUSSIA

<sup>2</sup>ESRF, France <e-mail: chumakov@esrf.fr>

<sup>3</sup> Inst. of Anal. Instrumentation, RAS, 198103 St.Petersburg, RUSSIA

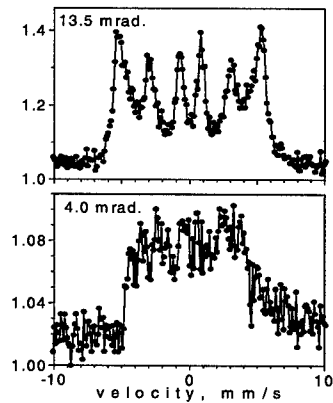
<sup>4</sup> Inst. of Phys. of Microstructure, RAS, 603600 Nizhny Novgorod, RUSSIA

<sup>5</sup> Chem. Inst., St.-Petersburg State Univ., 198904 St.-Petersburg, RUSSIA

There are a lot of methods for characterization of multilayers as a whole. But it is more difficult to get information about the surface or the bottom layer in this structure. Obviously these outer layers have another properties which sometimes influence sufficiently on their functions. This takes place for the multilayers which are created for the purpose of the nuclear monochromatization of synchrotron radiation. We present here the method for nondestructive depth selective analysis on nanometer scale: Mossbauer Reflectometry or in other words GIMS - Grazing Incidence Mössbauer Spectroscopy [NIM in Phys. Res. **B74**, 545 (1993); **B 103**, 351 (1995)].

We have tested Zr films as a possible  $\lambda/4$ -covering of resonant medium ( $^{57}\text{Fe}_x\text{Cr}_{1-x}$ ) for filtering of resonant frequencies in synchrotron radiation. The samples were prepared by sequential magnetron sputtering of  $^{57}\text{Fe}$  and Cr layers. The mixture of  $^{57}\text{Fe}$  and Cr was created only if the thicknesses  $^{57}\text{Fe}$  and Cr layers were less than 1 nm. In other cases we have got the  $^{57}\text{Fe}/\text{Cr}$  multilayer. The samples were investigated by X-ray reflectometry (the measurements were done for resonant wavelength 0.086 nm at ESRF) and by GIMS in energy (in St.-Petersburg) and time-domain (at ESRF).

Here we present the results for the sample Zr(10nm)/[ $^{57}\text{Fe}/\text{Cr} \bullet 26$ ]/Cr(50nm)/glass, which has not revealed an expected strong suppression of Rayleigh scattering, but has interesting Mossbauer properties. Two Mössbauer spectra of the secondary electron yield, shown in Fig., were measured for two grazing angles: near the Bragg angle of the multistucture (the period is 33 nm) and near the critical angle of the total external reflection. The difference in the value of magnetic hyperfine splitting in two spectra is clearly seen. The time delayed spectra of reflectivity for this sample has also shown the difference in quantum beat oscillations for different grazing angles. That is the another evidence that the value of hyperfine magnetic field is different for surface and inside layers of our multilayer.



**A DEPTH PROFILE STUDY OF THE STRUCTURE AND STRAIN DISTRIBUTION IN CHEMICALLY GROWN CU FILMS ON ALN**

Luz J. Martínez-Miranda<sup>1</sup>, Yiqun Li<sup>1</sup>, L.K. Kurihara<sup>2,3</sup> and G.M. Chow<sup>2</sup>

<sup>1</sup> Department of Materials and Nuclear Engineering, University of Maryland,  
College Park, MD 20742 USA

<sup>2</sup> Naval Research Laboratory, Washington, DC 20375, USA

<sup>3</sup> also at Potomac Research International, MD, USA

We have studied Cu coatings grown on AlN substrates via a polyol deposition method using grazing incidence X-ray (GIXS) techniques and small angle scattering techniques to determine the dependence of film structure on depth as well as the presence of nanometer size structures in the films. Small angle measurements indicate the presence of ordered structures in the order of 4 nm close to the surface of the films. Depth studies using different X-ray energies in combination with the GIXS technique suggest the first 20 to 60 nm of the film correspond to a textured region, with strains ranging between +0.1% to -0.6%. The azimuthal ordering in the plane of the films depends on the sample deposition time and the We will discuss the relation between the structure of the top layer of the coating and the mechanism of particle agglomeration and bonding at the substrate.

This work was supported partially by a NSF grant No. ECS-9710789, and by NRL and ONR nanostructured coatings programs. X-ray studies were performed at the National Synchrotron Light Source at Brookhaven National Laboratory, which is supported by the U.S. Department of Energy.

**GRAIN SIZE MEASUREMENT OF NANOCRYSTALLINE GOLD  
BY X-RAY DIFFRACTION METHOD**

*T. Inami<sup>1</sup>, M. Kobiyama<sup>1</sup>, S. Okuda<sup>2</sup>, H. Maeta<sup>3</sup> and H. Ohtsuka<sup>3</sup>*

<sup>1</sup> Faculty of Engineering, Ibaraki University, 4-12-1, Nakanarusawa,  
Hitachi, Ibaraki 316, JAPAN <inami@hit.ipc.ibaraki.ac.jp>

<sup>2</sup> Emeritus, University of Tsukuba, 1455-29 Arakawa-oki,  
Ami, Ibaraki 300-11, JAPAN

<sup>3</sup> Department of Materials Science and Engineering, Japan Atomic Energy Research  
Institute, Tokai-mura, Ibaraki 319, JAPAN <maeta@popsvr.tokai.jaeri.go.jp>

In evaluating thermal stability of nanocrystalline materials, grain size is a very important factor. Nanocrystalline metals prepared by the gas deposition method could be quite different in thermal stability because of no compaction process in preparing operation. Grain size of nanocrystalline gold prepared by the gas deposition method was studied by X-ray diffraction method for various preparing conditions and for various annealing.

Specimens of nanocrystalline gold were prepared by the gas deposition method at evaporation temperatures and He gas pressures in evaporation chamber ranging from 1700~1870 K and 650~1400 Torr, respectively. Annealing of specimens was made in vacuum (less than  $10^{-5}$  Torr) at temperatures ranging from 470~1120 K for 1h. X-ray diffraction profiles were measured using CuK $\alpha$  radiation. After removing K $\alpha_2$  peaks and instrumental broadenings, the crystal grain size was determined by the Warren-Averbach's method.

The mean grain size of as-prepared specimens was found to be in the range of 7 to 20 nm with no apparent dependence on the above preparation conditions. The specimens prepared under the conditions with evaporation temperatures >1770 K and He gas pressures <1000 Torr appeared to show a strong tendency to the preferred orientation. In such specimens, more grains seem to have (111) parallel to the specimen surface. The thermal stability of the specimens was found to be quite high, for 1h annealing, up to 770 K the mean grain sizes remained unchanged and were about 2 times of those of as prepared after 1070K. Significant grain growth occurred above 1100 K. This high thermal stability is in marked contrast with that of nanocrystalline pure metals prepared by the inert gas condensation and compaction method.

**ON THE THERMAL STABILITY OF NANOCRYSTALLINE PURE METALS**

*S. Okuda<sup>1</sup>, M. Kobiyama<sup>2</sup>, T. Inami<sup>2</sup> and S. Takamura<sup>2</sup>*

<sup>1</sup> Emeritus, University of Tsukuba, 1455-29 Arakawa-oki,  
Ami, Ibaraki 300-11, JAPAN

<sup>2</sup> Faculty of Engineering, Ibaraki University, 4-12-1, Nakanarusawa,  
Hitachi, Ibaraki 316, JAPAN <kobiyama@hit.ipc.ibaraki.ac.jp>

The thermal stability is an important property of nanocrystals not only from basic but also from practical viewpoints. In order to extract an essential property of nanostructures, we concentrate on nanocrystalline pure metals here. For nanocrystals prepared by the inert gas evaporation and compaction method which is most widely used now, numerous works have shown that nanocrystals are thermally very unstable, for example, nanocrystalline Cu (n-Cu) and n-Pd were recently reported to show a grain growth even at room temperature after prolonged period. However, it has been also reported that there are some very stable localized regions in nanocrystals. On the other hand, for n-Au prepared by the gas deposition method, some specimens showed a very high thermal stability. In the gas deposition method, nano sized particles are deposited on a substrate at high speed in low pressure He gas and no compaction process is included. Heavy deformation is known to make the thermal stability lower. We have studied the thermal stability of n-Au prepared by the gas deposition method by means of SEM, STM and TEM observations, X-ray diffraction, micro-hardness test and bending test. It was found that the thermal stability seemed to be higher for specimens with smaller initial grain size. For example, specimens with grain size of ~9 nm showed no grain growth after 1h annealing at 770 K and growth to twice even after 1070 K. The results seem to suggest that mechanical balance of boundaries in triple connections cause this high thermal stability. Based on these results, various factors controlling the thermal stability of nanocrystalline pure metals will be discussed in detail.

**RECOVERY PHENOMENA IN NANOCRYSTALLINE MATERIALS:  
DO GRAIN BOUNDARIES REALLY RELAX?**

*C. E. Krill, M. Meier and R. Birringer*

Universität des Saarlandes, FB 10 Physik, Gebäude 43, Postfach 151150,  
D-66041 Saarbrücken, GERMANY <krill@rz.uni-sb.de>

Owing to the large grain-boundary area contained in nanocrystalline materials, their overall properties can be highly sensitive to the detailed structural state of the boundary component. When a given nanocrystalline sample is synthesized by a highly non-equilibrium route such as by aerosol condensation+compaction or by ball milling. We might expect the as-prepared state of the resulting grain boundaries to be quite different from the quasi-equilibrium grain-boundary state in a fully 'relaxed' specimen. This should manifest itself through overall property changes that occur irreversibly and independently of grain growth.

There are numerous reports in the literature of such phenomena measured in nanocrystalline materials, including changes in the stored enthalpy, density, electrical resistivity and atomic-level co-ordination. Frequently, these observations have been interpreted as constituting evidence for the occurrence of structural relaxation in grain boundaries. We have examined the processes of relaxation and recovery in nanocrystalline Pt using low-temperature x-ray diffraction, differential scanning calorimetry and measurements of electrical resistivity. The results suggest that structural changes in the crystalline component—rather than in the grain boundaries—are primarily (though not necessarily exclusively) responsible for the observed relaxation effects.

**ADHESION BETWEEN NANOPARTICLES**

*Yimin Yao and Anders R. Thölén*

Dept. of Experimental Physics, Chalmers University of Technology,  
412 96 Göteborg, SWEDEN <tholen@fy.chalmers.se>

In bringing down the size of particles, being the constituents of nanostructured materials, the particles become more apt to adhere to one another. This effect makes handling of nanoparticles increasingly difficult with decreasing particle size.

The background for the current research program is to find out more about contact and adhesion of metal particles using modern methods for electron microscopy. Earlier investigations (1) have given a very clear picture of the physics when two particles meet and form contact. Due to the balance between surface, grain boundary and elastic energies contact is formed across a finite area, the size of which becomes relatively larger the smaller the particles. The accompanying stress field is clearly observed in the electron microscope and gives information about the contacting conditions. A very important factor for small metal particles is a most likely oxide coating on the particles which changes the conditions for contact. Thus oxide film formation and reduction (2) are also found to be very essential.

Our approach here is to get clean metal particles make contact in a controlled way and it is pursued along two different lines. The first method is to extract coherent cobalt precipitates from a cobalt-copper alloy and then allow them to meet. The second approach is to use existing particles and then anneal them in a reducing atmosphere. Results using a Philips CM200 FEG microscope will be reported.

1. Easterling K.E. and Thölén A.R., *Acta Met.* 20 (1972) 1001.
2. Sethi S.A. and Thölén A.R., *NanoStructured Materials*, 4 (1994) 903-913.

**X-RAY STUDY OF NANOCRYSTALLINE RIBBONS FeCuNbSiB  
SUBJECTED TO THE THERMOMECHANICAL TREATMENT**

*I.V. Gervasyeva<sup>1</sup>, H.J. Bunge<sup>2</sup>, K. Helming<sup>2</sup>, V.A. Lukshina<sup>2</sup> and I.V. Alexandrov<sup>3</sup>*

<sup>1</sup> Institute of Metal Physics of RAS, 18 Kovalevskaya str.,  
620219 Ekaterinburg, RUSSIA <domen@ifm.e-burg.su>

<sup>2</sup> Department of Physical Metallurgy, TU of Clausthal, 23 Grosser Bruch,  
D-38678 Clausthal-Zellerfeld, GERMANY

<sup>3</sup> Institute of Physics of Advanced Materials of Ufa State Aviation,  
TU 12 K.Marks Str., 450000 Ufa, RUSSIA

The nanocrystalline alloy FeCuNbSiB was produced by the annealing of the quenched amorphous ribbon at the temperature 530° C during 1 hour. This alloy shows high soft magnetic properties. The constant of magnetic anisotropy is close to zero. In the nanocrystalline alloy, subjected to annealing under loading at a temperature equal or higher of the crystallization temperature magnetic anisotropy is induced. A value of the constant of the magnetic anisotropy extremely increases when the thermomechanical treatment and the annealing for crystallization are overlapped.

In order to find out structure features accompanied this phenomenon X-ray study of texture, grain size and internal lattice microdistortions was undertaken.

There were studied the samples after following regimes of treatment:

- 1) Crystallization at the temperature 530° C during 1 hour;
- 2) Crystallization at the temperature 530° C during 1 hour under the loading 200 MPa;
- 3) The thermomechanical treatment at the temperature 530° C during 1 hour of the preliminary crystallized specimen.

Texture analysis was carried out by the method of integral pole figures on texture X-ray diffractometer with a position sensitive detector and a multichannel analyser.

The determination of a crystallite (coherently scattering domain) size and internal elastic microdistortions was carried out by the Warren-Averbach method (linear version). Preliminary investigations of ultrafine-grained materials showed an advantage of this method over the alternative x-ray methods in point of obtaining most reliable results.

Detail study of grain orientations in the samples after mentioned above regimes of treatments has not discovered any texture.

The use of the Warren-Averbach method for analysis of x-ray data of the investigated alloy showed that the grain size after variants of treatment 1-3 is almost the same (6-8 nm) and a value of internal elastic microdistortions extremely increases in the case of the overlapped treatment (2), and increase is not very much in the case of the sequential treatment (3).

**EXAFS STUDY ON NANOCRYSTALLINE  $\text{Fe}_{40}\text{Co}_{10}\text{Cu}_{50}$  ALLOY  
PROCESSED BY MECHANICAL ALLOYING**

*D.S. Yang, Y.G. Yoo, S.C. Yu and W.T. Kim<sup>1</sup>*

Department of Physics, Chungbuk National University,  
Cheongju 361-763, KOREA <scyu@cbucc.chungbuk.ac.kr>

<sup>1</sup> Department of Physics, Chongju University, Chongju360-764, KOREA

Metastable  $\text{Fe}_{40}\text{Co}_{10}\text{Cu}_{50}$  alloys were fabricated by mechanical alloying process from pure elemental powder. The mechanical alloying was performed in a high energy ball mill under an Ar atmosphere with the balls to powder weight ratio of 20:1. The processing times varied from 20 to 80 hours to observe the variation of structure. The structural changes during mechanical alloying process, and post heat treatment were examined by normal powder diffraction patterns taken with monochromatic MoK $\alpha$  radiation and EXAFS (Extended X-ray Absorption Fine Structure) spectroscopy for each step. The X-ray energy range for EXAFS experiments were above Fe, Co and Cu K-edge. The structural orderliness has been studied by the Fourier transform of the EXAFS spectra. EXAFS analysis provided information on both the short range and the long-range order. All the X-ray diffraction (XRD) peaks from  $\text{Fe}_{40}\text{Co}_{10}\text{Cu}_{50}$  alloys processed for 80 hours could be analyzed into a fcc nanocrystalline phase with grain size estimated about 10 nm. The EXAFS analysis verified that Fe and Co atoms replaced the Cu atom so that the nanocrystalline Fe-Co-Cu with fcc structure was formed by the mechanical alloying. Also we found that the nanocrystalline Fe-Co-Cu alloy was decomposed into bcc Fe-Co alloy and Cu by annealing process. These results were in good agreement with XRD analysis, showing a formation of nanocrystalline  $\text{Fe}_{40}\text{Co}_{10}\text{Cu}_{50}$  alloys with fcc crystal structure after 80 hours milling.

**ON THE STRUCTURE OF NANOCRYSTALLINE Pd  
BY MOLECULAR DYNAMICS SIMULATIONS AND X-RAY DIFFRACTION**

*P. Kebinski<sup>1,2</sup> and J. A. Eastman<sup>2</sup>*

<sup>1</sup> Materials Science Division, Argonne National Laboratory, Argonne, IL 60439, USA

<sup>2</sup> Forschungszentrum Karlsruhe, 76021 Karlsruhe, GERMANY

X-ray diffraction data from a 8.3 nm median grain-sized Pd sample were compared with the calculated diffraction spectrum of a computer-simulated uniform 7.8 nm grain-sized Pd microstructure grown from the melt by molecular-dynamics. While the experimental data show no evidence for the presence of interfacial disorder, X-ray data from the model microstructure contain clearly identifiable broad, amorphous-like peaks in addition to the normal crystalline Bragg peaks. The presence of atomic disorder at interfaces in the model microstructure is attributed to the chosen random high-angle misorientations between grains, which results in the formation of only high-energy GBs. In contrast, experimental processing conditions may allow neighbouring crystallites to rotate into lower energy misorientations, for which crystalline boundary structures are energetically preferred. This hypothesis is consistent with the recent mechanical properties studies of Sanders *et al* [1], in which it was speculated that observed orders-of-magnitude slower than expected creep rates in gas-condensed nanocrystalline Cu are due to the presence of a much higher than random fraction of twin or other low energy boundaries.

[1] P.G. Sanders *et al.*, *NanoStr. Mater.*, **9**, 433 (1997).

**SELF-ORGANIZATION OF FERROFLUIDS PREPARED  
USING SONOCHEMICAL IRRADIATION**

*Tanya Prozorov<sup>1</sup>, Ruslan Prozorov<sup>2</sup>, Kurrika V. P. M. Shafi<sup>2</sup> and Aharon Gedanken<sup>2</sup>*

<sup>1</sup> Department of Chemistry, Bar-Ilan University,  
Ramat-Gan 52900, ISRAEL <prozorr@ashur.cc.biu.ac.il>

<sup>2</sup> Institute for Superconductivity, Department of Physics, Bar-Ilan University,  
Ramat-Gan 52900, ISRAEL

We report on the two possibilities of the sonochemical synthesis of nanometer-size magnetic colloids. In the first method ferrofluids were produced using sonochemical irradiation of  $\text{Fe}(\text{CO})_5$  solution in decaline in the presence of a stabilizing agent, oleic acid (octadec-9-ene-1-carboxylic acid). In the second, *in-situ* method, sonochemical irradiation is applied to the decaline solution of  $\text{Fe}(\text{CO})_5$  and salt of high-molecular organic acids (like 2-ethyl-hexanoic acid) without adding the surfactant to a sonochemical cell. TEM study reveals that nanoparticles in as-prepared liquids are round-shaped and have uniform distribution with mean size of less than 20 nm. Magnetic measurements performed on frozen colloids exhibit superparamagnetic behavior. Additional TEM study for one-month aged colloids, revealed formation of acicular (ellipsoidal) particles of about 100 nm length and 20 nm in diameter. Magnetization measurements repeated at this time have demonstrated reduction of the magnetic signal, as compared to the fresh colloid. This is attributed to the significant enhancement of the shape anisotropy.

**CHARACTERIZATION OF BULK NANOSTRUCTURED MATERIALS  
THROUGH THE USE OF LOW-FREQUENCY  
INTERNAL FRICTION STUDIES**

*W.N. Weins, J.D. Makinson and R.J. DeAngelis*

Department of Mechanical Engineering The Center for Materials Research and Analysis  
University of Nebraska, Lincoln, Nebraska 68588-0656, USA  
<ww eins@unlinfo.unl.edu>

Low-frequency internal friction measurements have been made on a variety of bulk nanocrystalline copper and copper-iron materials which were prepared by mechanical milling and consolidation through hot isostatic pressing. Typically, nanostructures do not exhibit low-temperature dislocation damping peaks because of the lack of free dislocation structure in the heavily milled material. Studies also indicate that the nanocrystalline materials in general exhibit larger magnitude boundary-type damping peaks which are shifted to lower temperatures and higher activation energies than the same peak in an equivalent large-grained material. The presence of solid solution elements, however, appears to lower this energy appreciably, and parameters such as the log normal distribution function, which is indicative of the number of relaxation processes, does correlate with the extremely large boundary areas as found in the nanostructure materials. Annealing studies on the as-manufactured nanostructured materials have shown that internal friction can be used to follow the degradation of the nanostructure and will provide a semi-quantitative indication of the condition of the material.

**NEUTRON DIFFRACTION STUDIES OF CERIA-ZIRCONIA CATALYSTS  
PREPARED BY HIGH-ENERGY MECHANICAL MILLING***Enzo<sup>1</sup>, R. Frattini<sup>2</sup>, A. Primavera<sup>3</sup> and A. Trovarelli<sup>3</sup>*<sup>1</sup> Istituto Nazionale di Fisica della Materia e Dipartimento di Chimica dell'Università di Sassari, via Vienna 2, 07100 Sassari, ITALY <enzo@micromat.dipchim.uniss.it><sup>2</sup> Istituto Nazionale di Fisica della Materia e Dipartimento di Chimica Fisica dell' Università di Venezia, Dorsoduro 2137, 30123 Venezia, ITALY <frattini@unive.it><sup>3</sup> Dipartimento di Scienze e Tecnologie Chimiche, Università di Udine, via cotonificio 108, 33100 Udine, ITALY <trovarelli@dstc.uniud.it>

Ceria-based materials have been widely investigated in the last years owing to the broad range of applications in catalysis and in the preparation of advanced ceramic materials. The redox/catalytic properties of CeO<sub>2</sub> are strongly enhanced if isovalent cations such as Zr<sup>4+</sup> are introduced into its lattice by forming solid solutions. Usually these compounds are prepared via a conventional coprecipitation from the corresponding salts or using a sol/gel route, alternatively low-surface area materials are also produced via a high temperature firing of mixture of starting oxides. Recently the mechanical milling (MM) process has been extended to synthesize nanocrystalline CeO<sub>2</sub>-ZrO<sub>2</sub> in a wide composition range, starting from powders of the individual oxides. The structural analysis indicated that the milling process induces the formation of a solid solution with a contraction of the cell parameter of ceria based phases. Our preliminary X-ray diffraction studies have pointed out the formation of a cubic solid solution for CeO<sub>2</sub>-rich samples, and an increasing degree of tetragonality for higher ZrO<sub>2</sub> loading. Since the distinction between cubic vs. tetragonal phase may be controversial using X-rays, we have collected the neutron diffraction patterns of three [xCeO<sub>2</sub> + (1-x)ZrO<sub>2</sub>] mixtures (with x=0.2, 0.5, 0.8), produced with a SPEX 8000 high energy mixer/mill, after 9 h of milling and then have them subjected to in-situ annealing. The end-products displayed nanocrystalline features, so we have thought it useful to analyse the data with the Rietveld approach. The analysis of the diffraction patterns confirmed that the parental mixture is made up of cubic and monoclinic zirconia allotropes and of cubic ceria. For the [0.2CeO<sub>2</sub> + 0.8 ZrO<sub>2</sub>] mixture, after 9 h of MM we observed mainly one tetragonal Ce<sub>x</sub>Zr<sub>1-x</sub>O<sub>2</sub> solid solution, even if we can not disregard the existence of some nanocrystalline fraction (below 10% wt) in the monoclinic form. The location of O atoms in the tetragonal unit cell is such as to give M-O(M = Zr, Ce) nearest neighbour distances of ca 1.844 Å. For the equimolar mixture the end-products after 9 h are both the cubic and tetragonal structure of the Ce<sub>x</sub>Zr<sub>1-x</sub>O<sub>2</sub> solid solution. In the case of [0.8CeO<sub>2</sub> + 0.2ZrO<sub>2</sub>] mixture, the patterns of end-products are well accounted for mainly by just one cubic phase. Note that in the cubic zirconia phase the M-O distances are of 2.20 Å. In the solid solutions with Ce, these distances may be slightly elongated, owing to the larger lattice spacing measured for the unit cell. In situ annealing of end-products up to 1000°C makes larger the lattice parameters of both cubic and tetragonal phases, but subsequent cooling down to room temperature restore the structural parameters to their initial values. In addition, the peak broadening of phases decreases as a function of annealing temperature.

**THE STUDING OF PHASE COMPOSITION, CHARACTERISTICS OF  
THE STRUCTURE AND RANGE OF THE PARTICLE DIMENSIONS OF  
NANOSTRUCTURED IRON BY X-RAY DIFRACTION METHOD**

*A.L. Dzidzigury, V.V. Lyovina, D.V. Kuznetsov and D.I. Ryzhonkov*

Department of Theory of Metallurgical Processes, Moscow State University of Steel and  
Alloys, Leninsky prospect 4, Moscow, RUSSIA <levina@swi.misa.ac.ru>

We studied the peculiarities of phase composition, of structure and range of particle dimension of nanostructured (NS) iron, which was produced by means of reduction NS iron hydroxide ( $\alpha$ -FeOOH) in hydrogen at various temperatures and holding times. The FeOOH was produced by chemical dispersive method.

The dependence of phase composition on temperature and time of reduction was determined. The lattice constants were obtained. The average particle sizes and the particle size distributions were calculated. The anomaly of the broadening of X-ray reflections was detected. The ratio of physical broadening of two reflection degrees from one plane is close to 1.

The laws of change of the particle dimension from conditions of production was established. We suggested the mechanism of a particles amalgamation and the ways of production of the monodispersive NS iron powders.

### ELECTRON SPECTROSCOPY OF NANOSTRUCTURED LIQUID INTERFACES

*S. Södergren<sup>1</sup>, H. Rensmo<sup>2</sup>, K. Westermark<sup>1</sup>, G. Eriksson<sup>1</sup>, A. Henningsson<sup>1</sup>,  
A. Hagfeldt<sup>2</sup> and H. Siegbahn<sup>1</sup>*

<sup>1</sup>Department of Physics, University of Uppsala, Box 530,  
S-751 21 Uppsala, SWEDEN <first.secondname@fysik.uu.se>

<sup>2</sup>Institute of Physical Chemistry, University of Uppsala, Box 532,  
S-751 21 Uppsala, SWEDEN <first.secondname@fki.uu.se>

The structural properties of solid surfaces in contact with liquid solutions and the processes occurring at such interfaces are of fundamental interest in a large number of areas in current applied surface chemical physics. The mechanisms of the processes involved are generally found to be highly dependent on the nature of the surface-liquid interface. The electrochemistry of nanostructured transition metal oxide electrodes is one of the quickly expanding research areas since the demonstration of the usefulness of such electrodes in efficient photoelectrochemical solar cells [1]. A nanostructured electrode consists of interconnected nanocrystallites forming a porous structure (porosity around 50%). The significant property is the extremely large inner surface allowing for electrochemical reactions to take place in the entire volume of the electrode. The solar cell is only one of several potential applications of such electrodes. Recent papers in the area also report high charging capacities of nanostructured anatase titanium dioxide electrodes [2,3] when lithium is intercalated into the nanocrystals. Lithium intercalation in titanium dioxide also exhibits electrochromic properties. In order to maximize the reversibility and hence the long-term performance of such devices, it is of great interest to identify and monitor the interfacial charge transfer processes including potential side reactions. Subnanometer characterization including elemental and chemical information is thus desirable.

Electron spectroscopy has several attractive features for the study of the above mentioned processes. Applications to *in situ* prepared systems involving liquid interfaces are however comparatively complicated. One reason for this is the difficulty in handling the liquid phase in the context of sample surface preparation and the subsequent X-ray excitation and electron detection. In the present paper we present preparation methods which we have developed to monitor with electron spectroscopy the status of electrochemical surfaces, and the particular application to interfacial chemistry involving nanostructured transition metal oxide surfaces.

1. B. O'Regan and M. Grätzel, *Nature(London)*, **353**, 737 (1991)
2. A. Hagfeldt, N. Vlachopoulos and M. Grätzel, *J. Electrochem. Soc.*, **141**, L82 (1994)
3. L. Kavan, K. Kratochilova, and M. Grätzel, *J. Electroanal. Chem.*, **394**, 93 (1995)

**DISTRIBUTION OF THERMODYNAMIC PROCESSES  
CONTROLLING (NANO)CRYSTALLIZATION OF METALLIC GLASSES**

*K. Kristiakova and P. Svec*

Institute of Physics, Slovak Academy of Sciences, Dubravská cesta 9,  
842 28 Bratislava, SLOVAKIA <fyzikris@savba.sk>

A typical feature of modern materials, such as amorphous alloys, nanocrystal-formers, etc., is their metastable state which generally has to be stabilized or suitably controlled in order to obtain desired structure and properties of these materials. Alternatively, the knowledge of the processes controlling thermal and time stability of these materials and their transition to crystalline state provides vital information for detailed determination of thermodynamics and for identification of microstructural processes taking place during phase transitions and structural changes in general.

The methods of evaluation of thermodynamic processes during phase changes usually consist of the determination of either a single value of activation energy or of a spectrum of activation energies with an a-priori prescribed distribution, e. g. classical Arrhenius method, Avrami analysis, activation energy spectrum analysis, etc. On the other hand, results thus obtained indicate that the processes controlling e. g. crystallization of metallic glasses are neither simple nor unique; rather they exhibit a distribution reflecting the physics and thermodynamics of the material and the preparation procedure and are by no means sufficiently described by standard simple theoretical distributions.

A novel approach to this problem lies in the determination of the number of processes and their distributions without postulating the form of the distribution; this result can be achieved by analyzing the phase transition process monitored by changes of suitable physical properties such as specific heat, thermal capacity or electrical resistivity using a numerical Laplace transform method adapted to these purposes.

A theoretical analysis of the problem is presented; the results are applied to obtain the distribution of parameters controlling nanocrystallization of Finemet-based metallic glasses from changes of a suitable physical property.

**CORRELATION BETWEEN MICROSTRUCTURE AND  
SOFT-MAGNETIC PROPERTIES OF FeCuNbSiB BASED ALLOYS**

*A.M. Tonejc<sup>1</sup>, N. Ramšak<sup>2</sup>, A. Prodan<sup>2</sup>, S. Suriñach<sup>3</sup>, M.D. Baro<sup>3</sup> and A. Tonejc<sup>1</sup>*

<sup>1</sup> Faculty of Sciences, Department of Physics, Bijenička c. 32,  
POB 162, 10001 Zagreb, CROATIA

<sup>2</sup> Institute Josef Štefan, Jamova 39, SI-1000 Ljubljana, SLOVENIA

<sup>3</sup> Dep. Física, Universitat Autònoma de Barcelona, E-08193 Bellaterra, SPAIN

Rapid solidification from the melt is currently in wide spread of use to obtain metallic amorphous structures. These amorphous materials have quite interesting properties as soft magnetic materials. Due to their metastable nature, they tend to form different crystalline phases when heated above the crystallization temperature and the soft magnetic properties of these alloys deteriorate drastically after their crystallization. Recently Fe-based soft magnetic materials, consisting of a bcc structure with an ultrafine grain size and produced by controlled crystallization of their rapidly quenched metallic glass precursors, have attracted a great deal of attention from the viewpoints of materials science and new engineering materials.

In this work the influence of different heat treatments on the crystallization behaviour of two soft magnetic alloys  $\text{Fe}_{77.5-x}\text{Cu}_x\text{Nb}_3\text{Si}_{9.5+x}\text{B}_9$  ( $x=0, 4$ ) was investigated using different techniques: TEM, HREM, EDS and STM. From HREM examination some evidence on the grain interface structure and on nucleation and growth process was obtained. For the annealing conditions chosen it appeared that the overlapping of diffusion fields of neighbouring  $\alpha$ -Fe(Si) nano precipitates takes place provoking the impingement of the  $\alpha$ -Fe(Si) grains as a consequence. High resolution STM observations could reveal the presence of Cu and Nb, in the nanocrystalline grain boundaries. The microstructural studies have been correlated with the results obtained by means of X-ray diffraction, differential scanning calorimetry, thermogravimetry analysis under magnetic field and VSM measurements.

---

We thank Dr. G. Herzer, Vacuumschmelze GmbH, for providing the amorphous ribbons. The research reported in this work was partially supported by CICYT (project No. MAT94-0290-C03-01) which is acknowledged. The Autonomous University of Barcelona is also acknowledged for supporting A. Tonejc during her stay at the Department of Physics of UAB in Bellaterra.

---

**SURFACE REACTIVITY OF Ce-RICHED  
NANOPHASE Ce(Zr)O<sub>2</sub> COMPOUNDS**

*Tarja Turkki<sup>1</sup>, Michel L. Trudeau, Mamoun Muhammed<sup>1</sup> and M. Samy El-Shall<sup>2</sup>*

Emerging Technologies, Hydro-Quebec, 1800 Boul. Lionel-Boulet,  
Varennes, Quebec, J3X 1S1, CANADA <trudeaum@ireq.ca>

<sup>1</sup> Materials Chemistry Division, Royal Institute of Technology,  
SE-00 44 Stockholm, SWEDEN.

<sup>2</sup> Department of Chemistry, Virginia Commonwealth University,  
Richmond, VA 23284-2006, USA

Because of the presence of a high number of oxygen surface vacancies, cerium oxide is used commonly as a catalyst. Zirconium doping of cerium oxide was found to improve its thermal stability. A number of studies have revealed that catalytic properties are also improved in cerium oxide when the average crystallite size is decreased in the nanometer range. This improvement was related to an increase in oxygen surface vacancies in nanometer size crystals. In order to further improve materials properties, laser evaporation as well as chemical techniques (co-precipitation and solid state reaction) were used to synthesize nanostructured cerium-zirconium mixed oxides. For these samples, the average crystallite size was found to vary from about 5 nm, for laser evaporated samples, to about 30 nm in the case of solid state reacted materials. The oxygen storage capacity for these materials was found to be maximum for 20% zirconium doping. In this work we present a study of the surface chemical properties as well as reactivity of these different materials. X-ray photoelectron spectroscopy was used to study the chemical surface composition of the different nanostructured powders. After synthesis and oxidation at 600°C the surface Ce was found to be mainly present as Ce<sup>4+</sup> while Zr is present as ZrO<sub>2</sub>. The thermal surface reactivity was investigated using a reaction chamber attached directly to the XPS system. Reduction experiments were performed under a partial Ar-8%H<sub>2</sub> atmosphere between room temperature and 500°C. In this work we present a correlation between chemical surface changes and the oxygen storage capacity of cerium-riched Ce(Zr)O<sub>2</sub> compounds.

### **IDENTIFICATION OF NANOSTRUCTURES AT GRAIN SURFACES IN STANNOUS TUNGSTATE FILMS**

*J.L. Solis<sup>1</sup>, V. Lantto<sup>1</sup>, J. Frantti<sup>1</sup>, L. Häggström<sup>2</sup> and M. Wikner<sup>2</sup>*

<sup>1</sup>Microelectronics and Materials Physics Laboratories, University of Oulu,  
Linnanmaa, FIN-90570 Oulu, FINLAND

<sup>2</sup>Department of Physics, Uppsala University, P.O. Box 530, 75121 Uppsala, SWEDEN

Stannous tungstate,  $\text{SnWO}_4$ , crystallizes in the low-temperature,  $\alpha$ , and high-temperature,  $\beta$ , phases. They are extrinsic *n*-type semiconductors, similarly with the component phases  $\text{SnO}_2$  and  $\text{WO}_3$ , and also gas-sensitive oxides. The electrical conductivity of these oxides changes with concentration of various gas components in the ambient atmosphere that is the basis for gas sensing with the semiconductor gas sensors. However, in contrast to  $\text{SnO}_2$  that is the most common oxide semiconductor in gas sensors, tin appears in the divalent form,  $\text{Sn}^{2+}$ , in both  $\alpha$ - and  $\beta$ -structures of stannous tungstate. The easy oxidation of  $\text{Sn}^{2+}$  into the  $\text{Sn}^{4+}$  form makes possible a simple nanostructuring of the grain surfaces in gas-sensitive  $\text{SnWO}_4$  films by various heat treatments in oxygen containing atmospheres. It is then possible to tailor the gas-sensing properties of the films by different nano-scale phase structures at the grain surfaces in the films.

In our case, the size of different nanophases at the grain surfaces from the oxidation of  $\text{Sn}^{2+}$  into the  $\text{Sn}^{4+}$  form has been below the detection limit of x-ray diffraction. Therefore, we have used  $^{119}\text{Sn}$  Mössbauer (and also NMR) spectroscopy together with Raman spectroscopy as 'local' probes for the identification of the nanophases. Mössbauer spectroscopy (similarly with NMR), especially, as a very local probe for tin atoms gave valuable information of the nanophases in both  $\alpha$ - and  $\beta$ - $\text{SnWO}_4$ .

$\alpha$ - $\text{SnWO}_4$  thin films were prepared by reactive *dc* and *rf* magnetron co-sputtering of Sn and W, respectively, and screen-printing technique was used to fabricate thick films of both  $\alpha$ - and  $\beta$ - $\text{SnWO}_4$  powders. Conversion electron Mössbauer spectra (CEMS) were measured from sputtered thin films and Transmission Mössbauer spectra from stannous tungstate powders, which were used in the screen printing of the thick films. CEMS gives information, which is more surface sensitive.

**SELF-DIFFUSION IN HIGH-DENSITY NANOCRYSTALLINE Fe**

*Hisanori Tanimoto, Paul Farber, Roland W, rschum and Hans-Eckhardt Schaefer*

Institut für Theoretische und Angewandte Physik, Universität Stuttgart,  
Pfaffenwaldring 57, D-70550 Stuttgart, GERMANY  
<tanimoto@itap.physik.uni-stuttgart.de>

Fast atomic diffusion in nanostructured materials is both of interest for the study of the interfacial structures and of importance for the macroscopic properties as superplasticity. A recent  $^{59}\text{Fe}$  diffusion study suggests that  $^{59}\text{Fe}$  diffusivity in high-density n-Pd is slightly higher than that expected for the grain boundary diffusion by extrapolating high-temperature data for polycrystalline Pd. For further understanding of the diffusion phenomena in n-metals, we have carried out  $^{59}\text{Fe}$  self-diffusion measurements on high-density n-Fe.

Ultra-fine powders prepared by the gas condensation method are compacted at about 400 K with pressures of about 3 GPa in vacuum ( $10^{-7}$  Torr) yielding disks with a diameter of 8 mm and a thickness of about 0.15 mm. The density of the n-Fe disks measured by Archimedes method is 91 - 96 % of the polycrystalline Fe value reported and the mean grain size estimated from x-ray diffraction peak broadening is 19 - 38 nm.. The penetration depth profiles of the  $^{59}\text{Fe}$  tracer observed for high-density n-Fe at temperatures from 450 to 500 K are similar to those reported for  $^{59}\text{Fe}$  in high-density n-Pd. The temperature dependence of the self-diffusion coefficient determined by assuming a type C diffusion well agrees with the extrapolation of the high temperature data for the conventional grain boundary diffusion in polycrystalline Fe, suggesting that the effective activation enthalpy of self-diffusivity in high-density n-Fe is similar to that of the conventional grain boundary diffusion. Meanwhile, a concurrent grain growth of high-density n-Fe is found during diffusion annealing. It is considered that the structure of grain boundaries of high-density n-metals in the diffusion experiments resembles that of conventional grain boundaries in polycrystalline metals.

**THERMAL EVOLUTION OF BALL MILLED NANOCRYSTALLINE IRON**

*E. Bonetti, L. Del Bianco, L. Pasquini and E. Sampaolesi*

Dipartimento di Fisica, Università di Bologna and Istituto Nazionale per la Fisica della Materia, Viale Berti Pichat 6/2, I-40127 Bologna, ITALY <bonetti@df.unibo.it>

Pure iron powders have been ball milled in a vibratory mill down to about 10 nm crystallite size. The thermally induced structural evolution of the milled powders has been studied by a combination of X-ray diffraction (XRD), mechanical spectroscopy and differential scanning calorimetry (DSC) measurements.

The XRD investigation has been carried out on the as-milled powders and on powders previously subjected to 1-hour thermal treatments at selected temperature in the 300-900 K temperature range. The spectra have been analysed through the Warren-Averbach method and detailed information on the structural relaxation of the interfaces and on the grain growth process have been obtained. In particular, it has been found that the internal stress relaxes mainly between 570 and 620 K whereas a substantial increase in the mean grain dimension and a marked broadening of the grain size distribution occur at higher temperatures.

A good correlation with elastic modulus, internal friction and DSC measurements, performed on the as-milled powders as a function of the increasing temperature, has been established.

Moreover, in order to study the influence of the milling conditions on the structural parameters (including strain and grain size distribution) of the resulting nanocrystalline powders and on their subsequent structural evolution, similar experiments have been carried out on iron powders milled down to a comparable value of mean grain size, but in a planetary mill. Preliminary interesting results are presented.

**LOW-TEMPERATURE ISOTHERMAL SINTERING AND  
MICROSTRUCTURAL CHARACTERIZATION OF NANOCRYSTALLINE  
ZIRCONIA CERAMICS USING SMALL ANGLE NEUTRON SCATTERING**

*U. Betz<sup>1</sup>, A. Sturm<sup>1</sup>, J.F. Löffler<sup>2</sup>, W. Wagner<sup>2</sup>, A. Wiedenmann<sup>3</sup>, H. Hahn<sup>1</sup>*

<sup>1</sup> Darmstadt University of Technology, Department of Materials Science,  
Thin Films Division, Petersenstr. 23, 64287 Darmstadt, GERMANY  
*<hhahn@hrzpub.tu-darmstadt.de>*

<sup>2</sup> Paul Scherrer Institute, CH-5232 Villigen PSI, SWITZERLAND  
*<Werner.Wagner@psi.ch>*

<sup>3</sup> Hahn Meitner Institute, Glienicker Str. 100, D-1000 Berlin 39, GERMANY

Nanocrystalline powders of zirconia, yttria and alumina were synthesized by inert Gas Condensation and Chemical Vapor Condensation. Compacted samples of pure ZrO<sub>2</sub> and dispersion mixed ZrO<sub>2</sub> + 14 wt.% Al<sub>2</sub>O<sub>3</sub> and 5 mol% Y<sub>2</sub>O<sub>3</sub> + ZrO<sub>2</sub> were pressureless sintered in vacuum at 1100° C (0.4 T<sub>m</sub>) for 1, 2, 4 and 10 hours. Nearly full densities have been achieved in all of the three compositions with average grain sizes not exceeding 100 nm. Very small grain sizes of zirconia (< 30 nm) have been found for the composite due to a homogeneous distribution of alumina-phase particles hindering grain coarsening by pinning of the grain boundaries.

Complementary to X-ray diffraction and scanning electron microscopy, the microstructural evolution of the n-ceramics was investigated by small angle neutron scattering. Irregularities during the densification of monoclinic zirconia were verified by the scattering curves and attributed to effects due to phase transformation. From the quantitative analysis of the scattering data pore-size-distributions of the materials were obtained.

**LOCAL STRUCTURE IN NANOCRYSTALLINE ZIRCONIA**

*Markus Winterer and Vladimir Srdic*

Thin Films Division, Materials Science Department, Darmstadt University of  
Technology, Petersenstr. 23, D-64287 Darmstadt, GERMANY

Nanocrystalline materials are heterogeneously disordered due to atoms in particle surfaces and interfaces. Properties, for example ionic conductivity or plastic deformation behavior of nanocrystalline zirconia, depend on the local structure. EXAFS spectroscopy provides information on local structure independent of the degree of disorder.

Combining EXAFS spectroscopy with Reverse Monte Carlo (RMC) modeling we are able to extract pair distribution functions from the experimental data and supply structural models consistent with the experiments. Data analysis by RMC is model free, independent of the degree of disorder, uses the complete EXAFS spectrum and is not obstructed by anharmonic potentials, asymmetric or broad distribution functions. Therefore, EXAFS and RMC provide unbiased information on the local structure. Pair distribution functions and structural models determined are directly comparable to the results of other experimental or theoretical methods such as neutron scattering or molecular dynamics.

Results are discussed for powders and sintered ceramics of different grain sizes and origin, i.e. synthesized by Inert Gas Condensation and Chemical Vapor Synthesis and compared to neutron diffraction results.

**THE DOMINANCE OF STRESS ANISOTROPY ON GIANT  
MAGNETORESISTANCE IN NANOSTRUCTURED  $\text{La}_{0.7}\text{Mn}_{1.3}\text{O}_3$  FILMS**

*S.I. Khartsev, P. Johnsson and A.M. Grishin*

Department of Condensed Matter Physics, Royal Institute of Technology  
S-100 44 Stockholm, SWEDEN

Thickness dependence (over the range  $d = 400 - 90$  nm) of the magnetoresistance has been studied in the self-doped  $\text{La}_{0.7}\text{Mn}_{1.3}\text{O}_3$  films. Films have been deposited by dc-magnetron sputtering from the stoichiometric ceramic target onto the single crystal  $\text{LaSrGaO}_4$  substrates. Fabricated films have been found to be highly c-axis oriented with strong texture in the film plane. On the cleaved substrates ultrathin manganite film experiences the Volmer-Weber island growth, matches to the substrate crystallographic facets. Comprehensive XRD analyses revealed strong effects of the strain in ultrathin perovskites. Due to the strain the giant magnetoresistance peak of the ferromagnetic phase transition occurs at low temperatures and depends on the film thickness. Coalescence of separated islands on the cleaved substrates results in stress anisotropy and strong anisotropy of transport characteristics in ultrathin perovskites. With further deposition coalesced particles start to grow coherently, film changes c-axis orientation, strain decreases and film structure approaches to the bulk material. This results in ferromagnetic transition temperature increase, while the magnetoresistance in-plane anisotropy disappears. Full set of the experimental data has been well explained in the spin-polaron model of magnetotransport of doped perovskites.

### HIGH RESOLUTION STUDIES OF METALLIC NANOCRYSTALLINE MATERIALS

*P.J. Warren, F. Niu, M. Gögebakan, C. Weston, G.D.W. Smith and B. Cantor*

Department of Materials, University of Oxford, Parks Road, Oxford OX1 3PH, UK  
< paul.warren@materials.ox.ac.uk >

This paper will provide an overview of some current work in the Department of Materials at Oxford University on the characterisation of nanostructured materials.

Current projects include the study of amorphous and nanocrystalline materials produced by melt-spinning, sputter deposition and electrodeposition. In each case systematic variation of the process parameters was used to control the size, shape and distribution of the nanocrystalline product. The materials have been characterised by both x-ray diffraction and direct microstructural observations using high resolution electron microscopy and three-dimensional atom probe microanalysis.

A series of Al-Y<sub>x</sub>-Ni<sub>15-x</sub> amorphous/nanocrystalline alloys, of interest for high strength applications, have been produced by melt spinning. These materials typically form a fine distribution of 10-50nm α-Al nanocrystals during thermal ageing. The crystallisation behaviour has been characterised by DSC and the microstructural evolution observed during in-situ heating in the TEM. Atom probe measurements show the strong rejection of solute from the growing Al particles, forming a local enrichment of Y around the particles of 1-2nm in extent. This is thought to limit the particle size.

The opto-electronic properties of co-sputter deposited Si-Ag and Si-Al nanocomposite thin films have potential applications in optical sensors and gratings. As-deposited films consist of nano-sized Ag or Al particles embedded in an amorphous silicon matrix. The size of the particles is controlled by the composition, processing and heat treatment. In this way, the particle size can be used to tailor the optical and electrical properties such as interfacial plasma resonance and electrical resistivity.

More recently, we are starting to investigate the use of pulsed electrodeposition to form low-porosity deposits of nanocrystalline nickel and nickel alloys. Electrodeposition can be used to form both coatings and net-shape bulk products. Field ion microscopy is being used to observe the atomic structure of the nanocrystalline deposits and the size and shape of individual grains. Atom probe microanalysis is being used to identify the nature and distribution of impurities, particularly those segregated to the grain boundaries.

**MICROSTRUCTURAL EVOLUTION DURING MECHANICAL ALLOYING  
OF SUPERSATURATED SOLID SOLUTIONS**

*T.F. Grigorieva<sup>1</sup>, S.V. Tsybulya<sup>2</sup>, S.V. Cherepanova<sup>2</sup>, G.N. Kryukova<sup>2</sup>, V.V. Boldyrev<sup>1</sup>*

<sup>1</sup> Institute of Solid State Chemistry, Kutateladze 18, 630128 Novosibirsk, RUSSIA

<sup>2</sup> Boreskov Institute of Catalysts, Lavrentiev avenue 5, 630090 Novosibirsk, RUSSIA

The investigation of MA process in Ni-In, Ni-Bi, Cu-In, Cu-Sn systems showed that intermetallic compounds were formed at initial stage of process and then they interacted with metal-solvent resulting in the formation of supersaturated solid solutions [1]. The purpose of this work is study of microstructural evolution during this process. The object investigation was Ni-In system.

According to TEM results samples subjected to mechanochemical treatment possess the developed defect structure. There are numerous plane defects which are characteristic of the intermetallic phase. After treatment for 10 min the supersaturated solid solution formed, the main types of defects in the structure of alloy sample are stacking faults and microstrains. Prolonged treatment for 20 min leads to the increase of stacking faults; microstrains in this case are equally distributed over the volume of the isolated alloy particle.

The model diffraction patterns were calculated using program [2]. In this program the structure of crystal of distorted close packing can be simulated by the sequence of biperiodic layers with randomly distributed stacking faults and microstrains. Number of layers, their longitudinal size, density of stacking faults and average value of the random interlayer translations (that characterize the microstrains) are the variable parameters of the model. It was shown that the experimental and simulated X-ray powder diffraction patterns obtained with different models of the real structure of the sample treated for 10 min. Best fitting is realized by using a particle possessing the anisotropic size, high density of the microstrains and some concentration of the stacking faults. Long-range order into 1.1.1. direction of the close packing is better than of 1.1.0. direction. Size of coherent scattering domains and microstrain density indicate on this fact. At raising the time of mechanochemical treatment sizes of the coherent scattering domains increase a little bit whereas the microstrain density preserves. According to TEM data increase of the degree of long-range ordering seems to be associated with more regular distribution of the microstrains in the particle volume.

1. Grigorieva T.F., Barinova A.P., Ivanov E.Yu., Boldyrev V.V. «ISMANAM'96» (Proc. of Int. Symp. on metastable mechanically alloyed and nanocrystalline materials), Rome, Italy, 1996, p. 577-582.
2. Cherepanova S.V., Tsybulya S.V. 5<sup>th</sup> European Powder Diffraction Conference, Parma, Italy, 1997, p. 60.

**FORMATION AND BONDING OF PLATINUM NANOPARTICLES  
CONTROLLED BY HIGH ENERGY BEAM IRRADIATION***BingShe XU and Shun-ichiro TANAKA*

Tanaka Solid Junction Project, ERATO, Japan Science and Technology Corporation  
1-1-1 Fukuura, Kanazawa-ku, Yokohama 236, JAPAN

The formation and bonding of Pt nanoparticles controlled by high energy beam irradiation were investigated. Pt nanoparticles were prepared on amorphous carbon film by Ar<sup>+</sup> beam sputtering. The size of Pt nanoparticles ranges from 1 to 6 nm in diameter. It is clear that the size of Pt nanoparticles relates to the ion acceleration voltage, the ion beam current and the irradiation time. The Pt nanoparticle size increased at a high acceleration voltage and large ion beam current for the long irradiation times. On the other hand, the migration and bonding behaviors of these Pt nanoparticles were investigated using HRTEM by electron beam irradiation intensity of  $1-3.3 \times 10^{20}$  e/cm<sup>2</sup>·sec, on a stage at room-temperature. It was found that the adjacent Pt nanoparticles came into contact and bonded with necking. The structures of grain boundaries formed by bonding range from  $\Sigma 3$  to  $\Sigma 17b$ , with  $\Sigma 3$  boundaries being preferentially formed. The coalescence of several grains into a single grain through boundary and defect migration was induced by additional electron beam irradiation.

**ON MICROWAVE ABSORPTION PROPERTY OF SPHERICAL NANO-IRON POWDERS**

Boxiong Qin<sup>1</sup>, Gang Liu<sup>1</sup>, Dongsheng Gao<sup>2</sup> and Chongbin Pei<sup>3</sup>

<sup>1</sup> Dept. of Welding , College of Mechanical Eng., Tianjin University,  
Tianjin 300072, CHINA

<sup>2</sup> Zhenyuan Nanomaterials Engineering Inc., Weifang 261041, Shandong, CHINA

<sup>3</sup> Dept. of Mechanical Eng., Northwestern Polytechnical University,  
Xi'an 710072, Shaanxi, CHINA

The dynamic composite permeability and the microwave absorption loss of the spherical nano-Iron powders are measured in the frequency range of 8 GHz to 18 GHz. In this frequency range the imaginary part of magnetic permeability  $\mu_i''(\omega)$  is very low. With the frequency rising  $\mu_i''(\omega)$  decreases, nevertheless, the microwave absorption loss increases. The absorber consisting of nano-Iron powders (RAM), dispersing agent and epoxy resin binder is sprayed on the surface of duralumin plate, size 180mm×180mm. It is shown that the values of  $\sigma$  depend on the nanoparticle size, the coating of particles and the loading of nano-Iron powders dispersed in epoxy resin. If the loading is given more than 5g the sprayed surface of the testing piece reflects the microwave. It is found out that the nanoparticles with the microconstruction similar to the carbonyl Iron powders have good absorption property (<-5dBsm) in the frequency range of 10-18GHz.

**ANOMALOUS OPTICAL AND ELECTRIC PROPERTIES  
IN ASSEMBLIES OF NANOPOROUS COMPOSITES***Lide Zhang*

Institute of Solid State Physics, Chinese Academy of Sciences, Hefei 230031, CHINA

The latest progression of study on optical and electric properties of assemblies of nanoporous composites in our laboratory is reviewed. The main contents are as follows: (1) Enhancement effect of photoluminescence in assemblies of nano-ZnO particles/silica aerogels is observed. The luminescence intensities of these assemblies are 10~50 times higher than that of nanostructured ZnO bulks. (2) Intense green luminescence associated with the doping of  $\text{Al}^{+3}$  ions in nanoporous silica is systematically investigated. (3) Large red shifts of optical absorption edge from about 200 to 500 nm are found in assemblies of nano-Ag particles/nanoporous silica. The red shift amplitude becomes large with increasing the nano-Ag amount. The Energy gap,  $E_g$ , of these assemblies can be described by the energy gap expression of semiconductors:  $\alpha_0hv=A(hv-E_g)^2$ . (4) Reversible transparent to opaque changes occurs in nano-Ag particles/nano-porous silica with altering the humidity and temperature. In dry air at room temperature, the sample is transparent (shallow yellow). When the relative humidity is large that 65% the sample becomes opaque (black). After heating the sample at 580 K for 10 min, the sample is converted from the opaqueness to the transparency. (5) The negative resistance-temperature coefficient ( $\alpha$ ) and the electric conduction ( $\sigma$ ) of nano-Ag particles/nanoporous carbon solid can be modulated by variations of the diameter and the doping amount of Ag particles, respectively. When the Ag particle diameter is smaller than 5 nm, the absolute value of  $\alpha$  becomes large. With the increase of the doping amount of Ag particles,  $\sigma$  rises. The mechanisms of the above-mentioned anomalous optical and electric properties were discussed in detail.

**EFFECT OF SURFACE COATINGS AND MESOPOROUS CONFINEMENT  
ON PHOTOLUMINESCENCE OF NANO-ZnO PARTICLES**

*C.M. Mo<sup>1</sup> and L.D. Zhang<sup>2</sup>*

<sup>1</sup> Department of Materials Science and Engineering, University of Science and Technology of China, Hefei 230026, CHINA

<sup>2</sup> Institute of Solid State Physics, Chinese Academy of Sciences, Hefei 230031, CHINA

Nano-ZnO particles were prepared by pyrolysis of wrapped Zn(OH)<sub>2</sub> with polyethyleneglycol (PEG). Composites of nano-ZnO particles/nanoporous silica aerogels were obtained by pyrolysis of Zn(OH)<sub>2</sub> in nanopores of silica aerogels. For the above-mentioned two kinds of materials the enhancement effect of luminescence was observed. The luminescent intensity of nano-ZnO particles with coating of PEG is 3~4 times higher than that without coating. This luminescence enhancement phenomenon becomes much notable in composites of nano-ZnO particles/nanoporous silica. 50 times higher luminescence intensity in these composites was found in comparison with that in nanostructured ZnO bulks. The reasons of luminescence enhancement were discussed.

**PHOTOLUMINESCENCE OF DISPERSED  
NANO-Ce DOPED SILICA PARTICLES**

*Cai Weiping and Zhang Lide*

Institute of Solid State Physics, Academia Sinica, Hefei, 230031, CHINA

In this work, we investigated the luminescence properties of dispersed nano silica particles containing cerium. Nano-sized silica particles with Ce (molar ratio of Si:Ce=100) were put into the pores of pre-formed porous silica host by sol-gel technique, soaking and drying, and the assembly system of Ce-doped silica particles and the porous silica host was thus formed. The samples were characterized with the help of isothermal N<sub>2</sub> sorption experiment, and luminescence measurement was conducted over wavelength from 200 nm to 800 nm with excitation wavelength 250 nm.

It has been shown that the Ce-doped silica particles are mainly located into the pores with less than 7 nm in diameter; the distance between the adjacent particles is more than 600 nm along with channels of the host, indicating that the interaction between Ce-doped particles can be ignored. There exist two luminescent peaks at about 350 nm and 700 nm for both assembly system and bulk Ce-doped sample. The ratio of the integrated intensity for the two peaks is about 2. Both peaks originate from the same mechanism or the transition between 5d and 4f levels of Ce<sup>3+</sup>. What is more important is that the luminescence intensity for the nano Ce-doped silica is about 50 times higher than that of the bulk Ce-doped sample, which is attributed to the surface effect of the particles and the disappearance of the interaction between particles. Finally, Detailed analysis and discussion were made.

**FERROELECTRIC PHASE TRANSITIONS  
IN MATERIALS EMBEDDED IN POROUS MEDIA**

*E.V. Colla, A.V. Fokin, E.Yu. Koroleva, Yu.A. Kumzerov, B.N. Savenko and S.B.  
Vakhrushev*

A.F.Ioffe Phys.-Tech. Institute, 194021 St.Petersburg, RUSSIA

The physical properties of the dispersed solids are essentially different from those of the bulk materials. Particularly size effects result in the drastic changes of the phase transition features. But there is now the deficiency of the reliable experimental data for the really small particles (with diameter of about 10 nm and less) due to the difficulty of obtaining such nanoparticles.

We propose the method that permits to fabricate the large quantities of ferroelectric nanoparticles with diameters that may be varied from about 100 nm to 3-4 nm. This method is based on the embedding of the ferroelectric material into the porous medium from a melt, as well as from a water solution. Advantage of this method is the fact that it excludes any chemical processes during the sample preparation and thus it provides the possibility to produce the nanoscale fine particles by breaking down the bulk solids. The experiments were performed on "classical" ferroelectrics - NaNO<sub>2</sub>, KH<sub>2</sub>PO<sub>4</sub> (KDP) and Rochelle salt, embedded into the pores of artificial opals (strictly speaking we used not the opals but the pigs designed for jewelry opal production) and porous glasses (like Vycor one). Opal is composed of close packed amorphous SiO<sub>2</sub> spheres with a diameter of 250 nm. Such spheres packing produces two kind of "holes" between the spheres, the dominating pore size is about 100 nm and the secondary of 20 nm. It should be mentioned that using opal as porous matrix allows creating the spatially regular microparticles structure. The porous glasses with 7nm average size of pores were used. The volume amount of the ferroelectric material was about 30% of sample volume.

We present the preliminary experimental dielectric and neutron scattering results obtained on these materials. The low frequency dielectric measurements were carried out on a computer controlled dielectric spectrometer operating in frequency domain mode for NaNO<sub>2</sub>, KDP and Rochelle salt containing samples. The temperature dependencies of dielectric permittivity, corresponding to ferroelectric phase transition in dispersed materials, demonstrate that positions and magnitudes do not depend on measurement frequency (there were used three frequencies 1, 10 and 100 Hz). The significant shift of transition temperature from the bulk value for KDP particle samples was observed and KDP ferroelectric temperature dependency on the particle size was determined. The neutron scattering measurements on NaNO<sub>2</sub> were used to obtain the information on the critical temperature and the transition region smearing. The transition region reaches some tens of degrees and this behavior may be related to the effect of the fluctuations.

This work was supported by the RFFI grant N97-02-18267 and the Grant N 2-026/4 of the Programme «Physics of Solid State Nanostructures».

**MAGNETOIMPEDANCE EFFECT  
IN NANOCRYSTALLINE  $\text{Fe}_{92-x}\text{Zr}_7\text{B}_x\text{Cu}_1$  ( X = 6, 8, 10 ) ALLOYS**

*Heebok Lee, Yong-Kook Kim<sup>1</sup>, Taik-Kee Kim<sup>1</sup>, Seong-Cho Yu<sup>2</sup>, and Kyung-Seop Kim<sup>2</sup>*

Dept. Phys. Education, Kongju Nat'l. Univ., Kongju 314-701, KOREA

<sup>1</sup>Division of Material Sci., Chungnam Nat'l. Univ., Taejon 305-764, KOREA

<sup>2</sup>Dept. Phys., Chungbuk Nat'l. Univ., Chongju 361-763, KOREA

The magnetoimpedance of  $\text{Fe}_{92-x}\text{Zr}_7\text{B}_x\text{Cu}_1$  (X = 6, 8, 10) alloys have been measured to investigate the influence of the structural changes in the crystallization process as well as the changes of magnetic properties such as permeability, coercivity, magnetic anisotropy, etc. after thermal treatment. The frequency of magnetoimpedance measurement was ranging from 100 kHz to 10 MHz, and the current was fixed at 10 mA for all measurements. Annealing was performed at various temperatures (350°C, 450°C, and 550°C for 1 hr, respectively) with and without an applied magnetic field (5 kOe). The maximum magnetoimpedance ratio coincides with the softness of magnetic properties of thermally treated samples. The field annealing does not contribute to improve the magnetoimpedance effect in these nanocrystalline alloys. We have found that the changes of permeability as a function of the external DC magnetic field are mainly responsible for the magnetoimpedance effect.

**OPTICAL SPECTRA OF NANOCRYSTALLINE DIAMOND**

*V.S.Gorelik, A.V.Igo, S.N.Mikov and I.P.Puzov*

Ulyanovsk State Univer. 42 L.Tolstogo Str., Ulyanovsk, RUSSIA <igo@fesc.mv.ru>

The paper concerns Raman and two-photon excitation investigation of nanocrystalline diamond powders obtained by explosion synthesis. During experiments Raman spectra of three types of nano-diamonds obtained by different groups of technologists were recorded. To ensure experimental samples from over-heating and destruction they were prepared by immersing diamond powder in KBr matrix.

The experimental data shows a size-dependent broadening of fundamental line ( $1332\text{ cm}^{-1}$ ) and its shift to lower frequencies. Samples with average size of diamond crystallites about  $40\text{ \AA}$  show large broadening of fundamental line up to  $46\text{ cm}^{-1}$ . We note that intensities of luminescent background and Raman line increase simultaneously and reach their maximum during several hours.

The experimental data was compared with spectra calculated using model of "phonon confinement". To explain discrepancy between our experiments and model we have made our own phenomenological consideration of photon-phonon interaction in confined area. In contrast with "phonon confinement" model, our calculations were made without *a-priori* determined damping of phonon wave functions. Comparison of two models and experiments, ours and independent, shows that our model describes experimental results better when average size of particles is less than  $60\text{ \AA}$ .

We obtained luminescent spectra of samples, described above, in the range 400-500 nm using two-photon excitation technique with Cu-vapor-laser. We obtained two luminescent lines corresponding to well-known impurity centers N2 and N3 in diamond (360 and 440 nm respectively). We have made estimations the electron-phonon interaction energy (Huang-Rhys factor) for N2 impurity center. Its value was  $\approx 0.5$ , meanwhile, in bulk diamond this luminescence band has  $\approx 10$ .

### TRANSITION DYNAMICS IN NANOORDERED RELAXOR FERROELECTRICS

*E.A.Rogacheva<sup>1,2</sup>, S.G.Lushnikov<sup>2</sup>, I.G.Siny<sup>2,3</sup>, R.S.Katiyar<sup>3</sup>*

<sup>1</sup> Department of Electronics, Royal Institute of Technology, Electrum 229,  
SE-164 40 Kista, SWEDEN <katya@ele.kth.se>

<sup>2</sup> A.F.Ioffe Physical Technical Institute, Russian Academy of Sciences, 26  
Polytekhnicheskaja, 194021 St.Petersburg, RUSSIA <sgl@slush.ioffe.rssi.ru>

<sup>3</sup> Department of Physics, University of Puerto Rico, San Juan,  
PR 00931, USA <rkatiyar@upracd.upr.clu.edu>

Relaxor ferroelectrics or ferroelectrics with diffuse phase transitions form a specific group of challenging compounds which unexpected physical properties are tailored by order-disorder in the ion distribution. The whole ordering in relaxors is usually prevented by different reasons, such as the charge compensation, the random ion distribution, defects and others, whereas nanoordered regions seem to be a characteristic feature of such materials.

Raman scattering was used to study two model relaxor ferroelectrics,  $\text{PbMg}_{1/3}\text{Nb}_{2/3}\text{O}_3$  (PMN) with the 1:2 stoichiometric composition of  $\text{Mg}^{2+}$  and  $\text{Nb}^{5+}$  ions in the oxygen octahedrons and  $\text{PbSc}_{1/2}\text{Ta}_{1/2}\text{O}_3$  (PST) with the 1:1 stoichiometric composition of  $\text{Sc}^{3+}$  and  $\text{Ta}^{5+}$  ions. In spite of a different stoichiometric ratio the Raman spectra of both materials are consistent with the  $\text{Fm}3\text{m}$  space symmetry which implies the existence of similar 1:1 ordered clusters at least in nanoscale regions. The spectra show some anomalous features in the temperature range preceding a ferroelectric state, namely a broad central peak (e.g. an anomalous additional light scattering in a low frequency region) appears in PMN and a complex structure develops from the initially singlet  $\text{A}_{1g}$  mode in PST. Those phenomena are considered as the dynamic features in course of evolution of the relaxors to a ferroelectric state. Raman scattering gives evidence of a preceding phase in both PMN and PST. The selection rules for Raman scattering occur to be broken down in this preceding phase, so some information from the Brillouin zone appears in the spectra, namely a critical contribution to the broad central peak in PMN and to the initial singlet  $\text{A}_{1g}$  mode in PST. One should note that our studies showed preliminarily the existence of a central peak in PST as well as some traces of an additional structure around the  $\text{A}_{1g}$  mode in PMN. The existence of a special preceding phase is considered as a distinctive characteristic of the transition dynamics in relaxor ferroelectrics with ordered nanoscale clusters. The short-range-order arrangement prevents a ferroelectric transition from spreading throughout the sample volume if there is no additional effect of an external electric field. However, Raman scattering without any electric field is able to reveal a hidden phase transition dynamics in materials consisted of principal nanoscale regions.

Supported in part by DE-FG02-94ER75764 and NSF-OSR-9452893 Grants and RFBR Grant No.96-02-17859.

**NOVEL PROPERTIES OF IRON OXIDE NANOSYSTEMS AFFECTED  
BY INTERFACIAL INTERACTIONS**

*I.P. Suzdalev, Yu.V. Maksimov, V.N. Buravtsev and N.N. Semenov*

Institute of Chemical Physics of Russian Academy of Sciences,  
Kosyginia 4, Moscow 117977, RUSSIA <e-mail: suzdalev@chph.ras.ru>

New properties of the matter may appear when nanosystem is composed from nanoclusters: Several problems must be solved in order to obtain and describe these materials: 1) choice of appropriate methods of synthesis of nanosystems, 2) distinction of intercluster interactions, 3) selection of adequate methods for studying nanosystems.

The present report deals with the unusual properties of ferric oxide nanoclusters such as intercluster and intracluster dynamics, first and second order magnetic phase transitions. Nanoclusters are obtained by thermal (topochemical) decomposition of inorganic compounds and by microcapsulation of nanoclusters in pores of polymeric matrices. The study of nanosystems and the distinction of intercluster interactions are performed by Mössbauer spectroscopy, atomic force microscopy and thermodynamic analysis.

Two types of iron oxide nanoclusters are obtained: 1) weakly interacting gamma-ferric oxide nanoclusters with sizes  $d=1\text{-}5$  nm; 2) nanoclusters with  $d=10\text{-}50$  nm showing strong interfacial cluster-cluster interaction. Cluster microcapsulation gives rise to either non-interacting or interacting nanoclusters isolated in pores of hydrophobic (polysorbs) and hydrophilic sulphonated exchange resins with different pore sizes.

The size-dependent atomic dynamic properties of nanosystems are distinguished: an increase of intracluster atomic mobility, a decrease of cluster melting point with the decrease of cluster size, an appearance of the peculiar solid-liquid state in nanoclusters, an intercluster dynamics in pore described by the restricted Brownian diffusion model.

First order magnetic phase transitions with jump-like drop of magnetization are studied for strongly (interfacial) interacting gamma-ferric oxide nanoclusters ( $d=10\text{-}20$  nm) modified by carbon inclusion and for ferrihydrite clusters ( $d=1\text{-}3$  nm) isolated in pores of polysorb. For nanoclusters, possessing magnetostriction and compressibility, the first and second order magnetic phase transitions are interpreted in terms of thermodynamic model. For isolated ferric oxyhydroxide nanoclusters supported on sulphonated exchange resin, a shift in critical temperature of magnetic phase transition in clusters by 3-4 K is observed upon hydration and freezing and treated by thermodynamic analysis.

**COMPARATIVE STUDY OF THE GIANT MAGNETO-IMPEDANCE EFFECT  
IN AMORPHOUS AND NANOCRYSTALLINE GLASS-COVERED WIRES***H. Chiriac, T.-A. v↔ri, and C.S. Marinescu*

Natl. Inst. of R&amp;D for Technical Physics, 47 Mangeron Blvd., 6600 Iași 3, ROMANIA

The giant magneto-impedance (GMI) effect consists of strong changes in the high frequency impedance,  $Z$ , of a magnetic conductor with a small dc magnetic field,  $H_{dc}$ . The strongest GMI effect was observed in low magnetostrictive  $\text{Co}_{68.15}\text{Fe}_{4.35}\text{Si}_{12.5}\text{B}_{15}$  amorphous wires with diameters reduced down to 30 mm by cold drawing [1].

The aim of this paper is to perform a comparative study of the GMI effect in  $\text{Fe}_{73.5}\text{Cu}_1\text{Nb}_3\text{Si}_{13.5}\text{B}_9$  nanocrystalline glass-covered wires and  $\text{Co}_{68.15}\text{Fe}_{4.35}\text{Si}_{12.5}\text{B}_{15}$  amorphous glass-covered wires. The GMI measurements have been performed at frequencies of the driving ac current up to 10 MHz, on both glass-covered samples and samples after glass removal.

The most sensitive GMI response has been observed in  $\text{Fe}_{73.5}\text{Cu}_1\text{Nb}_3\text{Si}_{13.5}\text{B}_9$  nanocrystalline wires after glass removal, which display an MI ratio –  $DZ/Z = [Z(H_{dc} = 0) - Z(H_{dc} = 1 \text{ kA/m})]/Z(H_{dc} = 0)$  – of about 30%, larger than in the case of  $\text{Co}_{68.15}\text{Fe}_{4.35}\text{Si}_{12.5}\text{B}_{15}$  amorphous wires after glass removal (~20%). It is important to note that this value of the MI ratio is comparable to that of cold drawn CoFeSiB amorphous wires with 30 mm in diameter. On the other hand, the MI ratio of CoFeSiB amorphous glass-covered wires reaches to 17%, while in the case of FeCuNbSiB nanocrystalline glass-covered wires it reaches only 5%.

The results are explained on the grounds of local anisotropy distributions, by taking into account the magnetoelastic anisotropy in the case of amorphous wires, and the good soft magnetic properties, i.e. large permeability and reduced coercivity, in the case of nanocrystalline ones. The obtained results reveal the importance of good soft magnetic properties related to a sensitive GMI effect.

[1] L. V. Panina, K. Mohri, K. Bushida, and M. Noda, *J. Appl. Phys.* **76** (1994) 6198.

**FIELD AUTOELECTRONIC EMISSION FROM SUBMICROCRYSTALLINE NICKEL**

*L.R. Zubairov<sup>1</sup>, Yu.M. Yumaguzin<sup>2</sup>, R.Sh. Musalimov<sup>1</sup>, R.Z. Bakhtizin<sup>2</sup>, and  
R.R. Mulyukov<sup>1</sup>*

<sup>1</sup> Institute for Metals Superplasticity Problems of Russian Academy of Sciences,  
Khalturina 39, Ufa 450001, RUSSIA <radik@imspphys.bashkiria.su>

<sup>2</sup> Department of Physical Electronics, Bashkir State University, Frunze 32,  
Ufa 450074, RUSSIA

The submicrocrystalline structure was processed in nickel by severe plastic deformation. The microstructure was studied by transmission electron microscopy. Specific features of an electron structure of the processed samples were studied by a method of field autoelectron spectroscopy.

The samples in the form of foils were prepared by electrochemical polishing for transmission electron microscopy and for field electron spectroscopy they were prepared by electrochemical etching in the form of points. Measurements of field emission of electrons were made under super high vacuum ( $< 10^{-8}$  Pa) conditions in a special set containing an autoelectron projector and a dispersion power analyser with resolution no less than 30 meV. The obtained results for SMC Ni were compared with those for coarse-grained Ni samples.

Severe plastic deformation to the true logarithmic strain value  $e = 7$  results in formation of the SMC structure with a mean grain size of about 0.15  $\mu\text{m}$  and non-equilibrium grain boundaries. Power spectra of autoelectron for SMC samples significantly differ from spectra for coarse-grained samples and the ones calculated in a model of free electrons.

**THE PHOSPHORUS-DOPING EFFECT ON THE PHOTOLUMINESCENCE  
SPECTRA OF NANOSYSTEM SiO<sub>2</sub>:Si FABRICATED  
BY THE ION IMPLANTATION**

*D.I. Tetelbaum, O.N. Gorshkov, M.V. Stepikhova, S.A. Trushin, and K.A. Markov.*

Physico-Technical Research Institute of Nizhnii Novgorod State University,  
Gagarin prosp., 23/3, 603600, Nizhnii Novgorod, RUSSIA <maximov@nifti.nnov.su>

The SiO<sub>2</sub>:Si system (with silicon nanoinclusions) was produced by Si ion implantation into SiO<sub>2</sub> films on silicon substrates (150 keV,  $10^{17}$  cm<sup>-2</sup>). One party of the samples was additionally implanted with phosphorus at  $10^{16}$  cm<sup>-2</sup>. After ion implantation, the annealing at 1000°C (2 hours) was provided. The photoluminescence spectra (PLS) were obtained at 4-300 K for two kinds of the exciting light, namely 351 and 488 nm. It was established that PLS was dependent of the exciting light frequency: the peaks were situated at approximately 600 or 800 nm, respectively. The position of the peaks was essentially independent and their altitudes are only slightly dependent of temperature. The most prominent feature was the strong effect of phosphorus doping on PLS intensities: for the phosphorus-implanted samples, the peaks were several times as high as for the samples without phosphorus implantation. One of the possible explanation is the change of equilibrium filling of levels in the conduction band of the quantum dots that influence on the rate of radioactive transitions.

**FLUORESCENCE STUDY OF NANOCRYSTALLINE YSZ:Eu<sup>3+</sup> POWDERS**

*Yan-qi WANG, Xi-jun WU and Guo-long TAN*

Department of Materials Science and Engineering, Zhejiang University,  
Hangzhou 310027, CHINA <mse\_xjwu@ema.zju.edu.cn>

$\text{Y}_2\text{O}_3$  stabilized cubic  $\text{ZrO}_2$  doped by  $\text{Eu}_2\text{O}_3$ (YSZ:Eu<sup>3+</sup>) powders with an average grain size of 5 nm were synthesized with a co-precipitation method. YSZ:Eu<sup>3+</sup> powders with different average grain sizes were obtained by sintering the above powders at 800, 1000 and 1300°C respectively for 2 hours. Fluorescence spectra were measured under following different conditions: 1. excited with wave length 260 nm at room temperature, and 2. Excited with wave length 330 nm at 77 K. When the grain size of powders decreases fluorescence spectra show that: A. the main peak of 5D0 to 7F2 transition has a red shift, and another peak has a blue shift, B. the relative intensity of 5D0 to 7F1 transition decreases, and C. fluorescence intensity decreases. The results A and B indicate that Eu<sup>3+</sup> energy levels change with grain size. X-ray diffraction show that the crystal parameters of YSZ:Eu decrease with grain size . This is related with the enhanced internal pressure caused by surface stress. The decrease of fluorescence intensity with grain size is attributed to the large number of defects and unsaturated bonds on the surface of nanocrystalline YSZ:Eu.

**OPTICAL PROPERTIES OF THE FERROMAGNETIC SEMICONDUCTORS  
WITH THE PERIODIC NANOSTRUCTURES RODUCED  
BY COHERENT LIGHT BEAMS**

*O.Yu. Semchuk, L.G. Grechko, and V.M. Ogenko*

Institute of Surface Chemistry National Academy of Sciences of Ukraine,  
31 Nauka Avenue, 252022 Kyiv, UKRAINE <er@surfchem.freenet.kiev.ua>

In this paper the light reflection coefficient of the ferromagnetic semiconductor (FMSC) with a periodic nanostructures (superlattices), produced by coherent light beams (CLB) is calculated. It is shown that the presence of a periodic nanostructures will lead to the modulation the light absorption coefficient of the ferromagnetic semiconductors. Let us consider a wide-gap donor-type FMSC with mean carrier density  $n$  in the spin-wave temperature range placed in an external electric field  $F_0 \parallel OZ$ . This front surface  $x=0$  is illuminated by the several CLB's whose vector-potential in the material given as

$$\vec{A}(\vec{r}, t) = \sum_j A_j \cos(\omega t - \vec{k}_j \cdot \vec{r} - \varphi_j)$$

and their frequencies satisfy the inequality

$\bar{\varepsilon} \ll \hbar\omega \ll \varepsilon_g$  ( $\varepsilon_g$  is the energy-gap width,  $\bar{\varepsilon}$  -s the mean carrier energy). Under such conditions the CLB's gives rise to the formation of the periodic nanostructures-superlattices of the electron concentration, electric field strength, electron and magnon effective temperatures. From our calculation following that the presence of the periodic nanostructures (superlattices) will lead to the modulation of the light absorption and reflection coefficients of the FMSC, that could be detected by the changes of the outgoing intensity of the sensing waves passed through and scattered on the FMSC. Having analyzed the light reflection from the surface of the FMSC, we can take information about semiconductor surface conditions, existence of the some admixtures and sets of atoms, adatoms on the surface.

**THERMOELEMOTIVE FORCE IN NANOCRYSTALLINE WIRES***H.Chiriac and F.Barariu*

National Institute of R&D for Technical Physics,  
47 Mangeron Blvd., 6600 Iasi 3, ROMANIA <firuta@phys-iasi.ro>

Although the electrical and magnetic properties of the amorphous and nanocrystalline wires are generally known, there are less information about the thermoelectric properties of these materials. Recently we have reported the appearance of the thermoelectromotive force supplied by an amorphous-crystalline thermocouple for some amorphous materials [1,2].

The aim of this paper is to present some results on the thermoelectromotive force supplied by the junction of a thermocouple which consists of an amorphous wire and a wire in which the nanocrystalline phase have been induced by suitable annealing by Joule effect. This phenomenon has been studied on amorphous  $Fe_{73.5}Cu_1Nb_3Si_{13.5}B_9$  wires obtained by the rotating water quenching method. The results show that during the evolution of the crystallization process, a thermoelectromotive force appear at the ends of the thermocouple, which increases up to 0.8 mV in the nanocrystalline state with respect to the amorphous wire. The complete crystallization of the wire leads to an increase in the thermoelectromotive force up to 2 mV. The thermoelectromotive force of the nano- and crystalline wire are positive with respect to the amorphous one. The evolution of the crystallization process, controlled by means of the dc current and its maintaining duration, is well outlined by the evolution of the thermoelectromotive force, its quantitative determination being a very sensitive method for the study of the crystallization process. Comparative measurements on ribbons and wires having the same composition have been also performed.

- [1] H.Chiriac, F.Barariu, V.Nagacevschi, Jmmm 160 (1996) 239.
- [2] H.Chiriac, M.Sorohan, F.Barariu, J.Phys.D: Appl. Phys. 28 (1995) 831.

**A GAS-SENSING CoO/SiO<sub>2</sub> NANOCOMPOSITE**

*Naoto Koshizaki, Katsuya Yasumoto and Takeshi Sasaki*

National Institute of Material and Chemical Research, 1-1 Higashi,  
Tsukuba, Ibaraki 305-8565, JAPAN <koshizaki@nimc.go.jp>

Using co-sputtering and sol-gel methods, we developed a gas-sensing nanocomposite. CoO-dispersed SiO<sub>2</sub> (CoO/SiO<sub>2</sub>) nanocomposite films reversibly changed their optical transmittance by nitrogen oxide at 350 °C in the wavelength range from 400 to 800 nm. In the films sputtered from a SiO<sub>2</sub> target with CoO pellets on under an Ar atmosphere, cobalt oxide dots 4-8 nm in diameter were observed by a transmission electron microscope (TEM). NO sensitivity increased with increasing Co/Si atomic ratio, indicating that the Co component is an active material for transmittance change. However, after the heat-treatment at 600 °C, no transmittance change by NO was observed for the CoO/SiO<sub>2</sub> film though it still had nanoparticles embedded in a SiO<sub>2</sub> matrix. These results can be explained that the sensing properties are originated not only from the functional CoO nanoparticles which change their optical transmittance but also from nanopores which provide paths for gas molecules. Indeed, NO sensitivity increased with film thickness up to about 1 mm, indicating that the sensing process occurred in the interior of the film. Furthermore the columnar microstructure of the films observed by cross sectional SEM images disappeared along with this heat treatment at 600 °C. CoO/SiO<sub>2</sub> nanocomposite with similar structure having cobalt oxide dots about 10 nm in diameter can be also obtained by sol-gel method using Si(OC<sub>2</sub>H<sub>5</sub>)<sub>4</sub> and Co(NO<sub>3</sub>)<sub>2</sub>•6H<sub>2</sub>O as raw materials. Although this nanocomposite shows transmittance change by NO, the sensitivity was not so large and stable. Furthermore the wavelengths which showed the largest transmittance change in both CoO/SiO<sub>2</sub> nanocomposite films were about 400 nm for that prepared by co-sputtering and 600 nm for that by sol-gel method, respectively. A mechanism of optical transmittance change for co-sputtered CoO/SiO<sub>2</sub> nanocomposite is inferred that the octahedral divalent cobalt ions confined in CoO nanoparticles effectively interact with NO, resulting in the consumption of electronic sites which are involved in the optical absorption process.

**NANOSTRUCTURE AND PHOTOLUMINESCENCE PROPERTY  
OF Si/MgO AND Si/ZnO CO-SPUTTERED FILMS**

*Naoto Koshizaki, Hiroyuki Umebara, Takeshi Sasaki, Umapada Pal\* and  
Toshie Oyama*

National Institute of Materials and Chemical Research, 1-1 Higashi,  
Tsukuba, Ibaraki 305-8565, JAPAN <koshizaki@nimc.go.jp>

\*Instituto de Fisica, Universidad Autónoma de Puebla,  
Apdo. Postal J 48, Puebla, Pue. 72570, MEXICO

Nano-sized silicons, such as porous silicon and silicon nanoparticles, have attracted much attention because of their photoluminescence properties. Si/SiO<sub>2</sub> nanocomposite has been also studied as a new system having nano-sized silicon. The data and mechanism of photoluminescence, however, is still controversial for these systems. We have prepared composite films of Si/MgO and Si/ZnO by co-sputtering method to develop new photoluminescence materials. These composite films were obtained on SiO<sub>2</sub> substrate by sputtering of MgO or ZnO target (100mmf) with Si plates (5.15mm<sup>2</sup>) placed on. The changes in various properties with the increase in the number of Si plates were studied. For the Si/MgO system, while a sputtered MgO film was in the (200) orientation, XRD spectra of a film sputtered from the MgO target with 6 Si plates on showed a strong MgO(111) peak and no Si-derived peaks. By further increasing the number of Si plates up to 12, MgO(200) orientation was recovered with less crystallinity. The strong photoluminescence visible to naked eyes at 470 nm by UV light irradiation was observed only from the samples annealed above 500 °C and within the small range of Si content where the (111) orientation was observed. From the comparison with the data of Si/SiO<sub>2</sub> and Si/Al<sub>2</sub>O<sub>3</sub> nanocomposite systems, we concluded that the photoluminescence in the near infrared range observed in the Si/SiO<sub>2</sub> system resulted from the electron-hole recombination at the SiO<sub>x</sub> interface. The mechanism of photoluminescence in the visible region seems different from that in the near infrared region. For the Si/ZnO system, although the crystal structure monotonously became less structured with increasing the number of Si plates, the photoluminescence spectra were complicatedly changed. The correlation with the structure and photoluminescence will be discussed.

**PHOTOELECTROCHEMICAL BEHAVIOR OF ZnS QUANTUM DOTS MATERIALS WITH GUEST/HOST STRUCTURE**

*Ming Wu, Wenzhao Li, Xinyong Li, Wanzen Gu and Fudong Wang*

Dalian Institute of Chemical Physics, Chinese Academy of Sciences,  
Dalian, CHINA <wuming@ms.dicp.ac.cn>

Solid inclusion compounds exhibit a diversity of unique and important properties that have captivated the attention of scientists for several centuries. Recently, much of these attention have switched to a more interesting subject, that is to fabricate nanometer materials by inclusion techniques. It is expected that nanoscale molecular "container compound" can make possible the nano-fabrication with definite size and chemical interface. We previously reported that 1-nm ZnS particles could be obtained by embedding them into  $\beta$ -cyclodextrin (BCD) cavities and the resulting ZnS/BCD inclusion complex showed much high efficiency in photocatalysis as well as particular thermal behavior. This paper demonstrated the unique photoelectrochemical properties of the 1-nm ZnS included in BCD.

The photoelectric experimental results showed that the P-I or P-V response of the ZnS/BCD was approximately three times stronger than that for colloidal zinc sulfide samples. Since BCD molecule had no P-I response in the parallel experimental condition, the result thus suggested that the 1-nm ZnS with the guest/host structure had a better property of charge separation and that the host molecules had a possible synergic effect on surface charge transfer of the photo-generated carriers. A possible explanation of the above phenomena would be a different charge density for the different ZnS samples, as revealed by SAXS measurement in which the charge density of ZnS/BCD was observed to be 25% higher than that for the naked ZnS particle. Such a high charge density for ZnS/BCD sample was obviously coming from the space confinement due to BCD "container compound". Probe molecules like  $MV^{2+}$  and ROH ( $R=CH_3$ ,  $C_2H_5$  and  $C_3H_7$ ) were also employed to capture the photogenerated charges. From the observation of their fluorescence quenching and photocatalysis, we found that the interface between BCD and the included ZnS particles was of a better Ohmic contact and that BCD molecule would be a better electronic relay of charge transfer due to surface modification. These particular properties of the host molecules were believed to be an alternative explanation of the unique photoelectrochemical behavior of the ZnS/BCD samples. Moreover, the unique dot-line matrix, as observed by STM technique, of the ZnS/BCD solution sample would also have an impact on the photocurrent response. Therefore, both higher charge density for the guest (1nm ZnS quantum dots) and better Ohmic interfacial contact and charge relay for the host (BCD molecules) were believed to be the main reason for good photoelectrochemical behavior of the nanometer semiconductors with guest/host structure (ZnS/BCD).

**Acknowledgement.** This work was supported financially by the National Science Foundation of China (NSFC) under the grants No. 29473131 and by Key Projects from Chinese Academy of Sciences (CAS).

**STUDIES OF CUBIC AND HEXAGONAL ZnS QUANTUM DOTS**

*Neelesh Kumbhojkar, Shailaja Mahamuni and Anjali Kshirsagar*

Department of Physics, University of Pune, Pune 411 007, INDIA  
<neelesh@physics.unipune.ernet.in>

In recent years there is a growing interest in semiconducting quantum dots, both theoretically and experimentally. Molecular to bulk transition can be studied in this nano regime. Electronic and optical properties are size and shape dependent but not necessarily monotonic.

We have grown cubic as well as hexagonal ZnS quantum dots using a chemical route. Hexagonal ZnS quantum dots were synthesized using a high temperature synthesis route and were arrested by 1- *Thioglycerol* as a capping agent. Controlled and systematic temperature variation allows size variation. Size selective precipitation was used to separate these quantum dots. Cubic ZnS quantum dots were grown with *Thiophenol* as a capping agent.

Size quantization effects in these quantum dots are studied by optical absorption spectra that clearly exhibit a size dependent blue shift of about 30 nm. The sharp absorption peak at  $230(\pm 3)$  nm for smaller sized particles and that at  $260(\pm 3)$  nm for larger sized particles reveal narrow size distribution of these nanoparticles. Photoluminescence (PL) emission and excitation spectra are used to study the various energy levels. A size dependent shift is observed in the PL onset of the cubic quantum dots. Few subtle differences are observed in specific features of PL emission and excitation spectra of hexagonal and cubic phase. We have also studied changes in band structure of hexagonal and cubic phase.

These experimental results are compared with the theoretical calculations using pseudo potential band structure method.

**INVESTIGATION OF OPTICAL PROPERTIES OF NANO-SILICON  
USING PHOTOLUMINESCENCE AND RAMAN SCATTERING**

*S. Tripathy, S.K. Ghoshal, R.K. Soni and K.P. Jain*

Physics Department, Laser Technology Research Programme,  
Indian Institute of Technology, New Delhi - 110 016, INDIA

We have performed photoluminescence (PL) and Raman scattering measurements on Si nanocrystal-doped  $\text{SiO}_2$  thin films deposited by co-sputtering of Si and  $\text{SiO}_2$  on p-type Si (100) substrates annealed in Ar and  $\text{O}_2$  atmosphere. The broad luminescence band in red region is observed in the annealed samples and particle sizes are estimated from PL and Roman line shape analysis. Nanocrystalline Si particles are also fabricated by pulsed plasma processing technique on quartz substrates. Infra-red luminescence is observed from the as grown film at room temperature. Raman spectra from these films consists of a broad band superimposed on a sharp line near  $520 \text{ cm}^{-1}$  whose intensity, frequency and width depend on the particle size arises from the phonon confinement in the nanocrystalline silicon. For comparative study of optical properties of silicon nanostructures, we have also performed PL, Raman scattering and resonantly excited PL measurements on visible light emitting porous silicon prepared by anodic etching technique. An extensive computer simulation using empirical pseudopotential method has been carried out for 5 – 18 atoms Si clusters. Calculated band gap energies are close to our PL data.

---

**DIFFERENTIAL DILATOMETRY INVESTIGATION OF  
HYDROGEN SOLUTION IN NANOCRYSTALLINE PALLADIUM**

*C. Lemier and J. Weissmüller*

Universität des Saarlandes, Fachrichtung Technische Physik,  
Geb. 43B, D-66041 Saarbrücken, GERMANY

The reversible solubility of H in nanocrystalline  $\alpha$ -Pd-H, at given chemical potential  $\mu_H$ , is well known to be several times larger than that in the single crystal [1]. The increased solubility has been attributed to enrichment of hydrogen at grain boundaries, an effect that is suggested by standard grain boundary segregation isotherms. Mere grain boundary segregation, however, cannot be the whole story: X-ray diffraction data [2] show substantially increased lattice expansion, relative to the single crystal at same  $\mu_H$ , a finding that we argue to evidence that there is also a considerable solubility increase in the bulk of the nanocrystalline particles. Conventional theory of grain boundary segregation, based on fluid thermodynamics concepts that ignore the interaction of composition with stress or strain, offers no explanation for this effect.

Differential dilatometry, that is the combination of measurement of macroscopic expansion in a dilatometer with measurement of lattice constants by diffraction techniques, allows to determine separately the lattice strain and the change in grain boundary excess volume,  $\Delta\{V\}$ , as a function of  $\mu_H$ . The estimated resolution in  $\Delta\{V\}$  is of the order of  $10^{-4}$  nm. We present differential dilatometry data for hydrogen charging of nanocrystalline Pd prepared by inert gas condensation.

The computation of mean concentration and mean stress in bulk from the measured mean strain in bulk is based on the theory of open system elasticity [3]. A generalized capillary equation [4] describes the force balance between mean stress in bulk and interfacial stress, that is linked to the interfacial excess of hydrogen by a 'chemo-elastic' segregation isotherm.

Thus, analysis of the experimental data allows the deduction of experimental isotherms for the concentration in bulk and for the hydrogen excess at the boundaries. The results quantify the solubility increase in bulk and show that bulk and interfaces account for comparable fractions of the overall solubility increase in nanocrystalline Pd-H.

- 1; Mütschele, T., and Kirchheim, R., *Scripta Met.* **21** (1987), 135 - 140.
2. Eastman, J.A., Thompson, L.J., and Kestel, B.J., *Phys. Rev. B* **48** (1993), 84 - 92.
3. Larche, F., and Cahn, J.W., *Acta metall.* **21** (1973), 1051 - 1063.
4. Weissmüller, J., and Cahn, J.W.; *Acta mater.* **45** (1997), 1899-1906.

**STRONG COULOMB BLOCKADE  
IN RESISTIVELY ISOLATED TUNNEL JUNCTION**

*Wei Zheng , Jonathan R. Friedman , D.V. Averin , Siyuan Han \* and J.E. Lukens*

Department of Physics and astronomy, SUNY at Stony Brook,  
NY 11794, USA <zheng@onnes.physics.sunysb.edu>

Resistively isolated nano-scaled tunnel junctions are fabricated .We measured Coulomb - blockade current in resistively isolated ( $R_{\text{isol}} \gg R_K$  ) tunnel junctions with charging energy  $E_C$  much greater than the thermal energy . A zero - bias resistance  $R_0$  of up to  $10^4 R_T$  (The tunnel resistance of the bare junction) is obtained. For  $eV \ll E_c$ , the I-V curve for a given junction scales as a function of  $V/T$ , with  $I \propto V^\alpha (R_{\text{isol}})$  over a range of  $V$ . For  $T > 60$  mK, the data agree well with numerical calculations of the tunnelling rate that include environmental effects, and show the predicted power- law dependence of  $R_0(T)$ .

**ADSORPTION OF PSEUDOISOCYANINE AND TWO THIACARBOCYANINE  
DYES ON SILVER HALIDES NANOPARTICLES**

*L.Jeunieau and J. B.Nagy.*

Laboratoire de Résonance Magnétique Nucléaire, Facultés Universitaires Notre-Dame de la Paix, 61, rue de Bruxelles, 5000 Namur, BELGIUM  
<Laurence.Jeunieau@fundp.ac.be>

The nanoparticles are synthesized in a microemulsion system (AOT (sodium bis-2 ethylhexylsulfosuccinate) /Heptane/Water) and have an average size of 46 Å for the AgBr particles and of 32 Å for the AgCl particles. The influence of the dye adsorption on the stability of the particules has been specially investigated in the case of the pseudoisocyanine (PIC) adsorption. The molecules of pseudoisocyanine are replacing the molecules of the surfactant (AOT) on the surface of AgBr particles. The pseudoisocyanine, as well as the other cyanines, form aggregates (called J-aggregates) on the silver halides particles. This causes an instability in the silver bromide dispersion indeed: a large part of the surface will be unprotected by the surfactant and the particles finally coalesce. The stability can be improved by adding CTAB (Cetyltrimethylammonium bromide). The amount of CTAB influences the stability of the particles and the size of the J-aggregates. If an appropriate amount of CTAB is used, the particles remain stable for 30 days after the adsorption of pseudoisocyanine.

Two thiacarbocyanine dyes have also been adsorbed on silver halides nanoparticles. In order to have an insight on the adsorption of thiacarbocyanines on silver halides particles, an excess of halide or silver ions are used. Indeed, the adsorption could occur either by the interaction between the sulfur atom and the silver ion or by a Coulomb stabilization between the positive charge of the thiacarbocyanine and the negative charge of the halide ions. If the adsorption occurred by the interaction involving sulfur atoms, it would be favoured by an excess of silver ions. On the other hand, if the thiacarbocyanine is stabilized by coulombic attraction, it would be favored by an excess of halide ions. The results suggest that the adsorption occurred by an interaction between the sulfur atom and the silver ion in the case of silver bromide. Oppositely, for the silver chloride particles, the adsorption is favored by an excess of chloride, the coulombic interaction being the principal factor for adsorption. This difference has been attributed to a difference in the ionicity between the silver bromide and silver chloride nanoparticles.

**COMBINED EFFECTS OF GRAIN SIZE AND RESIDUAL STRAIN  
AS WELL AS IRON IMPURITIES ON THE MAGNETIC PROPERTIES  
OF BALL MILLED NICKEL**

*S. Szabó, D.L. Beke, M.Kis-Varga<sup>1</sup> and Gy. Kerekes<sup>1</sup>*

Department of Solid State Physics, L. Kossuth University,  
4010 Debrecen, P.O. Box 2, HUNGARY

<sup>1</sup>Institute of Nuclear Research of the Hungarian Academy of Sciences,  
4001 Debrecen, P.O. Box 51, HUNGARY

It is well-known that in the production of nanocrystalline metals the type of the contamination can be different e.g. for ball milling (metallic impurities from the ball: Fe, Cr) and for the vacuum condensation technique (light impurities, mainly oxygen). These can influence the magnetic properties measured as the function of the grain size,  $d$ . For example it was obtained, that the two Curie-temperatures measured in [1] were probably an artefact due to the oxygen contamination and not a real effect of the presence of a "grain-boundary phase" [2,3].

In this work it is shown that in nanocrystalline Ni - where iron contamination produced by ball milling is considerable [3] - during the milling process first the iron contamination in the form of small clusters happens. This leads to two Curie-temperatures,  $T_c$ , on the  $M(T)$  curves at the first heating-up circle, while a single  $T_c$  can be observed in the next heating up runs, because during the first circle a Ni(Fe) solid solution has been formed. Furthermore, using a similar procedure for the diminution of the residual strain,  $\epsilon$ , (but keeping the value of  $d$  almost unchanged) as in [4], the combined effects of the iron contamination as well as the residual strain and/or the grain size was also investigated for the coercitive force,  $H_c$ , and the saturation magnetisation,  $M_s$ . It was obtained that  $M_s$  and  $H_c$  are not sensitive to  $\epsilon$  and they change only if the grain size growths parallel with the formation of the Ni(Fe) solid solution.

- [1] Schaefer, H-E., Kisker, H., Kronmüller, H., Würschrum, Nanostructured Mat. **1**, 523 (1992)
- [2] Kisker, H., Gessmann, T., Würschrum, R., Kronmüller, H. H-E. Schaefer. Nanostructured Mat. **6**, 925 (1995)
- [3] Daróczy, L., Beke, D.L., Posgay, G., Kis-Varga, M., Nanostructured Mat. **6**, 981 (1995)
- [4] Eastmann, J.A., Beno, M.A., Knapp, G.S., Thompson, L.J., Nanostructured Mat. **6**, 543, (1995)

**CHARACTERIZATION OF BIOENGINEERED NANOSTRURES  
BY MULTIP TRIC OPTICAL ASSAY**

*Alexandra Bkzrukova*

Department of Biophysics, Department of Bioengineering, St. Petersburg  
State Technical University, St. Petersburg, 195251, RUSSIA <bezr@psb.usr.pu.ru>

Multiparametric optical assay (MOA) can provide further progress in studies of complex disperse systems such as liposomes carrying various substances (metals, enzymes, viruses, etc.), metallo-organic complexes, liquid crystals with surfactants, bloodsubstitutes and others engineered nanostructures.

MOA includes the nondistructive analysis of dispersions by different optical methods such as refractometry, absorbance, fluorescence, light scattering ( integral and differential, static and dynamic, unpolarized and polarized). Taking into account optical theory and results of study can help to elaborate methods for the on-line optical control of complex systems.

Our research has investigated different disperse systems: proteins, nucleoproteins, liposomes, lipoproteids, viruses, fat emulsions, bloodsubstitutes, latexes, liquid crystals, cells with various form and size, metal powders, barytes, kaolin, kimberlite clay, zeolites and mixtures - liquid crystals with surfactants, liposomes and viruses, mixtures of clay with cells, etc., by various optical methods.

One of the most actual problem is development of MOA for on-line environmental control for dangerous impurities - metals, oil, viruses, bacteria.

**MASS SPECTROMETRIC STUDY OF CLASTER FORMATION  
BETWEEN THE PROTEINS AND NUCLEIC ACIDS***I.K. Galetich and V.S. Shelkovsky*

B.Verkin Institute for Low Temperature Physics and Engineering,  
The National Academy of Sciences of Ukraine, Lenin avenue. 47,  
Kharkov 310164, UKRAINE <galetich@ilt.kharkov.ua>

Investigations of interaction in simple model systems are of fundamental importance for understanding of the mechanisms of molecular recognition and biopolymer functions.

Studies of small clusters which model interactions between components of nucleic acids and proteins on monomer level allow us to evaluate the role of particular atomic groups in protein - nucleic acid complex formation and, therefore, predict a variation in stability of the complex caused by a change in a biopolymer primary structure.

Present report is the next in the series of works in the frames of the problem of molecular recognition, in which the elementary interactions between the monomers of nucleic acids and proteins were studied on the model systems consisting of various nitrogen bases and acrylamide as a model of the side chains of Asn and Gln amino acids.

Thermodynamic parameters of interactions between the acrylamide and methylderivatives of Cytosine, Adenine and Guanine were obtained using a method of temperature dependent field ionization mass spectrometry. Under the mass spectrometric conditions the associates of the molecules were formed in the gas phase. The variation of temperature allowed to obtain relative association constants for the complexes of such molecules and to calculate the enthalpies of associates formation ( $\Delta H$ , kcal/mole) using Vant-Hoff plots.

The data obtained permits us to construct the stability sequence for the complexes between the acrylamide and methylderivatives of nitrogen bases:



A good agreement between experimental and theoretical data for the complexes of acrylamide with free atomic groups of various methylderivatives of nucleic acid bases was observed. These results can be used for estimation of the probability of recognition of the nucleic bases in single or double stranded DNA by amino acids Gln and Asn.

---

**SYNTHESIS AND SCALING UP OF THE NANOPOWDER PRODUCTION  
BY CHEMICAL CO-PRECIPITATION**

*Andrei A. Zagorodni, Yu Zhang, Lingna Wang and Mamoun Muhammed*

Materials Chemistry Division, Royal Institute of Technology,  
SE-100 44, Stockholm, SWEDEN <andreyz@matchem.kth.se>

Multi-element inorganic solid solutions are required in much modern area of techniques. In present work we established and scaled up the chemical production process of the Bi based precursor for HT superconductors.

Bi-based materials are well known superconducting system nowadays. However, still there is no any production of such materials in more than laboratory scale (several grams per one synthesise). The problem is in the complexity of the system due to multi-compound composition and requirements for the perfect homogeneity of the solid solution. Such solid solution is a "point compound" (considering the phase diagram). A co-precipitation was used to get the right product. The chemical system has no any buffer capacity toward the reagents used. It results in necessity of precise external multi-factor control. The process allowing the level of control down to 0.01 % was established. It allows producing the nano-structured material providing the quality required. The powder obtained has the homogenous chemical and physical properties. It results in highest quality of the superconductors produced as well as in reduction of the defective final product amount.

Scaling up of chemical processes is a significant problem in many technical applications. Since equilibria and chemical kinetics are controlling factors for small laboratory scale syntheses, the scaling up has to solve different problems of diffusion kinetics and dynamics. Precise control of large scale syntheses is impossible without computer operated system (in case of the buffer capacity absence). Hereby, the sensors and operated units response should be taken in account in complex with response of the chemical system. The automatic system including multi-channel process control was constructed. The target nano-phase can be produced in scale of kilograms per run and has been marketed.

**COMBINED NANOCRYSTALLINE MATERIAL WITH PIEZOELECTRIC CRYSTAL DETECTOR FOR APPLICATION IN GAS SENSOR**

*Hong-Ming Lin, Shiow-Feng Pan*

Dept. of Materials Engineering, Tatung Institute of Technology, Taipei 104, Taiwan  
[<hmlin@mse.ttit.edu.tw>](mailto:<hmlin@mse.ttit.edu.tw>)

Nanocrystalline (NC) Materials, exhibiting a large surface area, can be applied to gas sensors for its excellent surface characteristic is required. In this study, the 9 MHz AT quartz substrates are plated with gold on both side for electrical contacts and surface of quartz is doping with NC Pt, Pd, Au, Ag, with the mean particle size of about 10 nm which is directly deposited by gas evaporation method. Increasing the weight on the crystal surface will decrease the vibration frequency of quartz. The doping of NC particles on the quartz surface thereby increasing the absorption of gases that will enhance the sensitivity and selectivity of detecting gases.

To assist the base frequency stability of the piezoelectric quartz, the NC Pt, Pd, Ag and Au dopants are well spread, and extremely fine. Hitachi 800 TEM/STEM is used to analyze the particle sizes distribution and structure of NC Pt, Pd, Ag and Au. The QCM Analyzer detects the decreases of the vibration frequency under gas detection. This study will provided a new method, which combine the NC materials with piezoelectric crystal detector on gas sensing at the high temperature up to 300°.

---

**DETECTING CO AND NO<sub>2</sub> GASES BY NANOPHASE ZnO GAS SENSORS  
WITH NEURAL NETWORK TECHNIQUE**

*Shah-Jye Tzeng, Peng-Jan Hsiao, Hong-Ming Lin, and Wen-Li Tsai*

Dept. of Materials Engineering, Tatung Institute of Technology, Taipei 104, Taiwan  
<sjtzeng@alpha.cc.ntut.edu.tw>

Electrode effects on gas sensing properties have been examined by nanocrystalline zinc oxide sensor in this study. NC Zn is grown by the gas-condensation method in 5 mbar of helium atmosphere on the surface of gold or silver electrodes and then steps sintering to form nanocrystalline (NC) ZnO. The response time of NC ZnO sensor with Ag electrodes is fast in detecting NO<sub>2</sub> gas, but the sensitivity can not recovered to the background after turn off the NO<sub>2</sub> gas. This result indicates that Ag electrodes can be poisoned by NO<sub>2</sub> gas. The linear dynamic detecting range, response time, sensitivity and reliability of NC ZnO sensor with Au electrodes is comparable better than that of NC ZnO sensor with Ag electrodes.

The neural network technique is used in this study to recognize the response curve of the measured sensitivity for different gases. Using the back-propagation network and took the sensitivity of NC ZnO sensor at the time of 5, 10, 15, 20, 25, 30, 35, 40, 45 minutes to train, the neural network patterns can recognize CO and NO<sub>2</sub> precisely.

**STRUCTURAL AND CATALYTIC PROPERTIES  
OF Mn OXO-CLUSTERS SUPPORTED ON MESOPOROUS MCM-41***D. Gleeson, R. Burch and S.C.E. Tsang*

The Catalysis Research Centre, Department of Chemistry, University of Reading,  
Whitenights, Reading, RG6 6AD, UK

Mesoporous silicate produced by the co-operative assembly of silica and surfactants are characterized by large pores and large internal surface areas greater than any known molecular sieves [1]. The hexagonal channels are structurally well defined with a large number of surface hydroxyl groups which could provide reaction or nucleation sites for the entrapment of a wide variety of metal complexes. It thus provides a stable and reproducible environment for foreign material deposition.

At Reading, we are interested to use the mesoporous silica as a template for the deposition of reactive linings of chemical species through the surface reaction of Si-OH groups with various organometallic species. We prepared the first redox type of mesoporous silica MCM-41 supported catalyst via the surface immobilization of gaseous  $Mn_2(CO)_{10}$  using CVD techniques. This modified Mn-MCM-41 gave much higher catalytic activity in propene oxidation to carbon dioxide than that observed with bulk  $MnO_2$  and MnOx supported on conventional silica [2]. EXAFS studies clearly showed that the gaseous  $Mn_2(CO)_{10}$  upon immobilization resulted in dimeric  $Mn_2(CO)_8$  species anchored through two Mn-O-Si bonds. Upon the heat treatment in air, discrete dimeric Mn-oxo clusters resembling to  $Mn_2O_7$  grafted onto the internal walls of MCM-41 were formed [3]. These materials have been extensively characterised by FTIR, TPR, XRD, TEM, XPS and nitrogen physisorption. The correlation between structure and catalytic properties will also be discussed.

1. Presage, C.T.; Leonowicz, M.E.; Roth, W.J.; Vartuli, J.C. and Beck, J.S. *Nature* (1992) 359, 710
2. Burch, N.A. Cruise, D. Gleeson, S.C. Tsang, J. Chem. Soc., Chem. Comm., (1996) 951.
3. Burch, N.A. Cruise, D. Gleeson, S.C. Tsang, J. Mater. Chem., (1998) 8, 227.

### **IMMOBILIZATION OF NANOSTRUCTURED METAL COLLOIDS IN HYDROPHOBIC SOL-GEL MATERIALS**

*Markus Dugal and Manfred T. Reetz*

Max-Planck-Institut für Kohlenforschung, Kaiser-Wilhelm-Platz 1, 45470 Mülheim  
a.d. Ruhr, GERMANY <dugal@mpi-muelheim.mpg.de>

The synthesis of nanocomposite materials consisting of transition metal particles in the nanometer range dispersed in sol-gel materials has been a field of growing interest in the last 15 years. One major advantage of using the sol-gel-method for the development of heterogeneous catalysts lies in the high ability of controlling composition and structure of the carrier matrix[1].

Usually the active metal component is generated after formation of the carrier, e.g. by impregnation-reduction or thermal decomposition of encapsulated metal complexes[2]. However size and crystallinity of the resulting metal particles are difficult to control with these methods.

The presented work is the first example of an immobilisation of performed transition metal colloids in sol-gel materials[3]. The metal colloids used as precursors are stabilised by tetraalkylammonium salts and prepared by electrochemical reduction. This method, developed in our research group, allows the size selective synthesis of numerous transition metal colloids (e.g. Pd, Pt and Rh) in the nanometer range[4].

Encapsulation of the colloids was achieved by an optimised, fluoride catalysed sol-gel-process starting from alkylalkoxysilanes ( $R'SiOR_3$ ) and other alkoxides resulting in mesoporous metal(0)-xerogel or cryogel nanocomposites. Elemental analysis, REM, HRTEM,  $N_2$ -physisorption, CO-chemisorption,  $^{29}Si$ -CP-MAS-NMR, catalytic activity measurements and other techniques were applied to characterise the inorganic-organic hybride materials.

It was shown that the novel materials are useful catalytic tools in various organic reactions such as hydrogenations, the palladium catalysed *Heck* reaction and allylic substitution reactions.

A study about the influence of the matrix composition, with special respect to the hydrophobic group content, on structure and catalytic properties demonstrated that the materials exhibit new potentials in the selectivity control of heterogenously catalysed reactions.

- [1] M.A. Caqui, J.M. Rodriguez-Izquierdo, *J. Non-Cryst. Solids*, **1992**, *147&148*, 724
- [2] R.D. Gonzalez, T. Lopez, R. Gomez, *Catalysis Today*, **1997**, *35*, 293
- [3] M.Dugal, Diploma Thesis, *Gerhard-Mercator-Universität-GH-Duisburg*, July **1996**;
- [4] M.T. Reetz, W. Helbig, *J. Am. Chem. Soc.* **1994**, *116*, 7401

**THE EVIDENCE OF Ni NANOPARTICLES CATALYTIC ACTIVITY  
IN NiO REDUCTION.**

*M.I. Zacharenko, V.K. Yatsimirsky, V. Diyuk and S. Revo*

Chemistry department, Shevchenko University,  
Volodimirska 64, 252033 Kyiv, UKRAINE

The mechanism of catalytic action of nickel as an active catalyst of carbon monoxide oxidation is studied.

The processes of oxidation on nickel powder surface by oxygen at 623-973 K and of the reduction of nickel oxide by carbon monoxide at 623-703 K are considered.

It is established for nickel oxidation that the quantity of active centers increase with temperature decreasing. At  $T < 673$  K the dimension of NiO active centers is 10-12 nm.

It is evident that reaction of nickel oxide/reduction accelerates only after passing through Curie temperature (633 K) for nickel and becomes autocatalytical when transformation degree is above 0.5%.

A dimension of nickel active centers at transformation degree 0.5% is determined by measuring of magnetic susceptibility via temperature. It is established that the dimension of nickel active centers is 5-8 nm.

**FORMATION OF PARALLEL GOLD NANOWIRES  
BY SCANNING FORCE MICROSCOPY**

*M. Andersson, A. Iline, F. Stietz and F. Träger*

Fachbereich Physik, Universität Kassel, Heinrich-Plett-Str. 40,  
D-34132 Kassel, GERMANY <iline@physik.uni-kassel.de>

This paper reports an interesting mechanism through which a gold film can be converted into parallel Au nanowires by repeatedly scanning the tip of a force microscope over the surface. The highly oriented structures were obtained as follows. Gold films were grown on dielectric substrates such as CaF<sub>2</sub> or quartz by deposition of gold atoms from a thermal atomic beam generated by an electron beam evaporator. The substrate temperature was varied between 410 and 870 K. The flux of gold atoms, measured by a quartz crystal microbalance, was kept constant and areas of different coverage ranging from 2-40 monolayers (ML), were obtained on the substrate surface by appropriately choosing the position of a shutter in front of the sample. Subsequently, the samples were imaged by contact-mode scanning force microscopy (SFM) under ambient conditions. Initially, the films consisted of separated or closely arranged clusters. However, details of the original film morphology were difficult to determine because the tip often induced changes of the gold film. At low gold coverage, i.e. < 10 ML, the Au clusters are highly mobile. This gives rise to stripes in the initial images which originate from clusters moved over the surface by the SFM tip. Images of the same area recorded subsequently show larger aggregates at few places, preferentially at the edges of the imaged area. In contrast to this apparently random displacement of clusters, highly ordered structures of one-dimensional character were often formed during imaging of samples with larger gold coverage. These structures had the character of wires or chains of clusters and were mostly oriented under an angle of about 50-70° with respect to the fast scan direction. Typical dimensions of the wires were 5-10 nm high, 50-100 nm wide and several μm long. Network-like structures where the chains merge and branch out appear preferentially at the highest investigated coverages.

The displacement of individual clusters and the formation of ordered nanowires seem to be closely related to each other. At low coverages the clusters can stick to the tip and are translated over the surface until they reach an obstacle or the tip changes its scanning direction. Above a certain critical coverage of about 10 ML a large amount of gold is relatively rapidly collected at the tip. The gold can then be redeposited preferentially at larger objects on the substrate, for example the apex of a wire. If this is repeated for each scanline, wires grow with a small angle to the slow scan direction. The substrate temperature chosen during film growth appeared to influence the stability of the films and their propensity to transform. Samples grown at low temperatures could more likely be converted into wires as compared to films produced at higher temperatures, i.e. closer to thermodynamic equilibrium.

We finally mention that detailed investigation of the mechanism of transformation could provide a very useful method to generate novel, highly oriented Au nanostructures.

**METAL-POLYMER NANOCOMPOSITES  
AS NEW TYPE OF CHEMICAL SENSORS.**

*G.N Gerasimov, E.I. Grigor`ev, A.E. Grigor`ev, P.S Vorontsov, E.V. Nikolaeva,  
S.A. Zavjalov and L.I. Trakhtenberg*

Karpov Institute of Physical Chemistry, Vorontsovo Pole 10,  
103064 Moscow, RUSSIA <gerasim@cc.nifhi.ac.ru>

It was shown that metal-polymer nanocomposites are characterized by the tunnel charge transfer conductivity in the specific metal content ( $X_m$ ) range when value of conductivity (C) changes from C of polymer to C of metal in the vicinity of the percolation threshold. Tunnel C is very sensitive to barriers of charge transfer between metal particles. Such barriers alter, to one or another extent, under influence of substances adsorbed on particles from gaseous phase. Therefore it is believed metal-polymer composites can be used as chemical sensors.

This work is aimed at studying the sensor properties of metal containing poly-p-xylylene (PPX) films. The films were produced by co-condensation of p-xylylene monomer and metal vapors at 77 K followed by thermal solid-state polymerization of obtained co-condensate. P-xylylene monomers were prepared by pyrolysis of corresponding p-cyclophanes. Pb and Pd were chosen as metals. X-ray measurements showed such procedure allows to stabilize in PPX metal particles of size 3-10 nm depending on metal content( $X_m$ ).

Measurements of C of Pb-containing PPX shown these films do not have sensor properties. But films containing PbO-nanoparticles obtained by oxidation of Pb changed dramatically their C under influence of the water, ammonium, amine or alcohol traces in atmosphere. The sensitivity of films to substances mentioned depends strongly on  $X_m$ . Varying  $X_m$  one can prepare sensor films having the maximal selectivity for each of the substance together with the maximal sensitivity to this substance. Selectivity is not less than 100. The interval of measured concentration ranges between 0.5 to 100 mg/m<sup>3</sup>. The characteristic time of the signal appearance at contact of sensor with substance and that of the signal disappearance after removal of substance can be about of several seconds. That is unique parameter for sensors.

It was shown σ of PPX-films containing Pd nanocrystals sharply changes (on 5 or 6 orders) under action of molecular hydrogen.

The results of work show that metal-polymer nanocomposites can be considered as new promising chemical sensors.

**STRUCTURAL AND MAGNETIC PROPERTIES OF  
 $(Fe_{100-x}Co_x)_{73.5}Cu_1Nb_3Si_{13.5}B_9$  NANOCRYSTALLINE WIRES**

*H.Chiriac, F.Barariu, F.Vinai\*, I.Murgulescu, E.Ferrara\**

National Institute of R&D for Technical Physics, 47 Mangeron Blvd.,  
Iasi, ROMANIA <firuta@phys-iasi.ro>

\* Istituto Elettrotecnico Nazionale "Galileo Ferraris", Corso M. D'Azeglio,  
42 - 10125 Torino, ITALY <vinai@omega.ien.it>

Although many results on the production and properties of the nanocrystalline magnetic materials in the shape of ribbons have been previously reported, there is a lack of data in the field of wire-shaped nanocrystalline materials, due to the difficulty in obtaining the wires having this composition in the amorphous state.

The aim of this paper is to present some results on the production, structure and magnetic properties of the  $(Fe_{100-x}Co_x)_{73.5}Cu_1Nb_3Si_{13.5}B_9$  ( $x = 0, 5, 10, 20$ ) wires, both in the amorphous and nanocrystalline state.

We prepared amorphous wires of about 125  $\mu m$  in diameter by the in rotating water spinning method. The amorphous and the nanocrystalline states were checked by X-ray diffraction, DSC, and thermomagnetic measurements. The thermal treatments were performed in a conventional furnace, in vacuum.

We found that the substitution of Fe with Co leads to an increase in the wire glass-forming ability. For all studied alloys the thermal treatment performed above the crystallization temperature leads to the formation of the nanocrystalline structure with ultrafine grains of about 10 - 15 nm. The onset of crystallization for the nanocrystalline state has been shifted to higher values by increasing the Co content, from 505°C to 535°C. In the as-cast state all the wires present Large Barkhausen effect. The saturation magnetization slightly increases with the increase in the Co content. The nanocrystalline phase formation leads to an increase in the magnetic permeability and to a decrease of the coercive field. These changes are less important increasing the Co content. The increase in the Co content also produce an increase in the Curie temperature both in amorphous and nanocrystalline states. The magnetic properties of the wires are explained on the basis of the effect of annealing in correlation with the change in the values of the saturation magnetostriction.

**TAILORING THE MICROSTRUCTURE AND  
DEFECT CHEMISTRY IN NANOSTRUCTURED CERIUM OXIDE  
FOR OPTIMIZED GAS SENSOR PROPERTIES**

*Andreas Tschöpe and Rainer Birringer*

FB Physik, Universität des Saarlandes,  
Saarbrücken, GERMANY <antsch@rz.uni-sb.de>

The heterogeneous reaction between metal oxides and the gas phase is the basis for applications in gas-sensor devices. This interaction may involve (i) the exchange of lattice oxygen with the gas phase (redox-equilibrium) or (ii) trapping/injection of free electronic charge carriers in surface states (ionosorption). In both cases, the sensitivity of electrical conductance on charges in the gas phase is controlled by defect chemistry and the material's microstructure. In particular, the formation of space charge layers along interfaces is of fundamental importance for gas-sensor applications. Two examples will be used to demonstrate the advantage of tailoring the microstructure and defect chemistry in order to enhance gas sensitivity. Nanocrystalline dense acceptor-doped and nanoporous donor-doped cerium oxide were studied at various temperatures. Sensitivity of electrical resistance with respect to O<sub>2</sub>, CO, NO, CO<sub>2</sub> and SO<sub>2</sub> partial pressure was investigated. The discussion of the experimental results is based on a comparison of the grain size and the width of the space charge layer as the two most important tuning parameters.

**MONODISPERSED PALLADIUM CATALYSTS FOR HYDROGENATION**

*A. Zharmagambetova, S. Mukhamedzhanova, B. Selenova and I. Chanyshева*

Sokolskii Institute of Organic Catalysis and Electrochemistry, Kazakh Academy of Sciences, 142 Kunaev St., Almaty-480100, KAZAKHSTAN  
< adm@orgcat.academ. alma-ata.su>

Properties of heterogeneous catalysts depend on structure and sizes of active centres. Selective catalysts can be obtained by metal ion fixation on the surface of supports. Functional polymers can be used for this purpose. Macromolecule-metal complex (MMC) and the same complex fixed on MgO has been used to obtain monodispersed Pd catalysts for hydrogenation of propen-1-ol and 3-phenylpropen-1-ol. MMC was prepared by interaction of ethanol solutions of palladium chloride and polyvinylpyrildine (PVP). The Pd-PVP was fixed on MgO. The active phase of catalysts and their change during catalytic process was characterised by IR-spectrometry, electron microscopy, XPA, XPS methods.

Pd-PVP complex and the fixed one showed high activity and selectivity in alcohols hydrogenation in water at 25°C and atmospheric hydrogen pressure. These catalysts were stable. Reaction rate did not change at the repeated use of one and the same catalyst sample for hydrogenation of 10-30 portions of substrate. According to electron microscopy data the monodispersed Pd particles with 2.5-3.0 nm sizes are formed on the surface and inside the Pd-PVP complex. Pre-treatment of the complex with hydrogen in the reactor during 30 minutes leads to increase in the size of particles up to 8.0-10.0 nm. It is clearly visible in the electron photomicrographs that new palladium active centers consist of initial small particles. Catalyst used in hydrogenation of 30 portions of propen-1-ol is characterised by the same sizes of Pd particles as the pretreated one. XPA method confirms the obtained results. Thus, polymer chains of MMC prevent enlargement of Pd particles. Catalysts keep high activity during long time due to invariability of active centres' structure and sizes. According to XPS data the part of Pd (II) in initial Pd-PVP catalyst was reduced into Pd (O) during pre-treatment with hydrogen. IR-spectroscopy investigation of catalysts showed breakage of part of Pd-N bonds in Pd-PVP complex. The used sample was characterised by the same parameters as the pre-treated one. The only difference was in Pd (II): Pd (O) ratio. It is changed from 1:3 in reduced catalyst to 1:5 in used one. The MMC supported on MgO catalyst possesses similar properties but its stability is lower.

Thus, soluble functional polymers can be used to prepare active, selective and stable heterogeneous catalysts with monodispersed active phase.

**DISPERSED COPPER CATALYSTS  
FOR ACETYLENE COMPOUND HYDROGENATION**

*A. M.Pak, O.I.Kartonozhkina, S.K.Slepoval L.Komashko*

Sokolskii Institute of Organic Catalysis and Electrochemistry, Kazakhs Academy of Sciences, 142 Kunaev St., Almaty-480100, KAZAKHSTAN  
<adm@orgcat.academ. alma-ata.su>

Effectiveness of heterogeneous catalysts can be increased by fixation of small uniformed metal particles on supports. The effect of organic additives on formation of monodispersed copper catalysts has been studied in the present paper.  $\text{SiO}_2$ ,  $\text{MgO}$  and  $\gamma\text{-Al}_2\text{O}_3$  was used as support. The oxides were impregnated with organic additive (diethanolamine or polyvinylpyridine). Then copper salt was added to the pre-treated support. Both additives promote chemical fixation of metal ions and uniformed distribution of active phase on the surface of supports. Then catalysts' precursors with diethanolamine (DEA) were treated at 623K in  $\text{H}_2$  flow during 3 hours. The process leads to Cu (0) formation on the surface of support. There was not reduction of Cu (II) into Cu(0) in Cu-PVP supported catalysts in the same conditions. Because of this, the polymer-metal complexes on chosen oxides have been calcined at 473 K during 2 hours before reduction. The catalysts have been studied by electron microscopy, XPA, BET and IR spectroscopy methods.

According to the obtained data the most active catalysts were copper complexes fixed on  $\gamma\text{-Al}_2\text{O}_3$ . Both supported on alumina Cu catalysts with DEA or PVP are characterised by uniformed distribution of active phase on supports. Copper particle sizes are varied from 8 to 20 nm depending on the nature of organic additives. The prepared 10% Cu catalysts have been tested in the stereoselective hydrogenation of acetylene compounds at 393K and 8 MPa in ethanol. The only reaction product in the presence of both catalysts was cis-olefins. Higher activity in hydrogenation of 2-hexyne and 11-hexadecyne-1-ol was observed on catalyst pre-treated with PVP. Time of complete conversion of 11-hexadecyne-1-ol into cis-11-hexadecene-1-ol on this catalyst was 70 min. to compare with 135 min. on 10% Cu/ $\gamma\text{-Al}_2\text{O}_3$  pre-treated with DEA. According to electron spectroscopy investigations the active Cu-PVP/ $\gamma\text{-Al}_2\text{O}_3$  catalyst is characterised by smaller copper particles (around 8 nm) than pre-treated with DEA (20 nm). It can be assumed that the activity of Cu-PVP/ $\gamma\text{-Al}_2\text{O}_3$  would be higher, but calcination of the catalyst in air led to formation of coke that blocked active centres for activation of substrates.

Thus, stereoselective copper catalysts with monodispersed active phase can be obtained by pre-treatment of supports with organic compounds or functional polymers for preliminary chemical fixation of Cu(II) on the surface of support.

**INTENSITY-VOLTAGE CHARACTERISTICS OF METALLIC NANOWIRES**

*A. Correia, J.-L. Costa-Krämer, Y.W. Zhao and N. García.*

Lab. de Nanotecnología, CSIC, Serrano 144, 28006 Madrid, SPAIN

The phenomenon of conductance quantization (CQ) in units of  $G_0=2e^2/h$  was first observed at 0.6K in two-dimensional electron gas (2DEG) semiconductor structures. After then, CQ in metallic nanowires has constituted a field of increased interest. Theoretically predicted first as a step-like or oscillatory behavior of conductance in Scanning Tunneling Microscope (STM) calculations, it has been observed in wires made of different metals and produced by STM techniques, breaking a contact between macroscopic wires, and, using mechanically controllable break junctions. In all these experimental techniques, plateaus appear at quantized values of conductance showing that electron transport through metallic nanowires is ballistic and that the current is carried in quantized modes. Experiments involving thousands of consecutive measurements without any selection criterium have been performed showing that CQ is an actual phenomenon in metallic nanowires. Studies have been also performed on semimetals and first experimental evidence of CQ in bismuth at 4K has been recently reported. Another interesting subject is the nanowire structural characterization using either scanning or transmission electron microscopy.

In this work, we present experimental results for the room temperature I-V characteristics of gold nanowires whose zero current conductance is quantized. Several methods for producing nanowires have been used: (i)Using macroscopic metallic samples to form nanowires (in vacuum and at room temperature). (ii)Using STM at ambient pressure and room temperature. (iii)Using nanolithography in order to produce stabilized nanowires on a substrate.

We have analysed more thoroughly the I-V characteristics of nanoscopic contacts changing several parameters such as the formation technique or the structure around the nanowire (vacuum, air, polymer, substrate...). In all these experiments, a faster than linear increase of the current was observed, but at different threshold voltages depending on the situation: 0.1V for "free standing" nanowires (in air or vacuum), 0.3 to 0.5V for non "free standing", i.e., nanowires deposited on a substrate or embedded in a polymer.

**SYNTHESIS AND CHARACTERISATION OF  
CERIUM-ZIRCONIUM-CALCIUM OXIDES AND  
THEIR APPLICATION IN THREE WAY CATALYSTS.**

*Sara Hjelm<sup>1</sup>, Tarja Turkki<sup>1</sup>, Mamoun Muhammed<sup>1</sup> and Lothar Mussman<sup>2</sup>.*

<sup>1</sup> Materials Chemistry Division, Royal Institute of Technology,  
SE-100 44 Stockholm, SWEDEN

<sup>2</sup> Degussa AG, AK-FA-FE, Wolfgang, Postfach 13 45,  
D-834 03 Hanau, GERMANY <Lothar.Mussmann@degussa.de>

The Ce<sup>4+</sup> ion in ceria is easily reduced to Ce<sup>3+</sup>. This creates a nonstoichiometric oxide, CeO<sub>2.8</sub>, with oxygen vacancies in the crystal structure. The Ce<sup>3+</sup> is also readily reoxidised and this makes the material suitable as the oxygen storage component in automotive emission control catalysts. By doping, i.e. substituting cerium with cations of different size or lower valency, the formation of oxygen vacancies increases. The main target of this work was to study and develop doped ceria for use in three-way catalysts. It is desirable to improve the component oxygen release and storage properties as well as its ageing stability for a better and more durable performance of car catalysts. Ternary systems with cerium, zirconium and calcium were synthesised and investigated. The materials were characterised and the catalytic performance in fully formulated model catalysts was evaluated. TGA, XRD, TPR and BET techniques were used to study precursors and the calcined oxides. The model catalysts with the ternary oxide were evaluated as fresh and aged. Their static and dynamic oxygen storage capacities were studied in an oxygen pulse experiment and an oxygen/carbon monoxide pulse experiment. Model gas tests were performed to investigate their catalytic performance in a static and dynamic lambda sweep. This tests simulates conditions close to operating a real engine.

**QUANTUNIZED MAGNETIC DISKS FOR  
ULTRA-HIGH DENSITY MAGNETIC STORAGE**

*S.Y. Chou, L. Kong, L. Zhang, M. Li, and W. Wu*

NanoStructure Laboratory, Department of Electrical Engineering  
Princeton University, Princeton, NJ 08544, USA

Quantized magnetic disks (QMD)--a new paradigm for ultra-high density magnetic storage, that can overcome many limits of conventional magnetic thin film disks [1]. QMD consists of pre-fabricated discrete single-domain magnetic elements (e.g. array of bars or pillars) that have an identical shape and are uniformly embedded in a nonmagnetic disk. Due to its small size and shape anisotropy, each single-domain element has a quantized magnet moment with two possible stable magnetization direction. Each direction represents one binary bit of information. Perpendicular QMDs with nanoscale single-domain Ni pillars of 65 Gbit/in<sup>2</sup> density and longitudinal QMDs with Cr/Co/Cr bars of 30 Gbit/in<sup>2</sup> density have been fabricated. Magnetic force microscope (MFM) has written longitudinal QMDs of 10 Gbit/in<sup>2</sup> density and a 1000 coercively. The writing was perfect within the MFM writing window, even though there are no tracking and feedback in MFM, demonstrating the advantages of QMDs in relaxing the requirement on a write head. Nanoimprint lithography, a new approach for nanopatterning that has been used to fabricate QMDs with an area larger than one square-inch, will be presented.

- [1] S.Y. Chou, M.S. Wei, P.R. Krauss, and P.B. Fischer, "Study of Nanoscale Magnetic Structures Fabricated Using Lithography and Quantum Magnetic Disk", *J. Vac. Sci. and Tech.*, **B12**(6), 3695-3698, 1994

**HIGH ENERGY PRODUCTS AND HIGH COERCIVITY  
IN EXCHANGE COUPLED HARD/SOFT NANOCOMPOSITES***J.P. Liu, Y. Liu and D.J. Sellmyer*

Center for Materials Research and Analysis, University of Nebraska, Lincoln, NE, USA

Magnetic hysteresis and intergrain exchange coupling have been investigated in nano-scale composites consisting of hard and soft magnetic grains. The composite films were made by multilayer sputtering and subsequent thermal processing including rapid, multi-pulse annealing. Films of (fct)FePt:fccFe-Pt and CoPr:Co were systematically studied and were characterized by x-ray diffraction and TEM [1,2]. Magnetization measurements included initial curves, minor loops and temperature dependence of the magnetization. Qualitatively, exchange coupling of the type discussed by Skomski and Coey [3] was observed; as the fraction of soft phase increases the magnetization increases and coercivity decreases. With great attention to the thermal processing, very high energy products have been obtained in the two systems discussed above, viz. about 50 MGoe and 25MGoe, respectively. Mechanisms of magnetization reversal have been studied and there is evidence of both wall-pinning and nucleation, depending on microstructure. Prospects for further increase of energy products to still higher values will be discussed.

Research supported by DOE, AFOSR and CMRA.

1. J.P. Liu, et al., *J. Appl. Phys.* (in press).
2. J.P. Liu, et al., *Appl. Phys. Lett.* (in press).
3. R. Skomski and J.M.D. Coey, *Phys. Rev. B* 48, 15812 (1993).

**ENGINEERING OF NANOSTRUCTURED COMMERCIAL ALLOYS  
FOR STRUCTURAL APPLICATION.**

*V.S. Zhernakov, V.V. Latysh, V.V. Stolyarov and R.Z. Valiev*

Ufa State Aviation Technical University, K.Marksa 12, 450000 Ufa, RUSSIA  
*<vlst@ippm.rb.ru>*

One of the most important aspects in engineering of new structural alloys for motor car and aircraft industries is providing high technological and service properties: high ductility at low resistance to deformation during forming and then high structural strength and fatigue characteristics.

The promising way to obtain such properties is formation of nanostructures in commercial alloys. It is based on refinement of microstructure to nanometric sizes using methods of severe plastic deformation (SPD) and these results in improvement of material properties.

The present work deals with determining optimal regimes processing massive nanostructured samples out of a number of commercial alloys on titanium and aluminium base. Severe plastic deformation by equal channel angular (ECA) pressing is used for this fabrication. The work also deals with investigations of affects of nanostructure on technological and service properties of the alloys.

The effect of superplasticity at low temperatures and high strain rates is revealed during tensile tests of nanostructured alloys. This is very attractive for efficient forming of complex shape articles.

On the other hand, the properties resulted from processing by severe plastic deformation show that at room temperature nanostructured materials display very high strength and fatigue properties. This is connected not only with formation of ultrafine grains, but also with changes of phase composition of alloys during severe plastic deformation.

The obtained results are used for the demonstration of effective fabrication of a number of high strength pilot articles used in motor car and aircraft industries.

**STABILITY OF ALUMINA CERAMICS BONDED  
WITH NANOSCALED ALUMINA POWDERS**

R.J. Hellwig, J.-F. Castagnet and H. Ferkel

Institut für Werkstoffkunde und Werkstofftechnik, TU Clausthal, Agricolastr. 6,  
38678 Clausthal-Zellerfeld, GERMANY <hans.ferkel@tu-clausthal.de>

Nanoscaled alumina powder can be employed for diffusion bonding of alumina ceramics. The nanoscaled powder is generated by ablation of solid corundum samples with the pulsed radiation of a 1000 W Nd:YAG-laser followed by condensation of the vapour in a controlled atmosphere. Between two commercial microcrystalline alumina ceramics nanoscaled alumina powder is sandwiched, followed by uniaxially hot pressing of the assembly in vacuum at various pressures and temperatures up to 80 MPa and 1300°C. Several of these samples were additionally sintered in air at 1500°C for six hours without load. Four-point bending tests are carried out to determine the bending strength of the different joints. The specimens bonded without additional sintering show already bending strength comparable to commercial coarsened grained corundum. Post-sintering has almost no negative effect on the bending strength. The samples exhibit material failure not necessarily in the joint. The joints examined by SEM investigations directly after hot pressing exhibit a nanocrystalline structure with an average grain size less than 100 nm. The post-sintered samples show an extensive grain growth and the formation of submicron shrinkage voids in the interface.

**NANO-Ag AND NANO-Al (ALEX™ ) BASED INKS  
FOR CONTACTS TO SILICON SOLAR CELLS**

*Douglas L. Schulz<sup>1</sup>, Calvin J. Curtis<sup>1</sup>, David S. Ginley<sup>1</sup>,  
Vadim Z. Gandelsman<sup>2</sup> and Frederick Tepper<sup>2</sup>*

<sup>1</sup> National Renewable Energy Laboratory, 1617 Cole Blvd., Golden,  
CO 80401-3393, USA <dginley@nrel.nrel.gov>

<sup>2</sup> The Argonide Corporation, 240 Power Court, Suite 108,  
Sanford, FL 32771-9530, USA

Nanoparticle Al and Ag prepared by the exploding wire process have been used for contacts to p- and n-type Si, respectively. Toward this end, nano-Al and nano-Ag were printed as viscous inks to p-type and n-type Si films, respectively. After annealing these nano-Al/p-Si and nano-Ag/n-Si structures were heated above the eutectic temperatures (i.e., 645°C and 882°C, respectively), the subsequently formed metal contacts were characterized by IV. Figures 1a and 1b show the IV characterization of the annealed nano-Al/p-Si and nano-Ag/n-Si films, respectively. Each curve displays nearly linear behavior indicative of ohmic contact.

Physical properties characterization of the nanoparticles included transmission electron microscopy (TEM) and differential scanning calorimetry. TEM of the nano-Al powder showed two distinct fractions: (1) round spheres 100-300 nm in diameter, and (2) a mixed assemblage consisting of round spheres 100-150 nm in diameter and <50 nm particles. TEM selected area diffraction showed the nano-Al samples are polycrystalline with very little amorphous component. Initial results in the development of inks amenable to use in existing semiconductor contacting technologies will be discussed.

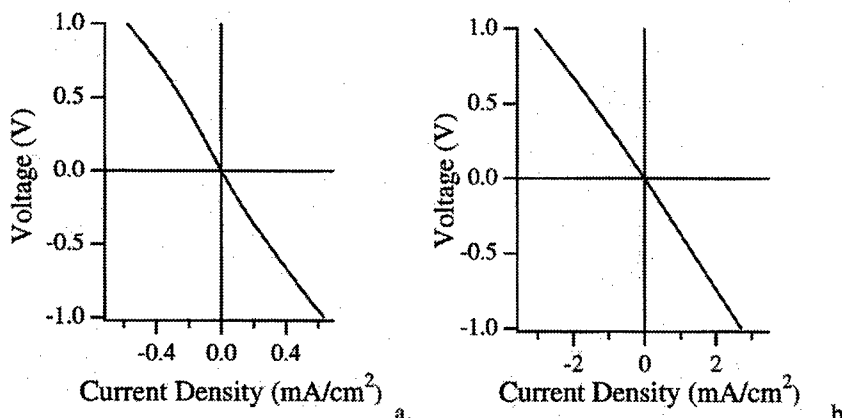


Figure 1. IV characterization for annealed (a) nano-Al on p-type Si and (b) nano-Ag on n-type Si.

**INTRINSIC AND EXTRINSIC EFFECTS IN NANOCRYSTALLINE MATERIALS AND SOME TECHNOLOGICAL CHALLENGES**

*Shankar M.L. Sastry<sup>1</sup>* and *Virgil Provenzano<sup>2</sup>*

<sup>1</sup> Washington University, Campus Box 1185, One Brookings Drive,  
St. Louis, MO 63130, USA <smls@mecf.wustl.edu>

<sup>2</sup> Naval Research Laboratory, Code 6320, 4555 Overlook Ave.,  
SW, Washington, DC 20375, USA

Mechanical properties of nanocrystalline materials synthesized by a variety of methods and consolidated by different processing routes have been attributed to nanocrystalline structure without due consideration given to the impurities present, nanoporosity of the consolidated products, and the nature of inter particle and inter agglomerate bonding. Contamination is a serious issue in processing of nanocrystalline materials; yet control and minimization of impurities such as carbon, oxygen, nitrogen, and hydrogen has not been adequately addressed in most of the investigations. Adsorbed impurities oxide films on particles surfaces and agglomeration of fine particles invariable result in poor inter particle and inter agglomerate bonding although the consolidated products may exhibit close to theoretical densities. Evaluation of properties of such nanocrystalline materials masks the 'intrinsic' effects of nanocrystalline and nanograin structure and leads to erroneous conclusions regarding nanocrystalline material behavior. Furthermore, because of the presence of 'extrinsic' effects mentioned above, the projected property enhancements for nanocrystalline materials have not been demonstrated thus far. Extensive hardness data has been generated but unfortunately, the tested specimens in most cases are impurity saturated, inadequately characterized, and poorly consolidated. Room temperature tensile properties and fracture toughness measurements are very sparse because in most cases the materials tested are brittle. Consolidation of nanocrystalline particles to fully dense compacts, while maintaining the fine structure of the starting powder has remained an elusive goal to researchers in the area. These issues have contributed to a rather slow progress in the development of nanocrystalline materials for structural applications. The paper will review the progress in the area, summarize key advances, identify key issues, and outline some of the recent successful approaches for timely resolution of the issues.

**HYDROGEN GAS EVOLUTION FROM NANOPARTICLES  
DISPERSED IN WATER IRRADIATED WITH  $\gamma$ -RAY**

*T. A. Yamamoto, S. Seino M. Katsura, K. Okitsu<sup>1</sup>, R. Oshima<sup>2</sup> and Y. Nagata<sup>2</sup>*

Department of Nuclear Engineering, Osaka University, 2-1 Yamadaoka,  
Suita, Osaka 565-0781, JAMPAN <takao@nucl.eng.osaka-u.ac.jp>

<sup>1</sup>Department of Materials Science and Engineering, Nagasaki University,  
1-14 Bunkyo, Nagasaki 852, JAPAN

<sup>2</sup>Research Institute for Advanced Science and Technology, Osaka Prefectural  
University, Gakuen, Sakai, Osaka 599-8570, JAPAN

Hydrogen gas evolution induced by g-ray irradiation of nanoparticles dispersed in aqueous solution was investigated by surveying hydrogen yields of various kinds of particle materials. Hydrogen gas was detected by a gas chromatography system after an irradiation of the sample solution in a closed vial using a  $^{60}\text{Co}$   $\gamma$ -source. Irradiation of 3.2 kGy was performed at room temperature. We have found that the titania particles known as a highly photo-catalytic material, mainly in anatase structure with average diameter of 21 nm, has a low evolution yield just slightly higher than the background hydrogen evolution due to water radiolysis, while  $\alpha$ - and  $\gamma$ -alumina showed a much higher yield, about 20 times of the background. A part of mechanism of the hydrogen evolution may be understood as an extrapolation of that of the photo-catalysis, in which holes and electrons created by photons play roles as respectively oxidizing and reducing species to electrolyse water on the particle surface. However, since the g-photon has an energy far higher than those involved in the ordinary photo catalysis, many other processes should be taken into account, such as electron removal from and incident to the particle, radicals formation from the radiolysis, etc.

**EVALUATION OF MECHANICAL PROPERTIES IN NANOMETER SCALE  
USING AFM-BASED NANOINDENTATION TESTER**

*Kensuke Miyahara, Nobuo Nagashima, Takahito Ohmura and Saburo Matsuoka*

National Research Institute for Metals, JAPAN <miyahara@nrim.go.jp>

A nanoindentation hardness apparatus was developed on the basis of an atomic force microscope to evaluate mechanical properties of microstructures. This tester can obtain both force-penetration depth curves and topographic images. Devised features were to use a lever which is held on both sides and has a three-sided pyramidal diamond tip in the center, to measure vertical displacement at the center of the lever and to add an actuator for force control. The diamond tip works as both an AFM tip and indenter.

Force-penetration depth curves represent mechanical properties of specimens. However, because of indentation size effect, the hardness values obtained by such nanoindentation tester is greater than the bulk hardness. We have measured force curves of several metallic single crystals and found good correlation between the curves and Vickers hardness values. An empirical formula for Vickers hardness is proposed in order to remove the size effect.

Using this tester, mechanical properties of drawn steel wires will be also studied.

**Authors Index****A**

Abe, H.	<b>6-6</b>	74	Antonova, M.	<b>P3-45</b>	538
Abe, M.	<b>2-5</b>	53	Anuradha, T.V.	<b>3-2</b>	57
Abinandanan, T.A.	<b>P1-29</b>	229	Arnaud d'Avitaya, F.	<b>P2-31</b>	371
Abrosimova, G.E.	<b>P3-3</b>	496		<b>P2-64</b>	404
	<b>P3-4</b>	497	Arnold, W.	<b>19-4</b>	131
Acharya, D.P.	<b>P1-31</b>	231		<b>IP-18</b>	177
	<b>P2-108</b>	450	Aronin, A.S.	<b>P3-3</b>	496
Adhikari, S.	<b>P1-79</b>	279		<b>P3-4</b>	497
Afanas'ev, A.	<b>P3-13</b>	506	Arrot, A.S.	<b>12-1</b>	97
Agladze, O.V.	<b>P3-46</b>	539	Ascencio.J.A.	<b>10-1</b>	89
Agnew, S.R.	<b>IP-27</b>	186	Astakhov, M.V.	<b>P1-89</b>	289
Ågren, J.	<b>IP-26</b>	185	Atteridge, D.	<b>P2-65</b>	405
Ahn, K.H.	<b>P1-51</b>	251	Averin, D, V,	<b>P3-96</b>	588
Aizikovich, S.M.	<b>P2-77</b>	419	Avoyan, A.	<b>PL-3</b>	46
Åklint, T.	<b>P2-10</b>	350	Ayyub, P.	<b>10-3</b>	91
Aldinger, F.	<b>P1-43</b>	243	Azzaoui, M.E.	<b>P2-4</b>	344
Alexander, G.	<b>P2-52</b>	392	<b>B</b>		
Alexandrov, I.V.	<b>P1-12</b>	212	Baba, K.	<b>6-6</b>	74
	<b>P3-9</b>	502	Babanov, Yu.A.	<b>P3-17</b>	510
	<b>P3-54</b>	547	Babich, M.	<b>P2-148</b>	490
Alexe, M.	<b>24-4</b>	159	Bakhshai, A.	<b>P1-77</b>	277
Alexeenko, A.A.	<b>P2-59</b>	399	Bakhtizin, R.Z.	<b>P3-85</b>	577
Aliev, A.E.	<b>P1-129</b>	328	Bakonyi, I.	<b>P3-30</b>	523
Aliev, F.G.	<b>18-1</b>	123	Balamurugan, B.	<b>P1-31</b>	231
	<b>P2-99</b>	441	Baldokhin, Yu.V.	<b>P1-24</b>	224
Allard, Jr	<b>12-2</b>	98	Ballesteros, C.	<b>22-3</b>	144
Altherr, A.	<b>4-5</b>	65	Balogh, J.	<b>P3-44</b>	537
Alvarez, M.P.	<b>10-1</b>	89	Barariu, F.	<b>P3-89</b>	581
Alymov, M.I.	<b>P2-27</b>	367		<b>P3-108</b>	601
	<b>P2-124</b>	466	Barinova, A.P.	<b>P1-90</b>	290
Amils, X.	<b>IP-14</b>	173		<b>P1-91</b>	291
Andersson, M.	<b>P3-106</b>	599	Barker, J.	<b>IP-29</b>	188
Andersson, M.L.	<b>15-3</b>	110	Barker, J.G.	<b>15-3</b>	110
Andersson, M.T.	<b>P2-10</b>	350	Baró, M.D.	<b>IP-14</b>	173
	<b>P2-11</b>	351		<b>P3-24</b>	517
	<b>P2-119</b>	461	Bartz, K.	<b>P3-63</b>	556
Andersson, T.G.	<b>P2-61</b>	401	Bassani, F.	<b>4-5</b>	65
Andreeva, M.A.	<b>P3-48</b>	541		<b>P2-31</b>	371
Andrievskaya, E.R.	<b>P1-121</b>	320	Bauer, H.-D.	<b>P2-64</b>	404
Andrievski, R.A.	<b>15-1</b>	108	Baughman, R.H.	<b>17-6</b>	121
Angiolini, M.	<b>P2-89</b>	431		<b>23-1</b>	147
				<b>7-2</b>	77

**Authors Index**

Baytinger, E.	<b>P2-26</b>	366	Bochenkov, V.E.	<b>P2-115</b>	457
Bazylinski, D.A.	<b>P2-151</b>	493	Bochkin, A.M.	<b>P1-62</b>	262
Beat, M.	<b>24-3</b>	158	Boero, M.,	<b>9-3</b>	85
Beck, Ch.	<b>IP-16</b>	175	Bogdanova, L.P.	<b>P2-46</b>	386
	<b>4-3</b>	63	Bogomolov, V.N.	<b>IP-7</b>	166
Becker, M.	<b>P2-65</b>	405	Boiko, G.,	<b>P2-41</b>	381
Begin-Colin, S.	<b>P1-50</b>	250	Boikov, Y.A.	<b>IP-32</b>	191
	<b>P3-41</b>	534	Bokhimi, X.	<b>P3-18</b>	511
Beke, D.L.	<b>P2-152</b>	590		<b>P3-19</b>	512
Beketov, I.	<b>P1-16</b>	216	Boldyrev, V.V.	<b>P3-72</b>	565
Belogurov, S.	<b>P2-114</b>	456	Boman, M.	<b>4-6</b>	66
Belykh, V.D.	<b>P1-91</b>	291	Bomk, O.I.	<b>P2-12</b>	352
BenderKoch, C.	<b>P1-65</b>	265	Bomze, Yu.V.	<b>P2-38</b>	378
Bennemann, K.H.	<b>6-2</b>	70		<b>P2-48</b>	388
Berdon, P.	<b>P2-103</b>	445	Bonard, J.-M.	<b>IP-37</b>	196
Berger, A.	<b>P1-54</b>	254	Bonder, M.	<b>P1-64</b>	264
Bergues, J.M.	<b>P2-43</b>	383	Bonetti, E.	<b>IP-24</b>	183
Berkowitz, A.E.	<b>17-4</b>	119		<b>P2-136</b>	478
Berry, F.J.	<b>12-5</b>	101		<b>P2-137</b>	479
Berthier, S.	<b>P2-109</b>	451		<b>P3-67</b>	560
Berzhanova, S.K.	<b>P1-103</b>	410	Bonny, V.	<b>P3-35</b>	528
Betancourt-Riera, R	<b>P2-43</b>	383	Bordyyuk, E.	<b>P1-36</b>	236
Betz, U	<b>P2-149</b>	491	Borgmeier, O.	<b>P2-111</b>	453
	<b>P3-68</b>	561	Borgohain, K.	<b>P2-49</b>	389
Beuer, H.K.	<b>P1-32</b>	232	Borisov, B.F.	<b>P1-131</b>	330
Beulen, M.	<b>P3-38</b>	531	Bork, D.	<b>P2-144</b>	486
Bezrukova, A.G.	<b>P3-98</b>	591	Börner, I.	<b>P1-100</b>	300
Bhattacharya, P.	<b>P1-94</b>	294	Boukos, N	<b>P2-9</b>	349
Bi, H.	<b>P1-2</b>	202	Bovin, J.-O.	<b>2-6</b>	54
Bill, J	<b>P1-43</b>	243		<b>IP-22</b>	181
Billas, I.M.L.	<b>P2-8</b>	348	Branz, W	<b>9-3</b>	85
	<b>9-3</b>	85		<b>P2-8</b>	348
Birringer, R.	<b>P2-110</b>	452	Braun, H.-B.	<b>19-5</b>	132
	<b>1-2</b>	48		<b>P2-113</b>	455
	<b>P3-52</b>	545	Breese, K.	<b>P1-137</b>	336
	<b>P3-110</b>	602	Bremers, H.	<b>P3-13</b>	506
Bizios, R.	<b>23-7</b>	153	Brinzanik, R.	<b>6-2</b>	70
Blaginina, L.A.	<b>P3-17</b>	510	Brjezinskaya, M	<b>P2-26</b>	366
Blin, J.	<b>4-5</b>	65	Brodova, I.G.	<b>P2-121</b>	463
Bobbert.P.A.	<b>10-5</b>	93	Brodova, I.	<b>P3-11</b>	504
Bobrysheva, N.	<b>P2-44</b>	384	Brossmann, U.	<b>P2-120</b>	462
	<b>P2-86</b>	428	Browning, V.	<b>17-5</b>	120

**Authors Index**

Broyer, M.	<b>P2-7</b>	347	Chattopadhyay, K.	<b>P1-29</b>	229
Bruynsraede, Y.	<b>18-1</b>	123		<b>P1-94</b>	294
	<b>P2-99</b>	441		<b>P2-71</b>	413
Buchstab, E.I.	<b>P2-42</b>	382		<b>P2-97</b>	439
Bugaev, A.S.	<b>P2-34</b>	374	Chattopadhyay, S.	<b>10-3</b>	91
Bunge, H.J.	<b>P3-54</b>	547	Chen, Y.	<b>IP-12</b>	171
Buranbaev, M.	<b>P2-41</b>	381		<b>P1-107</b>	306
Buravtsev, V.N.	<b>P3-83</b>	575	Chen, Y.-J.	<b>P1-7</b>	207
Burch, Ch.	<b>IP-16</b>	175		<b>P1-8</b>	208
Burch, R.	<b>22-4</b>	145		<b>P1-95</b>	295
	<b>P3-103</b>	596	Chen, Y.Y.	<b>P2-36</b>	376
Busmann, H-G	<b>P1-96</b>	296		<b>P3-1</b>	494
Bykov, Yu.	<b>P1-14</b>	214		<b>10-4</b>	92
<b>C</b>					
Caër, G.Le	<b>P1-50</b>	250	Cherepanova, S.V.	<b>P3-72</b>	565
	<b>P3-33</b>	526	Cherkaoui, R.	<b>17-2</b>	117
	<b>P3-41</b>	534	Cherkasova, V.G.	<b>P2-47</b>	387
Cai, W.P.	<b>P3-78</b>	570	Chernykh, L.V.	<b>P1-15</b>	215
Campari, E.G.	<b>IP-24</b>	183	Chesnokov	<b>P1-123</b>	322
	<b>P2-137</b>	479	Chew, C.H.	<b>P3-16</b>	509
Campora, J.	<b>4-1</b>	61	Chezhina, N.	<b>P2-86</b>	428
Campos, N.Ay.	<b>P3-33</b>	526	Chinnasamy, C.N.	<b>P2-97</b>	439
Cannas, C.	<b>P1-139</b>	338	Chiriac, H.	<b>P2-97</b>	439
Canton, P.	<b>12-3</b>	99		<b>18-4</b>	126
Cantor, B.	<b>P3-71</b>	564		<b>P1-110</b>	309
Capitán, M.	<b>P3-47</b>	540		<b>P1-120</b>	319
Carlsson, J-O	<b>4-6</b>	66		<b>P2-107</b>	449
Carlstöm, E.	<b>P1-74</b>	274		<b>P2-116</b>	458
Caro, A.	<b>20-5</b>	137		<b>P3-84</b>	576
	<b>P3-34</b>	527		<b>P3-89</b>	581
Carpenter, E.E.	<b>4-2</b>	62	Chmelik, F	<b>P3-108</b>	601
Carrot, G.	<b>P1-40</b>	240	Choa, Y.H.	<b>P2-81</b>	423
Carter, W.C.	<b>6-5</b>	73	Chong, P.F.	<b>P1-136</b>	335
Cassagneau, T.	<b>1-1</b>	47	Chopra, H.D.	<b>P3-16</b>	509
Chaiken, A.	<b>19-1</b>	128	Chou, S.Y.	<b>19-1</b>	128
Chaim, R.	<b>P1-9</b>	209		<b>16-2</b>	115
	<b>P3-2</b>	495	Chow, G.M.	<b>P3-115</b>	607
Chang, H.C.	<b>10-4</b>	92		<b>P2-57</b>	397
Chanyshева, J.	<b>P3-111</b>	603	Chow, P.Y.	<b>P3-49</b>	542
Charnaya, E.V.	<b>P1-131</b>	330	Christodoulides, J.	<b>P3-16</b>	509
	<b>P2-90</b>	432	Christodoulides, J.A.	<b>IP-41</b>	200
	<b>P2-147</b>	489	Chuev, M.	<b>P1-98</b>	298
				<b>P3-13</b>	506

**Authors Index**

Chumakov, A.I.	<b>P3-48</b>	541	Dennis, J.R.	<b>23-4</b>	150
Chuvil'deev, V.N.	<b>P2-122</b>	464	Deppert, K.	<b>2-6</b>	54
	<b>P2-123</b>	465	Derevyankin, A.I.	<b>P1-123</b>	322
Claeson, T.	<b>IP-32</b>	191	Diaz, D.	<b>P2-50</b>	390
Colla, E.V.	<b>P3-79</b>	571	Dierstein, A.	<b>4-3</b>	63
Compagnini, G.	<b>P2-16</b>	356	DiTolla, F.D.	<b>P2-32</b>	372
Costa, B.F.O.	<b>P3-33</b>	526	Diyuk, V.	<b>P3-105</b>	598
CostaFilho, R.N.	<b>6-7</b>	75	Djurkovic, G.	<b>P1-1</b>	201
Cottam, M.G.	<b>6-7</b>	75	Dligatch, S.	<b>P1-97</b>	297
Craighead, H.G.	<b>10-5</b>	93	Dmitrenko, I.M.	<b>P2-47</b>	387
Crespo, D.	<b>P2-128</b>	470	Dmitriev, A.I.	<b>P2-96</b>	438
	<b>P3-47</b>	540		<b>P2-143</b>	485
Crnjak-Orel, Z.	<b>IP-17</b>	176	Dmitruk, N.	<b>P2-2</b>	342
Cui, C.	<b>23-1</b>	147		<b>P2-39</b>	379
	<b>7-2</b>	77	Dobatkin, S.V.	<b>P2-127</b>	469
Curcic, R.	<b>P1-1</b>	201	Doerner, M.	<b>24-3</b>	158
Curran, C.	<b>24-4</b>	159	Dominguez, M.	<b>4-1</b>	61
Curtis, C.J.	<b>23-5</b>	151	D'Orazio, F.	<b>17-2</b>	117
	<b>P3-119</b>	611	Dorfman, A.M.	<b>P1-117</b>	316
Czap, N.	<b>P1-10</b>	210	Dormann, J.L.	<b>17-2</b>	117
	<b>9-2</b>	84		<b>P2-89</b>	431
Cziraki, A.	<b>P3-30</b>	523	Dorofeev, G.A.	<b>P1-116</b>	315
<b>D</b>					
Dalmazio, L.	<b>P1-83</b>	283	Doukellis, G	<b>P2-9</b>	349
DanDahlberg, E.	<b>17-1</b>	116	Dowding, R.J.	<b>21-3</b>	140
	<b>P2-151</b>	493	Doyama, M.	<b>P1-73</b>	273
Danilov, V.A.	<b>IP-32</b>	191	Dragieva, I.	<b>P1-25</b>	225
Danilyuk, A.F.	<b>P1-123</b>	322	Draie, G.	<b>P3-26</b>	519
Dantas, S.O.	<b>7-2</b>	77	Dramicanin, M.	<b>P1-38</b>	238
Dauwe, C.	<b>15-6</b>	113	Drmanjic, S.	<b>P2-45</b>	385
Davidovich, V.I.	<b>P1-70</b>	270	Drost, W.-G.	<b>P1-27</b>	227
DeAngelis, R.J.	<b>P3-58</b>	551	Du, L.	<b>P1-54</b>	254
DeArmitt, C.	<b>P1-137</b>	336	Du, Y.W.	<b>P1-58</b>	258
Debrezeni,	<b>P1-11</b>	211		<b>P2-78</b>	420
Dedukh, L.M.	<b>19-1</b>	128	Dubois, J.M.	<b>P3-8</b>	501
Degen, A.	<b>P1-59</b>	259	Dugal, M.	<b>P2-15</b>	355
deJonge, W.J.M.	<b>18-5</b>	127	Duhaj, P.	<b>P3-104</b>	597
Dekany, I.	<b>P1-11</b>	211	Dupuis, V.	<b>P2-132</b>	474
Del Barco, E.	<b>P2-88</b>	430	Dutta, J.	<b>P2-6</b>	346
Del Bianco, L.	<b>22-3</b>	144	Dvoynenko, M.M.	<b>7-1</b>	76
Del Bianco, L.	<b>P2-136</b>	478		<b>P2-39</b>	379
	<b>P3-67</b>	560	Dzhardimalieva, G.I.	<b>P2-14</b>	354

**Authors Index**

Dzidziguri, E.L.  
Dzidzigury, A.L.

**P1-63** 263  
**P3-60** 553

**E**

Eastman, J.A.  
Ebihara, K.  
Ebihara, K.  
Eckert, J.  
Edelstein, A.S.  
Efimova, E.A.  
Egorov, A.Yu.  
Egorov, S.  
Eibeck, P.  
Eickman, J.  
Eifert, T.  
Eklund, P.C.  
Ekström, M.  
El-Shall, M.S.  
Elihn, K.  
Elliott, B.R.  
Engbers, G.H.M.,  
Enzo, S.  
Eppler, A.  
Erb, U.  
Erb, U.  
Eremeev, A.  
Erenburg, A.I.  
Eriksson, G.  
Erts, D.  
Esaki, L.  
Estournes, C.

**IP-27** 186  
**P3-56** 549  
**P2-52** 392  
**6-6** 74  
**IP-9** 168  
**P1-100** 300  
**P1-101** 301  
**P1-124** 323  
**17-5** 120  
**P1-23** 223  
**P2-54** 394  
**P1-14** 214  
**6-4** 72  
**5-1** 67  
**P2-111** 453  
**9-1** 83  
**P2-92** 434  
**11-1** 94  
**P1-57** 257  
**P3-64** 557  
**4-6** 66  
**IP-27** 186  
**IP-6** 165  
**12-3** 99  
**P3-59** 552  
**PL-3** 46  
**7-5** 80  
**IP-29** 188  
**P1-14** 214  
**P2-48** 388  
**P3-61** 554  
**IP-32** 191  
**PL-2** 45  
**P1-28** 228  
**P3-29** 522

**F**

Fadeeva, V.I.  
Fagnent, S.  
Falco, C.M.  
Falk, L.K.L.  
Fan, C.,  
Farber, P.  
Farkas, D.  
Fecht, H.J.  
Federeci, J.C.  
Federenko, A.I.  
Feijen, J.  
Fendler, J.H.  
Fenelonov, V.V.  
Fenouchka, B.V.  
Ferkel, H.  
Fernandez, A.  
Ferrara, E.  
Fiorani, D.  
Fissan, H.  
Fitz-Gerald, J.  
Flink, S.  
Fogel, N.Ya.  
Fokin, A.V.  
Fokin, V.N.  
Folks, L.  
Foner, S.  
Frank, W.  
Frantti, J.  
Frattini, R.

**P1-33** 233

**P1-108** 307

**P3-32** 525

**P2-109** 451

**5-1** 67

**P1-74** 274

**14-2** 105

**P3-66** 559

**20-5** 137

**P3-34** 527

**P2-74** 416

**10-2** 90

**P2-48** 388

**IP-6** 165

**1-1** 47

**P1-123** 322

**P1-106** 305

**P1-104** 303

**P3-118** 610

**4-1** 61

**P1-109** 308

**P3-108** 601

**17-2** 117

**P2-89** 431

**2-7** 55

**4-6** 66

**14-1** 104

**P1-140** 339

**P3-38** 531

**P2-38** 378

**P2-42** 382

**P2-47** 387

**P2-48** 388

**P3-79** 571

**P1-92** 292

**24-3** 158

**17-4** 119

**15-4** 111

**P3-65** 558

**12-3** 99

## Authors Index

Frattini, R.	<b>P3-59</b>	552	Gervasyeva, I.V.	<b>P3-54</b>	547
Friedman, J.R.	<b>P3-96</b>	588	Gerward, L.	<b>P2-106</b>	448
Friedrich, J.	<b>P2-131</b>	473	Ghoshal, S.K.	<b>P3-94</b>	586
Friedrichs, B.	<b>P3-14</b>	507	Giaever, I.	<b>PL-1</b>	44
Frickeri, A.	<b>P3-38</b>	531	Gianella, S.	<b>IP-14</b>	173
Frindt, R.F.	<b>P1-112</b>	311	Ginley, D.S.	<b>23-5</b>	151
Frolov, V.D.	<b>IP-37</b>	196		<b>P3-119</b>	611
Fu, Y.	<b>P3-6</b>	499	Girhardt, T.	<b>P2-84</b>	426
Fuchs, J.	<b>7-3</b>	78		<b>P3-14</b>	507
Fukaya, T.	<b>P1-68</b>	268	Girot, T.	<b>P1-50</b>	250
<b>G</b>					
Galetich, I.K.	<b>P3-99</b>	592	Gitzovich, V.N.	<b>P1-85</b>	285
Galez, P.	<b>P1-42</b>	242	Gleeson, D.	<b>22-4</b>	145
Gan, L.M.	<b>P3-16</b>	509		<b>P3-103</b>	596
Gandelsman, V.Z.	<b>P3-119</b>	611	Gleiter, H.	<b>9-5</b>	87
Gao, D.	<b>P3-75</b>	567	Glezer, A.M.	<b>12-4</b>	100
Gao, H.	<b>P1-140</b>	339		<b>P2-142</b>	484
Gao, L.	<b>P1-26</b>	226	GloriantT.	<b>P3-3</b>	496
Gao, Y.	<b>P3-5</b>	498	Glumac, N	<b>P1-8</b>	208
	<b>P3-12</b>	505		<b>P1-95</b>	295
Garcia, A.	<b>17-2</b>	117	Gögebakan, M.	<b>P3-71</b>	564
	<b>P2-89</b>	431	Gold, J.	<b>P2-63</b>	403
Garcia, N.	<b>16-1</b>	114	Gómez, R.	<b>P3-19</b>	512
	<b>P3-113</b>	605	GoncharenkoA.V.	<b>P2-39</b>	379
García-Ruiz, A.	<b>P3-18</b>	511	Gopinathan, C.	<b>P1-79</b>	279
Garrido, V.	<b>P2-128</b>	470	Gordeev, N.Yu.	<b>P2-54</b>	394
	<b>P2-128</b>	470	Gorelik, V.S.	<b>P3-81</b>	573
	<b>P3-47</b>	540	Gornakov, V.	<b>19-1</b>	128
Gartz, M.	<b>IP-39</b>	198	Gorodetskaya, T.A.	<b>P1-123</b>	322
Gasivo, V.S.	<b>IP-10</b>	169	Gorshkov, O.N.	<b>P3-86</b>	578
Gavarri, J-R	<b>P1-41</b>	241	Göthelid, M.	<b>IP-26</b>	185
Ge, S.H.	<b>P2-72</b>	414	Grabias, A.	<b>P1-33</b>	233
Gedanken, A.	<b>2-3</b>	51		<b>P2-84</b>	426
	<b>P2-58</b>	398		<b>P2-140</b>	482
	<b>P2-134</b>	476	Grabovetskaya, G.P.	<b>P2-94</b>	436
	<b>P3-57</b>	550	Graf, T.	<b>P2-85</b>	427
Gerasimov, G.N.	<b>P1-126</b>	325	Granqvist, C.G.	<b>21-4</b>	141
	<b>P3-107</b>	600	Grebel, H.	<b>10-2</b>	90
Germanenko, I.	<b>11-1</b>	94	Grechko, L.G.	<b>P2-3</b>	343
Gerocs, I.	<b>P3-30</b>	523		<b>P3-88</b>	580
Gerold, U.	<b>P3-23</b>	516	Greer, A.L.	<b>P3-3</b>	496

## Authors Index

Grenthe, I.	<b>P1-80</b>	280	<b>H</b>	
Grigor'ev, A.E.	<b>P1-126</b>	325	Ha, G.H.	<b>P1-46</b> 246
	<b>P3-107</b>	600		<b>P3-40</b> 533
Grigor'ev, E.I.	<b>P1-126</b>	325	Hadjipanayis, G.C.	<b>19-2</b> 129
Grigor'ev, E.I.	<b>P3-107</b>	600		<b>IP-41</b> 200
Grigorieva, T.F.	<b>P1-90</b>	290		<b>P1-98</b> 298
	<b>P1-91</b>	291		<b>P1-118</b> 317
	<b>P3-72</b>	565	Hagfeldt, A.	<b>P3-61</b> 554
Grimaud, C-M	<b>P2-119</b>	461		<b>P3-65</b> 558
Grinkevych, K.E.	<b>P1-23</b>	223	Häggström, L.	<b>IP-26</b> 185
Grishin, A.M.	<b>P2-150</b>	492	Haglund, S.	<b>IP-36</b> 195
	<b>P3-70</b>	563	Hahn, H.	<b>P1-87</b> 287
	<b>6-6</b>	74		<b>P2-69</b> 409
Gromov, V.	<b>P1-81</b>	281		<b>P3-73</b> 411
Gromov, V.E.	<b>P2-21</b>	361	Hahn, H.	<b>P2-72</b> 414
Gromova, A.V.	<b>P2-21</b>	361		<b>P2-149</b> 491
Grönbeck, H.	<b>IP-28</b>	187		<b>P3-68</b> 561
Groza, J.R.	<b>21-1</b>	138		<b>P3-96</b> 588
Gryaznov, M.Y.	<b>P2-122</b>	464	Han, S.	<b>P2-63</b> 403
Gu, W.	<b>P3-92</b>	584	Hanarp, P.	<b>P2-10</b> 350
Guan, Z.	<b>P2-98</b>	440	Hanson, M.	<b>P1-133</b> 332
Gubin, S.P.	<b>23-9</b>	155	Harabe, T.	<b>4-3</b> 63
Gui, L.	<b>P1-5</b>	205	Härti, W.	<b>P2-92</b> 434
Guille, J.L.	<b>P1-28</b>	228	Hartmann, O.	<b>11-3</b> 96
GuizardC.	<b>P1-83</b>	283	Hasegawa, S.	<b>9-2</b> 84
Gunderov, D.V.	<b>P2-80</b>	422	Hasoon, F.S.	<b>12-2</b> 98
Günther, B.,	<b>P1-96</b>	296	He, L.	<b>9-2</b> 84
Guo, J.	<b>P1-5</b>	205	Heben, M.J.	<b>P1-10</b> 210
Guo, J.K.	<b>P1-26</b>	226		<b>23-6</b> 152
Guo, L.	<b>16-2</b>	115	Hedberg, L.	<b>IP-31</b> 190
Gupta, V.V.	<b>20-4</b>	136		<b>P2-40</b> 380
Gurin, V.S.	<b>P2-59</b>	399	Hedlund, J.	<b>P2-144</b> 486
Gurzhi, R.N.	<b>P2-100</b>	442	Heijtjans, P.	<b>13-2</b> 103
Gustavsson, F.	<b>P2-10</b>	350	Heim, U.	<b>9-3</b> 85
Gvozdikov, V.M.	<b>P2-145</b>	487	Heinebrodt, M.	<b>P2-8</b> 348
Gvozdikova, M.V.	<b>P2-145</b>	487	Heintz, M.	<b>4-5</b> 65
Gvozdover, R.S.	<b>P3-46</b>	539	Heitjans, P.	<b>P2-129</b> 471
			Helfen, L.	<b>1-2</b> 48
			Hellmig, R.J.	<b>P3-118</b> 610
			Helming, K.	<b>P3-54</b> 547
			Hempelmann, R.	<b>IP-16</b> 175

## Authors Index

Hempelmann, R.	<b>P2-98</b>	440	Huisman, B-H	<b>P3-38</b>	531
	<b>P2-110</b>	452	Hupe, O.	<b>P3-13</b>	506
	<b>P2-111</b>	453	Hutchison, J.L.	<b>IP-7</b>	166
	<b>4-3</b>	63	Hwu, H.H.	<b>P3-109</b>	340
Henningsson, A.	<b>P3-61</b>	554	Hwu, Y.	<b>P1-105</b>	304
Hernandez, J.M.	<b>P2-88</b>	430		<b>P2-75</b>	417
Hernando, A.	<b>22-3</b>	144	Hyakkai, M.	<b>P2-146</b>	488
Herr, U.	<b>20-2</b>	134	Hyomi, K.	<b>5-1</b>	67
	<b>P2-131</b>	473			
Hesse, D.	<b>24-4</b>	159	I		
Hesse, J	<b>P2-85</b>	427	Iasonna, A.	<b>2-2</b>	50
	<b>P2-84</b>	426	Idrisiva, S.	<b>P1-86</b>	286
	<b>P3-14</b>	507	Idzikowski, B.	<b>P2-132</b>	474
Heyer, M.	<b>P1-60</b>	260		<b>P2-140</b>	482
Higberg, K.	<b>3-1</b>	56	Igo, A.I.	<b>P3-81</b>	573
Hilborn, J.	<b>P1-40</b>	240	Ikegami, T.	<b>P2-52</b>	392
Hilger, A.	<b>IP-39</b>	198	Il'chenko, L.G.	<b>P2-12</b>	352
Hirvi, K.P.	<b>IP-23</b>	182		<b>P2-29</b>	369
Hjelm, S.	<b>P3-114</b>	606	Il'chenko, V.V.	<b>P2-12</b>	352
Hoell, A.	<b>P3-22</b>	515		<b>P2-29</b>	369
Hoffmann, W.D.	<b>P1-131</b>	330	Iline, A.	<b>P2-11</b>	351
Hofmann, H.	<b>P1-40</b>	240		<b>P3-106</b>	599
	<b>7-1</b>	76	Illy, S.	<b>P2-15</b>	355
Hofmeister, H.	<b>P1-53</b>	253	Ilver, L.	<b>P2-61</b>	401
	<b>P1-54</b>	254	Imperatori, P.	<b>P2-89</b>	431
	<b>7-1</b>	76	Inami, T.	<b>P3-51</b>	544
Holtwick, R.	<b>P1-132</b>	331		<b>P2-130</b>	472
Hono, K.	<b>IP-4</b>	163		<b>P3-50</b>	543
	<b>P3-7</b>	500	Inokuma, T.	<b>11-3</b>	96
Hornyak, L.	<b>P1-10</b>	210	Inoue, A.	<b>14-2</b>	105
Hornyak,G.L.	<b>9-2</b>	84		<b>IP-40</b>	199
Horillo, M.C.	<b>P3-21</b>	514	Iqbal, Z	<b>10-2</b>	90
Horvath, M.P.	<b>P1-77</b>	277		<b>7-2</b>	77
Hou, M.	<b>P2-4</b>	344	Irkaev, S.M.	<b>P3-48</b>	541
	<b>P2-25</b>	365	Ishikawa, M.	<b>P1-69</b>	269
Houriet, R.	<b>7-1</b>	76	Iskakova, Y.L.	<b>P2-22</b>	362
Howard, J.	<b>23-4</b>	150	Islamgaliev, R.K.	<b>P2-81</b>	423
Hsiao, P-J.	<b>P3-102</b>	595		<b>P3-10</b>	503
Hsu, S-L.	<b>P2-20</b>	360	Ito, S.	<b>IP-1</b>	160
Huang, B.	<b>IP-5</b>	164	Ivanov, E.Yu.	<b>P1-90</b>	290
Huang, GZ	<b>P2-36</b>	376	Ivanov, G.V.	<b>P1-70</b>	270
Huch, V.	<b>P1-49</b>	249	Ivanov, K.V.	<b>P2-94</b>	436

**Authors Index**

Ivanov, K.V.	<b>P2-95</b>	437	Jokanovic, V.	<b>P1-1</b>	201
Ivanov, M.G.	<b>P3-15</b>	508		<b>P1-27</b>	227
Ivanov, V.	<b>P1-14</b>	214		<b>P2-17</b>	357
	<b>P1-16</b>	216	Jolivet, J.P.	<b>17-2</b>	117
	<b>P1-18</b>	218		<b>P2-30</b>	370
Ivanova, L.Y.	<b>IP-8</b>	167	Jones, B.	<b>24-3</b>	158
Ivashko, S.V.	<b>P2-115</b>	457	Jones, K.M.	<b>9-2</b>	84
Ivchenko, V.A.	<b>18-3</b>	125	Jönsson, B.J.	<b>P1-32</b>	232
Iwama, S.	<b>P1-68</b>	268	Jorda, J.L.	<b>P1-42</b>	242
<b>J</b>			Josell, D.	<b>6-5</b>	73
Jacobsen, K.W.	<b>P2-32</b>	372		<b>IP-2</b>	161
Jacques, R.G.S.	<b>P3-21</b>	514	José-Yacamán, M.	<b>P1-2</b>	202
Jain, K.P.	<b>IP-25</b>	184		<b>P1-3</b>	203
	<b>P3-94</b>	586	Julbe, A.	<b>P1-83</b>	283
Janackovic, Dj.	<b>P1-27</b>	227	Julia, A.	<b>P2-88</b>	430
	<b>P2-17</b>	357	<b>K</b>		
Jang, L.Y.	<b>P3-1</b>	494	Kadikova, A.H.	<b>P1-116</b>	315
Jankowski, A.	<b>5-2</b>	68	Kakimoto, K.I.	<b>P1-43</b>	243
Järås, S.	<b>P1-83</b>	283	Kalinenko, A.N.	<b>P2-100</b>	442
Jartych, E.	<b>P2-83</b>	425		<b>P2-101</b>	443
Jaskiewicz, P.	<b>P2-141</b>	483	Kaloshkin, S.D.	<b>P1-24</b>	224
Jena, P.	<b>8-2</b>	82		<b>P2-24</b>	364
	<b>IP-13</b>	172	Kalyanaraman, R.	<b>21-3</b>	140
Jensen, P.J.	<b>6-2</b>	70	Kamei, S-I	<b>P1-69</b>	269
Jeunieau, L.	<b>P3-97</b>	589	Kang, WT	<b>P2-36</b>	376
Jeyadevan, B.	<b>IP-1</b>	160	Kapoor, S.	<b>IP-33</b>	192
Jiang, J.S.	<b>P1-26</b>	226		<b>P1-135</b>	334
Jiang, J.Z.	<b>12-5</b>	101	Kaptas, D.	<b>P3-44</b>	537
	<b>P1-26</b>	226	Kapustin, M.G.	<b>P1-89</b>	289
	<b>P1-65</b>	265	Kaputkina, L.M.	<b>P2-127</b>	469
	<b>P2-105</b>	447	Karabutov, A.V.	<b>IP-37</b>	196
	<b>P2-106</b>	448	Karppinen, M.	<b>P1-76</b>	276
Jin, X.M.	<b>P3-8</b>	501	Kartonozhkina, O.I.	<b>P3-112</b>	604
Jin, Z.-H.	<b>P2-33</b>	373	Kartuzov, V.V.	<b>P1-23</b>	223
Jin, Z.Q.	<b>P2-78</b>	420	Kasemo, B.	<b>23-6</b>	152
	<b>P3-8</b>	501	Kasuya, A.	<b>IP-1</b>	160
Jockel, J.,	<b>P1-102</b>	302	Kataby, G.	<b>P2-58</b>	398
Johansson, C.	<b>P2-10</b>	350	Katalin,	<b>P1-11</b>	211
John, V.T.	<b>4-2</b>	62	Katiyar, R.S.	<b>P3-82</b>	574
Johnsson, P.	<b>P2-150</b>	492	Katsura, M.	<b>P1-133</b>	332
	<b>P3-70</b>	563		<b>P1-134</b>	333

## Authors Index

Katsura, M.	<b>P3-121</b>	613	Kim, C.G.	<b>P2-138</b>	480
Katz, J.D.	<b>P1-70</b>	270	Kim, H.J.	<b>IP-21</b>	180
Kaufman, J.	<b>24-3</b>	158	Kim, J.-C.	<b>P1-127</b>	326
Kauppinen, J.P.	<b>IP-23</b>	182	Kim, K.S.	<b>IP-21</b>	180
Kavecansky, V.	<b>P2-132</b>	474		<b>P3-80</b>	572
Kawasaki, K.	<b>P1-69</b>	269	Kim, S.H.	<b>P1-64</b>	264
Kazakov, M.A.	<b>P2-127</b>	469	Kim, S.Y.	<b>P1-51</b>	251
Kear, B.H.	<b>22-5</b>	146		<b>P1-113</b>	312
	<b>P1-6</b>	206	Kim, W.T.	<b>P3-55</b>	548
	<b>P1-7</b>	207	Kinbara, A.	<b>IP-15</b>	174
	<b>P1-8</b>	208	Kinnunen, K.M.	<b>IP-23</b>	182
	<b>P1-95</b>	295	Kioussis, N.	<b>5-2</b>	68
Keblinski, P.	<b>9-5</b>	87	Kiraly, Z.	<b>P1-11</b>	211
	<b>P3-56</b>	549	Kirillova, N.	<b>P1-36</b>	236
Keghalian, P.	<b>6-3</b>	71		<b>P1-37</b>	237
Keiderling, U.	<b>P3-23</b>	516	Kir'janov, Y.V.	<b>P3-3</b>	496
Keis, K.	<b>P1-118</b>	317		<b>P3-4</b>	497
Keller, N.	<b>P3-29</b>	522	Kirkpatrick, E.	<b>P1-64</b>	264
Kemény, T.	<b>P3-44</b>	537	Kis-Varga, M.	<b>P2-152</b>	590
Kerekes, Gy.	<b>P2-152</b>	590	Kiseleva, T.Yu.	<b>P1-63</b>	263
Kester, E.	<b>19-4</b>	131	Kislov, V.V.	<b>23-9</b>	155
Khadar, M.A.	<b>P1-128</b>	327	Kiss, L.B.	<b>21-4</b>	141
Khairullin, I.	<b>7-2</b>	77	Kiss, L.F.	<b>P3-44</b>	537
	<b>23-1</b>	147	Kita, E.	<b>P2-146</b>	488
Khait, Yu.L.	<b>P2-18</b>	358	Kitagawa, M.	<b>IP-15</b>	174
Khaleel, A.	<b>P1-111</b>	310	Kitamoto, Y.	<b>2-5</b>	53
Khanna, S.N.	<b>8-2</b>	82	Klabunde, K..	<b>7-4</b>	79
	<b>IP-13</b>	172		<b>P1-25</b>	225
Khapikov, A.	<b>19-1</b>	128		<b>P1-44</b>	244
Kharlamov, A.	<b>P1-36</b>	236		<b>P1-111</b>	310
	<b>P1-37</b>	237	Knorr, P.	<b>P1-115</b>	314
Khartsev, S.I.	<b>P2-150</b>	492	Kobayashi, T.	<b>IP-15</b>	174
	<b>P3-70</b>	563	Kobelev, N.P.	<b>P2-121</b>	463
Khavryutchenko, V.D.	<b>P2-35</b>	375	Kobiyama, M.	<b>P2-130</b>	472
Kholmanov, I.N.	<b>P1-129</b>	328		<b>P3-50</b>	543
Khotinov, V.A.	<b>P2-125</b>	467		<b>P3-51</b>	544
Khrustov, V.	<b>P1-14</b>	214	Kobzar, A.A.S.	<b>P2-143</b>	485
	<b>P1-16</b>	216	Koch, M.	<b>P1-60</b>	260
KIJIMA, K.	<b>P1-30</b>	230	Koch, M.G.	<b>P3-27</b>	520
Kikineshi, A.	<b>P2-53</b>	393	Kodama, R.H.	<b>17-4</b>	119
Kim, B.K.	<b>P1-46</b>	246		<b>17-5</b>	120
	<b>P3-40</b>	533	Ködderitzsch, P.	<b>P1-53</b>	253

## Authors Index

Kogure, Y.	<b>8-1</b>	81	Kotov, N.A.	<b>3-3</b>	58
Koinuma, M.	<b>P1-130</b>	329	Kotov, Yu.	<b>P1-14</b>	214
Koivusaari, J.	<b>P1-93</b>	293	Kotov, Y.	<b>P1-16</b>	216
Kolesnikova, A.L.	<b>P2-23</b>	363		<b>P1-17</b>	217
Kolesov, V.V.	<b>23-9</b>	155		<b>P3-15</b>	508
Kolobkova, E.V.	<b>IP-19</b>	178	Kovac, J.	<b>P2-132</b>	474
Kolobov, G.P.	<b>P2-94</b>	436	Kovalchuk, I.A.	<b>P1-37</b>	237
Kolobov, Y.R.	<b>P2-93</b>	435	Kovalyova, E.G.	<b>P2-5</b>	345
	<b>P2-95</b>	437	Kovsh, A.R.	<b>P2-54</b>	394
Kolosov, V.Yu.	<b>15-2</b>	109	Kovtyukhova, N.	<b>P2-55</b>	395
Koltsov, S.	<b>P1-81</b>	281	Krämer, J.L.C.	<b>P3-113</b>	605
Koltypin, Y.	<b>P2-134</b>	476	Krasikov, I.V.	<b>P1-23</b>	223
Komashko, L.	<b>P3-112</b>	604	Krasilnikov, N.A.	<b>P2-127</b>	469
Kong, L.	<b>P3-115</b>	607	Krasnowski, M.	<b>P1-108</b>	307
Konov, V.I.	<b>IP-37</b>	196	Krasovskii, E.E.,	<b>P1-102</b>	302
Konygin, G.N.	<b>P1-55</b>	255	Kreibig, U.	<b>IP-39</b>	198
	<b>P1-116</b>	315	Krenev, L.I.,	<b>P2-77</b>	419
Kopcewicz, M.	<b>P2-84</b>	426	Kresin, V.V.	<b>20-1</b>	133
Kopcewicz, M.	<b>P2-85</b>	427	Kresin, V.Z.	<b>20-1</b>	133
	<b>P2-140</b>	482	Krill, C.E.	<b>1-2</b>	48
Kopchatov, V.I.	<b>P2-54</b>	394		<b>P3-52</b>	545
Kopeliovich, A.I.	<b>P2-100</b>	442		<b>P2-110</b>	452
	<b>P2-101</b>	443	Kristiakova, K.	<b>P3-62</b>	555
Kop'ev, P.S.	<b>P2-54</b>	394	Krüger, J.K.	<b>P1-132</b>	331
Kopylov, V.I.	<b>21-2</b>	139	Kruis, F.E.	<b>2-7</b>	55
	<b>P2-122</b>	464		<b>4-6</b>	66
Korin, E.	<b>P2-121</b>	463	Kryukova, G.N.	<b>P1-91</b>	291
KormiletsV.	<b>P2-26</b>	366		<b>P3-72</b>	565
Korobeinikov, A.Yu	<b>18-3</b>	125	Kshirsagar, A.	<b>P3-93</b>	585
Koroleva, E.Yu.	<b>P3-79</b>	571	Kübler, A.	<b>P1-101</b>	301
Korshunov, S.M.	<b>P2-34</b>	374	Kubota, H.	<b>IP-22</b>	181
Korznikov, A.V.	<b>P1-86</b>	286	Kuchumova, E.S.,	<b>P2-21</b>	361
Korznikov, V.A.	<b>P2-125</b>	467	Kudaikulova, S.	<b>P2-41</b>	381
Kosec, M.	<b>P1-38</b>	238	Kudrenitskis, I.	<b>P2-114</b>	456
Koshizaki, N.	<b>P1-130</b>	329	Kuijpers, N.C.W.	<b>18-5</b>	127
	<b>P3-90</b>	582	Kulikov, L.M.	<b>P1-23</b>	223
	<b>P3-91</b>	583		<b>P2-96</b>	438
Kosoroukov, P.	<b>P1-36</b>	236		<b>P2-143</b>	485
Kostic-Gvozdenovic, Lj	<b>P1-27</b>	227	Kulshreshtha.S.K.	<b>IP-33</b>	192
Kostorz, G.	<b>19-5</b>	132		<b>P1-135</b>	334
Kotchetov, G.A.	<b>P3-32</b>	525	Kumbhojkar, N.	<b>P3-93</b>	585
Kotov, N.A.	<b>P2-50</b>	390	Kumzerov, Yu., A.	<b>P3-79</b>	571

## Authors Index

Kurata, Y.	<b>11-3</b>	96	Lee, J.S.	<b>P1-113</b>	312
Kurihara, L.	<b>P1-66</b>	266		<b>P1-114</b>	313
Kurihara, L.K.	<b>P2-57</b>	397		<b>P1-115</b>	314
Kurihara, L.K.	<b>P3-49</b>	542	Lee, P-Y.	<b>P1-105</b>	304
Kuruvilla, B.A.	<b>P2-60</b>	400		<b>P2-75</b>	417
	<b>P2-67</b>	407	Lee, SF.	<b>P2-36</b>	376
Kusano, E.	<b>IP-15</b>	174	Lee, T.K	<b>10-4</b>	92
Kuzel, E.	<b>P2-81</b>	423	Leiserowitz, L.	<b>P2-37</b>	377
Kuzmichev, S.D.	<b>P2-34</b>	374	Lembke, U.	<b>P3-22</b>	515
Kuznetsov, A.	<b>P2-12</b>	352	Lemier, C.	<b>P3-95</b>	587
Kuznetsov, D.V.	<b>P1-63</b>	263	Lepeshkina, T.	<b>P2-2</b>	342
	<b>P3-60</b>	553	Leppävuori, S.	<b>IP-38</b>	197
Kuznetsov, V.L.	<b>IP-37</b>	196		<b>P1-93</b>	293
	<b>P1-123</b>	322	Lerme, J.	<b>P2-7</b>	347
			Lerner, M.I.	<b>P1-70</b>	270
			Leslie-Pelecky, D.L.	<b>P1-64</b>	264
<b>L</b>					
Lahav, M.	<b>P2-37</b>	377		<b>P2-133</b>	475
Lahiri, R.	<b>10-3</b>	91	Levi, S.	<b>P3-38</b>	531
Lang, M.	<b>IP-18</b>	177	Levoska, J.	<b>IP-38</b>	197
Langer, V.	<b>P2-48</b>	388		<b>P1-93</b>	293
Lantto, V.	<b>P1-76</b>	276	Li, G.H.	<b>P1-99</b>	299
	<b>P3-65</b>	558	Li, J.	<b>P2-72</b>	414
Lashkarev, G.V.	<b>P2-96</b>	438	Li, M.	<b>P3-115</b>	607
Lashkarev, G.V.	<b>P2-143</b>	485	Li, S.	<b>4-2</b>	62
Latuch, J.	<b>P2-141</b>	483		<b>11-1</b>	94
Latysh, V.V.	<b>P1-12</b>	212	Li, W.	<b>P3-92</b>	584
	<b>P3-117</b>	609	Li, W.H.	<b>10-4</b>	92
Lau, M.L.	<b>20-4</b>	136	Li, Weifeng	<b>P1-111</b>	310
	<b>IP-5</b>	164	Li, X.	<b>P3-92</b>	584
Lauer, St.	<b>P2-98</b>	440		<b>P3-5</b>	498
Lavernia, E.J.	<b>20-4</b>	136		<b>P3-12</b>	505
	<b>IP-5</b>	164		<b>P3-49</b>	542
Lavernia, J.	<b>P1-78</b>	278	Li, Z.	<b>IP-20</b>	179
Lazar, K.	<b>P1-32</b>	232		<b>P1-58</b>	258
Lecerf, N.	<b>P1-48</b>	248		<b>P3-6</b>	499
leCoutre, A.	<b>P1-132</b>	331	Liao, S.-C.	<b>P1-7</b>	207
LEDOUX, M.J.	<b>P3-29</b>	522	Lin, H-M	<b>P1-105</b>	304
Lee, D.W.	<b>P1-46</b>	246		<b>P2-20</b>	360
	<b>P3-40</b>	533		<b>P2-20</b>	360
Lee, G.G.	<b>P1-46</b>	246		<b>P2-75</b>	417
	<b>P3-40</b>	533		<b>P3-101</b>	594
Lee, J.S.	<b>P1-51</b>	251	Lin, H-M	<b>P3-102</b>	595

**Authors Index**

Lin, JJ	<b>P2-36</b>	376	Lukshima, V.A.	<b>P3-54</b>	547
Lin, K.J.	<b>P2-90</b>	432	Luo, C.P.	<b>24-2</b>	157
	<b>P2-147</b>	489	Lushnikov, S.G.	<b>P3-82</b>	574
Lin, K.Y.	<b>10-4</b>	92	Lutz, T.	<b>P1-28</b>	228
Lin, Y.S.	<b>10-4</b>	92	Iyakh, E.N.	<b>P1-72</b>	272
Lindquist, S.-E.	<b>P1-118</b>	317	Lyakhov, N.Z.	<b>P1-90</b>	290
Lin, X.P.	<b>P2-105</b>	447		<b>P1-91</b>	291
Liou, Y,	<b>P2-36</b>	376	Lyovina, V.V.	<b>P1-63</b>	263
Lipovskii, A.A.	<b>IP-19</b>	178		<b>P3-60</b>	553
Liu, G.	<b>P2-76</b>	418			
	<b>P3-75</b>	567			
Liu, J.P.	<b>P3-116</b>	608	<b>M</b>		
Liu, L.M.	<b>7-2</b>	77	Ma, E.	<b>12-2</b>	98
Liu, W	<b>P1-47</b>	247	Maase, M.	<b>P3-28</b>	521
Liu, W.C.	<b>10-4</b>	92	Macek, J.	<b>P1-59</b>	259
Liu, Y.	<b>24-2</b>	157	Macht, M-P	<b>P1-122</b>	321
	<b>P3-116</b>	608	Madurga, V.	<b>P3-23</b>	516
Livage, J.	<b>P2-30</b>	370	Maeta, H.	<b>P3-50</b>	543
Livinsh, M.	<b>P3-45</b>	538	Magini, M.	<b>2-2</b>	50
Löffler, J.F.	<b>15-6</b>	113	Magnusson, M.H.	<b>2-6</b>	54
	<b>19-5</b>	132	Magonov, S.	<b>3-3</b>	58
	<b>P2-113</b>	455	Mahamuni, S.	<b>P2-49</b>	389
	<b>P3-68</b>	561		<b>P3-93</b>	585
Lomayeva, S.F.	<b>P1-116</b>	315	Maiorova, O.A.	<b>P2-102</b>	444
Lomello-Tafin, M.	<b>P1-42</b>	242	Majetich, S.	<b>17-3</b>	118
Long, J.W.	<b>15-3</b>	110	Makhlof, S.H.	<b>17-4</b>	119
López, T.	<b>P3-19</b>	512	Makino, A.	<b>IP-40</b>	199
Lovas, A.	<b>P3-30</b>	523	Makinson, J.D.	<b>P3-58</b>	551
Loychenko, S.V.	<b>P1-37</b>	237	Maksimov, Yu.V.	<b>P3-83</b>	575
Lozovan, M.	<b>P1-110</b>	309	Malic, B.	<b>P1-38</b>	238
	<b>P2-116</b>	458	Malinowski, N.	<b>9-3</b>	85
Lu, K.	<b>15-5</b>	112		<b>P2-8</b>	348
	<b>P2-33</b>	373	Mallouk, T.E.	<b>P2-55</b>	395
	<b>P3-37</b>	530	Malm, J.-O.	<b>2-6</b>	54
Lu, L.Y.	<b>P2-78</b>	420	Mamiya, H.	<b>P2-112</b>	454
Luapunov, V.V.	<b>P1-72</b>	272	Manukhin, A.	<b>P3-11</b>	504
Lubitz, P.	<b>17-5</b>	120		<b>P2-121</b>	463
Lucari, F.	<b>17-2</b>	117	Marcin, J.	<b>P2-132</b>	474
Lucas, E.	<b>P1-44</b>	244	Marinescu, C.S.	<b>18-4</b>	126
Luck, R.	<b>P3-37</b>	530		<b>P3-84</b>	576
Lueken, H.	<b>P2-111</b>	453	Marinsek, M.	<b>P1-122</b>	321
Lukens, J.E.	<b>P3-96</b>	588	Markov, K.A.	<b>P3-86</b>	578

## Authors Index

Markushev, M.V.	<b>P2-102</b>	444	Michel, T.	<b>15-4</b>	111
Martin, J.E.	<b>22-2</b>	143	Michels, A.	<b>1-2</b>	48
Martin, J.L.	<b>P2-43</b>	383		<b>IP-29</b>	188
Martin, T.P.	<b>P2-8</b>	348	Mikaelyan, K.N.	<b>P2-23</b>	363
	<b>9-3</b>	85	Mikhailik, O.M.	<b>P1-55</b>	255
Martinez-Miranda, L.J.	<b>P3-49</b>	542		<b>P1-117</b>	316
Massobrio, C.	<b>9-3</b>	85	Mikhailov, M.Yu.	<b>P2-38</b>	378
Mastalir, A.	<b>P1-11</b>	211		<b>P2-42</b>	382
Masumoto, T.	<b>IP-40</b>	199		<b>P2-47</b>	387
Mathur, S.	<b>P1-49</b>	249	Mikhailov, S.B.	<b>P2-125</b>	467
Mathur, S.	<b>4-3</b>	63	Mikhailova, M.	<b>P2-86</b>	428
Matsubara, H.	<b>P1-21</b>	221	Mikhailova, S.S.	<b>P1-55</b>	255
Matsumoto, T.	<b>P1-52</b>	252		<b>P1-116</b>	315
Matsumoto, Y.	<b>P1-130</b>	329	Mikov, S.N.	<b>P3-81</b>	573
Matsuoka, S.	<b>P3-122</b>	614	Miller, M.M.	<b>17-5</b>	120
Matyja, H.	<b>P1-33</b>	233	Millot, N.	<b>P3-41</b>	534
	<b>P1-108</b>	307	Milovzorov, D	<b>11-3</b>	96
	<b>P3-31</b>	524	Mishak, A.	<b>P2-53</b>	393
	<b>P3-32</b>	525	Mishra, P.	<b>IP-25</b>	184
Mayo, M.J.	<b>IP-11</b>	170	Misra, S.	<b>P2-68</b>	408
Mayo, W.E.	<b>P1-7</b>	207	Mitchler, P.D.	<b>17-1</b>	116
McCormic, P.G.	<b>4-4</b>	64	Mittal, J.P.	<b>IP-33</b>	192
McCormick	<b>P1-47</b>	247		<b>P1-135</b>	334
McMichael, R.D.	<b>IP-29</b>	188	Miyahara, K.	<b>P3-122</b>	614
McNiff, E.J.	<b>17-4</b>	119	Mizsei, J.	<b>P1-76</b>	276
Medvedev, A.	<b>P1-16</b>	216	Mizubayashi, H.	<b>14-4</b>	107
Mehta, B.R.	<b>P1-31</b>	231	Mizukoshi, Y.	<b>P1-13</b>	213
	<b>P2-108</b>	450	Mo, C.M.	<b>P3-77</b>	569
Meier, M.	<b>P3-52</b>	545	Mocellin, A.	<b>P1-50</b>	250
Melinon, P.	<b>6-3</b>	71	Moga, A.E.	<b>P1-120</b>	319
	<b>P2-6</b>	346	Möller, A.	<b>P1-87</b>	287
Melnichenko, I.M.	<b>P2-59</b>	399		<b>6-4</b>	72
Ménard, S.	<b>P2-31</b>	371	Molochnikov, L.S.	<b>P2-5</b>	345
	<b>P2-64</b>	404	Monty, C.J.A.	<b>P1-67</b>	267
Meng, G.W.	<b>9-6</b>	88	Moodera, J.S.	<b>18-5</b>	127
Menon, A.	<b>24-1</b>	156	Moon, I.-H.	<b>P1-127</b>	326
Menshikova, S.V.	<b>P2-46</b>	386	Morales, A.	<b>P3-18</b>	511
Merkert, P.	<b>P3-73</b>	411		<b>P3-19</b>	512
Merzbacher, C.I.	<b>15-3</b>	110	Moravsky, A.P.	<b>P1-92</b>	292
Meyer, F.	<b>4-3</b>	63	Mordkovich, V.Z.	<b>P1-4</b>	204
Meyer, U.	<b>P1-96</b>	296	Morosov, Y.N.	<b>P1-39</b>	239
Michel, D.	<b>P1-131</b>	330	Mørup, S.	<b>12-5</b>	101

**Authors Index**

Mørup, S.	<b>P1-65</b>	265	Nam, J.G.	<b>P1-115</b>	314
	<b>P2-106</b>	448	Nanda, J.	<b>P2-60</b>	400
Moser, A.	<b>24-3</b>	158	Nanto, H.	<b>P2-67</b>	407
Moshchalkov, V.V.	<b>18-1</b>	123	Naser, J.	<b>IP-15</b>	174
Moskovits, M.	<b>P1-9</b>	209	Natter, H.	<b>P1-104</b>	303
Mu{evi, I.	<b>IP-17</b>	176		<b>P2-98</b>	440
Muhammed, M	<b>P1-84</b>	284		<b>P2-110</b>	452
	<b>P1-80</b>	280	Nayak, S.K.	<b>8-2</b>	82
	<b>P1-83</b>	283	Nazarov, A.A.	<b>P2-28</b>	368
	<b>P1-138</b>	337	Neagu, M.	<b>P2-107</b>	449
	<b>P3-64</b>	557	Necula, F.	<b>P1-120</b>	319
	<b>P3-100</b>	593	Nedeljkovic, J.M.	<b>P2-45</b>	385
	<b>P3-114</b>	606	Negrier, M.	<b>P2-6</b>	346
Mukhamedzhanova, S.	<b>P3-111</b>	603	Nemukhin, A.V.	<b>13-1</b>	102
Mukoseev, A.G.,	<b>P3-25</b>	518	Neu, V.	<b>17-6</b>	121
Mulas, G.	<b>12-3</b>	99	Neuendorf, R.	<b>IP-39</b>	198
Mulyukov, R.R.	<b>P2-125</b>	467	Ng, C.B.	<b>P1-125</b>	324
	<b>P3-17</b>	510	Ni, T.	<b>P2-50</b>	390
	<b>P3-85</b>	577	Niarchos, D.	<b>IP-41</b>	200
Muñoz, J.S.	<b>IP-14</b>	173	Nihoul, G.	<b>P1-71</b>	271
Murashkin, M.Yu.	<b>P2-102</b>	444	Niihara, K.	<b>9-4</b>	86
Murayama, A.	<b>5-1</b>	67		<b>P1-136</b>	335
Murgulescu, I.	<b>P3-108</b>	601	Niihara, K.	<b>P3-43</b>	536
Murin, I.V.	<b>P1-85</b>	285	Nikitenko, V.	<b>19-1</b>	128
Murzakaev, A.	<b>P1-16</b>	216	Nikitina, E.A.	<b>P2-35</b>	375
Musalimov, R.Sh.	<b>P2-28</b>	368	Niklasson, G.A.	<b>10-5</b>	93
	<b>P3-85</b>	577		<b>21-4</b>	141
Mushnikov, N.V.	<b>IP-10</b>	169		<b>P1-22</b>	222
Musinu, A.	<b>P1-139</b>	338		<b>P2-91</b>	433
Mussman, L.	<b>P3-114</b>	606		<b>P2-118</b>	460
<b>N</b>					
Nagashima, N.	<b>P3-122</b>	614	Nikolaeva, E.V.	<b>P3-107</b>	600
Nagata, Y.	<b>P1-13</b>	213	Nishimaki, K.	<b>P1-133</b>	332
	<b>P3-121</b>	613		<b>P1-134</b>	333
Nagy, J.B.	<b>P3-97</b>	589	Niu, F.	<b>P3-71</b>	564
Nakagava, T.	<b>P1-133</b>	332	Nogués, J.	<b>IP-14</b>	173
Nakahira, A.	<b>P1-30</b>	230	Nogués, M.	<b>17-2</b>	117
Nakajima, S.	<b>IP-22</b>	181	Nordholm, S.	<b>IP-28</b>	187
Nakatani, I.	<b>P2-112</b>	454	Noskova, N.I.	<b>IP-34</b>	193
Nakayama, T.	<b>P1-136</b>	335		<b>P1-86</b>	286
Nam, J.G.	<b>P1-114</b>	313	Novakova, A.A.	<b>P2-70</b>	412
				<b>P1-63</b>	263
				<b>P3-46</b>	539

**Authors Index**

Novaro, O.	<b>P3-19</b>	512	Osmolovski, M.	<b>P2-44</b>	384	
Nozaki, T.	<b>8-1</b>	81		<b>P2-86</b>	428	
Nozdrin, A.	<b>P1-18</b>	218		<b>P2-87</b>	429	
<b>O</b>			Otten, F.	<b>2-7</b>	55	
Obraztsova, E.D.	<b>IP-37</b>	196	Ou, H.	<b>P3-6</b>	499	
O'Connor, C.J.	<b>4-2</b>	62	Ovari, T.-A.	<b>18-4</b>	126	
	<b>P1-45</b>	245		<b>P3-84</b>	576	
Odawara, O.	<b>P1-69</b>	269	Ovid'ko, I.A.	<b>P2-23</b>	363	
Odokienko, I.I.	<b>P1-23</b>	223	Oyama, T.	<b>P3-91</b>	583	
Ogenko, V.M.	<b>P3-88</b>	580	<b>P</b>			
Ohgami, T.	<b>IP-22</b>	181	Padella, F.	<b>2-2</b>	50	
Ohmae, S.	<b>P1-134</b>	333	Pak, A.	<b>P3-112</b>	604	
Ohmura, T.	<b>P3-122</b>	614	Pakhomov, A.B.	<b>P2-104</b>	446	
Ohnuma, M.	<b>IP-4</b>	163	Pal, U.	<b>P3-91</b>	583	
	<b>P3-7</b>	500	Palma, P.	<b>4-1</b>	61	
Ohshita, K.	<b>P1-68</b>	268	Palmer, R.E.	<b>P2-119</b>	461	
Ohtsuka, H.	<b>P3-50</b>	543	Palpant, B.	<b>P2-7</b>	347	
Okada, T.	<b>12-5</b>	101	Palumbo, G.	<b>7-5</b>	80	
Okazaki, M.	<b>P1-52</b>	252	Palyok, V.	<b>P2-53</b>	393	
Okitsu, K.	<b>P3-121</b>	613	Pan, S-F.	<b>P3-101</b>	594	
Oku, T.	<b>IP-22</b>	181	Panagiotopoulos, I.	<b>IP-41</b>	200	
	<b>9-4</b>	86	Pande, B.M.	<b>P1-135</b>	334	
Okuda, S.	<b>P2-130</b>	472	Paranin, S.	<b>P1-16</b>	216	
	<b>P3-50</b>	543	Parker, F.T.	<b>17-4</b>	119	
	<b>P3-51</b>	544	Parrinello, M.	<b>9-3</b>	85	
OldeRiekerink, M.B.	<b>IP-6</b>	165	Pasquini, L.	<b>IP-24</b>	183	
Oleszak, D.	<b>P2-83</b>	425		<b>P2-137</b>	479	
	<b>P3-31</b>	524				
Ollivier, P.J.	<b>P2-55</b>	395		<b>P3-67</b>	560	
Olofsson, L.	<b>IP-31</b>	190	Pavlikyanov, E.	<b>P1-25</b>	225	
Olsen, J.S.	<b>P2-106</b>	448	Pavlovská, M.	<b>P2-2</b>	342	
Olsson, E.	<b>P2-10</b>	350	Pei, C.	<b>P3-75</b>	567	
Onodera, H.	<b>IP-4</b>	163	Pekala, K.	<b>P2-141</b>	483	
	<b>P3-7</b>	500	Pekala, M.	<b>P2-83</b>	425	
Onyestiyak, Gy.	<b>P1-32</b>	232	Pekola, J.P.	<b>IP-23</b>	182	
Orlovic, A.	<b>P1-27</b>	227	Pellarin, M.	<b>P2-7</b>	347	
Ortega, R.J.	<b>18-2</b>	124	Pennycook, S.J.	<b>P1-140</b>	339	
Oshima, R.	<b>P1-13</b>	213	PérezdeLandazábal, I	<b>18-2</b>	124	
	<b>P3-121</b>	613	Perez, A.	<b>6-3</b>	71	
Osipov, V.V.,	<b>P3-15</b>	508		<b>P2-6</b>	346	
Osmolovski, M.	<b>IP-8</b>	167	Perriat, P.	<b>P3-41</b>	534	

## Authors Index

Persson, S, H.M.	<b>IP-31</b>	190	Prados, C.	<b>19-2</b>	129
Petkov, V.	<b>P3-24</b>	517	Prangnell, P.B.	<b>P2-102</b>	444
Petrikov, V.D.	<b>IP-19</b>	178	Presz, A.	<b>P1-34</b>	234
Petronis, S.	<b>23-6</b>	152	Prevel, B.	<b>P2-7</b>	347
Petrov, A.	<b>P2-114</b>	456	Primavera, A.	<b>P3-59</b>	552
Petrov, V.A.	<b>P2-62</b>	402	Prochorov, K.A.	<b>P3-48</b>	541
Petrov, Y.I.	<b>IP-3</b>	162	Prodan, A.	<b>P3-63</b>	556
Petrunin, V.A.	<b>P2-21</b>	361	Prokopenko, V.B.	<b>P2-59</b>	399
Petrunin, V.F.	<b>P3-42</b>	535	Proksch, R.	<b>P2-151</b>	493
Petteghem, S.V.	<b>15-6</b>	113	Provenzano, V.	<b>23-2</b>	148
Pham-Huu, C.	<b>P3-29</b>	522		<b>P1-66</b>	266
Phillpot, S.R.	<b>9-5</b>	87		<b>P3-120</b>	612
Piccaluga, G.	<b>P1-139</b>	338	Prozorov, R.	<b>P2-58</b>	398
Pignataro, B	<b>P2-16</b>	356		<b>P2-134</b>	476
Pignolet, A.	<b>24-4</b>	159		<b>P3-57</b>	550
Pillong, F.	<b>4-5</b>	65	Prozorov, T.	<b>P2-134</b>	476
Pimenov, S.M.	<b>IP-37</b>	196		<b>P3-57</b>	550
Pinchuk, A.M.	<b>P2-12</b>	352	Prusov, A.N.	<b>P3-36</b>	529
Pinchuk, V.M.	<b>P2-12</b>	352	Puglisi, O	<b>P2-16</b>	356
Pineda, E.	<b>P3-47</b>	540	Pustovit, V.N.	<b>P2-3</b>	343
Ping, D.H.	<b>P3-7</b>	500	Puzov, I.P.	<b>P3-81</b>	573
Pirjamali, M.	<b>P1-83</b>	283	Pyshmintcev, I.Yu.	<b>P2-125</b>	467
Pirttiaho, L.	<b>P1-76</b>	276		<b>Q</b>	
Pletnev, M.A.	<b>P1-117</b>	316	Qi, Min	<b>P2-74</b>	416
Plotnikov, P.G.	<b>P1-131</b>	330	Qian, Z.	<b>P2-79</b>	421
Plummer, C.	<b>P1-40</b>	240	Qin, B.	<b>P2-76</b>	418
Pogany, L.	<b>P1-77</b>	277		<b>P3-75</b>	567
Pomogailo, A.D	<b>P1-61</b>	261	Quek, C.H.	<b>P3-16</b>	509
	<b>P1-62</b>	262		<b>R</b>	
	<b>P2-13</b>	353	R., Mikov	<b>P2-81</b>	423
	<b>P2-14</b>	354	Raab, G.I.	<b>P1-12</b>	212
Pomogailo, S.I.	<b>P2-14</b>	354	Rabe, U.	<b>19-4</b>	131
Ponpandian, N.	<b>P2-97</b>	439	Radaelli, P.	<b>12-3</b>	99
Portilla, M.	<b>P3-18</b>	511	Ragulya, A.V.	<b>P1-121</b>	320
Portnoy, V.K.	<b>P3-31</b>	524	Rajh, T.	<b>P2-45</b>	385
	<b>P3-32</b>	525	Ralchenko, V.G.	<b>7-2</b>	77
Potty, S.N.	<b>P1-128</b>	327	Ramasamy, S.	<b>IP-30</b>	189
Povstugar, V.I.	<b>P1-55</b>	255	Ramin, D.	<b>P2-84</b>	426
	<b>P1-116</b>	315		<b>P2-117</b>	459
	<b>P1-117</b>	316	Ramsak, N.	<b>P3-63</b>	556
Pozarov, A.S.	<b>IP-37</b>	196			
Pradell, T.	<b>P3-47</b>	540			

## **Authors Index**

Ranganathan, S.	<b>3-2</b>	57	RomaniukV.R.	<b>P2-39</b>	379
Rao, B.K.	<b>8-2</b>	82	Romanov, A.E.	<b>P2-23</b>	363
	<b>IP-13</b>	172	Ronda, A.	<b>P2-64</b>	404
Rao, K.V.	<b>17-7</b>	122	Rosén, A.	<b>IP-28</b>	187
	<b>P2-138</b>	480		<b>P2-10</b>	350
	<b>P2-150</b>	492	Roshko, R.M.	<b>17-1</b>	116
	<b>P2-151</b>	493	Roth, M.	<b>P2-111</b>	453
Ratochka, I.V.	<b>P2-94</b>	436	Rouanet, A.	<b>P1-67</b>	267
	<b>P2-95</b>	437	Roubin, M.	<b>P1-71</b>	271
Ravi, B.G.	<b>P1-9</b>	209	Rozenberg, A.S.	<b>P1-61</b>	261
	<b>P3-2</b>	495	Ruffer, R.	<b>P3-48</b>	541
Ravishankar, N	<b>P1-29</b>	229	Rullang, F.	<b>P1-60</b>	260
Read, D.	<b>IP-2</b>	161	Rusu, F.	<b>P1-110</b>	309
Reddy, B.V.	<b>8-2</b>	82		<b>P2-116</b>	458
Reddy, E.P.	<b>P1-109</b>	308	Ryu, G.-H.	<b>P2-138</b>	480
	<b>4-1</b>	61	Ryu, S.-S.	<b>P1-127</b>	326
Reetz, M.T.	<b>P3-27</b>	520	Ryzhonkov, D.I.	<b>P3-60</b>	553
	<b>P3-28</b>	521			
	<b>P3-104</b>	597			
Reimann, K.	<b>P3-39</b>	532	S., Obraztsova	<b>P2-81</b>	423
Reinhoudt, D.N.	<b>P3-38</b>	531	Saenger, D.U.	<b>20-3</b>	135
Rellinghaus, B.	<b>2-7</b>	55	Sagel, A.	<b>P2-74</b>	416
Rensmo, H.	<b>P1-118</b>	317	SainteCatherine, M.C.	<b>P2-109</b>	451
	<b>P3-61</b>	554	Sakai, S.	<b>14-4</b>	107
Reuben, A.J.	<b>P2-19</b>	359	Sakai, Y.	<b>P1-68</b>	268
Revenko, R.	<b>P2-151</b>	493	Sakamoto, K.	<b>P1-119</b>	318
Revo, S.	<b>P3-105</b>	598	Salaschenko, N.N.	<b>P3-48</b>	541
Rickerby, D.G.	<b>23-2</b>	148	Salmeron, Miquel	<b>19-3</b>	130
	<b>P3-21</b>	514	Salunke, H.G.	<b>P1-135</b>	334
Riehemann, W	<b>P2-84</b>	426	Samatov, O.M.	<b>P1-17</b>	217
	<b>P2-117</b>	459		<b>P3-15</b>	508
Rieke, R.D.	<b>P1-64</b>	264	Sampaolesi, E.	<b>IP-24</b>	183
Riera, R.	<b>P2-43</b>	383		<b>P2-137</b>	479
Robertson, A.	<b>7-5</b>	80		<b>P3-67</b>	560
Rödel, J.	<b>P3-73</b>	411	Samwer, K.	<b>P2-131</b>	473
Rogachev, A.A.	<b>P2-56</b>	396	Sanchez-Lopez, J.C.	<b>P1-109</b>	308
Rogacheva, E.A.	<b>P3-82</b>	574	SanchezLopez, J.C.	<b>4-1</b>	61
Rojas, T.C.	<b>P1-109</b>	308	Sandagi, R.K.	<b>22-5</b>	146
	<b>4-1</b>	61	Sanders, P.G.	<b>IP-27</b>	186
Rojo, J.M.	<b>22-3</b>	144	Sandomirsky, V.B.	<b>P2-62</b>	402
Roldan, E.	<b>4-1</b>	61	Sarma, D.D.	<b>P2-60</b>	400
Rolison, D.R.	<b>15-3</b>	110		<b>P2-67</b>	407

**Authors Index**

Sarnatskii, V.M.	<b>P2-90</b>	432	Schulz, D.L.	<b>23-5</b>	151
	<b>P2-147</b>	489		<b>P3-119</b>	611
Sasaki, T.	<b>P1-130</b>	329	Schur, D.V.	<b>P1-92</b>	292
	<b>P3-90</b>	582	Schurack, F.	<b>IP-9</b>	168
	<b>P3-91</b>	583	Schwitzgebel, G.	<b>13-2</b>	103
	<b>P2-146</b>	488		<b>P1-60</b>	260
Sastray, S.M.L.	<b>14-3</b>	106	Scipione, G.	<b>IP-24</b>	183
	<b>P1-66</b>	266		<b>P2-137</b>	479
	<b>P3-120</b>	612	Scott, J.F.	<b>24-4</b>	159
Satoh, A.	<b>IP-15</b>	174	Segers, D.	<b>15-6</b>	113
Saul, A.	<b>P2-31</b>	371		<b>P3-35</b>	528
Sauques, L.	<b>P2-109</b>	451	Seidel, M.	<b>P1-100</b>	300
Savenko, B.N.	<b>P3-79</b>	571	Seifried, S.	<b>P2-69</b>	409
Savini, L.	<b>P2-136</b>	478	Seino, S.	<b>P3-121</b>	613
Sayagues, M.J.	<b>P1-109</b>	308	Seip, C.T.	<b>4-2</b>	62
Scechtmann, D.	<b>IP-2</b>	161		<b>P1-45</b>	245
Schadler, L.S.	<b>P1-125</b>	324	Selenova, B.	<b>P3-111</b>	603
Schaefer, H.E.	<b>15-4</b>	111	Sella, C.	<b>P2-109</b>	451
	<b>P2-120</b>	462	Sellmyer, D.J.	<b>24-2</b>	157
	<b>P3-39</b>	532		<b>P3-116</b>	608
	<b>P3-66</b>	559	Semchuk, O.Yu.	<b>P3-88</b>	580
Schalek, R.	<b>P2-133</b>	475	Semenov, V.G.	<b>P1-85</b>	285
Scharwaechter, P.	<b>15-4</b>	111		<b>P2-51</b>	391
Schattke, W.	<b>P1-102</b>	302		<b>P2-87</b>	429
Schenider, J.J.	<b>9-2</b>	84	Semenov, V.G.	<b>P3-48</b>	541
Schimid, G.	<b>9-4</b>	86	Semjonov-Kobzar, A.A.	<b>P1-23</b>	223
Schiottz, J.	<b>P2-32</b>	372		<b>P1-106</b>	305
Schlörke, N.	<b>P1-20</b>	220		<b>P2-96</b>	438
Schmelzer, M.	<b>P2-98</b>	440	Senet, P.	<b>P2-25</b>	365
	<b>P2-110</b>	452	Sergeev, B.M.	<b>13-1</b>	102
Schneider, J.J.	<b>P1-10</b>	210		<b>P3-36</b>	529
Schneider, P.	<b>P3-73</b>	411	Sergeev, G.B.	<b>13-1</b>	102
Schoeman, B.J.	<b>3-1</b>	56		<b>P1-39</b>	239
Scholl, M.	<b>P2-65</b>	405		<b>P2-115</b>	457
	<b>P2-66</b>	406		<b>P3-36</b>	529
Scholz, S.M.	<b>P1-40</b>	240	Sergeev, I.A.	<b>P2-51</b>	391
Schuller, I.	<b>6-1</b>	69	Serikov, V.V.	<b>IP-10</b>	169
Schultz, L.	<b>17-6</b>	121	Serova, N.A.	<b>P2-77</b>	419
	<b>IP-9</b>	168	Serventi, A.M.	<b>P3-21</b>	514
	<b>P1-20</b>	220	Sethuram, K.	<b>21-3</b>	140
	<b>P1-101</b>	301		<b>P1-73</b>	273
	<b>P1-124</b>	323	Seynaeve, E.	<b>P2-99</b>	441

**Authors Index**

Shabashov, V.A.	<b>P3-25</b>	518	Sivamohan, R.	<b>IP-1</b>	160
Shabatina, T.I.	<b>13-1</b>	102	Skala, D.	<b>P1-27</b>	227
	<b>P1-39</b>	239	Skandan, G.	<b>P1-8</b>	208
Shafi, K.V.P.M.	<b>P3-57</b>	550		<b>P1-95</b>	295
Shafi, Kurikka.V.P.M.,	<b>2-3</b>	51	Skorokhod, V.V.	<b>P1-121</b>	320
Shammazov, A.M.	<b>P2-103</b>	445	Skorvanek, I.	<b>P2-132</b>	474
Shapiro, A.J.	<b>19-1</b>	128	Skripkin, M.Yu.	<b>P1-15</b>	215
Sharma, S.K.	<b>P1-31</b>	231	Slepov, S.K.	<b>P3-112</b>	604
Shebanovs, L.	<b>P3-45</b>	538	Smirnov, E.P.	<b>P1-82</b>	282
Sheka, E.F.	<b>P2-35</b>	375	Smirnov, V.	<b>P2-44</b>	384
Shelekhov, E.V.	<b>P1-24</b>	224	Smirnov, V.M.	<b>3-4</b>	59
Shelkovsky, V.S.	<b>P3-99</b>	592		<b>P1-85</b>	285
Sheshadri, K	<b>10-3</b>	91		<b>P2-46</b>	386
Shevchenko, N.B.	<b>P1-98</b>	298		<b>P2-90</b>	432
Shevchenko, S.I.	<b>P2-139</b>	481		<b>P2-147</b>	489
Shi, J.L.	<b>P2-79</b>	421	Smith, G.B.	<b>P1-97</b>	297
Shiang, H-G	<b>P2-36</b>	376		<b>P2-19</b>	359
Shih, H.C.	<b>IP-35</b>	194	Smith, G.D.W.	<b>P3-71</b>	564
Shiomii, K.	<b>P1-133</b>	332	Södergren, S.	<b>P3-61</b>	554
Shiplyak, M.	<b>P2-53</b>	393	Soderlund, J.	<b>21-4</b>	141
Shkunov, M.	<b>23-1</b>	147	Södervall, U.	<b>P2-120</b>	462
Shorshorov, M.Kh.	<b>P2-27</b>	367	Soifer, L.	<b>P2-121</b>	463
Shorubalko, I.	<b>P3-45</b>	538	Soifer, Y.M.	<b>P2-121</b>	463
Shourie, S.	<b>P1-84</b>	284	Soldatov, E.S.	<b>23-9</b>	155
Shtol'ts, A.	<b>P1-16</b>	216	Solis, J.L.	<b>P3-65</b>	558
Shul'ga, Yu.M.	<b>P1-92</b>	292	Solntsev, V.P.	<b>P1-106</b>	305
Shull, R.D.	<b>19-1</b>	128	Solntseva, T.A.	<b>P1-106</b>	305
	<b>IP-29</b>	188	Solomin, V.A.	<b>P1-72</b>	272
Sibieude, F.	<b>P1-67</b>	267	Somorjai, G.A.	<b>PL-3</b>	46
Sidorenko, A.S.	<b>P2-42</b>	382	Song, I.Y.	<b>IP-21</b>	180
Sieber, H.	<b>17-5</b>	120	Soni, R.K.	<b>P3-94</b>	586
Siegbahn, H.	<b>P3-61</b>	554	Sorenson, Ch.	<b>7-4</b>	79
Siegel, R.W.	<b>23-7</b>	153	Sorokin, L.M.	<b>IP-7</b>	166
	<b>P1-125</b>	324	Sorokoumov, V.E.	<b>P2-34</b>	374
Siirola, E.	<b>23-3</b>	149	Sosnin, O.V.	<b>P2-21</b>	361
Siller, L.	<b>P2-119</b>	461	Sotelo, J.A.	<b>P1-22</b>	222
Simon, U.	<b>P1-102</b>	302	Spaczter, M.	<b>20-5</b>	137
Simopoulos, A.	<b>5-2</b>	68		<b>P3-34</b>	527
Singh, R.K.	<b>14-1</b>	104	Spasic, P.	<b>P2-17</b>	357
	<b>P1-140</b>	339	Spassov, T.	<b>P3-24</b>	517
Siny, I.G.	<b>P3-82</b>	574	Spatz, J.P.	<b>6-4</b>	72
Sipatov, A.Yu.	<b>P2-48</b>	388	Spinu, L.	<b>17-2</b>	117

**Authors Index**

Spule, A.	<b>P3-45</b>	538	Sun, X.K.	<b>P1-3</b>	203
Srdic, V.V.	<b>IP-36</b>	195	Suriñach, M.D.	<b>P3-63</b>	556
	<b>P3-69</b>	562	Suriñach, S.	<b>IP-14</b>	173
Srinawasan, D	<b>P2-71</b>	413		<b>P3-24</b>	517
Starrost, F.,	<b>P1-102</b>	302	Sutherland, D.	<b>P2-63</b>	403
Stavroyiannis, S.	<b>IP-41</b>	200	Suzdalev, I.P.	<b>P3-83</b>	575
Stelmukh, I.V.	<b>P1-89</b>	289	Svec, P.	<b>P3-62</b>	555
Stepanenko, N.B.	<b>P1-103</b>	410	Swagten, H.J.M.	<b>18-5</b>	127
Stepikhova, M.V.	<b>P3-86</b>	578	Sweeney, S.M.	<b>IP-11</b>	170
Sternberg, A.	<b>P3-45</b>	538	Swygenhoven, H.Van	<b>15-6</b>	113
Sterte, J.	<b>3-1</b>	56		<b>20-5</b>	137
	<b>P2-40</b>	380		<b>P3-34</b>	527
Stetzenko, A.N.	<b>P2-47</b>	387		<b>P3-35</b>	528
Stietz, F.	<b>11-2</b>	95	Sysoev, A.N.	<b>P2-122</b>	464
	<b>P2-1</b>	341	Syzdykova, A.	<b>P2-41</b>	381
	<b>P2-11</b>	351	Szabo, D.V.	<b>7-3</b>	78
	<b>P3-106</b>	599		<b>P3-20</b>	513
Stoeva, S.	<b>P1-25</b>	225	Szabó, S.	<b>P2-152</b>	590
Stoimenov, P.	<b>P1-25</b>	225	Szewczak, E.	<b>P1-34</b>	234
Stolyarov, V.V	<b>P3-117</b>	609		<b>P1-35</b>	235
	<b>P2-80</b>	422	Szucs, A.	<b>P1-11</b>	211
	<b>P2-82</b>	424			
Stopic, S.	<b>P1-75</b>	275	<b>T</b>		
Stoynov, Z.	<b>P3-26</b>	519	Tajika, M.	<b>P1-21</b>	221
Strikha, V.I.	<b>P2-12</b>	352	Takacs, L.	<b>P1-77</b>	277
Strutt, P.R.	<b>P1-6</b>	206	Takahashi, H.	<b>IP-1</b>	160
	<b>P3-19</b>	512	Takamura, S.	<b>P3-51</b>	544
Stuke, M.	<b>P2-1</b>	341	Takano, K.	<b>17-4</b>	119
Sturm, A	<b>P3-68</b>	561	Takeuchi, A.	<b>14-2</b>	105
Su, Z.	<b>P2-72</b>	414	Tamou, Y.	<b>P1-19</b>	219
Subbash, G.	<b>21-3</b>	140	Tan, G.	<b>IP-20</b>	179
	<b>P1-73</b>	273		<b>P1-56</b>	256
Suber, L.	<b>P2-89</b>	431		<b>P3-87</b>	579
Suda, Y.	<b>6-6</b>	74	Tanaka, S	<b>P2-73</b>	415
	<b>21-3</b>	140	Tanaka, S.-I.	<b>2-1</b>	49
Sudarshan, T.S.	<b>P1-73</b>	273		<b>P1-19</b>	219
Suganuma, K.	<b>9-4</b>	86		<b>P3-74</b>	566
	<b>IP-22</b>	181	Tang, K.	<b>P3-6</b>	499
Sukhostavskaya, O.V.	<b>P2-127</b>	469	Tang, S.L.	<b>P2-78</b>	420
Sun, X.Ch.	<b>P1-2</b>	202		<b>P3-8</b>	501
	<b>P1-3</b>	203	Tang, W.	<b>P2-78</b>	420
Sun, X.K.	<b>P1-2</b>	202	Tanimoto, H.	<b>14-4</b>	107

## Authors Index

Tanimoto, H.	<b>P2-146</b>	488	Trakhtenberg, L.I.	<b>P1-126</b>	325
	<b>P3-66</b>	559		<b>P3-107</b>	600
Tarasov, B.P.	<b>P1-92</b>	292	Treilleux, M.	<b>P2-7</b>	347
	<b>P3-46</b>	539	Trifonov, A.S.	<b>23-9</b>	155
Tasaki, A.	<b>P2-146</b>	488	Tripathy, S.	<b>P3-94</b>	586
Tast, F.	<b>9-3</b>	85	Tronc, E.	<b>17-2</b>	117
	<b>P2-8</b>	348	Tropsha, Y.	<b>3-3</b>	58
Taylor, R.S.	<b>P2-135</b>	477	Trovarelli, A.	<b>P3-59</b>	552
Tcherdyntsev, V.V.	<b>P1-24</b>	224	Trudeau, M.L.	<b>3-5</b>	60
	<b>P2-24</b>	364		<b>P3-64</b>	557
Tejada, J.	<b>P2-76</b>	418	Trushevsky, S.M.	<b>P1-89</b>	289
	<b>P2-88</b>	430	Trusin, S.A.	<b>P3-86</b>	578
Tellkamp, V.L.	<b>P1-78</b>	278	Tsai, S.H.	<b>IP-35</b>	194
Temst, K.	<b>P2-99</b>	441	Tsai, T.G.	<b>IP-35</b>	194
Tepper, F.	<b>P1-70</b>	270	Tsai, W-L.	<b>P1-105</b>	304
	<b>P3-119</b>	611		<b>P3-102</b>	595
Terent'ev, S.V.	<b>P2-139</b>	481		<b>P2-75</b>	417
Terlingen, J.G.A.,	<b>IP-6</b>	165	Tsakalakos, Th.	<b>5-2</b>	68
Tesche, B.	<b>P3-28</b>	521		<b>P2-9</b>	349
Testa, A.M.	<b>P2-89</b>	431	Tsang, S.C.E.	<b>22-4</b>	145
Tetelbaum, D.I.	<b>P3-86</b>	578		<b>P3-103</b>	596
Thölén, A.R.	<b>15-2</b>	109	TschöpeA.	<b>P3-110</b>	602
	<b>P3-53</b>	546	Tsellaermaer, V.Ya	<b>P2-21</b>	361
Thomas, R.	<b>24-2</b>	157	Tsenev, N.K.	<b>P2-103</b>	445
Thordson, J.V.	<b>P2-61</b>	401	Tsouris,P	<b>P2-9</b>	349
Thurnauer, M.C.	<b>P2-45</b>	385	Tsunawakit, Y.	<b>P1-119</b>	318
Thurston, T.R.	<b>22-2</b>	143	Tsunekawa, S.	<b>IP-1</b>	160
Tiberto, P.	<b>P2-136</b>	478	Tsuzuki, T.	<b>4-4</b>	64
Tien, C.	<b>P2-90</b>	432	Tsvetkova, T.	<b>P2-148</b>	490
	<b>P2-147</b>	489	Tsybulya, S.V.	<b>P3-72</b>	565
Tillement, O.	<b>P2-15</b>	355	Tuallon, J.	<b>P2-6</b>	346
Tohji, K.	<b>IP-1</b>	160	Tung, C-Y.	<b>P2-75</b>	417
Tomilin, I.A.	<b>P1-24</b>	224	Turkki, T.	<b>P1-83</b>	283
	<b>P2-24</b>	364		<b>P3-64</b>	557
Tomut, M.	<b>P2-107</b>	449		<b>P3-114</b>	606
Tonejc, A.	<b>P3-63</b>	556	Turquat, Ch.	<b>P1-71</b>	271
Tonejc, A.M.	<b>P3-63</b>	556	Tyunina, M.	<b>IP-38</b>	197
Toppari, J.J.	<b>IP-23</b>	182		<b>P1-93</b>	293
Tousimi, K.	<b>23-8</b>	154	Tzeng, S-J.	<b>P1-105</b>	304
Träger, F.	<b>P2-1</b>	341		<b>P3-102</b>	595
	<b>P2-11</b>	351		<b>P2-75</b>	417
	<b>P3-106</b>	599			

**Authors Index****U**

Uimin, M.A.	<b>18-3</b>	125	Vayssieres, L.	<b>P1-118</b>	317
Ulman, Avi.	<b>P2-58</b>	398	Vegge, T.	<b>P2-30</b>	370
Umeshara, H.	<b>P3-91</b>	583	Veith, M.	<b>P2-32</b>	372
Unruh, H.G.	<b>IP-16</b>	175		<b>4-3</b>	63
Unruh, K.M.	<b>P2-135</b>	477		<b>4-5</b>	65
Urse, M.	<b>P1-110</b>	309	Venger, E.F.	<b>P1-48</b>	248
	<b>P1-120</b>	319	Venkatasubramanian, R.	<b>P1-49</b>	249
	<b>P2-116</b>	458	Vergaga, J.	<b>P2-39</b>	379

Uskokovic, D.

	<b>P1-27</b>	227	Verkin, B.I.	<b>P2-139</b>	481
	<b>P1-75</b>	275	Vialle, J.L.	<b>P2-7</b>	347
	<b>P2-17</b>	357	Viereck, J.	<b>P2-1</b>	341

Ustinov, V.M.

	<b>P2-54</b>	394	Vijayalakshmi, R.	<b>IP-33</b>	192
			Vijayalakshmi, S.	<b>10-2</b>	90

**V**

Vakhrushev, S.B.	<b>P3-79</b>	571	Vinai, F.	<b>P2-136</b>	478
Valdre, G.	<b>23-2</b>	148		<b>P3-108</b>	601

	<b>2-4</b>	52	Vincze, I.	<b>P3-44</b>	537
	<b>23-2</b>	148	Viswanath, R.N.	<b>IP-30</b>	189
	<b>P2-81</b>	423	Vogel, V.	<b>23-4</b>	150
	<b>P2-82</b>	424	Volkova, E.G.	<b>IP-34</b>	193
	<b>P2-127</b>	469	Vollath, D.	<b>7-3</b>	78

	<b>P3-9</b>	502	Volodin, A.	<b>P2-99</b>	441
	<b>P3-117</b>	609	Voronkov, G.P.	<b>P1-85</b>	285
	<b>P1-41</b>	241	Voronov, O.A.	<b>22-5</b>	146
	<b>P1-42</b>	242	Vorontsov, P.S.	<b>P1-126</b>	325
	<b>P1-71</b>	271		<b>P3-107</b>	600

Valtchev, K.	<b>P1-48</b>	248	Vovk, E.V.	<b>P1-39</b>	239
vanderKlink, J.	<b>P3-35</b>	528			

VandeVeerdonk, R.J.M.	<b>18-5</b>	127		<b>W</b>	
VanHaesendonck, C.	<b>P2-99</b>	441	Wäckelgård, E	<b>P2-91</b>	433
vanHeerden, D.	<b>IP-2</b>	161	Wagner, J.	<b>4-3</b>	63
vanVeggel, F.C.J.M.	<b>P3-38</b>	531	Wagner, W.	<b>15-6</b>	113
Vardeny, V.Z.	<b>23-1</b>	147		<b>19-5</b>	132

Varga, L.K.	<b>17-7</b>	122		<b>P2-113</b>	455
	<b>P1-32</b>	232		<b>P3-35</b>	528
	<b>P1-77</b>	277		<b>P3-68</b>	561
	<b>P3-30</b>	523	Wahlberg, S.	<b>P1-80</b>	280
	<b>P3-44</b>	537		<b>P1-138</b>	337

Vargas, W.	<b>P2-118</b>	460	WakaiF.	<b>P1-43</b>	243
Varghese, V.	<b>P1-29</b>	229	Wakayama, Y.	<b>2-1</b>	49

## **Authors Index**

Wang, B.W.	<b>P3-8</b>	501	Wikner, M.	<b>P3-65</b>	558
Wang, F.	<b>P3-92</b>	584	Wilcoxon, J.P.	<b>22-2</b>	143
Wang, J.	<b>P1-5</b>	205	Wilson, W.R.	<b>P2-135</b>	477
Wang, L.	<b>P3-100</b>	593	Winter, R.	<b>P2-129</b>	471
Wang, M.	<b>P1-84</b>	284	Winterer, M.	<b>IP-36</b>	195
	<b>P1-138</b>	337		<b>P1-88</b>	288
Wang, S.K.	<b>P2-104</b>	446		<b>P2-69</b>	409
Wang, T.M.	<b>P2-72</b>	414		<b>P3-69</b>	562
Wang, Y.	<b>IP-20</b>	179	Witek, A.	<b>P1-34</b>	234
	<b>P1-58</b>	258	Wittborn, J.	<b>P2-151</b>	493
	<b>P2-126</b>	468	Woldt, E.	<b>P3-14</b>	507
	<b>P3-87</b>	579	Wolf, D.	<b>9-5</b>	87
Wang, Z.C.	<b>10-4</b>	92	Wolf, H.	<b>P2-98</b>	440
Wäppling, R.	<b>P2-10</b>	350	Wu, C.Y.	<b>P2-36</b>	376
	<b>P2-92</b>	434		<b>P2-105</b>	447
Warren, P.J.	<b>P3-71</b>	564	Wu, M.	<b>P3-92</b>	584
Wassermann, E.F.	<b>2-7</b>	55	Wu, W.	<b>P3-115</b>	607
Webster, T.J.	<b>23-7</b>	153	Wu, X.	<b>IP-20</b>	179
Weertman, J.R.	<b>IP-27</b>	186		<b>P1-56</b>	256
Wei, F.L.	<b>P2-72</b>	414		<b>P1-58</b>	258
Wei, W.	<b>P1-2</b>	202		<b>P2-126</b>	468
	<b>P1-3</b>	203		<b>P3-87</b>	579
Weib, B.	<b>P1-20</b>	220	Würschum, R.	<b>15-4</b>	111
	<b>P1-100</b>	300		<b>P2-120</b>	462
Weins, W.N.	<b>P3-58</b>	551		<b>P3-66</b>	559
Weissbuch, I.	<b>P2-37</b>	377	Wynn, P.	<b>12-5</b>	101
Weissmuller, J.	<b>IP-29</b>	188	Wyrzykowski, J.W.	<b>P1-34</b>	234
	<b>P3-95</b>	587		<b>P1-35</b>	235
Weller, D.	<b>24-3</b>	158			
Wenzel, T.	<b>P2-1</b>	341	<b>X</b>		
Werkmeister, K.-St.	<b>P1-60</b>	260	Xenoulis.A	<b>P2-9</b>	349
Wesseling, E.	<b>17-1</b>	116	Xiao, J.Q.	<b>P2-135</b>	477
Westergren, J.	<b>IP-28</b>	187	Xiao, T.D.	<b>P1-6</b>	206
Westerman, K.	<b>P3-61</b>	554		<b>P3-19</b>	512
Weston, C.	<b>P3-71</b>	564	Xing, L.Q	<b>P1-100</b>	300
Westreich, P.	<b>P1-112</b>	311		<b>P1-124</b>	323
White, C.W.	<b>10-2</b>	90	Xu, B.	<b>P2-73</b>	415
Wichert, Th	<b>P2-98</b>	440		<b>P3-74</b>	566
Wiedenmann, A.	<b>19-5</b>	132			
	<b>P3-22</b>	515			
	<b>P3-23</b>	516			
	<b>P3-68</b>	561			

**Authors Index****Y**

Ya, V. **P2-21** 361  
Yacaman, M.J. **10-1** 89  
Yamagata, Y. **P2-52** 392  
Yamaguchi, S. **P3-43** 536  
Yamamoto, T.A. **P1-134** 333  
**P1-13** 213  
**P1-133** 332  
**P1-136** 335  
**P3-121** 613  
Yamashita, J.Y. **P3-45** 538  
Yamazato, M. **P2-52** 392  
Yan, X. **P2-104** 446  
Yang, D. **P1-112** 311  
Yang, D.S. **P3-55** 548  
Yang, X.L. **P1-26** 226  
Yang, Z. **P2-72** 414  
**P3-6** 499  
Yanovsky, A.V. **P2-100** 442  
**P2-101** 443  
Yao, Y.D. **10-4** 92  
**P2-36** 376  
**P2-75** 417  
**P3-1** 494  
Yao, Yimin **P3-53** 546  
Yartys, V.A. **P1-92** 292  
Yasumoto, K. **P3-90** 582  
Yatsimirsky, V.K. **P3-105** 598  
Yavari, A.R. **23-8** 154  
Yelsukov, E.P. **P1-55** 255  
**P1-116** 315  
Yermakov, A.Ye **18-3** 125  
**IP-10** 169  
Ying, J.Y. **22-1** 142  
**P3-109** 340  
Yogo, K. **P1-69** 269  
Yokotsuka, T **8-1** 81  
Yoo, S.H. **21-3** 140  
**P1-73** 273  
Yoo, Y.G. **P3-55** 548  
Youngdahl, C.J. **IP-27** 186

**Yu, J.H.**

Yu, M. **24-2** 157  
Yu, R.H. **P2-135** 477  
Yu, S.C. **IP-21** 180  
**P2-138** 480  
**P3-55** 548  
**P3-80** 572  
Yumaguzin, Yu.M. **P3-85** 577  
Yurgelevych, I. **P2-148** 490  
Yuzephovich, O.I. **P2-38** 378  
**P2-42** 382  
**P2-47** 387

**Z**

Zabashta, L. **P2-2** 342  
Zacharenko, M.I. **P3-105** 598  
Zagorodni, A.A. **P3-100** 593  
Zagorskii, V.V. **13-1** 102  
**P2-115** 457  
Zaichenko, S.G. **P2-142** 484  
Zaikovskii, V.I. **IP-37** 196  
**P1-123** 322  
Zaitsev, S.V. **P2-54** 394  
Zajkov, N.K. **IP-10** 169  
Zakharenko, M. **P2-148** 490  
Zakharov, N.D. **24-4** 159  
Zakhidov, A.A. **7-2** 77  
**23-1** 147  
Zarur, AndreyJ. **P3-109** 340  
Zaslavskaya, T.N. **IP-7** 166  
Zavjalov, S.A. **P1-126** 325  
**P3-107** 600  
Zeng, W. **P1-5** 205  
Zhang, D. **7-4** 79  
Zhang, H. **P1-58** 258  
Zhang, J.R. **P2-78** 420  
Zhang, L. **P3-76** 568  
**P3-115** 607  
Zhang, L.D. **9-6** 88  
**P1-99** 299  
**P3-77** 569

**Authors Index**

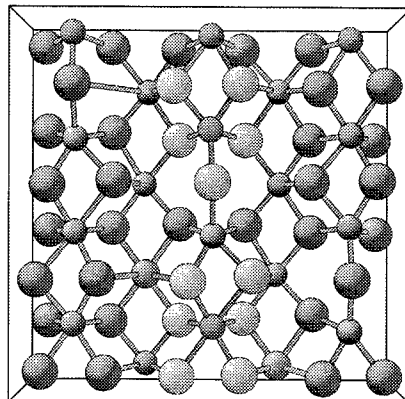
Zhang, L.D.	<b>P3-78</b>	570
Zhang, S.Y.	<b>P3-8</b>	501
Zhang, T.	<b>P3-5</b>	498
	<b>P3-12</b>	505
Zhang, W.	<b>16-2</b>	115
Zhang, X.	<b>P2-76</b>	418
Zhang, Yu	<b>P1-84</b>	284
	<b>P3-100</b>	593
Zhang, Z	<b>P1-138</b>	337
Zhao, Y.W.	<b>P3-113</b>	605
Zharmagambetova, A.	<b>P3-111</b>	603
Zheng, W.	<b>P3-96</b>	588
Zhernakov, V.S.	<b>P3-117</b>	609
Zhou, F.	<b>P3-37</b>	530
Zhuang, L.	<b>16-2</b>	115
Zhubanov, B.	<b>P1-72</b>	272
	<b>P2-41</b>	381
	<b>P1-103</b>	410
Zhukov, A.E.	<b>P2-54</b>	394
Ziolo, R.	<b>P2-88</b>	430
Zivanovic, P.	<b>P1-1</b>	201
Zsebök, O.	<b>P2-61</b>	401
Zubairov, L.R.	<b>P3-85</b>	577
Zubarev, A.Y.	<b>P2-22</b>	362
Zurawicz, J.K.	<b>P2-83</b>	425
Zver'kova, I.I.	<b>P3-4</b>	497

# The Materials Research Consortium on Clusters and Ultrafine Particles

Established in 1990, one of eleven (now eight) Swedish Materials Research Consortia.

The *objective* of the Consortium is to develop physical and chemical methods to synthesize, process, and characterize materials assembled from clusters or nanoparticles. The Consortium is made up of groups from Chemistry, Physics, and Materials Science, with both Experimental and Theoretical efforts.

*Calculation of the structure of calcium-doped cerium oxide used to simulate the reactivity of doped nanoparticles. The large balls represent oxygen atoms, the green balls calcium, and the smallest balls cerium. The cerium sites which theory indicates are induced by the presence of calcium are indicated in blue. It is at such sites that the increased reactivity is found to originate, offering an explanation of the observed effect for the particles synthesized at KTH as part of the Consortium program.*



Our *approach* consists of a combined Experimental-Theoretical program in **three main areas: Size-Selected Clusters, Nanophase Materials, and Nanostructured Electrodes**. Projects range from controlled synthesis of clusters to the synthesis and processing of nanostructured materials, supported by comprehensive characterization capabilities. The activities in the Consortium include an important component of basic experimental research, which expedites the connection to a strong theoretical effort. Characterisation tools include advanced electron spectroscopies, both UHV and at liquid/solid interfaces.

Groups within the Consortium *collaborate* with scientists in Europe (both networks such as Joule, TMR, etc.) and bilaterally. Several patents have been obtained under the research programme, and industrial companies, both national and international, are directly involved in several projects.

The Consortium Leader is Prof. Nils Mårtensson, MAX-Lab/Uppsala Univ., and the Board of Directors consists of Dr. Gunnar Brandt, Sandvik Coromant AB, (Chair), Dr. Bjerne Clausen, Haldor Topsøe A/S, Dr. Anders Hagfeldt, Uppsala Univ., Prof. Mamoun Muhammed, Royal Inst. of Tech.. The Coordinator is Dr. Paul Brühwiler, Uppsala Univ.. To contact us or learn more, use our WWW address: <<http://xray.uu.se/cluster/>>.



KUNGL  
TEKNISKA  
HÖGSKOLAN

## Kungliga Tekniska Högskolan, KTH

Kungl Tekniska Högskolan, KTH, in Stockholm, Sweden is a technical university with first-class education and research. It provides one-third of Sweden's capacity for engineering studies and technical research at post-secondary level. KTH has about 11 000 students and 2 800 employees and about 1 300 active post-graduate students. KTH trains architects and engineers at Master's and Bachelor's level, as well as doctors and licentiates.

KTH is organised in six faculties and a college of applied engineering:

- Architecture, Surveying and Civil Engineering (including School of Architecture)
- Electrical Engineering and Information Technology
- Chemistry and Chemical Engineering
- Mechanical and Materials Engineering (including School of Industrial Management)
- Engineering Physics
- College of Engineering

There are some 35 departments, each possessing a wide and comprehensive scientific competence for research and undergraduate education.

The undergraduate programmes and the research activities cover a broad spectrum, from natural sciences to all branches of technology including architecture, industrial economics, urban planning, work science and environmental technology. There are also two and three years engineering programmes, vocational higher education and programmes for subsequent and continuing education.

KTH provides study programmes leading to a Master of Science degree (in Swedish civilingenjör) in the following areas:

- Architecture
- Chemical Engineering
- Civil Engineering
- Computer Science
- Electrical Engineering
- Engineering Physics
- Industrial Economics and Management
- Materials Technology
- Mechanical Engineering
- Surveying
- Vehicle Engineering

KTH is very active in the European educational programmes Erasmus/Socrates and Tempus and is extensively involved in the European research programmes.

Higher education studies lead to Tekn Lic (two years) and Tekn Dr (four years) diploma. Both end with a thesis of which the latter must be defended in public. A list of the last twelve months' doctoral theses has been included in the end of this book.

KTH cooperates extensively with various national research centres and industrial research institutes and KTH has a well-developed research and educational network with universities and colleges all over the world.

Kungliga Tekniska Högskolan  
SE-100 44 Stockholm  
Visitors: Valhallavägen 79  
URL: <http://www.kth.se>



Teknikvetenskapliga  
Forskningsrådet  
Swedish Research Council  
for Engineering Sciences

The Swedish Research Council for Engineering Sciences (TFR) is a Swedish authority under the auspices of the Ministry of Education and Science. It was established in 1990 and its main purpose is to encourage and support the basic engineering sciences in Sweden. This is mainly done through a variety of grants, for which Swedish scientists are invited to apply once a year. TFR allocates annually about SEK 240 million. The proposals are assessed and ranked according to scientific quality, relevance for society and the scientific competence of the research team. It is mandatory that research results from funded projects be published.

TFR is responsible for supporting engineering research of industrial relevance, with emphasis on the education of graduate students and knowledge transfer. TFR also formulates policies for research and graduate education within the engineering sciences, and provides the Swedish government and its ministries with evaluations of these and related areas.

Policy-making, evaluations, and the handling of applications for grants are managed by a board of directors and a secretariat. The rules of nomination to the board are regulated by the government. The board of directors has one chair-person, ten members and ten deputy members, altogether 21 persons. Seven of these members and their corresponding deputy members are professors, elected by leading Swedish scientists. The chair-person and the other members (and corresponding deputy members) are appointed by the government. The secretariat consists of one secretary general (a professor), who is elected by the board of directors, a director of secretariat (an associate professor) and a staff of research officers, administrators, accountant and computer support.



Nobel Committees for Physics and Chemistry  
The Royal Swedish Academy of Sciences

## The Royal Swedish Academy of Sciences

The Royal Swedish Academy of Sciences is an independent, non-governmental organization founded in 1739. In 1998, the Academy has about 350 Swedish and 164 foreign members. The major aims of the Academy, are to promote research in mathematics and the natural sciences. These aims are achieved by stimulating national and international scientific cooperation; through seven scientific institutes; by publishing scientific journals; by distributing scientific information; and by promoting contact between scientists and society at large.

The Academy provides independent scientific advice to policy makers, ensures that scientific evidence and scientific considerations are included in the public debate, and prepares and submits proposals for science policy priorities, which can be used, for example, by the government. These activities are carried out mainly within the Academy's ten classes and special committees. The members take initiatives to symposias and official reports. They meet at the Academy every second week when lectures, open to the public, are held.

The Academy plays an active role in enhancing worldwide cooperation with scientists. Agreements concerning scientific cooperation have been reached with foreign academies all over the world.

To support and encourage school teachers the Academy arranges teachers' days with front line lectures, awards prizes and provides research information. *Science for everyone* is a project aiming to improve science teaching in the lower school levels.

One important task for the Academy is administration of the Swedish national committees which handle the contacts with the International Council of Scientific Unions (ICSU). A worldwide ICSU activity, housed at the Academy, is the *International Geosphere-Biosphere Programme: A Study of Global Change (IGBP)*. The aim of this programme is to describe and understand the interactive physical, chemical, and biological processes that regulate the total Earth system, the unique environment that it provides for life, the changes that are occurring in this system, and the manner in which they are influenced by human activities.

The Academy follows worldwide environmental development through its advisory body the *Environmental Committee*. The committee work, supported by its secretariat, includes both surveillance, identification, and investigation of current environmental problems.

Through the Academy, Sweden has a long tradition in polar research. The Academy's *Polar Committee* was established to coordinate, initiate, and support Swedish polar research. The Committee acts as an advisory board for the *Swedish Polar Research Secretariate*, a governmental authority for the promotion of Swedish polar research.

Prizes and grants are awarded annually from about 100 funds held in trust by the Academy. The Nobel Prizes in Physics and Chemistry have been awarded by the Academy since 1901, the Prize in Economic Sciences in memory of Alfred Nobel since 1968 and the Crafoord Prize since 1982.

Current information can be obtained at <http://www.kva.se>

**Only the best connections  
can lead to your congress.**

